Master Thesis, Department of Geosciences

The first attempt to correlate the migrated bitumen from the Helgeland Basin cores to Devonian source rocks and oils from the UK Orcadian Basin

-Is there a Devonian Orcadian type basin offshore Norway?

Anders Rønningen

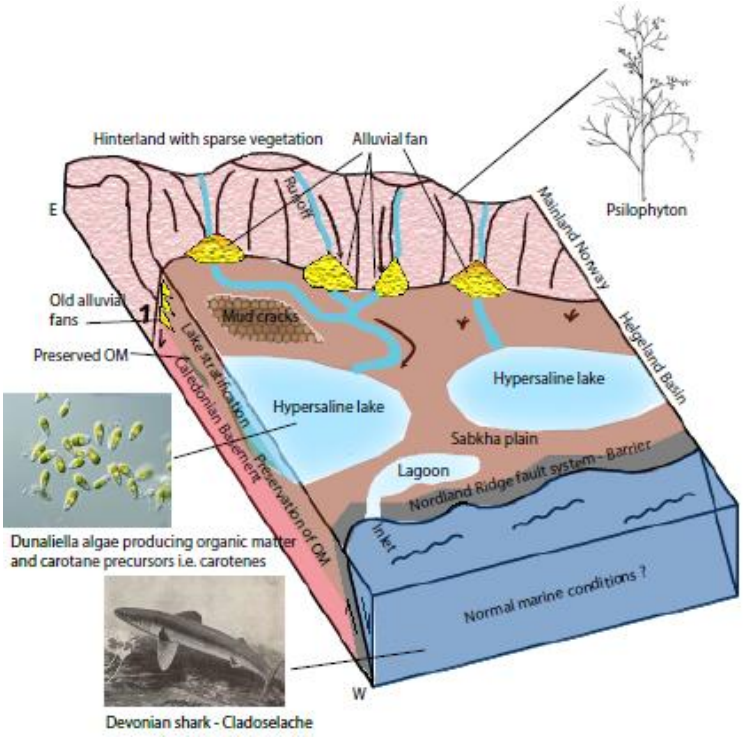

UNIVERSITY OF OSLO

FACULTY OF MATHEMATICS AND NATURAL SCIENCES

The first attempt to correlate the migrated bitumen fron the Helgeland Basin cores to Devonian source rocks and oils from the UK Orcadian Basin

-Is there a Devonian Orcadian type basin offshore Norway?

Anders Rønningen

Master Thesis in Geosciences

Discipline: Petroleum Geology and Petroleum Geophysics (PEGG)

Department of Geosciences

Faculty of Mathematics and Natural Sciences

University of Oslo

June, 2015

Tutor(s): Assoc. Prof. Dag A. Karlsen

This work is published digitally through DUO – Digitale Utgivelser ved UiO

http://www.duo.uio.no

It is also catalogued in BIBSYS (http://www.bibsys.no/english)

Abstract

A key focus of this thesis is if migrated bitumen from Lower to Middle Jurassic and Cretaceous age sandstones in the 6609/11-1, 6610/7-1 and the 6609/5-1 wells in the Helgeland Basin might originate from Devonian source rock strata. For a possible comparison of source rock facies has nine outcrop samples collected from the Orkneys been used alongside with the Beatrice oil from Moray Firth as references of the lacustrine Middle Devonian organofacies present in the Orcadian Basin, Also, oils from the Judy Field and the Embla Field were included in this investigation as their geochemical signature differs from the typical Kimmeridge derived oils on the Norwegian Shelf, which in this study is represented by the NSO-1 oil i.e. oil from the Oseberg Field.

Analytical methods i.e. GC-FID and GC-MS were used to generate characterization parameters used for indicating the maturity and also the type of organofacies of bitumen samples and the oil samples. In addition, TOC and Rock-Eval analysis were performed on the source rock samples for assessing the quality i.e. the kerogen type and the generative potential, and also for obtaining additional maturity information.

Based on the TOC and Rock-Eval analysis, the HI of the five highest quality source rocks samples is in the range of 313 mg HC/g TOC to 397 mg/ HC/g TOC and those values corresponds to type II kerogen and the overall generative potential of the same five samples is categorized as good to very good, i.e. the TOC values in the range of 1.48wt.% to 2.79wt.%. The four other samples scores lower in both quality and/or generative potential. Of the nine source rock samples in total, only one scores below the minimum criteria for being categorized as a source rock, i.e. a TOC value of at least 0.5wt%.

All the three wells i.e. 6609/11-1, 6610/7-1 and 6609/5-1 from which the bitumen bitumen samples studied in this thesis were isolated show evidence of having received migrating oils from a source rock that correlates with the geochemistry of the lacustrine Middle Devonian source rocks of the general Orcadian Basin source rock facies. In particular is the positive identification of β-carotane in the 6609/11-1, 6610/7-1 and 6609/5-1 wells of the highest interest as this biomarker is a type component for the Devonian lacustrine systems.

It is thus concluded that there are Devonian source rock systems present in the Helgeland Basin which are of sufficient magnitude to generate and migrate oil into the studied sandstones which are of Early to Middle Jurassic and Cretaceous age.

In addition to oil from the likely Middle Devonian source rock, well 6609/11-1 also contains migrated oil from a terrestrially derived source rock and the upper section in well 6610/7-1 (depth 2661m to 2668.5m) and also well 6609/5-1 contains migrated bitumen (oil) which is clearly sourced form a marine derived source, i.e. the Late Jurassic Kimmeridge equivalent. The bitumen samples in the lower section of well 6610/7-1 (depth 2713.8 to 2715m) bears no resemblance of influence from lacustrine Middle Devonian source rocks, but are interpreted to have been sourced mainly from terrestrially derived source rocks, and there is also indications for co-sourcing from the Late Jurassic Kimmeridge equivalent source rocks.

Furthermore, oils representing the Embla Field, the Judy Field and the Oseberg Field, are interpreted to have been mixed in the reservoir with petroleum from a lacustrine Middle Devonian source rock equivalent. Also this is totally new information as such has never been described, and it is inferred that such palaeo-oil must have escaped from the Oseberg Field reservoir and the Judy Field reservoirs long before the arrival of the present oil charges. It is thus inferred that also in the drainage areas of Oseberg, Embla and Judy are the Devonian basins which have generated oil.

Concerning the maturity, the source rock bitumen samples from the Orkneys are considered marginally mature, and the Helgeland Basin bitumen samples, the Judy oil, the Beatrice oil and the Oseberg oil are considered to be at maturity levels which corresponds to the middle of the oil window. The Embla oil is highly mature, with a maturity level corresponding to the later part of the oil window.

The maturity from the lowest to the highest is as follows: The source rock bitumen samples from the Orkneys - NSO-1 (Oseberg) - Beatrice - 6609/11-1 - Judy - 6610/7-1 upper section - 6610/7-1 lower section - 6609/5-1 - Embla.

Acknowledgements

I would like to thank my supervisor Dr. Dag A. Karlsen for his great teaching skills in the petroleum systems course earlier in the master degree, which encouraged me to catch the interest of organic geochemistry. I would also thank him for giving me the opportunity to write such an interesting thesis, for this I am really grateful. He has also been of great support throughout the whole period of thesis working, and has been an excellent source for guidance and also a really helpful discussion partner.

I would also thank Kristian Backer-Owe for helpful discussions and guidance related to practical lab work and also for providing articles and templates and a special thanks to Dr. John Flett Brown for providence of source rock samples from the Orkneys, thus making this thesis possible, and for his helpful comments. Also thanks to Tesfamariam Berhane Abay for lab guidance and assistance, Zagros Matapour for lab assistance and Benedict Lerch for providing me with additional templates.

Finally, I would like to thank my fellow students and good friends for interesting discussions and for having made the period of my master degree a great time.

Oslo, June 2015

Anders Rønningen

Table of Contents

1. Introduction

1.1 Introduction

Petroleum plays on the Norwegian continental shelf (NCS) and in the UK – sector have mostly been related to Jurassic source rocks, the most important being the Kimmeridge equivalent, the so-called "hot-shale" from Late Jurassic. However, with discoveries of petroleum sourced from Palaeozoic sources having been reported, e.g. the Beatrice Field (Peters et al. 1989, Bailey 1990) and the Clair Field (Mark et al., 2008), both fields located in the UK-sector and sourced from the Orcadian Basin Middle Devonian lacustrine source rock, it was brought to attention that there could be other important source rocks contributing commercial quantities of hydrocarbons in the UK sector and also on the NCS in regions where the Kimmeridge equivalent is still immature.

1.2 Introduction Helgeland Basin

A few wells in the Helgeland Basin area, located outside mainland Norway in the Norwegian Sea at latitudes of 66-67°N have been drilled, but all have been reported dry. However, some hydrocarbon shows in well 6609/11-1, 6609/5-1 and 6610/7-1 have been reported (NPD, 2015a). Intervals in the sandstone core from well 6609-11/1 was stained with hydrocarbons and the geochemical signature was reported to differ from the typical NCS oils from the nearby Haltenbanken, having what seems to be a terrestrial or lacustrine origin instead of marine and was reported as of older age than Jurassic (Karlsen et al. 1995). Schou et al. (1983) suggested a mature Kimmeridge equivalent as the most likely main source for the hydrocarbons stained in intervals in the sandstone core in well 6610/7-1, but they did not exclude a possible second source for the three studied core samples from depths 2661.6m, 2668.05m and 2706m.

The oldest penetrated formations in the Norwegian Sea have been penetrated in shallow cores close to mainland Norway and these formations are of Late Permian age (Bugge et al., 2002) while the wells drilled in the Helgeland Basin have only encountered formations of Triassic and younger age. As a consequence, it is not proven whether there are sedimentary rocks of Devonian age with source rock potential present in the Helgeland Basin area. However, when considering the presence of Devonian rocks in Hornelen Basin onshore western part of Norway (Duncan and Buxton 1995), in the Barents Sea e.g. the western coast of Novaya Zemlya (Guo et al. 2010) and on Bjørnøya

(Gjelberg 1981), on Svalbard (Elvevold et al. 2007) and on East Greenland (Surlyk 1990), plus the known post-Caledonian palaeographical symmetry between Norway and East Greenland, it is not unlikely that Devonian strata with possible source rock potential is present also in the Helgeland Basin area in the Norwegian Sea. The Devonian age reservoir units with also a paleo-petroleum as described by Abay et al. (2014) is furthermore evidence to underline the potential for Devonian age petroleum systems on the Norwegian Offshore Continental Shelf.

Furthermore, based on seismic data, and correlation with East Greenland, presence of Devonian rocks in the Norwegian Sea can be presumed (Bukovics and Ziegler 1985), at least in depocenter areas (e.g. possibly in the Helgeland Basin) where accommodation space from the reactivation of Caledonian thrusts in Devonian was created (Pedersen et al., 2006). It is thus a possibility that the hydrocarbon shows in the Helgeland Basin could originate from an equivalent to the organic rich source rock from Middle Devonian in the Orcadian Basin, as it would be expected that the Devonian source rocks if present in the area, has surpassed the minimum maturity required for petroleum expulsion.

1.3 Thesis objectives

In this MSc thesis, further investigations of the Helgeland Basin bitumen from well 6609/11-1 with unusual geochemical signature reported in Karlsen et al. (1995) will be performed. Bitumen samples from selected depths in well 6609/11-1, 6610-7/1 and 6609/5-1 will be compared to diagnostic biomarkers from the Middle Devonian source rock bitumen samples from southern Orkneys for investigating possible similarities in geochemical signature that points towards the potential existence of Middle Devonian source rocks in areas of the Helgeland Basin. Furthermore, the Helgeland Basin bitumen samples will also be compared to the typical North Sea oil (NSO-1) and oil from the Beatrice Field as references for the marine Late Jurassic Kimmeridge equivalent and Middle Devonian lacustrine sourced oil respectively. Oils from the Embla Field and the Judy Field from the North Sea is also included in this study, as they differ in composition from the more common Kimmeridge equivalent sourced oils and possible linkage to Middle Devonian source rocks for the former and latter will thus be investigated.

The main objectives in this thesis will be as follows:

- To investigate the potential that the bitumen samples of the Helgeland Basin might be related to the organo-facies typified by the Middle Devonian source rocks from the

Orcadian Basin in the based on diagnostic biomarkers and δ13C isotope data, and try to determine the main source if possible if there are indications of co-sourcing.

- To investigate if analytical data from selected oils in the North Sea, conventionally believed to be sourced 100% from Jurassic source rocks, might in fact also contain Devonian hydrocarbon signatures. If so found, this might thus extend our understanding of Devonian source rock kitchens on the Norwegian shelf.
- To evaluate the quality of the Middle Devonian source rock bitumen samples and the associates potential source rocks from the Orkneys based on biomarkers and also TOC and Rock-Eval analysis, and to assess variations within the source rock unit.
- To assess the maturity differences of the bitumen samples within the Helgeland Basin and compare to internally the geochemistry of the NSO-1, the Beatrice oil and the Orkney source rock bitumen samples.

2. Geological setting

Chapter 2 gives an overview of the Orcadian Basin and Devonian source rock units within the basin, plus the maturation history of the area. Furthermore will the Helgeland Basin be briefly introduced. The outline is as follows:

2.1 Introduction of the Orcadian Basin

2.2 The stratigraphical units of the Devonian deposits i.e. the Old Red Sandstone (ORS)

2.3 Maturation history of the Orcadian Basin

2.4 Source rock potential of the ORS

2.5 Geological setting of the Norwegian Sea with emphasis on theDevonian time in the Helgeland Basin

2.1 Introduction of the Orcadian Basin

Outcrops of Devonian sediments have been located in the area around Moray Firth i.e. in the Caithness and Inverness in the Scottish Highland and on the Orkney and Shetland Islands in the UK - sector; this greater area was referred to as the Orcadian Basin by Marshall et al., (1986). Later publication by Ziegler (1990) proposed that the Orcadian basin extended from Moray Firth across the northern North Sea and to the Hornelen basin in Norway where it was earlier reported presence of minor lacustrine sequences (Steel et al., 1985), but little information about the area in between was known at that time. Later, well 9/16-3 was drilled on the western flank of the Beryl Embayment (see Figure 2.1) and encountered Middle Devonian rocks which were interpreted as a part of the Orcadian basin, and thus provided an important link of the extent of the Orcadian basin eastwards towards mainland Norway (Duncan and Buxton, 1995). Mark et al., (2008) defined the Orcadian Basin to extend from the Inner Moray Firth in west, the Shetland Islands in north and across the northern North Sea to mainland Norway in the east (see Figure 2.1).

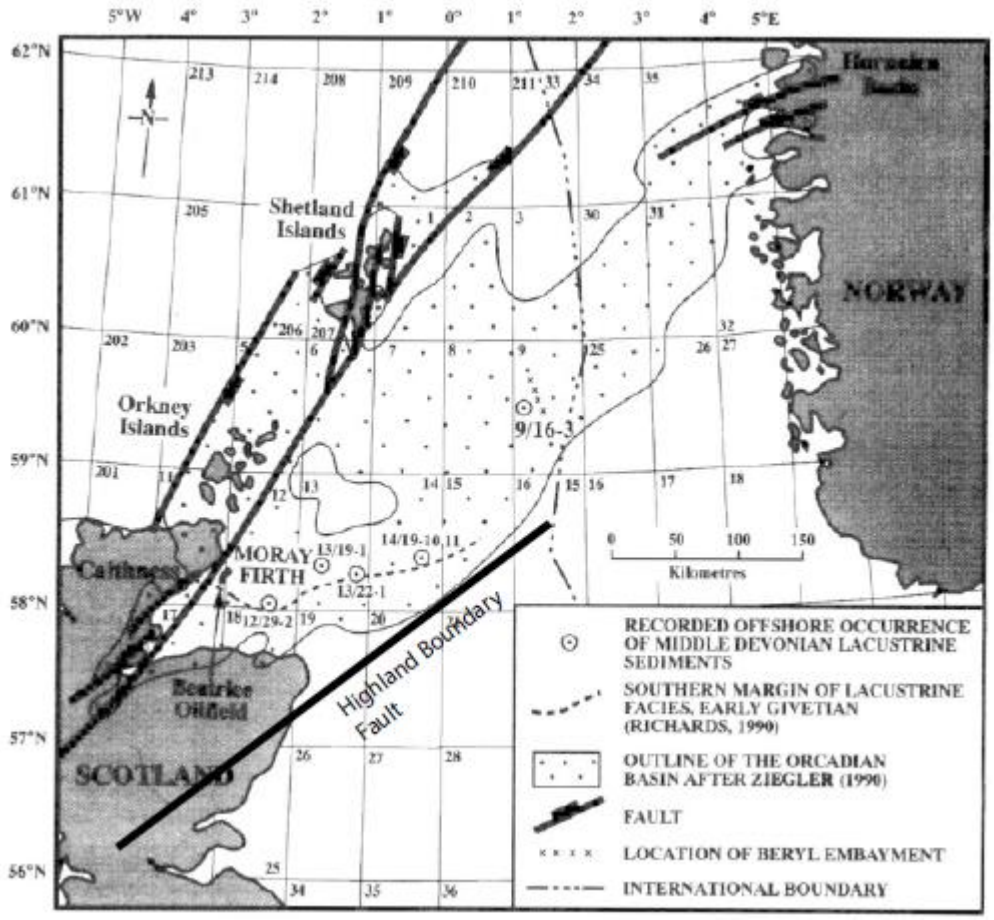

Figure 2.1: The outline of the Orcadian Basin (modified from Duncan and Buxton, 1995). Notice that the outline extends onto mainland Norway i.e. Solund-Fensfjord in the East and the southern boundary defined by the Highland Boundary Fault which acted as a barrier that prevented mixing with marine water from the south.

The Orcadian Basin is a result from the collapse of the Caledonian Orogeny that caused reactivation of fault zones which lead to rifting that created several linked halfgrabens which defines the basin (Mark et al., 2008). The deposits in the Orcadian Basin are of Devonian age, have an average thickness of 3-4 km, and are named the Old Red Sandstone (ORS). The Devonian sediments were deposited in a hot and arid continental setting with lacustrine, alluvial fans and braided fluvial plan environments (Downie, 2009).

2.2 The stratigraphical units of the Devonian deposits i.e. the Old Red Sandstone (ORS)

The ORS is subdivided into a lower, middle and upper unit, which roughly corresponds to the Lower, the Middle and the Upper Devonian respectively (Trewin, 1989). The lithostratigraphical units of the ORS in the Caithness and Orkney area are shown in Figure 2.2. The Lower ORS comprises generally

in the proximal parts of the basin a conglomerate facies which was deposited by alluvial fans formed at the rift basin margins, and this facies is located on the fault scarps, while playa lake sediments were formed in the more distal parts of the basin (Trewin, 1989). In the locality of Yesnaby on the Orkneys there is presence of aeolian cross-bedded sandstones which could serve as potential reservoirs (Trewin, 1989).

The Lower – Middle ORS boundary is mostly an unconformity which was caused by events of folding, faulting, uplift and erosion in the late Lower Devonian to early Middle Devonian time (Trewin, 1989). In the Caithness area, the boundary is possibly conformable and this area acted as an area of deposition of the Caithness flagstone group at the time when other areas in the basin were eroded. Later, in Middle Devonian, the deposition of the Achanarras fish beds, extended to include the whole area from Moray Firth, Inverness, Caithness, Orkney and Shetland (Trewin, 1989) and because of the wide extent of those beds; they are used as a reference for correlation of the Orcadian Basin (Hillier and Marshall, 1992).

In the Stromness Flagstone Formations (see Figure 2.2), repeated cycles of shallow – deep lake leaded to organic rich laminated calcareous siltstone deposits of so-called fish-bed lithology during periods of deep water (Trewin, 1989); fish-carcasses are preserved in some intervals during periods of anoxic conditions, caused by thermal stratification of the lake (Trewin, 1985). During periods with shallower water levels, the organic richness of the deposits drops while the input of fine-grained sand increases, and the lake-floor eventually becomes exposed to air as seen from the presence of dessication cracks (Trewin, 1989). The alteration between a playa lake and a permanently stratified lake was a process driven by variations in the precipitation to evaporation ratio which resulted from the weakening or strengthening of the seasonal monsoon by climatic cycles (Marshall et al., 2011).

Above the flagstone group, i.e. the Eday Marl (see Figure 2.2), there is a transition towards more aeolian and fluvial dominated facies which are related to a sabkha environment, while the lacustrine laminites are only seen at the base of the formation at the time when precipitation exceeded evaporation (Marshall et al., 2011). After the short lifespan of the stratified lake, the evaporation surpassed the precipitation, and restricted the water depth of the lake, and thus did not allow development of a stratified water column again (Marshall et al., 2011). South from the Orcadian Basin, the water was of a marine character e.g. as seen in the Devonian marine carbonates in the Embla Field, and a physical barrier i.e. the Highland Boundary Fault which marks the southern boundary of the Orcadian Basin (see Figure 2.1), prevented mixing with the lacustrine water in the Orcadian Lake (Marshall et al., 2011). However, In late Givetian time, events of marine incursions in

the Orcadian Lake caused by flooding of the Highland Boundary fault and thus allowing mixing of lacustrine and marine water, have been reported as seen from intervals with restricted marine/marine fauna in the Roeberry Member and more significantly in the Berstane Member from Eday Marl Formation (see Figure 2.2) (Marshall et al., 2011). The Upper ORS is in general dominated by widespread fluvial sandstones (Trewin, 1989).

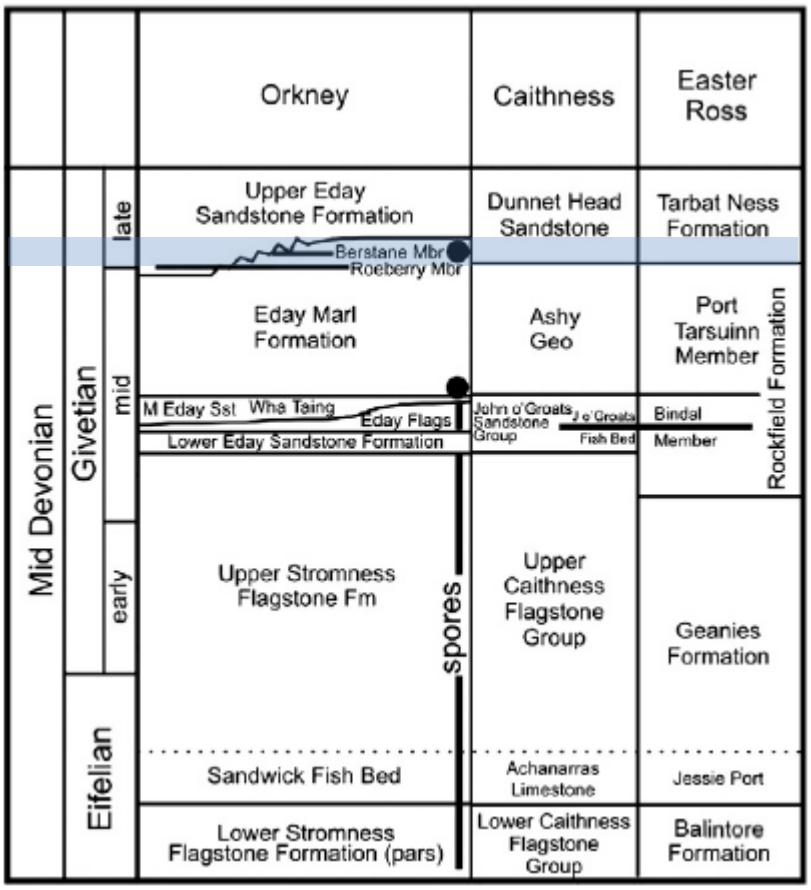

Figure 2.2: The ORS lithostratgraphic units in the Caithness and Orkney areas in the Orcadian basin (modified from Marshall et al., 2011). The period which comprises known events of marine incursions into the Orcadian Basin is outlined in blue.

2.3 Maturation history of the Orcadian Basin

Concerning the maturation history, some of the areas in the Orcadian Basin are believed to have matured at a fast pace, having steep geothermal gradients that typically occurs in a rift basin setting (Mark et al., 2008). From the presence of reservoir petroleum that were heated in situ by Permian dykes in the Orkneys, it is proposed that the Devonian lacustrine source rock entered the oil window as early as in latest Devonian to Middle Carboniferous (Astin, 1990) and that migration had already taken place by Late Carboniferous time (Mark et al. 2008). The Devonian source rocks in the

Caithness and Orkney areas reached maximum burial during Late Carboniferous time before the region was subjected to uplift, resulting in cooling of the source rocks with the consequence of no further oil generation from around 280 Ma. (Astin, 1990; Parnell et al., 1998). Geothermal history from Orkney samples shows that the temperature drops from 110°C 340 Ma. to 80°C 200 Ma. (Mark et al., 2008). Trewin (1989) suggested that deposition of Mesozoic sediments could lead to sufficient burial depth for petroleum generation from Devonian source rocks offshore Scotland, but considered it unlikely that the source rocks west from the Helmsdale fault could reach sufficient depths because of limited thickness of Mesozoic and Tertiary overburden.

2.4 Source rock potential of the ORS

Regarding source rock potential of the ORS in the Orcadian Basin, the Middle Devonian contains significant portions of highly organic rich deposits, while there are only some present in the Lower Devonian due to the more limited extent (Marshall, 1986). The organic matter consists mainly of amorphous organic matter which corresponds to kerogen type I (Trewin, 1989) as reflected in the high hydrogen index for the two Devonian samples (933 mg HC/g TOC and 609 mg HC/g TOC) (see Table 7.2) from Peters et al. (1989), although the latter was classified as type II by the authors based on the combination of the hydrogen index and oxygen index. The organic matter originated mainly from an algal source (Duncan and Hamilton, 1988) and was deposited during periods with anoxic conditions and high salinity levels of the lake.

2.5 Geological setting of the Norwegian Sea with emphasis on the Devonian time in the Helgeland Basin

Following the late to post-Caledonian orogeny, a period of extension events was initiated in the Norwegian Sea in Devonian with succeeding rifting events in Late Palaeozoic, Triassic, Jurassic, Cretaceous and the subsequent Late Cretaceous to Early Eocene rifting event which leaded to the opening of the Norwegian Sea (Osmundsen et al., 2002). The outline of basins in the Norwegian Sea i.e. the east-northeast to west-southwest extension as seen for e.g. the Helgeland Basin and the Vøring Basin (see Figure 2.3) was controlled by the fault system which developed during Devonian to Carboniferous and the continuous faulting in Permian and Early Triassic confined the variations in the sediment depositional pattern (Osmundsen et al., 2002).

Little is known about the distribution of sedimentary rocks of older age than Late Permian in the Helgeland Basin in the Norwegian Sea, as the older formations have not been physically encountered i.e. penetrated in wells, but formations from Devonian to Late Permian age are inferred on seismic data, and can be correlated from East Greenland (see section 1.2). From seismic data, Osmundsen et al. (2002) identified stratigraphy below the Trøndelag Platform, and based on the development of the basins and the creation of accommodation space in Devonian, the authors presumed that the stratigraphy represent strata of Devonian-Carboniferous age.

Furthermore, Bugge et al. (2002) suggested that an anhydrite unit from the Upper Permian Foldvik Creek Group represented redeposited and reworked sediments from a sabkha environment, and also that Late Permian shallow marine red sandstones were actually reworked and redeposited sediments of possibly Late Devonian age.

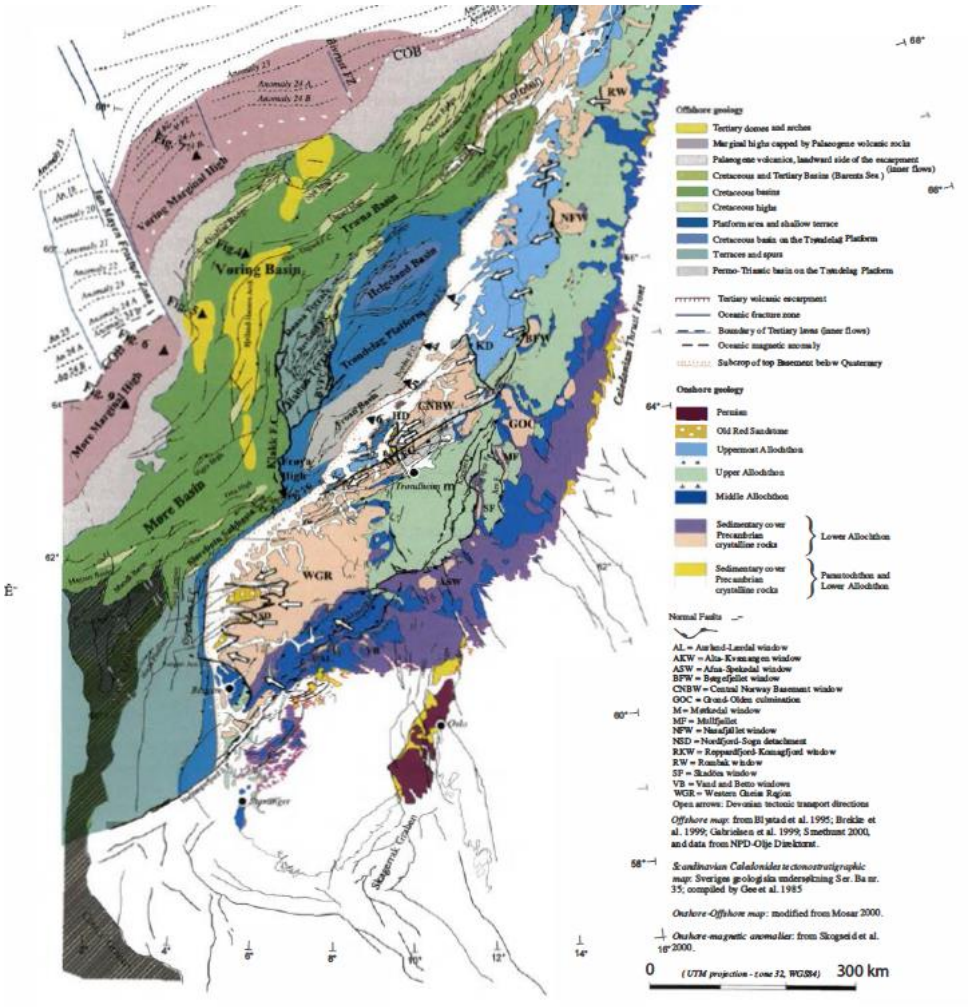

Figure 2.3: Overview of the structural elements and the nomenclature on the Norwegian Shelf, with emphasis on the Norwegian Sea (From Osmundsen et al., 2002). Notice the east-north east to west-southwest extension of the basins e.g. as for the Helgeland Basin.

3. Sample set and well description

In this chapter, the samples, i.e. both the core samples, the outcrop samples and the oils used in this thesis will be presented and the studied wells from the Helgeland Basin will be briefly introduced. This chapter will be presented as follows:

3.1 Areas of this study

3.2 Source rock samples from the Orcadian Basin at the Orkneys.

3.3 Samples from selected wells in the Helgeland Basin area

- 3.3.1. Overview of samples from the Helgeland Basin area
- 3.3.2. Description of selected wells in the Helgeland Basin area

3.4 Additional oils i.e. from the Oseberg Field (NSO-1 referece oil), the Embla Field, the Beatrice Field and the Judy Field

3.1 Areas of this study

The general region from where the samples originate are shown in Figure 3.1. The Helgeland Basin area (Figure 3.2), and the Orcadian Basin area (Figure 3.3) is marked with red and purple respectively. The samples studied in this MSc thesis and the respective coordinates are listed in Table 3.1.

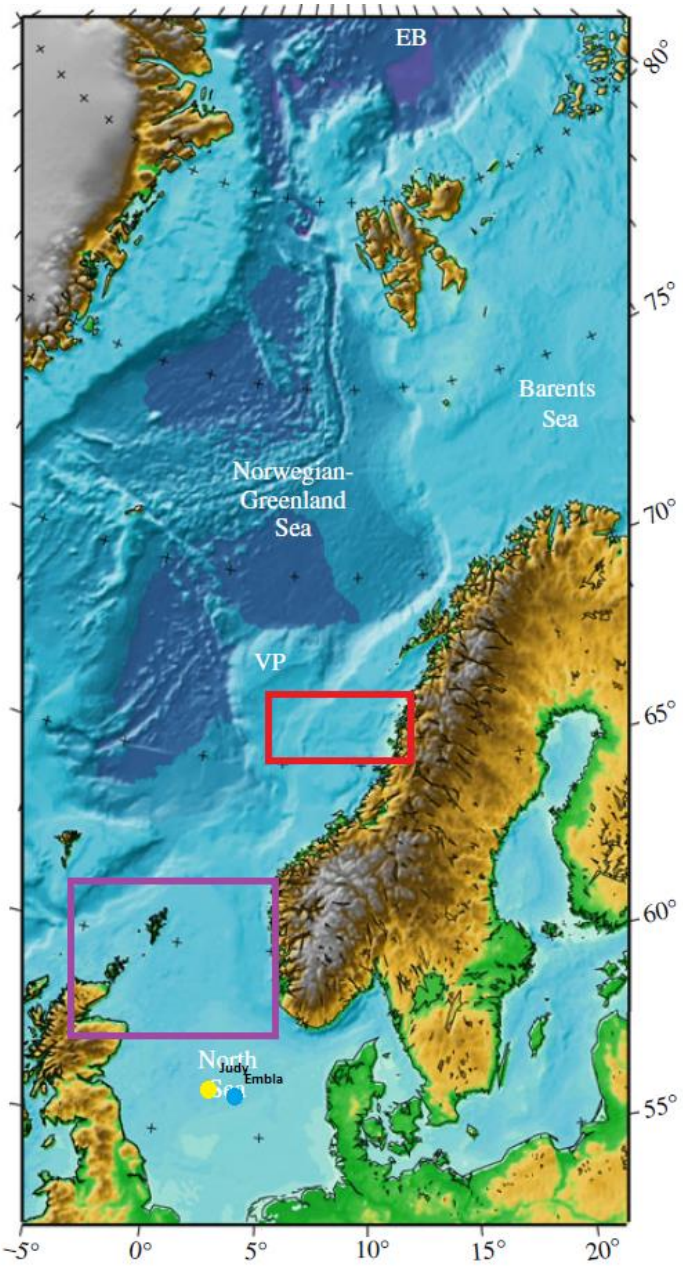

Figure 3.1: Map of the NCS and UK-sector (modified from Faleide et al., 2010). The Judy and Embla Fields are marked with yellow and blue color respectively. The Helgeland Basin area (Figure 3.2) is highlighted with a red color and the Orcadian Basin (Figure 3.3) is highlighted with purple color. The outlines of the basins are based on the areas of main focus in this thesis.

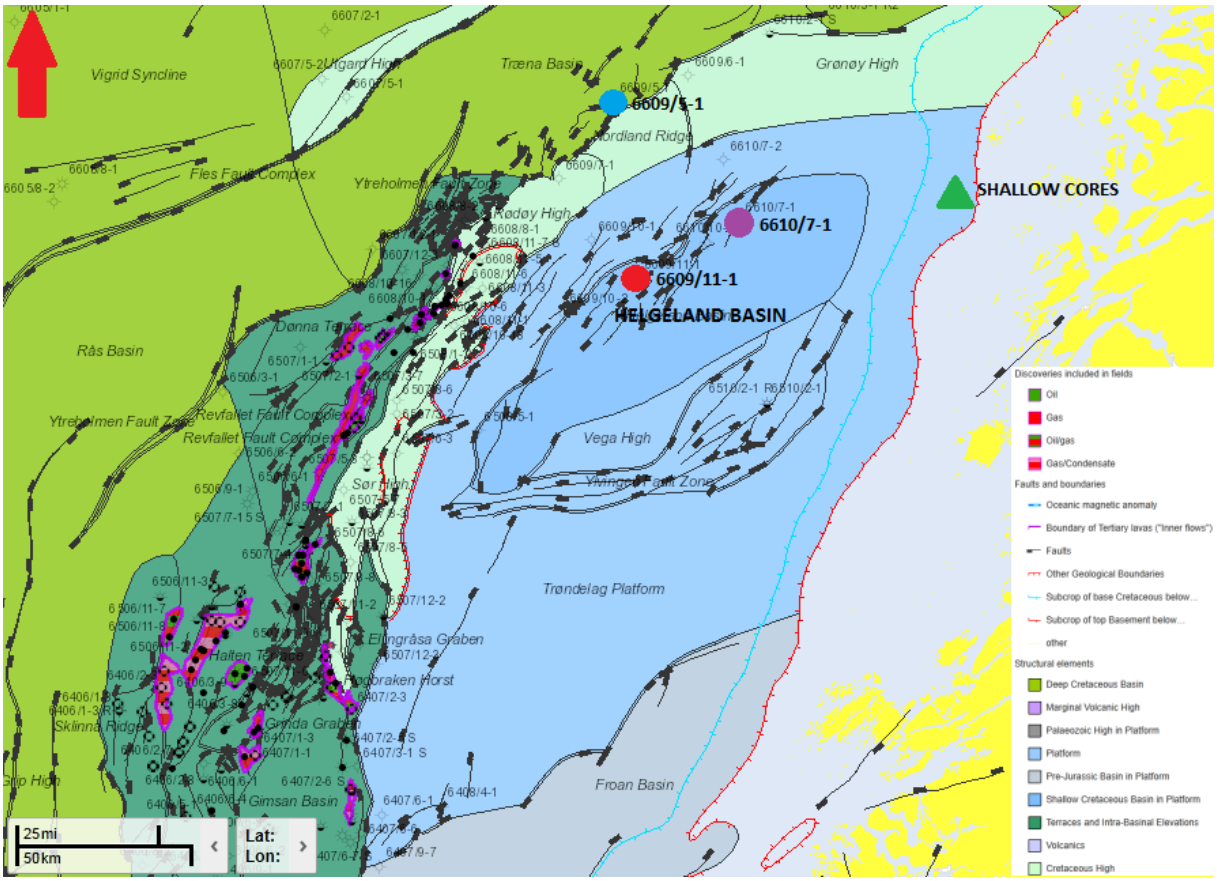

Figure 3.2: Map of the Helgeland Basin area in the Norwegian Sea. Well 6609/11-1, 6610/7-1 and 6609/5-1 are marked with red, purple and blue dots respectively. The green triangle corresponds to the shallow cores studied by Bugge et al. (2002). Notice nearby hydrocarbon reservoirs on the Halten and Dønna Terrace, and that no discoveries have been made in the Helgeland Basin (modified from NPD 2015b).

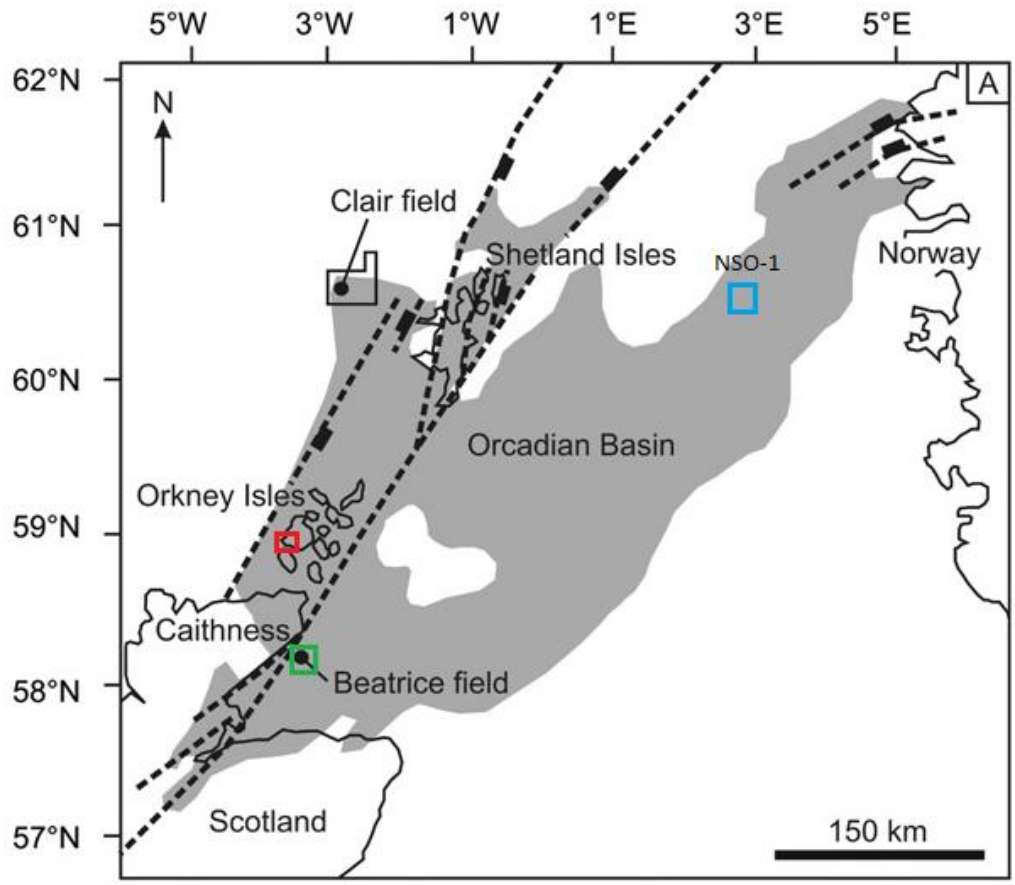

Figure 3.3: Illustration showing the location of the Beatrice Field (green square), the Oseberg Field (blue square, with the standard North Sea Oil (NSO-1)) and the locality of the source rock samples from the Orkney Isles studied in this thesis (red square) and the outline of the Orcadian Basin (modified from Mark et al., 2008). The Clair Field with its Upper ORS and Lower Carboniferous reservoir rocks represents the Northwesternmost known extent of the Orcadian Basin towards the Atlantic Ocean. To the East, The Solund-Fensfjord Devonian Basin is seen trending onshore Norway where sandstones and conglomerates of an intra-montana setting (Helgesen, 2008) represents the Norwegian manifestation of the Orcadian Basin development as seen in e.g. the Orkneys and Inner Moray Firth. Not shown in this map, but to the SE, the Embla Field (see Figure 3.1) on the NCS has been shown to contain both a Palaeozoic derived oil and a Jurassic derived oil in its Permian and Devonian reservoir rocks and rhyolites (Abay et al., 2014.) In addition are the Silurian and Lower Devonian? of the Oslo Graben clear manifestations of a Silurian to Devonian clastic development onshore Norway.

3.2 Source rock samples from the Orcadian Basin at the Orkneys.

Nine shaly outcrop samples represents the Middle Devonian lake and lagoonal source rock development at the location of West Shore Stromness, Orkneys (see Figure 3.1 and Figure 3.3) and will be referred to as O-1 (001/2013), O-2 (002/2013), O-3 (003/2013), O-4 (004/2013), O-5 (005/2013), O-6 (006/2013), O-7 (007/2013), O-20 (020/2013) and O-21 (021/2013) (original name in brackets). O-1 and O-2 were collected from the Sandwick fishbed, the Orkney equivalent to the

Achannaras fishbeds in the Orcadian Basin (see Figure 2.2), while the others are from lake laminites (Brown, unpubl.). The source rock bitumen samples are displayed in Figure 3.4

Figure 3.4: Illustration showing the DCM:MeOH (see section 4.2, Analytical Methods) extracts of the crushed source rock samples. A darker colour is in general a proxy for the organic bitumen extract.

3.3 Samples from selected wells in the Helgeland Basin area

3.3.1 Overview of samples from the Helgeland Basin area

Five visually stained sandstone samples assumed to contain migrated bitumen were taken from the sandstones from the Lower Jurassic Tilje Formation (NPD 2015a) from a core in the dry well 6609/11-1 from the Helgeland Basin, Norwegian Sea and will be referred to as A-1 (2557m), A-2 (2559m), A-3 (2559.9m), A-4 (2560m) and A-5 (2561m). A-5 is from the same well and depth as the sample studied by Karlsen et al. (1995). Seven samples are from two core intervals in the dry well 6610/7-1 from the Helgeland Basin where also slight staining was observed, and these will be referred to as B-1 (2661m), B-2 (2662.2m), B-3 (2668.5m), B-4 (2713.8m), B-5 (2714m), B-6 (2714.5m) and B-7 (2715). The DCM:MeOH extracts from 6609/11-1 and 6610/7-1 are displayed in Figure 3.5.

Figure 3.5: Extracted bitumen samples from sandstones in the dry wells 6609/11-1 and 6610/7-1 in the Helgeland Basin. As observed are most of the core extracts very dark in colour and this reflect usually a rich organic extract. The extracts were made using a Soxtec apparatus and the extraction media was DCM and MeOH (93:7 vol) (see section 4.2, Analytical Methods).

The samples from well 6610/7-1 are subdivided into an upper (B-1 to B-3) and a lower (B-4 to B-7) section due to the gap of 45.3m between B-3 and B-4 and also the different geochemical signature. Also, the two intervals are collected from two different formations i.e. the B-1 to B-3 samples are collected from the Ile Formation sandstones of Early to Middle Jurassic age, while the B-4 to B-7 samples are collected from the Ror Formation sandstones of Early Jurassic age (NPD, 2015a). Two already extracted samples are from the Cretaceous Cromer Knoll Group sandstones (NPD, 2015a) from a core in well 6609/5-1 from the Trænabanken area in the Norwegian Sea, and will be referred to as C-1 (3009m) and C-2 (3011m). All the depths of the different samples are shown in brackets.

3.3.2 Description of selected wells in the Helgeland Basin area

The location of the three selected wells 6609/11-1, 6610/7-1 and 6609/5-1 are shown in Figure 3.2 (red, purple and blue dots respectively), and the respective latitudes and longitudes are displayed in Table 3.1.

6609/11-1

According to NPD (2015a), well 6609/11-1 was drilled in 1983 on the north-western side of the Helgeland Basin, and the well was located on a structural high horst block with a southwest-northeast trend. The purpose of this well was to test the quality of reservoir sandstones of Late Triassic to Middle Jurassic in this region; therefore it was not drilled further down than to 3068 m when Late Triassic sediments were encountered.

NPD (2015a) reports that residual hydrocarbons were discovered in the Late Triassic and in the Lower Jurassic sequences, but the only recorded oil show was in a core taken from depth 2559.7-2560.9 m. Well 6609/11-1 was later in 1983 abandoned and reported as dry

6610/7-1

Well 6610/7-1 was drilled in 1983 on a tilted fault block structure in the Helgeland Basin. The purpose of this well was to investigate possible hydrocarbon potential of the Helgeland Basin and also to acquire information about the stratigraphy. The main interest was the sandstone packages of Early to Middle Jurassic age. This well was drilled to a depth of 3333 m, where it encountered Late Triassic sediments (NPD, 2015a).

Cores and cuttings from Lower Jurassic sandstones from 2656m to 2715m depth contained hydrocarbon shows. This well was abandoned and reported as dry later in 1983 (NPD, 2015a).

6609/5-1

Well 6609/5-1 was drilled on a structural horst in the Trænabanken area in the Norwegian Sea in 1984. The purpose of this well was mainly to evaluate sandstones of Late Triassic to Early Jurassic age. Indications of hydrocarbon were observed in Early Cretaceous sandstones and siltstones at a depth of 2195m. Similar observations were made in the intervals of 2580m to 2595m and 2856m to 2904m and at 2987m. The interval between 3009m and 3020m had hydrocarbon shows and was cored. There were also weak shows in the Triassic in the interval from 3154 to 3496m. The well was drilled down to 3600m. In 1985, well 6609/5-1 was abandoned and reported as dry (NPD, 2015a).

Sample list:

Table 3.1: Table showing the label, sample type and location of every sample included in this thesis.
***Values from Brown (unpubl.), ¤Values from NPD (2015a), #Values are from well 2/7-20, NPD (2015a), &Values are from well 30/6-1, NPD (2015a), ^Values are from Adu and Petersen (2011), %Values are from National Geospatial-Intelligence Agency (2015).**

Sample name.	Label	Sample type	Location
001/2013	O-1	Outcrop	N58° 57.207 W3° 19.156*
002/2013	O-2	Outcrop	N58° 57.201 W3° 19.247*
003/2013	O-3	Outcrop	N58° 57.015 W3° 18.096*
004/2013	O-4	Outcrop	N58° 57.005 W3° 18.130*
005/2013	O-5	Outcrop	N58° 57.007 W3° 18.160*
006/2013	O-6	Outcrop	N58° 57.000 W3° 18.191*
007/2013	O-7	Outcrop	N58° 56.997 W3° 18.203*
020/2013	O-20	Outcrop	N58° 57.044 W3° 18.662*
021/2013	O-21	Outcrop	N58° 57.057 W3° 18.697*
NSO-1	NSO-1	Oil	N60° 33’15.1’’ E2° 46’38.36’’&
Beatrice JK-00-101	Beatrice	Oil	N58° 07’00’’ W3° 05’00’’^
Embla D-2	Embla	Oil	N56° 20’0.1 E3° 14’54.7’’#
Judy 3017-A-8 DSTS 63187	Judy	Oil	N56° 42’ 30’’ E2° 19’00’’%
6609/11-1_2557m	A-1	Core	N66° 8’ 13.9’’ E9° 33’47.89’’¤
6609/11-1_2559m	A-2	Core	N66° 8’ 13.9’’ E9° 33’47.89’’¤
6609/11-1_2559.9m	A-3	Core	N66° 8’ 13.9’’ E9° 33’47.89’’¤
6609/11-1_2560m	A-4	Core	N66° 8’ 13.9’’ E9° 33’47.89’’¤
6609/11-1_2561m	A-5	Core	N66° 8’ 13.9’’ E9° 33’47.89’’¤
6610/7-1_2661m	B-1	Core	N66° 17’ 32.82’’E10° 16’52.92’’¤
6610/7-1_2662.2m	B-2	Core	N66° 17’ 32.82’’E10° 16’52.92’’¤
6610/7-1_2668.5m	B-3	Core	N66° 17’ 32.82’’E10° 16’52.92’’¤
6610/7-1_2713.8m	B-4	Core	N66° 17’ 32.82’’E10° 16’52.92’’¤
6610/7-1_2714m	B-5	Core	N66° 17’ 32.82’’E10° 16’52.92’’¤
6610/7-1_2714.5m	B-6	Core	N66° 17’ 32.82’’E10° 16’52.92’’¤
6610/7-1_2715m	B-7	Core	N66° 17’ 32.82’’E10° 16’52.92’’¤
6609/5-1_3009m	C-1	Core	N66° 37’42.73’’ E9° 24’52.17’’¤
6609/5-1_3011m	C-2	Core	N66° 37’42.73’’ E9° 24’52.17’’¤

3.4 Additional oils i.e. from the Oseberg Field (NSO-1 referece oil), the Embla Field, the Beatrice Field and the Judy Field

Oils from the Beatrice Field and the Judy Field, both in the UK-sector, and the Embla Field were also included in the sample set. The standard North Sea oil from the Oseberg Field was included as a reference of a Kimmeridge/Draupne/Spekk derived oil and will be referred to as NSO-1

4. Analytical methods

This chapter presents methods that were used in this thesis, and is outlined in the following order:

4.1 Introduction of analytical methods

4.2 Preparation and extraction of samples

4.3 GC-FID

4.4 Molecular sieving

4.5 GC-MS

4.6 Rock-Eval and TOC

4.7 δC13 isotope analysis

4.1 Introduction of analytical methods:

Geochemical analysis is performed for assessing the characterization and differentiation of bitumens, oils and gases, and such data can be used for correlation studies between source rock extracts and oils, or for oil. A series of different methods for performing detailed and rapid geochemical analysis is available; e.g. GC-FID and GC-MS. Parameters reflecting e.g. the source rock maturity and the source rock facies can be ascertained and used for obtaining a better understanding of the relationship between oils and source rocks in a basin. Reservoir alteration processes such as the level of biodegradation and water washing may also be determined and the geochemical information is thus providing an improved petroleum system understanding of the basin. Quality of the organic matter and also quantity and maturity can be assessed from TOC and Rock-Eval analysis, and δC13 isotope data provides additional information regarding marine/non-marine input.

The standard North Sea oil (NSO) is used as reference oil in the GC-FID and GC-MS analysis to make sure that the equipment works correctly, since the peak distributions in the chromatograms of this oil is already known. The respective peaks are also identified in NSO-1 which is then used as a reference for peak identification of compounds in other samples.

4.2 Preparation and extraction of samples

The source rock samples are crushed into a fine powder before geochemical analysis can be carried out. This is first done manually to obtain fragments of about 0.5 cubic centimeters and these rock fragments are then crushed in a sling mill.

The extraction of bitumen from the crushed samples is carried out in an extraction unit, named Soxtec System HT 1043 extraction unit from Tecator. The powder from the individual samples is weighted before filled into pre-extracted cellulose cartridges and the cartridges are covered with wool for preventing loss of the samples during the solvent boiling stage. Approximately 7.1g and 9.1g of powder are used for the extraction of the source rock samples and reservoir rock samples respectively.

A solvent of 93% dichloromethane (DCM) and 7% methanol is used for extraction (cf. Karlsen and Larter 1991). For removing sulfur from the samples, copper activated by HNO_3 is introduced to the solvent before boiling (cf. Azhar, 2012).

The solvents, maximum six at the time, are heated to 90 degrees Celsius and the source rock samples are boiling for one hour, then rinsed for two hours while the reservoir rock samples are boiling for 30 minutes and rinsed for one hour. The last step of preparation is to concentrate the solvent. The DCM is evaporating in contact with air, but this is a slow process. To speed up the evaporation, nitrogen gas is blown over the solvents and extracts, while inside the extraction cups, to assist in the evaporation. The concentrated extracts can then be geochemically analyzed.

4.3 GC-FID

GC-FID (Gas Chromatography – Flame Ionization Detector) is a tool used for identification, differentiation and quantification of important components in petroleum e.g. n-alkanes, isoprenoids and toluene (Abay, 2010). The machine works in the way that the sample is vaporized before its different molecules are being separated in a chromatographic column (Abay, 2010). A nitrogen carrier gas is being utilized.

The chromatographic column is being held at an initial temperature of 80°C in 1min, and then heated to 320°C with an increase of 4.5°C/min, then running at constant temperature for 25min. The different type of molecules have a different traveltime throughout the column, depending on their chemical properties; Those with short chains, low boiling points and high vapor pressure will travel faster relative to the molecules which are more branched (Abay, 2010). When exiting the column, the molecules are identified with a flame ionization detector which provides the information to a computer that records the data. The output gas chromatogram is a plot of signal intensity versus time. Figure 4.1 from Abay (2010) (modified from Pedersen, 2002) illustrates the different steps of the procedure in a GC-FID analysis.

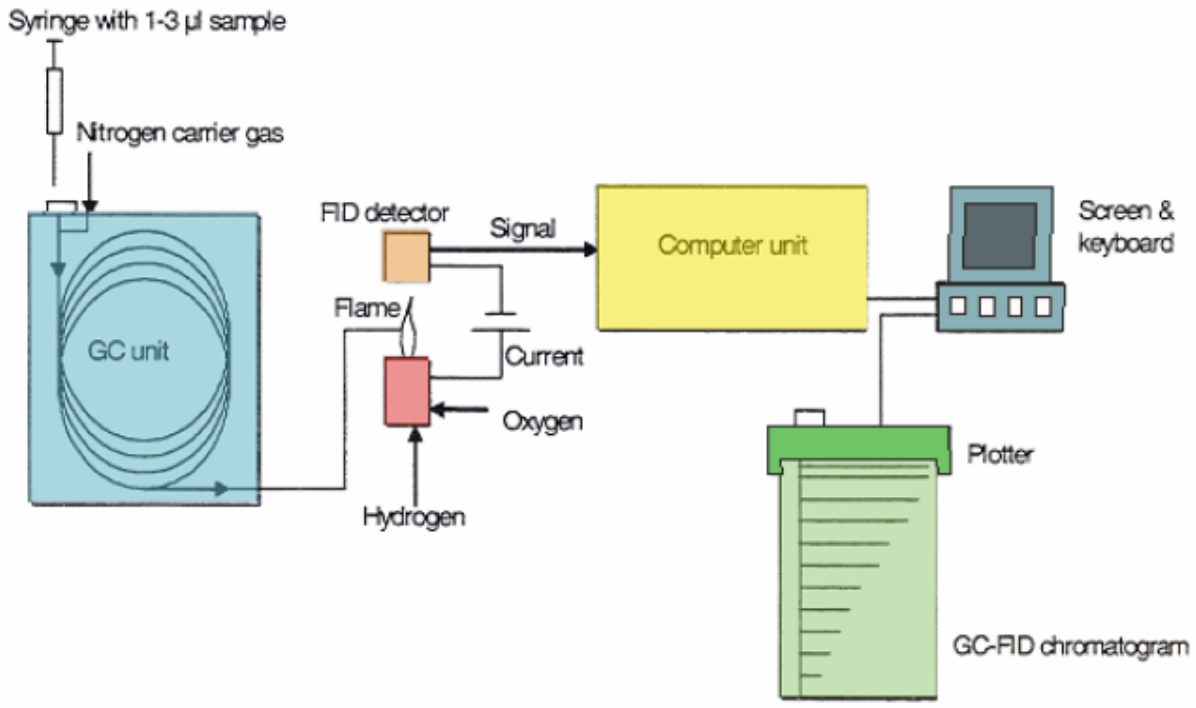

Figure 4.1: Illustration of the different components in a GC-FID machine (from Abay 's (2010) modified version from Pedersen, 2002).

4.4 Molecular sieving

Before GC-MS is carried out, molecular sieving is normally performed because there will be interference between the signals of the biomarkers of interest and n-alkanes in the GC-MS if not sieved. Removing of n-alkanes from the extract will effectively improve reliability of the results from analysis (Peters et al., 2005), since the diluted biomarkers will be more concentrated. The molecular sieving functions that the long chained n-alkanes will fit the pores in the molecules of the sieves and become trapped while the larger molecules will be unaffected by the sieving, as they are too big for

the pores (Abay, 2010). After the sieving, the extract is enriched in biomarkers and aromatics while ideally 100 % depleted in n-alkanes (Abay, 2010).

4.5 GC-MS

GC-MS (Gas Chromatography-Mass Spectrometry) is the principal tool used for identification and quantification of biomarkers (Peters et al., 2005). As for GC-FID, the molecules from the samples are separated first in GC-MS in the gas chromatograph. The mass spectrometer is able to identify different compounds by ionization and mass analysis separately as the different types of molecules have a different traveltime throughout the GC (Abay, 2010). Every molecule is being broken and ionized by the MS which is then able to detect the ionized broken molecules from their mass (m) to charge (z) ratio (m/z) (Peters et al., 2005). The resulting chromatogram from the computer shows relative abundance of ions with one specific m/z ratio versus time (Abay, 2010). Figure 4.2 from Pedersen (2002) shows each step of the procedure in the GC-MS analysis. Many of the biomarkers of interest have different m/z ratios, and can therefore be identified and quantified when studying the chromatogram (Abay, 2010).

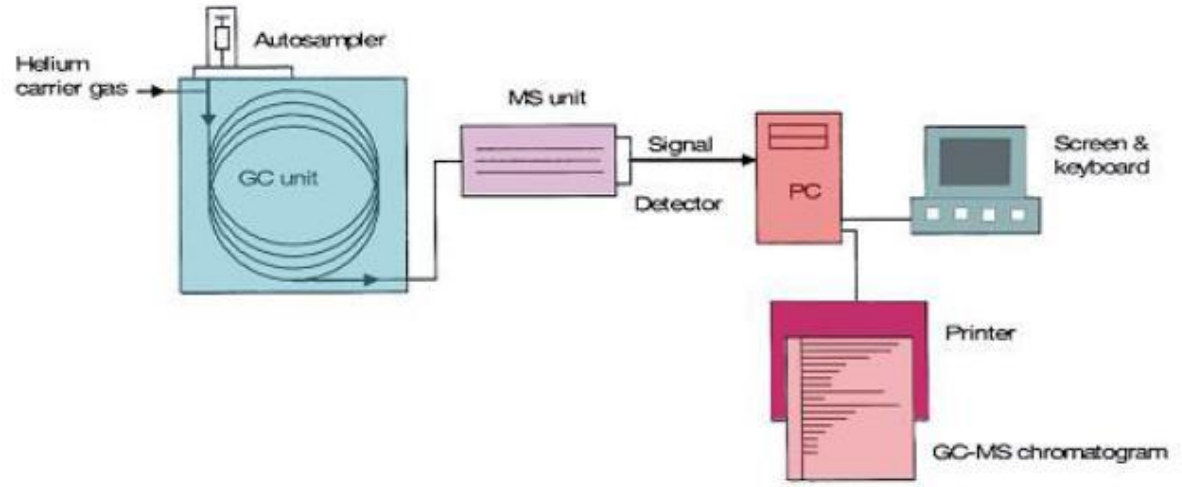

Figure 4.2: Illustration of the different components in a GC-MS machine (from Pedersen, 2002).

The peaks that represent different molecules in the respective m/z chromatogram can be measured and thus provides information about biomarker distributions. From those measurements, different parameters which can indicate maturity, source and facies can be calculated (Abay, 2010).

On the first run, the chromatographic column was set to an initial temperature of 40°C that was held for 1 min, and then the temperature was increased with 20°C/min up to 180°C and 1.7°C/min

up to a maximum temperature of 310°C which was held for 40.53 min. Additional m/z ratios to the standards that were included was 558 (β-carotane) and 560 (γ-carotane).

The β-carotane molecule of great interest in this thesis i.e. the prime lacustrine Middle Devonian marker, was only dectected in the source rock bitumen samples (except from O-4), NSO-1 and C-1 and C-2 from well 6609/5-1. Therefore, the reservoir rock samples without positive identification of β-carotane were concentrated further and the Embla oil, the Beatrice oil and the Embla oil were analyzed as whole oils i.e. they were diluted with DCM in the first run. The rest of the reservoir rock extracts were added to the leftovers from the first GC-MS run and then concentrated. The additional extracts were not sieved as the only purpose of the second run was to identify β-carotane. The temperature settings for the chromatographic column in the second run was a more steep temperature gradient from 180°C and onwards (4°C/min instead of 1.7°C/min) and a higher maximum temperature of 330°C (increase of 20°C). The maximum temperature of 330°C was held for 50min.

4.6 Rock-Eval and TOC

Rock-Eval is a method for evaluation of maturity and petroleum potential of the selected sample (Peters 1986). The sample is subjected to pyrolysis i.e. it is heated to sufficient temperatures for yielding petroleum, first liberating the bitumen, then at higher temperatures cracking the kerogen which then yields additional petroleum compounds (Peters, 1986). From the pyrolysis, peaks representing already generated hydrocarbons in the sample i.e. the S1 peak, hydrocarbons generated through additional cracking of kerogen during pyrolysis i.e. the S2 peal and amount of released CO_2 from the sample i.e. the S3 peak (Peters 1986). The temperature at which the highest peak intensity of S2 occurs is referred to as T_{max}. Values for TOC (Total Organic Content), HI (Hydrogen Index) and OI (Oxygen Index) are ascertained from this analysis.

4.7 δ13C isotope analysis

Isotope analysis provides estimations of the relative enrichment or depletion of different isotopes relative to the most common (e.g. C13 to C12 carbon) and can provide useful additional information alongside the diagnostic biomarkers for correlation studies.

Isotope composition is ascertained with an online combustion system which converts the samples into gases i.e. CO_2, H_2O, N_2 and SO_2 which are then trapped and separated in a linked elemental analysis unit and an isotope ratio mass spectrometer which measures isotope ratios (Hoefs, 2009). The high conversion rates for the samples based on the high operative combustion temperatures guarantees a quantitative representation of isotope configurations (Hoefs, 2009).

5. Interpretation parameters

The analytical methods described in chapter 4, provide results which in turn can be used to generate geochemical parameters for investigating source rock maturity at the time of expulsion of oils, or the maturity of given source rocks, parameters for estimating the organic facies of the depositional environment represented by the oils or source rock samples, and also parameters employed to evaluate biodegradation. The parameters will be discussed in this chapter in the following order:

5.1 Organic geochemical facies and maturity paramters based on GC-FID

- 5.1.1. The n-alkane distribution
- 5.1.2. The pristane/phytane ratio
- 5.1.3. The ratios of pristane/n-C17 and phytane/n-C18
- 5.1.4. The Carbon Preference Index (CPI) and the Odd/Even Predominance (OEP)
- 5.1.5. Specific molecular compounds such as β-carotane and γ-carotane

5.2 Organic geochemical facies and maturity parameters based on GC-MS

- 5.2.1 The terpanes
- 5.2.2 The steranes
- 5.2.3 The triaromatic steroids
- 5.2.4 The monoaromatic steroids
- 5.2.5 The phenanthrene, methylphenanthrenes and methylbenzothiopenes
- 5.2.6 The standard parameters concerning maturity and organic facies
- 5.2.7 Other parameters

5.3 Interpretation paramters based on Rock-Eval and TOC

5.4 Interpretation parameter, δ13C

5.1 Organic geochemical facies and maturity parameters based on GC-FID

GC-FID analysis is performed to estimate the n-alkane envelope and for identification of n-alkanes and isoprenoids like pristane and phytane. The pattern of the n-alkanes, mainly the C15+ fraction, and the relationship with isoprenoids can indicate facies, maturity and also biodegradation (Tissot and Welte, 1984).

5.1.1 The n-alkane distribution

The baseline of the GC-FID chromatogram will be elevated due to increasing amount of UCM (Unresolved Complex Mixture) if the sample has been subjected to biodegradation, and can thus provide information whether the sample has been biodegraded or not. The UCM comprises some of the most complex organic compounds on Earth, therefore it is almost impossible to identify specific compounds on the chromatograms (Sutton et al., 2005). The n-alkanes will also be more depleted relative to isoprenoids like pristane and phytane as the degradation of compounds is selective (Tissot and Welte, 1984). If biodegradation is severe, the n-alkanes will approach depletion, and at even more extensive degradation will the same occur for the isoprenoids. Identification of n-alkanes in the NSO-1 reference GC-FID chromatograms are shown in Figure 5.1

5.1.2 The Pristane/phytane ratio

The main source of the two isoprenoids pristane (C19) and phytane (C20) is the isoprenoid side chain of chlorophyll i.e. the C20-phytol side chain (Tissot and Welte, 1984). Formation of either pristane or phytane from phytol is dependent on whether the depositional environment is oxic or anoxic; oxic conditions lead to oxidation of the alcohol phytol to an acid which is later decarboxylated resulting in the C19-compound pristane, while anoxia favours phytane formation via direct reduction of the C20-acid to phytane (Peters et al., 2005). A pristane/phytane ratio below 0.8 is an indicator of saline or hypersaline environment which is associated with deposition of evaporites and carbonates, a ratio above 3.0 indicates a terrigeneous source rock palaeo-depositional environment with oxygen being present (Peters et al., 2005). Identification of the pristane (Pr) and phytane (Ph) peaks are shown in Figure 5.1.

5.1.3 The ratios of Pristane/n-C17 and phytane/n-C18

Due to the lower boiling points of the isoprenoid structure compared to n-alkanes, the C19-compound pristane will elute just after n-C17, and phytane will elute just following n-C18. It only became possible to separate these isoprenoids from the associated n-alkanes in the early 1980s following development of capillary GC-columns (Tissot and Welte, 1984). The concentration of the isoprenoids pristane and phytane will decrease relative to the concentration of n-C17 and n-C18 respectively in the oil window as a result of increased n-alkane generation from the kerogen (Tissot et al., 1971) i.e. the isoprenoids becomes diluted. It is also the case that the branched isoprenoids are less thermally stable than the n-alkanes which lack tertiary carbon (a carbon atom bound directly to three others). Thus, these two isoprenoid/n-alkane ratios can be used as maturity parameters. These ratios have their limitations however, the type of source input (Alexander et al., 1981) and also biodegradation (Tissot and Welte, 1984) affects the ratios, and the usage is therefore limited to oils and bitumens that are related and not biodegraded.

5.1.4 The Carbon Preference Index (CPI) and the Odd/Even Predominance (OEP)

The ratio between odd-numbered and even-numbered n-alkanes is given as the amount of odd to even n-alkane molecules (Tissot and Welte, 1984) and is a maturation indicator but is also affected by source input. The Carbon Preference Index (CPI) was introduced by Bray and Evans (1961) and the improved ratio Odd/Even Predominance by Scalan and Smith (1970) with the advantage of the possibility to being calibrated for both shorter and longer n-alkanes. Those parameters have in common that oils or extracts have values way below/above 1.0 when immature while they are approaching 1.0 during maturation (Peters et al., 2005), but values of 1.0 does not prove alone that the sample is mature. Values below 1.0 give indications of either a carbonate environment or a hypersaline depositional environment of the source while values above 1.0 points towards a silisiclastic source or lacustrine environment. The reason for this is that the bio-precursor molecule is an even numbered fatty acid. This fatty acid is decarboxylated to give rise to odd-numbered n-alkanes via alpha-cleavage in a silisiclastic environment, while in carbonates and evaporates beta-cleavage is dominating with the loss of two carbon atoms, thus maintaining the even-predominance (Tissot and Welte, 1984).

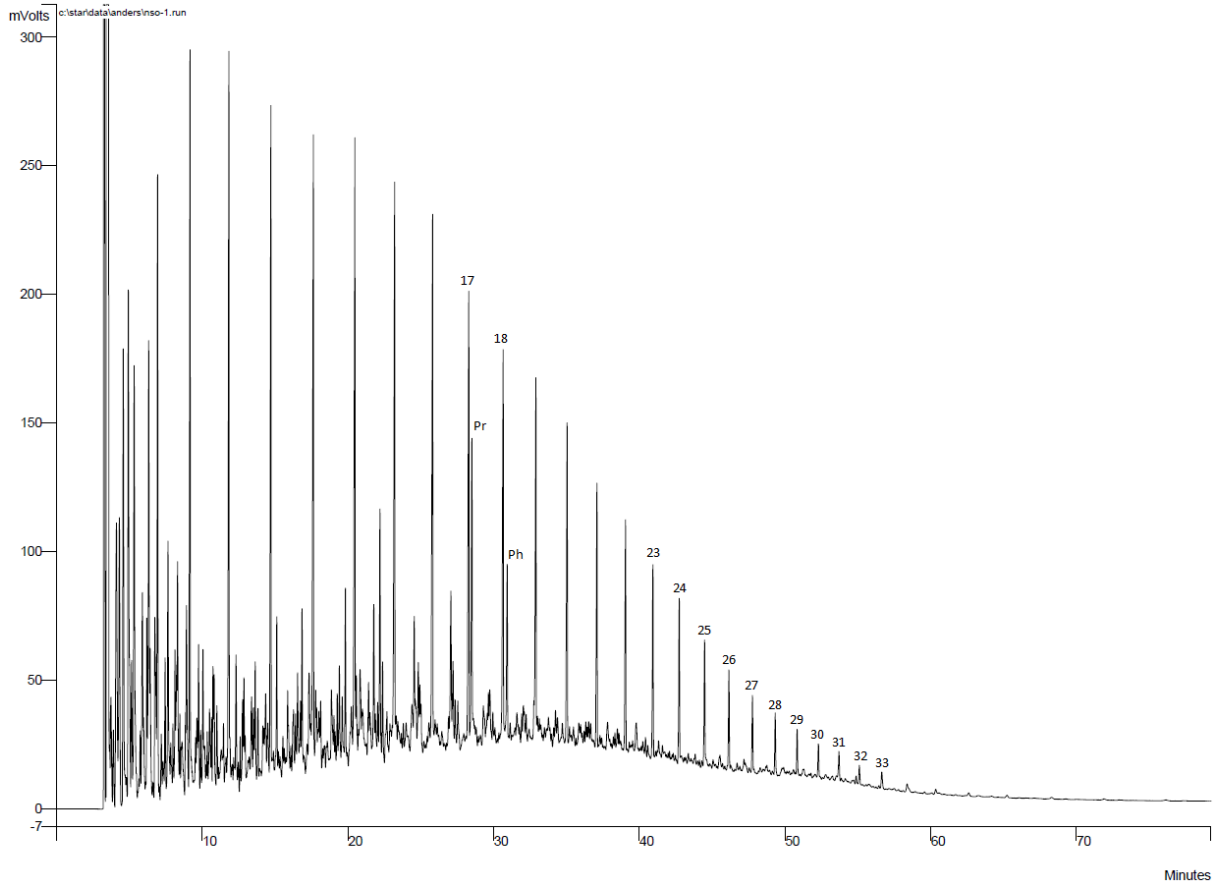

Figure 5.1: GC-FID chromatogram for NSO-1 and identification of n-alkanes (numbers), pristane (Pr) and phytane (Ph). Note also the front-end-biased type n-alkane profile and the asymthotic n-alkane profile extending beyond n-C33.

5.1.5 Specific molecular compounds such as β-carotane and γ-carotane

The presence of β-carotane and γ-carotane in oils or source rock extracts indicates saline anoxic lacustrine and highly restricted marine settings (Peters et al., 2005). Carotenoids which originate from plant pigment (Ben-Amotz et al., 1989) most typically in *dunaliella* which is an unicellular algae that thrives in hypersaline waters, are easily oxidized and are thus rarely found in deposited sediments, but if the conditions are highly reducing, those compounds may be preserved (Peters et al., 2005). Their branched alkane structure with a methyl-group on every fourth carbon atom makes these C40 structures prone to thermal degradation i.e. these compounds will not occur in high proportions in highly mature oils. Still, traces of these compounds in oils have a very diagnostic source rock facies signature and this is why their detection is of paramount importance for facies evaluations. β-carotene, the unsaturated precursor to β-carotane, reacts with sulfur under anoxic marine conditions but is reduced to β-carotane in anoxic lacustrine conditions with low sulfur content (Peters et al., 2005).

β-carotane is usually the most abundant of the carotenoids and is less thermally stable relative to γ-carotane but more resistant against biodegradation, resulting in an increase of γ-carotane/ β-carotane with increased maturity and decrease if biodegraded (Jiang and Fowler 1986). Peters et al. (2005), states that this relationship is also dependent on the type of source input. Identification of β-carotane and γ-carotane is shown in the GC-FID chromatogram of O-2 (see Figure 5.2).

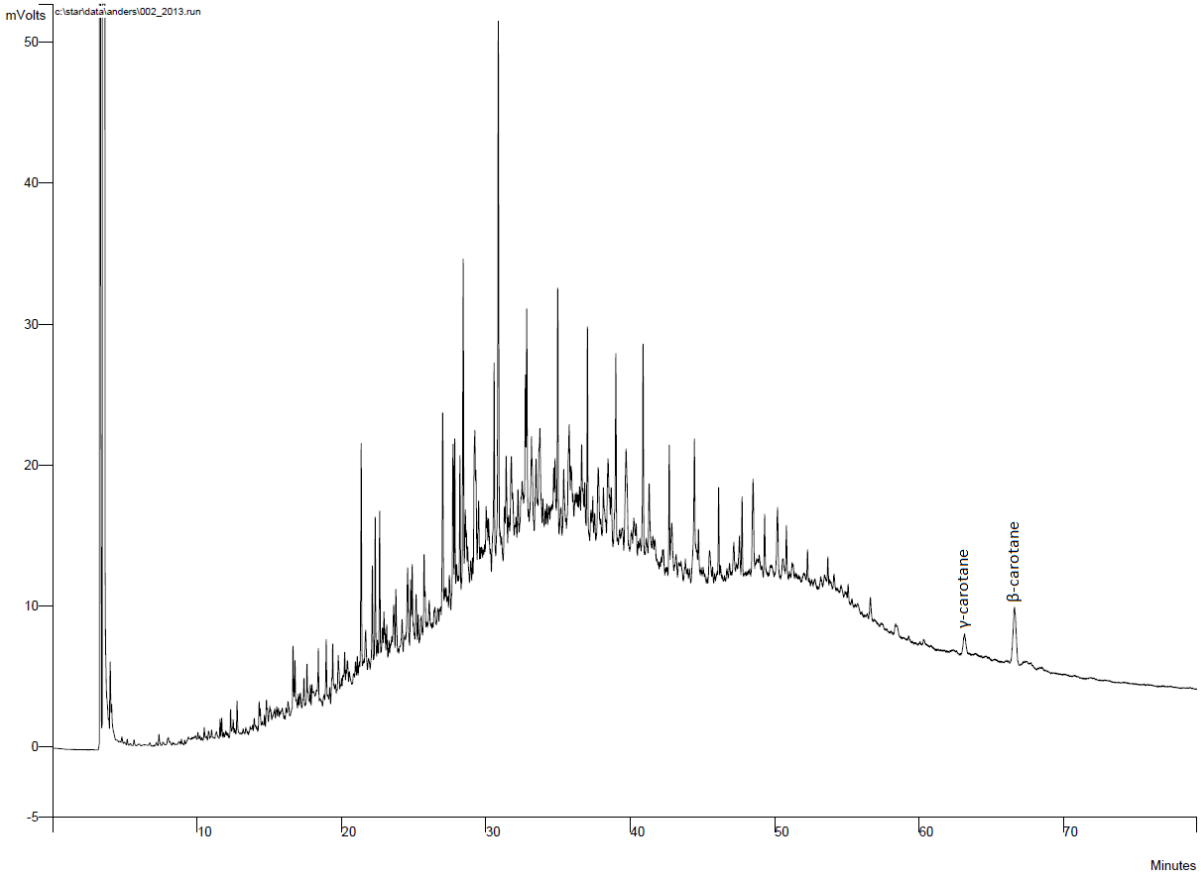

Figure 5.2: Identification of β-carotane and γ-carotane in the GC-FID chromatogram of sample O-2 i.e. one of the lacustrine lake samples from the Orkneys. Also shown are pristane (Pr), phytane (Ph) and normal alkanes from n-C17 to n-C35.

5.2 Organic geochemical facies and maturity parameters based on GC-MS

A series of individual interpretation parameters from chromatograms are based on mass to charge ratios as provided by GC-MS analysis, see Table 5.8 in section 5.2.6 and section 5.2.7. Specific compounds in the saturated fraction are identified in m/z = 177, m/z = 191, m/z = 217, and m/z = 218 The saturated fraction is identified in m/z 177, 191, 217 and 218 while in the aromatic fraction

are the following ions utilized: m/z = 178, m/z = 192, m/z = 198, m/z = 231 and m/z = 253. The peak labels used in this thesis are the same as in the NIGOGA guide. Carotanes are identified in m/z = 125, m/z = 558 and m/z = 560.

5.2.1 The terpanes

The terpane group is identified in m/z = 177 and m/z = 191 and falls in under the saturated hydrocarbon fraction. Table 5.1 and 5.2 lists different peaks and the corresponding names for m/z 177 and 191 respectively. The reference chromatogram of NSO-1 from m/z = 177 (Figure 5.3) and m/z = 191 (Figure 5.4) shows identification of the peaks.

Table 5.1: Peak label of the biomarker compound from m/z = 177 with its full name.

Peak	Name
25nor28αβ	17α(H), 21β(H)-25-28-30-trisnorhopane

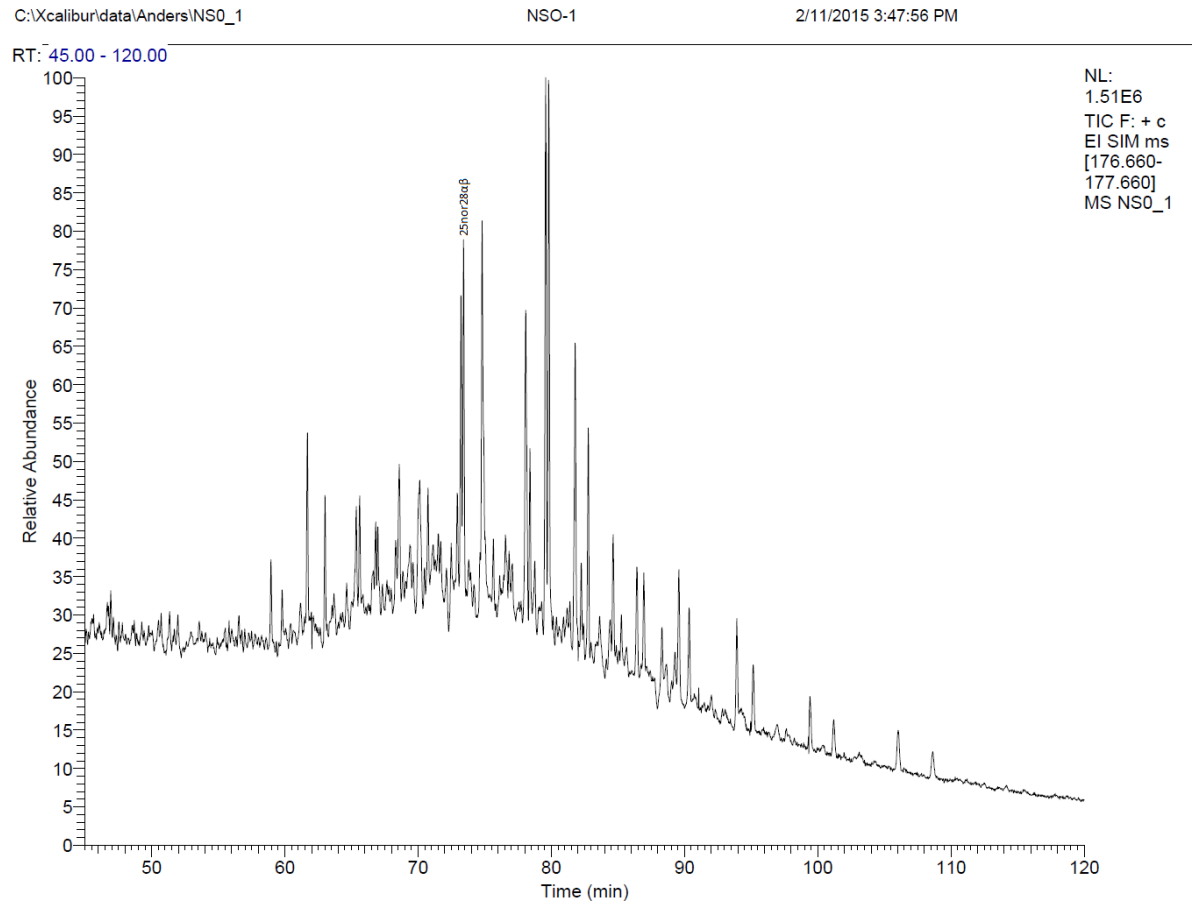

Figure 5.3: Identification of 25-28-30-trisnorhopane in m/z = 177 of NSO-1. This compound is also formed by biodegradation of normal hopanes e.g from 28-30-bisnorhopane.

Table 5.2: List of different peaks from m/z = 191 and their respective names and composition.

Peak	Stereochemistry	Name	Composition
23/3		Tricyclic terpane	$C_{23}H_{42}$
24/3		Tricyclic terpane	$C_{24}H_{44}$
25/3	17R + 17S	Tricyclic terpane	$C_{25}H_{46}$
24/4		Tetracyclic terpane	$C_{24}H_{42}$
26/3	R + S	Tricyclic terpane	$C_{26}H_{48}$
28/3	R + S	Tricyclic terpane	$C_{28}H_{52}$
29/3	R + S	Tricyclic terpane	$C_{29}H_{54}$
27Ts		18α (H) trisnorneohopane	C_{27}
27Tm		17α (H) trisnorneohopane	C_{27}
28αβ		17α(H), 21β(H)-28-30-bisnorhopane	$C_{28}H_{48}$
29αβ		17α(H), 21β(H) norhopane	$C_{29}H_{50}$
29Ts		18α (H) norneohopane	C_{29}
30d		15α-methyl-17α (H) diahopane	$C_{30}H_{52}$
29βα		17β (H), 21α (H) normoretane	$C_{29}H_{50}$
30αβ		17α (H), 21β (H) hopane	$C_{30}H_{52}$
30βα		17β (H), 21α (H) moretane	$C_{30}H_{52}$
30G		Gammacerane	
31αβS		17α (H), 21β (H) homohopane	$C_{31}H_{54}$
31αβR		17α (H), 21β (H)homohopane	$C_{31}H_{54}$

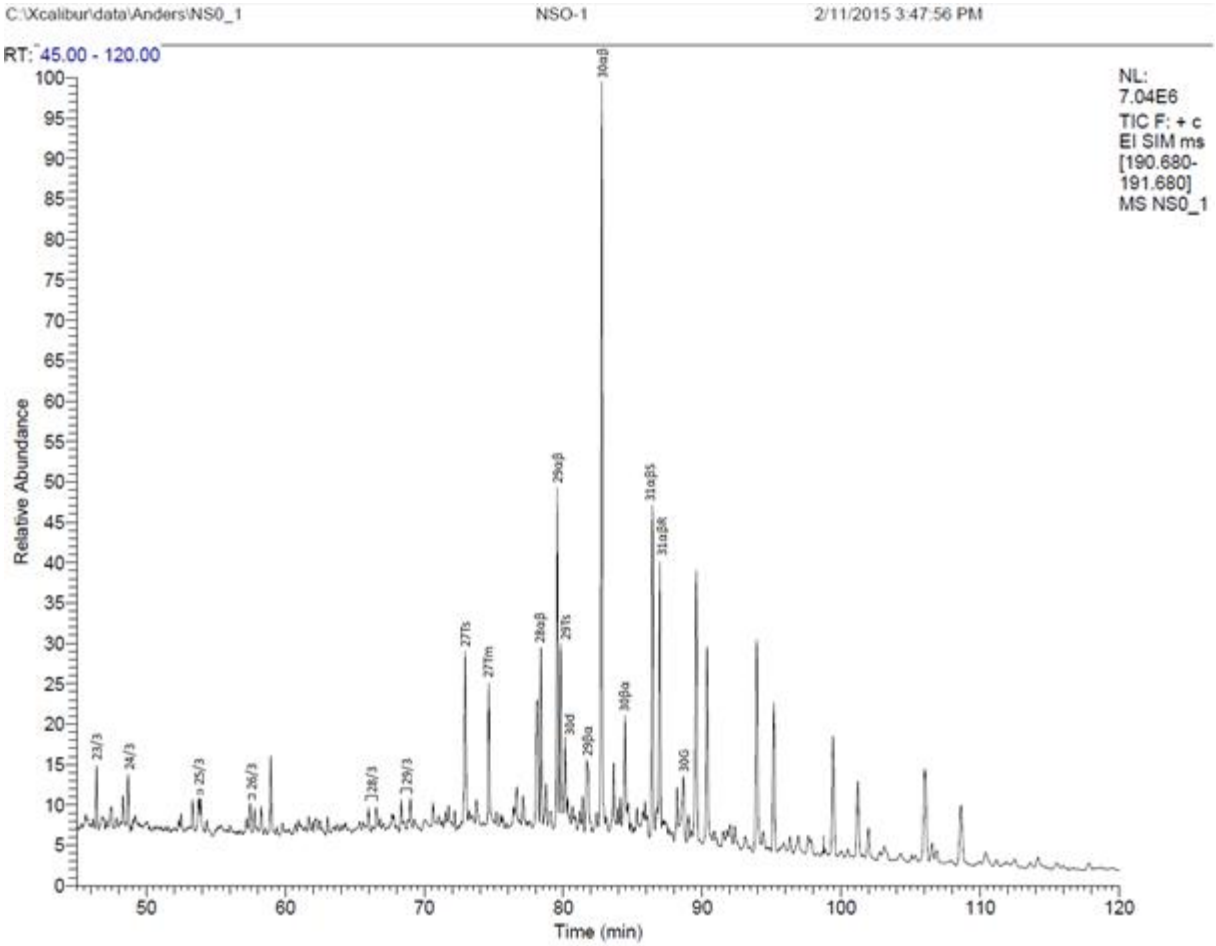

Figure 5.4: Identification of different peaks which corresponds to the biomarker compounds listed in Table 5.2 from the m/z = 191 chromatogram of NSO-1. Their main use is for assessing the organic facies and also for maturity estimates.

5.2.2 The steranes

The sterane group is a part of the saturated hydrocarbon fraction and is identified in both m/z = 217 and m/z = 218. Table 5.3 and Table 5.4 list the peaks identified in m/z = 217 and m/z = 218 respectively. The NSO-1 reference chromatogram shows the identification of the peaks in m/z = 217 (Figure 5.5) and m/z 218 (Figure 5.6). Some of the peaks are identified in both m/z = 217 and m/z = 218.

Table 5.3: Overview over different peaks from m/z = 217 and their respective names and compostions.

Peak	Name	Composition
27αβS	13β(H), 17α(H), 20(S)-cholestane (diasterane)	$C_{27}H_{48}$
27αβR	13β(H), 17α(H), 20(R)-cholestane (diasterane)	$C_{27}H_{48}$
29ααS	24-ethyl-5α(H), 14α(H), 17α(H), 20(S)-cholestane	$C_{29}H_{52}$
29ββR	24-ethyl-5α(H), 14β(H), 17β(H), 20(R)-cholestane	$C_{29}H_{52}$
29ββS	24-ethyl-5α(H), 14β(H), 17β(H), 20(S)-cholestane	$C_{29}H_{52}$
29ααS	24-ethyl-5α(H), 14α(H), 17α(H), 20(R)-cholestane	$C_{29}H_{52}$

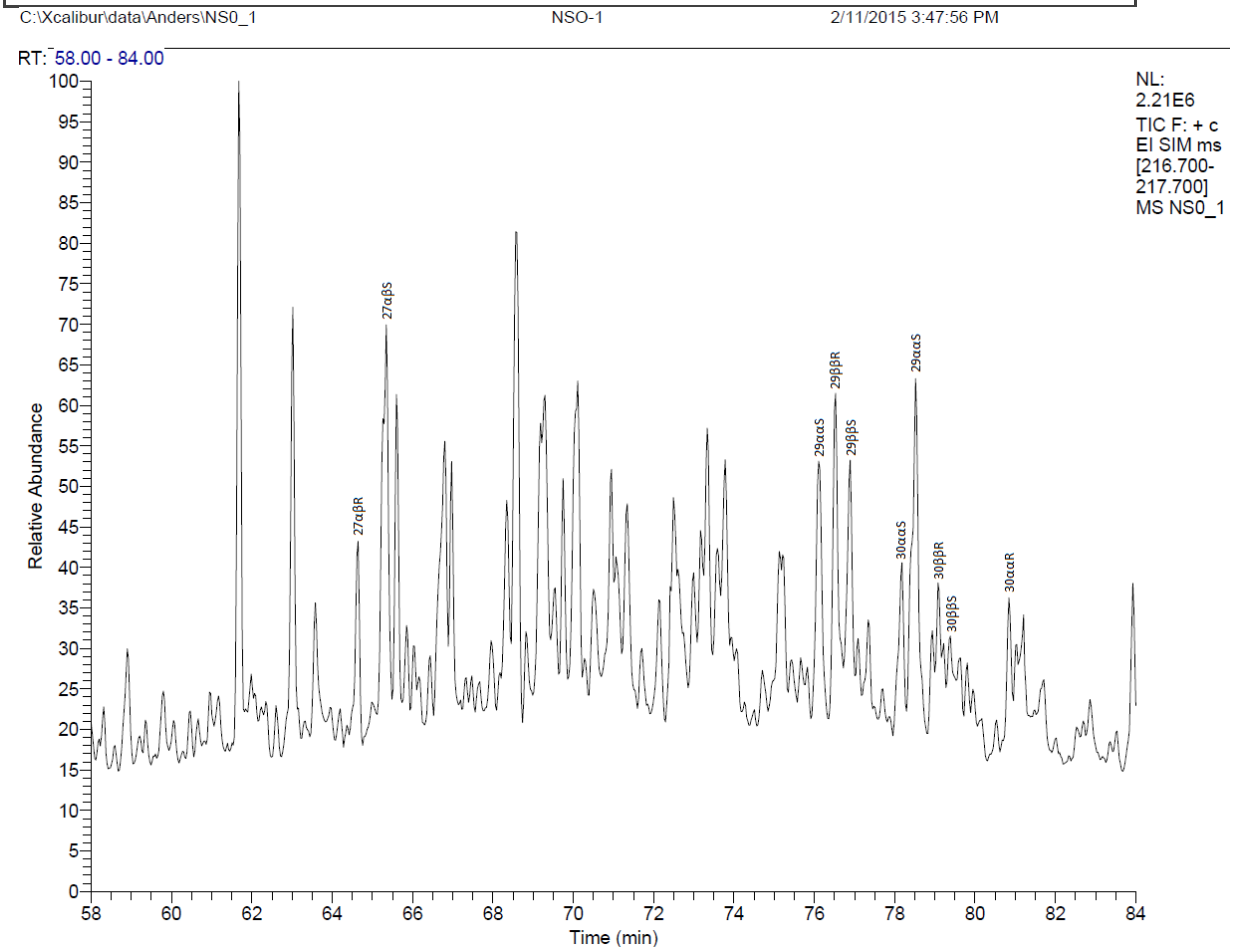

Figure 5.5: Peak identification of the biomarker compounds listed in Table 5.3 in the m/z = 217 chromatogram from the reference sample NSO-1.

Table 5.4: Overview over different peaks from m/z = 218 and their respective names and compositions.

Peak	Name
27ββR	5α(H), 14β(H), 17β(H), 20(R)-cholestane
27ββS	5α(H), 14β(H), 17β(H), 20(S)-cholestane
28ββR	24-methyl-5α(H), 14β(H), 17β(H), 20(R)-cholestane
28ββS	24-methyl-5α(H), 14β(H), 17β(H), 20(S)-cholestane
29ββR	24-ethyl-5α(H), 14β(H), 17β(H), 20(R)-cholestane
29ββS	24-ethyl-5α(H), 14β(H), 17β(H), 20(S)-cholestane
30ββR	24-propyl-5α(H), 14β(H), 17β(H), 20(R)-cholestane
30ββS	24-propyl-5α(H), 14β(H), 17β(H), 20(S)-cholestane

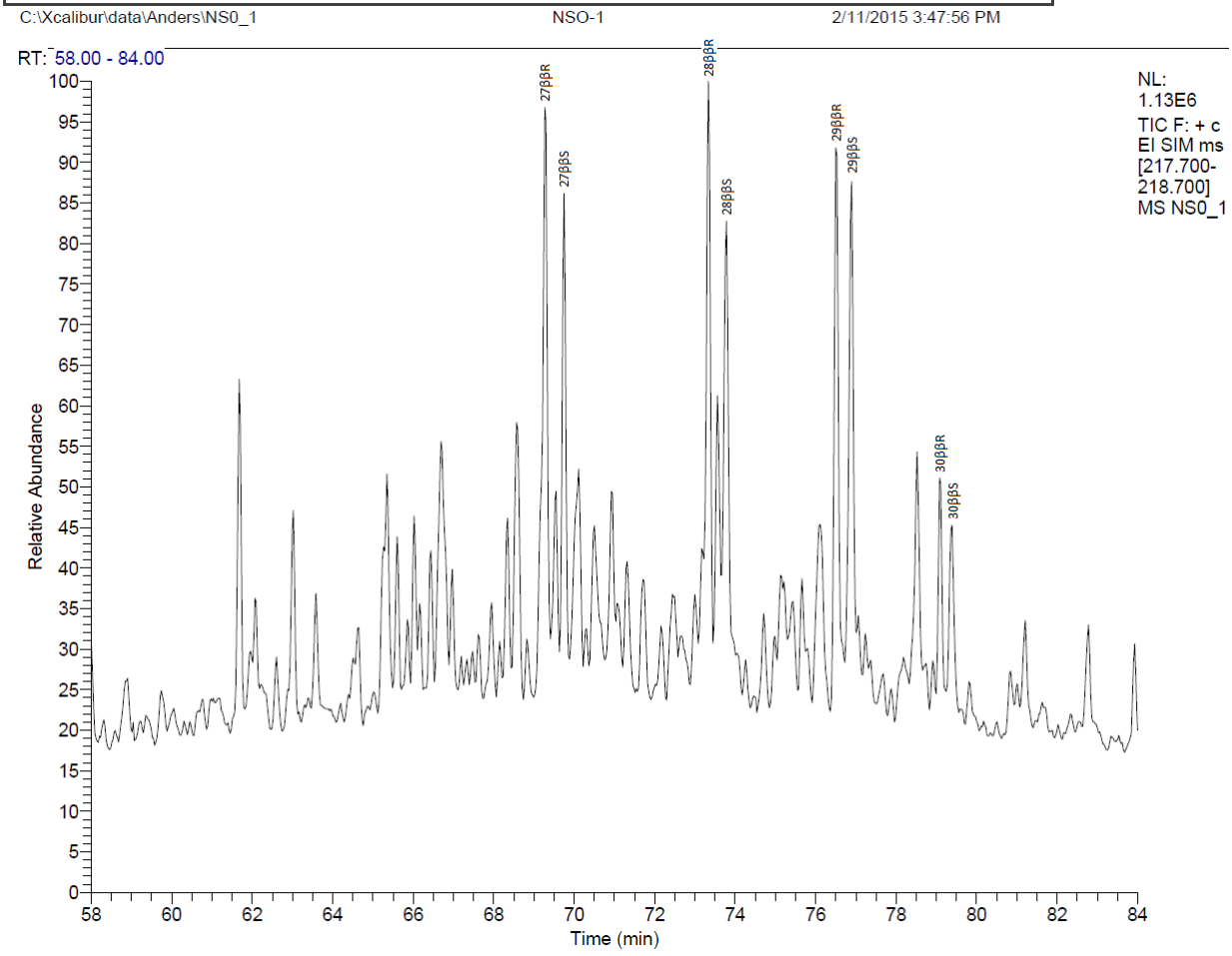

Figure 5.6: Peak identification of the biomarker compounds listed in Table 5.4, in the m/z = 218 chromatogram from the reference sample NSO-1.

5.2.3 The triaromatic steroids

The triaromatic steroid group is a part of the aromatic hydrocarbon fraction, and is identified in m/z = 231. The peaks of relevance are listed in Table 5.5 and the identifications in the chromatograms are shown in Figure 5.7. Their main use in organic geochemistry is as maturity indicators because short-chained triaromatic steroids are more thermally stable than those with longer chains (Beach et al., 1989).

Table 5.5: Overview of identified peaks in m/z = 231.

Peak	R_1	R_2
C20TA	CH_3	H
RC28TA	$R(CH_3)$	C_8H_{17}

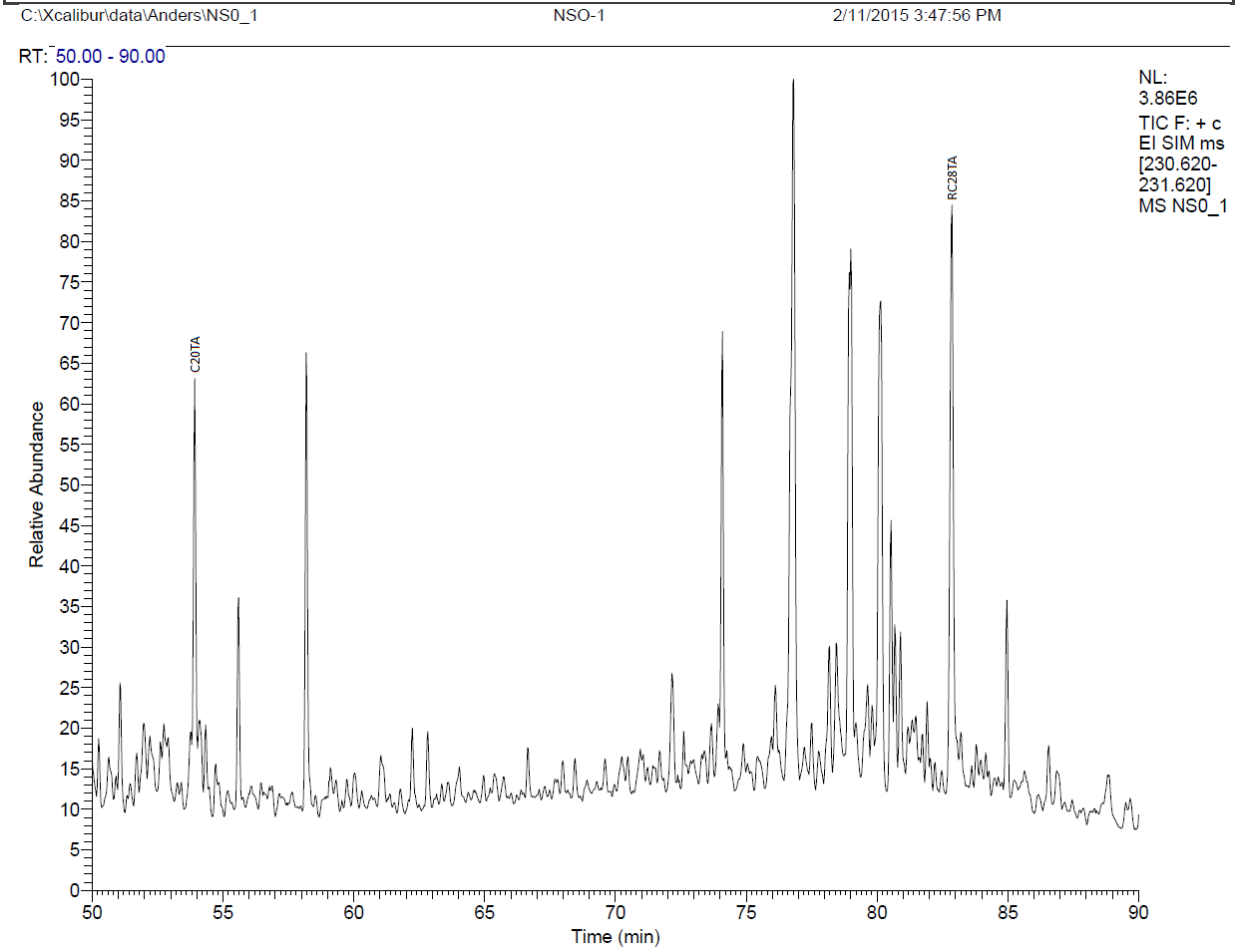

Figure 5.7: Peak identification of the biomarker compounds listed in Table 5.5 in NSO-1 chromatogram from m/z = 231. The peak height of the C20 compond will increase relative to the C28 compound in response to increased maturity.

5.2.4 The monoaromatic steroids

The monoaromatic stereoid group falls into the aromatic hydrocarbon fraction and is identified in the m/z = 253 chromatogram. These compounds form from steroids in the early diagenetic environment by aromatization (Tissot and Welte, 1984). The peaks of relevance are listed in Table 5.6 and the peak identification in the chromatogram is shown in Figure 5.8. The compounds in this family are used together with the tri-aromatic steroids as maturity indicators because the monoaromatic steroids will aromatize to tri-ring steroids with increased maturity (Peters et al., 2005).

Table 5.6: List of the different peaks identified from m/z = 253

Peak Group	R1	R2	R3	R4	Peak
H1	α(H)	CH_3	$S(CH_3)$	C_2H_5	$\alpha SC_{29}MA$
H1	α(H)	CH_3	$R(CH_3)$	CH_3	$\alpha RC_{28}MA$
H1	β(H)	CH_3	$R(CH_3)$	C_2H_5	$\beta RC_{29}MA$
H1	bCH_3	H	$R(CH_3)$	C_2H_5	$\beta RC_{29}DMA$

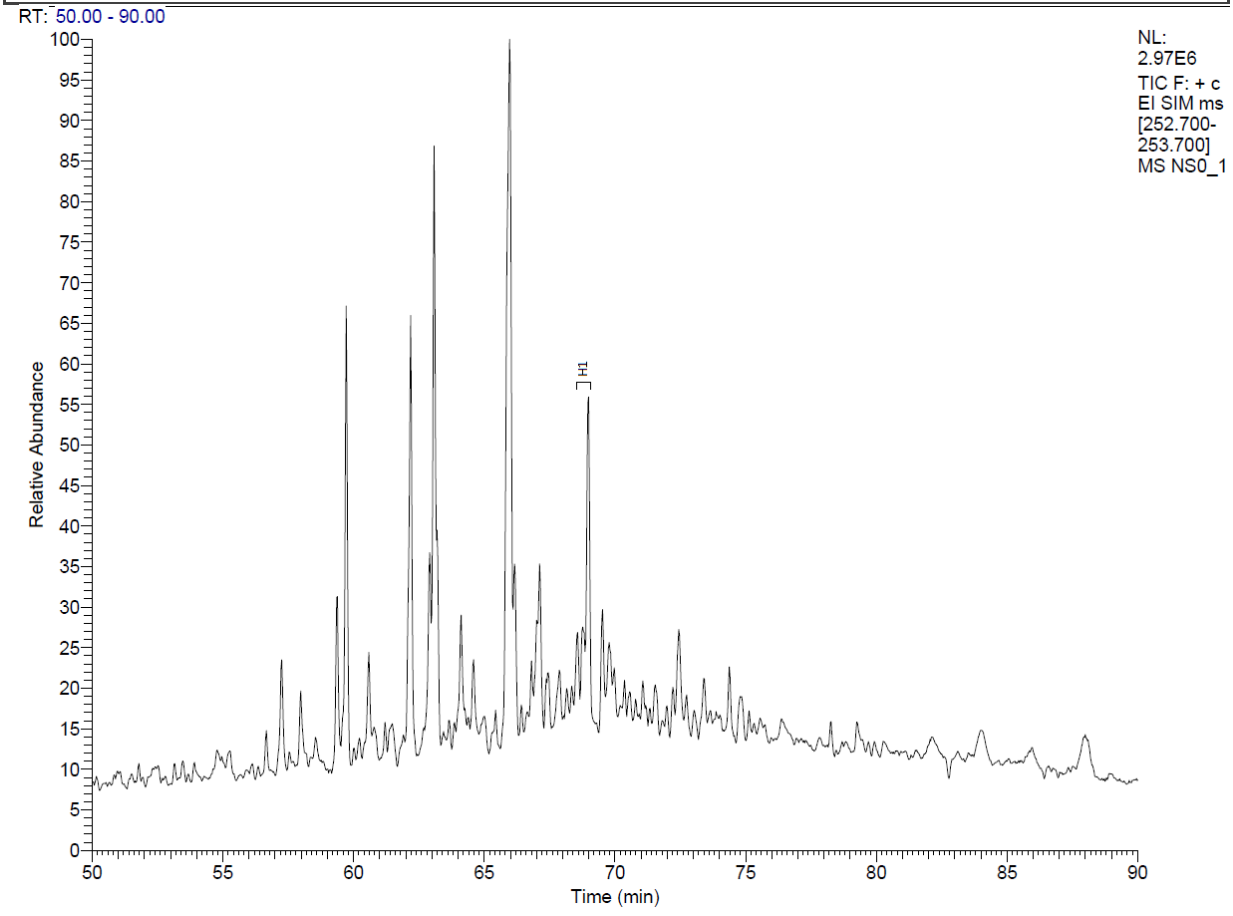

Figure 5.8: Peak identification of biomarker compounds listed in Table 5.6 in the m/z = 253 chromatogram of the NSO-1 reference oil.

5.2.5 The phenanthrene, methylphenanthrene and methyldibenzothiophenes

Phenanthrene, methylphenanthrene and methyldibenzothiophene are aromatic hydrocarbons identified in m/z 178, m/z = 192 and m/z = 198 respectively, and the peaks of relevance is listed in Table 5.7. Figure 5.10 shows the identification of m/z = 178, m/z = 192 and m/z = 198 in the reference chromatogram from NSO-1. Methylphenanthrene is a fuzed tri-aromatic moiety with 14 C atoms. Methylphenanthrene is the methylated analog of phenanthrene i.e. a C15 with 4 main isomers (1, 2, 3 and 9, see Figure 5.9, left for isomer positions), and methyldibenzothiopene is a sulfur-aromatic unit with 13 C atoms and one sulfur atom and 4 main isomers (1, 2, 3 and 4, see Figure 5.9, right for isomer positions). These compounds are all used mainly for maturity estimates as some isomers are more thermally stable than others, see below:

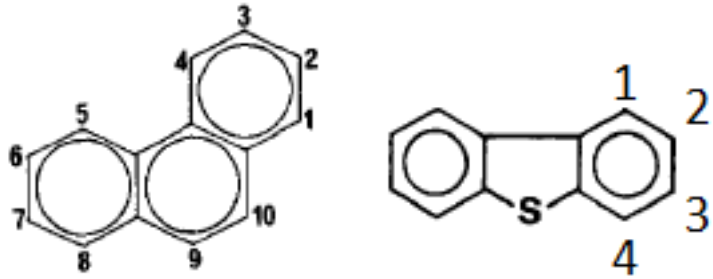

Figure 5.9: To the left: Illustration of the chemical structure of the phenanthrene molecule and the possible isomer positions of the methyl side-chain (from Kvalheim et al., 1987). To the right: Illustration of the chemical structure of the dibenzothoiphene molecule and the possible isomer positions of the methyl side-chain (modified from Radke, 1988).

Table 5.7: List of identified peaks from the different m/z ratios.

m/z	Peak	Name
178	P	Phenanthrene
192	3-MP	3-Methylphenanthrene
192	2-MP	2-Methylphenanthrene
192	9-MP	9-Methylphenanthrene
192	1-MP	1-Methylphenanthrene
198	4-MDBT	4-Methyldibenzothiophene
198	(3+2)-MDBT	3+2-Methyldibenzothiophene
198	1-MDBT	1-Methyldibenzothiophene

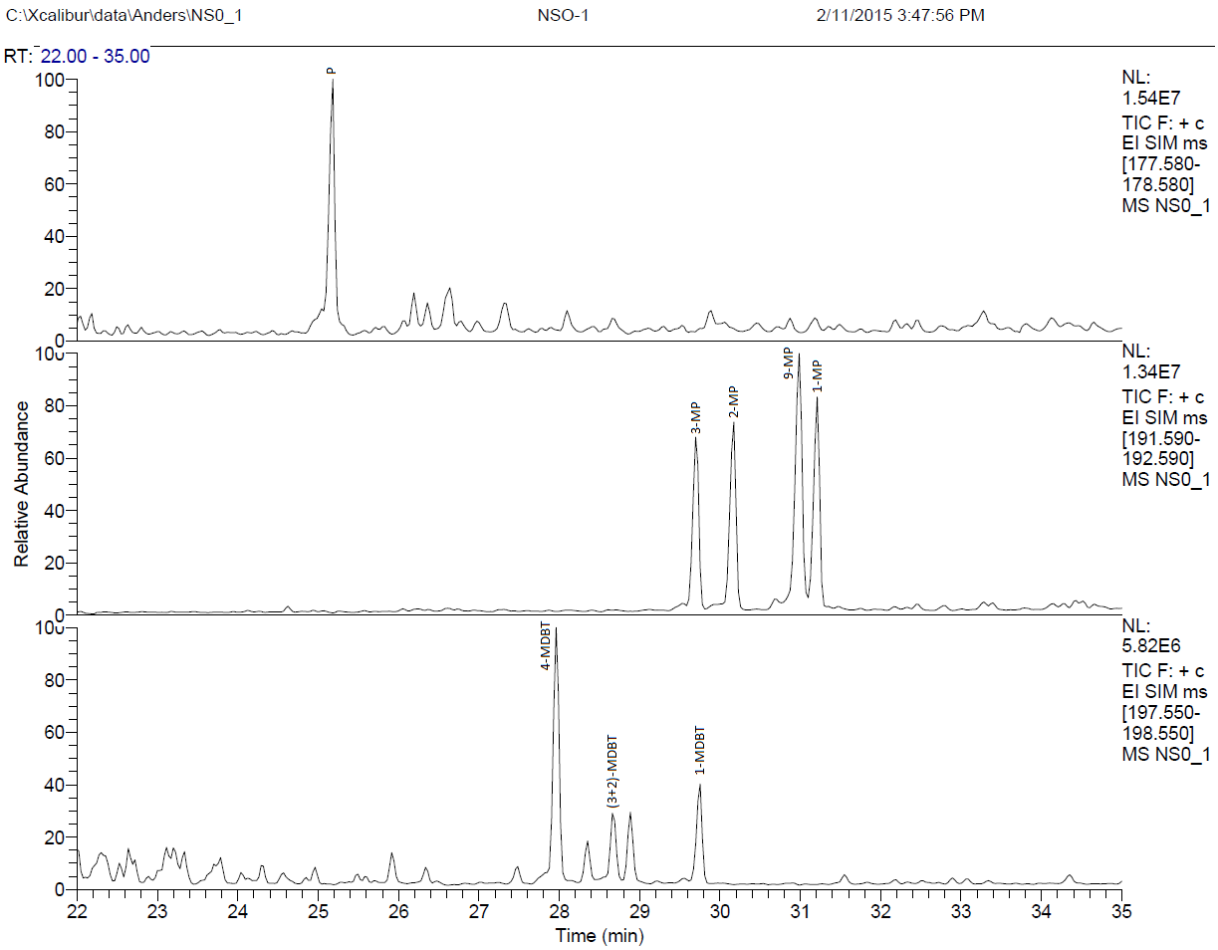

Figure 5.10: Identification of peaks in the m/z = 178 (phenanthrene), m/z = 192 (methylphenanthrenes) and m/z = 198 (methyldibenzothiophenes) chromatograms of the NSO-1 reference.

5.2.6 The Standard parameters concerning maturity and organic facies

The “standard parameters” are referred to the 27 parameters listed in Table 5.8, and will be briefly explained in this subchapter. The maturity ranges of selected maturity parameters are shown in Figure 5.11. Note in this figure that the most parameters are non-linear in maturity.

Table 5.8: Overview of the 27 "standard parameters" from GC-MS used to evaluate source rock maturity and the organic facies of the palaeo-depositional environment.

No.	Parameter
1	Ts/(Ts+Tm), (Seifert and Moldowan, 1978)
2	Diahopane/(diahopane + normoretane), (Cornford et al., 1980)
3	22S/(22S+22R) homohopane, (Mackenzie et al., 1980)
4	C30-hopane/(C30-hopane + C30 morethane), (Mackenzie et al., 1985)
5	29Ts/(29Ts + norhopane) (Moldowan et al., 1991)
6	28-30-bisnorhopane/(28-30-bisnorhopane + norhopane) (Wilhelms and Larter, 1994)
7	C23-C29 tricyclic terpanes/C30αβ-hopane (modified from Mello et al., 1988)
8	C24 tetracyclic terpane/C30 αβ-hopane (Mello et al., 1988)
9	Hopane/sterane ratio, (Mackenzie et al., 1984)
10	ββ/(ββ+αα) of C29 (20R+20S) sterane isomer, (Mackenzie et al., 1980)
11	20S/(20S+20R) of C29 5α(H), 14α(H), 17α(H) steranes, (Mackenzie, 1984)
12	Diasteranes/ (diasteranes+regular steranes), (Seifert and Moldowan, 1978)
13	% C27 of C27+C28+C29ββ-cholestanes, (Moldowan et al., 1985)
14	% C28 of C27+C28+C29ββ-cholestanes, (Moldowan et al., 1985)
15	% C29 of C27+C28+C29ββ-cholestanes, (Moldowan et al., 1985)
16	C20/(C20 +C28) triaromatic steroids (TA) (Mackenzie et al., 1985)
17	C28 TA/(C28 TA + C29 MA) (Peters and Moldowan, 1993)
18	MPR = 2-MP/1-MP, (Radke et al., 1982b)
19	Methyl phenanthrene index, MPI1 (MPI1 = 1.5 (3-MP + 2-MP)/(P + 9-MP + 1-MP), (Radke et al., 1982a)
20	20. MPDF = (3-MP + 2-MP)/ (3-MP + 2-MP + 1-MP + 9-MP), (Kvalheim et al., 1987)
21	MDR = 4-MDBT /1-MDBT, (Radke, 1988)
22	Rm (1) = 1.1*log10MPR + 0.95, (Radke, 1988)
23	%Rc = 0.6*MPI 1 + 0.4, (Radke, 1988)
24	%Ro = 2.242*MPDF - 0.166, (Kvalheim et al., 1987)
25	Rm(2)= 0.073*MDR+0.51, (Radke, 1988)
26	3-MP/4MDBT, (Hughes et al., 1995)
27	MDBTs/MPs, (Radke et al., 2001)

1. Ts/(Ts+Tm)

When entering catagenisis (vitrinite reflectivity >0.5%R_o c.f. Tissot and Welte, 1984), Tm is less stable than Ts with increased maturity, hence the ratio will increase for more mature samples compared to those which are less mature (Seifert and Moldowan, 1978). However, the Ts/(Ts+Tm) is also affected by the type of source of the sample (Moldowan et al., 1986) and carbonate-derived oils have been reported to score very low in this ratio (cf. Peters et al., 2005). Bitumen samples from hypersaline source rocks shows typically unusual high Ts/(Ts+Tm) values (e.g Rullkötter and Marzi, 1988).Therefore, the Ts/(Ts + Tm) is a more reliable maturity parameter when comparing petroleum from the same type of organic facies (Peters et al., 2005).

2. Diahopane/(diahopane + normoretane)

It is indicated that this ratio is related to maturity, and high ratios corresponds to high maturities, but may also indicate input of terrestrial material (Peters and Moldowan, 1993).

3. 22S/(22S+22R) homohopane

The 22R hopane, being less stable than 22S at maturation levels from immature to early oil generation, leads to an early increase in the 22S/(22S+22R) ratio until it equilibrates around 0.6 (0.57-0.62)(Seifert and Moldowan, 1980). Ratios in the range of 0.50-0.54 indicates samples around the start of the oil window, while ratios at equilbrium (0.57-0.62) indicates maturity corresponding to the main oil generation phase or beyond (Peters et al., 2005). As a consequence of the early equilibration of this ratio, it is only useful for immature and early oil generating source rocks and sedimentary samples, and all oils have full isomerized values.

4. C30-hopane/(C30-hopane + C30-morethane)

The compound 17 β,21α (H) morethane (30βα) is thermally less stable compared to 17α, 21β (H) hopane, leading to a faster decrease in abundance of the former compared to the latter with increasing maturity, resulting in an increase of the ratio. This ratio is also dependent on the type of organic matter to the source rock; Rullkötter and Marzi (1988) reported that bitumens sourced from a hypersaline source rock had higher morethane/hopane ratios compared to adjacent shales.

Considering maturity, it has been reported morethane/hopane ratios for immature bitumens of about 0.8, while mature source rocks show a range in the values from 0.05 to 0.15 (Mackenzie et al., 1980; Seifert and Moldowan, 1980).

5. 29Ts/(29Ts+norhopane)

29Ts is thermally more stable than norhopane and this ratio can therefore be used as a maturity parameter towards maturities which corresponds to late oil generation (Moldowan et al., 1991).

6. Bisnorhopane/(Bisnorhopane + norhopane)

The 28-30-bisnorhopane/(28-30-bisnorhopane+norhopane) ratio is a facies parameter. High concentrations of the 25-30-bisnorhopane (BNH) compound can indicate anoxic conditions during source rock depositions (Katz and Elrod, 1983), but the observations of concentrations also in e.g. Middle Jurassic coal samples which are associated with non-anoxic organofacies shows that BNH is not reliable as a sole anoxia indicator (Justwan et al., 2006). It also has to be noted that low concentrations of BNH not necessarily excludes an anoxic depositional environment (Peters et al., 2005). BNH is not bound to the kerogen but is provided by bitumen in the source rock (Moldowan et al., 1984), resulting in a drastic drop in BNH concentration caused by intitiation of kerogen cracking when entering oil window. Therefore, the 28-30-bisnorhopane/(28-30-bisnorhopane+norhopane) ratio is only useful for correlation of samples which have maturities in roughly the same range (Peters et al., 2005).

7. C23-C29 tricyclic terpanes/C30αβ hopane

The ratio of C23-C29 tricyclic terpanes to C30αβ hopane is a maturity parameter. The combination of the fact that tricyclic terpanes are more thermally stable than hopanes (Peters et al., 1990) and are liberated from kerogen at higher temperatures (Aquino Neto et al., 1983), results in a higher ratio for more mature samples, and a drastic increase at maturities exceeding vitrinite reflectivity of 0.75% (Van Graas et al 1990). Still, this ratio is also highly influenced by the gas to oil ratio of petroleums (GOR) and is always higher in condensates which are higher in GOR (Karlsen et al., 1995). However, the tricyclic terpane abundance is also determined by salinity (Mello, 1988), thus limiting its usefulness to differentiate organic facies.

8. C24 tetracyclic terpane/C30αβ hopane

Hopanes are seemingly less resistant to maturation and also biodegradation compared to tetracyclic terpanes (Peters et al., 2005) thus the C24 tetracyclic terpane/C30αβ hopane ratio will increase during maturation, and it will also increase due to degradation caused by bacterial activity.

9. Hopane/sterane ratio

Sediments which are rich in steroids are usually associated with marine or lacustrine environments, and hopane/sterane ratios which are low indicates a planktonic derived source while high ratios indicates a more terrestrial dominated source (Tissot and Welte, 1984).

10. ββ/(ββ+αα) of C29 (20R+20S) sterane isomer

As maturity increases, isomerization of the regular steranes 20S and 20R leads to an increase of this ratio from values close to zero towards equilibrium values is reached close to 0.7 (0.67-0.71) (Seifert and Moldowan, 1986). Even though this parameter seemingly is not affected by the type of source input, it has been reported that lab experiments indicates otherwise (Peters et al., 1990), but it is still useful as a maturity parameter up until peak oil generation (Peters et al., 2005).

11. 20S/(20S+20R) of C29 5α(H), 14α(H), 17α(H) steranes

C29 5α(H), 14α(H), 17α(H) steranes are isomerized with increasing maturation and this leads to a rise of the 20S/(20S+20R) ratio from 0 to approximately 0.52-0.55 (Seifert and Moldowan, 1986). This ratio may also be affected by factors like type of organic facies and biodegradation (Peters et al., 2005).

12. Diasteranes/ (diasteranes+regular steranes)

Diasterane/regular sterane ratios can be used to distinguish between petroleum sourced from carbonates and silisiclastic source rocks (Mello et al., 1988), and can therefore be used as a source parameter. Low diasterane to regular steranes ratio normally corresponds to a clay-poor carbonate source rock, and high ratios corresponds accordingly to clay-rich source rocks, but high ratios may also be caused by high maturity (Seifert and Moldowan, 1978) and biodegradation (Seifert and Moldowan, 1979).

13, 14 and 15

Parameter 13, 14 and 15 corresponds to C27ββS i.e. C27 cholestane, C28ββS i.e. C28 cholestane and C29ββS i.e. C29 cholestane respectively, and their distribution relative to each other is plotted in a ternary diagram which indicates type of facies (Moldowan et al., 1985).

16. C20/(C20 +C28) triaromatic steroids (TA)

The C20/(C20 + C28) triaromatic steroid (TA) ratio is sensitive to increasing maturity and is thus useful as a maturity indicator. Laboratory heating experiments shows a faster degradation of the

longer chained C28 TA compound compared to the C20 TA compound (Beach et al., 1989), and this ratio will thus increase during maturation.

17. C28 TA/(C28 TA + C29 MA)

As a source rock matures, the monoaromatic steroids are aromatized to triaromatic steroids i.e. the ratio increases from 0 to 1 and this ratio is therefore a maturity parameter and is valid for immature to mature samples (Peters et al., 2005).

18. MPR = 2-MP/1-MP

The ratio of the isomer 2-MP to 1-MP is kept constant up until 0.95%R_m., with further increase in maturity a predominance of 2-MP can be noticed (Radke et al., 1982b). This ratio can thus be used as a maturity indicator for mature oils/source rocks.

19. Methyl phenanthrene index 1, MPI1 (MPI1 = 1.5 (3-MP + 2-MP)/(P + 9-MP + 1-MP)

Radke et al. (1982a) and Radke and Welte (1983) observed that the 3-MP and 2-MP isomers are more resistant to thermal alteration compared to the 1-MP and 9-MP isomers. The methyl phenanthrene index is thus a maturity parameter, shows good correlation with vitrinite reflectivity (Radke et al., 1982a), and can therefore be calibrated with vitrinite reflectivity (see parameter 23). Radke and Welte (1983) noticed a positive linear relationship in the range of 0.65%R_m to 1.35%R_m and a negative linear relationship in the range of 1.35%R_m to 2.00%R_m, however, the later publication from Szcerba and Rospondek (2010) did not indicate a negative trend starting from maturity levels corresponding to 1.35%R_m. If a sample lacks vitrinite which is typical for samples containing mainly kerogen type I (Tissot and Welte, 1984), %R_m can be estimated from MPI1 (Peters et al., 2005). However, more recently, the usefulness of this parameter has been considered lower due to additional effects on the ratio, e.g. from the redox potential of the sedimentary rocks (Szcerba and Rospondek, 2010).

20. MPDF = (3-MP + 2-MP)/ (3-MP + 2-MP + 1-MP + 9-MP)

This is a maturity parameter and was introduced by Kvalheim et al. (1987), and is like parameter 19 based on the fact that the 3-MP and 2-MP isomers are more thermally stable compared to the 1-MP and 9-MP isomers. The difference from parameter 19 is that this parameter is solely based on methylphenanthrenes (phenanthrene, peak P, is not included in this ratio).

21. MDR = 4-MDBT /1-MDBT

1-MDBT is less thermally stable compared to 4-MDBT, and their relationship is therefore useful as a maturity parameter (Radke, 1988). In the maturity range of 0.4 to 0.7 vitrinite reflectivity, MDR values below 1.0 are common for oil prone source rocks, while source rocks which comprise type III kerogen shows MDR values around 2.5 (Radke et al., 1986). This difference gives the opportunity to distinguish between different types of organic facies in some cases.

*22. Rm (1) = 1.1*log10MPR + 0.95*

MPR = 2-MP/1-MP (parameter 18) can be calibrated against vitrinite reflectivity and parameter 22 shows this relationship (from Radke, 1988).

*23. %R c = 0.6*MPI 1 + 0.4*

This parameter shows the relationship between the MPI1 (Methyl Phenanthrene Index 1) i.e. parameter 19 and vitrinite reflectivity and is valid at least for vitrinite reflectivities between 0.7%R_c and 1.3%R_c (Radke et al., 1986).

*24. %R o = 2.242*MPDF – 0.166*

Parameter 24 shows the relationship between parameter 20 and vitrinite reflectivity (from Kvalheim et al., 1987).

*25. Rm(2)= 0.073*MDR+0.51*

Parameter 25 shows the relationship between parameter 21 and vitrinite reflectivity (from Radke, 1988).

26. 3-MP/4MDBT:

The 3-MP/4MDBT ratio (3-MP from m/z = 192 and 4MDBT from m/z = 198) is a facies parameter which plotted together with the Pr/Ph ratio can indicate different facies cf. Figure 6.3 (Hughes et al., 1995)

27. MDBTs/MPs:

MDBTs/MPs, (sum of peaks 4-MDBT, (2+3) MDBT and 1-MBDT from m/z = 198 divided by the sum of peaks 3-MP, 2-MP, 9-MP and 1-MP from m/z = 192) is a facies parameter giving indication of lithology of the source rock; values above 1 indicate carbonates, values below 1 indicate shale (see Hughes plot, Figure 6.2) (Hughes et al., 1995)

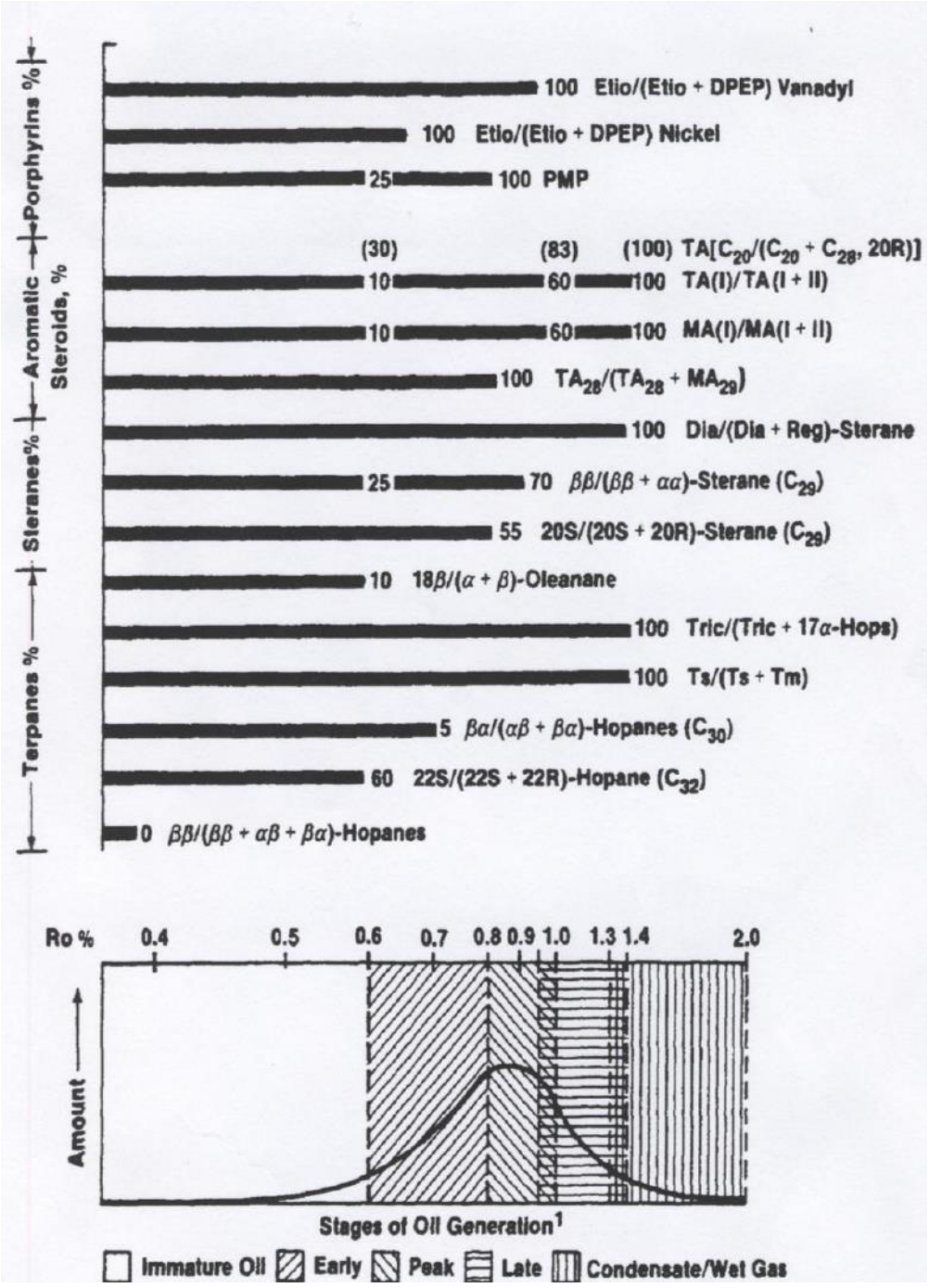

Figure 5.11: Validity range of different biomarker maturity parameters, corresponding to the oil window indicated by the %R_o values (from Peters and Moldowan, 1993)

5.2.7 Other parameters

BNH/C30 hopane

The BNH/C30 hopane ratio functions as a supplement to the BNH/C29 ratio and is thus used for the same purpose (see parameter 6).

Gammacerane index (gammacerane/C_{31} 22R hopane)

Gammacerane is an indicator of stratification of the water column in non-marine and marine depositional environments often caused by variations in salinity, and is thus a typical indicator of hypersalinity or more generally abnormal salinity during sediment deposition making it a useful parameter for distinguishing different sources for petroleum (Peters et al., 2005). Sabkha environments will often score high in this parameter, and it is generally high for Permian derived marine source rock systems, e.g. the Upper Permian Irati Shales from the Parana Basin in Brazil (Peters et al., 2005) and the Retort member, comprising phosphatic shale, from the Middle-Upper Permian Phosphoria Formation, at Little Sheep Creek located in Montana, USA (Dahl et al., 1993). The gammacerane index was one of the ratios Peters et al. (1989) used for their interpretation of the Beatrice oil being co-sourced by Middle Devonian source rocks, as the gammacereane index was an intermediate between the lower valued Jurassic source rocks and the higher valued Middle Devonian source rocks which can range in salinity from lacustrine to sabkha environments and source rock settings are often associated with cyclic evaporative lakes and also lagoonal depositional environments (Marshall et al., 2011).

β and γ-carotane

GC-MS detects lower abundance of carotanes than GC-FID, therefore specific m/z ratios were selected for identification of the different molecules; m/z = 558 for β-carotane and m/z = 560 for γ-carotane. The daughter-ion of the carotanes, m/z = 125 is also included and both β-carotane and γ-carotane can be identified in this chromatogram. Identification of β and γ-carotane after the first run (Figure 5.12) and second run (Figure 5.13) is shown in GC-MS chromatograms from O-21 and Beatrice respectively (see section 4.5. for explanation for the reason behind two runs). Notice a peak which coincides with the retention time of β-carotane also in the m/z 560 chromatograms.

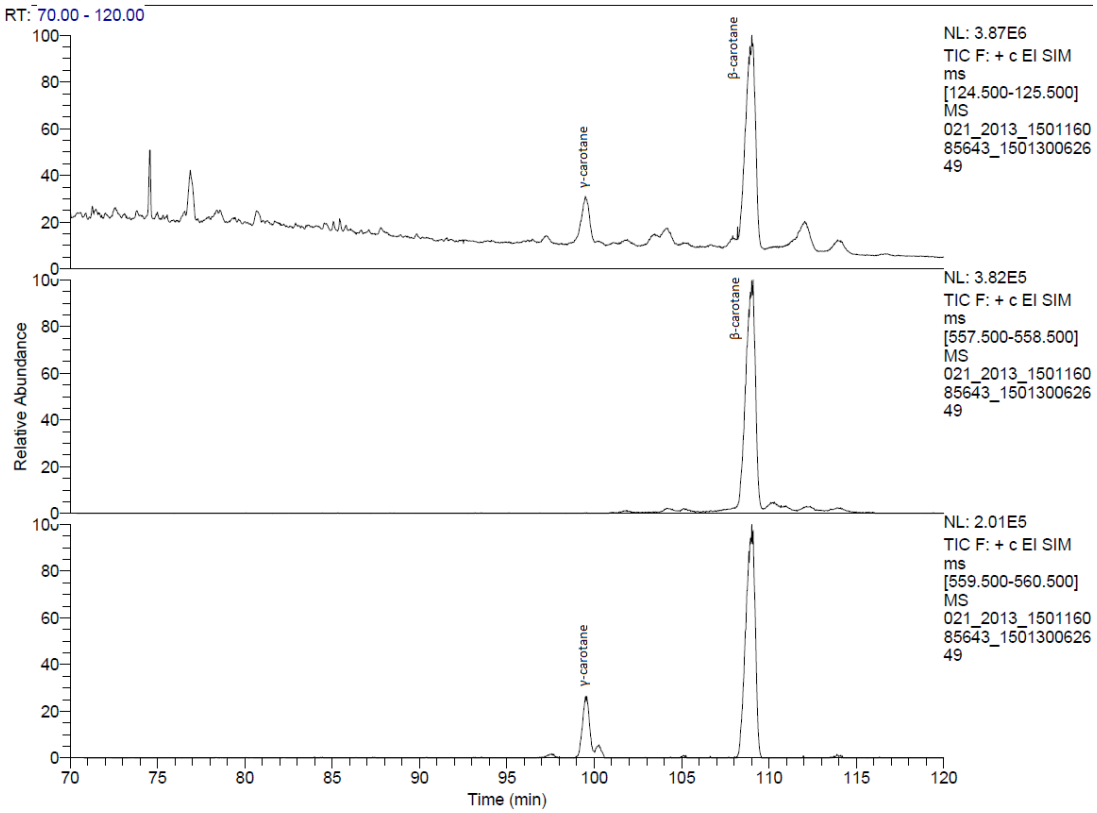

Figure 5.12: Positive Identification of β-carotane and γ-carotane in the GC-MS chromatogram of O-21, i.e. one of the lacustrine lake samples from the Orkneys.

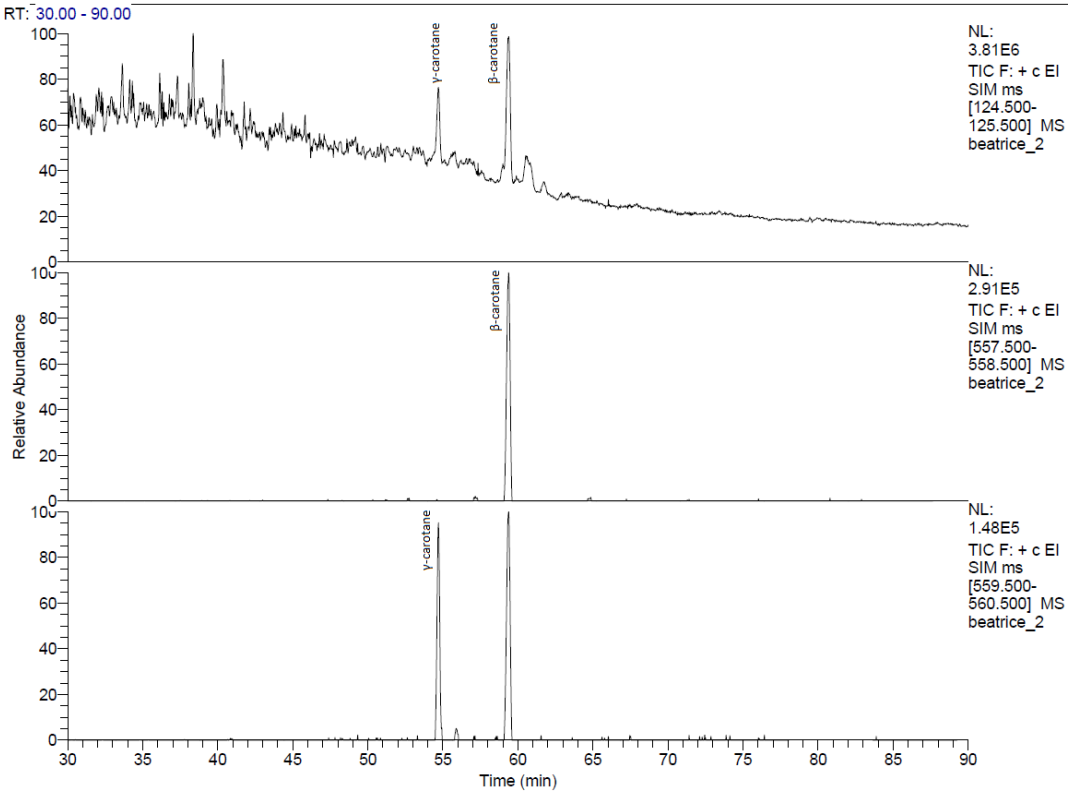

Figure 5.13: Positive identification of β-carotane, and γ-carotane in the GC-MS chromatogram of Beatrice.

C26/C25 tricyclic terpane ratio and C31 22R/C30 hopane ratio

Lacustrine source rocks generally shows higher C26/C25 tricyclic terpane ratios compared to marine source rocks. Statistics from more than 500 different crude oil samples worldwide, plotted in Figure 5.14 (cf. Peters et al. 2005) shows a tendency for lacustrine sourced oils mostly to have a C26/C25 ratio above 1.4 while marine shales commonly shows ratios below 1.3 thus making this ratio a great support when separating marine sourced oils from lacustrine sourced oils. The C26/C25 ratio was in Peters et al. (2005) plotted against C31 22R/C30 hopane ratio; lacustrine source rocks show in general low C31 22R/C30 ratios compared to oils derived from marine shales, marls and carbonates which shows higher values (Figure 5.14). Peters et al. (2005) states that the C31 22R/30 hopane ratio alone is not an adequate tool for distinguishing lacustrine from other type of source rock depositional environments, but when plotted together with C26/C25 tricyclic terpane ratio it becomes easier to differentiate the different sources. Values above 0.2 are common for the marine shales; it should be above 0.25 when considering the certainty of separating marine shales from lacustrine sourced oils where the bulk of the samples have values below 0.25.

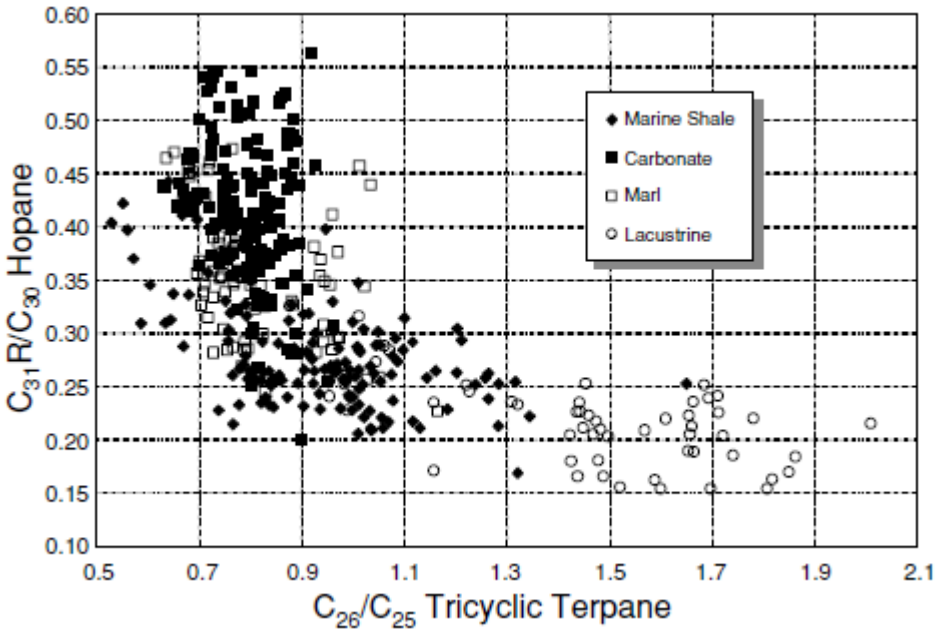

Figure 5.14: Relationship between C26/C25 tricyclic terpane and C31 R/C30 hopane for more than 500 oils worldwide (from Peters et al. 2005), which indicates that oils from carbonate source rock facies will not score high in both the C26/C25 tricyclic terpane and C31 R/C30 hopane parameter. Oils from lacustrine source rock facies scores in general high in the C26/C25 tricyclic terpane ratio and low in the C31 R/C30 hopane ratio.

C30 sterane

Presence of C30 sterane is a strong indicator of marine source, while absence indicates a non-marine or lacustrine source (Moldowan et al., 1985).

25-28-30-Trisnorhopane

The 25-28-30-trisnorhopane (TNH) compound is like BNH diagnostic for anoxic conditions (Peters et al 2005). If the organic matter is subjected to microbial degradation, BNH is altered and may be converted into TNH (Peters et al., 2005), thus making TNH a great asset in such cases.

5.3 Interpretation parameters based on Rock-Eval and TOC

During maturation, kerogen cracking leads to the progressive elimination of carbon structures bonded to the kerogen via bonds with lower activation energies and as such will the overall S2 signal diminish with the progress of increasing maturity, resulting in a lower S2 peak and a shift of the T_{max} of the S2 signal towards a higher temperature (Tissot et al., 1987). The S2 peak may be affected by effects from the mineral matrix i.e. clay minerals tend to absorb oil-prone kerogen compounds, which results in an underestimation and the S2 value from samples which shows low organic content is more likely to be affected (Peters, 1986).

Thermal breakdown of kerogen is dependent on the kerogen type and also sulfur content; Type I has a narrow range of activation energies, Type II has a broader range than I and III has a broader range than II (Tissot et al., 1987). The generation of petroleum is therefore dependent on type of source input; T_{max} can be used as a maturity indicator if the kerogen type is known. However, the narrow range of activation energies for type I kerogen results in almost all transformation at the same temperature, making T_{max} more or less useless as a maturity indicator for this kerogen type.

TOC (Total Organic Content) is a measure of the quantity of the organic matter in the sample, HI (Hydrogen Index) is a measure of the quality of the kerogen i.e. the generative quantity of the TOC, and the OI (Oxygen Index) is a measure of the quantity of mg CO_2/ g TOC and is thus related to S3 and the generative potential (S1+S2). The PI (Production Index) reflects the transformation of the kerogen to oil and gas and is defined as S1/(S1 + S2) (cf. Peters, 1986).

5.4 Interpretation parameter, δ13C

Marine organic matter is more enriched in the C13 isotope relative to terrestrial organic matter, resulting in organic matter from a terrestrial source being isotopically lighter compared to organic matter from a marine source (Galimov, 1980). The difference of 3-5 $^{o}/_{oo}$ leads to C13 isotope analysis providing helpful additional information for correlation between source rocks and oils.

Usually, given approximately the same maturity, the extractable organic matter (bitumen) has δ13C values that is about 0-1.5$^{o}/_{oo}$ lighter compared to kerogens, and crude oils has about 0-1.5$^{o}/_{oo}$ lower values compared to the bitumen of the source rock (Peters et al., 2005), but Galimov (1980) noted that there was no noticeable difference between kerogen and bitumen until Carboniferous time and the associated widespread terrestrial floras that are so typical for the Carboniferous.

6. Results

This chapter will present the selected interpretation parameters which are described in chapter 5 and the scaled down chromatograms from the analytical methods described in chapter 4 (the different peaks from the chromatograms are identified in chapter 5). The full-scale chromatograms are presented in the appendix. The outline of this chapter is as follows:

6.1 GC-FID results

- 6.1.1. The source rock bitumen samples from the Orkneys
- 6.1.2. Oils from the Oseberg Field (NSO-1), the Embla Field, the Beatrice Field and the Judy Field.
- 6.1.3. The bitumen extracts from well 6609/11-1
- 6.1.4. The bitumen extracts from well 6610/7-1
- 6.1.5. The bitumen extracts from well 6609/5-1

6.2 GC-MS results

- 6.2.1. The source rock bitumen samples from the Orkneys
- 6.2.2. Oils from the Oseberg Field (NSO-1), the Embla Field, the Beatrice Field and the Judy Field.
- 6.2.3. The bitumen extracts from well 6610/11-1
- 6.2.4. The bitumen extracts from well 6610/7-1
- 6.2.5. The bitumen extracts from well 6609/5-1

6.3 TOC and Rock-Eval results for source bitumen rock samples

6.4 δ13C isotope analysis results

6.5 Scaled-down GC-FID and GC-MS chromatograms

6.1 GC-FID results

Values from the parameters based on GC-FID analysis (see section 4.3) are presented in the results and listed in Table 6.1 and the parameter descriptions are presented in section 5.1. Scaled-down GC-FID chromatograms are shown in section 6.5 and the full-scale versions are found in Appendix A.

6.1.1 The source rock bitumen samples from the Orkneys

O-1

The O-1 sample shows a Pr/n-C17 and Ph/n-C18 ratio of 0.52 and 1.58 respectively and has a Pr/Ph ratio of 0.27 which is the lowest for the entire dataset (see Table 6.1). The most prominent n-alkane-peaks are in the range from n-C17 to n-C25 (see Figure 6.4) and the abundance of C30+ n-alkanes is low. All the odd/even predominance indexes are found to be above 1. The observed peaks at the retention time of 63min and 67min corresponds to γ-carotane and β-carotane respectively.

O-2

Sample O-2 has a Pr/n-C17 and Ph/n-C18 ratio of 2.45 and 2.70 respectively a Pr/Ph ratio of 0.61. The most prominent n-alkane-peaks are in the range from n-C18 to n-C23, but the n-alkanes are predominated by the isoprenoids (see Figure 6.5). There is also some contribution from n-alkanes in the C30+ fraction. A hump around n-C20 probably representing UCM is observed. A trend of slight odd n-alkane predominance is observed in O-2 but CPI1 falls clearly below 1 (0.86) (see Table 6.1). γ-carotane and β-carotane are detected at the retention times of 63min and 67min respectively.

O-3

The Pr/n-C17 and Ph/n-C18 ratios for sample O-3 are 0.65 and 0.90 respectively, and the Pr/Ph ratio is 0.44. There is a predominance of n-alkane-peaks from n-C19 to n-C25 and no presence of n-alkanes below n-C15 (see Figure 6.6). There is also a significant abundance of n-C30+ present in O-3. All CPI indexes are above 1 (see Table 6.1). The peak which corresponds to β-carotane is detectable around 67min retention time.

O-4

Pr/n-C17, Ph/n-C18 and Pr/Ph ratios for O-4 are 0.44, 1.07 and 0.34 respectively. The most prominent n-alkane-peaks are in the range from n-C18 to n-C23 (see Figure 6.7) and the abundance of longer chained n-alkanes (>n-C30) is relatively high. All CPI indexes are found to be above 1 (see Table 6.1).

O-5

O-5 has the lowest Pr/n-C17 ratio of the source rock samples with the value 0.33, and the second lowest Ph/n-C18 ratio with 0.51. The Pr/Ph ratio of O-5 is 0.67. The n-alkane-peaks in the range

from n-C17 to n-C20 (see Figure 6.8) are most prominent and all CPI indexes are above 1 (see Table 6.1). The n-alkane envelope for the n-C20 plus fraction has a concave shape.

O-6

Sample O-6 shows a Pr/n-C17 and Ph/n-C18 ratio of 0.67 and 0.49 respectively and has a Pr/Ph ratio of 0.67. The Ph/n-C18 ratio is the lowest of the source rock samples. The most prominent n-alkane-peaks are in the range from n-C20 to n-C27 (see Figure 6.9). There is no presence of n-alkanes below n-C15. All CPI indexes are found to be above 1 (see Table 6.1). The detected peaks at 63 min and 67min retention time correspond to γ-carotane and β-carotane respectively.

O-7

The Pr/n-C17 and Ph/n-C18 ratio for O-7 are 0.82 and 0.78 respectively and the Pr/Ph ratio is 0.78. A predominance of n-alkanes in the range from n-C18 to n-C22 is observed (see Figure 6.10), and all CPI indexes are above 1 (see Table 6.1). The n-alkane envelope for the n-C20 plus fraction has a concave shape and the n-c30+ fraction is of low abundance.

O-20

Sample O-20 shows a Pr/n-C17 and Ph/n-C18 ratio of 0.67 and 0.94 respectively and has a Pr/Ph ratio of 0.58. The most prominent n-alkane-peaks are in the range from n-C17 to n-C25 but are predominated by an unidentified peak at the retention time of around 22min (see Figure 6.11). All CPI indexes are found to be above 1 (see Table 6.1).

O-21

O-21 has Pr/n-C17, Ph/n-C18 and Pr/Ph ratio of 0.60, 0.72 and Pr/Ph ratio of 0.71. The n-alkane peaks in the range from n-C17 to n-C23 predominates and all CPI indexes are above 1 (1.03-1.49) (see Table 6.1). An unidentified peak which predominate the n-alkanes is detected around 22min retention time. Other unidentified peaks with high intensities are observed from around 5min to 9min retention time (see Figure 6.12).

6.1.2 Oils from the Oseberg Field (NSO-1), the Embla Field, the Beatrice Field and the Judy Field

NSO-1

NSO-1 shows a Pr/n-C17 and Ph/n-C18 ratio of 0.61 and 0.41 respectively and has a Pr/Ph ratio of 1.7. The most prominent n-alkane-peaks are in the range from n-C9 to n-C10 (see Figure 6.13). The

n-alkane envelope has a concave shape as the decrease in peak intensity relative to increasing n-alkane number flattens out. All CPI indexes are found to be above 1 (see Table 6.1).

Embla

The Embla oil shows a Pr/n-C17 and Ph/n-C18 ratio of 0.55 and 0.49 respectively, the Pr/Ph ratio is 2.42. The most prominent n-alkane-peaks are in the range from n-C11 to n-C15 (see Figure 6.14). The Embla oil shares the typical concave n-alkane envelope that is found in the NSO-1 chromatogram. All CPI indexes are found to be above 1 (see Table 6.1).

Beatrice

The values from the ratios Pr/n-C17, Ph/n-C18 and Pr/Ph are 0.27, 0.12 and 2.42 respectively. The most prominent n-alkane-peaks are in the range from n-C9 to n-C11 (see Figure 6.15) but significant amounts of n-C25+ is also observed. All CPI indexes are found to be above 1 (1.07-1.36) (see Table 6.1). An unidentified peak with about same intensity as pristane is located between n-C14 and n-C15 at the retention time of 22 min.

Judy

The Judy oil shows a Pr/n-C17 and Ph/n-C18 ratio of 0.38 and 0.27 respectively and has a Pr/Ph ratio of 1.69. The n-alkane envelope has a similar concave-shape trend to NSO-1 and the most prominent n-alkane-peaks are in the range from n-C9 to n-C11 (see Figure 6.16). The CPI indexes are found to be above 1 (see Table 6.1).

6.1.3 The bitumen extracts from well 6609/11-1

A-1

A-1 shows a Pr/n-C17 and Ph/n-C18 ratio of 1.61 and 1.23 respectively and has a Pr/Ph ratio of 1.54. The most prominent n-alkane-peaks are in the range from n-C13 to n-C15 (see Figure 6.17) and the CPI indexes are found to be below 1 except from CPI (1.27) (see Table 6.1). The intensity of n-alkanes is in general low compared with the background bleeding (baseline of GC-FID chromatogram).

A-2

A-2 shows a Pr/n-C17 and Ph/n-C18 ratio of 0.36 and 0.17 respectively and has a Pr/Ph ratio of 1.29. A-2 has a predominance of n-alkanes in the range from n-C21 to n-C23 and a rapid decrease in n-

alkane peak intensities for shorter and longer chains (see Figure 6.18). The CPI indexes are found to be above 1 (see Table 6.1).

A-3

The Pr/n-C17 and Ph/n-C18 ratio for A-3 are 0.33 and 0.17 respectively and the Pr/Ph ratio is 1.00. The most prominent n-alkane-peaks are in the range from n-C23 to n-C27 (see Figure 6.19), but there is also a significant contribution from n-C28+ shown in the n-C17/n-C31 ratio of 0.10 (lowest ratio in the entire sample list, see Table 6.1). All the CPI indexes are above 1 (1.11-1.27).

A-4

Sample A-4 shows a Pr/n-C17 and Ph/n-C18 ratio of 1.10 and 0.71 respectively and has a Pr/Ph ratio of 2.11. The most prominent n-alkane-peaks are in the range from n-C13 to n-C15 (see Figure 6.20). All of the CPI indexes are found to be at or below 1 (see Table 6.1). The peak intensities of the n-alkanes are in general low compared to the background bleeding i.e the baseline of the GC-FID chromatogram.

A-5

The A-5 sample has a Pr/n-C17 and Ph/n-C18 ratio of 0.17 and 0.08 respectively and a Pr/Ph ratio of 1.60. A-5 is characterized by high n-alkane abundance which is reflected in high peak intensities, and the most prominent n-alkane-peaks are in the range from n-C22 to n-C25 (see Figure 6.21), but there is also significant abundance of longer chained n-alkanes. The CPI indexes are above 1 (1.10-1.28).

6.1.4 The bitumen extracts from well 6610/7-1

B-1

Sample B-1 shows a Pr/n-C17 and Ph/n-C18 ratio of 0.70 and 0.63 respectively and has a Pr/Ph ratio of 1.13. B-1 has a broad range of high intensity n-alkane peaks, which is observed in the predominance of n-alkane-peaks in the range from n-C16 to n-C24 (see Figure 6.22), and the peak intensities for longer chained n-alkanes are also relatively high. All of the CPI indexes are found to be above 1, if excluding OEP (0.96) (see Table 6.1)

B-2

B-2 shows a Pr/n-C17 and Ph/n-C18 ratio of 0.71 and 0.61 respectively and has a Pr/Ph ratio of 0.93. The most prominent n-alkane-peaks are in the range from n-C19 to n-C24 (see Figure 6.23), but

there is also high abundance of longer chained n-alkanes. All of the CPI indexes are above 1, except from OEP (0.98) (see Table 6.1).

B-3

The Pr/n-C17, Ph/n-C18 and Pr/Ph ratios for sample B-3 are 0.82, 0.73 and 0.78. The n-alkane peaks are most prominent in the range from n-C20 to n-C24 (see Figure 6.24) and also n-alkanes with longer chains are abundant. All the CPI indexes show values above 1, except from OEP (0.94) (see Table 6.1)

B-4

Sample B-4 shows a Pr/n-C17 and Ph/n-C18 ratio of 0.64 and 0.29 respectively and has a Pr/Ph ratio of 2.57. A predominance of n-alkane-peaks in the range from n-23 to n-C27 is observed, also is high abundance of the longer chained n-alkanes, and the n-alkanes in range of n-C16 to n-C19 are depleted relative to n-C12 to n-C15 (see Figure 6.25). All the CPI indexes are found to be above 1, except from OEP (0.90) (see Table 6.1)

B-5

B-5 has a Pr/n-C17 and Ph/n-C18 ratio of 0.54 and 0.18 respectively and a Pr/Ph ratio of 3.91. The most prominent n-alkane-peak is n-C13 and the n-alkane envelope shows a concave trend starting from n-C17 towards longer chained components (see Figure 6.26) and the significance of n-alkanes with length from n-C25 is low. The CPI indexes are found to be above 1 i.e. ranging from 1.16 to 1.37 (see Table 6.1).

B-6

Sample B-6 shows a Pr/n-C17 and Ph/n-C18 ratio of 0.48 and 0.15 respectively and has a Pr/Ph ratio of 4.29 which is the highest value of the dataset. The n-alkane envelope shows a concave trend starting from n-C17 towards longer chained components, the most prominent n-alkane-peak is n-C13 (see Figure 6.27) and the significance of n-alkanes with length from n-C25 is low. All the CPI indexes are found to be clearly above 1 i.e. ranging from 1.26 to 1.50 (see Table 6.1).

B-7

The Pr/n-C17 and Ph/n-C18 ratio for B-7 are 0.63 and 0.27 respectively and the Pr/Ph ratio is 4.25. The most prominent n-alkane-peak is n-C13 and there is a rapid drop in intensity from n-C13 to n-C18 (see Figure 6.28) and n-alkanes of with at least C20 are of low abundance. All the CPI indexes are found to be clearly above 1 i.e. ranging from 1.33 to 1.75 (see Table 6.1).

6.1.5 The bitumen extracts from well 6609/5-1

C-1

Sample C-1 shows a Pr/n-C17 and Ph/n-C18 ratio of 0.53 and 0.29 respectively and the Pr/Ph ratio is 0.90. The n-alkane-peaks in the range from n-C20 to n-C25, which also shows a hump in baseline probably caused by UCM, predominate in C-1 (see Figure 6.29) and the abundance of n-C26+ are higher than the abundance of short chained n-alkanes below C18. All the CPI indexes are found to be above 1 except from OEP (0.99) (see Table 6.1).

C-2

C-2 has Pr/n-C17 and Ph/n-C18 ratios of 0.50 and 0.24 respectively and a Pr/Ph ratio of 1.09. The most prominent n-alkane-peaks are in the range from n-C20 to n-C23 and the intensities for longer chained n-alkanes drops with a concave trend from n-C23 (see Figure 6.30). All CPI indexes are found to be above 1 (see Table 6.1).

Table 6.1: Table showing values from selected parameters from GC-FID (see section 5.1 for parameter descriptions).
[1]: CPI = $(C_{25}+C_{27}+C_{29}+C_{31}+C_{33})/(C_{26}+C_{28}+C_{30}+C_{32}+C_{34})$, [2]: CPI1 = $2(C_{23}+C_{25}+C_{27}+C_{29})/(C_{22}+2(C_{24}+C_{26}+C_{28})+C_{30})$
[3]: OEP = $(C_{25}+6C_{27}+C_{29})/(4C_{26}+4C_{28})$ (from Peters et al., 2005)

Sample	Pr/n-C17	Ph/n-C18	Pr/Ph	CPI[1]	CPI1[2]	OEP[3]
O-1	0.52	1.58	0.27	1.30	1.03	1.06
O-2	2.45	2.70	0.61	1.47	0.86	1.11
O-3	0.65	0.90	0.44	1.31	1.16	1.05
O-4	0.44	1.07	0.34	1.27	1.11	1.08
O-5	0.33	0.51	0.67	1.45	1.06	1.05
O-6	0.67	0.49	0.67	1.19	1.18	1.05
O-7	0.82	0.78	0.78	1.41	1.10	1.05
O-20	0.67	0.94	0.58	1.29	1.17	1.04
O-21	0.60	0.72	0.71	1.49	1.22	1.03
NSO-1	0.61	0.41	1.7	1.25	1.05	1.02
Embla	0.55	0.49	1.53	1.29	1.06	1.03
Beatrice	0.27	0.12	2.42	1.36	1.29	1.07
Judy	0.38	0.27	1.69	1.35	1.16	1.07
A-1	1.61	1.23	1.54	1.27	0.94	0.98
A-2	0.36	0.17	1.29	1.61	1.48	1.10
A-3	0.33	0.17	1.00	1.27	1.25	1.11
A-4	1.10	0.71	2.11	1.00	0.77	0.74
A-5	0.17	0.08	1.60	1.28	1.28	1.10
B-1	0.70	0.63	1.13	1.18	1.04	0.96
B-2	0.71	0.61	0.93	1.17	1.07	0.98
B-3	0.82	0.73	0.78	1.15	1.06	0.94
B-4	0.64	0.29	2.57	1.09	1.10	0.90
B-5	0.54	0.18	3.91	1.37	1.21	1.16
B-6	0.48	0.15	4.29	1.50	1.32	1.26
B-7	0.63	0.27	4.25	1.75	1.33	1.33
C-1	0.53	0.29	0.90	1.29	1.25	0.99
C-2	0.50	0.24	1.09	1.36	1.29	1.02

6.2 GC-MS Results

The calculated parameters from the GC-MS analysis (see section 4.5) for every sample are listed in Table 6.2, Table 6.3 and Table 6.4. The parameters 1-27 from Table 6.2 and Table 6.3 are labeled in Table 5.8 and all the GC-MS parameters are described in section 5.2.6 and the parameters in Table 6.4 are described in section 5.2.7. Scaled-down GC-MS chromatograms are shown in section 6.5 and the full-scale versions are found in Appendix B. The values from parameter 2, parameter 4, parameter 5, parameter 8, parameter 10, parameter 11, parameter 16, and parameter 17 were not included in the discussion.

6.2.1 The source rock bitumen samples from the Orkneys

O-1

The Ts/(Ts/Tm) ratio of sample O-1 is found to be 0.78, the distribution of C27-C29 regular steranes are 15%, 43% and 42% respectively, the hopane/sterane ratio is 1.74 and the gammacerane index is 1.00. The 28-30-bisnorhopane (BNH)/norhopane ratio is 0.25 and the C26/C25 tricyclic terpane and C31 22R/C30 hopane ratios are 1.47 and 0.19 respectively. The vitrinite reflectivity values from parameters 22-25 for O-1 are 0.50, 0.55, 0.18 and 0.74 respectively. β-carotane and γ-carotane are identified in the m/z = 125 chromatogram, but only the former is detectable in the chromatogram of specific m/z ratio (558). The O-1 chromatograms are shown in Figure 6.4 and in Appendix B.

O-2

O-2 shows a Ts/(Ts/Tm) ratio of 0.74 and has a C27-C29 regular sterane configuration of 15%, 45% and 40% respectively. The hopane/sterane ratio and the gammacerane index are 1.88 and 0.91 respectively and the BNH/norhopane ratio is 0.19. O-2 has a C26/C25 tricyclic terpane ratio of 1.33 and a C31 22R/C30 hopane ratio of 0.18. O-2 has values of 0.28, 0.53 and 0.14 from the vitrinite reflectivity parameters 22-24. Both the γ-carotane and β-carotane are detected in the m/z = 125 chromatogram, but the peak intensities of the former and latter are low in the chromatograms of m/z = 560 and m/z = 558 respectively. The O-2 chromatograms are shown in Figure 6.5 and in Appendix B.

O-3

The Ts/(Ts/Tm) ratio of sample O-3 is 0.75 and the distribution of C27-C29 regular steranes are 0%, 0% and 100% respectively. The hopane/sterane ratio is not possible to measure due to lack of steranes. O-3 has a gammacerane index of 0.43, BNH/norhopane ratio of 0.16, C26/C25 ratio of 1.52 and a C31 22R/C30 hopane ratio of 0.22. The vitrinite reflectivity values from parameters 22-24 for O-3 are 0.26, 0.55 and 0.21 respectively. γ-carotane is easily identified in the m/z = 125 chromatogram, but not detectable in the m/z = 560 chromatogram, while β-carotane is easily identified in both the m/z = 125 and m/z = 558 chromatograms. The O-3 chromatograms are shown in Figure 6.6 and in Appendix B.

O-4

The Ts/(Ts/Tm) ratio of sample O-4 is found to be 0.58 which is the lowest value of the Orkney source rock bitumen samples. O-4 has a C27-C29 regular sterane configuration of 43%, 22% and 35% respectively, a hopane/sterane ratio of 3.43 and the gammacerane index is found to be 0.26 which is the lowest value of the source rock bitumen samples from the Orkneys. The BNH/norhopane ratio is 0.09 and is the lowest of the source rock samples. O-4 has also the lowest C26/C25 tricyclic terpane ratio of the source rock samples with 0.82 and has a C31 22R/C30 hopane ratio of 0.21. The vitrinite reflectivity value from parameters 22-24 are 0.40, 0.56 and 0.26 respectively. Positive identification of β-carotane is seen in the chromatograms of m/z = 125 and m/z = 558, although the peak intensities are low. Due to the unusually low intensities of the carotanes and also the much lower C26/C25 tricyclic terpane ratio than what is typical for lacustrine organofacies (see Figure 5.14) and the other Orkney source rock bitumens and the Beatrice oil which all represents this facies type, the O-4 sample will not be of major concern in the discussion. The O-4 chromatograms are shown in Figure 6.7 and in Appendix B.

O-5

The ratio of Ts/(Ts/Tm) for O-5 is given as 0.82 and the distribution of C27-C29 regular steranes are 14%, 51% and 36% respectively. O-5 shows the lowest hopane/sterane ratio of the source rock bitumen samples of 0.79 and the highest value of the source rock bitumen samples from the Orkneys from the gammacerane index which is 2.57. The BNH/norhopane ratio is found to be 0.21, the C26/C25 tricyclic terpane ratio is 1.15 and the C31 22R/C30 hopane ratio of O-5 is 0.22. O-5 has values of 0.42, 0.56, 0.21 and 0.90 from the vitrinite reflectivity parameters 22-25. Both γ-carotane

and β-carotane are identified in the chromatograms of m/z = 125, and m/z = 560 and m/z = 558 respectively. The O-5 chromatograms are shown in Figure 6.8 and in Appendix B.

O-6

O-6 has a Ts/(Ts/Tm) ratio 0.68 which is the second lowest value of the source rock samples and the distribution of C27-C29 regular steranes are 42%, 0% and 58% respectively. The hopane/sterane ratio is 5.46, the gammacerane index is 0.36 and the BNH/norhopane ratio is 0.13. The C26/C25 tricyclic terpane and C31 22R/C30 hopane ratios are 1.13 and 0.23 respectively. O-6 shows values of 0.18, 0.53, 0.13 and 0.65 from the vitrinite reflectivity parameters 22-25. In the m/z = 125 chromatogram, peaks corresponding to γ-carotane and β-carotane are detected, and γ-carotane is also present in the m/z = 560 chromatogram. Interestingly, β-carotane is not present in m/z = 558 but it is detected in m/z = 560. The O-6 chromatograms are shown in Figure 6.9 and in Appendix B.

O-7

The Ts/(Ts/Tm) ratio of sample O-7 is found to be 0.82, the C27-C29 regular sterane configurations are 4%, 56% and 40% respectively, the hopane/sterane ratio is 2.51 and the gammacerane index is 1.33. BNH/norhopane, C26/C25 tricyclic terpane and C31 22R/C30 hopane ratios of O-7 are 0.21, 1.35 and 0.21 respectively. The vitrinite reflectivity value from parameters 22-24 are 0.68, 0.69 and 0.57 respectively. Positive identification of γ-carotane (the m/z = 125 chromatogram) and β-carotane (the m/z = 125 and m/z = 558 chromatograms) are noticed. The O-7 chromatograms are shown in Figure 6.10 and in Appendix B.

O-20

The Ts/(Ts/Tm) ratio of sample O-20 is 0.88 which is the highest value of the source rock samples and the distribution of C27-C29 regular steranes are 35%, 0% and 65% respectively. O-20 has also the highest hopane/sterane ratio value of the source rock bitumen samples from the Orkneys with 13.65. The gammacerane index is 1.43 and the BNH/norhopane ratio is 0.15. The C26/C25 tricyclic terpane and C31 22R/C30 hopane ratios are 1.8 and 0.17 respectively, the former is tied with the value from O-21 for being the highest and the latter is second lowest of the entire sample set. O-20 has values of 0.40, 0.57 and 0.20 from the vitrinite reflectivity parameters 22-24. Both γ-carotane and β-carotane are easily identified in the chromatograms of m/z = 125, and also in m/z = 560 and m/z = 558 respectively but those peak intensities are low compared to the background noise. The O-20 chromatograms are shown in Figure 6.11 and in Appendix B.

O-21

O-21 has a Ts/(Ts/Tm) ratio of 0.86 which is the second highest value of the source rock samples and the C27-C29 regular sterane configurations are 14%, 49% and 37% respectively, the hopane/sterane ratio is 3.04 and the gammacerane index is 1.25. The BNH/norhopane ratio is found to be 0.10 and is the second lowest value of the source rock samples from the Orkneys. O-21 has the highest C26/C25 tricyclic terpane ratio of the sample set with 1.8, which is tied with O-20 and also the lowest C31 22R/C30 hopane ratio of the sample set with 0.12. The vitrinite reflectivity value from parameters 22-25 are 0.43, 0.52, 0.12 and 0.72 respectively. Both γ-carotane and β-carotane are easily identified in the chromatograms of m/z = 125, and m/z = 560 and m/z = 558 respectively. The O-21 chromatograms are shown in Figure 6.12 and in Appendix B.

6.2.2 Oils from the Oseberg Field (NSO-1), the Embla Field, the Beatrice Field and the Judy Field

NSO-1

The Ts/(Ts+Tm) ratio of the NSO-1 oil is found to be 0.55 which is lower compared to all of the source rock bitumen samples from the Orkneys as is the gammacerane index value of 0.14. The distribution of C27-C29 regular steranes are 33%, 32% and 35% respectively, the hopane/sterane ratio is 2.00. NSO-1 has a BNH/norhopane ratio of 0.35 which is higher than the entire sample set if excluding the upper section of well 6610/7-1 (B-1 to B-3), C26/C25 tricyclic terpane ratio of 0.81 and a C31 22R/C30 hopane ratio of 0.37. The vitrinite reflectivity value from parameters 22-25 are 0.89, 0.83, 0.81 and 0.70 respectively. β-carotane is identified in the m/z = 558 chromatogram, and also detected in the m/z 125 chromatogram. The NSO-1 chromatograms are shown in Figure 6.13 and in Appendix B.

Embla

The Embla oil has a Ts/(Ts+Tm) ratio of 0.90 which is the highest value of the entire sample set and has a C27-C29 regular sterane distribution of 38%, 28% and 34% respectively. The hopane/sterane ratio is 0.33 which is the lowest value of the entire sample set and the gammacerane index is 0.55. Embla has a BNH/norhopane ratio of 0.30 and C26/C25 tricyclic terpane and C31 22R/C30 hopane ratios of 0.81 and 0.51 respectively. Embla has values of 1.12, 1.08, 1.06 and 1.94 from the vitrinite reflectivity parameters 22-25. γ-carotane is not detectable in the m/z = 125 chromatogram, but

easily identified in the m/z = 560 chromatogram. The Embla chromatograms are shown in Figure 6.14 and in Appendix B.

Beatrice

The Ts/(Ts+Tm) ratio of Beatrice is found to be 0.58, the distribution of C27-C29 regular steranes are 21%, 37% and 43% respectively, the hopane/sterane ratio is 5.70, the gammacerane index is 0.33 and the BNH/norhopane ratio is found to be 0.08. The C26/C25 tricyclic terpane ratio of Beatrice is 1.23 and the C31 22R/C30 hopane ratio is 0.23. The vitrinite reflectivity value from parameters 22-25 are 0.88, 0.73, 0.76 and 0.71 respectively. γ-carotane and β-carotane are easily identified in the m/z = 125 chromatogram and the former and latter is also easily identified in the m/z = 560 and m/z = 558 chromatograms respectively. The Beatrice chromatograms are shown in Figure 6.15 and in Appendix B.

Judy

The Ts/(Ts+Tm) ratio of Judy is found to be 0.77, C27-C29 regular steranes configurations are 37%, 31% and 32% respectively and the hopane/sterane ratio is 2.02. The gammacerane index and BNH/norhopane ratios are 0.14 and 0.09 respectively. Judy has a C26/C25 tricyclic terpane ratio of 0.81 and a C31 22R/C30 hopane ratio of 0.37. The vitrinite reflectivity value from parameters 22-25 are 0.94, 0.86, 0.83 and 0.82 respectively. Although the peak intensities are low, γ-carotane and β-carotane are detectable in the m/z = 560 and m/z = 558 chromatograms respectively. The Judy chromatograms are shown in Figure 6.16 and in Appendix B.

6.2.3 The bitumen extracts from well 6610/11-1

A-1

A-1 has a Ts/(Ts+Tm) ratio of 0.52, the distribution of C27-C29 regular steranes are 36%, 26% and 39% respectively, the hopane/sterane ratio is 2.07 and the gammacerane index is 0.21. A-1 shows the lowest ratio of BNH/norhopane with 0.07 and has C26/C25 tricyclic terpane and C31 22R/C30 hopane ratios of 0.64 and 0.35 respectively. A-1 has values of 1.09, 0.75, 0.94 and 0.82 from the vitrinite reflectivity parameters 22-25. The A-1 chromatograms are shown in Figure 6.17 and in Appendix B.

A-2

The Ts/(Ts+Tm) ratio of A-2 is found to be 0.60, and the configuration of C27-C29 regular steranes are 25%, 33% and 42% respectively, the hopane/sterane ratio is 1.55, the gammacerane index is 0.13 and BNH/norhopane is 0.11. A-2 has a C26/C25 tricyclic terpane ratio of 2.5 which is clearly the highest value from the sample set and a C31 22R/C30 hopane ratio of 0.26. The vitrinite reflectivity value from parameters 22-25 are 1.00, 0.74, 0.81 and 0.74 respectively. β-carotane is identified in the m/z = 558 chromatogram, although the peak intensity is quite low. The A-2 chromatograms are shown in Figure 6.18 and in Appendix B.

A-3

The Ts/(Ts+Tm) ratio of A-3 is found to be 0.59 and the distribution of C27-C29 regular steranes are 26%, 33% and 41% respectively. The hopane/sterane, gammacerane index and BNH/norhopane ratios are 17.58, 0.16 and 0.11 respectively. A-3 has the highest hopane/sterane ratio of the entire sample set. The C26/C25 tricyclic terpane and C31 22R/C30 hopane ratios are 1.5 and 0.24 respectively. A-3 has values of 0.93, 0.71, 0.74 and 0.78 from the vitrinite reflectivity parameters 22-25. The A-3 chromatograms are shown in Figure 6.19 and in Appendix B.

A-4

A-4 has a Ts/(Ts+Tm) ratio of 0.55, and the C27-C29 regular sterane configurations are 29%, 26% and 45% respectively. The hopane/sterane ratio is 5.69, the gammacerane index is 0.23 and BNH/norhopane ratio is calculated to be 0.13. The C26/C25 tricyclic terpane and C31 22R/C30 hopane ratios are 1.13 and 0.22 respectively. A-4 has values of 1.03, 0.67, 0.87 and 0.91 from the vitrinite reflectivity parameters 22-25. The A-4 chromatograms are shown in Figure 6.20 and in Appendix B.

A-5

The Ts/(Ts+Tm) ratio of A-5 is found to be 0.61 and the distribution of C27-C29 regular steranes are 30%, 35% and 35% respectively. A-5 has hopane/sterane ratio of 10.82 and gammacerane index of 0.18. The BNH/norhopane, C26/C25 tricyclic terpane and C31 22R/C30 hopane ratios are 0.13, 1.17 and 0.34 respectively. The vitrinite reflectivity value from parameters 22-25 are 1.00, 0.79, 0.78 and 0.76 respectively. Positive identification of β-carotane in the m/z = 558 chromatogram is noticed. The A-5 chromatograms are shown in Figure 6.21 and in Appendix B.

6.2.4 The bitumen extracts from well 6610/7-1

B-1

The Ts/(Ts+Tm) ratio of B-1 is found to be 0.28, the distribution of C27-C29 regular steranes are 36%, 31% and 32% respectively and the hopane/sterane ratio is 1.28. The gammacerane index and BNH/norhopane ratio are 0.10 and 0.37 respectively. B-1 has a C26/C25 tricyclic terpane ratio of 0.64 and a C31 22R/C30 hopane ratio of 0.55 which is the second highest value from the entire sample set. The vitrinite reflectivity value from parameters 22-25 are 1.04, 0.80, 0.92 and 0.70 respectively. β-carotane is detected in the m/z = 558 chromatogram and TNH and C30 steranes are detected in the m/z = 177 and 218 chromatograms respectively. The B-1 chromatograms are shown in Figure 6.22 and in Appendix B.

B-2

B-2 has a Ts/(Ts+Tm) ratio of 0.26 and a configuration of C27-C29 regular steranes which are 37%, 31% and 32% respectively, the hopane/sterane ratio is 1.29 and the gammacerane index is 0.11. The BNH/norhopane, C26/C25 tricyclic terpane and C31 22R/C30 hopane ratios are 0.39, 0.70 and 0.51 respectively. B-2 has values of 1.05, 0.81, 0.92 and 0.70 from the vitrinite reflectivity parameters 22-25. β-carotane is positively identified in the m/z = 558 chromatogram, TNH is identified in the m/z = 177 chromatogram and C30 steranes are easily detected in the m/z = 218 chromatogram. The B-2 chromatograms are shown in Figure 6.23 and in Appendix B.

B-3

B-3 has a Ts/(Ts+Tm) ratio of 0.27 and the distribution of C27-C29 regular steranes are 38%, 31% and 31% respectively. The hopane/sterane ratio, gammacerane index and BNH/norhopane ratio are 1.17, 0.13 and 0.39 respectively. B-3 has a C26/C25 tricyclic terpane ratio of 0.77 and a C31 22R/C30 hopane ratio of 0.56 which is the highest value from the entire sample set. The vitrinite reflectivity value from parameters 22-25 are 0.98, 0.85, 0.87 and 0.65 respectively. β-carotane is positively identified in the m/z = 558 chromatogram and TNH and C30 steranes are detected in the m/z = 177 and 218 chromatograms respectively. The B-3 chromatograms are shown in Figure 6.24 and in Appendix B.

B-4

The Ts/(Ts+Tm) ratio of B-4 is found to be 0.34, the distribution of C27-C29 regular steranes are 28%, 26% and 46% respectively, the hopane/sterane ratio is 2.97 and the gammacerane index is 0.22. The BNH/norhopane ratio is calculated to be 0.15 and the C26/C25 tricyclic terpane and C31 22R/C30 hopane ratios are 0.29 and 0.31 respectively. B-4 has values of 0.92, 0.65, 0.82 and 0.72 from the vitrinite reflectivity parameters 22-25. From the m/z = 177 chromatogram, TNH is positively identified as the most intense peak, and C30 steranes although having low peak intensities are detectable in the m/z = 218 chromatogram. The B-4 chromatograms are shown in Figure 6.25 and in Appendix B.

B-5

The Ts/(Ts+Tm) ratio B-5 is found to be 0.33, the C27-C29 regular sterane configurations are 26%, 26% and 48% respectively, the hopane/sterane ratio is 4.84 and the gammacerane index is 0.25. B-3 has BNH/norhopane ratio of 0.15, C26/C25 tricyclic terpane ratio of 0.16 and a C31 22R/C30 hopane ratio of 0.40. The vitrinite reflectivity value from parameters 22-25 are 0.94, 0.70, 0.86 and 0.92 respectively. THN is present as an intense peak in the m/z = 177 chromatogram and the C30 steranes are positively identified in the m/z = 218 chromatogram. The B-5 chromatograms are shown in Figure 6.26 and in Appendix B.

B-6

B-6 has a Ts/(Ts+Tm) ratio of 0.31 and a C27-C29 regular steranes distribution of 22%, 26% and 51% respectively. The hopane/sterane ratio is 6.14 and the gammacerane index is 0.29. The BNH/norhopane, C26/C25 tricyclic terpane and C31 22R/C30 hopane ratios are 0.15, 0.13 and 0.36 respectively. B-6 has the lowest C26/C25 tricyclic terpane ratio of the entire sample set. The vitrinite reflectivity value from parameters 22-25 are 0.96, 0.69, 0.87 and 0.95 respectively. TNH is easily detectable in m/z = 177, and C30 steranes can be observed in the m/z = 218 chromatogram. The B-6 chromatograms are shown in Figure 6.27 and in Appendix B.

B-7

The Ts/(Ts+Tm) ratio of B-7 is 0.21, the distribution of C27-C29 regular steranes are 23%, 29% and 48% respectively, the hopane/sterane ratio is 7.34 and the gammacerane index is 0.26. B-7 has BNH/norhopane ratio of 0.15, C26/C25 tricyclic terpane ratio of 0.15 and a C31 22R/C30 hopane

ratio of 0.32. The C26/C25 tricyclic terpane ratio is the second lowest from the sample set. B-7 has values of 0.86, 0.66, 0.77 and 0.76 from the vitrinite reflectivity parameters 22-25. From the m/z = 177 chromatogram, TNH is positively identified as the most intense peak, and C30 steranes are detected in the m/z = 218 chromatogram. The B-7 chromatograms are shown in Figure 6.28 and in Appendix B.

6.2.5 The bitumen extracts from well 6609/5-1

C-1

The Ts/(Ts+Tm) ratio of C-1 is found to be 0.58 and the C27-C29 regular sterane configurations are 33%, 33% and 34% respectively, the hopane/sterane ratio is 7.34 and the gammacerane index is 0.13. C-1 has BNH/norhopane ratio of 0.20, C26/C25 tricyclic terpane ratio of 0.95 and a C31 22R/C30 hopane ratio of 0.22. The vitrinite reflectivity value from parameters 22-25 are 1.05, 0.69, 0.99 and 0.78 respectively. β-carotane is easily detected in the m/z = 558 chromatogram, and also possibly in the m/z = 125 chromatogram. The C-1 chromatograms are shown in Figure 6.29 and in Appendix B.

C-2

C-2 has a Ts/(Ts+Tm) ratio of 0.53 and a distribution of C27-C29 regular steranes which are 35%, 32% and 33% respectively. The hopane/sterane ratio and gammacerane index are 2.45 and 0.18 respectively. The BNH/norhopane, C26/C25 tricyclic terpane and C31 22R/C30 hopane ratios are 0.24, 0.39 and 0.31 respectively. C-2 has values of 0.84, 0.62, 0.64 and 1.01 from the vitrinite reflectivity parameters 22-25. Positive identification of β-carotane is seen in the m/z = 558 chromatogram and also possibly the m/z = 125 chromatogram. TNH is positively identified in the m/z = 177 chromatogram, and the C30 steranes are easily seen in the m/z = 218 chromatogram. The C-2 chromatograms are shown in Figure 6.30 and in Appendix B.

Table 6.2: Values of the GC-MS parameters 1-14 for all the samples. ND = No Data. The parameters are listed in Table 5.8 and described in section 5.2.6.

Sample	1	2	3	4	5	6	7	8	9	10	11	12	13	14
O-1	0.78	0.93	0.56	0.77	0.49	0.25	9.22	0.19	1.74	0.59	0.64	0.28	15	43
O-2	0.74	0.90	0.56	0.78	0.46	0.19	8.80	0.21	1.88	0.61	0.63	0.29	15	45
O-3	0.75	0.68	0.52	0.85	0.41	0.16	6.64	0.27	ND	ND	ND	ND	0	0
O-4	0.58	0.62	0.53	0.88	0.29	0.09	2.40	0.20	3.43	0.69	0.70	0.50	43	22
O-5	0.82	0.79	0.53	0.78	0.56	0.21	14.06	0.78	0.79	0.63	0.47	0.28	14	51
O-6	0.68	0.71	0.51	0.84	0.34	0.13	3.62	0.20	5.46	ND	ND	0.49	42	0
O-7	0.82	0.85	0.50	0.72	0.44	0.21	17.82	0.54	2.51	ND	ND	0.36	4	56
O-20	0.88	0.84	0.56	0.79	0.50	0.15	12.50	0.33	13.65	ND	ND	0.49	35	0
O-21	0.86	0.80	0.56	0.83	0.40	0.10	15.12	0.36	3.04	0.63	0.53	0.18	14	49
NSO-1	0.55	0.56	0.54	0.86	0.36	0.35	0.61	0.11	2	0.49	0.43	0.34	33	32
Embla	0.90	0.86	0.47	0.66	0.76	0.30	7,1	0.85	0.33	0.58	0.48	0.49	38	28
Beatrice	0.58	0.72	0.59	0.87	0.34	0.08	0.68	0.10	5.7	0.58	0.45	0.25	21	37
Judy	0.77	0.76	0.61	0.90	0.45	0.09	0.65	0.09	2.02	0.59	0.45	0.37	37	31
A-1	0.52	0.45	0.51	0.86	0.25	0.07	0.82	0.11	2.07	0.44	0.24	0.16	36	26
A-2	0.60	0.78	0.59	0.88	0.41	0.11	0.22	0.07	1.55	0.57	0.41	0.29	25	33
A-3	0.59	0.80	0.58	0.89	0.42	0.11	0.20	0.07	17.58	0.59	0.41	0.28	26	33
A-4	0.55	0.61	0.58	0.87	0.38	0.13	0.58	0.14	5.69	0.50	0.34	0.28	29	26
A-5	0.61	0.76	0.55	0.84	0.44	0.13	0.43	0.17	10.82	0.53	0.46	0.35	30	35
B-1	0.28	0.50	0.57	0.90	0.22	0.37	0.40	0.06	1.28	0.51	0.43	0.23	36	31
B-2	0.26	0.48	0.58	0.90	0.23	0.39	0.35	0.06	1.29	0.49	0.44	0.23	37	31
B-3	0.27	0.45	0.55	0.87	0.25	0.39	0.45	0.09	1.17	0.49	0.44	0.25	38	31
B-4	0.34	0.60	0.59	0.84	0.26	0.15	0.44	0.13	2.97	0.51	0.42	0.30	28	26
B-5	0.33	0.48	0.61	0.81	0.24	0.15	0.45	0.08	4.84	0.44	0.40	0.22	26	26
B-6	0.31	0.42	0.62	0.81	0.23	0.15	0.29	0.04	6.14	0.42	0.41	0.18	22	26
B-7	0.21	0.36	0.61	0.82	0.19	0.15	0.24	0.06	7.34	0.39	0.39	0.15	23	29
C-1	0.58	0.67	0.60	0.87	0.41	0.20	1,01	0.08	2.26	0.49	0.40	0.44	33	33
C-2	0.53	0.54	0.58	0.84	0.42	0.24	0.78	0.12	2.45	0.49	0.35	0.44	35	32

Table 6.3: Values of the GC-MS parameters 15-27 for all the samples. ND = No Data. The parameters are listed in Table 5.8 and described in section 5.2.6.

Sample	15	16	17	18	19	20	21	22	23	24	25	26	27
O-1	42	0.67	0.82	0.39	0.25	0.16	3.14	0.50	0.55	0.18	0.74	2.53	0.05
O-2	40	0.59	0.59	0.25	0.22	0.14	ND	0.28	0.53	0.14	ND	3.37	0.02
O-3	100	1	ND	0.24	0.24	0.17	ND	0.26	0.55	0.21	ND	2.94	0.04
O-4	35	1	ND	0.32	0.26	0.19	ND	0.40	0.56	0.26	ND	4.4	0.03
O-5	36	0.66	0.64	0.33	0.27	0.17	5.40	0.42	0.56	0.21	0.90	3.87	0.03
O-6	58	0.42	0.66	0.20	0.21	0.13	1.94	0.18	0.53	0.13	0.65	2.33	0.06
O-7	40	0.47	0.63	0.57	0.48	0.33	ND	0.68	0.69	0.57	ND	ND	ND
O-20	65	ND	ND	0.32	0.28	0.16	ND	0.40	0.57	0.20	ND	3.89	0.02
O-21	37	0.83	0.70	0.33	0.20	0.13	2.88	0.43	0.52	0.12	0.72	2.69	0.04
NSO-1	35	0.42	0.63	0.88	0.71	0.43	2.55	0.89	0.83	0.81	0.70	1.56	0.22
Embla	34	0.88	0.22	1.44	1.14	0.55	19.63	1.12	1.08	1.06	1.94	2.28	0.14
Beatrice	43	0.52	0.70	0.86	0.55	0.41	2.74	0.88	0.73	0.76	0.71	3.86	0.08
Judy	32	0.70	0.65	0.98	0.76	0.44	0.42	0.94	0.86	0.83	0.82	2.23	0.13
A-1	39	0.45	0.27	1.34	0.58	0.49	4.25	1.09	0.75	0.94	0.82	2	0.15
A-2	42	0.18	0.69	1.11	0.57	0.44	3.22	1	0.74	0.81	0.74	3.9	0.08
A-3	41	0.14	0.68	0.95	0.52	0.40	3.75	0.93	0.71	0.74	0.78	4.33	0.08
A-4	45	0.47	0.62	1.19	0.45	0.46	5.52	1.03	0.67	0.87	0.91	2.45	0.12
A-5	35	0.27	0.53	1,1	0.65	0.42	3.36	1	0.79	0.78	0.76	5.54	0.05
B-1	32	0.16	0.32	1.21	0.67	0.48	2.65	1.04	0.80	0.92	0.70	2.7	0.11
B-2	32	0.16	0.34	1.24	0.69	0.48	2.58	1.05	0.81	0.92	0.70	2.5	0.12
B-3	31	0.16	0.36	1.07	0.75	0.46	1.86	0.98	0.85	0.87	0.65	5.03	0.08
B-4	46	0.37	0.67	0.94	0.41	0.44	2.84	0.92	0.65	0.82	0.72	3.03	0.09
B-5	48	0.52	0.41	0.98	0.50	0.46	5.56	0.94	0.7	0.86	0.92	3.82	0.09
B-6	51	0.45	0.47	1.01	0.49	0.46	6.04	0.96	0.69	0.87	0.95	2.72	0.10
B-7	48	0.35	0.61	0.83	0.43	0.42	3.43	0.86	0.66	0.77	0.76	8.5	0.05
C-1	34	0.23	0.63	1.23	0.49	0.51	3.72	1.05	0.69	0.99	0.78	2.09	0.18
C-2	33	0.09	0.62	0.80	0.31	0.36	6.83	0.84	0.62	0.64	1.01	0.92	0.27

Table 6.4: Table showing the other selected parameters from GC-MS. The parameters are described in section 5.2.7.

Sample	Gammacerane Index	C26/C25 tricyclic terpane	C31 22R/C30 hopane	BNH/C30 hopane
O-1	1	1.47	0.19	0.14
O-2	0.91	1.33	0.18	0.11
O-3	0.43	1.52	0.22	0.11
O-4	0.26	0.82	0.21	0.05
O-5	2.57	1.15	0.22	0.16
O-6	0.36	1.13	0.23	0.08
O-7	1.33	1.35	0.21	0.14
O-20	1.43	1.8	0.17	0.1
O-21	1.25	1.8	0.12	0.06
NSO-1	0.14	0.81	0.37	0.24
Embla	0.55	0.81	0.51	0.21
Beatrice	0.33	1.23	0.23	0.05
Judy	0.14	1.09	0.30	0.04
A-1	0.21	0.64	0.35	0.05
A-2	0.13	2.5	0.26	0.06
A-3	0.16	1.5	0.24	0.06
A-4	0.23	1.13	0.22	0.08
A-5	0.18	1.17	0.34	0.09
B-1	0.10	0.64	0.55	0.32
B-2	0.11	0.70	0.51	0.32
B-3	0.13	0.77	0.56	0.34
B-4	0.22	0.29	0.31	0.11
B-5	0.25	0.16	0.40	0.09
B-6	0.29	0.13	0.36	0.1
B-7	0.26	0.15	0.32	0.11
C-1	0.13	0.95	0.22	0.12
C-2	0.18	0.39	0.31	0.15

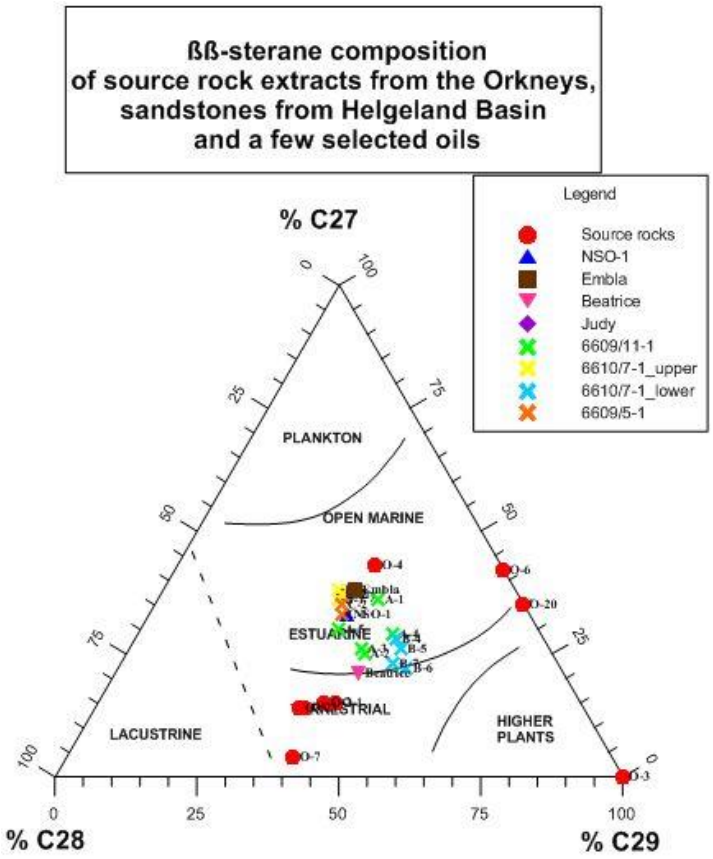

Figure 6.1: Ternary diagram showing the relative distribution of C27-C29 steranes and the relation to different types of facies.

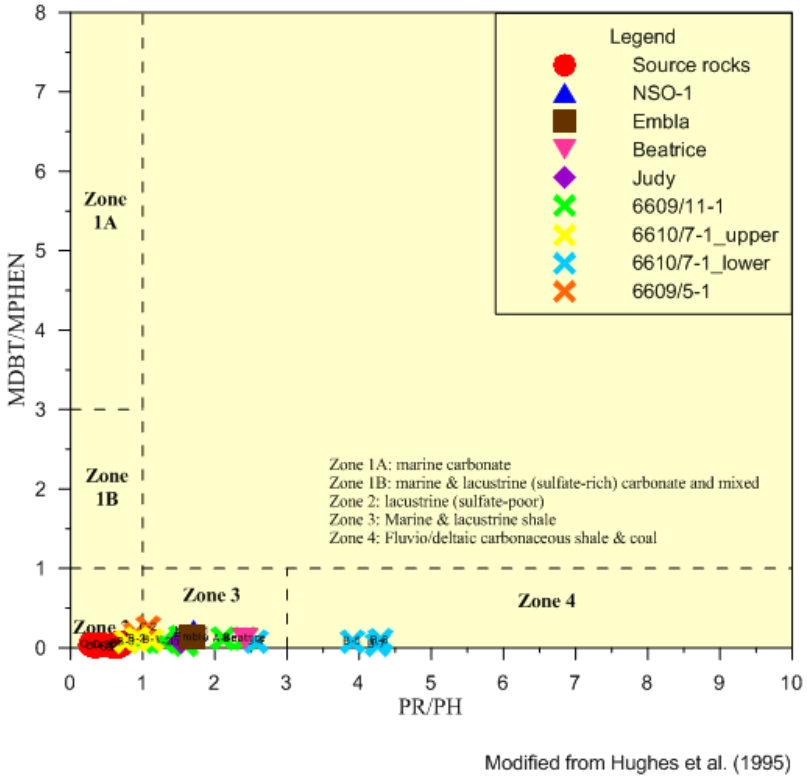

Figure 6.2: Figure showing the MDBT/MPHEN ratio plotted against the Pr/Ph ratio and relative to different types of facies.

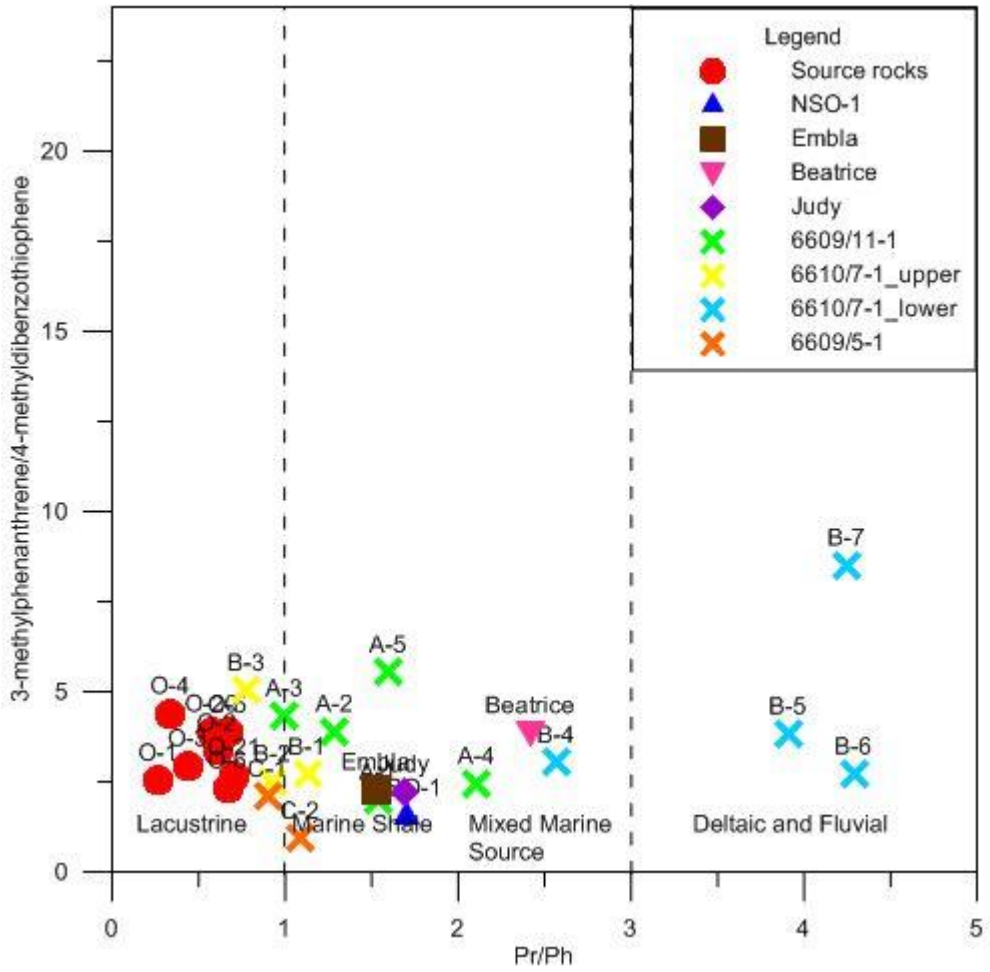

Figure 6.3: Plot of 3-methylphenanthrene/4-methuyldibenzothiophene (perameter 26) versus the Pr/Ph ratio and the relation to different types of facies is shown. The advantage of this plot over the Hughes-plot (Figure 6.2) is that it is easier to visually differentiate between the different samples in the figure.

6.3 TOC and Rock-Eval results for source rock bitumen samples

TOC and Rock-Eval analysis (see section 4.6) provides information about source rock quality and maturity and is thus important when evaluating source rock potential and is also useful for determining if the petroleum generation has been initiated. The results from TOC and Rock-eval analysis are listed in Table 6.5, and parameter descriptions are presented in section 5.3.

O-1

Sample O-1 shows S1 and S2 values of 0.46 mg/g and 6.35 mg/g respectively, it reaches T_{max} at 438°C and has a TOC of 1.75wt.% and HI of 363 mg HC/g TOC.

O-2

The S1 and S2 values given for O-2 are 0.48 mg/g and 5.51 mg/g respectively. O-2 reaches T_{max} at 437°C and has a TOC of 1.48wt.% and HI of 372 mg HC/g TOC.

O-3

O-3 has S1 and S2 values of 0.00 mg/g and 0.29 mg/g respectively. O-3 reaches T_{max} at 429°C and has TOC and HI values of 0.33wt.% and 88 mg HC/g TOC. It has to be noted that O-3 shows the lowest S1, S2, TOC and HI, while the OI value is the highest of the source rock bitumen samples from the Orkneys (207 mg CO_2/g TOC)

O-4

Sample O-4 shows S1 and S2 values of 0.04 mg/g and 3.24 mg/g respectively, it reaches T_{max} at 426°C and has a TOC of 1.48wt.% and HI of 219 mg HC/g TOC.

O-5

The S1 and S2 values are 0.34 mg/g and 6.10 mg/g respectively for sample O-5 and T_{max} is reached at 442°C. The TOC is 1.95wt.% and HI is 313 mg HC/g TOC.

O-6

Sample O-6 shows S1 and S2 values of 0.03 mg/g and 0.89 mg/g respectively. O-6 reaches T_{max} at 425°C and has TOC of 0.36wt.% and HI of 245 mg HC/g TOC.

O-7

O-7 has S1 and S2 values of 0.17 mg/g and 1.51 mg/g respectively and it reaches T_{max} at 430°C. The TOC and HI is 0.74wt.% and 205 mg HC/g TOC respectively.

O-20

Sample O-20 shows S1 and S2 values of 0.59 mg/g and 8.17 mg/g respectively, it reaches T_{max} at 443°C, has a TOC of 2.46wt.% and HI of 332 mg HC/g TOC.

O-21

The S1 and S2 values given for O-21 are 0.43 mg/g and 11.08 mg/g respectively. The T_{max} temperature is reached at 442°C. The TOC and HI values, which are both the highest of the samples, are 2.79wt.% and 397 mg HC/g TOC respectively.

Table 6.5: Table showing the results from TOC and Rock-eval analysis for all the source rock bitumen extracts from the Orkneys representing Middle Devonian lacustrine lake deposits.

Sample	S1	S2	S3	T_{max}(°C)	S1+S2	S1/(S1+S2)	S2/S3	HI	OI	TOC(%)
O-1	0.46	6.35	0.56	438	6.81	0.07	11.34	363	32	1.75
O-2	0.48	5.51	0.22	437	5.99	0.08	25.05	372	15	1.48
O-3	0.00	0.29	0.68	429	0.29	0.00	0.43	88	207	0.33
O-4	0.04	3.24	0.34	426	3.28	0.01	9.53	219	23	1.48
O-5	0.34	6.10	0.19	442	6.44	0.05	32.11	313	10	1.95
O-6	0.03	0.89	0.42	425	0.92	0.03	2.12	245	116	0.36
O-7	0.17	1.51	1.00	430	1.68	0.10	1.51	205	136	0.74
O-20	0.59	8.17	0.42	443	8.76	0.07	19.45	332	17	2.46
O-21	0.43	11.08	0.27	442	11.51	0.04	41.03	397	10	2.79

6.4 δC13 isotope analysis results

Four of the bitumen extracts from the Orkneys representing the Middle Devonian lacustrine source rocks, were selected for δC13 isotope analysis (see section 4.7 for analysis description and section 5.4 for interpretation parameter description) and the results are listed in Table 6.6 together with the values for the bitumen extracts from sandstone in well 6609/7-1 at depth 2561m (Karlsen et al. 1995) and from well 6610/7-1 (Schou et al. 1983). The Kimmeridge equivalents representing Late Jurassic age from well 6610/7-1 (Schou et al. 1983) and the Orcadian Basin (Peters et al. 1989) are included as references for a marine signature.

The Late Jurassic Kimmeridge source rock equivalent encountered in well 6610/7-1 has δ13C isotope values from the saturated fraction (SAT) of -30.3$^{o}/_{oo}$ and the aromatic fraction (ARO) of -29.6$^{o}/_{oo}$. The bitumen from depth 2661.6m (intermediate between depths of B-1 and B-2) has δ13C isotope values of -31.1$^{o}/_{oo}$ and -29.0$^{o}/_{oo}$ for the SAT and ARO fraction respectively, the bitumen from depth 2668.05m (0.45m shallower depth than B-3) has δ13C isotope values in the SAT fraction of -31.3$^{o}/_{oo}$ and ARO fraction of -30.6$^{o}/_{oo}$ and the bitumen from depth 2706m has δ13C isotope values for SAT which is -31.4$^{o}/_{oo}$ and ARO which is -30.5 $^{o}/_{oo}$. No δ13C data is available from the lower section in well 6610/7-1 i.e. from 2713.8m to 2715m corresponding to the depth interval from B-4 to B-7. Two samples from well 6610/7-1 representing the Lower Jurassic coals has δ13C isotope values for SAT which is -29.0$^{o}/_{oo}$ and -28.5$^{o}/_{oo}$ and ARO which is -28.0 $^{o}/_{oo}$ and -26.6 $^{o}/_{oo}$

It is noted that the Kimmeridge equivalent from Schou et al. (1983) is isotopically lighter than the Kimmeridge equivalent from Peters et al. (1989) and that the $\delta 13C_{OIL}$ of A-5 (6609/7-1_2561m) is on par with the values of the source rocks.

Table 6.6: Table showing δ13C isotope values for selected samples representing the Middle Devonian Lacustrine source rocks (O-1, O-2, -5 and O-21), the Late Jurassic Kimmeridge equivalent (Kimmeridge_Orcadian and 6610/7-1_Kimmeridge), the Lower Jurassic coals from the Åre Formation (6610/7-1_Lower Jurassic coals 1 and 6610/7-1_Lower Jurassic coals 2) the Beatrice oil and bitumen samples from the Helgeland Basin area (A-5 (6609/7-1_2561m, 6610/7-1_2661.6m, 6610/7-1_2668.05m and 6610/7-1_2706m). *The value is from Karlsen et al. (1995). +The value is from Schou et al. (1983). ^The value is from from Peters et al. (1989).

Sample	$\delta 13C_{OIL}$	$\delta 13C_{SAT}$	$\delta 13C_{ARO}$
O-1	-32.8‰		
O-2	-32.4‰		
O-5	-32.0‰		
O-21	-33.1‰		
A-5 (6609/7-1_2561m)*	-32.2‰		
Kimmeridge_Orcadian^	-28.32‰		
Beatrice oil^	-31.77‰		
6610/7-1_Kimmeridge+		-30.3‰	-29.6‰
6610/7-1_Lower Jurassic coals 1+		-29.0‰	-28.0‰
6610/7-1_Lower Jurassic coals 2+		-28.5‰	-26.6‰
6610/7-1_2661.6m+		-31.1‰	-29.0‰
6610/7-1_2668.05m+		-31.3‰	-30.6‰
6610/7-1_2706m+		-31.4‰	-30.5‰

6.5 Scaled-down GC-FID and GC-MS chromatograms

This section will present scaled down chromatograms from GC-FID and selected m/z chromatograms from GC-MS for every sample. The full scale chromatograms are presented in Appendix A (GC-FID) and Appendix B (GC-MS).

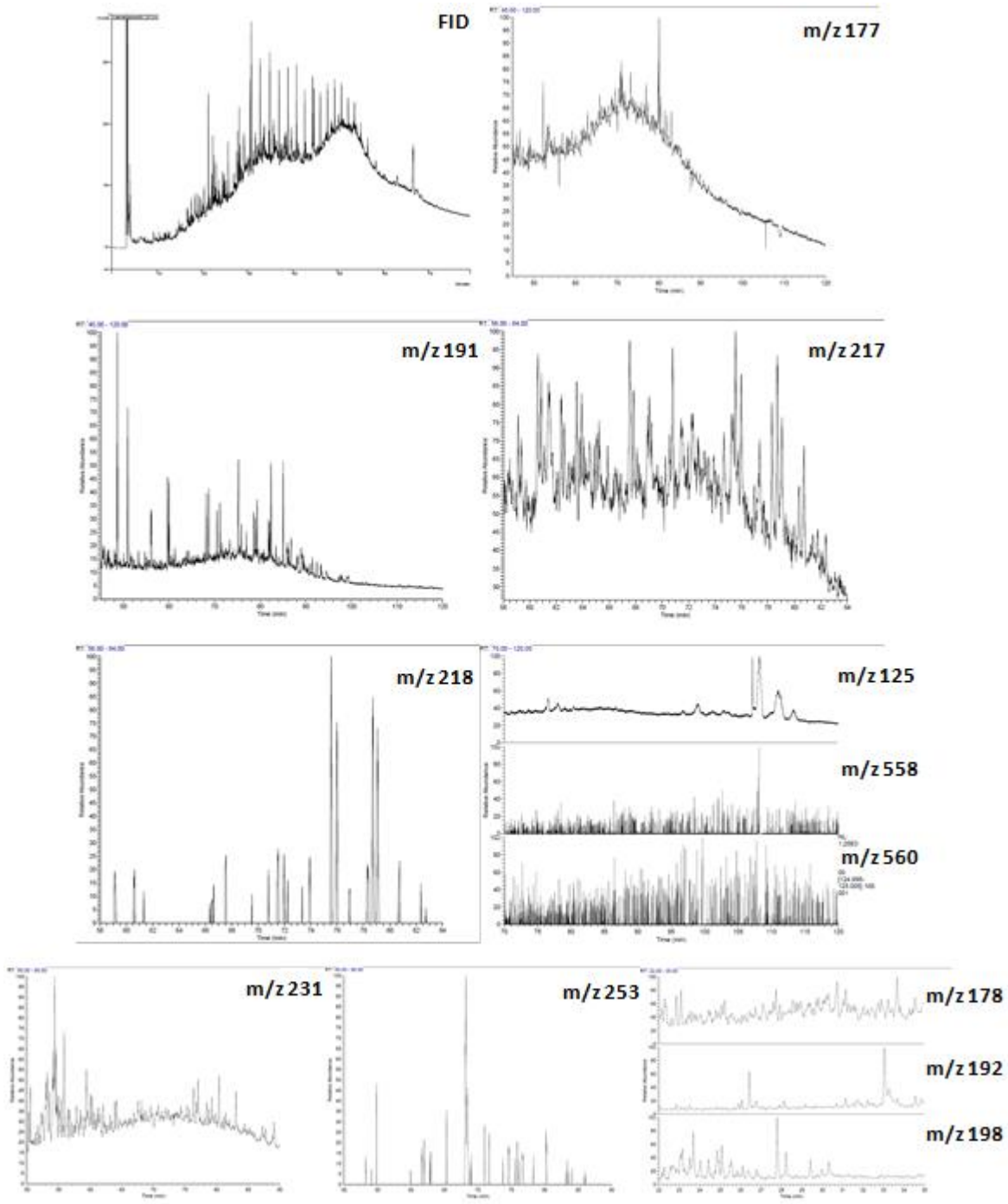

Figure 6.4: Scaled down GC-FID and GC-MS chromatograms for O-1.

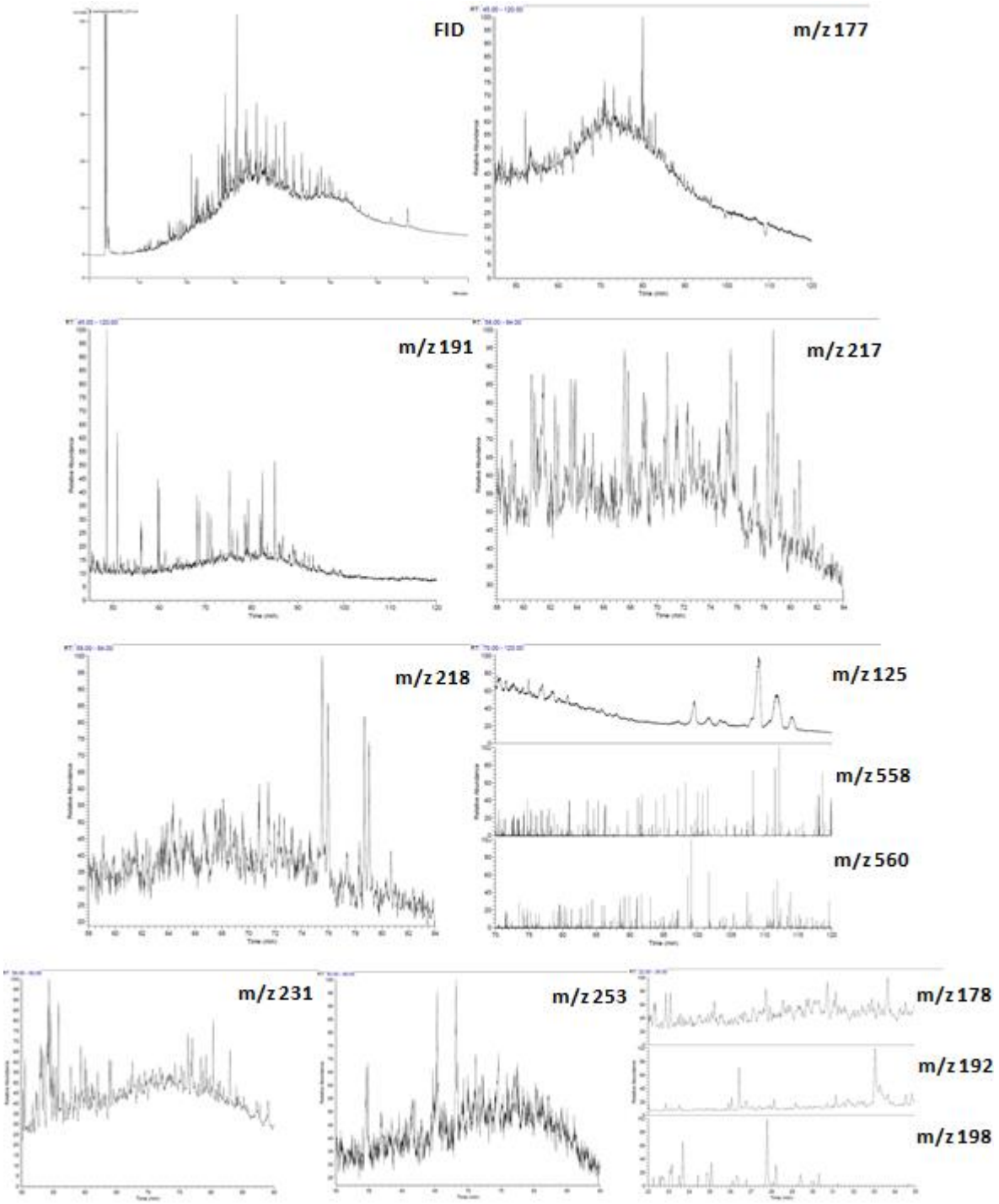

Figure 6.5: Scaled down GC-FID and GC-MS chromatograms for O-2.

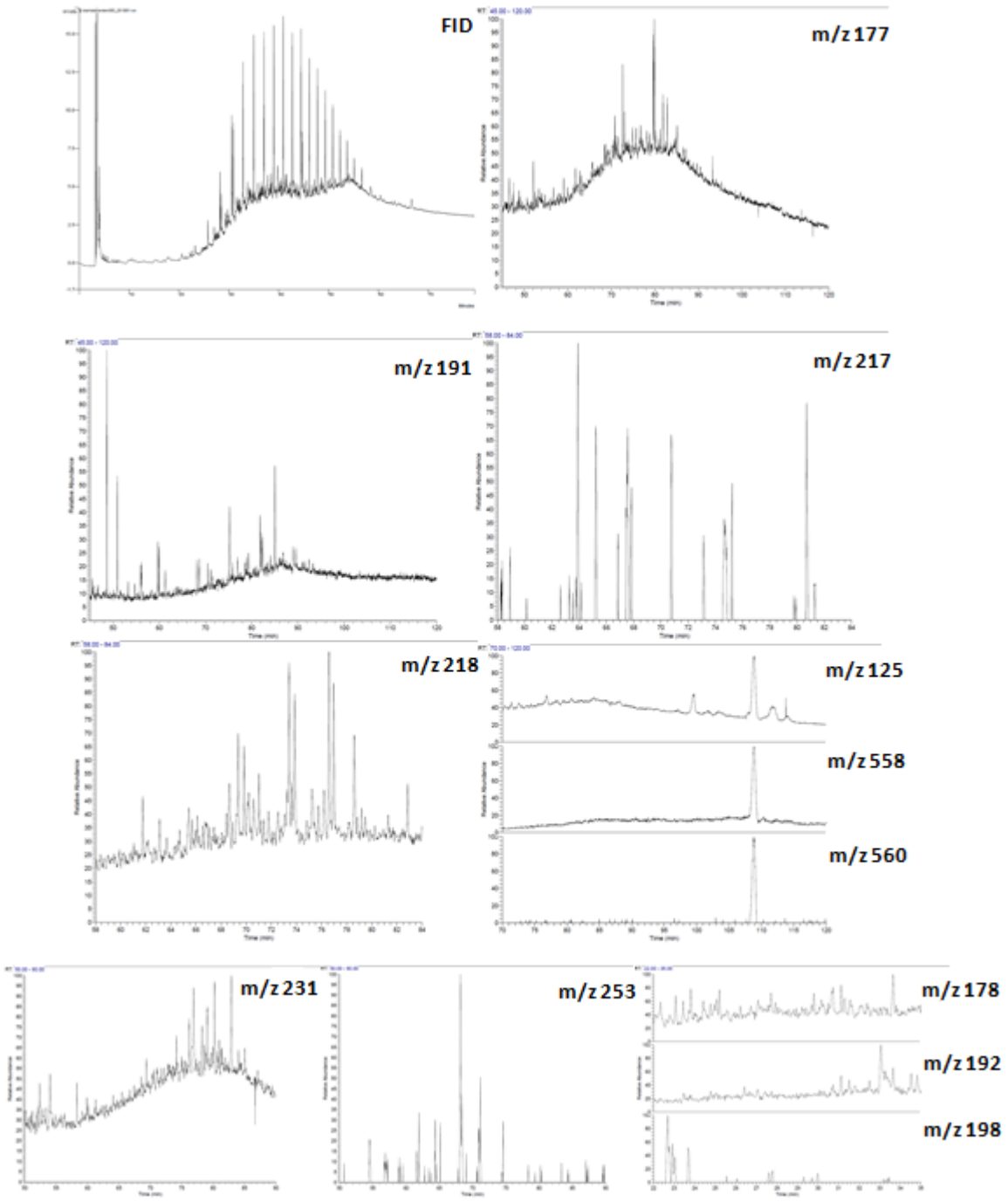

Figure 6.6: Scaled down GC-FID and GC-MS chromatograms for O-3.

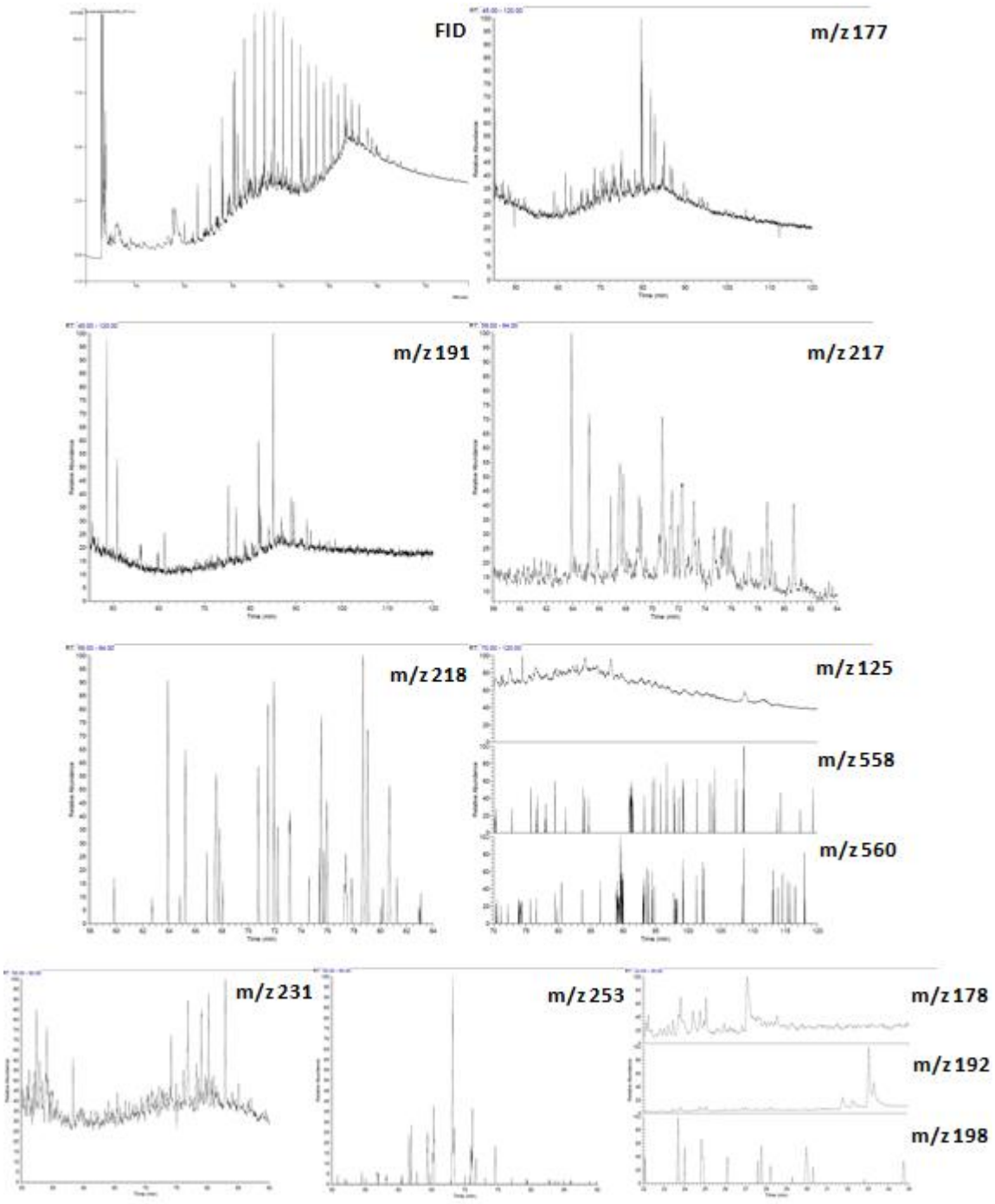

Figure 6.7: Scaled down GC-FID and GC-MS chromatograms for O-4.

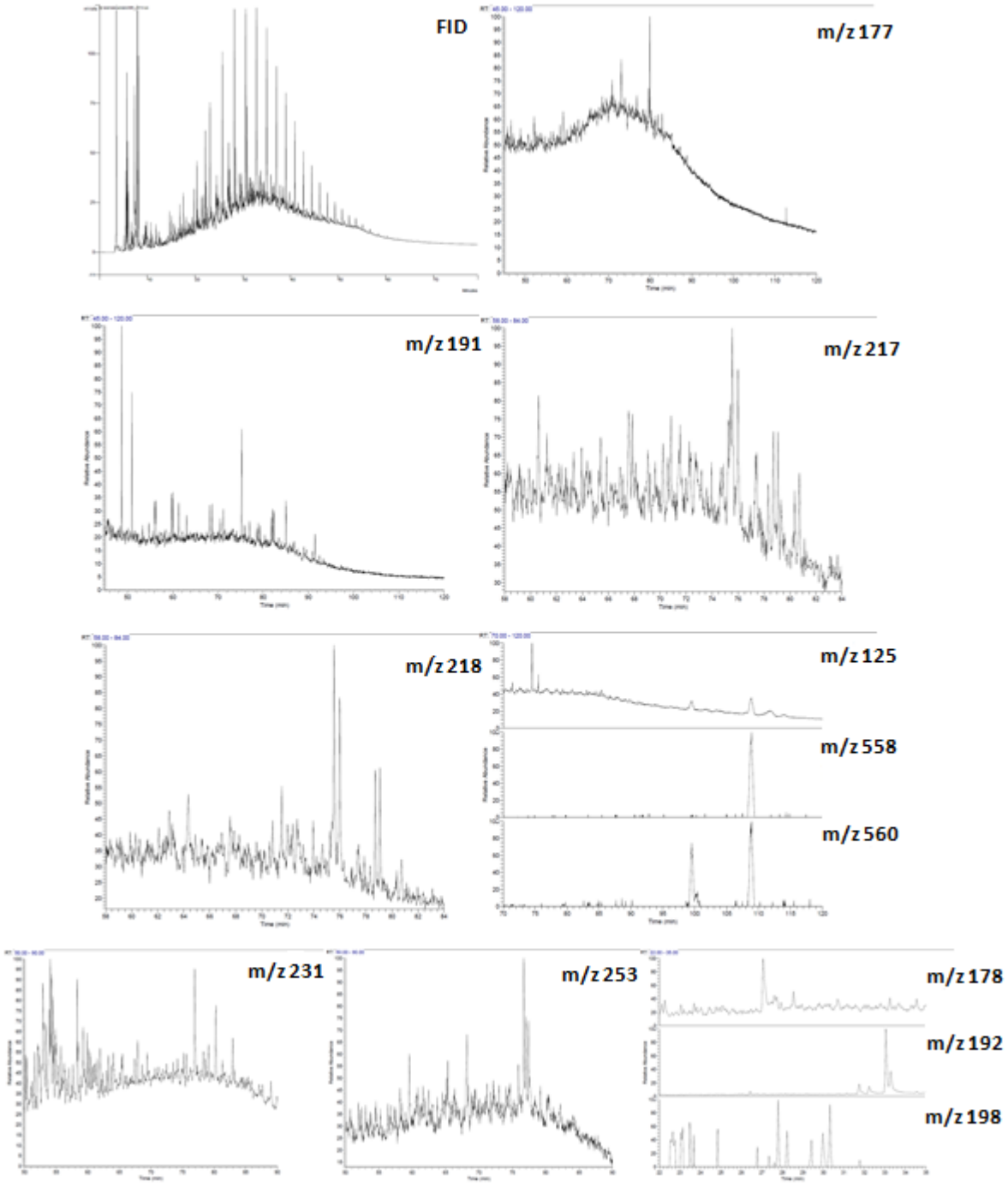

Figure 6.8: Scaled down GC-FID and GC-MS chromatograms for O-5.

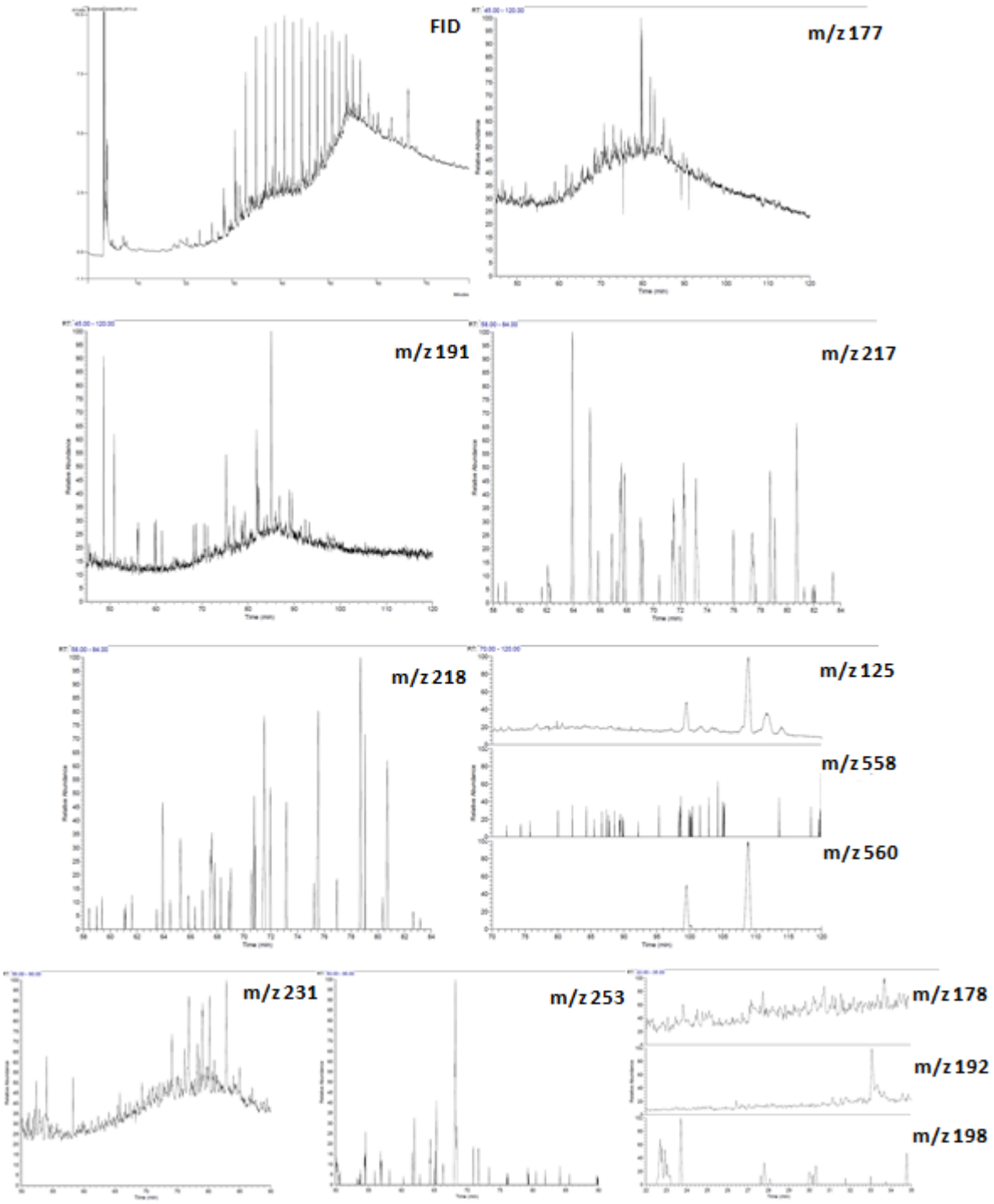

Figure 6.9: Scaled down GC-FID and GC-MS chromatograms for O-6.

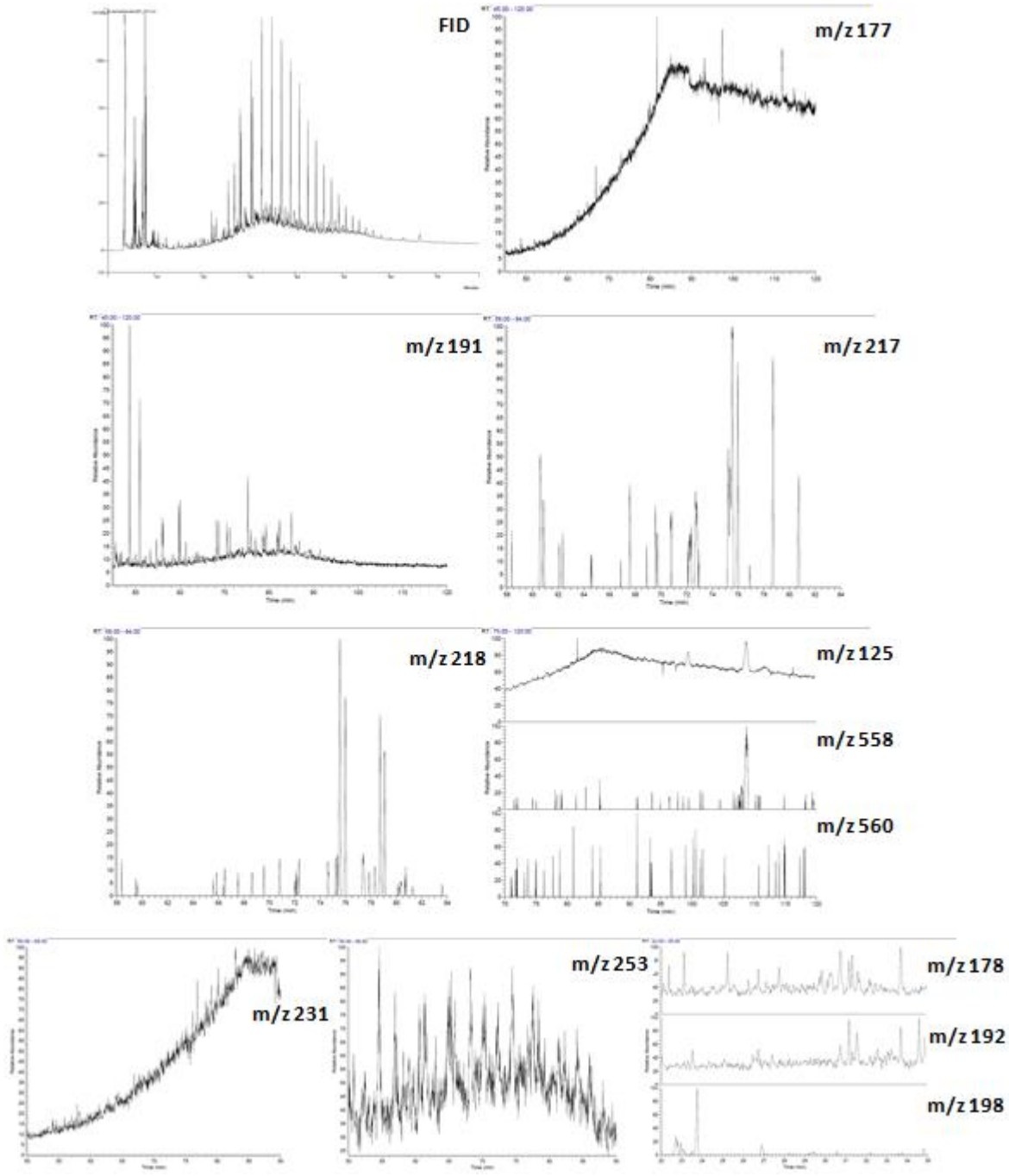

Figure 6.10: Scaled down GC-FID and GC-MS chromatograms for O-7.

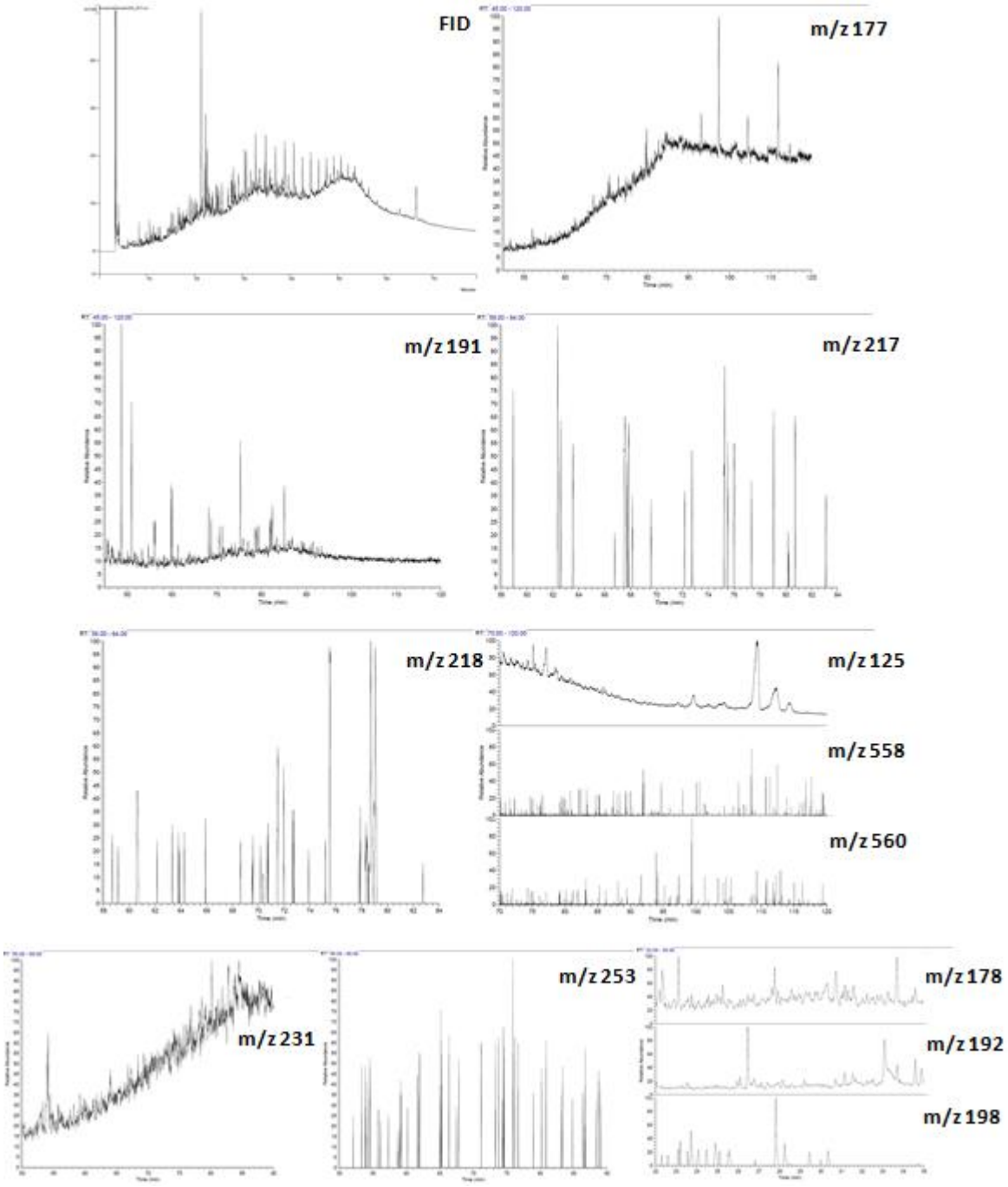

Figure 6.11: Scaled down GC-FID and GC-MS chromatograms for O-20.

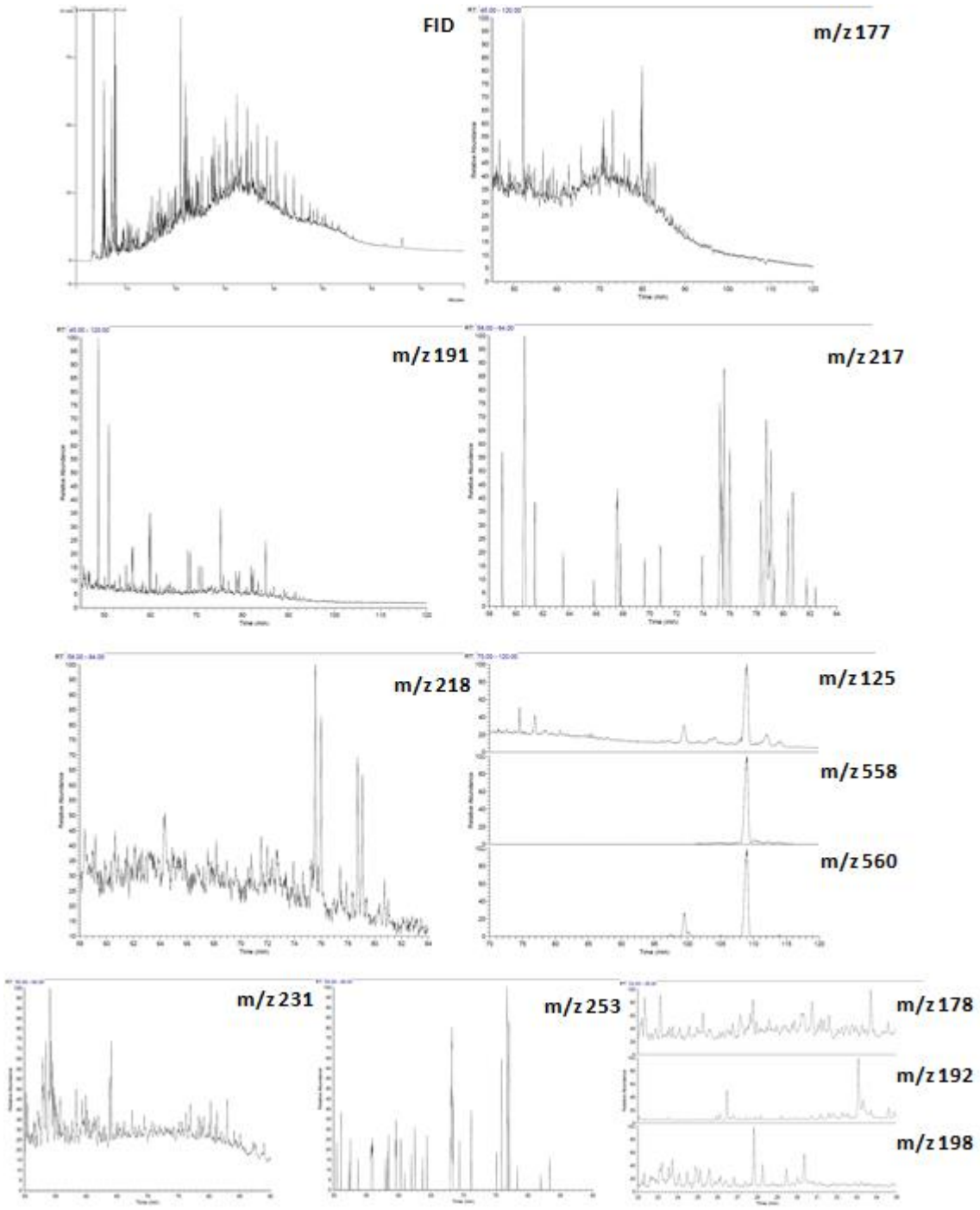

Figure 6.12: Scaled down GC-FID and GC-MS chromatograms for O-21.

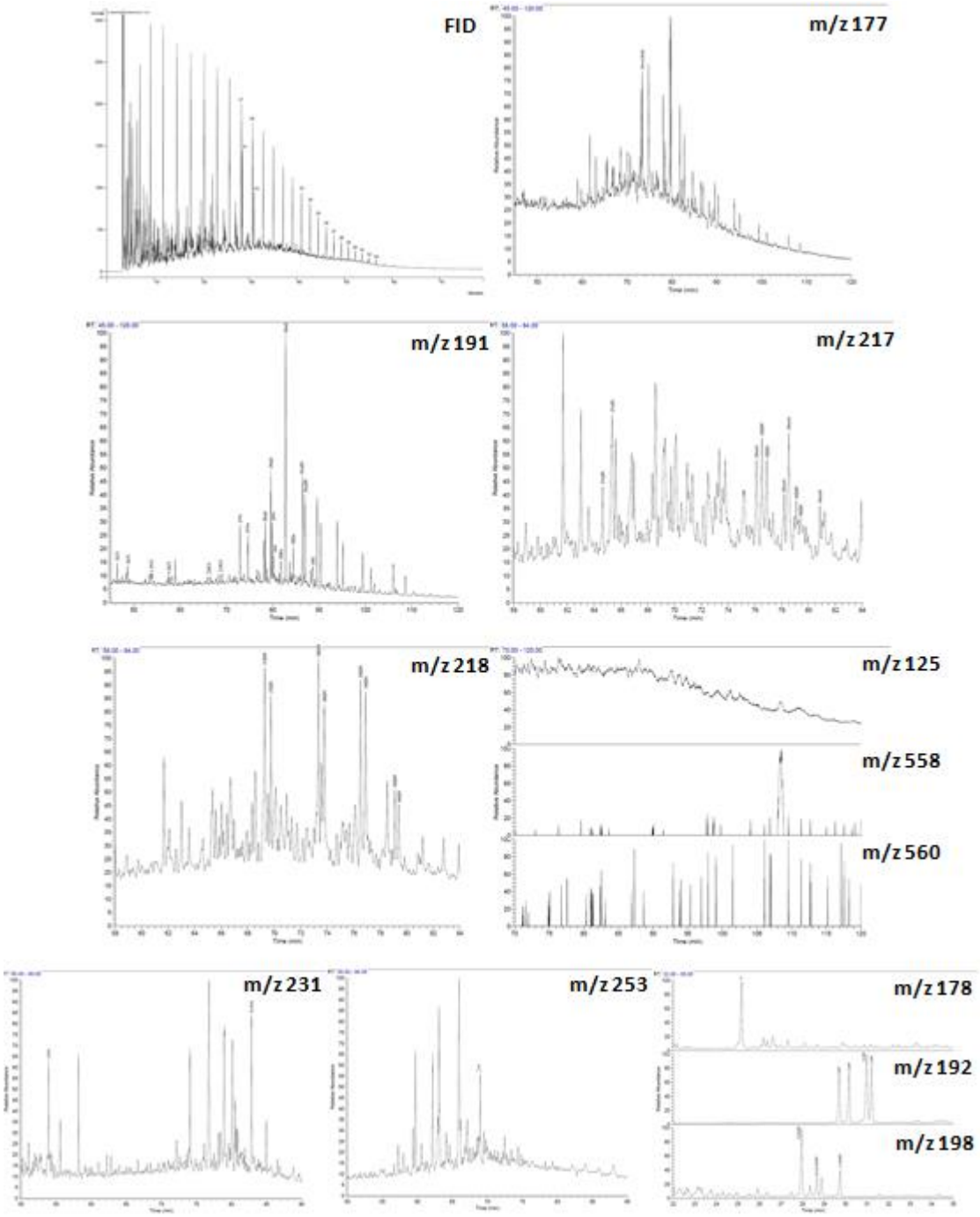

Figure 6.13: Scaled down GC-FID and GC-MS chromatograms for the NSO-1 oil.

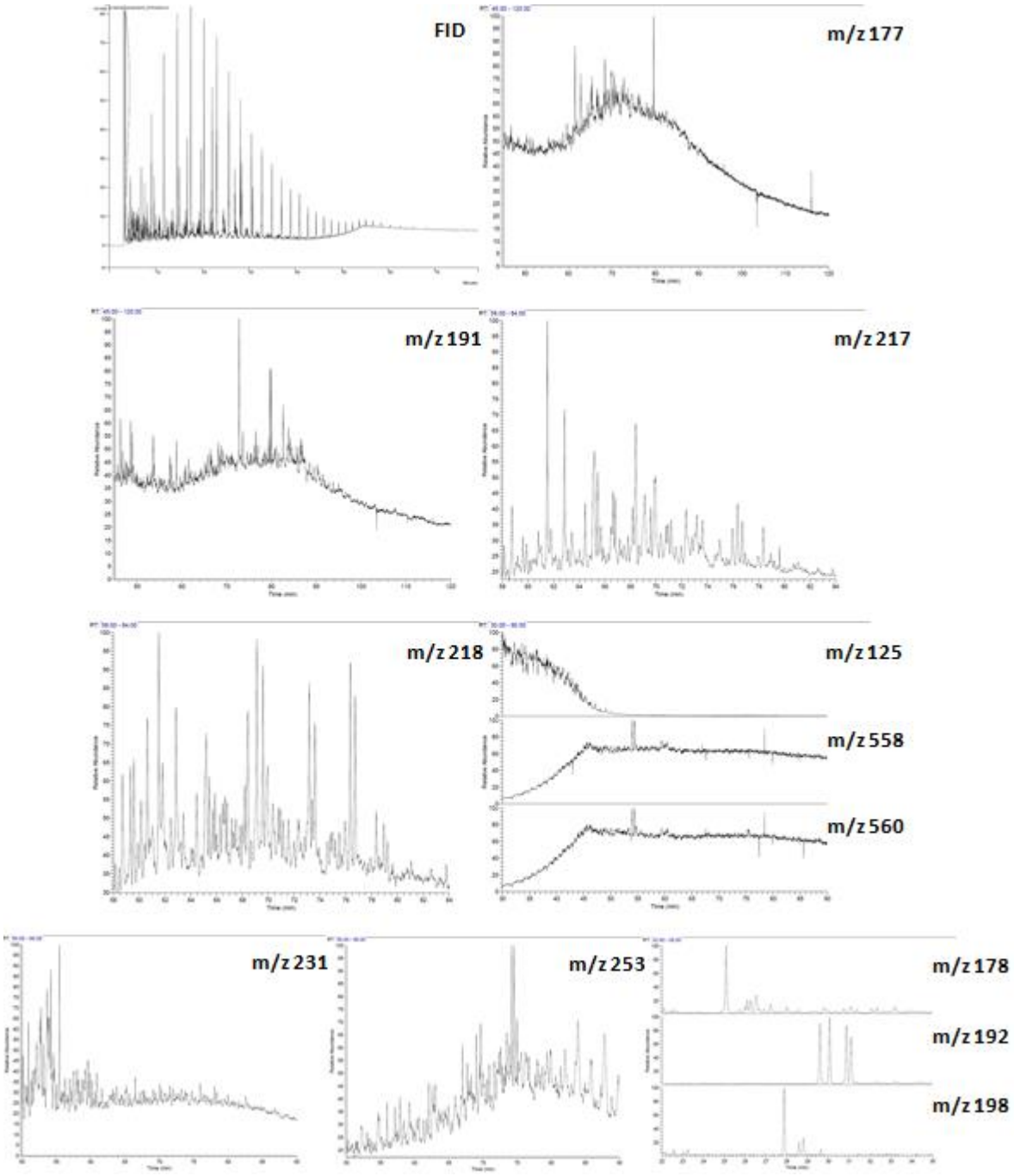

Figure 6.14: Scaled down GC-FID and GC-MS chromatograms for the Embla oil.

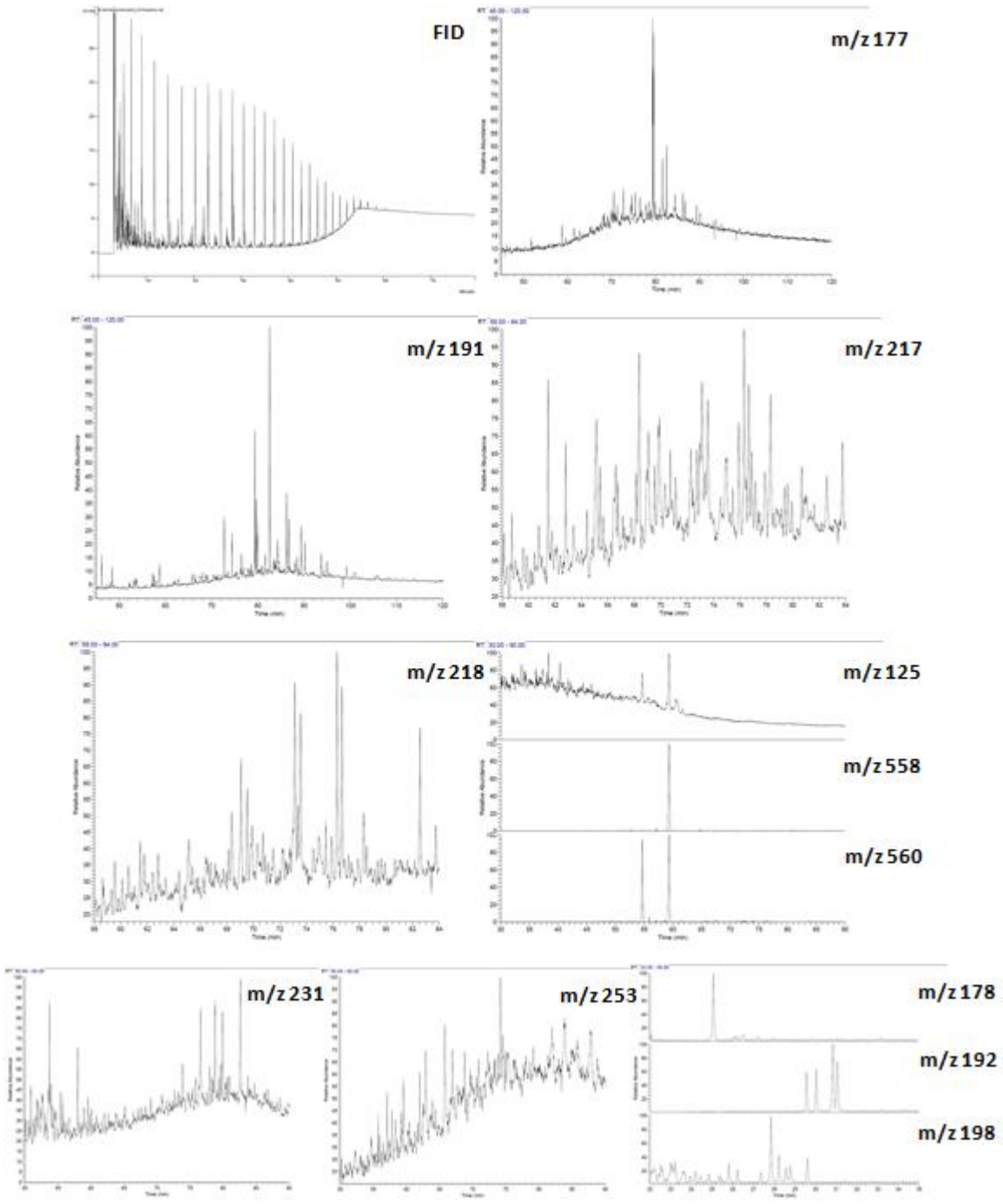

Figure 6.15: Scaled down GC-FID and GC-MS chromatograms for the Beatrice oil.

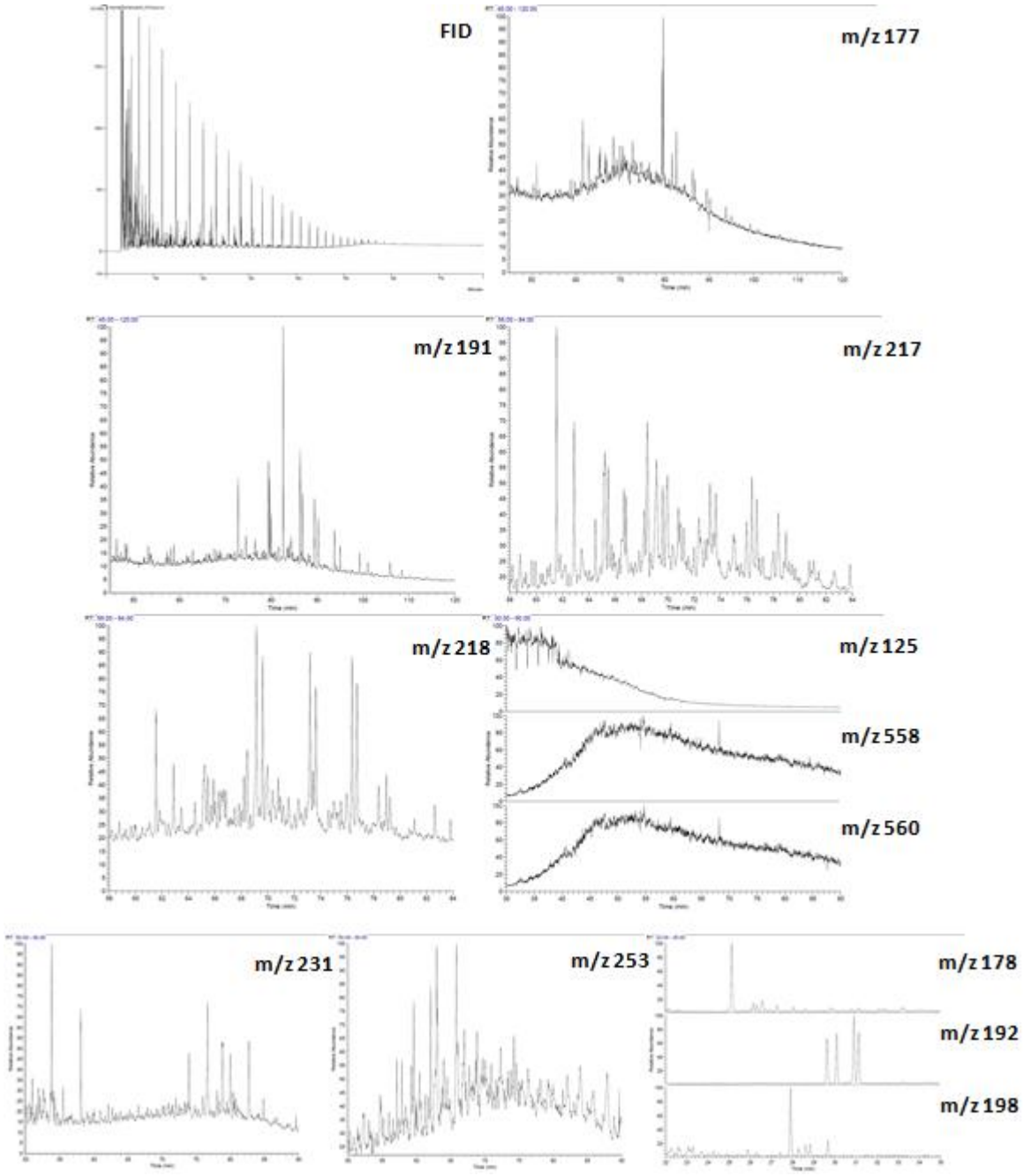

Figure 6.16: Scaled down GC-FID and GC-MS chromatograms for the Judy oil.

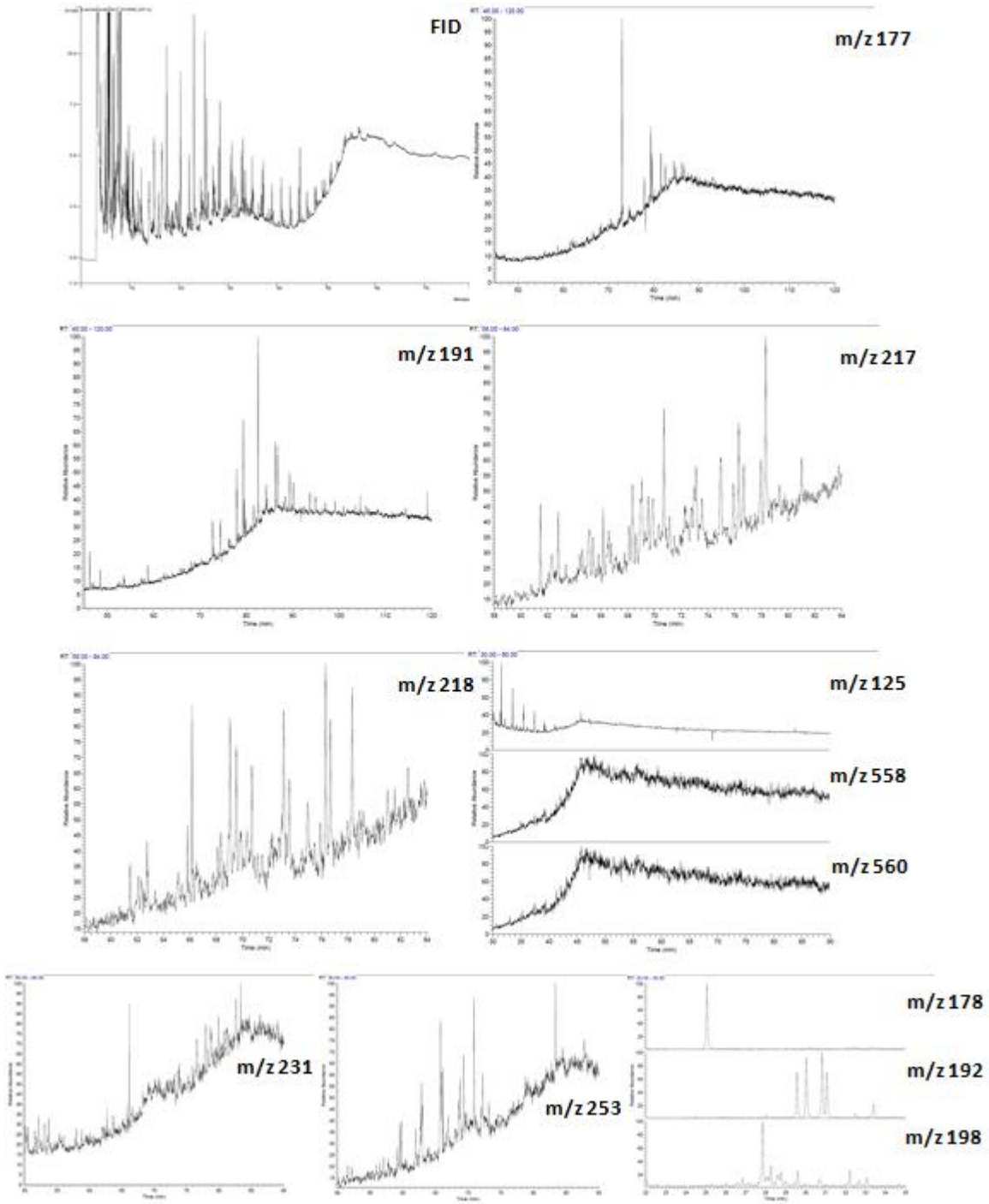

Figure 6.17: Scaled down GC-FID and GC-MS chromatograms for A-1.

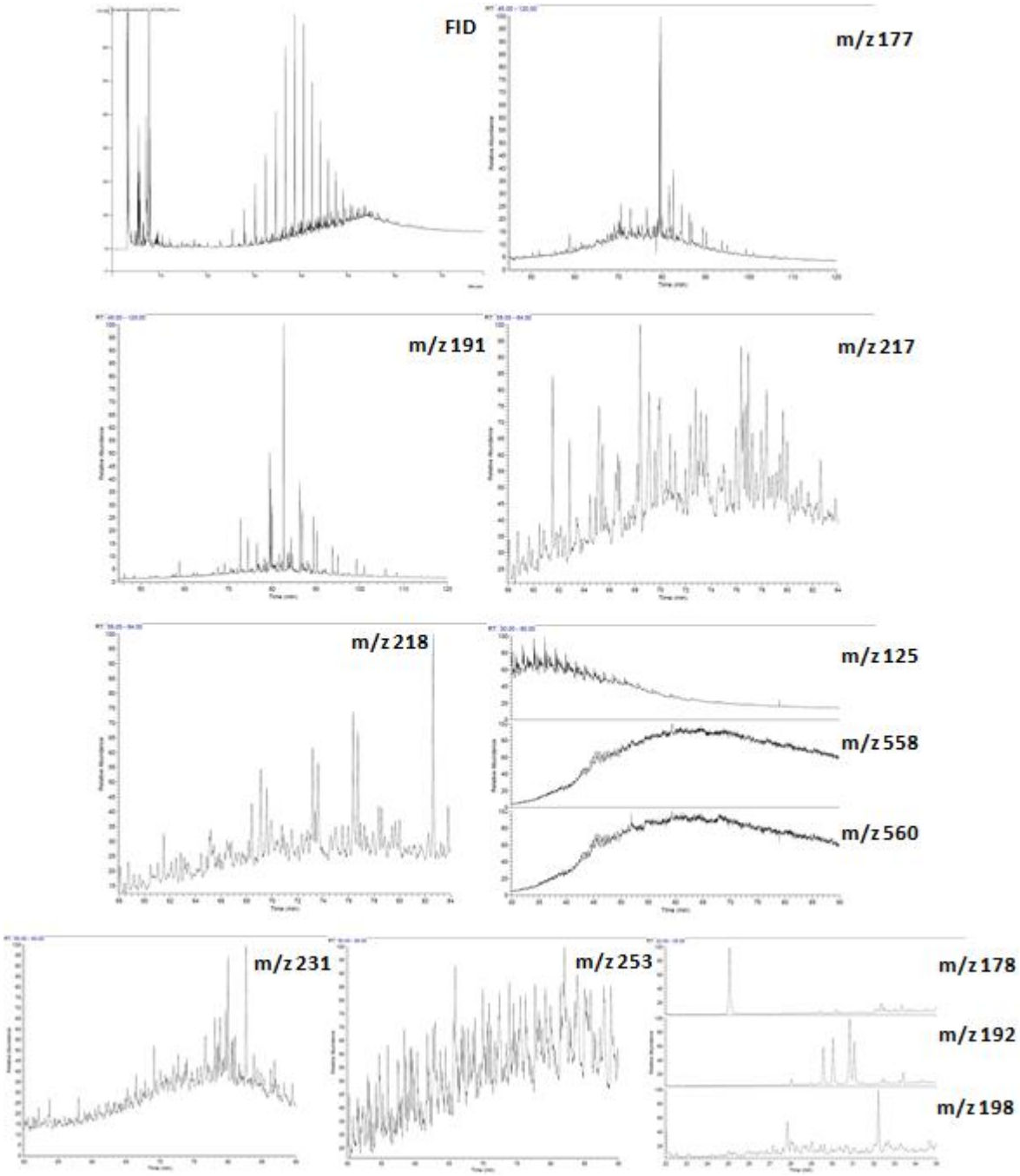

Figure 6.18: Scaled down GC-FID and GC-MS chromatograms for A-2.

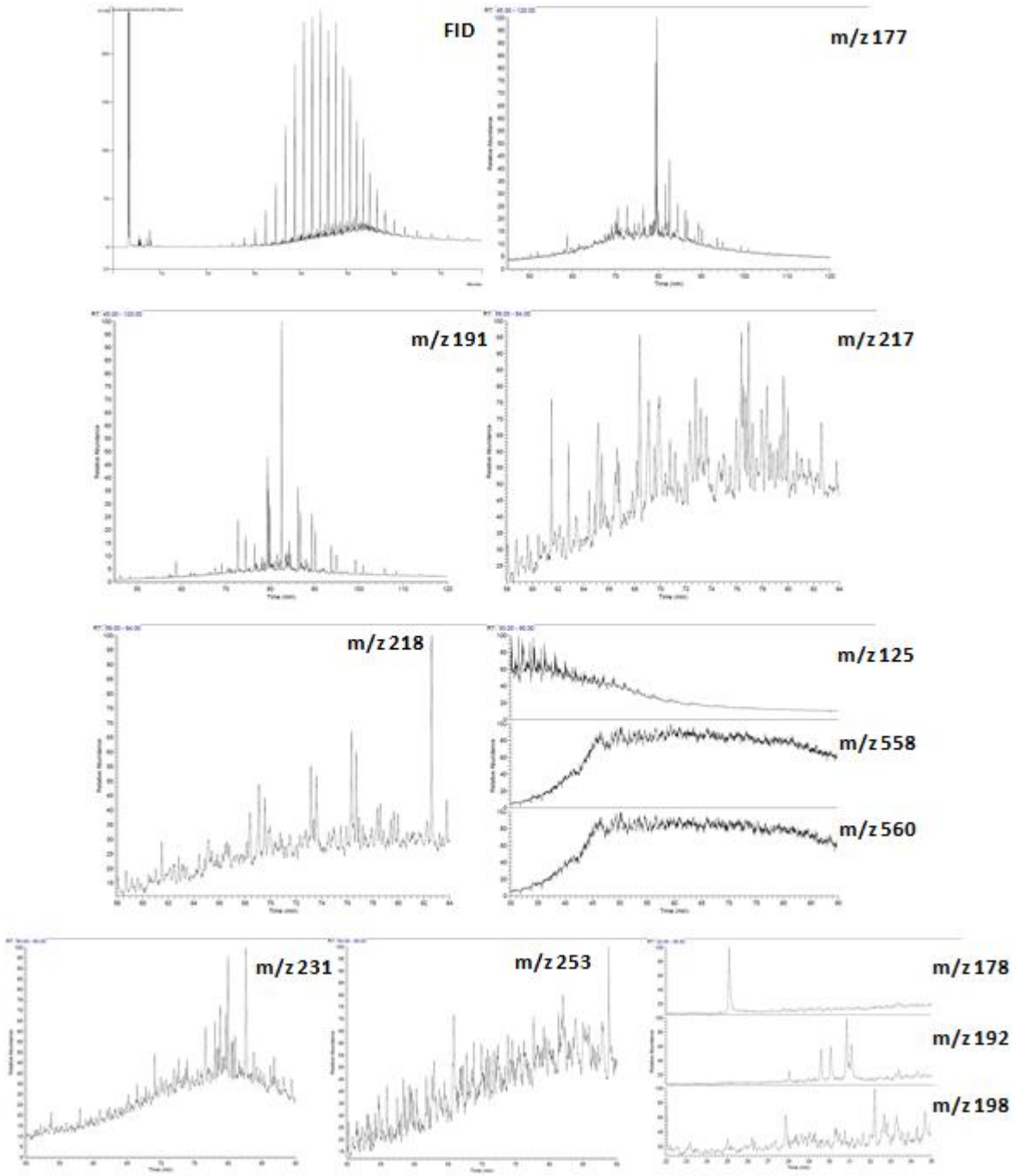

Figure 6.19: Scaled down GC-FID and GC-MS chromatograms for A-3.

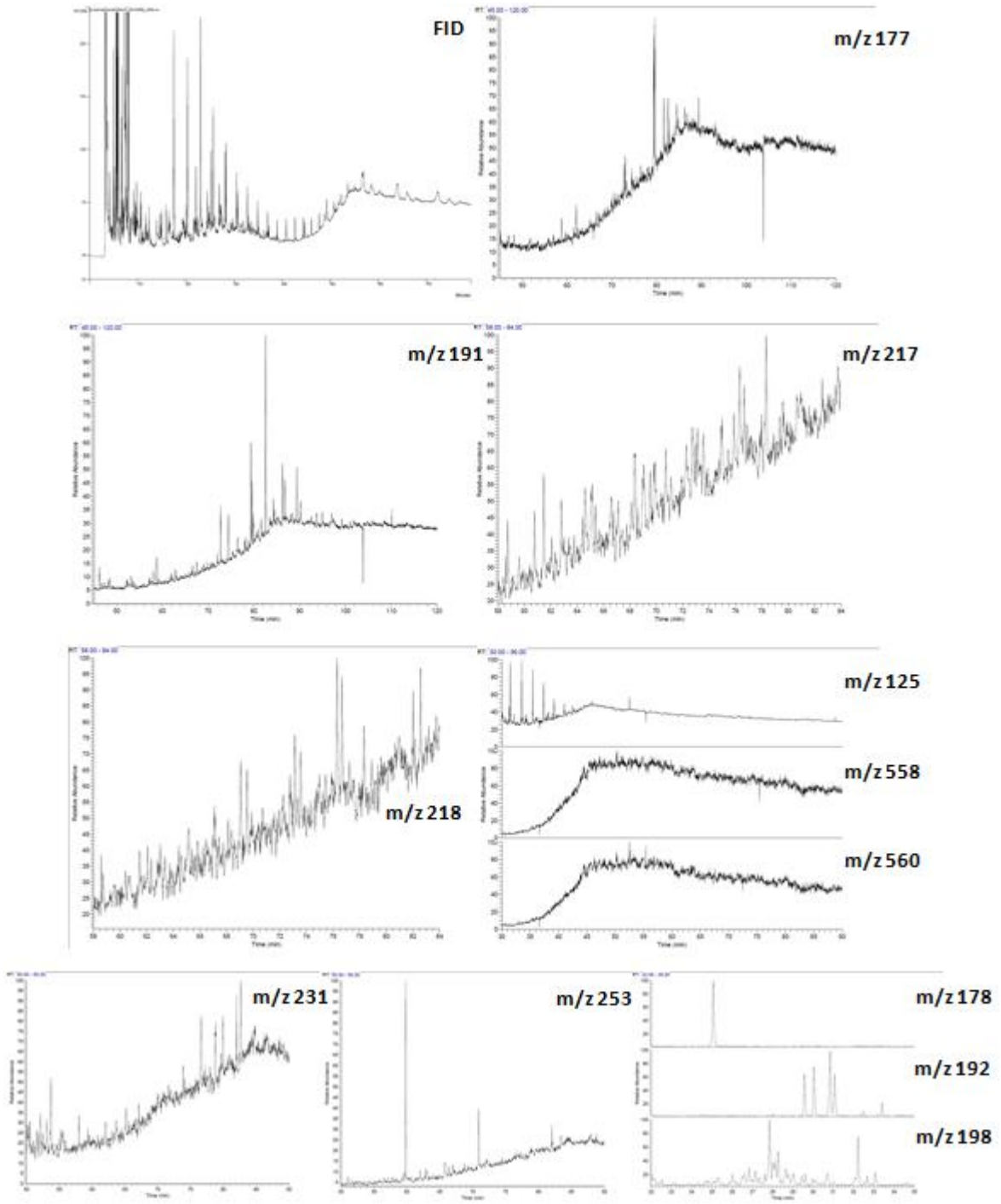

Figure 6.20: Scaled down GC-FID and GC-MS chromatograms for A-4.

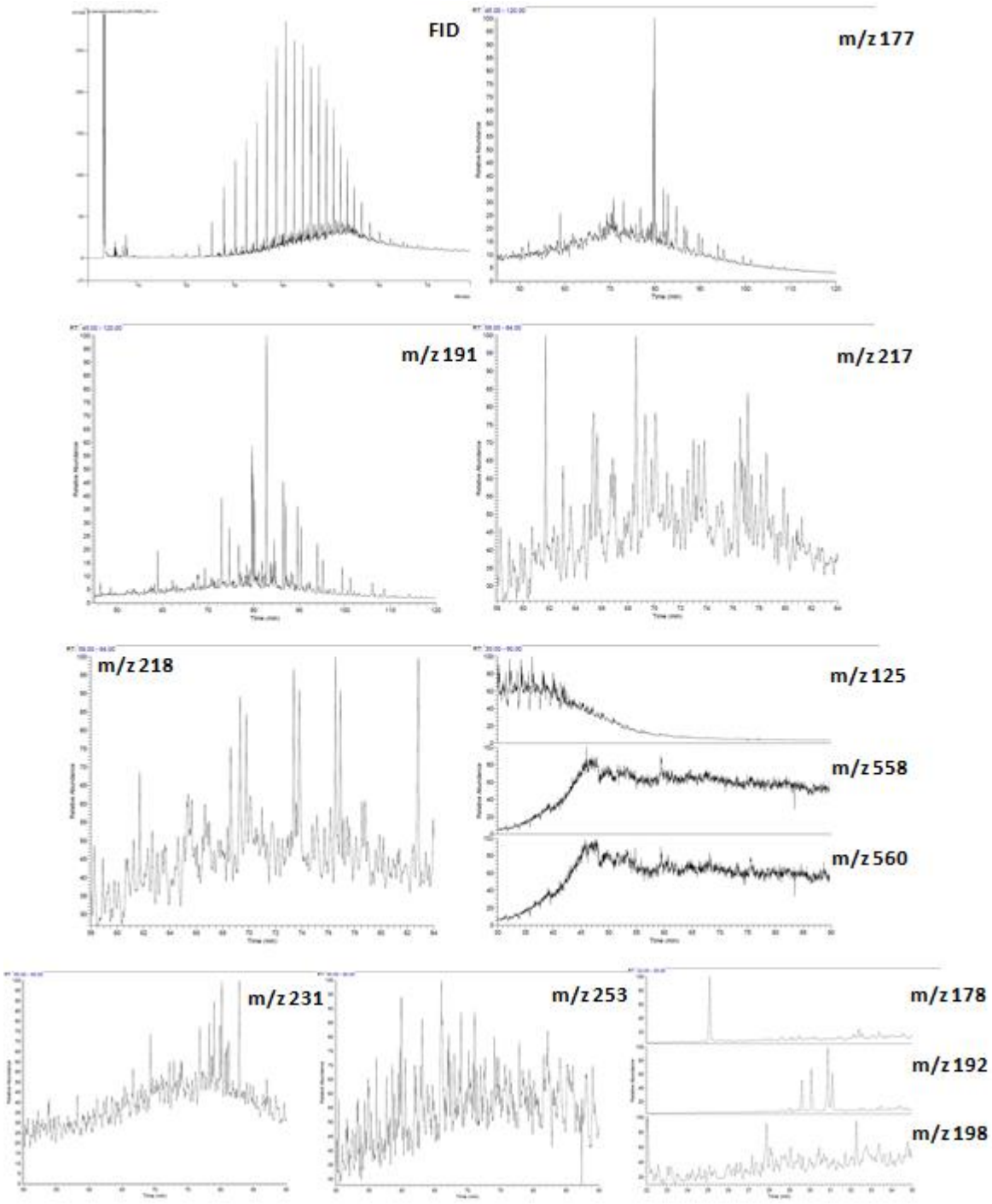

Figure 6.21: Scaled down GC-FID and GC-MS chromatograms for A-5.

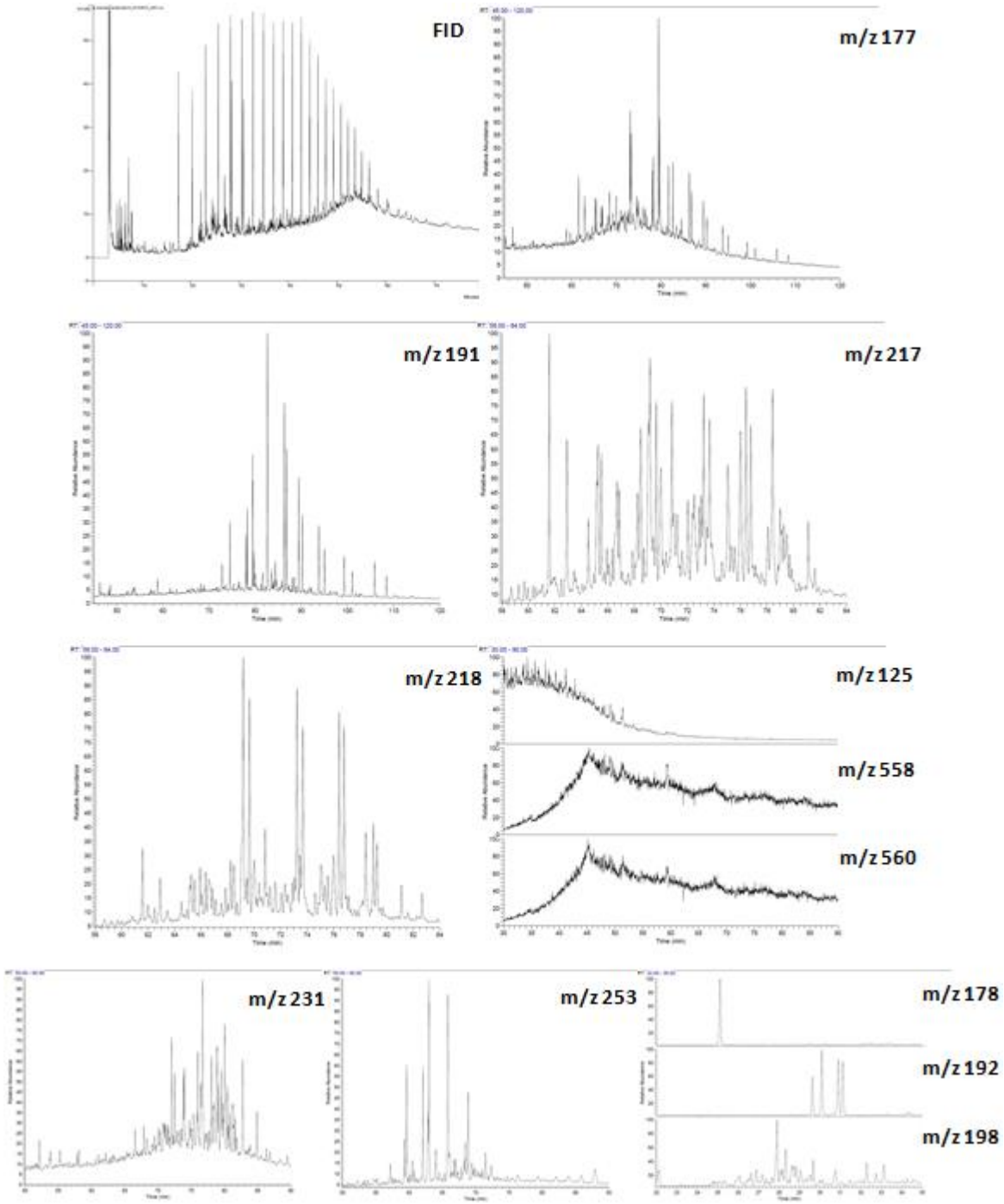

Figure 6.22: Scaled down GC-FID and GC-MS chromatograms for B-1.

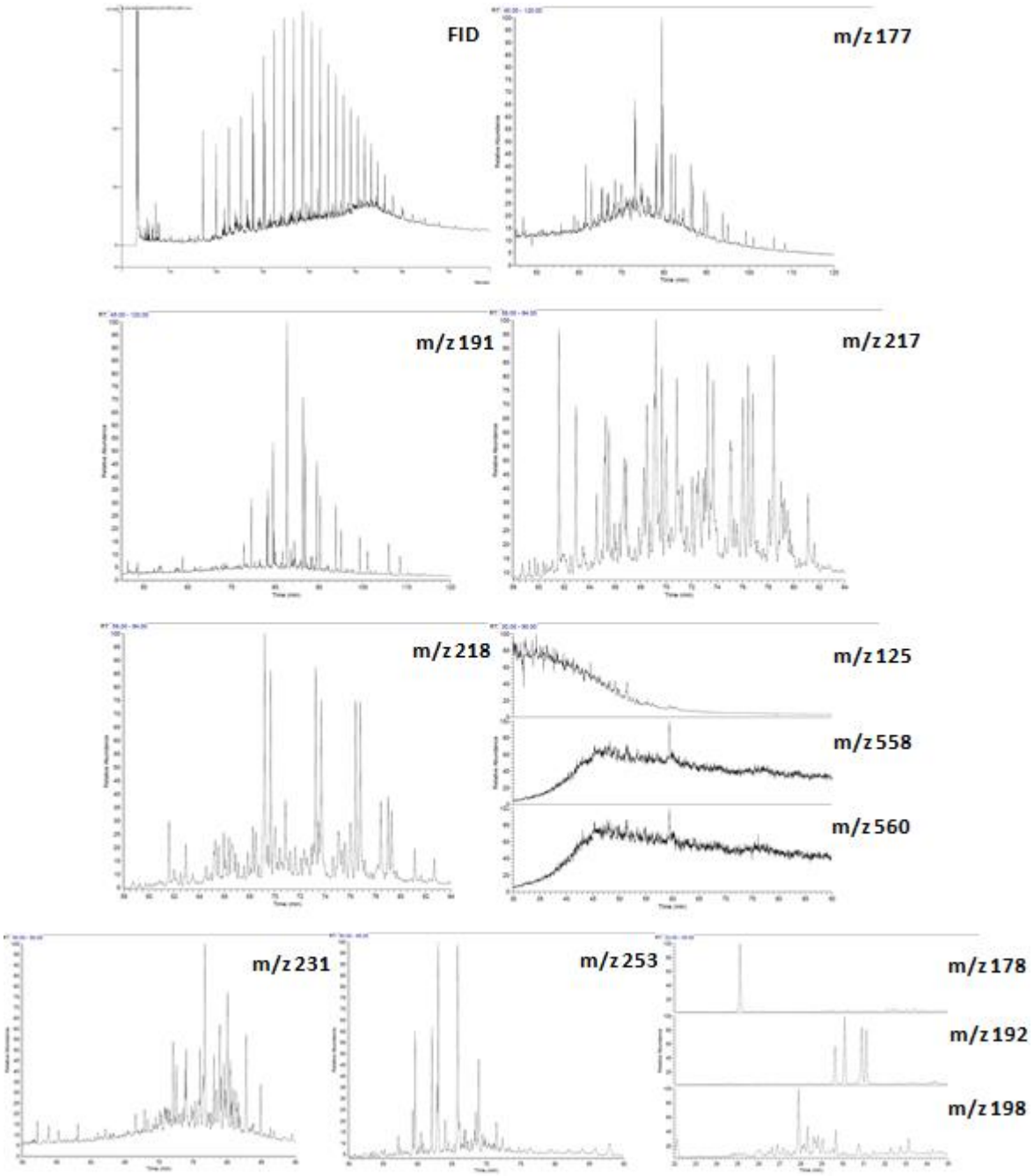

Figure 6.23: Scaled down GC-FID and GC-MS chromatograms for B-2.

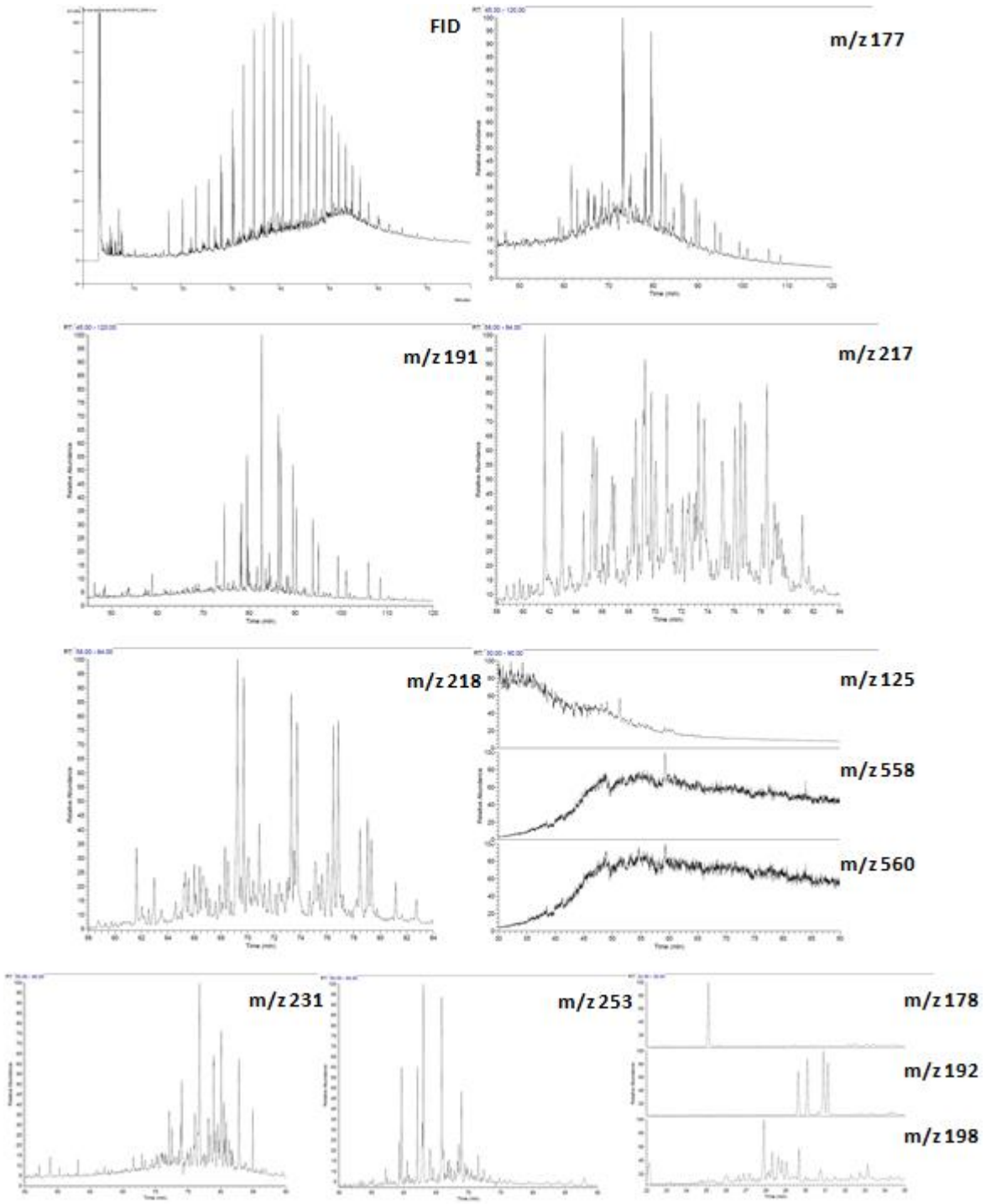

Figure 6.24: Scaled down GC-FID and GC-MS chromatograms for B-3.

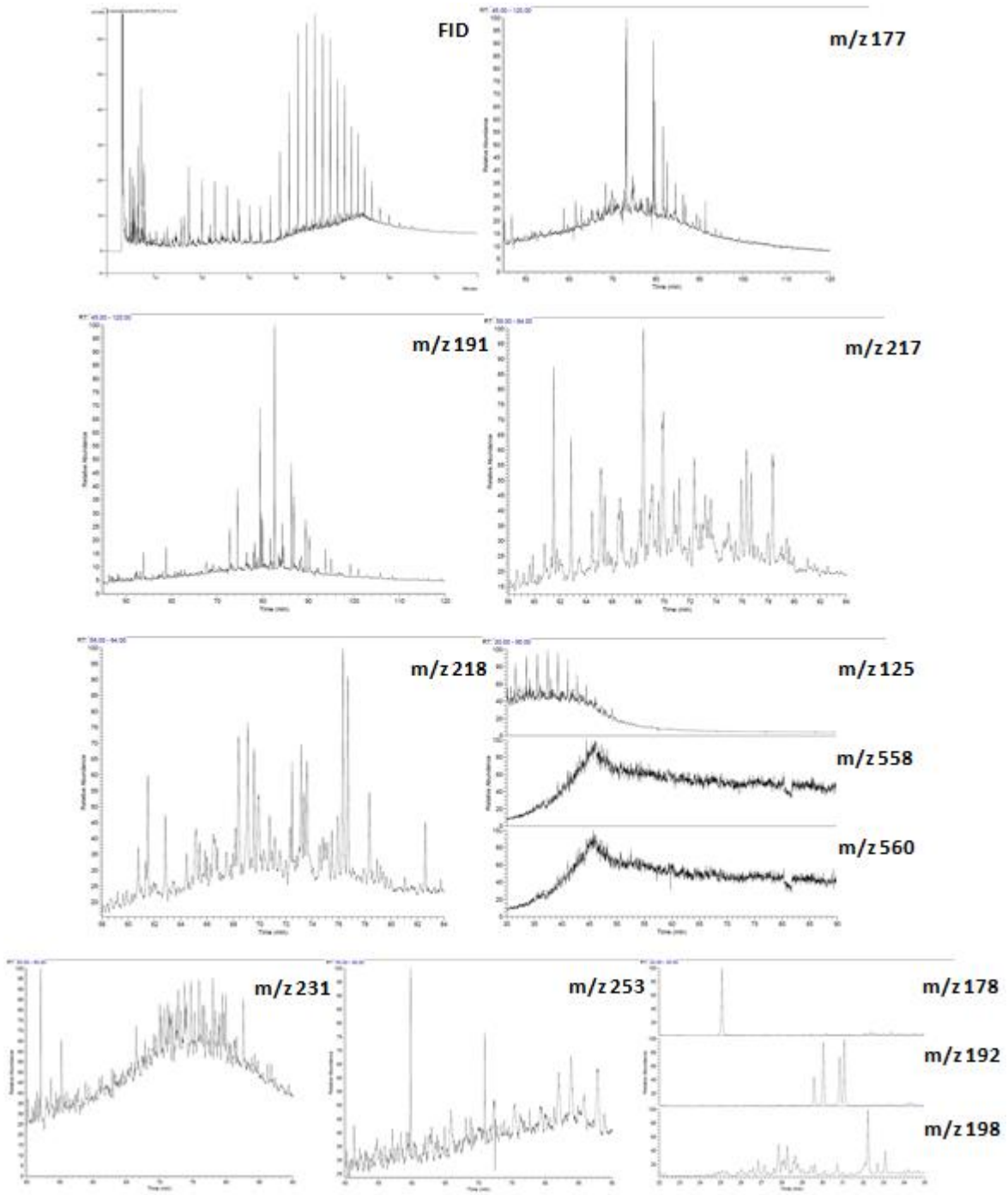

Figure 6.25: Scaled down GC-FID and GC-MS chromatograms for B-4.

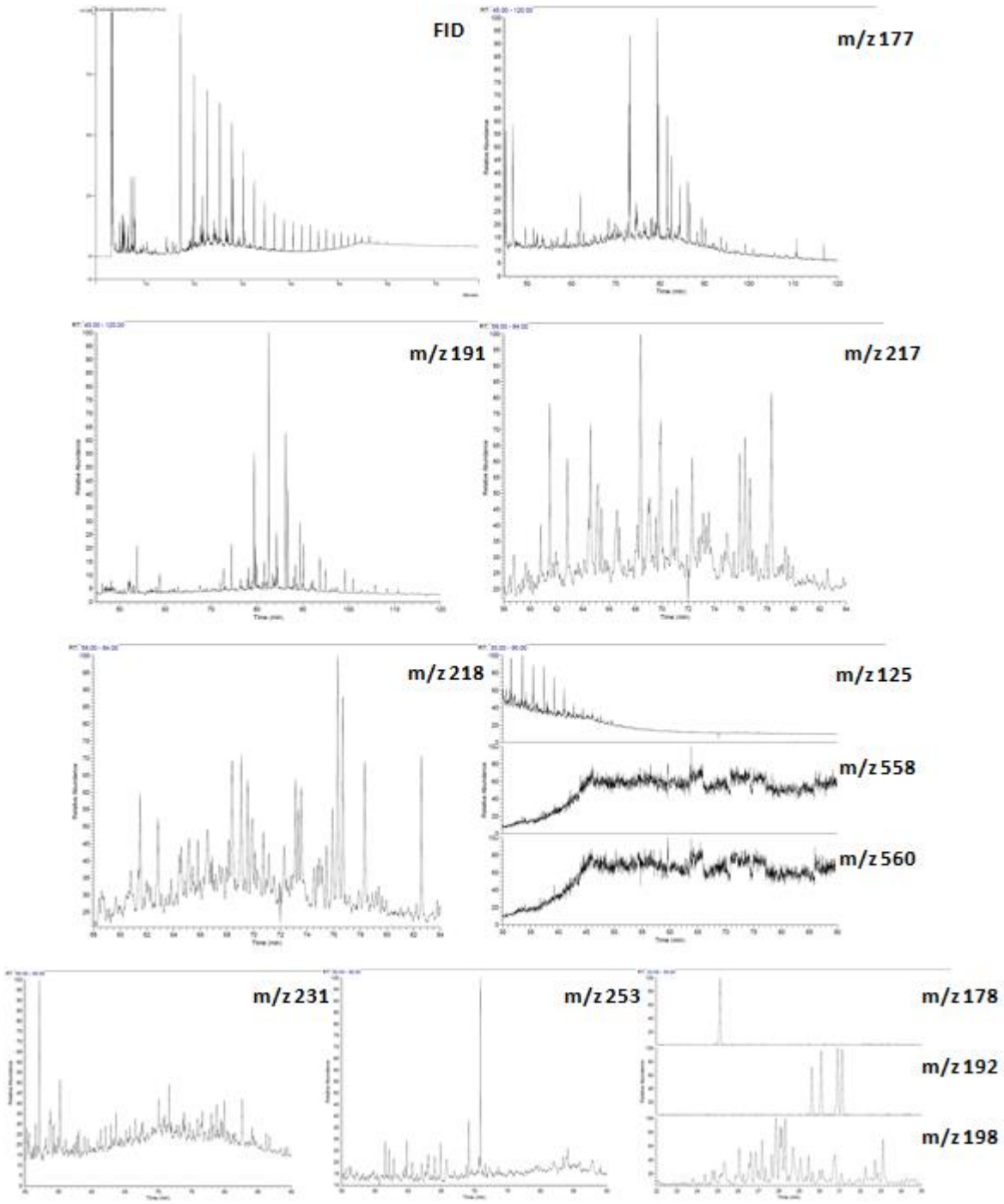

Figure 6.26: Scaled down GC-FID and GC-MS chromatograms for B-5.

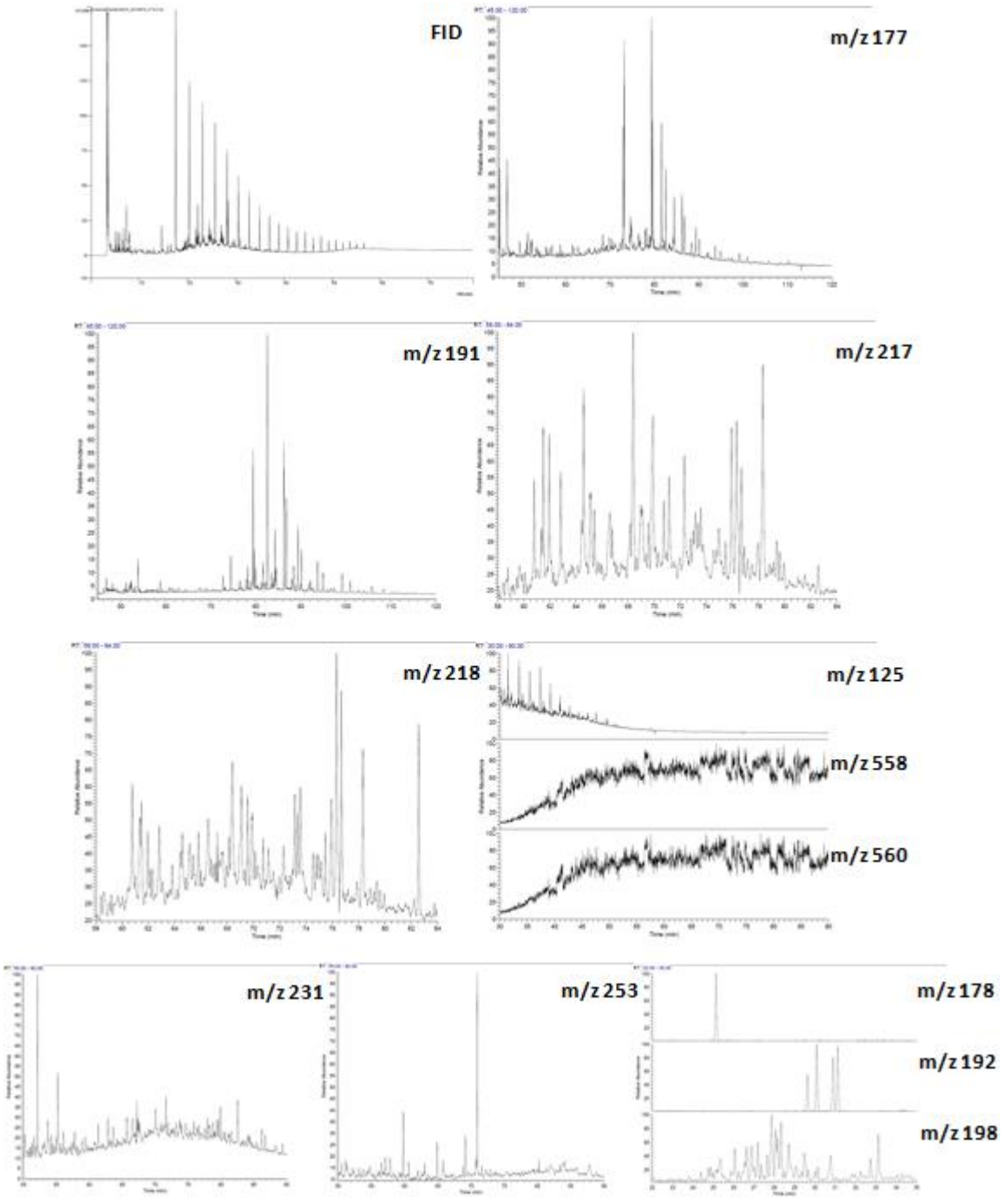

Figure 6.27: Scaled down GC-FID and GC-MS chromatograms for B-6.

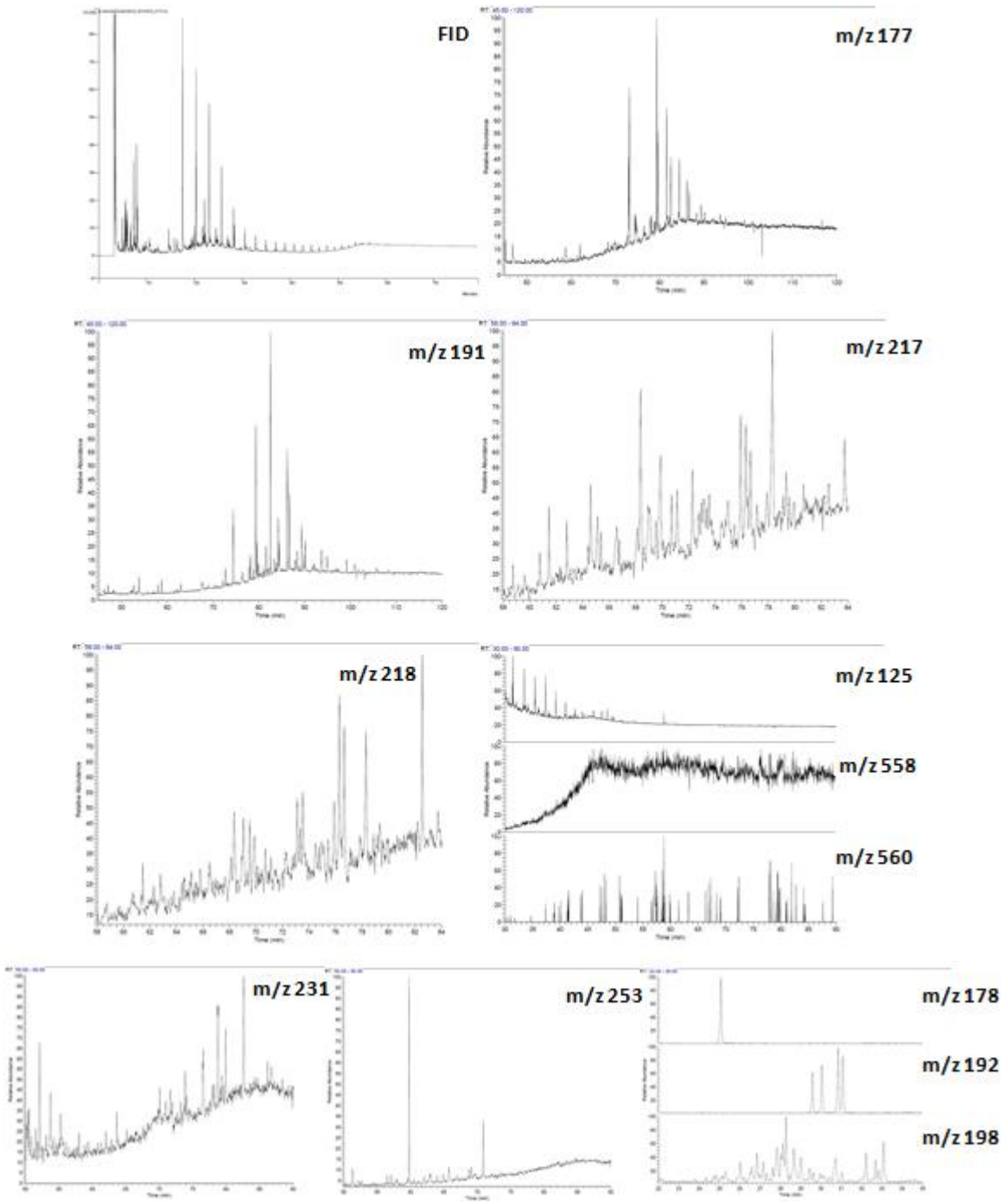

Figure 6.28: Scaled down GC-FID and GC-MS chromatograms for B-7.

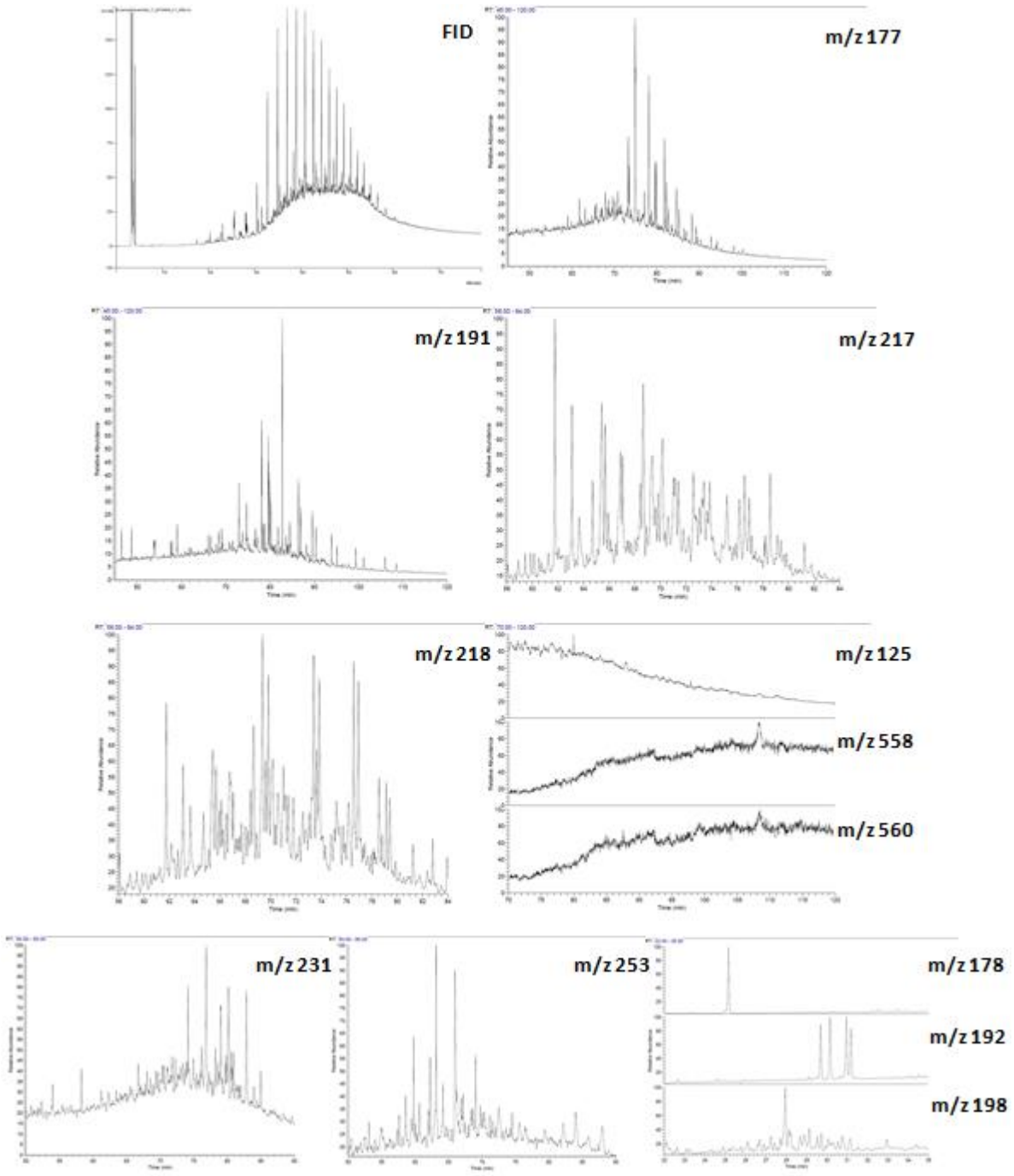

Figure 6.29: Scaled down GC-FID and GC-MS chromatograms for C-1.

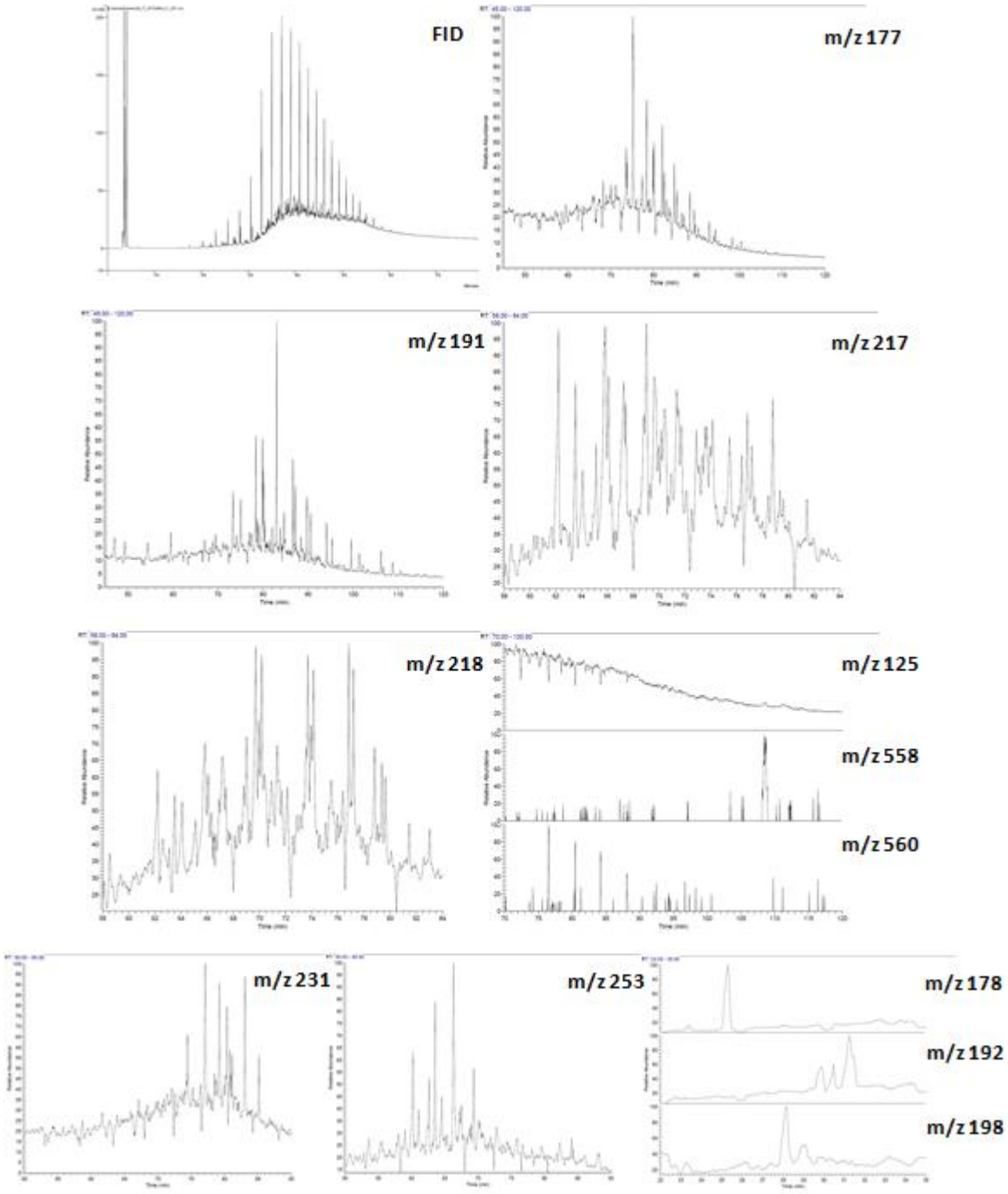

Figure 6.30: Scaled down GC-FID and GC-MS chromatograms for C-2.

7. Discussion

This chapter contains a discussion concerning maturity and facies aspects of the samples in this study based on the results which are presented in chapter 6. In particular will the maturity differences between the source rock bitumen samples from the Orkneys which represents Middle Devonian lacustrine source rocks, the marine Kimmeridge equivalent represented by the NSO-1 oil and the bitumen samples from the Helgeland Basin. The differences regarding the quality of organic matter and the generative potential between the Orkney source rock bitumen samples will also be investigated. The different viable source rocks in the Helgeland Basin, and their inferred maturity as based on the migrated bitumen, will be briefly discussed, and the parental source rock or source rocks for all the Helgeland Basin bitumen samples will be ascertained, based on the analytical geochemical methods described in chapter 4 and the results from chapter 6. The oils representing the Embla Field, the Judy field and the Oseberg Field (NSO-1) will also be discussed briefly, regarding the possible linkage to parental lacustrine Middle Devonian source rocks. This chapter is outlined as follows:

7.1 δ13C isotope analysis of selected source rock bitumen samples from the Orkneys, compared to the literature i.e. the Helgeland Basin bitumen samples, the Middle Devonian bitumen samples, plus bitumen samples representing the Late Jurassic Kimmeridge equivalent and the Beatrice oil

7.2 TOC and Rock-Eval analysis of the source rock bitumen samples from the Orkneys

7.3 Maturity discussion of the Orkney source rock bitumen samples, the Helgeland Basin bitumen samples in comparison to the Oseberg oil and the Beatrice oil and also the oils from the Judy Field and the Embla Field

- 7.3.1. The maturities of the source rock bitumen samples from the Orkneys
- 7.3.2. The maturity of the reference oil, NSO-1
- 7.3.3. The maturity of the oil from the Beatrice Field
- 7.3.4. The maturities of the bitumen extracts from well 6609/11-1
- 7.3.5. The maturities of the bitumen extracts from well 6610/7-1 upper section
- 7.3.6. The maturities of the bitumen extracts from well 6610/7-1 lower section
- 7.3.7. The maturities of the bitumen extracts from well 6609/5-1
- 7.3.8. Summary of the maturity discussion
- Challenges related to oil-source rock correlations due to effects from maturity

7.4 Overview of organic facies parameters, i.e. main diagnostic markers of the possible source rocks in the Helgeland Basin.

- 7.4.1. The Middle Devonian Orcadian Basin equivalent

- 7.4.2. The Late Jurassic Kimmeridge equivalent
- 7.4.3. The main diagnostic biomarkers for indicating positive relation to Middle Devonian or Late Jurassic source rocks
- 7.4.4. Possible coal derived Lower Carboniferous source rock
- 7.4.5. Possible Late Permian source rock
- 7.4.6. Possible Lower Triassic source rock
- 7.4.7. Possible coal derived Lower and Middle Jurassic source rocks

7.5 Tricyclic terpanes

7.6 Discussion of organofacies for the source rock bitumen samples from the Orkneys

7.7 Discussion of of organofacies for the bitumen extracts from well 6609/11-1

- 7.7.1. Discussion of potential sources for the bitumen extracts from well 6609/11-1
- 7.7.2.Summary of the organofacies for well 6609/11-1

7.8 Discussion of organofacies for the bitumen extracts from well 6610/7-1 upper section

- 7.8.1. Discussion of potential sources for the bitumen extracts from the upper section in well 6610/7-1
- 7.8.2. Summary of the organofacies for the upper section in well 6610/7-1

7.8 Discussion of organofacies for the bitumen extracts from well 6610/7-1 lower section

- 7.9.1. Discussion of potential sources for the bitumen extracts from the lower section in well 6610/7-1
- 7.9.2. Summary of the organofacies for the lower section in well 6610/7-1

7.10 Discussion of organofacies for the bitumen extracts from well 6609/5-1

- 7.10.1. Discussion of potential sources for the bitumen extracts from well 6609/5-1
- 7.10.2. Summary of the organofacies for well 6609/5-1

7.11 Discussion of the linkage to Middle Devonian source rocks for oils from the Embla Field, the Oseberg Field and the Judy Field

- 7.11.1. Oseberg (NSO-1)
- 7.11.2. Embla
- 7.11.3. Judy

7.12 Summary of the organofacies discussion

7.1 δ13C isotope analysis of selected source rock bitumen samples from the Orkneys, compared to the literature i.e. Helgeland Basin bitumen samples, Middle Devonian bitumen samples, plus bitumen samples representing the Late Jurassic Kimmeridge equivalent and the Beatrice oil

The immature Late Jurassic bitumen from Schou et al. (1983) is isotopically lighter than the more mature Late Jurassic bitumen from Peters et al. (1989) cf. Table 6.6. The latter is more mature, which results in heavier δ13C values for the saturated fraction (Peters and Fowler, 2002), and a heavier saturated fraction relative to the aromatic fraction (Tissot and Welte, 1984), leading to the observed enrichment of δ13C for the latter. The oil-stained sandstone samples from the Helgeland Basin will be compared to the δ13C value of the latter due to more comparable maturities, thus making it a more viable option for limiting the effects caused by variations in maturity.

Regarding the stable carbon analysis of the four selected Orkney source rock bitumen samples, the values are on par with the value for A-5 (6609/11-1_2561m from Karlsen et al., 1995), cf. Table 6.6. When comparing those values to the value for a typical Kimmeridge equivalent source (-28.32$^{o}/_{oo}$, Peters et al., 1989) and the Lower Jurassic coals, it is clear that contribution from a standard Kimmeridge equivalent source should be insignificant for A-5 as the Kimmeridge is about 3.9$^{o}/_{oo}$ more enriched in the δ13C isotope. The same argument is also valid for excluding the Lower Jurassic coals as a contributor to A-5, as it is shows heavier δ13C values than the Kimmeridge equivalent (see Table 6.6).

The isotopic composition of oils and bitumen samples are normally intermediate between the SAT and ARO fractions as the former and latter comprises the bulk of the sample in most cases and can be tentatively approached by assuming the value similar to the weighted mean i.e. 70% x δ13C sat + 30% x δ13C = δ13C total oil (Peters et al., 2005). When compared to the marine Kimmeridge equivalent (-28.32$^{o}/_{oo}$) and the Orkney source rock bitumen samples which have δ13C values of EOM in the range of -32.0$^{o}/_{oo}$ to -33.1$^{o}/_{oo}$, it is noted that the bitumen from selected depths of 2661.6m and 2668.05m in the upper section of 6610/7-1, and also from depth 2706m in between the upper and lower section are isotopically lighter than the marine Kimmeridge equivalent and Lower Jurassic coals, and heavier than the Beatrice oil and the Orkney source rock bitumen samples. This observation may suggest that the upper interval of well 6610/7-1 is co-sourced by

equivalents to the lacustrine Middle Devonian source rocks and the marine Kimmeridge Late Jurassic source rocks or coal derived Lower Jurassic source rocks.

Although being a great asset in correlation studies, the data from δC13 isotope supports, but does not prove a relation between two oils if difference in the δ13C value is below $1^{o}/_{oo}$, since the effects from maturation on related oils may account for the more mature oils becoming up to maximum $2\text{-}3^{o}/_{oo}$ heavier (Peters et al., 2005). From the histogram distribution of δ13carbon isotope values from 107 North Sea oils and bitumens (see Figure 7.1), a distinct separation is shown between the oils/bitumens which are related to the marine Late Jurassic source rocks and the oils/bitumens which are related to the lacustrine Middle (and Lower) Devonian source rocks and this observation shows that the values δC13 isotope analysis thus may prove to be very useful in particular for the correlation studies in this thesis as the commonly encountered Jurassic sourced oils are clearly differentiated from the Middle Devonian lacustrine source rocks which are of main concern.

Peters et al. (1989) noted that the δC13 isotope value of the Beatrice oil was intermediate between the values from the Middle Devonian and Middle Jurassic source rocks respectively, both which are located in the Moray Firth area, and this observation gave support to their co-sourcing interpretation. The same authors did also calculate the percentage of contribution from the Middle Devonian and Middle Jurassic source rocks to the Beatrice oil based on the C13 isotope data.

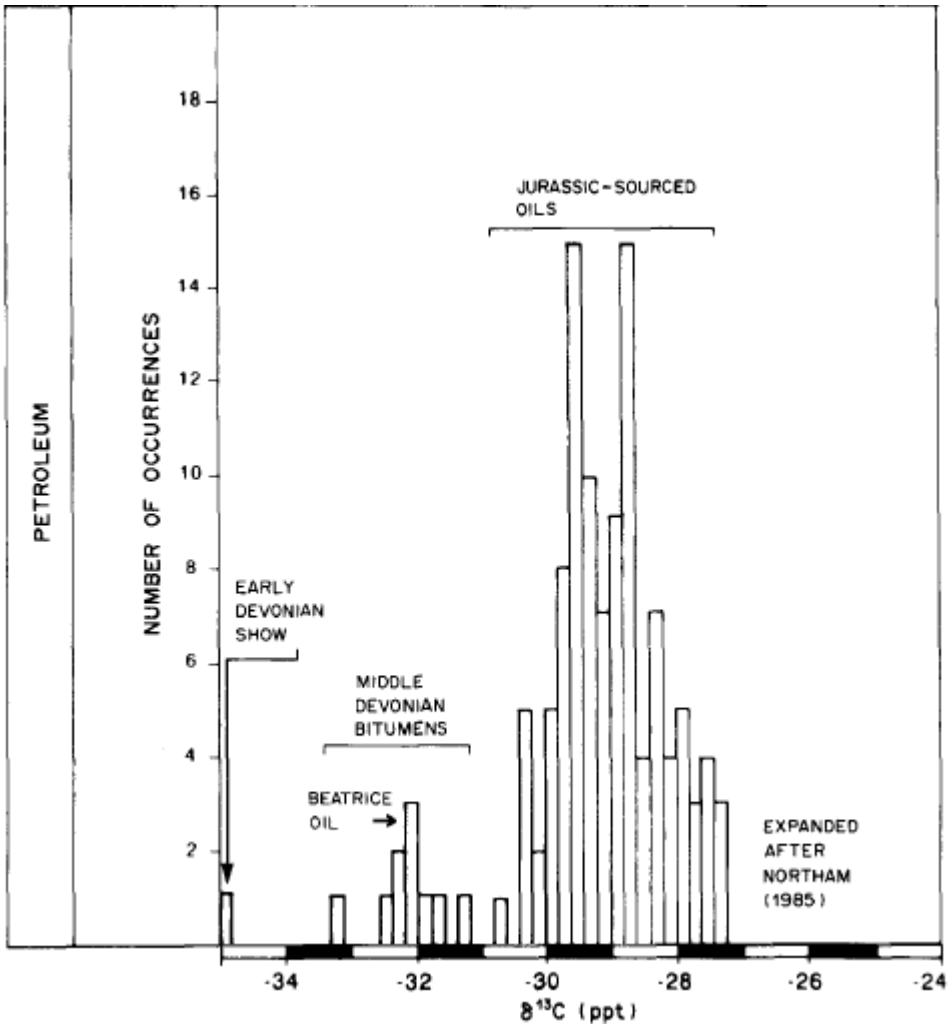

Figure 7.1: Histogram which shows the distribution of δ13C values for 107 oils and bitumens from the North Sea (modified from Bailey et al., 1990). Notice the distinct separation in δ13C values between the lacustrine Middle Devonian derived organofacies and the marine Late Jurassic derived organofacies.

7.2 TOC and Rock-Eval analysis of the source rock bitumen samples from the Orkneys

From the results of TOC and Rock-Eval analysis (see section 6.4 and Table 6.5), it is clear that there are great variations in the organic matter quality between the source rock bitumen samples from the Orkneys which represents Middle Devonian lacustrine lake deposits. HI values range from 88mg HC/g TOC to 397mg HC/g TOC and the TOC values range from 0.33wt.% to 2.79wt.%. Traditionally TOC values of 0.5wt.% and 0.3wt.% were regarded as cut of values for a carbonate and silisiclastic rocks respectively to be classified as a source rock (Tissot and Welte, 1984). However, at present day the cut of values are assigned the same value i.e. 0.5wt.% (cf. Peters et al.,

2005) and the classification from Peters and Cassa (1994) operates with the same minimum source rock criteria value for carbonate rocks and silisiclastic rocks (see Table 7.1).

The plots of HI versus OI (the modified van Krevelen diagram) cf. Figure 7.2 (left) and HI versus T_{max} (Figure 7.2, right) are used for categorizing the samples based on the type of organic matter i.e. the kerogen type and those plots may also be useful as maturity indicators. However, kerogen classification is troublesome for highly matured samples as all kerogen types approach graphite composition in the late catagenesis stage i.e. maturities corresponding to the post-oil generation (Tissot and Welte, 1984) i.e. the gas generating zone starts around R_o = 1.4% (see Figure 5.11), and thus becomes hard to distinguish as illustrated in the merging of the kerogen pathways in Figure 7.2. Still for the present samples, kerogen classification based on HI is anyways reliable for the early mature source rock samples from the Orkneys (see section 7.3.1 for maturity discussion).

The OI is in general relatively low for most of the samples (≤32 mg CO_2/g TOC) but exceeds values of 100 for three samples; O-3 shows 207 mg CO_2/g TOC, O-6 shows 116 CO_2/g TOC and O-7 shows 136 CO_2/g TOC. The three mentioned samples are also those that showed the lowest petroleum generative potential during pyrolysis, they have the lowest TOC values and they all fall into the poor petroleum potential range of TOC, S1 and S2 based on the classification from Peters and Cassa (1994) cf. Table 7.1. Sample O-4 shows a good TOC value, but shows a only fair S2 and a poor S1 value which indicate that it overall has only a moderate source rock potential.

Table 7.1: Parameter ranges and the corresponding petroleum potential of source rocks (from Peters and Cassa, 1994).

Potential	TOC (wt. %)	S_1 (mg/g)	S_2 (mg/g)
Poor	<0.5	<0.5	<2.5
Fair	0.5-1	0.5-1	2.5-5
Good	1-2	1-2	5-10
Very Good	2-4	2-4	10-20
Excellent	>4	>4	>20

The bitumen samples O-1, O-2, O-5, and O-20 all show good source rock potentials, based on the yield of petroleum during pyrolysis i.e. the S2 value is in between 5mg/g and 10mg/g. However, the S1 parameter indicates only poor potential for all the mentioned samples except from O-20 which shows fair potential. This indicates that the source rocks are only marginally mature, and that the maturity is insufficient for petroleum expulsion. All of the source rock bitumen samples from the Orkneys are at the onset of or into the early oil generating phase (see section 7.3.1. for maturity discussion), and those samples will thus score low in petroleum potential based on S1. The O-20

bitumen sample falls into the very good potential category based on the TOC value of 2.46wt%, while the O-1, O-2, and O-5 bitumen samples falls into the good potential range based on TOC values which are in the range from 1.48wt.% to 1.95wt.%..

The O-21 bitumen sample shows the highest TOC, S2 and HI values of the source rock samples, and has thus the best source rock potential. The TOC (2.79wt.%) and S2 (11.08mg/g) values corresponds to the very good potential range (see Table 7.1), while S1 (0.43mg/g) falls into the poor potential range as O-21 is only in the early oil generating phase.

The HI value of O-3 (88mg HC/g TOC) is much lower than the second lowest i.e. of O-7 (205mg HC/g TOC) and third lowest i.e. of O-4 (219mg HC/g TOC), and based on this parameter combined with the highest OI and also the lowest TOC, it can be concluded that O-3 shows by far the lowest source rock potential of all the Orkney source rock bitumen samples as it scores the lowest in both quality (HI) and generative potential (TOC), and does also not fulfill the criteria for being classified as a source rock i.e. the TOC value of O-3 is below the 0.5wt.%.threshold. It is worth mentioning that this outcrop sample has been weathered (Brown, unpubl.), which could explain why it has the lowest overall potential and quality.

Regarding the quality of the organic matter i.e. the kerogen type, the HI values for the O-6 and O-7 bitumen samples correspond to type II/III kerogen while the HI value for O-3 corresponds to type III kerogen. The O-4 bitumen sample has a comparable HI value to the O-6 bitumen sample and the former and latter and also the O-7 bitumen sample can be classified as type II/III kerogen, but higher TOC gives the O-4 sample a better potential overall compared to the two others. The bitumen samples O-1, O-2, O-5, O-20 and O-21 all have HI which corresponds to type II kerogen (see Table 7.2).

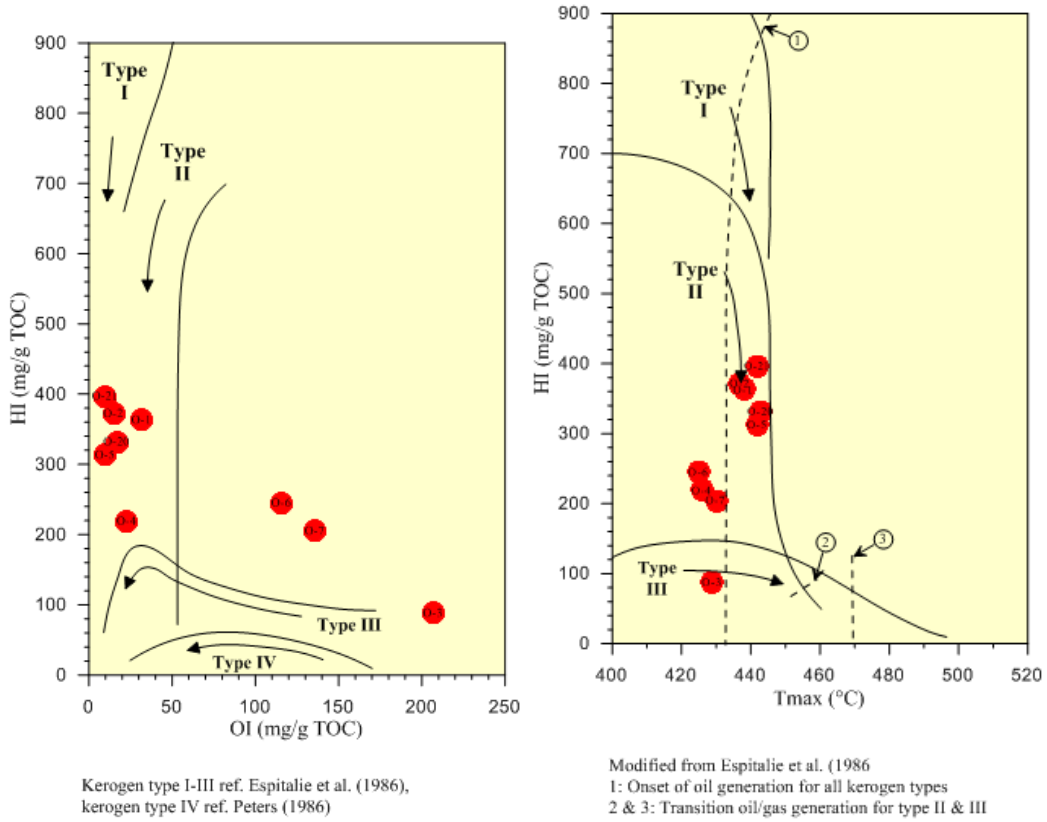

Figure 7.2: Modified van Krevelen diagram of HI vs OI to the left and HI vs Tmax to the right, and the corresponding kerogen-type zones. Land plant evolution (vascular plants) was still limited in the Middle Devonian, and the region in question was partly a desert, and this might be considered concerning the validity of OI as a kerogen indicator in this dataset and the figure to the right is thus possibly more accurate for determining the correct kerogen type.

Table 7.2: Table showing the parameter ranges and the corresponding kerogen type and hydrocarbon products at the peak maturity of source rocks (from Peters and Cassa, 1994).

Kerogen	HI (mg hydrocarbon/g TOC)	S2/S3	Product at peak maturity
I	>600	>15	Oil
II	300-600	10-15	Oil
II/III	200-300	5-10	Oil/gas
III	50-200	1-5	Gas
IV	<50	<1	None

The Lacustrine source rocks in the Orcadian Basin is mostly associated with kerogen type I (Trewin, 1989), therefore the HI for the samples representing this area was expected to exceed values of 600mg HC/g TOC which is the minimum criteria for type I kerogen based on the classification from Peters and Cassa (1994). However, none of the Orkney bitumen samples fulfills this criterion, and can thus not be categorized as type I kerogen based on the HI. The S2 to S3 ratio (see Table 6.5) which alongside the HI estimates quality, indicates higher quality of the best rated source rock bitumen samples compared to the latter parameter. Based on the S2/S3 parameter, the bitumen

samples O-2, O-5, O-20 and O-21 qualifies for kerogen type I, O-1 falls into the kerogen type II range (same as for HI) and O-4 falls into kerogen type II/III (same as for HI). O-3, O-6 and O-7 falls into lower quality kerogen based on S2/S3 compared with HI i.e. O-3 falls into kerogen type IV based on S2/S3 (kerogen type III based on HI), while O-6 and O-7 falls into kerogen type III (II/III based on HI).

A high S3 peak results in a high OI value as the latter is related to the former and this is diagnostic for kerogen type III which consists of woody material (Tissot and Welte, 1984). The low OI for the source rock samples compared to HI in general can thus be explained by the low abundance of woody material in Middle Devonian, as the formation of woody material was not fully developed until Late Devonian (Schweingruber et al., 2006). As a consequence, the usefulness of S2/S3 as a source rock quality parameter is limited because the criteria values used for categorizing the respective kerogen types are not calibrated for the Middle Devonian flora. The kerogen type classification is thus solely based on the HI. However, the OI is still useful as a supplement to the HI for distinguishing source rock quality within the source rock samples and does mostly agree with latter for the classification of quality.

Dahl et al., (2004) proposed a relationship which utilizes data from TOC and Rock-Eval analysis to indicate the percentage of oil generation and the percentage of gas generation in source rocks. The TOC-values are plotted against the S2 values, and the HI is derived from a regression line which is an estimate from the average values of the HI of the organic matter and is calibrated to the relative abundance of oil prone and gas prone compounds which are assigned fixed values (Dahl et al., 2004). Due to the change in HI during increased maturation of the source rock (see Figure 7.2) which is an effect from kerogen-cracking, the relationships need to be adjusted for more mature source rocks, otherwise would source rocks appear as they are of lower quality as they matures (Dahl et al., 2004). The Orkney source rock bitumen samples are plotted in the TOC versus S2 crossplot (see Figure 7.3). The plot which is not calibrated for the transformation ratio of kerogen (TR) is used on the bitumen samples, as they are only considered marginally mature (see section 7.3.1 for maturity discussion) i.e. insignificant transformation of kerogen has occurred, hence the usage of the plot with TR value equal to 0.

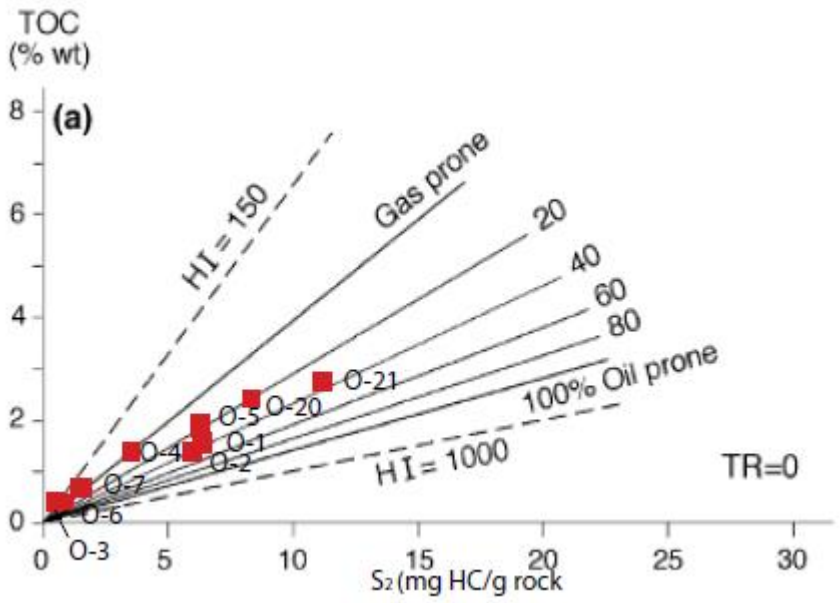

Figure 7.3: Plot of the TOC versus the S2 yield during pyrolysis, and the corresponding percentage of gas and oil generative potential for the Orkney source rock bitumen samples, based on the presumption of no transformation prior to the pyrolysis i.e. TR = 0 (the plot is from Dahl et al., 2004). Notice that even the best rated source rock sample i.e. O-21 is likely to yield more gas than oil.

From Figure 7.3, it is shown that the Orkney source rock bitumen samples show a higher potential for generating gas than for generating oil, and even the highest rated source rock bitumen samples i.e. O-1, O-2, O-5, O-20 and O-21 are more gas-prone than oil-prone as the percentage of oil generative potential does not exceed 40 %. The same samples are classified as oil-prone after the criterias from Peters and Cassa (1994), thus meaning that the latter classification may be slightly misleading or that the plot from Dahl et al., (2004) is not properly calibrated. However, it is important to keep in mind that some transformation of kerogen has occurred i.e the S1/(S1 + S2) ratio does equal 0 only for O-3 and ranges from 0 to 0.10 (O-7), meaning that the actual oil-proneness is slightly higher than what is proposed from Figure 7.3 and closer to the classification from Peters and Cassa (1994). Furthermore, the oil-prone classified source rock bitumen samples fall into the lower part of the HI range of type II kerogen (see Table 7.2 and Table 6.5), meaning that those samples are only slightly more oil-prone than gas prone. Thus would the determination of the oil-proneness from Figure 7.3, if properly calibrated for the true kerogen transformation ratio and the classification based on Peters and Cassa (1994) be of close approximation relative to each other.

Summary of the source rock potential i.e. quantity based on TOC and S2 from Table 7.1 and kerogen type i.e. quality based on HI from Table 7.2:

O-1: Good potential, kerogen type II, oil prone.

O-2: Good potential, kerogen type II, oil prone.

O-3: Poor potential, kerogen type III, gas prone.

O-4: Fair potential, kerogen type II/III, oil/gas prone.

O-5: Good potential, kerogen type II, oil prone.

O-6: Poor potential, kerogen type II/ III, oil/gas prone.

O-7: Poor potential, kerogen type II/III, oil/gas prone.

O-20: Good potential, kerogen type II, oil prone.

O-21: Very good potential, kerogen type II, oil prone.

The O-1 and O-2 bitumen samples both represent the Sandwick fishbed (Brown, unpubl.), an equivalent to the Achanarras fish bed, which was deposited during periods of deep water in the lake. The seven other source rock samples i.e. O-3, O-4, O-5, O-6, O-7, O-20 and O-21 are associated with lake laminites.

O-5 and O-6 are associated with large and thin stromatolites respectively (Brown, unpubl.) and O-5 was probably deposited at water depths of only a few meters in areas close to the lake margin and protected from clastic input (Trewin, 1989). O-6 was situated at the proximal parts of the lake like O-5, but was unlike the latter probably not shielded against clastic input as seen in the low gammacerane index of 0.36 (O-5 has in comparison 2.57) and the much higher OI of 207 mg CO2 /g TOC (O-5 has in comparison 10 mg CO2 / g TOC). The low gammacerane index of O-6 suggests that the lake was not stratified at the depositional location i.e. circulation of the water column probably caused by nearby rivers which could provide clastic sediments and thus also terrestrially derived kerogen type III organic matter which would cause the observed elevated OI value for this bitumen sample. The very low Pr/Ph ratio of O-3 which is 0.44 does conflict with the OI and the gammacerane index, as circulation of the water column normally would result in oxidizing conditions leading to much higher Pr/Ph ratios and also higher phenanthrene abundance (see maturity discussion, section 7.3.1). A natural explanation for the low Pr/Ph ratio in co-occurrence

with high OI value and a low gammacerance index value is that the concentration of atmospheric oxygen was low during Devonian due to the fact that the establishment of life on land was still in its early stages (cf. Schweingruber et al., 2006) i.e. the oxygen release into the atmosphere from photosynthesis was still of relatively low-scale. Despite the circulation of the water column, the circulating fresh water from the upper part of the water column would not be enriched in oxygen and thus would the reducing conditions on the lake floor prevail despite the events with water column circulation which lead to the deposition of terrestrially derived organic matter.

O-3 shares the same pattern as O-6 i.e. high OI (207 mg CO2/g TOC), low gammacerane index (0.43) and low Pr/Ph ratio (0.44), and was thus most likely also deposited in a proximal part of the lake, unprotected agaist clastic input. O-7 does also show a high OI (136 mg CO2/g TOC), however the high gammacerane index of 1.33 suggests that the lake was stratified i.e. which leads to the interpretation that O-7 was deposited in a more distal part of the lake as compared to O-3 and O-6, but still with close enough proximity to land for terrestrially derived organic matter to be deposited.

The O-20 and O-21 bitumen samples are associated with sections with lots of fish remains and the locality of the latter has also some large examples. The preservation of larger fish remains might explain the greater generative potential of O-21 relative to O-20.

The source rock bitumen samples which are related to different depositional settings within the lake shows that good quality source rocks were not limited to one or a few specific depositional conditions, but could be more widespread within the entire lake system.

7.3 Maturity discussion of the Orkney source rock bitumen samples, the Helgeland Basin bitumen samples in comparison to the Oseberg oil and the Beatrice oil and also the oils from the Judy Field and the Embla Field

7.3.1 The maturities of the source rock bitumen samples from the Orkneys

The source rock bitumen samples have not reached the isomerization equilibrium of the homohopanes i.e. the 22S/(22S+22R) values are below the range of 0.57 to 0.62 (see Table 6.2), implying that those samples have not reached maturity levels corresponding to the main oil

generation phase. However, the source rock bitumen samples show values above 0.5 which indicates maturities corresponding to the early oil generating phase.

The suggestion that the maturities of the Orkney source rock bitumen samples correspond to the early oil generating phase is supported by the vitrinite reflectivity calibrated parameter 23, i.e. MPI1 (all values except from O-7 are slightly above 0.5) cf. Table 6.3, and the low PI ($S_1/(S_1+S_2)$) ratios (see Table 6.5) which reflect that only a small portion of petroleum from the total potential has been generated. Parameter 25 i.e. the vitrinite reflectivity calibrated parameter based on MDR (see Table 6.3) gives higher estimates of vitrinite reflectivity compared to the other vitrinite reflectivity parameters (22-24) for the source rock bitumen samples. However, it is clear that the values in the range of 0.65%R_m to 0.90%R_m seen from parameter 25 and also the Ts/(Ts+Tm) ratios in general (see Figure 7.5) overestimates the maturity since those values corresponds to the main oil generating phase i.e. significant amounts of petroleum should have been generated which is not the case as seen from the low PI (S1/S1+S2), the low MPI values in the range from 0.52%R_c to 0.69%R_c and also the low MPDF i.e. parameter 24 values in the range from 0.12%R_o to 0.57%R_o

The unusual low vitrinite reflectivity values from parameter 24 are shown in Figure 7.6 and Figure 7.8 where the values are plotted against parameter 23 and parameter 25 respectively, and result from the low phenanthrene abundance compared to the methylphenanthrenes as illustrated in the former figure, as the only major difference between parameter 24 and parameter 23 is the inclusion of phenanthrene in addition to the methylphenanthrenes for the former parameter (see parameter 19 and parameter 20 in section 5.2.6). Also, the vitrinite reflectivity parameters shows good correlation in the maturity range of 0.7%-1.3% vitrintite reflectance, while irregularities has been reported in the early oil generating phase i.e. maturity of 0.5%-0.7% vitrintite reflectance (Radke et al., 1986) which is consistent with the poor correlation between the vitrinite reflectivity parameters observed for the source rock bitumen samples (see Figure 7.6, Figure 7.7 and Figure 7.8).

Furthermore, it has been reported that the phenanthrene concentration is influenced by the redox potential of the source rock, and is encriched relative to methylphenanthrenes in secondary oxidation processes by metal-bearing solutions in the source rock matrix (Püttmann et al., 1989) and also from lower microbial degradation (Budzinski et al., 2000) and lower TOC values (Szczerba and Rospondek, 2010). Low phenanthrene abundances are associated with highly reducing facies and are caused by ionic or radical demethylation reactions (Szcerba and Rospondek, 2010). The observed low abundance of phenanthrenes in the source rock bitumen samples is thus a result from

the highly reducing facies which is inferred from the indication of a reducing facies type in Figure 7.4 and also by the very low Pr/Ph ratios (see Table 6.1).

7.3.2 The maturity of the reference oil, NSO-1

The NSO-1 oil has a comparable 22S/(22S+22R) homohopane ratio to the source rock bitumen samples from the Orkneys (see Table 6.2), and the value is below the equilibrium range. However, parameter 22, 23 and 24 clearly shows that NSO-1 is more mature than the source rock bitumen samples (see Table 6.3), indicated from the values in the range of 0.81-0.89 corresponding to vitrinite reflectivity, and thus suggesting maturity of NSO-1 corresponding to the middle of the oil window. Parameter 1 and 7 clearly suggests otherwise, but as those two parameters are affected by type of organic matter in the source rock, their validity is thus low in this case.

Parameter 25 shows slightly lower maturity (0.7%R_c) compared to the other vitrinite calibrated parameters (see Figure 7.7 and Figure 7.8 for comparison with parameter 23 and parameter 24 respectively), but it is based on parameter 21 which is also affected by organic facies type. This is reflected in the higher values for the source rock bitumen samples compared to NSO-1 as the source rock bitumen samples are related to another type of organofacies i.e lacustrine. The facies influence on parameter 21 and 25 which causes the low maturity estimates is confirmed from the fact that the NSO-1 oil has migrated from a source rock (the sandstone reservoir has no source rock potential to generate the petroleum) i.e. the source rock has reached sufficient maturity for expelling petroleum, unlike the source rock bitumen samples from the Orkneys.

7.3.3 The maturity of the oil from the Beatrice Field

The Beatrice oil has reached the isomerization equilibrium of homohopanes, i.e. the 22S/(22S+22R) homohopane ratio which is 0.59 (see Table 6.2) is in the equilibrium range of 0.57-0.62. The homohopane (parameter 3) versus MPDF (parameter 20) plot (see Figure 7.5) indicate only a slight maturity difference between the oil from Beatrice and the NSO-1 oil. The Beatrice oil scores slightly lower overall compared to NSO-1 regarding the vitrinite reflectivity values based on the parameters 22-24 which points towards the former being slightly less mature than the latter while parameter 25 indicates otherwise (see Figure 7.6, Figure 7.7 and Figure 7.8 for comparison of parameter 23 versus parameter 24, parameter 25 versus parameter 23 and parameter 25 versus parameter 24 respectively). The Pr/n-C17 versus Ph/n-C18 plot (see Figure 7.4) also indicates that the Beatrice oil is more mature than the NSO-1 oil, as the former shows much lower ratios of pristane and phytane

relative to n-C17 and n-C18 respectively but the low abundance of isoprenoids is most likely diagnostic for the organofacies related to this oil. To summarize, the Beatrice oil shows about the same maturity as NSO-1 i.e. corresponding to the middle of the oil zone, and is perhaps slightly less mature compared to the latter, and the observed differences in facies parameters between those oils should not be significantly influenced by effects from maturity.

7.3.4 The maturities of the bitumen extracts from well 6609/11-1

The Ts/(Ts+Tm) ratios of the A-1 to A-5 bitumen samples suggest maturities corresponding to the early oil window (see Figure 7.9), but the 22S/(22S+22R) homohopane parameter values has reached equilibration values of 0.57-0.62 for all the samples except from A-1 (0.51) and A-5 (0.55) (see Table 6.2), suggesting that they have reached maturities corresponding to at least the middle of the oil zone. This is supported by parameter 22 (MPR) which shows values corresponding to vitrinite reflectivity in the range of 0.93%R_m to 1.09%R_m, and thus also suggesting that A-1 and A-5 shows maturites corresponding to the middle of the oil window (see Figure 5.11). When compared to the NSO-1 oil, the values for A-1 to A-5 from parameter 22 and parameter 25 (MDR) are slightly higher in general, while the values from parameter 23 (MPI) are slightly lower and the values from parameter 24 (MPDF) are on par (see Table 6.3). The higher 22S/(22S+22R) ratio and the slightly higher trend of the vitrinite calibrated parameters in general suggests that the bitumen samples from well 6609/11-1 are slightly more mature than NSO-1.

The Pr/n-C17 versus Ph/n-C18 plot (see Figure 7.4) shows a wide variation within well 6609/11-1 and both the lowest and highest Pr/n-C17 and Ph/n-C18 ratios of the Helgeland Basin samples originate from bitumen samples which represents this well. The isoprenoid intensities relative to those of the n-alkanes of A-5, are comparable to those observed in the Beatrice oil and are of lower magnitude than all the other samples from the Helgeland Basin, indicating a much high maturity for this sample, and this thus conflicts with the other maturity parameters mentioned. A-1 and A-4 is on the other side off the scale and they are both characterized by a relatively high abundance of isoprenoids relative to the n-alkanes, which suggests much lower maturies than the maturities indicated by other parameters e.g. the homohopane isomerization ratio. Also the phenanthrene abundances are high in A-1 and A-4 as seen from the underestimation of maturities from parameter 23 relative to parameter 24 (see Figure 7.6). The low intensity of n-alkanes and isoprenoids relative to the hump i.e. background bleeding in the GC-FID chromatograms suggests that those two samples contain low concentrations of petroleum, and this is most likely responsible for the high

values, as small changes in abundance of isoprenoids or n-alkanes would greatly affect the ratios. The bitumen samples A-2, A-3 and A-5 have comparable maturity values from parameter 23 and parameter 24, suggesting moderate abundance of phenanthrene relative to the mehtylphenanthrenes. Also, the vitrinite calibrated parameter 25 shows in general approximately the same maturity for A-2, A-3 and A-5 (see Figure 7.7 and Figure 7.8). It is noticed that only the A-2 and A-5 bitumen samples, which are interpreted to be related to the Beatrice oil (see section 7.7) shares almost the same relation concerning parameter 23 versus parameter 25 and also very similar relations concerning parameter 23 versus parameter 24 and parameter 24 versus parameter 25.

7.3.5 The maturities of the bitumen extracts from well 6610/7-1 upper section

The bitumen samples B-1 to B-3 which represents the upper section of well 6610/7-1 are characterized by extremely low Ts/(Ts+Tm) values (0.26 to 0.28, see Table 6.2) and low diasteranes/(diasteranes+steranes) ratios, and both parameters indicate that B-1 to B-3 are immature (see Figure 7.9). However, as the bitumen do not originate from the sandstone samples, it is clear that the former and latter parameter do not provide maturity estimates which are realistic, but a potential for in-situ contamination exists. Also, both the Ts/(Ts+Tm) and the diasteranes/(diasteranes+steranes) maturity parameters are affected by facies type and oils derived from carbonate facies tend to score low in both ratios. The homohopane isomerization is on the brink of equilibrium for B-1 i.e. the 22S/(22S+22R) homohopane parameter is 0.57, has reached equilibrium for B-2 (0.58) and is not equilibrated for B-3 (0.55). However, it is indicated that all the samples has reached maturities corresponding to the middle of the oil zone by the vitrinite reflectivity calibrated parameters 22-24, while parameter 25 shows slightly lower values of (0.65%R_c to 0.70%R_c) and is on par with NSO-1 (0.70%R_c), cf. Table 6.3. Parameter 25 is clearly underestimating the maturity which is illustrated in the plot of parameter 24 versus parameter 25 (see Figure 7.8), as maturities necessary for expulsion of the migrated petroleum from the parental source rocks corresponds typically to avitrinite reflectivity value of at least 0.8%R_o (pers. comm. Karlsen, 2015).

The parameters 22-24 and also parameter 3 i.e the (22S/22S+22R) homohopane ratio suggests that B-1, B-2 and B-3 are slightly more mature than NSO-1. On the contrary, the Pr/n-C17 to Ph/n-C18 plot suggests that B-1 to B-3 could be less mature than NSO-1 (see Figure 7.4) but this observation could also indicate biodegradation. However, the difference shown in Figure 7.4 is not substantial and the GC-FID chromatograms for B-1 to B-3 (see Figure 6.22, Figure 6.23, Figure 6.24 and

Appendix A) show no significant abundance of UCM, meaning that the biodegradation should not be very significant.

7.3.6 The maturities of the bitumen extracts from well 6610/7-1 lower section

The bitumen samples B-4 to B-7 which represents the lower section of well 6610/7-1 are like the samples from the upper section of the same well characterized by low Ts/(Ts+Tm) ratios and low diasteranes/(diasteranes + steranes) ratios, suggesting that they are immature, and thus underestimates the maturity (see Figure 7.9). As earlier discussed in section 7.3.5, those maturity parameters are affected by the type of facies, and the observed underestimations from those parameters are also diagnostic for oils which are derived from carbonate source rocks. All the four samples have reached the equilibrium range of the 22S/(22S+22R) homohopane ratio (see Table 6.2), suggesting maturities for those samples corresponding to the main oil generating phase. Parameter 22 (all values above 0.8%R_m) supports this observation, as does parameter 23 in general (values above 0.8%R_c exept from B-7), cf. Table 6.3. The parameters 22-24 also suggests that the lower section of well 6610/7-1 is slightly more mature than the upper section, supported by 22S/(22S+22R) ratios which are more clearly into the equilibration range of isomerization. Also the Pr/n-C17 vs Ph/n-C18 plot (see Figure 7.4) indicates higher maturity for the lower section of well 6610/7-1 compared to the upper section of the same well. The opposite trend for B-4 to B-7 is shown as compared to the upper section, regarding the parameter 23 versus parameter 24 plot (see Figure 7.6). Although both parameter 23 and parameter 24 shows lower values for B-4 to B-7 than B-1 to B-3 overall, the relative abundance of phenanthrene relative to the methylphenanthrenes is higher for B-4 to B-7 compared to B-1 to B-3, resulting in a greater underestimation of maturity from parameter 23 relative to parameter 24. The phenanthrene abundance is related to the redox potential of the sedimentary rock (see maturity discussion of source rocks, section 7.3.1), and the much higher oxidizing potential of the sedimentary rocks related to B-4 to B-7 compared to e.g the source rock bitumen samples and also higher oxidizing potential compared to B-1 to B-3, is also shown in the higher Pr/Ph ratios (see Table 6.1) and also the plot in Figure 7.4. The underestimation of vitrinite reflectivity from parameter 23 is also shown in the plot versus parameter 25 (see Figure 7.7). The plot of parameter 25 versus parameter 24 on the other hand shows good correlation for B-4 to B-7 (see Figure 7.8).

7.3.7 The maturities of the bitumen extracts from well 6609/5-1

Both C-1 and C-2 which represents well 6609/5-1 show maturities corresponding to the middle of the oil window, as suggested from the equilibrated isomerization of homohopanes i.e. the 22S/(22S+22R) ratio (parameter 3, see Table 6.2), and also parameter 22 i.e. MPR (values above 0.8%R_m, see Table 6.3). The Ts/(Ts + Tm) ratio (see Figure 7.9) indicates lower maturities which corresponding to the early oil window. Interestingly, parameter 24 points towards C-1 being more mature than C-2, while in parameter 25 the opposite is shown (see Figure 7.8). However, due to contamination of C-2 (see section 7.10.1), the peaks in the m/z = 178, m/z 192, m/z = 198 chromatograms (see Figure 6.30 and appendix B) are not well resolved and are responsible for this observed difference. Also both parameter 23 and parameter 24 are clearly underestimating the maturity for C-2 (see Figure 7.6). As a consequence, neither of the vitrinite reflectivity calibrated parameters i.e. MPR, MPI1, MPDF and MDR of C-2 is reliable and can thus not be used for maturity assessment of well 6609/5-1. Also observed from Figure 7.6 is the clear underestimation of maturity from parameter 23 relative to parameter 24 for C-1 i.e C-1 has a high abundance of phenanthrene. The high phenanthrene abundance which indicates oxidizing conditions conflicts however with the low Pr/Ph (0.90) ratio and also the Pr/n-C17 vs Ph/n-C18 ratio (see Figure 7.4) which indicates more reducing conditions. The reasons behind those conflicting observations will be further discussed in section 7.10.

The C-1 and C-2 bitumen samples are slightly more mature than NSO-1, based on parameter 3 and the Pr/n-C17 versus Ph/n-C18 plot (see Figure 7.4), but the high MPDF ratio of C-1 clearly classifies this sample as more mature (see Figure 7.5).

7.3.8 Summary of the maturity discussion

The maturity of the samples is ranked from the lowest to the highest: The Orkney source rocks - NSO-1 - Beatrice - 6609/11-1 - Judy - 6610/7-1 upper section - 6610/7-1 lower section - 6609/5-1 - Embla.

The maturity plot of parameter 20 versus parameter 3 (Figure 7.5) shows the maturity of the samples relative to each other, and represents the overall maturity classification fairly well.

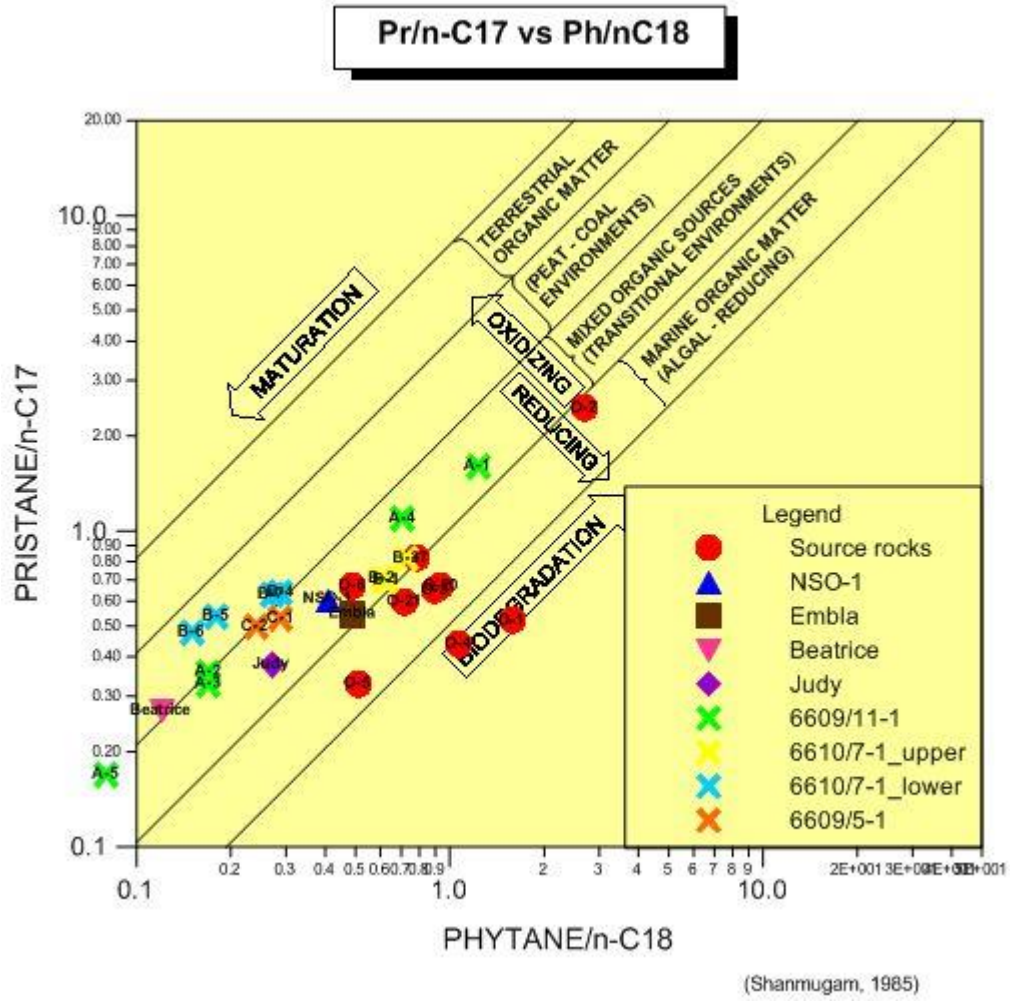

Figure 7.4: Plot of Pr/n-C17 versus Ph/n-C18 (see Table 6.1 for values) relative to maturity, biodegradation and depositional environments. Note that the source rock bitumen samples in general plot in a highly reducing organofacies, which is also related to the low phenanthrene abundance in those samples. The Beatrice oil shows an unusual low Pr/n-C17 ratio and Ph/n-C18 ratio which may be related to the facies type and it is also noted that the A-5 bitumen sample and to some extent also A-2 and A-3 share this pattern which could indicate that the Beatrice oil and those two bitumen samples are related. Furthermore, the positive indentification of β-carotane in A-2 and A-5 which strongly indicates a relation to lacustrine Middle Devonian source rocks supports that the unusually low Pr/n-C17 and Ph/n-C18 ratios are linked to this type of organofacies.

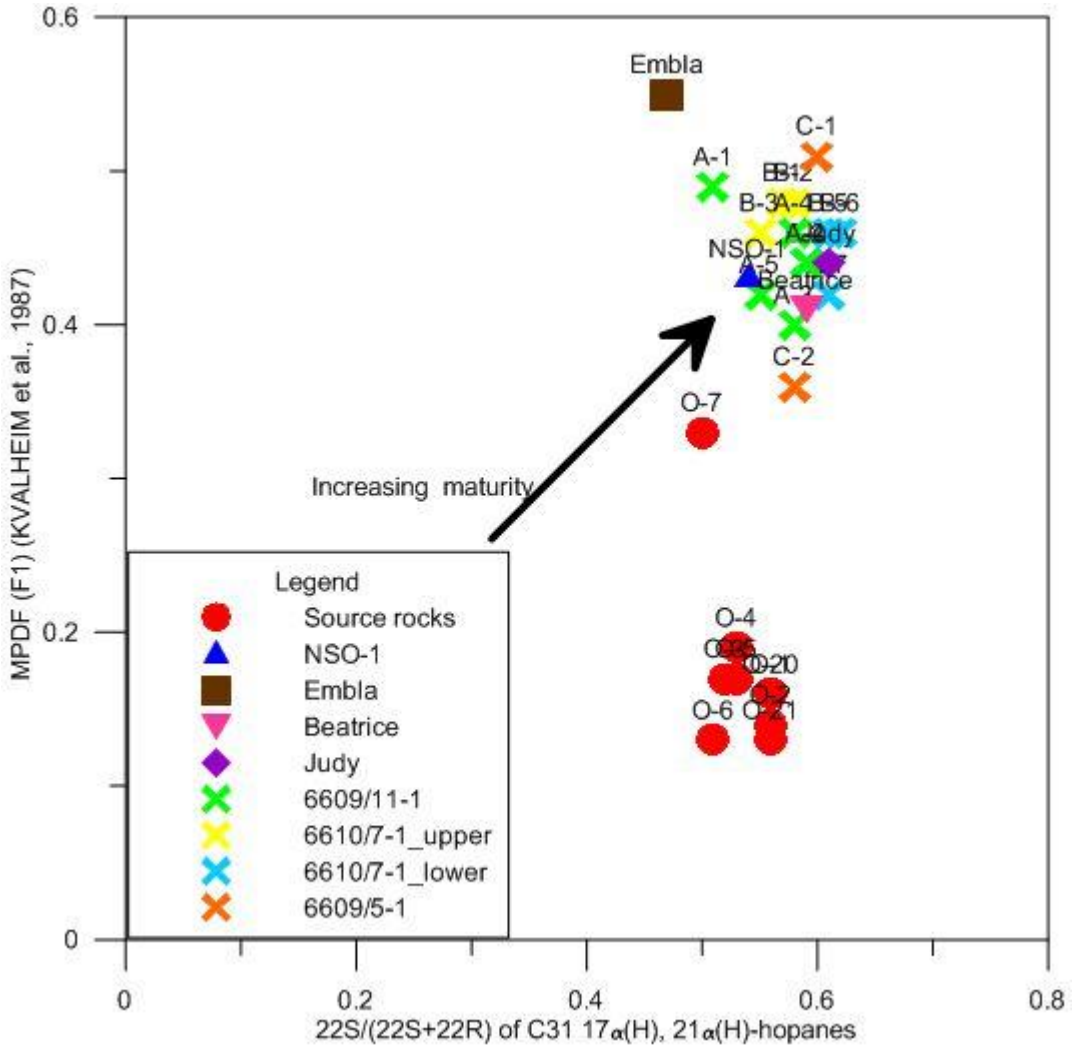

Figure 7.5: Maturity plot based on values from parameter 20 i.e. MPDF (see Table 6.3) and parameter 3 i.e. 22S/(22S+22R) of C31 17α(H), 21α (H)-hopanes (see Table 6.2) from GC-MS. Notice how well the maturity differences indicated in this figure coincides with the overall maturity classification of the samples relative to each other and it is clear that the source rock bitumen samples from the Orkney are significantly less mature than the oils and also the bitumen samples from the Helgeland Basin area.

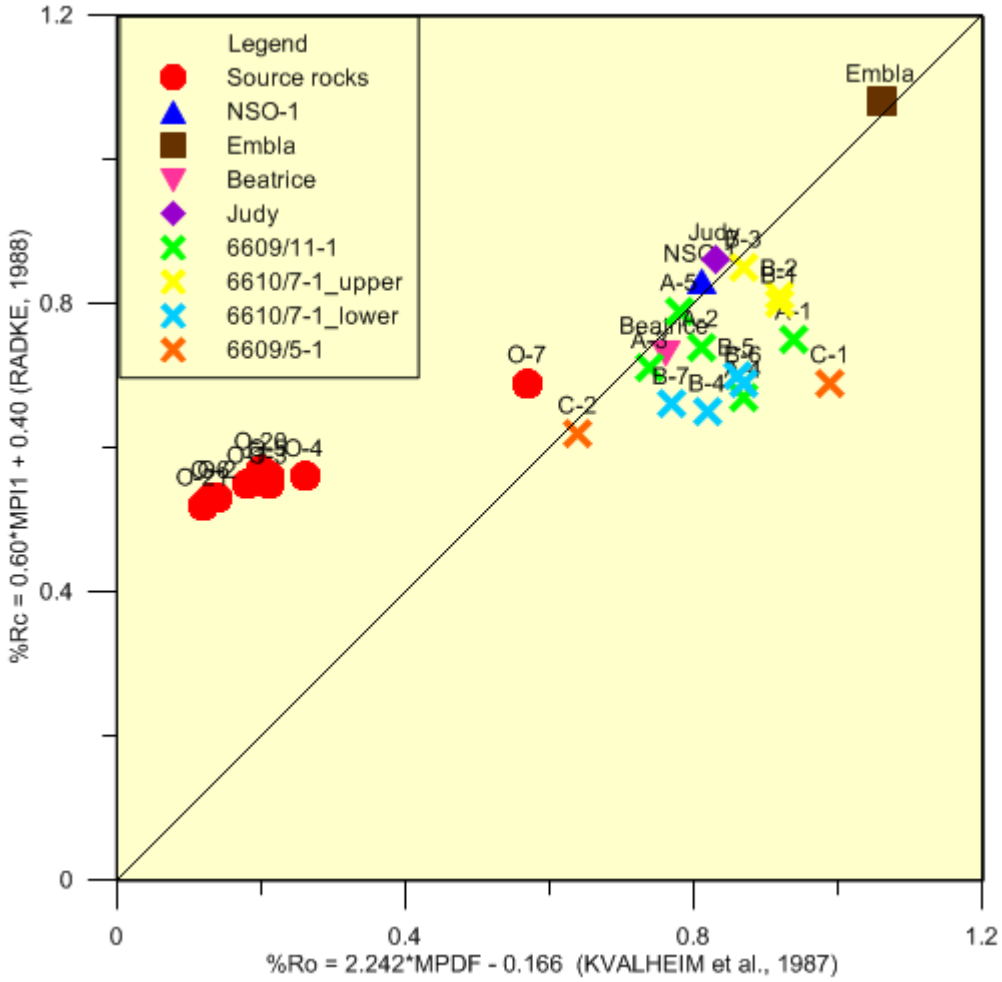

Figure 7.6: Plot of the vitrinite reflectivity calibrated parameters 23 (MPI1) versus 24 (MPDF). Notice the underestimation of the maturites of the source rock bitumen extracts from parameter 23 relative to 24 and the slightly opposite trend for the Helgeland Basin bitumen samples. The maturity estimates of all the oil samples i.e. NSO-1, Judy, Embla and Beatrice are almost identical from parameter 23 and parameter 24.

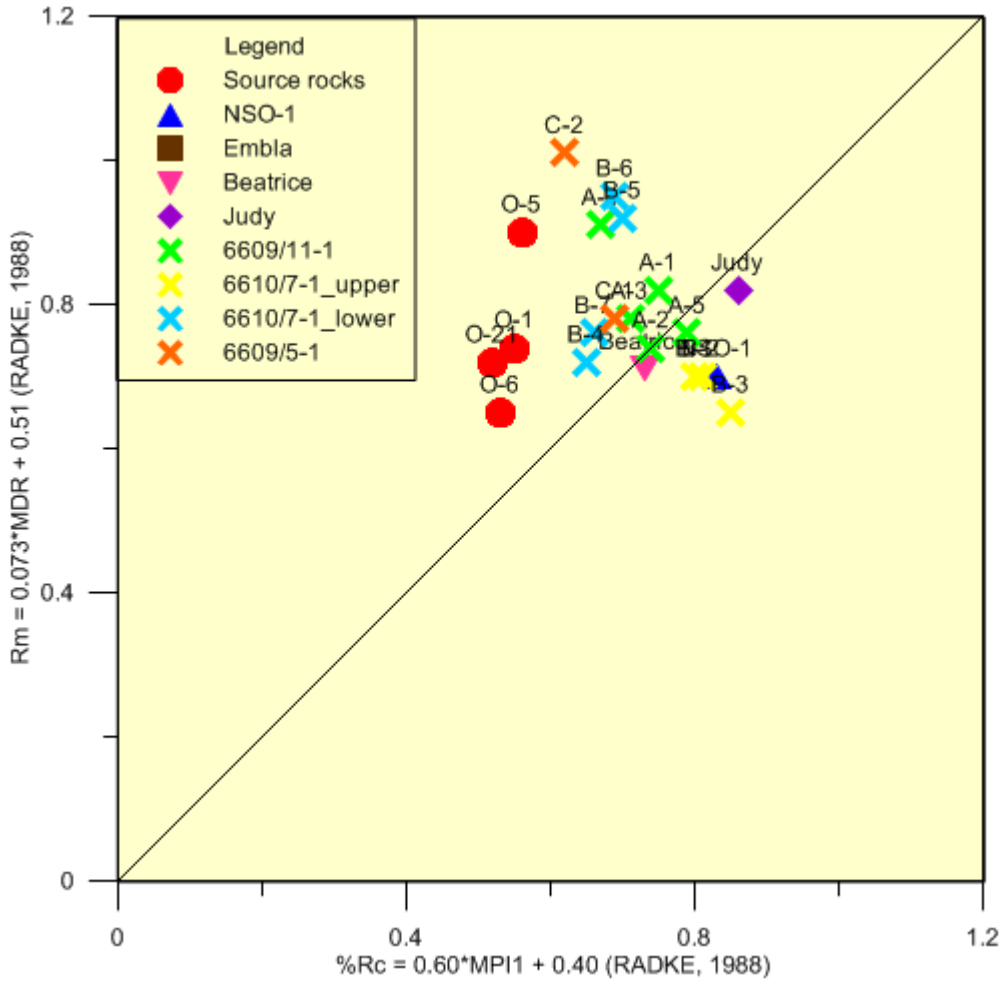

Figure 7.7: Plot of the vitrinite reflectivity calibrated parameters 25 (MDR) versus 23 (MPI). Notice the underestimation of the maturites for the source rock bitumen extracts from parameter 25 relative to 23 which is also seen in the Helgeland Basin bitumen samples except from those representing the upper section of well 6610/7-1. Four of the source rock bitumen samples i.e. O-2, O-3, O-4, O-7 and O-20 are not seen in this plot due to lack of the 2 and 3-methyldibenzothiophene isomers (the denominator in the parameter 21ratio which parameter 25 is based on equals 0). The Embla oil is not seen in this plot due to its extreme parameter 25 value of 1.94.

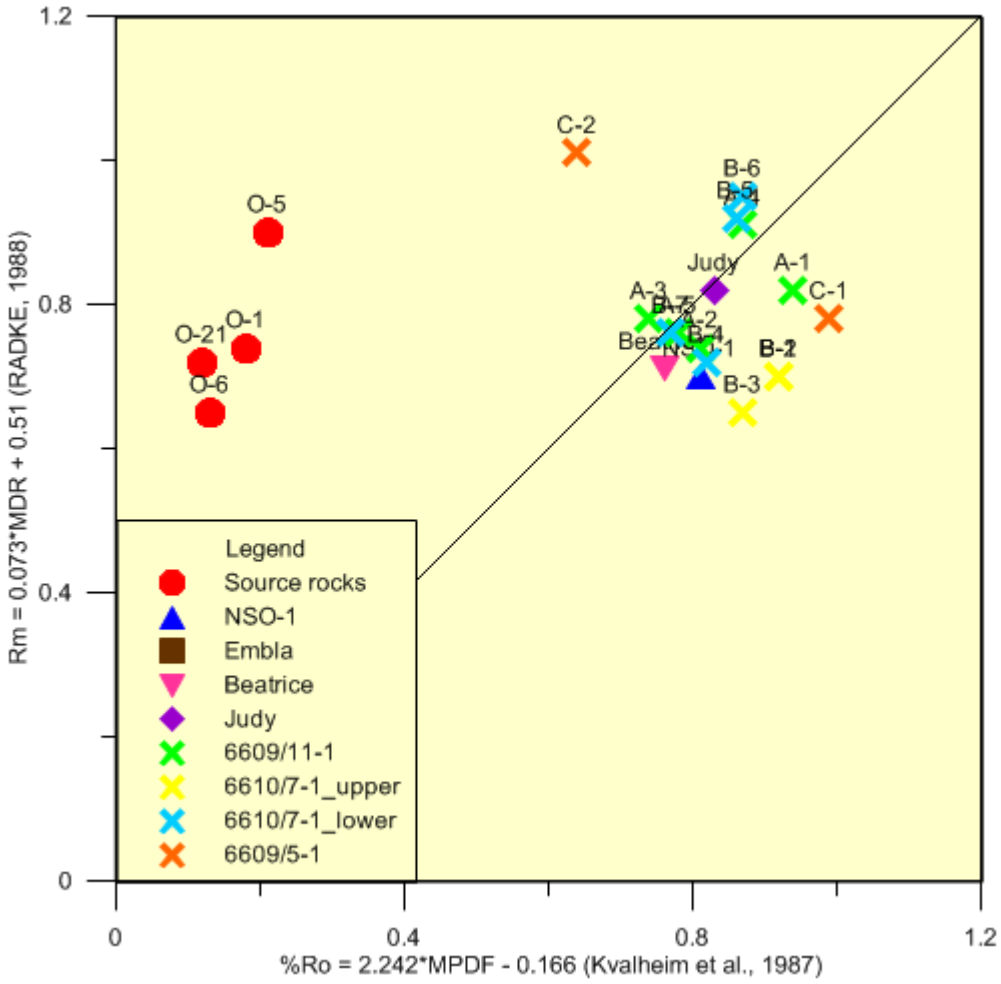

Figure 7.8: Plot of the vitrinite reflectivity calibrated parameters 25 (MDR) versus 24 (MPDF). Notice the underestimation of the maturites of the source rock bitumen extracts from parameter 24 relative to 25. Four of the source rock bitumen samples i.e. O-2, O-3, O-4, O-7 and O-20 are not seen in this plot due to lack of the 2 and 3-methyldibenzothiophene isomers (the denominator in parameter 21 which parameter 25 is based on equals 0). The Embla oil is not seen in this plot due to its extreme parameter 25 value of 1.94.

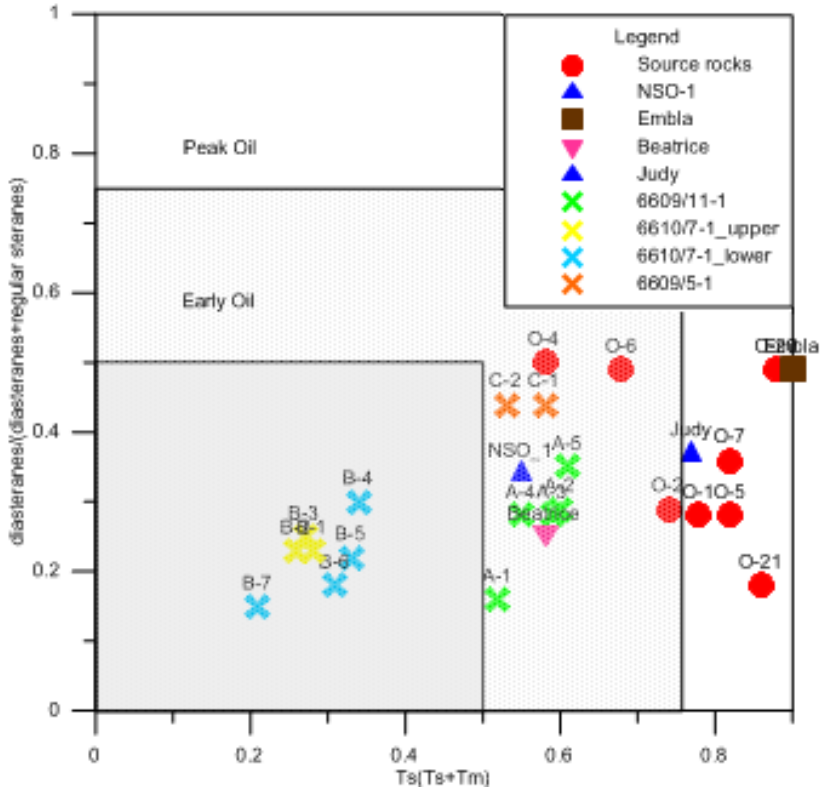

Figure 7.9: Maturity plot based on parameter 12 i.e. diasteranes/(diasteranes+regular steranes) versus parameter 1 i.e. Ts(Ts+Tm) (see Table 6.2), and corresponding values for the onset and peak of the oil window. Notice how parameter 1 and 12 underestimates the maturity for all the samples representing well 6610/7-1. Parameter 1 clearly overestimates the maturity of the source rock bitumen samples (excluding O-4 and O-6), as the S1 value from the TOC and Rock-Eval analysis (see section 7.2) shows that the source rocks from the Orkneys up until present day have generated only small amounts of petroleum. However, unusual high Ts/(Ts+Tm) values for source rock bitmens are also related to hypersaline organofacies. As the Orkney source rock bitumen samples, excluding O-4 and O-6 and probably also O-3 (although not shown in the figure due to no data from parameter 12) are related to hypersaline organofacies as seen from e.g. the in general high gammacerane index values (0.91 to 2.57) and very low Pr/Ph ratios (0.27 to 0.78), thus the observed high Ts/(Ts+Tm) values result from the facies type. The gammacerane index of O-4 and O-6 are clearly lower i.e. 0.26 and 0.36, suggesting that those source rocks are not related to hypersaline organofacies, and this most likely causes the Ts/(Ts+Tm) ratio to be lower in comparison to those which are related to the hypersaline organofacies despite the similar maturities.

7.3.9 Challenges related to oil-source rock correlations due to effects from maturity

Many of the parameters which are used for estimating organofacies and depositional environments are also affected by maturation (see chapter 5 for explanation of the different parameters). Therefore, precautions have to be taken when investigating potential relationships between oils and source rock bitumen samples with different maturity. When determining the maturity of the source rock bitumen samples from the Orkneys relative to the bitumen samples from the Helgeland Basin area and the NSO-1 oil, it is important to keep in mind that the type of facies does also affect

some of the maturity parameters and thus limiting the parameter usefulness when comparing samples that does not originate from related facies, and co-sourcing will also cause complications.

The migrated petroleum found in reservoirs represents a range of maturity as the migration of petroleum into the reservoir is continuous during the ongoing maturation of the source rock kitchen, and since the geochemical signature of the petroleum changes i.e. different molecules are formed at different maturity stages, the petroleum composition may thus not represent the composition of the parental source rock with a given maturity level (Peters et al., 2005).

7.4 Overview of organic facies paramters, i.e. main diagnostic markers of the possible source rocks in the Helgeland Basin

7.4.1 The Middle Devonian Orcadian Basin equivalent

A possible source rock in the Helgeland Basin is an equivalent to the Middle Devonian source rocks present in the Orcadian Basin (see section 1.2). The most diagnostic features of the Middle Devonian lacustrine lake deposits are presence of carotanes, low δ13C isotope values i.e. isotopically light values (values below -31$^{o}/_{oo}$ are common, see Table 6.6 and Figure 7.1), and also a C26/C25 tricyclic terpane ratio of at least 1.1 (see Table 6.4) is common. As seen from the Orkney bitumen samples, low Pr/Ph ratios (seems diagnostic for the lacustrine Middle Devonian organofacies. However, the relatively high Pr/Ph ratio of the Beatrice oil (2.42) does limit the usefulness of Pr/Ph for distinguishing the Middle Devonian lacustrine source from marine and terrestrial sources , although it is important to remember that the Beatrice oil was not solely sourced from the Middle Devonian source as it has a second Middle Jurassic source with a higher Pr/Ph ratio (Pr/Ph ratio of 1.38, Peters et al.,(1989)) which could partly explain the elevated Pr/Ph ratio of this oil compared to the Orkney bitumen samples.

7.4.2 The Late Jurassic Kimmeridge equivalent

The Late Jurassic Kimmeridge equivalent is the most common source for petroleum on the NCS (e.g. Ravnås et al., 2000), and can thus not be ruled out when it comes to potential source rocks on the shelf, and its existence is physically proven in the Helgeland Basin i.e. an immature source rock interval corresponding to the Kimmeridge equivalent was encountered in well 6610/7-1 (Schou et al., 1983). Some of the most diagnostic markers representing the Late Jurassic Kimmeridge source

rock equivalent are the presence of C30 steranes, 28-30-bisnorhopane (BNH) and 25-28-30-trisnorhopane (TNH) (Peters et al., 1989).

7.4.3 The main diagnostic biomarkers for indicating positive relation to Middle Devonian or Late Jurassic source rocks

γ-carotane and/or β-carotane were in this study found to be present in the GC-FID chromatogram and/or the GC-MS chromatograms from all of the Middle Devonian source rock bitumen samples from the Orkneys and the Beatrice oil which is sourced from Middle Devonian (see section 6.1 and 6.2). Thus, the presence of γ and/or β-carotane is diagnostic of equivalents to the parental lacustrine Middle Devonian source rocks. The C26/C25 tricyclic terpane ratio is relatively high, above 1.1 for the Orkney source rock bitumen samples (except from O-4) and the Beatrice oil, and the C31 22R/C30 hopane ratio is below 0.25. Especially the former, but also the latter parameter is helpful for identification of Middle Devonian sourced oils as the values differ from typical worldwide marine oils (see Figure 5.14) and the NSO-1 oil (C26/C25 of 0.81 and C31 22R/C30 hopane of 0.37). The tricyclic terpane abundance (parameter 7, Table 6.2) is salinity driven and is also affected by marine influence (see tricyclic terpane discussion, section 7.5), and it is observed that the O-6 source rock bitumen sample and especially the O-4 source rock bitumen sample shows low abundance of the tricyclic terpane compounds compared to other Orkney source rock bitumen samples, although the abundance is higher than in the Beatrice oil. O-6 and O-4 also shows the two lowest C26/C25 values of the source rock bitumen samples (1.13 and 0.82 respectively), and shows values closer to the those from the bulk of marine oils (see Figure 5.14). High hopane/sterane ratios are common, as seen in the Beatrice oil and in the Orkney samples in general, however O-1, O-2 and especially O-5 shows low ratios. Despite the great observed variations in the hopane/sterane ratio seen for the source rock bitumen samples, high hopane/sterane ratios are more diagnostic for the lacustrine Middle Devonian organofacies. It is noted that commercial quantities of oils such as the oil in the Beatrice Field is always sourced from a large stratigraphic interval of source rocks which gives mean values of biomarker parameters, while individual source rock lamina will represent only a small stratigrahic interval. Thus, the Beatrice oil gives a more certain general representation of the typical hopane/sterane ratio for the Middle Devonian organofacies than only a few (nine) outcrop source rock samples.

The main diagnostic biomarkers used to indicate marine derived Late Jurassic Kimmeridge equivalent source rocks are the TNH, BNH and the C30 steranes (e.g. Peters et al., 1989). Despite that the BNH compound is considered as being a common marker for Late Jurassic Kimmeridge

derived extracts and oils e.g. as seen in the NSO-1 oil (see Figure 5.4), variations within the parental source rocks may occur as reported from e.g. Justwan et al., (2005) as the samples collected from the Southern Viking Graben contained none or only small amounts of BNH in the lower part of the Draupne Formation i.e. the Kimmeridge equivalent in the North Sea while the upper part of the Draupne Formation on the other hand showed the more common characteristically high abundance of BNH. The same observations were reported e.g. from the Great Balder Area and the lower section of the Draupne formation related to restricted marine syn-rift setting is more dominated by terrestrially derived kerogen type III organic matter than the upper section related to post-rift open marine settings and mostly comprises organic matter of kerogen type II quality (Justwan and Dahl, 2005).This enlightens that the BNH compound is not a specific biomarker for the Late Jurassic Kimmeridge equivalent source rocks in general, but is for the most confined to the source rock intervals which are related to the open marine organofacies.

The strength of the BNH, TNH and C30 steranes markers are that unlike as seen in the marine Late Jurassic Kimmeridge equivalent, the Middle Devonian source rocks shows only insignificant abundances, and it is thus also possible to indicate from the presence of those markers a second source rock contribution from the marine Late Jurassic Kimmeridge equivalent if a Middle Devonian source already has been ascertained e.g. from the presense of carotanes. Also, a characteristic concave algal dominated n-alkane envelope (see Figure 5.1) can be seen in the GC-FID chromatogram for marine derived non-biodegraded oils.

7.4.4 Possible coal derived Lower Carboniferous source rock

Since the oldest encountered formations in the Helgeland Basin area are of Late Permian age (see section 1.2), it is either proved or disproved the presence of Carboniferous strata with possible source rock potential. However, the presence of pre-Permian strata including the Carboniferous in the Norwegian Sea and perhaps also in the Helgeland Basin is presumed based on seismic data and by correlation from East Greenland (Bukovics and Ziegler, 1985). Thus, it is a possibility for the presence of coal-bearing Carboniferous strata with oil generative potential in the Helgeland Basin, like the coals of Early Carboniferous age which have been encountered e.g. on the Finnmark Platform in the southern Barents Sea (van Koeverden et al., 2010).

The diagnostic features of the Lower Carboniferous coal derived source rocks are the low abundance of C27 cholestanes as compared to C28 and C29 cholestanes i.e. below 20%, high Pr/Ph

ratios ranging from 3-7), indications of oxic depositional conditions from the Pr/n-C17 versus Ph/n-C18 plot and high waxiness i.e. abundance of long chained n-alkanes (van Koeverden et al., 2010).

7.4.5 Possible Late Permian source rock

Bugge et al. (2002) studied two shallow core successions in the eastern margin of the Trøndelag platform close to mainland Norway and east off the Helgeland Basin area (see Figure 3.2) and detected two laminated mudstone intervals of Late Permian age with source rock potential. The two mudstone intervals could possibly be correlated with two mudstone intervals found in the Ravnefjeld Formation in East Greenland (Bugge et al., 2002). There is also a possibility that a more mature Late Permian source rock interval could act as a source rock kitchen if present at greater depths in the Helgeland Basin relative to the marginally mature Late Permian source rock (R_o = 0.5% to 0.6%) that was detected in the shallow core successions. The proximity of the shallow cores to mainland Norway is reflected in the terrestrial character of the laminated mudstones and the low to moderate quality of the organic matter (HI average of 114mg/g TOC and 185mg/g TOC in the lower and upper interval respectively), but the quality may improve in the more distal parts of the sedimentary basin (Bugge et al., 2002) e.g. in the Helgeland Basin.

The Late Permian source rock encountered in the shallow cores are characterized by a high enrichment in the δ C13 isotope (-28.7$^{o}/_{oo}$ to -24.8$^{o}/_{oo}$), Pr/Ph ratios in the range of 1.8 to 2.6, a slight predominance of C29 cholestanes over C27 cholestanes and also a slight predominance of 27Tm over 27Ts. Another diagnostic feature is the slight odd n-alkane predominance and the low waxiness i.e. low abundance of long-chained n-alkanes, and high to very high relative concentration of tricyclic terpanes, and among them among them the 28/3 (“u”) and 29/3 (“v”) isomers (cf. Bugge et al., 2002) and as such is there no ground for correlation to the Helgeland Basin bitumen samples studied in this thesis.

7.4.6 Possible Lower Triassic source rock

Thin intervals with TOC up to 2.8wt % and HI up to 450mg/g were detected in a Lower Triassic turbidite unit in the shallow core succession in the eastern margin of the Trøndelag platform close to mainland Norway and east from the Helgeland Basin area (cf. Bugge et al., 2002). From the kerogen composition, Bugge et al., (2002) suggested a marine depositional setting with a close proximity to the coast. Bugge et al., (2002) mentioned that for the Lower Triassic being a capable for generating petroleum in the area, the thin organic rich intervals of 0.5cm to 1.5cm would have

to thicken into the more distal parts of the basin, but there is no evidence for such thickening. Due to the apparent non-thickening of the Lower Triassic source rocks, it should be of insignificant importance in the Helgeland Basin, and based on this assumption and the lack of geochemical data, no further investigations of this particular source rock will be performed in this thesis.

7.4.7 Possible coal derived Lower and Middle Jurassic source rocks

Lower Jurassic coaly intervals with source rock potential from the Åre Formation have been encountered in well 6609/11-1 (NPD, 2015a) and in well 6610/7-1 (cf. Schou et al 1983), which is thus physical proof for the existence of this source rock type in the Helgeland Basin. The two sample cuttings from the depths of 3035m – 3050m and 3148m from well 6610/7-1 represents the Lower Jurassic coals and are characterized by very high Pr/Ph ratios i.e. ratios of 5.6 to 6.1 respectively and a high waxiness (see Figure 7.10). Furthermore, the δ13C isotope values of the Åre Formation coals from well 6610/7-1 are in the range from -28.5/$_{oo}$ to -29.0/$_{oo}$ (SAT) and -26.6/$_{oo}$ to -28.0/$_{oo}$ (ARO) and there is a strong predominance of the C29 cholestanes from the m/z = 218 chromatogram of the cuttings at depth 3050m (c.f. Schou et al., 1983).

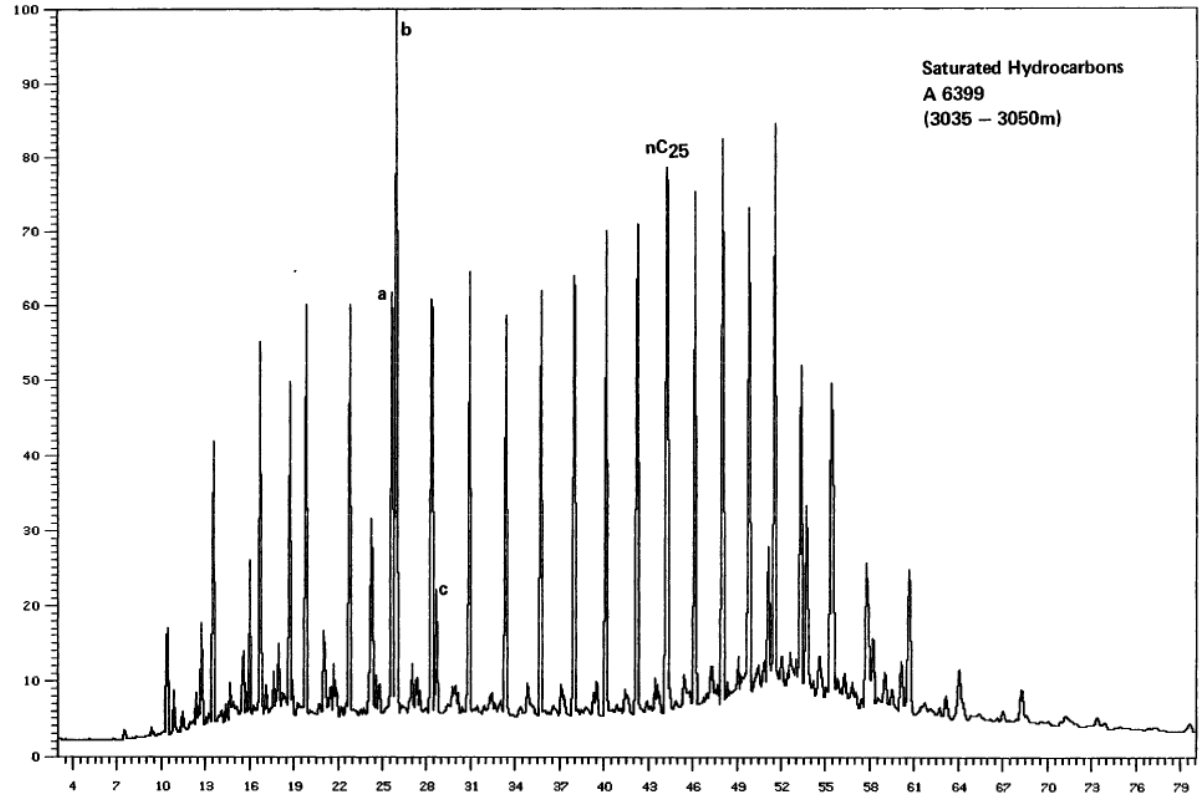

Figure 7.10: GC-FID chromatogram for Lower Jurassic coals from depth-interval of 3035m to 3050m in well 6610/7-1 (from Schou et al., 1983). Notice the high waxiness of this coal-derived sample and the very high Pr/Ph ratio of 5.6 (pristane is labelled as peak b and phytane is labelled as peak c)

Middle Jurassic coals with source rock potentials have been encountered in northeastern Greenland and also on mainland Norway i.e. the Kvæfjord coal e.g. on the Andøya Island in the Nordland county (Petersen et al, 2013), and have proven to contribute commercial quantities of petroleum in the UK-sector i.e .the Middle Jurassic Brora coals acts as a co-source for the Beatrice oil (Peters et al., 1989). Thus it is also possible that coal derived source rocks from the Middle Jurassic could be present also in the Helgeland Basin, however as Middle Jurassic formations with source rock potential were not encountered in either well 6609/11-1 and well 6610/7-1 from the Helgeland basin and fact that the entire Jurassic strata is missing in well 6609/5-1 from the Trænabanken (NPD, 2015a) the probability of existence of source rocks of this age in the Helgeland Basin area is thus limited but still not completely ruled out. Despite the possibility of the existence of a Middle Jurassic source rock kitchen outside from the Helgeland Basin which could have contributed with long-migrated petroleum into the basin, further investigations of a possible parental Middle Jurassic source rocks for the migrated bitumen samples from the Helgeland Basin area will not be carried out in this thesis.

7.5 Tricyclic terpanes

There is an important notice concerning the tricyclic terpane abundance in the dataset; only the Middle Devonian source rock bitumen samples from the Orkneys show high abundance while all the Helgeland Basin bitumen samples show very low abundance in comparison, pointing towards that there is no relation between the Middle Devonian source rock equivalent from the Orkneys and all the Helgeland Basin bitumen samples.

The Beatrice oil is co-sourced from the lacustrine Middle Devonian source rocks located in the Orcadian Basin (Peters et al., 1989), but does not contain significant amounts of tricyclic terpanes, which are so characteristic of the studied source rock samples from the Orkneys in general. Also the Middle Devonian source rock bitumen samples from Peters et al. (1989) and Bailey (1990) were reported to contain low amounts of tricyclic terpanes comparable to the Beatrice oil. The samples used as references for the Middle Devonian source rocks in Peters et al., (1989) originated from Inner Moray Firth, about 20 km east from the Beatrice Field.

Mello (1988) suggested that there was a linkage between high abundance of tricyclic terpanes and salinity; too low salinity (freshwater conditions) and too high salinity (hypersaline marine conditions) would lead to a suppression, while intermediate salinity conditions e.g saline lacustrine or marine carbonate settings would provide favorable conditions for the tricyclic terpane precursors.

The Middle Devonian source rock bitumen samples from Orkney are characterized by high relative abundances of tricyclic terpanes compared to the C30 hopane (range of 2.4 to 17.82, see parameter 7, Table 6.2), and the wide range probably reflects variations in the salinity level in the lake during the deposition of the Middle Devonian source rocks, caused by the variations in the precipitation/evaporation ratio in the lake as reported by Marshall et al. (2011). The marine NSO-1 oil on the other hand shows low abundance of tricyclic terpanes as seen from the values of 0.61 from parameter 7. Those observations agrees with the observation of high abundance of tricyclic terpanes in samples related to hypersaline lacustrine settings and low in hypersaline marine settings as was reported from De Grande et al. (1993). It is important to take note that the two source rock bitumen samples with the lowest generative potential (S1+S2) i.e. O-3 (0. 29) and O-6 (0.92) (see Rock-Eval and TOC discussion, section 7.2), also shows very low abundances of tricyclic terpanes i.e. 6.64 and 3.62 respectively while the other source rock bitumen samples containing higher quality organic shows ratios between 8.80 and 17.82 (when excluding O-4). O-3 and O-6 were thus probably deposited during periods with either lowered or elevated salinity levels of the lake. The low gammacerane index for O-3 and O-6 indicate that the lake was not stratified at the time of deposition, and thus could lighter water with lower salinity levels, most likely origninating from rivers due to the enhanced input of terrestrial material (see section 7.2) circulate to the lakefloor and lead to the observed suppression in the tricyclic terpane abundance.

The observed low abundance of tricyclic terpanes in the Inner Moray Firth Middle Devonian source rock bitumen samples from Peters et al. (1989) and Bailey et al. (1990) is most likely a result of the salinity being increased to levels which provided unfavorable conditions for tricyclic terpane precursors. Events of marine incursions into the Orcadian Lake from the south in Late Givetian in Middle Devonian has been reported (Marshall et al., 2011), which could lead to a sufficient elevation of the salinity, and thus cause the observed low abundance in tricyclic terpanes e.g. as seen in the Beatrice oil. Although the marine influence on the lake seemed to restrict the tricyclic terpane abundance, the presence of γ-carotane and β-carotane e.g. in the Beatrice oil suggests together with the insignificant abundance of diagnostic marine biomarkers like C30 steranes, BNH

and TNH that normal marine conditions did not develop in the Orcadian Lake when the source rocks which sourced the Beatrice oil were deposited. This observation coincides with the interpretation of a restricted marine (Marshall et al., 2011) depositional setting in the area at the time of marine incursions.

The first marine incursion into the Orcadian Basin has been dated at the boundary between mid and late Givetian in upper Middle Devonian (Marshall et al., 2011). The source rock samples from the Orkneys represent formations deposited before the first marine incursion (Sandwick Fish Bed was deposited in Eifelian in lower Middle Devonian) i.e. conditions were still favorable for tricyclic terpane formation at that time.

An important question is whether the salinity levels were sufficiently elevated (lowering of salinity levels would result in deposition of poor quality source rocks) e.g. by events of possible marine incursions for limiting tricyclic terpane abundance, when the possible Middle Devonian source rock was deposited in the Helgeland Basin area. Are the source rock bitumen samples with high tricyclic terpane abundance more representable for the likely Middle Devonian source rocks in the Helgeland Basin area than those used in Peters et al. (1989) and Bailey et al. (1990), and the signature found in the Beatrice Oil? If this assumption is true, it would be expected that if the hydrocarbon shows in the Helgeland basin originated from an equivalent to the source rock bitumen samples from the Orkneys and the tricyclic terpane abundance in the Helgeland Basin bitumen samples would thus be more on par with those of the Orkney source rock bitumen samples. The presence of carotanes combined with the low tricyclic terpane abundance could then be explained by an escape of the Middle Devonian palaeo-oil and the carotanes would thus only represent remnants of the escaped oil as is interpreted for the NSO-1 oil (see section 7.11.1), the Judy oil (see section 7.11.4) and the Embla oil (see sectoun 7.11.2) the bulk of the present day oil is from a completely different source which is characterized by a low tricyclic terpane ratio. It is also important to remember that the tricyclic terpane abundance observed in the nine source rock samples from the Orkneys does not necessarily represent the bulk of the source rocks in this area, as the number of samples are relatively few plus the fact that great variations in abundance are seen within the formation (see section 7.4.3).

Due to the proximity of the Helgeland Basin to mainland Norway compared to the Inner Moray Firths proximity to Scotland and Orkney, the basinwise location of the former is possibly an analog to the latter and thus situated in the more central and perhaps also deeper parts of the lake. Therefore, the conditions in the Helgeland Basin were probably similar to the conditions in Inner

Moray Firth e.g. regarding accommodation space and depositional pattern and also the grainsize of the sediments (conglomerates and coarse grained sandstone are normally distributed within the proximal parts of the basin, with closer proximity to the hinterland). Possible events with marine incursions also in the Helgeland Basin could cause mixing with marine water, leading to the lakes approaching similar salinity levels as in the Orcadian Lake, and thus cause the observed low tricyclic terpane abundance in combination with the presence of carotanes as are seen in some of the Helgeland Basin bitumen samples and in the oil from the Beatrice Field.

7.6 Discussion of organofacies for the source rock bitumen samples from the Orkneys

The Middle Devonian source rock bitumen samples from the Orkneys are characterized by a very high abundance in tricyclic terpanes compared to the Beatrice oil and also the source rock bitumen samples from Peters et al. (1989) which also represents Middle Devonian source rock deposits in the Orcadian Basin. This observed variation in tricyclic terpanes is most likely driven by variations in salinity within the Orcadian Basin, as the production of tricyclic terpane precursors is limited by too low e.g. freshwater lacustrine and too high salinity e.g. hypersaline marine. As the source rock bitumen samples from the Orkneys are few in numbers (nine in total), they may not represent their respective formations as the formations are not homogenous which is seen in the great variations in e.g. the hopane/sterane ratios, the tricyclic terpane abundance (although the lowest value is much higher than the value seen for the Beatrice oil), and in the C27-C29 cholestane configuration e.g. no presence of C28 cholestanes in O-3, O-6 and O-20 (see Figure 6.1). It is important to remember that the Beatrice oil represents the average configuration of a large interval of source rocks, and it is also noticed that the Beatrice oil has a C27-C29 cholestane configuration which is roughly intermediate between the Orkney bitumen samples as seen in Figure 6.1.

Another striking difference between the source rock bitumen samples from the Orkneys and the Middle Devonian source rocks from Peters et al. (1989) is the low HI for the former (see TOC and Rock-Eval discussion, section 7.2), compared to the common type I kerogen as reported in the literature e.g. Trewin (1989) (see section 2.4) which is confirmed in the high HI for the Middle Devonian samples from Peters et al. (1989). Furthermore the gammacerane index is found to be much higher for the source rock bitumen samples from the Orkney in general (see Table 6.4) compared to the Beatrice oil.

Despite the observed differences between the source rock bitumen samples from the Orkneys, the Beatrice oil and also the source rock bitumen samples from Peters et al. (1989), the former does belong to a similar organofacies i.e. hypersaline lacustrine, based on the values from both the C26/C25 tricyclic terpane ratio and the C31 22R/C30 ratio (see section 7.4.3) which are associated with lacustrine organofacies (see Figure 5.14) and most importantly the high abundance of the carotane family represented by both γ-carotane and β-carotane. Furthermore, a lacustrine derived organofacies is indicated for all the Orkney Figures from the pr/ph ratio (see Figure 6.2 and Figure 6.3). However, some of the Orkney bitumen samples are also significantly affected by terrestrially derived organic matter i.e. O-3, O-6 and O-7 as seen from e.g. the high OI. Based on no significant presence of the diagnostic marine markers i.e. C30 steranes, BNH and TNH, a relation to marine-derived organofacies can thus be excluded for the Orkney source rock bitumen samples.

7.7 Discussion of organofacies for the bitumen extracts from well 6609/11-1

7.7.1 Discussion of potential sources for the bitumen extracts from well 6609/11-1

The bitumen samples which represent well 6609/11-1 show Pr/Ph ratios in the range from 1.00 (A-3) to 2.11 (A-4), reflecting great variations within a few cm as the depth difference between A-3 and A-4 is only 10 cm. The samples plot clearly in the marine and lacustrine shale zone in the Hughes plots (see Figure 6.2) except from A-3 which plots at the transition line between the lacustrine (sulfate-poor) zone and the marine and lacustrine shale zone. Also, Figure 6.2 shows that the MDBTs/MPs ratios are clearly below 1 for all samples, which together with the general odd predominance of n-alkanes except from in A-4 (see Table 6.1), strongly suggests that there is no influence from a carbonate source and neither of the viable parental source rocks presented in section 7.4 are related to carbonate derived organofacies. However, A-4 (and also A-1) shows low concentration of petroleum, illustrated by the low peak intensities of n-alkanes in the respective GC-FID chromatograms (see Figure 6.17 and Figure 6.20), and this is likely to affect the calculated ratios as a small change in the peak intensity of a given compound would change the ratio more drastically. It can thus be concluded that even predominance is not representative for well 6609/11-1. A-3 and A-5 and to less degree A-2 are represented by a significant portion of n-alkanes with at least 25 carbon atoms (see Figure 6.19, Figure 6.21 and Figure 6.18), giving the bitumen samples a waxy character. High abundance of the n-C25 fraction is diagnostic for non-marine organic matter

e.g. higher plants (Tissot and Welte, 1984), and the observed n-alkane patterns suggest thus a terrestrially derived source. The significant contribution from the C25+ fraction is also observed in the source rock bitumen samples from the Orkneys and also in the Beatrice oil and the observed n-alkane pattern as seen in A-2, A-3 and A-5 can thus possibly be caused by an equivalent to the Middle Devonian source rocks from the Orcadian Basin.

The C27-C29 cholestane (ββ-isomers of the C27-C29 steranes) distribution is slightly biased towards C29 for A-2, A-3 and A-4, A-1 has the least input of C28 while A-5 plots close to NSO-1 on the ternary diagram (Figure 6.1). The C30 steranes are only present in insignificant amounts in all the five bitumen samples from well 6609/11-1, suggesting no significant input from a marine derived source and supports the interpretation by Karlsen et al. (1995) where they suggested a non-marine source rock as a source for A-5. This is supported by the low BNH abundance as the BNH to C30 hopane ratios of A-1 to A-5 is in the range of 0.05 to 0.09 compared to the marine derived NSO-1 oil which shows a value of 0.24. The validity of the BNH parameter is good as the difference in values between the bitumen samples representing well 6609/11-1 and the NSO-1 oil is significant and the additional dilution effects on BNH in the slightly more mature samples of A-1 to A-5 are most likely insufficient for causing the observed difference. Furthermore, the high hopane/sterane ratios which are comparable to the ratio seen for the Beatrice oil (see parameter 9, Table 6.2) and observed in A-3, A-4 and A-5 supports a main non-marine source.

The δC13 value of A-5 (see Table 6.6) was used as an argument by Karlsen et al. (1995) for suggesting a non-marine source as the A-5 bitumen is significantly more depleted in the C13 isotope than marine sourced oils e.g. the Kimmeridge equivalent. It has to be noted that the δC13 value of A-5 is on par with the values for the Middle Devonian lacustrine source rock bitumen samples from the Orkneys and is thus indicating a possible relation between the former and the latter. No isotope data is available for the four other samples, but the lack of marine diagnostic biomarkers, i.e. BNH, TNH and C30 steranes excludes the marine Late Jurassic source rock as a contributor for all the five bitumen samples which represents well 6609/11-1.

The β-carotane compound is clearly detected in A-5 (see Figure 6.21) and it is also detectable in A-2 (see Figure 6.18), it is however not possible to detect β-carotane in A-1, A-3 and A-4. The presence of β-carotane in A-5 and A-2 suggests a contribution from a hypersaline lacustrine derived source i.e. the lacustrine Middle Devonian source rocks most likely provided the β-carotane seen in the two bitumen samples. The absence of γ-carotane in A-2 and A-5 could indicate biodegradation (see section 5.1.5), but the shape of the GC-FID chromatograms shows otherwise and is supported by

the Pr/n-C17 vs Ph/n-C18 plot as the ratios bear no resemblance of being underestimated as they are much higher than the value from the only slightly less mature NSO-1 oil which is not biodegraded (see Figure 7.4).

The gammacerane index values for A-2 (0.13) and A-5 (0.18) are quite low compared to values from the Orkney source rock bitumen samples (0.91-2.57, if excluding the three samples O-3, O-4 and O-6 with the worst overall potential). The low gammacerane index together with higher Pr/Ph ratios for A-2 and A-5 of 1.29 and 1.60 respectively compared to the source rocks (0.34-0.78) could indicate a mixture of hypersaline lacustrine derived oils and terrestrial derived oils, and if including the latter organofacies, the Pr/Ph ratio will be elevated and the gammacerane index lowered as is seen for the A-2 and A-5.

The C26/C25 tricyclic terpane ratios for A-2 is 2.5 are much higher than 1.4 which is the minimum criteria for strong indication of lacustrine input i.e. the bulk of lacustrine source rock samples have values above 1.4 (see Figure 5.14). Interestingly, this value is much higher for A-2 (2.5) than for the Beatrice oil (1.23) and also all the source rock samples from the Orkneys (highest observed value of 1.8 in the O-20 and O-21 samples). The C26/C25 tricyclic terpane ratio of A-5 (1.17) is below the 1.4 threshold but is still on par with the source rock bitumen samples and the Beatrice oil, thus indicating input of lacustrine derived petroleum. The C31 22R/C30 hopane ratio of A-2 is close to the 0.25 threshold (lacustrine source rocks shows values below 0.25 in general, see Figure 5.14), supporting the suggestion of a lacustrine source based on C26/C25 tricyclic terpane ratio. Interestingly, A-5 shows a C31 22R/C30 hopane ratio of 0.34, which is higher than the 0.25 threshold and is unlike the C26/C25 tricyclic terpane ratio not on par with the source rock samples and the Beatrice oil that show ratios in the range of 0.12 to 0.23.

The main terrestrial derived contributor to the bitumen samples in well 6609/11-1 is most likely neither the Carboniferous nor the Lower Jurassic coals. Although the coals share the waxiness as is seen in the bitumen samples A-1 to A-5, the much higher Pr/Ph combined with lower predominance of C27 cholestanes for the Carboniferous coals (see section 7.4.4) and the much heavier δ1C value of the Lower Jurassic coal as compared to A-5, suggests that there is no relation between the coals and the source rock bitumen samples which represent well 6609/11-1.

7.7.2 Summary of organofacies for well 6609/11-1

Despite the Pr/Ph ratios being lower than the 3.0 threshold (values above 3 points strongly towards a terrestrial source) with a good margin for all samples and the zone plotting in the Hughes plot (Figure 6.2) and in Figure 6.3, there is a strong indication of a sole terrestrial source for A-1, A-3 and A-4 and a terrestrial co-source for A-2 and A-5. The interpretation of a terrestrial source is based on the high hopane/sterane ratios for 6609/11-1 in general (above 5 for A-3, A-4 and A-5) combined with a predominance of C29 cholestane over C27 cholestane and C28 cholestane for all samples excluding A-5, no significant abundance of the marine biomarkers i.e C30 steranes, BNH and TNH, the low gammacerane index values and a significant contribution from the C25+ fraction of n-alkanes in general, plus no carotanes present. The presence of carotanes in only A-2 and A-5, the C26/C25 tricyclic ratios which are comparable to those seen for the source rock bitumen samples and also the Beatrice oil, plus moderate Pr/Ph and the intermediate placement between more terrestrial dominated environments, and the source rock bitumen samples from Orkney which is also on par with the Beatrice oil in the Pr/n-C17 vs Ph/n-C18 plot (Figure 7.4), suggests a second Middle Devonian source for those two bitumen samples.

7.8 Discussion of organofacies for the bitumen extracts from well 6610/7-1 upper section

7.8.1 Discussion of potential sources for the bitumen extracts from the upper section in well 6610/7-1

The three bitumen samples from the depths of 2661m (B-1), 2662,2m (B-2) and 2668,5m (B-3), which represents the upper section of well 6610/7-1, show similar C27-C29 cholestane configurations to the configuration seen in the NSO-1 oil, which is reflected in the C27-C29 ternary diagram (see Figure 6.1). The bitumen samples B-1, B-2 and B-3 also show presence of C30 steranes (see m/z= 218 chromatograms in Figure 6.22, Figure 6.23 and Figure 6.24), with relative intensities compared to the C27-C29 cholestanes which are similar to the relative intensity of C30 steranes seen for NSO-1, thus suggesting a significant influence from marine-derived organic matter. The Middle Devonian lacustrine source rock, represented by the source rock bitumen samples from Orkneys and the Beatrice oil only show traces of C30 steranes and can thus not provide the observed quantities.

The unusually low Ts/(Ts+Tm) ratios and diasteranes/(diasteranes+regular steranes) ratios (see maturity discussion, section 7.3.5) indicate a relation to parental carbonate derived source rocks. However, the MDBTs/MPs ratios for B-1 to B-3 are clearly below 1 (see Figure 6.2) and two out of three carbon preference indexes (see Table 6.1) points towards odd predominance. Both the former and latter observation indicate no significant contribution from a carbonate source, and from those two observations and the fact that neither of the viable source rocks (see section 7.4) are related to carbonate derived organofacies, a carbonate derived source of the B-1 to B-3 bitumen samples can thus be excluded.

The gammacerane index values for B-1, B-2 and B-3 are 0.10, 0.11 and 0.13 respectively and are slightly lower than seen for the NSO-1 oil (0.14), much lower than values from the source rock bitumen samples with good quality (0.91-2.57, excluding O-3, O-4 and O-6) and also lower than the value seen for the Beatrice oil (0.33). The Pr/Ph ratios are low for the three samples as compared to NSO-1 (1.70) and there is a trend of a decrease in the Pr/Ph ratio with increasing depth, as B-1 shows the highest value of 1.13 while the deeper B-2 and B-3 shows 0.93 and 0.78 respectively. If the Pr/Ph ratio drops below the 0.8 threshold, it is indicative for a hypersaline depositional environment for the parental source rocks. From the observed low Pr/Ph values of B-1 to B-3, the Lower Carboniferous and Lower Jurassic coals with Pr/Ph ratios above 5 (see section 7.4.7) can be excluded as sources of the migrated petroleum.

The β-carotane compound has been detected in the bitumen samples of B-1, B-2 and B-3, and is thus strongly indicating parental lacustrine Middle Devonian source rocks. Schou et al. (1983) suggested a Late Jurassic Kimmeridge equivalent as a main/sole source for the B-1 to B-3 section, but the authors did not find β-carotane because GC-MS was not used specifically to find β-carotane i.e. m/z = 125, m/z = 558 and m/z = 560 chromatograms were not generated. Also, the β-carotane concentrations in the bitumen samples are too low to be detected in GC-FID (see Appendix A, GC-FID chromatograms for B-1 to B-3). The observed n-alkane patterns for B-1 to B-3 are more biased towards longer chained n-alkanes than seen for the Beatrice oil, thus giving the bitumen samples which represent the upper section of well 6610/7-1 a more waxy character compared to the latter.

In the Hughes plot (see Figure 6.2), both B-2 and B-3 plot in the lacustrine sulfate poor zone, while B-1 plots in the marine and lacustrine shale zone. When comparing the Pr/Ph ratios of the three samples to the values for the source rock bitumen samples from the Orkneys (0.27-0.78), B-1 (1.13) and B-2 (0.93) show higher ratios, while B-3 (0.78) is on par with the source rock bitumen sample with the highest ratio (O-7).

The BNH compound is identified as a prominent peak for B-1, B-2 and B-3 in their respective m/z = 191 chromatograms and is comparable to the peak intensity seen in the m/z = 191 chromatogram from the NSO-1 oil. The BNH/C30 hopane ratios for B-1 (0.32), B-2 (0.32) and B-3 (0.34) are all higher than for NSO-1 (0.24), despite that the three extracts are slightly more mature than NSO-1 (see the maturity discussion, section 7.3.5). The same pattern is observed from the BNH/(BNH + norhopane) ratio (see parameter 6, Table 6.2). The B-1, B-2 and B-3 bitumen samples do also show prominent TNH peaks in the m/z = 177 chromatograms (another diagnostic marker for the marine Late Jurassic Kimmeridge equivalent and the NSO-1 oil). Furthermore the hopane/sterane ratios for B-1 to B-3 are very low in general compared to the hopane/sterane ratios for Beatrice oil and the source rock bitumen samples from the Orkneys (see Table 6.2), thus supporting the interpretation of a significant contribution of a marine planktonic derived source to those samples.

Schou et al. (1983) suggested a mixed source for the sandstone core at 2661.6-2661.64m (corresponding fairly well to B-1) and it is observed from their chromatograms that BNH (peak Z in Figure 7.11) is much less prominent compared to the two chromatograms from depths 2668.05-2668.12m (corresponding to B-3) and is thus differing from B-1 to B-3 and 2706-2706.05m. However, Schou et al. (1983) believed that this possible mixing is caused by hydrocarbon contamination from claystones nearby. The possible local contamination in only the shallowest sandstone core from Schou et al. (1983) is supported by the 0.64m shallower B-1 having BNH intensities on par with B-2 and B-3 and also the two deeper core samples from Schou et al. (1983), indicating that the upper interval is in overall represented by high BNH abundance.

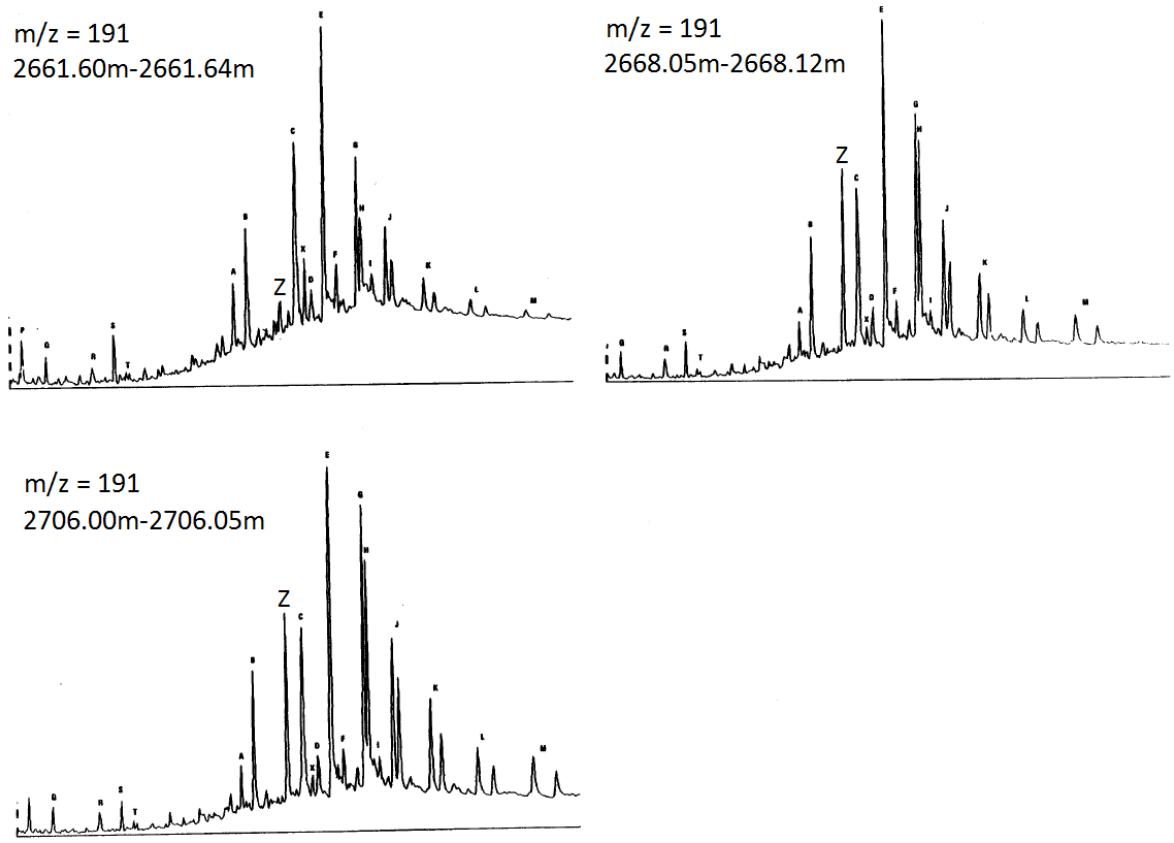

Figure 7.11: m/z = 191 chromatograms from the three sandstone core intervals from Schou et al. (1983). The low Z-peak intensity in the m/z = 191 chromatogram for the 2661.60m-2661.64m interval was proposed by Schou et al., (1983) to be caused by contamination from nearby claystones.

7.8.2 Summary of the organofacies for the upper section in well 6610/7-1

The intermediate δ13C values and intermediate Pr/Ph ratios in between the Middle Devonian source rock bitumen samples and Late Jurassic oil for the upper section of well 6610/7-1 (illustrated in Figure 6.3) plus the presence of both β-carotane and the relatively high abundance of both C30 steranes, BNH and TNH plus low hopane/sterane ratios suggests a mixing between a lacustrine derived Middle Devonian source and a marine derived Late Jurassic Kimmerdige equivalent source for B-1 to B-3, and the Late Jurassic Kimmeridge equivalent acts as the main contributor of the present day petroleum in place. However, B-1 to B-3 show a more waxy character than the Beatrice oil and also the source rock bitumen samples from the Orkney which does conflict with the co-source interpretation as the n-alkane pattern should be intermediate between the two sources.

7.9 Discussion of organofacies for the bitumen extracts from well 6610/7-1 lower section

7.9.1 Discussion of potential sources for the bitumen extracts from the lower section in well 6610/7-1

The four bitumen samples B-4 to B-7 which represents the lower section in well 6610/7-1 i.e the depth from 2713.8m to 2715m, are characterized by high Pr/Ph ratios. B-4 shows a Pr/Ph ratio of 2.57 while the three others have Pr/Ph values above the 3.0 threshold i.e B-5 shows 3.91, B-6 shows 4.29 and B-7 shows 4.25 which points towards major input of organic matter from a terrestrial derived source which was deposited under oxic conditions. In the Hughes plot (see Figure 6.2) B-5 to B-7 plots in the fluvial/deltaic carbonaceous shale and the coal zone while B-4 plots in the marine and lacustrine shale zone. B-4 to B-7 all plot in the peat-coal environment in the Pr/n-C17 vs Ph/n-C18 plot (Figure 7.4) and this supports the observations from the Hughes plot and the values from the Pr/Ph ratios which indicate a source with terrestrial derived character. B-4 to B-7 shows MDBT/MPs ratios clearly below 1 and in combination with the observation of odd predominance of n-alkanes, no significant contributions from a carbonate source can be presumed despite the indication of a carbonate derived source from the unusual low Ts/Ts+Tm and diasteranes/(diasteranes+regular steranes) ratios. To support the exclusion of a potential carbonate source is that no possible viable carbonate derived source rocks are located in the area (see section 7.4). Regarding the n-alkane patterns, B-4 differs from B-5 to B-7 as there is significant contribution from the n-C25+ fraction which gives the former more waxy character, while the others show a more similar configuration to the one seen in NSO-1.

Interestingly, the gammacerane index values for the B-4 to B-7 bitumen samples are high in general (0.22-0.29) compared to the other samples representing the Helgeland Basin area (0.10-0.23), while the Pr/Ph ratio on the other hand is much higher (2.57 to 4.29 for B-4 to B-7 and 0.78-2.11 for the other Helgeland Basin samples). Normally it would be expected that higher gammacerane index values results in lower Pr/Ph ratios, as gammacerane is diagnostic for stratified lake settings which is also associated with anoxic conditions resulting in low Pr/Ph ratios.

A clear predominance of C29 cholestanes compared to C27 and C28 cholestanes is observed in B-4 to B-7, and the bitumen samples plot closer to the higher plants and terrestrial zones in the ternary diagram compared to the NSO-1 oil (see Figure 6.1). The C30 sterane compounds which are strong indicators for input from a marine derived source, and found abundant in the NSO-1 oil, are less

significant for the bitumen samples B-4 to B-7, but still noticeable which indicates some contribution of marine derived organic matter to those samples. The high hopane/sterane ratio (2.97 to 7.34) and insignificant amounts of BNH (BNH/C30 hopane ratios of 0.09-0.11) on the other hand suggests no significant contribution from marine derived source rocks. The high hopane/sterane ratio could be an indication of input of terrestrial derived and/or microbial reworked material (Tissot and Welte, 1984). The presence of the TNH compound in the m/z = 177 chromatograms of B-4 to B-7 indicates that the secondary effect elevated the hopane/sterane ratio further, as there is evidence from microbially activity based on the reworking of BNH to TNH by microbes (Peters et al., 2005), as BNH is depleted. TNH is associated with anoxic marine conditions and suggests together with the high abundance of gammacerane and presence of C30 steranes that a terrestrial source could not be the only source for the B-4 to B-7 bitumen samples. An interpretation of a contribution of petroleum that has later been microbially reworked from a Late Kimmeridge source rock equivalent seems viable based on those observations.

The β-carotane compound is not present in the B-4 to B-7 bitumen samples which strongly points towards the conclusion of none contribution from the lacustrine Middle Devonian source rocks. The combination of low C26/C25 tricyclic terpane and high C31 22R/C30 hopane ratios (see Table 6.4) shows a significant difference from the typical values which are diagnostic for worldwide lacustrine derived oils (see Figure 5.14), the source rock bitumen samples from the Orkneys, the Beatrice oil and also typical values for worldwide oils from carbonate and marine shales. This observation support the interpretation of no contribution from the lacustrine Middle Devonian source rocks and carbonate source rocks and also confirms that the Kimmeridge equivalent could not be the main source.

It is noted that there is a relationship between higher Pr/Ph and higher hopane/sterane ratio for B-4 to B-7 and an increasing trend with increasing depths. The abundance of C30 steranes relative to C27-C29 cholestanes from B-4 to B-7 on the other hand decreases (see m/z = 218 chromatograms for B-4 to B-7, appendix) and there is also a slight trend towards a stronger predominance of C29 cholestanes. From those observations, a tendency of decreasing influence from a marine source, and increasing influence of a terrestrial source is indicated for B-4 to B-7.

The discussed markers which point towards a terrestrial source for the bitumen samples which represents the lower section of well 6610/7-1 would suggest also a significant contribution from the n-C25+ fraction in the GC-FID chromatograms which is so diagnostic for land-derived organic matter. However, the n-alkane patterns of B-5 o B-7 clearly conflicts with the interpretation of a terrestrial

source and the observed patterns are more comparable to the pattern seen in the NSO-1 oil. Thus can the Carboniferous coals and also the Lower Jurassic coals be excluded as a source for B-5 to B-7 despite the similar low abundance in C27 cholestanes and comparable Pr/Ph ratios (see section 7.4.4 and the indication of organofacies zone in Figure 6.1). B-4 shows a n-alkane pattern which is typical for terrestrially sourced oils and bitumens (see Figure 6.25), and it is thus more similar to the pattern seen for the coals (see Figure 7.10) but the much lower Pr/Ph ratio of B-4 (2.57) than the coals (the Lower Jurassic coal sample seen in Figure 7.10 has a Pr/Ph ratio of 5.6) excludes possible parental coal-derived source rocks also for this bitumen sample

7.9.2 Summary of the organofacies for the lower section in well 6610/7-1

The observation of high Pr/Ph ratios, very low C26/C25 tricyclic terpane ratios and high C31 22R/C30 hopane ratios, high hopane/sterane ratios, no presence of β-carotane, the high Pr/n-C17 vs Ph/n-C18 relationship, plus a predominance of C29 over C27 and C28 cholestanes leads to the suggestion of a terrestrially derived main source of hydrocarbons for B-4 to B-7, for B-5 to B-7. The relatively high gammacerane index values combined with the presence of C30 steranes, TNH and no significant amounts of BNH suggests a second infill of hydrocarbons that was later microbially reworked and originated from a marine Late Jurassic Kimmeridge source equivalent. The marine source has contributed a smaller portion of the total volume of the migrated petroleum at greater depths within the lower section of well 6610/7-1.

7.10 Discussion of organofacies for the bitumen extracts from well 6609/5-1

7.10.1 Discussion of potential sources for the bitumen extracts from well 6609/5-1

Both the bitumen samples from well 6609/5-1, from depth 3009m (C-1) and 3011m (C-2) respectively, show a similar configuration as the NSO-1 oil regarding the C27-C29 cholestanes (see m/z = 218 chromatograms of C-1, C-2 and NSO-1 in Appendix B) and plot thus close to NSO-1 in the ternary diagram (Figure 6.1). The configuration of C30 steranes relative to C27-C29 cholestanes seen in C-1 and C-2 are also comparable to NSO-1, which suggests input of marine derived organic matter into C-1 and C-2.

The gammacerane index for C-1 (0.13) and C-2 (0.18) is also on par with NSO-1 (0.14). The β-carotane compound is detected in both C-1 and C-2 which is indicative of a hypersaline lacustrine or restricted marine depositional environment for the parental source rocks. Concerning the Hughes plot (see Figure 6.1), C-1 plots in the lacustrine zone while C-2 which has higher Pr/Ph ratio (1.09 while C-1 has 0.90) plots in the marine and lacustrine shale zone, however close to the transition to lacustrine shale zone. The NSO-1 oil has in comparison higher Pr/Ph ratio (1.7). C-1 and C-2 have intermediate Pr/Ph ratios between the source rocks (0.27-0.78) and NSO-1 and much lower than the Beatrice oil (2.42).

The BNH compound is a relatively prominent peak in the NSO-1 oil (BNH to C30 hopane ratio of 0.24) while less prominent in C-1 and C-2. However, there is still significant contribution of BNH in C-1 and C-2 as seen in the BNH to C30 hopane ratios which are 0.12 and 0.15 respectively. The TNH compound is also present in both samples but is as BNH less prominent than in the NSO-1 oil. The BNH to C30 hopane ratios are slightly higher for C-1 and C-2 when compared to the average for the source rock bitumen samples from the Orkney (0.11), but because C-1 and C-2 are more mature (see maturity discussion, section 7.3) and BNH rapidly becomes diluted due to infill of additional petroleum i.e. non biomarker compounds from the source rock kitchen as it matures, the BNH contribution is more important than this small difference suggests. The same pattern is seen in the values from the BNH/(BNH+norhopane) ratio (see parameter 6, Table 6.2). The relatively low C26/C25 tricyclic terpane ratio of 0.95 of sample C-1 agrees with the BNH abundance observations that the main source is of marine character as the value is closer to the bulk of oils derived from marine shales compared to lacustrine derived oils (see Figure 5.14).

The C26/C25 tricyclic terpane ratio of C-2 (0.39) is very low compared to C-1, but the calculated value is affected by interference in the m/z = 191 chromatogram (see Figure 7.12) which drastically reduces the peak intensities of the C26 compounds i.e the 26/3R and 26/3S isomers (see Figure 5.4 for peak identification). This observed depression is caused by contamination of the sample from siloxanes (m/z = 73) originating from the silica septa (cf. Wang, 2006), and the calculated C26/C25 tricyclic terpane ratio from C-2 will thus not be taken into account.

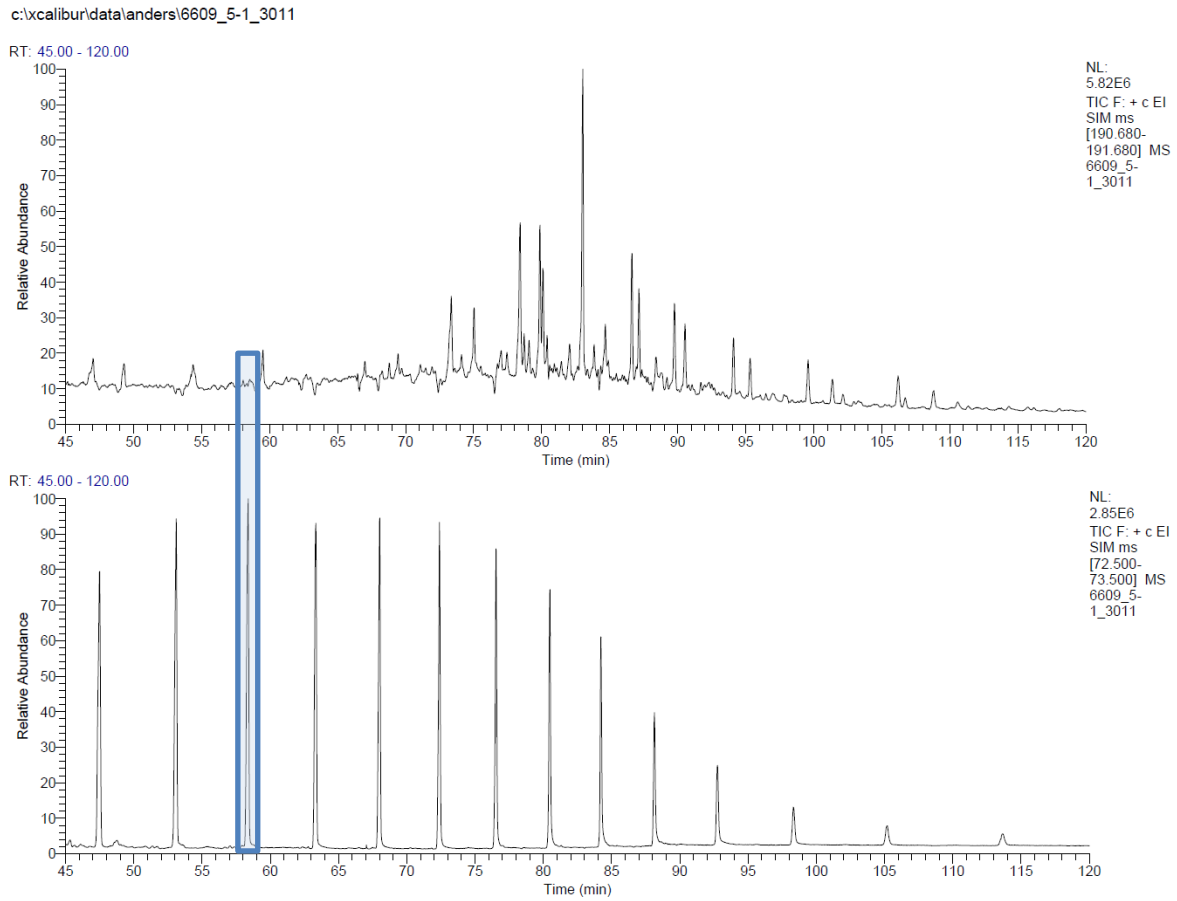

Figure 7.12: Contamination of the m/z = 191 chromatogram (upper) from the C-2 sample, seen as depressions in the base line caused by interference from the siloxane peaks (lower chromatogram, m/z = 73).The retention time for one of the siloxane peaks coincides with the retention times of the C26 tricyclic terpanes (outlined in blue), and affects thus the C26/C25 tricyclic terpane ratio.

The bitumen samples C-1 and C-2 both show a waxy character as seen in their respective GC-FID chromatograms (see Figure 6.29, Figure 6.30 and appendix B), pointing towards significant contributions from a non-marine source, i.e. most likely the Middle Devonian lacustrine source rocks due to the presence of β-carotane and the low Pr/Ph ratios which excludes the waxy coal derived Lower Carboniferous and Lower Jurassic sources. The hopane/sterane ratios for C-1 and C-2 are intermediate between the NSO-1 oil and the Beatrice oil, supporting the interpretation of co-sources from the lacustrine derived Middle Devonian source rock and marine derived Late Jurassic source rocks but values closer to the former indicates a marine-derived main source.

The C-1 bitumen shows a high abundance of phenanthrene relative to the methylphenanthrenes, indicating that oxidizing conditions has developed, as seen from the underestimation of maturity from parameter 23 compared to parameter 24 (see Figure 7.6). However, the low Pr/Ph ratio of 0.90 conflicts with the high phenanthrene abundance as a low value of the former is associated

with a low abundance of the latter. The high phenanthrene abundance of C-1 does also conflict with the interepted sources i.e. the lacustrine Middle Devonian organofacies represented by the Orkney bitumen samples and the Beatrice oil, and the marine Late Jurassic Kimmeridge equivalent organofacies represented by NSO-1 both shows a much lower relative abundance of phenanthrene.

The demethylation of the methylphenanthrenes were probably enhanced by water washing into the reservoir i.e. the interpretion of water washing is indicated from the presence of UCM in the GC-FID chromatogram (see Figure 6.29 and Appendix B). The influx of water carried metal-bearing solutions and bacterias into the reservoir and thus allowed secondary oxidation (see section 7.3.1) and also microbial degradation while at the same time the original Pr/Ph rato was not altered significantly as either of those two compounds are clearly preferred by bacterial degradation. Thus does the Pr/Ph ratio of the C-1 bitumen sample give a better representation of the parental source, than the phenanthrene abundance.

7.10.2 Summary of the organofacies for well 6609/5-1

The intermediate Pr/Ph ratios in between the source rock bitumen samples from the Orkney and the NSO-1 oil for C-1 and C-2 cf. Figure 6.3, plus the presence of β-carotane which is a Middle Devonian marker and C30 steranes, BNH and TNH which are the Kimmeridge equivalent markers suggests a mixing between a Middle Devonian and Late Jurassic source for the Lower Cretaceous sandstone at depths 3009m and 3011m in well 6609/5-1. The abundance of C30 steranes relative to C27-C29 cholestanes (see m/z 218), the BNH and the TNH abundance, the C26/C25 tricyclic terpane ratios, hopane/sterane ratios plus the distribution of C27-C29 cholestanes (see ternary diagram, Figure 6.1) suggests that the marine Late Jurassic source is the main contributor, despite that the C-1 and C-2 bitumen samples have a waxy character comparable to the Beatrice oil, as seen from the high abundance of n-alkanes with at least 25 carbon atoms.

7.11 Discussion of the linkage to Middle Devonian source rocks for oils from the Embla Field,the Oseberg Field and the Judy Field

7.11.1 Oseberg (NSO-1)

The for the first time positive identification of the β-carotane compound in the reference oil NSO-1 from the Oseberg Field in the North Sea (see the m/z = 558 chromatogram in Figure 6.13), leads to the interpretation of an oil-charge event prior to the infill of the marine derived Late Jurassic oil, probably from the lacustrine Middle Devonian source rocks. The palaeo-oil most likely escaped from the reservoir long before the second infill event, as the NSO-1 oil at present day has a completely different signature i.e. marine than the lacustrine Middle Devonian source rocks. It is interpreted that the heavy C40 β-carotane compound (cf. Peters et al., 2005) was left in the reservoir as residue in the sandstone of Middle Jurassic age (NPD, 2015a), and then dissolved into the Late Jurassic Kimmeridge equivalent oil from the second oil charge. The γ-carotane compound is absent in NSO-1, suggesting that the palaeo-oil was subjected to biodegradation as γ-carotane is less resistant to biodegradation compared to β-carotane (Jiang and Fowler, 1986). The biodegraded palaeo-oil would if still present elevate the baseline in the GC-FID chromatogram as is observed e.g. in the GC-FID chromatograms from bitumen samples which represents the palaeo-oils in the Embla reservoir (Abay et al., 2014). However, the UCM hump is not detectable which confirms that the palaeo-oil escaped from the Oseberg reservoir.

Although the palaeo-oil is believed to have escaped before the second oil charge i.e. with oil derived from the marine Kimmeridge equivalent, the palaeo-oil probably caused an increase in the efficiency of migration of the second infill into the reservoir as secondary migration of petroleum is improved by the already oil-saturated pathways, and the pathways would also enhance porosity preservation within the reservoir (Karlsen and Skeie, 2006).

Many of the rotated fault blocks in the northern North Sea was uplifted by planar normal faulting at an early stage after the Middle Jurassic – Earliest Cretaceous rifting, leading to exposure and erosion (Badley et al., 1988). The uplift explains the biodegradation of the palaeo-oil as the reservoirs would be situated at shallow depths, and thus leading to a drop in temperature to below the 70°C threshold (60-80°C), which enabled biodegradation (Peters et al. 2005) and this coincides with the observed depletion of γ-carotane in the oil as this compound is favoured over β-carotane for bacterial degradation. The erosion would eventually lead to seal breakage (if a seal was

established), and thus enabling the palaeo-oil to escape from the reservoir. The palaeo-oil in the Oseberg Field was therefore most likely lost sometime in Early Cretaceous.

7.11.2 Embla

An infill event of petroleum sourced from a Palaeozoic source rock has been reported to have occurred in the Devonian reservoirs of the Embla Field, southern North Sea (Pedersen et al., 2007, Ohm et al., 2012 and Abay et al., 2014). It has also been reported that the reservoirs in the Embla Field shares many features as the Devonian co-filled Clair Field and Beatrice Field (cf. Abay et al., 2014). The new discovery of γ-carotane in the Embla Field (see m/z = 560, Figure 6.14) points towards a contribution from an equivalent to the Middle Devonian lacustrine source rocks from the Orcadian Basin, thus supporting the interpretations by Abay et al., 2014).

The depletion of the β-carotane compound and at the same time the presence of the γ-carotane compound for this highly mature oil (all vitrinite reflectivity calibrated maturity parameters 22-25 shows values above 1, see Table 6.3) supports the observation of Jiang and Fowler (1986) that the latter is more thermally resistant than the former. However, it was reported by Abay et al. (2014) that this palaeo-oil was biodegraded due to the presence of UCM in the GC-FID chromatogram, but as γ-carotane is still present unlike in the palaeo-oil from the Oseberg Field, the Embla palaeo-oil has probably been subjected to less severe biodegradation than the Oseberg palaeo-oil. In the producible oil from the Embla Field however, UCM is not detectable in the GC-FID chromatogram which indicates that the palaeo-oil contributes only a small portion of the present day oil volume. This interpretation is supported by the lack of long-chained n-alkanes which are so typical for the Middle Devonian source rocks, and also the C26/C25 tricyclic terpane ratio and C31 22R/C30 hopane ratio of 0.81 and 0.55 respectively which clearly differs from the typical values for worldwide lacustrine derived oils, the Middle Devonian source rock bitumen samples from the Orkneys and the Beatrice oil (see Figure 5.14 and Table 6.4).

7.11.3 Judy

Both the β-carotane compound and the γ-carotane compound are detected in the Judy oil, which leads to the suggestion of a lacustrine Middle Devonian source co-source. The intensities of β-carotane and γ-carotane are about the same, approximately $1.2*10^4$ in total (see m/z = 558 and m/z= 560 chromatograms of Judy in appendix B) and is about half of the β-carotane intensity in NSO-1 which is $2.02*10^4$ (see m/z = 558 chromatogram of NSO-1 in appendix B) The Judy oil is

slightly more mature than NSO-1, indicated by the Pr/n-C17 versus Ph/n-C18 plot (see Figure 7.4)), parameter 3 versus 20 plot (Figure 7.5) and the parameters 22-24 (0.02 to 0.05 higher, see Table 6.3) from GC-MS.

Modelling of the burial depth history of the Judy Field reservoir sandstones of Middle Triassic age shows a slow burial rate until 90Ma., when the burial rate started to accelerate, and a rapid burial of 1.7 km over the last 3Ma. (see Figure 7.13) (Swarbrick et al., 2000). The main difference between the burial histories of the Judy Field Middle Triassic reservoir and the Oseberg Field Middle Jurassic reservoir is that there are no indications of uplift and exposure for the former, which would lead to probably a more severe biodegradation of the palaeo-oil as seen in the latter from the depletion of γ-carotane. The Judy Field reservoir is located on a horst structure, and was situated at a shallow depth of less than 600m until 80Ma. (Swarbrick et al., 2000), and possible salt structures situated below i.e. Permian Zechstein salts? might have prevented significant burial rates. It is not unlikely that the possible lacustrine Middle Devonian source rocks below the reservoir were buried to insufficient depths for expelling petroleum until more recent due to the slow burial rates, but the depths of the lows nearby to the Judy Field horst structure could be sufficient for a Devonian source rock kitchen to form and source the Middle Triassic sandstones before a trap structure was established and thus allow the palaeo-oil to escape from the reservoir.

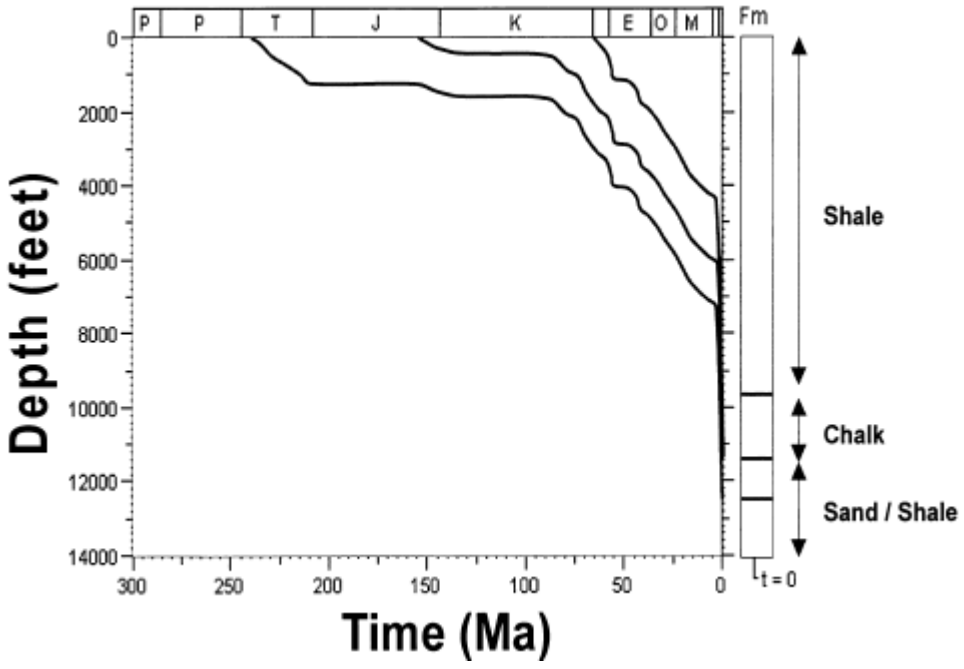

Figure 7.13: Reconstructed burial history for a well in the Judy Field (from Swarbrick et al., 2000). The Triassic curve corresponds to the depth of the Middle Triassic Judy Field at the given time. Notice the slow burial rate up until 80Ma. and the abrupt acceleration of burial rate over the last few Ma.

The heavy carotane compounds which originated from the escaped palaeo-oil were left as residue in the sandstones and then dissolved into the oil from the later infill, i.e a similar history of events as interpreted for the Oseberg palaeo-oil. The palaeo-oil was most likely biodegraded at the time when the Triassic reservoir was situated at shallow depths, but not as severe as the palaeo-oil in the Oseberg Field, as there is unlike in the Oseberg oil still γ-carotane left in the Judy oil. The ratio of γ-carotane to β-carotane is about 1 today (see peak intensities in m/z = 558 and m/z = 560 chromatograms of Judy in Appendix B) probably because the rapid burial of the reservoir from Pleistocene to present resulted in an increase of the maturity and thus leaded to a decrease in the β-carotane abundance relative to the abundance of γ-carotane. The maturity effect would therefore reduce or nullify the effect from biodegradation on the ratio.

The low intensities of the carotane compounds together with the C27-C29 cholestane configuration which is about the same as seen in the NSO-1 oil (Figure 6.1) combined with the presence of C30 steranes, strongly suggests a marine signature of the Judy oil and the carotanes represents only remnants of the escaped palaeo-oil. The interpretation of an escaped palaeo-oil is supported by a slow burial rate and the GC-FID chromatogram, as the biodegraded palaeo-oil would elevate the UCM and there is no such noticeable elevation (see Figure 6.16). Furthermore, the waxiness is not consistent with the waxiness seen for the lacustrine Middle Devonian source rocks i.e. the Judy oil has a low abundance of the n-C25+ fraction and shares the same convave n-alkane envelope as seen in the marine NSO-1 oil which supports the conclusion of a marine derived main contributor of the present day geochemical configuration.

7.12 Summary of the organofacies discussion

The presence of a Middle Devonian source rock kitchen in the Helgeland Basin area is presumed based on the strong evidence of Devonian geochemical signatures found in the bitumen samples from well 6609/11-1, well 6610/7-1 and well 6609/5-1. Furthermore, also a terrestrially derived source rock kitchen of unknown age is indicated from the geochemical signatures found in the B-5 to B-7 bitumen samples which represents the lower section of well 6610/7-1. The terrestrial main source in well 6609/11-1 is also of unknown age, as the bitumen samples from this well show geochemical signatures which are different from the terrestrially derived Lower Jurassic and Carboniferous coals, suggesting that they are not related.

Although found immature in well 6610/7-1 (cf. Schou et al., 1983), also the Kimmeridge equivalent, proves to have reached maturities sufficient for petroleum expulsion in other areas of the Helgeland Basin (or in areas of relatively close proximity to the west i.e. long distance migration of petroleum), which is an interpretation based on the marine diagnostic markers found present in bitumen samples from well 6610/7-1 and also 6609/5-1.

The Middle Devonian palaeo-environemt in the Helgeland Basin is interpretated to be as seen in Figure 7.14. The climate was hot and arid, and the deposition of coarse grained sediments was for the most confined to the areas which were located close to the hinterland. Hypersaline stratified lacustrine lakes with no or little communication to marine waters, with low sedimentation and with production and preservation of organic matter are presumed to have existed. During periods when evaporation exceeded precipitation complete evaporation of the lakes may have occured, as illustraded by the appearance of mudcracks in Figure 7.14.The fault system situated at the Nordland Ridge are presumed to have acted as a physical barrier in a similar way as the Highland Boundary Fault in the Orcadian Basin (see section 2.1 and Figure 2.1), which shielded the basin against mixing with marine waters with the hypersaline lakes, but possible inlets which enabled the establishments of lagoons with a restricted marine organofacies in the Helgeland Basin is not ruled out.

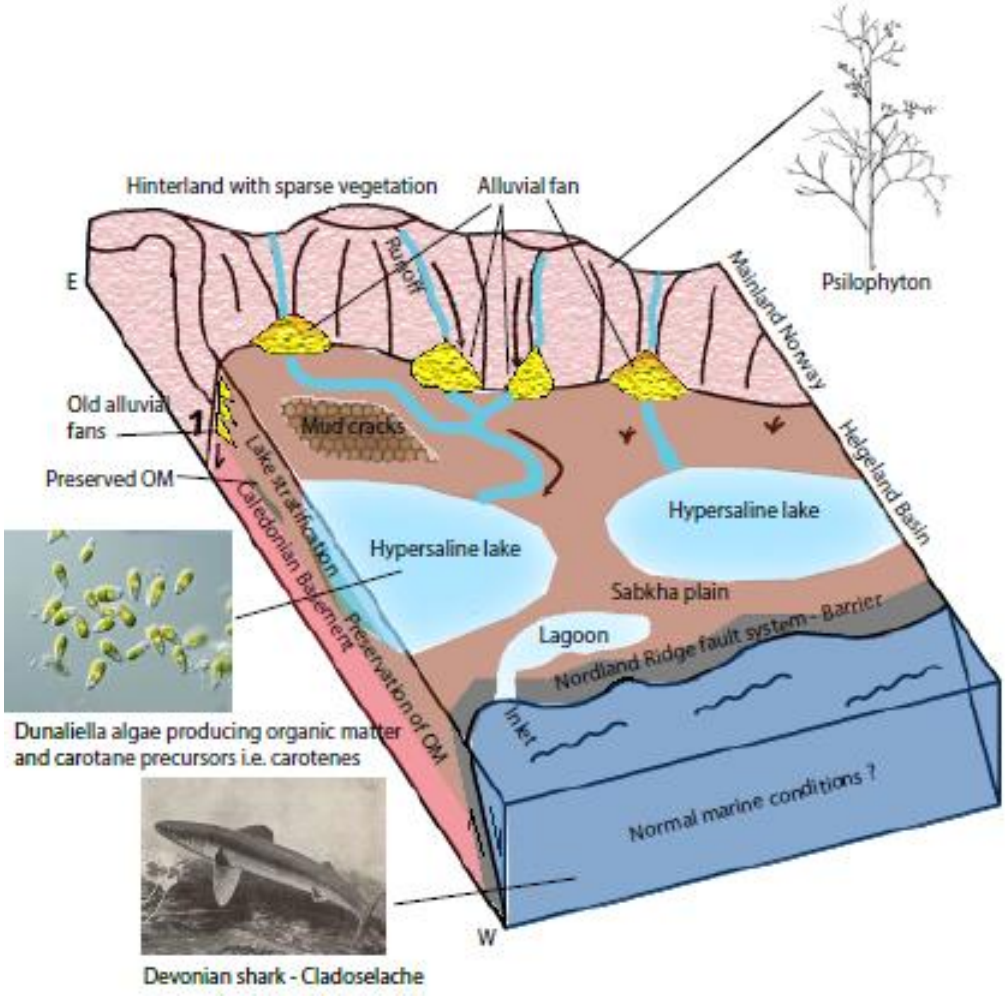

Figure 7.14: Interpretation of the palaeo-environment in the Helgeland Basin area during Middle Devonian (the figure is modified from Pedersen et al., 2006 and the pictures are from Wikipedia 2015a i.e. Devonian shark – *Cladoselachte,* Wikipedia 2015b i.e. *Dunaliella* algae and Wikipedia 2015c i.e. *Psilophyton*).

When considering the investigation of a potential linkage to the lacustrine Middle Devonian source rocks for the Judy oil and the Embla oil, the presence of carotanes in those oils more or less proves a relationship. Furthermore, the positive identification of β-carotane in the reference NSO-1 i.e. the Oseberg oil also relates this oil to the lacustrine Middle Devonian source rocks. However, most of the palaeo-oil in the Judy Field and the Oseberg Field and also probably the Embla Field escaped the reservoirs before the second oil-charge with marine Late-Jurassic Kimmeridge derived oils

8. Summary and conclusion

In this work has novel geochemical data been generated for lacustrine source rock units at the Orkneys and the data has been compared to new analytical data on a series of reference oils from the North Sea, including the Beatrice oil from the Moray Firth offshore UK. In addition was migrated bitumen isolated from sandstone units in the three Helgeland Basin wells 6609/11-1, 6610/7-1 and 6609/5-1 with special focus on the potential existence of hitherto unknown lacustrine markers of the carotane family as known from the Beatrice oil and the Orcadian Basin. This chapter will comprise a summary of important observations and interpretations and will also contain a brief summary of other localities which shows evidence of Palaeozoic sources as reported from the literature, plus a conclusion from this thesis work. This chapter will be outlined as follows:

8.1 The observations based on the Helgeland Basin samples, and their implications for the understanding of Devonian filled basins, offshore Norway

8.2 Differences between the organofacies of the Orkney source rocks and the equivalent in the Helgeland Basin

8.3 The β-carotane versus γ-carotane relationship

8.4 Summary of the thesis objectives

8.5 Evidences for a Palaezoic source in other areas

8.6 Conclusions

8.1 The observations based on the Helgeland Basin samples, and their implications for the understanding of Devonian filled basins, offshore Norway

The carotanes found for the first time to be present in core bitumen extracts from well 6609/11-1, 6610/7-1 and 6609/5-1 in the Helgeland Basin is very strong evidence to suggest that these core extracts were sourced from lacustrine Middle Devonian source rock kitchens of the same general organofacies as found for the Beatrice oil, the well-known bitumens of the Orcadian Basin and also our own source rock samples from the Orkneys. This correlation is also supported by the characteristically low tricyclic terpane abundance in the Helgeland samples, which is identical to that observed in the Beatrice oil. This correlation is further supported by the waxiness i.e. significant portions of long-chained n-alkanes, low isoprenoid abundances (especially for A-5), low enrichment of the C13 isotope and also comparable hopanes to steranes ratios.

The suggestion of a Middle Devonian source rock kitchen in the Helgeland Basin may indicate that depositional basins on the NCS which comprises Devonian strata with possible source rock potential are more common than previously assumed, and this assumption should encourage investigations of specific Middle Devonian source rock biomarkers (e.g. the carotane family) also in other basinal areas.

8.2 Differences between the organofacies of the Orkney source rocks and the equivalent in the Helgeland Basin

The organofacies of the Orkneys source rocks are characterized by high abundance of tricyclic terpanes, high isoprenoid abundances (even though lower maturity compared to the Helgeland samples may account for all this observed difference in abundances) and also in general low hopanes to steranes ratio, and would thus slightly differ from the Middle Devonian source rock equivalent in the Helgeland Basin which shows a more similar geochemical signature as seen from the Beatrice oil.

8.3 The β-carotane versus γ-carotane relationship

The relationship of β-carotane versus γ-carotane which was reported by Jiang and Fowler (1986), i.e. the former being more resistant to biodegradation and the latter being more resistant to thermal maturation, is confirmed in this thesis as observed from the depletion of β-carotane in the highly mature Embla oil, while γ-carotane is depleted in the Oseberg oil which was situated in a reservoir subjected to uplift and erosion which in turn allowed severe biodegradation of the palaeo-oil.

8.4 Summary of the thesis objectives

- The hydrocarbons in well 6609/11-1 originate from a terrestrial source, and samples A-2 plus A-5 are concluded to have a second lacustrine Middle Devonian source origin based on the presence of β-carotane. The bitumen found in the upper section of 6610/7-1 (B-1 to B-3) are probably co-sourced by the lacustrine Middle Devonian source and a Kimmeridge equivalent source, and the same is suggested for the C-1 and C-2 bitumen samples in well 6609/5-1. The lower section of 6610/7-1 contains bitumen samples (B-4 to B-7) which are

concluded to have been mainly sourced by a terrestrially derived source, with a secondary contribution from a Kimmeridge equivalent source rock.

- The presence of carotanes in the Embla Field and Judy Field which are both located outide the outline of what is considered the Orcadian Basin at present day, suggests a Middle Devonian source for the former and latter and thus that the area affected by the Middle Devonian source rock kitchen expands further to the south across the southern limit of the Orcadian Lake i.e. High Boundary Fault (Marshall et al., 2011) and into the zone which had presence of marine water in Middle Devonian (long distance migration of petroleum?). The carotane presence in the Oseberg Field, confirms the correlation of the Orcadian Basin into this area.

- Concerning the source rock samples from the Orkneys, the kerogen type of the organic matter in the source rock is based on Rock-Eval and TOC evaluations concluded to represents Middle Devonian lacustrine lake deposits with input varying from type II to type III kerogen, and the extracted bitumen samples collaborates this conclusion with the bulk of the bitumen samples classified as type II, and are thus of lower quality than the common type I organic matter seen in the Middle Devonian source rock deposits in the Orcadian Basin. The generative potential of the source rocks varies from poor to good, the TOC values are in the range from 0.33 wt.% to 2.79 wt.% and the S2 values in the range of 0.89 mg/g to 11.08 mg/g (see Table 6.5), and the bulk of the samples classified as having good potential (See Table 7.1). In comparison, the minimum criterias for categorizing a rock unit as a source rock after Peters and Cassa (1994) are TOC value of at least 0.5 wt. % and also a S2 yield of at least 2.5 mg/g.

- Based on a series of maturity parameters, the source rock bitumen samples are classified as marginally mature, while the Helgeland Basin bitumen samples and the oils representing the Beatrice Field, the Oseberg Field, the Judy Field and Embla Field are categorized as mature, i.e. in the peak oil, and concerning Embla the late peak oil window.

8.5 Evidences for a Palaezoic source in other areas

Beside the Beatrice Field and the indications of a very strong set of evidences for a Palaeozoic source for some of the Helgeland Basin bitumen samples and the Oseberg Field in this thesis plus confirmation of a Palaeozoic, i.e. probably Middle Devonian based on γ-carotane in the Embla oil, there have been found evidences of hydrocarbon originating from Palaeozoic sources in other areas. The Clair field which is located north -west from Shetland Islands on the brink of the outline of the Orcadian Basin (see Figure 3.3) has been partly filled with Palaeozoic oil, most likely originating from the Middle Devonian (Mark et al., 2008). In the Solund – Fensfjorden Devonian Basin situated at the easternmost area of the Orcadian Basin on mainland Norway, remnants of pyrobitumen that is thought to once be Palaeozoic oils but at present day overcooked, have been reported (Helgesen 2008). Furthermore, residual bitumen samples of most likely Palaeozoic age and with a marine character (Pedersen et al., 2007) has been observed also in other regions in Scandinavia, e.g. in Upper Ordovician limestones in the Oslo Graben (Dons, 1956), in Ordovician carbonates at Siljan (e.g. Vlierboom et al., 1986), in Precambrian sandtones at Gävle and in granitic basement in Jämtland (see Figure 8.1).

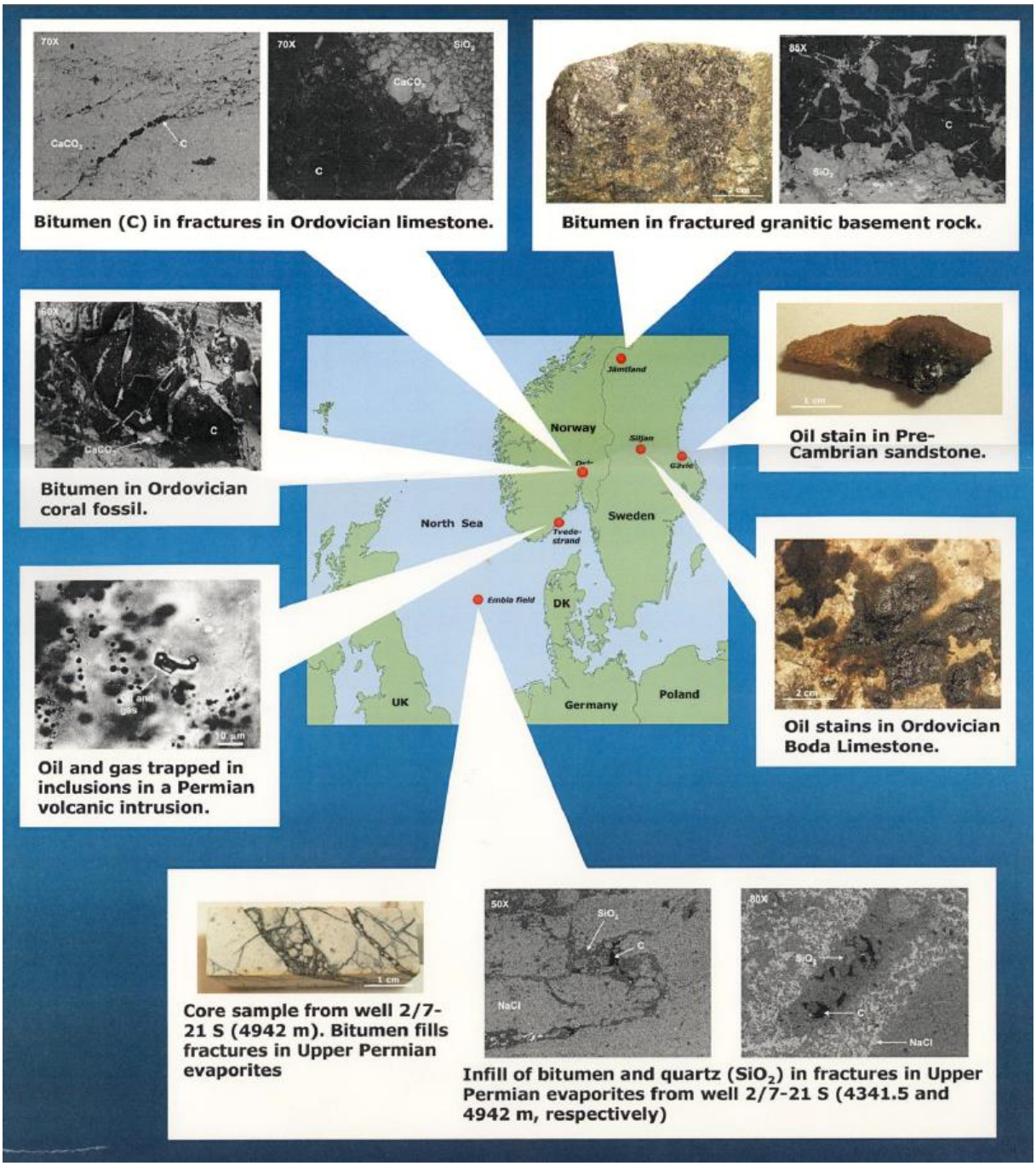

Figure 8.1: Overview of different known localities in Scandiavia with presence of bitumens which can be related to Palaeozoic sources (from Pedersen 2002).

8.6 Conclusions

Presence of carotanes in the Embla Field, Judy Field and some of the selected Helgeland Basin bitumen samples suggests the existence today of an extensive Middle Devonian source rock kitchen which extends from what is at present day considered as part of the Orcadian Basin, covering areas further to the south in the North Sea and also expanding into the Helgeland Basin in the Norwegian Sea. The cumulative irrefutable evidences of bitumen sourced from Middle Devonian source rocks as observed from the presence of β-carotane in the Oseberg Field, which is located within what is at present day considered the Orcadian Basin, strengthens a model with several Palaeozoic source rock basins on the NCS and not only within the Helgeland Basin. Why these compounds have not before been identified in the Oseberg oil is hard to tell, but most likely is this simply reflecting our modern and improved instrumentations and a willingness to look also for the less likely geochemical parameters. The observation of β-carotane in the Oseberg Field does also improve the certainty of correlating the Orcadian Basin across the Northern North Sea eastwards from the Moray Firth/Scotland area towards mainland Norway.

The residual bitumens from the lacustrine Middle Devonian source rocks as represented by the presence of the carotane family, and found present in oils from reservoirs on structural highs e.g. in the Judy Field and the Oseberg Field did most likely increase the secondary migration efficiency of the second infill, i.e. the Late Jurassic Kimmeridge equivalent and did also enhance preservation of porosity.

It is possible that the Middle Devonian source rock kitchen expands even further north from the Helgeland Basin on the NCS and into Lofoten and Vesterålen but as those areas are not yet opened for exploration, this topic will thus remain unresolved in the near future. However, the northward extent of the hypersaline lacustrine source rocks, which are present in the Orcadian Basin, towards the Barents Sea could be limited by the greater change in palaeo-latitude and this may account for a lower probability of similar climatic settings i.e. hot and arid as in the Orcadian Basin during Middle Devonian.

When all evidence and indications of Palaeozoic sourcing across the NCS and the UK-sector are put together, and also discoveries of residual bitumens on mainland Norway and Sweden, one starts to envisage the outline of much more complex Palaeozoic source rock systems, some of which may be active today in regions where the Jurassic source rocks are non-existent or marginally mature and

this might be of commercially great importance as seen from the Beatrice Field and also the Clair Field.

References

Abay, T.B, 2010. *Vertical variation in reservoir core geochemistry*. Master thesis, University of Oslo, 284pp.

Abay, T.B., Karlsen, D.A. and Ohm, S.E., 2014. *Vertical variations in reservoir geochemistry in a palaeozoic trap, Embla Field, offshore Norway.* Journal of Petroleum Geology, Vol. 37, Issue 4, 349-372.

Adu, R.O. and Petersen, T., 2011. *Danish Sustainable Offshore Decommisioning Project – Background report of Danish and other North Sea fields and platforms due for decommissioning*. Offshore Centre Denmark, 21pp.

Alexander, R., Kagi, R.I. And Woodhouse, G.W., 1981. *Geochemical Correlation of Windalia Oil and Extracts of Winning Group (Cretaceous) Potential Source Rocks, Barrow Subbasin, Western Australia.* The American Association of Petroleum Geologists Bulletin 65, 235-250.

Aquino Neto, F.R., Trendel, J.M., Restle, A., Connan, J. and Albrecht, P.A., 1983. *Occurrence and formation of tricyclic and tetracyclic terpanes in sediments and petroleums*. In: Advances in Organic Geochemistry 1981 (Bjorøy, M., Albrecht, C., Cornford, C., et al., Eds.). John Wiley & Sons, New York, 659-676.

Astin, T.R., 1990. *The Devonian lacustrine sediments of Orkney, Scotland; implications for climate cyclicity, basin structure and maturation history.* Journal of the Geological Society, London, Vol. 147, 141-151.

Azhar, H, 2012. *Petroleum geochemistry of the so-called "dry wells" off mid-Norway; clues to ignored and overlooked petroleum systems*. Master thesis, University of Oslo, 129pp.

Badley, M.E, Price, J.D, Rambech Dahl, C. and Agdestein, T., 1988. *The structural evolution of the northern Viking Graben and its bearing upon extensional modes of basin formation*. Journal of the Geological Society, 455-472.

Bailey, N.J.L., Burwood, R. and Harriman, G.E., 1990. *Application of pyrolysate carbon isotope and biomarker technology to organofacies definition and oil correlation problems in North Sea basins.* Advances in Organic Geochemistry 1989, Organic Geochemistry Vol. 16, Nos 4-6, 1157-1172.

Beach, F., Peakman, T.M., Abbott, G.D., Sleeman, R. and Maxwell, J.R., 1989. *Laboratory thermal alteration of triaromatic steroid hydrocarbons.* Organic Geochemistry, Volume 14, Issue 1, 109-111.

Ben-Amotz, A., Shaish, A. and Avron, M., 1989. *Mode of Action of the Massively Accumulated β-Carotene of Dunaliella bardawil in Protecting the Alga against Damage by Excess Irradiation*. Plant physiology, Vol. 91, Issue 3, 1040-1043

Bray, E.E. and Evans, E.D., 1961. *Distribution of n-paraffins as a clue to recognition of source beds.* Geochimica et Cosmochimica Acta, Vol. 22, 2-15.

Budzinski, H., Nadalig, T., Raymond, N., Matuzahroh, N. and Gilewicz, M., 2000. *Evidence of two metabolic pathways for degradation of 2-Methylphenanthrene by spingomonas sp. Strain (2MPII).* Environmental Toxicology and Chemistry, Vol. 19, No. 11, 2672-2677.

Bugge, T., Ringås, J.E.,Leith, D.A., Mangerud, G., Weiss, H.M. and Leith, T.L, 2002. *Upper Permian as a new play model on the mid-Norwegian continental shelf: Investigated by shallow stratigraphic drilling*. The American Association of Petroleum Geologists Bulletin 86, No. 1, 107-127.

Bukovics, C. and Ziegler, P.A., 1985. *Tectonic development of the Mid-Norway continental margin.* Marine and Petroleum Geology, Vol. 2, 2-22.

Dahl, B., Bojesen-Koefoed, J., Holm, A., Justwan, H., Rasmussen, E. and Thomsen E., 2004. *A new approach to interpreting Rock-Eval S_2 and TOC data for kerogen quality assessment*. Organic Geochemistry, Vol. 35, 1461-1477.

Dahl, L, Moldowan, M. and Sundararaman, P., 1993. Relationship of biomarker distribution to depostional environment: Phosphoria Formation, Montana, U.S.A. Organic Geochemistry, Vol. 20, No. 7, 1007-1017.

De Grande, S.M.B., Aquino Neto, F.R. and Mello, M.R., 1993. *Extended tricyclic terpanes in sediments and petroleums.* Organic Geochemistry, Vol. 20, No. 7, 1039-1047.

Dons, J.A., 1956. *Coal blend and uranifierous hydrocarbon in Norway*. Norsk Geologisk Tidsskrift, v. 36, 250-266.

Downie, R.A., 2009. *Devonian*. In: Glennie, K.W. (Ed.), *Petroleum Geology of the North Sea: Basic Concepts and Recent Advances, Fourth Edition.* Blackwell Science Ltd, 85-103.

Duncan, A.D and Hamilton, R.F.M., 1988. *Palaeolimnology and organic geochemistry of the Middle Devonian in the Orcadian Basin*. In: Fleet, A.J., Kelts, K. and Talbot, M.R. (eds.), *Lacustrine Petroleum Source Rocks*, Geological Society Special Publication No. 40 , 173-201.

Duncan, W.I. and Buxton, N.W.K., 1995. *New evidence for evaporitic Middle Devonian lacustrine sediments with hydrocarbon source potential on the East Shetland Platform, North Sea.* Journal of the Geological Society, London, Vol. 152, 251-258.

Elvevold, S., Dallmann, W. and Blomeier, D., 2007. *Geology of Svalbard*. Norwegian Polar Institute, 38pp.

Faleide, J.I., Bjørlykke, K. and Gabrielse, R.H., 2010. *Geology of the Norwegian Continental Shelf.* In: Bjørlykke, K. (ed.), *Petroleum Geoscience: From Sedimentary Environments to Rock Physics.* Springer-Verlag Berlin Heidelberg. 467-499.

Galimov, E.M., *1980. 13C/12C in kerogen*. In: Durand, B. (ed.), *Kerogen – Insoluble Organic Matter from Sedimentary Rocks*. Editions Technip, Paris, 271–299.

Gjelberg, J.G., 1981: *Upper Devonian (Famennian) - Middle Carboniferous succession of Bjørnøya. A study of ancient alluvial and coastal marine sedimentation*. Norsk Polarinstitutt, 67pp.

Guo, Li, Schekoldin, R. and Scott, R., 2010. *The Devonian succession in northern Novaya Zemlya, Artic Russia: sedimentology, palaeogeography and hydrocarbon occurrence.* Journal of Petroleum Geology, Vol. 33, Issue 2, April, 105-122.

Helgesen, L., 2008. *Possible remnants after Hydrocarbons in Serpentinized Ultramafics from the Solund-Fensfjorden Devonian Basin Western Norway – Abiogenic vs. Biogenic Origin.* Master thesis, University of Oslo, 107pp.

Hillier, S. and Marshall, J.E.A., 1992. *Organic maturation, thermal history and hydrocarbon generation in the Orcadian Basin, Scotland.* Journal of the Geological Society, London, Vol. 149, 491-502.

Hoefs, J., (2009). *Stable Isotope Geochemistry (*6th ed.) Springer-Verlag, New York, 285 pp.

Hughes, W.B., Holba, A.G. And Dzou, L.I.P, 1995. *The ratios of dibenzothiophene to phenanthrene and pristane to phytane as indicators of depositional environment and lithology of petroleum source rocks.* Geochimica et Cosmochimica Acta, Vol. 59, No. 17, 3581-3598.

Jiang, Z., and Fowler, M.G., 1986. *Carotenoid-derived alkanes in oils from northwestern China.* Organic Geochemistry, Vol. 10, Issue 4-6, 831-839.

Justwan, H. and Dahl, B., 2005. *Quantitative hydrocarbon potential mapping and organofacies study in the Greater Balder Area, Norwegian North Sea*. In: Dore', A.G. and Vining, B.A., (eds.), *Petroleum Geology: North-West Europe and Global Perspectives – Proceedings of the 6th Petroleum Geology Conference,* Geological Society, London, 1317-1329.

Justwan, H., Dahl, B., Isaksen, G.H. and Meisingset, I., 2005. *Late to Middle Jurassic source facies and quality variations, South Viking Graben, North Sea*. Journal of Petroleum Geology, Vol. 28, Issue 3, 241-268.

Justwan, H., Dahl, B. and Isaksen, G.H., 2006. *Geochemical characterization and genetic origin of oils and condensates in the South Viking Graben, Norway*. Marine and Petroleum Geology, Vol. 23, 213-239.

Karlsen, D.A. and Larter, S.R., 1991. *Analysis of petroleum fractions by TOC-FID: applications to petroleum resveroir description*. Organic Geochemistry, Vol. 17, No. 5, 603-617.

Karlsen, D.A., Nyland, B., Flood, B., Ohm, S.E., Brekke, T., Olsen, S. and Backer-Owe, K, 1995. *Petroleum geochemistry of the Haltenbanken, Norwegian continental shelf.* In Cubitt, J.M. and England, W. A. (eds.), 1995, *The Geochemistry of Reservoirs*, Geological Society Special Publication No. 86, 203-256.

Karlsen, D.A. and Skeie, J.E., 2006. *Petroleum migration, faults and overpressure, part I: Calibrating basin modelling using petroleums in traps – A review*. Journal of Petroleum Geology, Vol. 29, Issue 3, 227-256.

Katz, B.J. and Elrod, L.W., 1983. *Organic geochemistry of DSDP Site 467, offshore California, Middle Miocene to Lower Pliocene strata.* Geochimica et Cosmochimica Acta, Vol. 47, 389-396.

Kvalheim, O.M., Telnaes, N., Bjørseth, A. and Christy, A.A., 1987. *Interpretation of Multivariable Data: Relationship between phenanthrenes in Crude Oils*. Chemometrics and Intelligent Laboratory systems Vol. 2, 149-153.

Mackenzie, A.S., Patience, R.L. And Maxwell, J.R., 1980. *Molecular parameters of maturation in the Toarcian shales, Paris Basin, France-I. Changes in the configurations of acyclic isoprenoid alkanes, steranes and triterpanes.* Geochimica et Cosmochimica Acta Vol. 44, 1709-1721.

Mark, D.F., Green, P.F., Parnell, J., Kelley, S.P., Lee, M.R. and Sherlock, S.C., 2008. *Late Palaeozoic hydrocarbon migration through the Clair field, West of Shetland, UK Atlantic margin.* Geochimica et Cosmochimica Acta 72 (2008), 2510-2533.

Marshall, J.E.A., Brown, J.F. and Hindmarsh, S., 1986. *Hydrocarbon source rock potential of the Devonian rocks of the Orcadian Basin.* Scott. J. Geol. 21, (3), 301-320.

Marshall, J.E.A, Brown, J.F. and Astin, T.R., 2011. *Recognizing the Taghanic Crisis in the Devonian terrestrial environment and its implications for understanding land-sea interactions.* Palaeogeography, Palaeoclimatology, Palaeoecology 304, 165-183.

Mello, M.R., 1988. *Geochemical and Molecular Studies of the Depositional Environments of Source Rocks and their Derived Oils from the Brazilian Marginal Basins*. Ph.D thesis, Bristol University, 240pp.

Mello, M.R., Telnaes, N., Gaglianone, P.C., Chicarelli, M.I., Brassel, S.C. And Maxwell, J.R., 1988. *Organic geochemical characterization of depositional palaeoenvironments of source rocks and oils in Brazilian marginal basins.* Organic Geochemistry, Vol. 13, Nos. 1-3, 31-45.

Moldowan, J.M., Seifert, W.K., Arnold, E. and Clardy, J., 1984. *Structure proof and significance of stereoisometric 28,30-bisnorhopanes in petroleum and petroleum source rocks.* Geochimica et Cosmochimica Acta Vol. 48, 1651-1661.

Moldowan, J.M., Seifert, W.K. And Gallegos, E.J., 1985. *Relationship Between Petroleum Composition and Depositional Environment of Petroleum Source Rocks.* The American Association of Petroleum Geologists Bulletin Vol. 69, No. 8, 1255-1268.

Moldowan, J.M., Sundararaman, P. and Schoell, M., 1986. *Sensitivity of biomarker properties to depositional environment and/or source input in the Lower Toarcian of SW-Germany*. Organic Geochemistry, Vol. 10, 915-926.

Moldowan, J.M., Fago, F.J., Carlson, R.M.K., Young, D.C., Duyne, G.V., Clardy, J., Schoell, M., Pillinger, C.T. And Watt, D.S., 1991. *Rearranged hopanes in sediments and petroleum.* Geochimica et Cosmochimica Acta, Vol. 55, 3333-3353.

National Geospatial-Intelligence Agency, 2015, *Judy Oil Field: United Kingdom*. Available at http://www.geographic.org/geographic_names/name.php?uni=97889&fid=6477&c=united_kingdom, last visited 05.29.2015.

NPD, 2015a. *Factpages*. Available at: http://factpages.npd.no/factpages/, last visited 05.27.2015.

NPD 2015b. *Factmaps.* Available at: http://gis.npd.no/FactMaps/sl_20/?Viewer=FactMaps_20, last visited 05.27.2015.

Ohn, S.E., Karlsen, D.A., Phan, N.T., Strand, T. and Iversen, G., 2012. *Present Jurassic petroleum charge facing Paleozoic biodegraded oil; geochemical challenges and potential upsides, Embla Field, North Sea*. The American Association of Petroleum Geologists Bulletin, Vol. 96, 1189-1212.

Osmundsen, P.T., Sommaruga, A., Skilbrei, J.R. and Olesen, O., 2002. *Deep structure of the Mid Norway rifted margin.* Norwegian Journal of Geology, Vol. 82, No. 4, 205-224.

Parnell, J., Carey, P. and Monson, B., 1998. *Timing and temperatureof decollement on hydrocarbon source rock beds in cyclic lacustrine successions.* Palaeogeography, Palaeoclimatology, Palaeoecology 140, 121-134.

Pedersen, J.H. 2002. *Atypical oils and condensates of the Norwegian Continental Shelf – an Organic Geochemical Study*. Cand. Scient. Thesis in Geology, University of Oslo, Norway, 236 pp.

Pedersen, J.H., Karlsen, D.A., Lie, J.E., Brunstad, H. and di Primio, R., 2006. *Maturity and source-rock potential of Palaeozoic sediments in the NW European Northern Permian Basin*. Petroleum Geoscience, Vol. 12, 13-28.

Pedersen, J.H., Karlsen, D.A., Spjeldnæs, N., Backer-Owe, K., Lie, J.E. and Brunstad, H., 2007. *Lower Palaeozoic petroleum from southern Scandinavia: Implications to a Paleozoic petroleum system*

offshore Norway. American Association of Petroleum Geologists Bulletin Vol. 91, No. 8 (August 2007), 1189-1212.

Peters, K. E., 1986. *Guidelines for evaluating petroleum source rock using programmed pyrolysis.* The American Association of Petroleum Geologists Bulletin, Vol. 70, No. 3, 318–329.

Peters, K.E., Moldowan, J.M., Driscole, A.R. and Demaison, G.J., 1989. *Origin of Beatrice Oil by Co-Sourcing from Devonian and Middle Jurassic Source Rocks, Inner Moray Firth, United Kingdom.* The American Association of Petroleum Geologists Bulletin Vol. 73, No. 4, 454-471.

Peters, K.E., Moldowan, J.M. and Sundararaman, P., 1990. *Effects of hydrous pyrolysis on biomarker thermal maturity parameters: Monterey Phosphatic and Siliceous members*. Organic Geochemistry, Vol. 15, No. 3, 249-265.

Peters, K.E. and Moldowan, J.M.,1993. *The Biomarker Guide. Interpreting Molecular Fossil* .In: *Petroleum and Ancient Sediments*. Englewood Cliffs, Prentice-Hall, N.J, 363pp.

Peters, K.E. and Cassa, M.R., 1994. *Applied source rock geochemistry*. In: L.B. Magoon and W.G. Dow. (eds.), *The Petroleum System – From Source to Trap*. American Association of Petroleum Geologists Memoir, Vol. 60, 93-120.

Peters, K.E. and Fowler, M.G., 2002. *Applications of petroleum geochemistry to exploration and reservoir management*. Organic Geochemistry Vol. 33, 5-36.

Peters, K.E., Walters, C.C., and Moldowan, J.M., 2005. *The Biomarker Guide second edition.* Cambridge University Press, 1155pp.

Petersen, H.I., Øverland, J.A., Solbakk, T., Bojesen-Koefoed, J.A. and Bjerager, M., 2013. *Unusual resinite-rich coals found in northeastern Greenland and along the Norwegian coast: Petrographic and geochemical composition*. International Journal of Coal Geology 109-110, 58-76.

Püttman, W., Merz, C. and Speczik, S., 1989. *The secondary oxidation of organic material and its influence on Kupferschiefer mineralization of southwest Poland*. Applied Geochemistry, Vol. 4, 151-161.

Radke, M., 1988. *Application of aromatic compounds as maturity indicators in source rocks and crude oils*. Marine and Petroleum Geology, Vol. 5, 224-236.

Radke, M., Welte, D.H. and Willsch, H., 1982a. *Geochemical study on a well in the Western Canada Basin: relation of the aromatic distribution pattern to maturity of organic matter*. Geochimica et Cosmochimica Acta, Vol. 46, 1-10.

Radke, M., Willsch, H. and Leythaeuser, D., 1982b. *Aromatic components of coal: relation of distribution pattern to rank*. Geochimica et Cosmochimica Acta, Vol. 46, 1831-1848.

Radke, M. and Welte, D. H., 1983. *The methylphenanthrene index (MPI). A maturity parameter based on aromatic hydrocarbons*. In: Bjorøy, M., Albrecht, C., Cornford, C., et al., (eds.), *Advances in Organic Geochemistry 1981,* John Wiley & Sons, New York, 504–512.

Radke, M., Welte, D.H. and Willsch, H., 1986. *Maturity parameters based on aromatic hydrocarbons: Influence of the organic matter type.* Organic Geochemistry, Vol. 10, 51-63.

Ravnås, R., Nøttvedt, A., Steel, R.J. and Windelstad, J. 2000. *Syn-rift sedimentary architectures in the Northern North Sea*. Geological Society, London, Special Publications, 133-177.

Rullkötter, J. and Marzi, R., 1988. *Natural and artificial maturation of biological markers in a Toarcian shale from northern Germany.* Advances in Organic Geochemistry 1987, Organic Geochemistry, Vol. 13, Nos 4-6. 639-645.

Scalan, E.S. and Smith, J.E., 1970. *An improved measure of the odd-even predominance in the normal alkanes of sediment extracts and petroleum*. Geochimica et Cosmochimica Acta, Vol. 34, Issue 5, 611-620.

Schou, L., Akernes, J. and Hustad, E., 1983. *Source rock/Hydrocarbon Staining Correlation in Well 6610/7-1.* Continental shelf institute, Norway. 99 pp.

Schweingruber, F.H., Börner, A. and Schulze, E.D., 2006. *Atlas of Woody Plant Stems – Evolution, Structure, and Environmental Modifications*. Springer Verlag. 218pp.

Seifert, W.K. and Moldowan, J.M., 1978. *Applications of steranes, terpanes and monoaromatics to the maturation, migration and source of crude oils.* Geochimica et Cosmohimica Acta, Vol. 42, 77-95.

Seifert, W.K. and Moldowan, J.M., 1979. The effect of biodegradation on steranes and terpanes in crude oils. Geochimica et Cosmochimica acta, 43, 111-126.

Seifert, W.K. and Moldowan, J.M., 1980. *The effect of thermal stress on source-rock quality as measured by hopane stereochemistry*. Physics and Chemistry of the Earth, Vol. 12, 229-237.

Seifert, W.K. and Moldowan, J.M., 1986. *Use of biological markers in petroleum exploration*. In: Johns, R.B. (ed.), *Methods in Geochemistry and Geophysics Vol. 24*, Elsevier, Amsterdam, 261-290.

Steel, R., Siedlecka, A. and Roberts, D., 1985. *The Old Red Sandstone Basins of Norway and their deformation; a review.* In: Gee, D.G. and Sturt, B.A., (eds.), *The Caledonide Orogen – Scandinavia and Related areas*. J. Wiley, Chinchester, 293-315.

Surlyk, F., 1990. *Timing, style and sedimentary evolution of Late Palaeozoic-Mesozoic extensional basins of East Greenland.* In: Hardman, R.F.P. and Brooks, J., (eds.), *Tectonic Events Responsible for Britain's Oil and Gas Reserves*. Geological Society Special Publication No. 55, 107-125.

Sutton, P.A., Lewis, C.A., and Rowland, S.J., 2005. *Isolation of individual hydrocarbons from the unresolved complex hydrocarbon mixture of a biodegraded crude oil using preparative capillary gas chromatography*. Organic Geochemistry, Vol. 36, Issue 6, 963-970.

Swarbrick, R.E., Osborne, M.J., Grunberger, D., Yardley, G.S., Macleod, G., Aplin, A.C., Larter, S.R., Knight, I., Auld, H.A., 2000. *Integrated study of the Judy Field Block 30/7a) – an overpressured Central North Sea oil/gas field*. Marine and Petroleum Geology Vol. 17, 993-1010.

Szczerba, M. and Rospondek, M.J., 2010. *Controls on distributions for methylphenanthrenes in sedimentary rock extracts: Critical evaluation of existing geochemical data from molecular modelling*. Organic Geochemistry, Vol. 41, 1297-1311.

Tissot, B., Califet-Debyser, Deroo, G. and Oudin, J.L., 1971. *Origin and Evaluation of Hydrocarbons in Early Toarcian Shales, Paris Basin, France.* The American Association of Petroleum Geologists Bulletin 55, No. 12, 2177-2193.

Tissot, B.P. and Welte, 1984. *Petroleum formation and Occurrence* (2nd ed.). Springer-Verlag, 699pp.

Tissot, B.P., Pelet, R. and Ungerer, PH., 1987. *Thermal History of Sedimentary Basins, Maturation Indices, and Kinetics of Oil and Gas Generation.* The American Association of Petroleum Geologists Bulletin, Vol. 71, No. 12, 1445-1466.

Trewin, N.H., 1985. *Mass mortalities of Devonian fish – the Achanarras Fish Bed, Caithness.* Geology today, Vol. 1, Issue 2, 45-49.

Trewin, N.H., 1989. *The petroleum potential of the Old Red Sandstone of northern Scotland.* Scott. J. Geol. 25, (2), 201-225.

Van Graas, G.W., 1990. *Biomarker maturity parameters for high maturities: Calibration of the working range up to the oil/condensate threshold.* Organic Geochemistry, Vol. 16, No 4-6, 1025-1032.

Van Koeverden, J.H., Karlsen, D.A., Schwark, L., Chpitsglouz, A. and Backer-Owe, K, 2010. *Oil-prone Lower Carboniferous coals in the Norwegian Barents Sea: Implications for a Palaeozoic petroleum system*. Journal of Petroleum Geology, Vol. 33, Issue 2, 1-28.

Vlierboom, F.W., Collini, B. and Zumberge, J.E., 1986. *The occurrence of petroleum in sedimentary rocks of the meteor impact crater at Lake Siljan, Sweden*. Organic Geochemistry Vol. 10, No 1-3, 153-161.

Wang, Y., 2006. *How Pierced PTFE/Silicone Septa Affect GC-MS Experiments*. American Laboratory, 4pp.

Wikipedia, 2015a. *Picture of Devonian shark – Cladoselache*. Available at: http://en.wikipedia.org/wiki/Cladoselache, last visited 05.28.2015.

Wikipedia, 2015b. *Picture of Dunaliella alga.* Available at: http://en.wikipedia.org/wiki/Dunaliella, last visited 05.28.2015.

Wikipedia, 2015c. *Picture of Psilophyton*. Available at: http://en.wikipedia.org/wiki/Psilophyton, last visited 05.28.2015.

Ziegler, P.A., 1990. Geological Atlas of Western and Central Europe (2nd ed.). Shell International Petroleum Maatschappij BV, 256pp.

Appendix A: GC-FID chromatograms

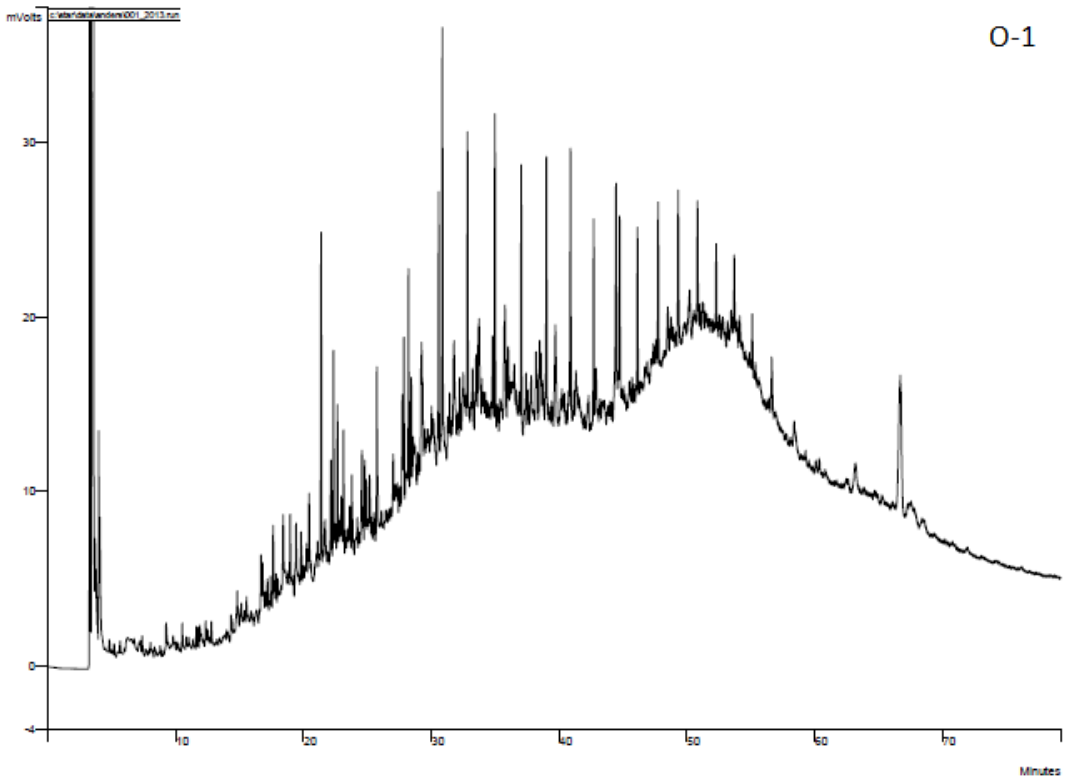

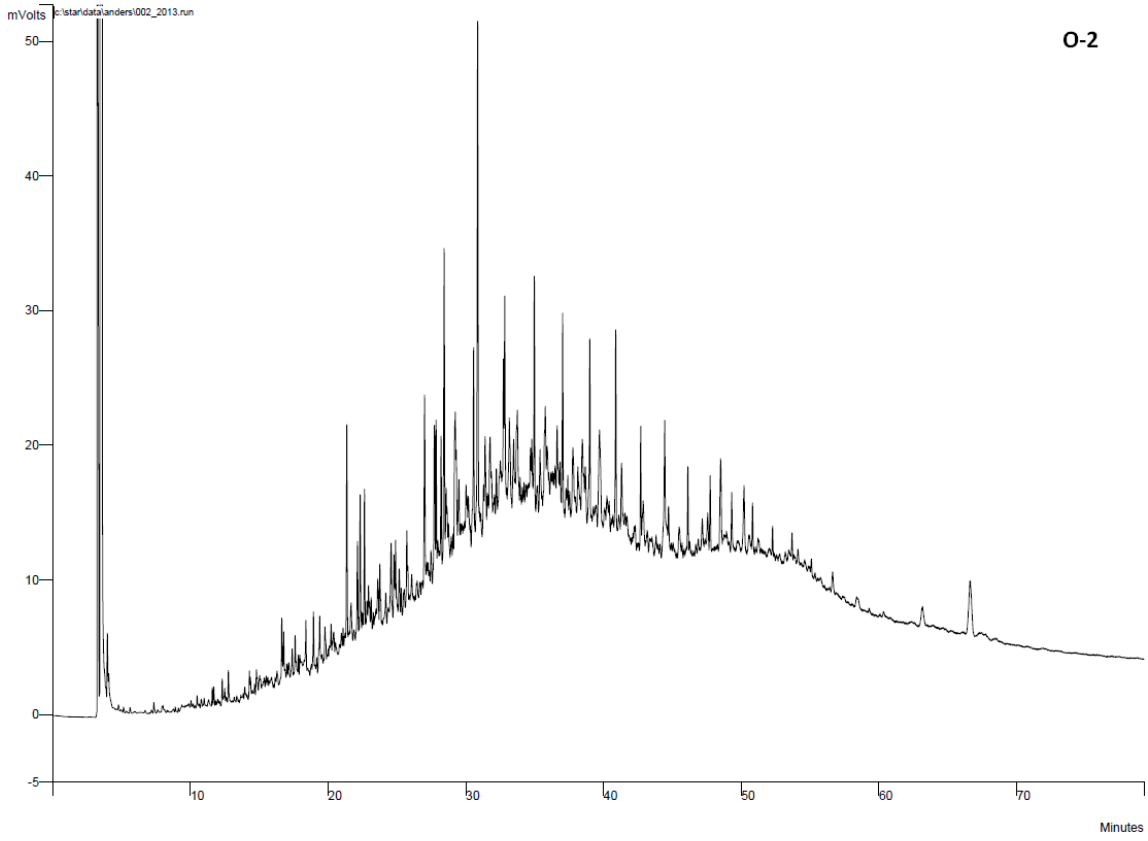

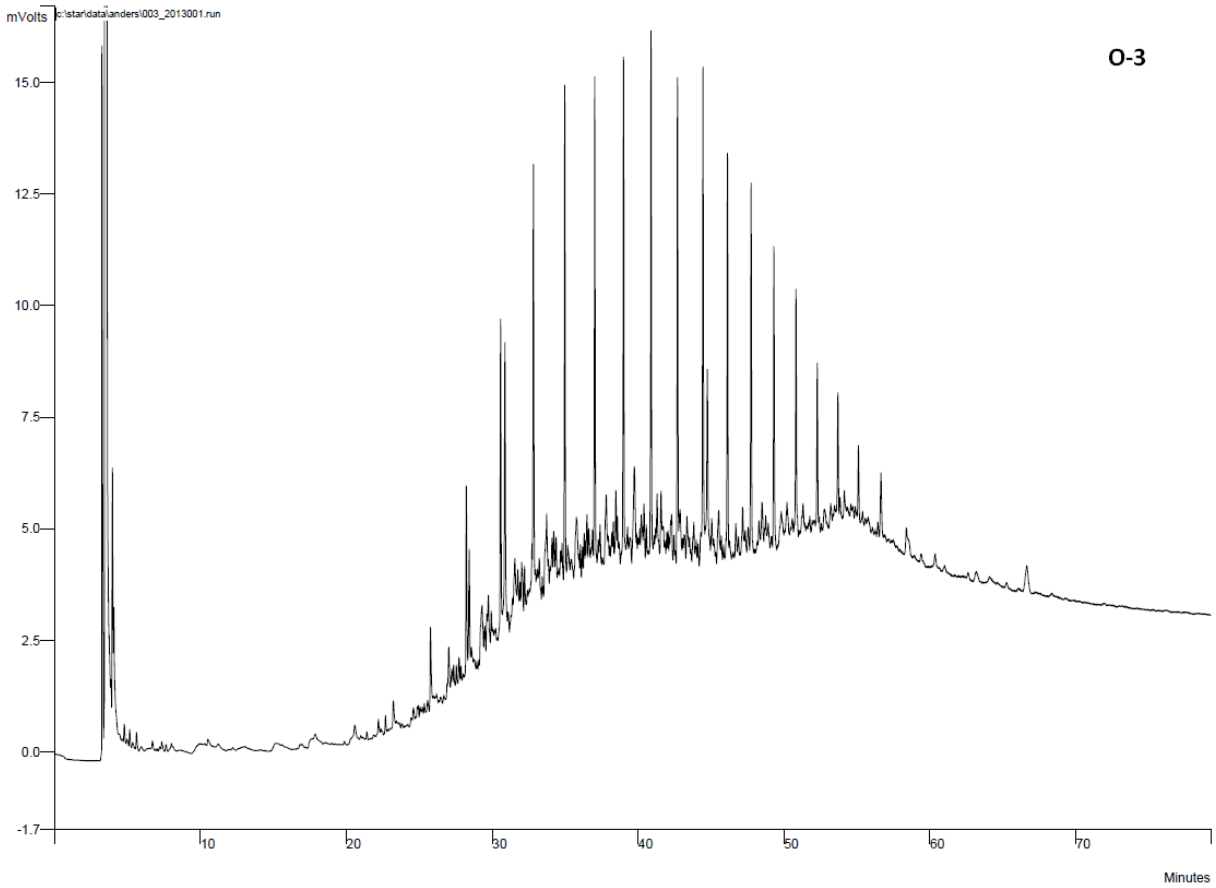
mVolts
c:\star\data\anders\003_2013001.run
O-3
15.0
12.5
10.0
7.5
5.0
2.5
0.0
-1.7
10
20
30
40
50
60
70
Minutes

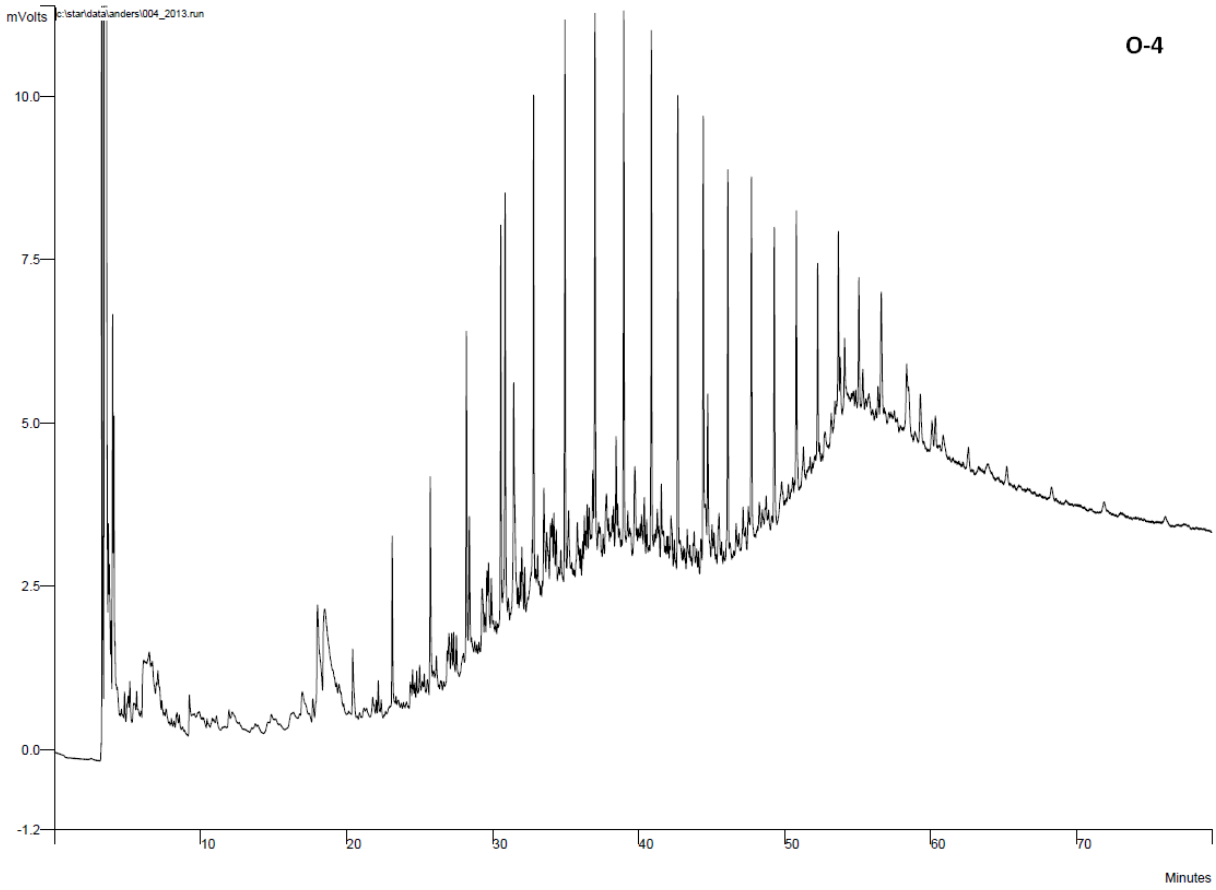
mVolts
c:\star\data\anders\004_2013.run
O-4
10.0
7.5
5.0
2.5
0.0
-1.2
10
20
30
40
50
60
70
Minutes

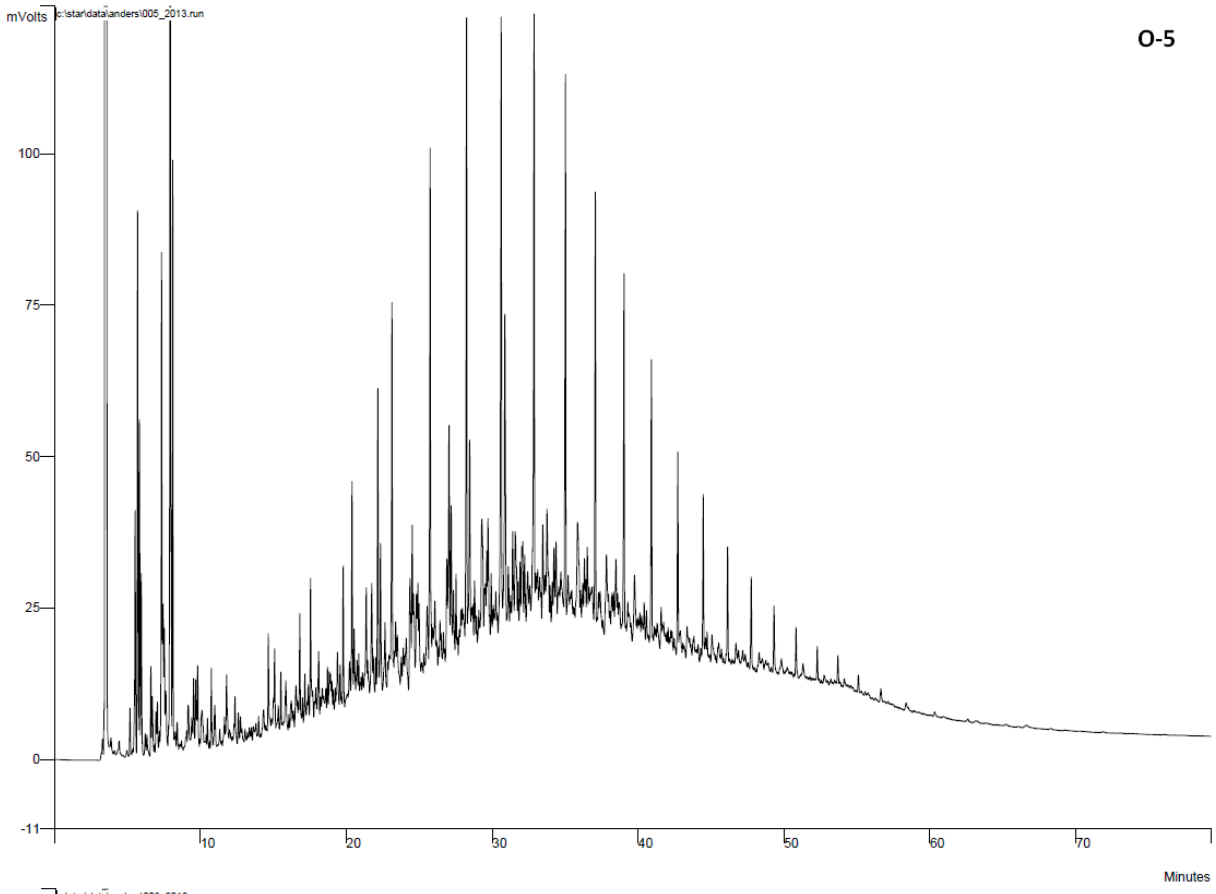
mVolts
c:\star\data\anders\005_2013.run
O-5
100
75
50
25
0
-11
10
20
30
40
50
60
70
Minutes

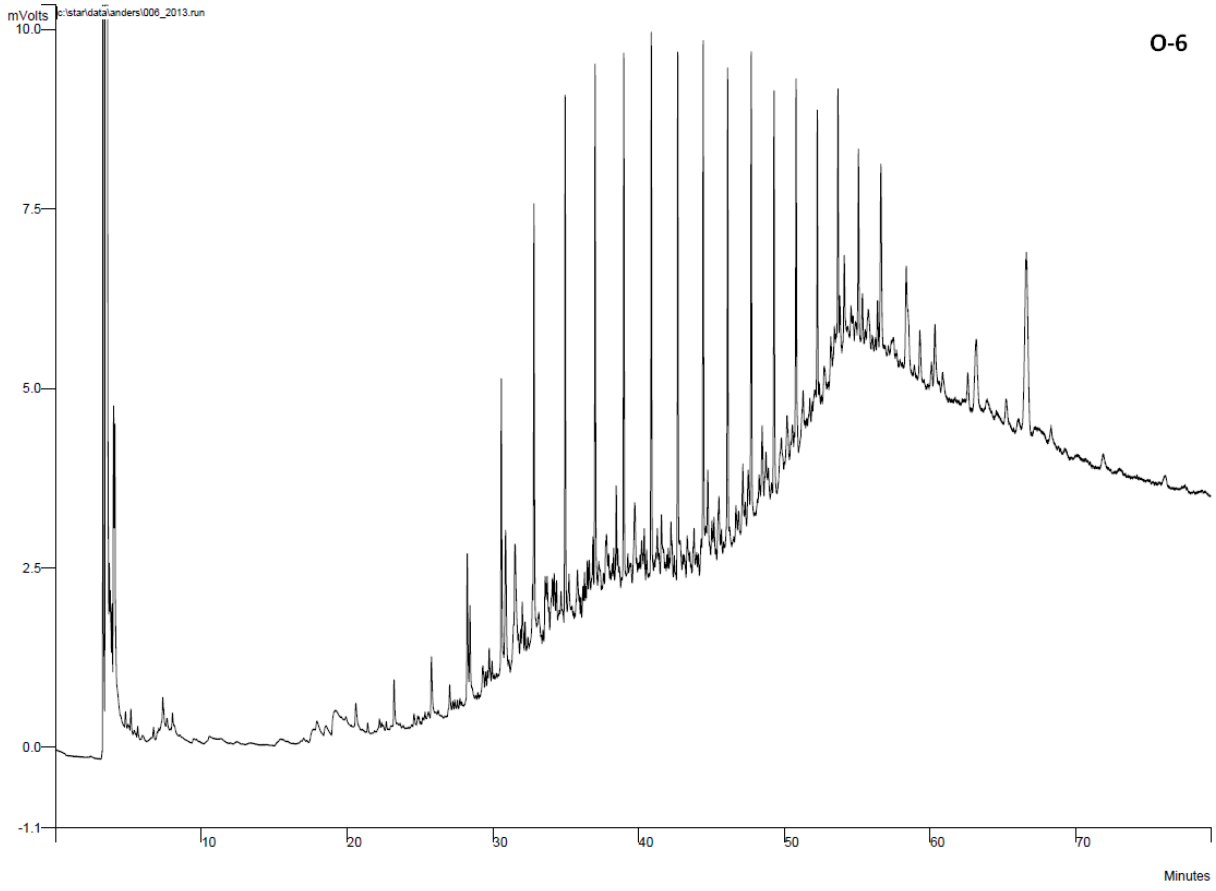
mVolts
c:\star\data\anders\006_2013.run
O-6
10.0
7.5
5.0
2.5
0.0
-1.1
10
20
30
40
50
60
70
Minutes

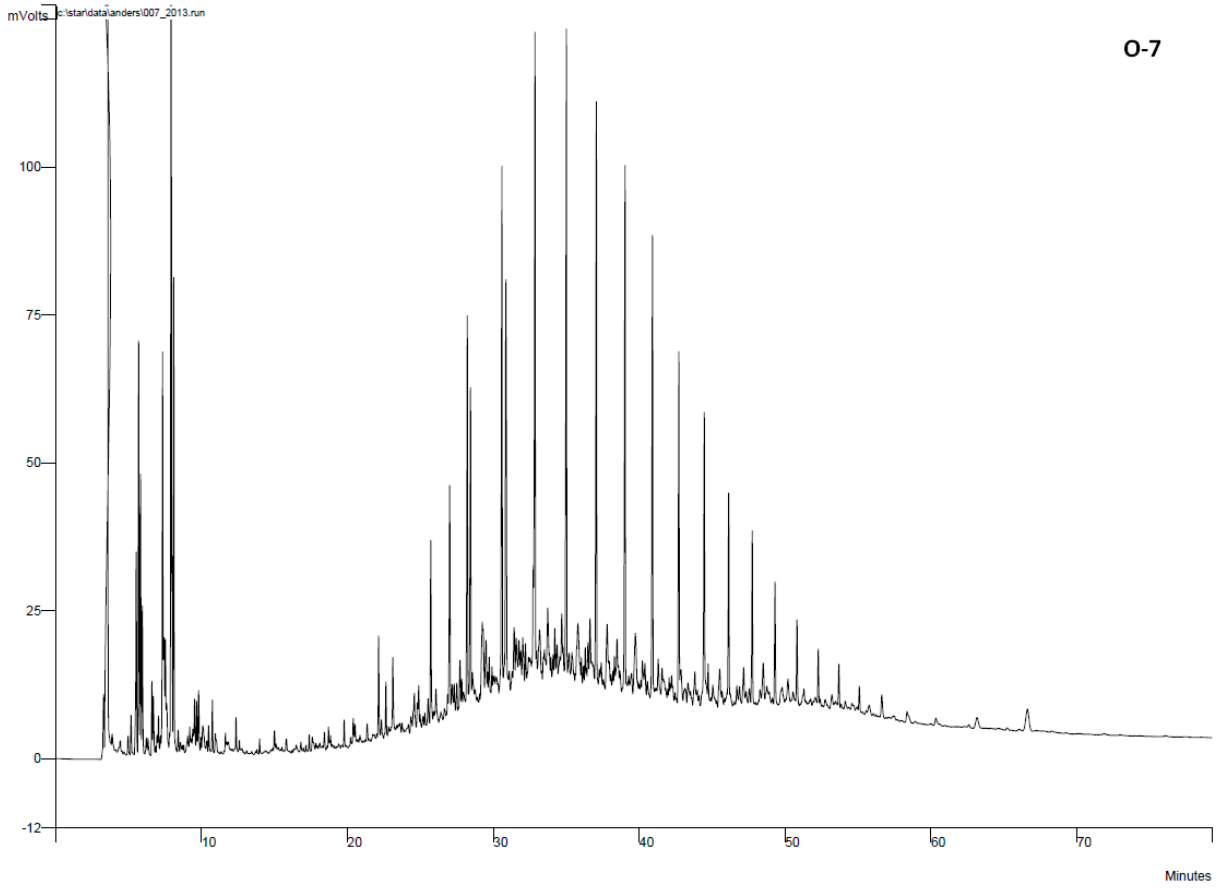
mVolts
c:\star\data\anders\007_2013.run
O-7
100
75
50
25
0
-12
10
20
30
40
50
60
70
Minutes

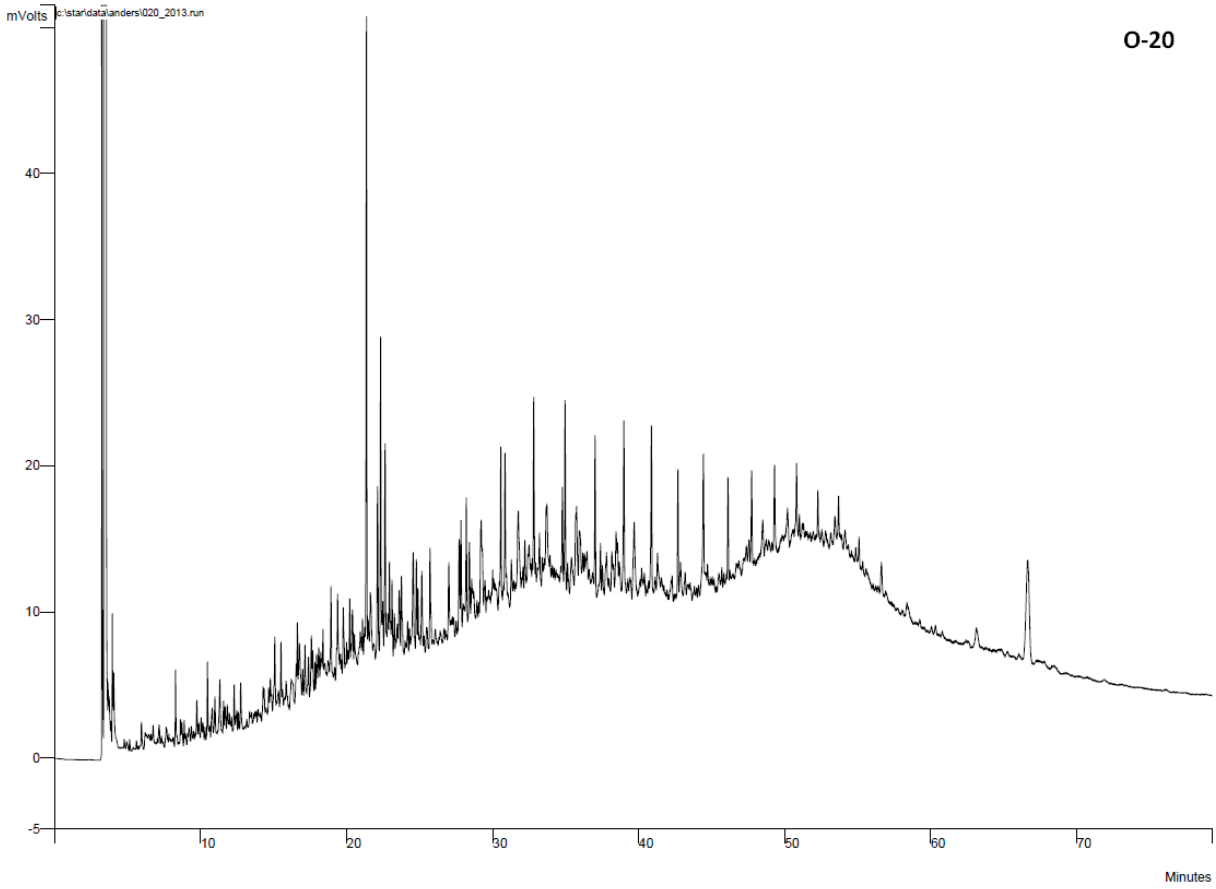
mVolts
c:\star\data\anders\020_2013.run
O-20
40
30
20
10
0
-5
10
20
30
40
50
60
70
Minutes

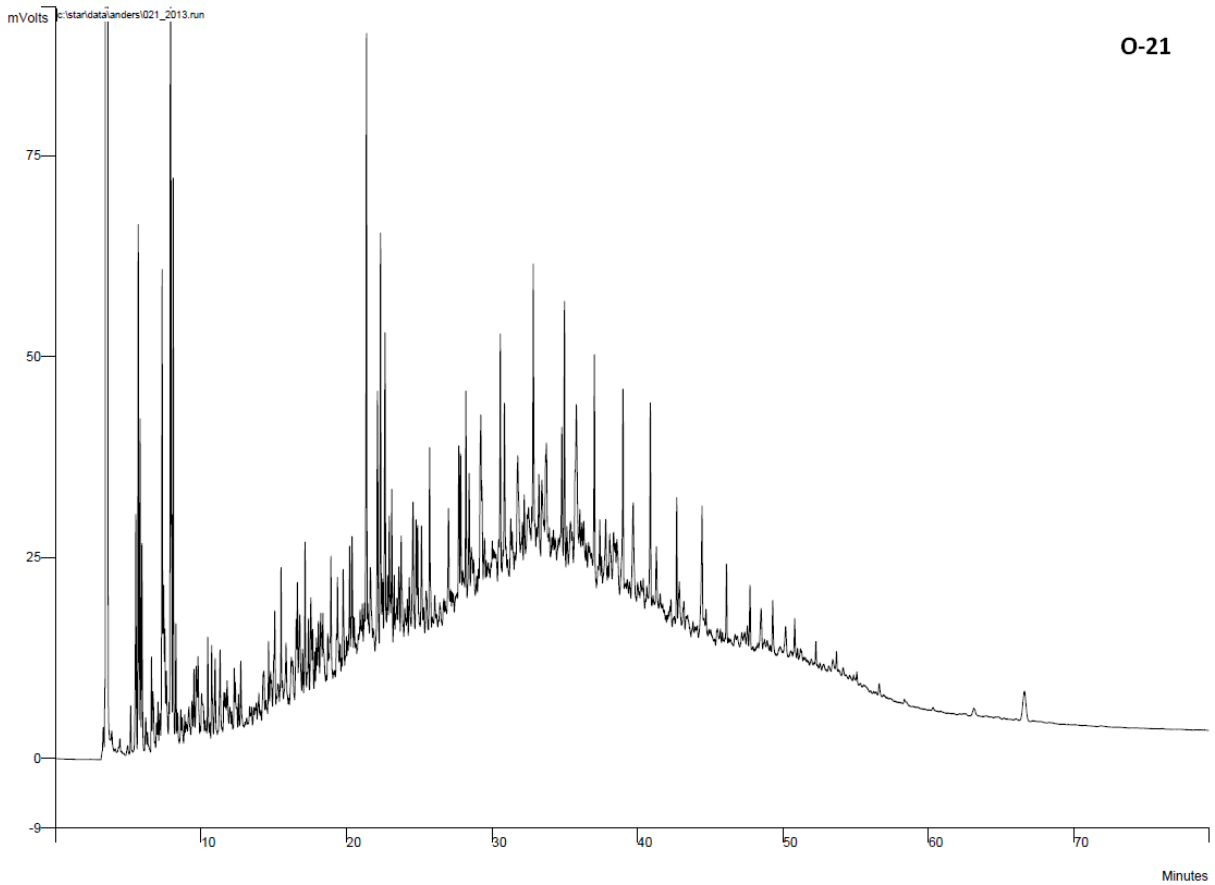
mVolts
c:\star\data\anders\021_2013.run
O-21
75
50
25
0
-9
10
20
30
40
50
60
70
Minutes

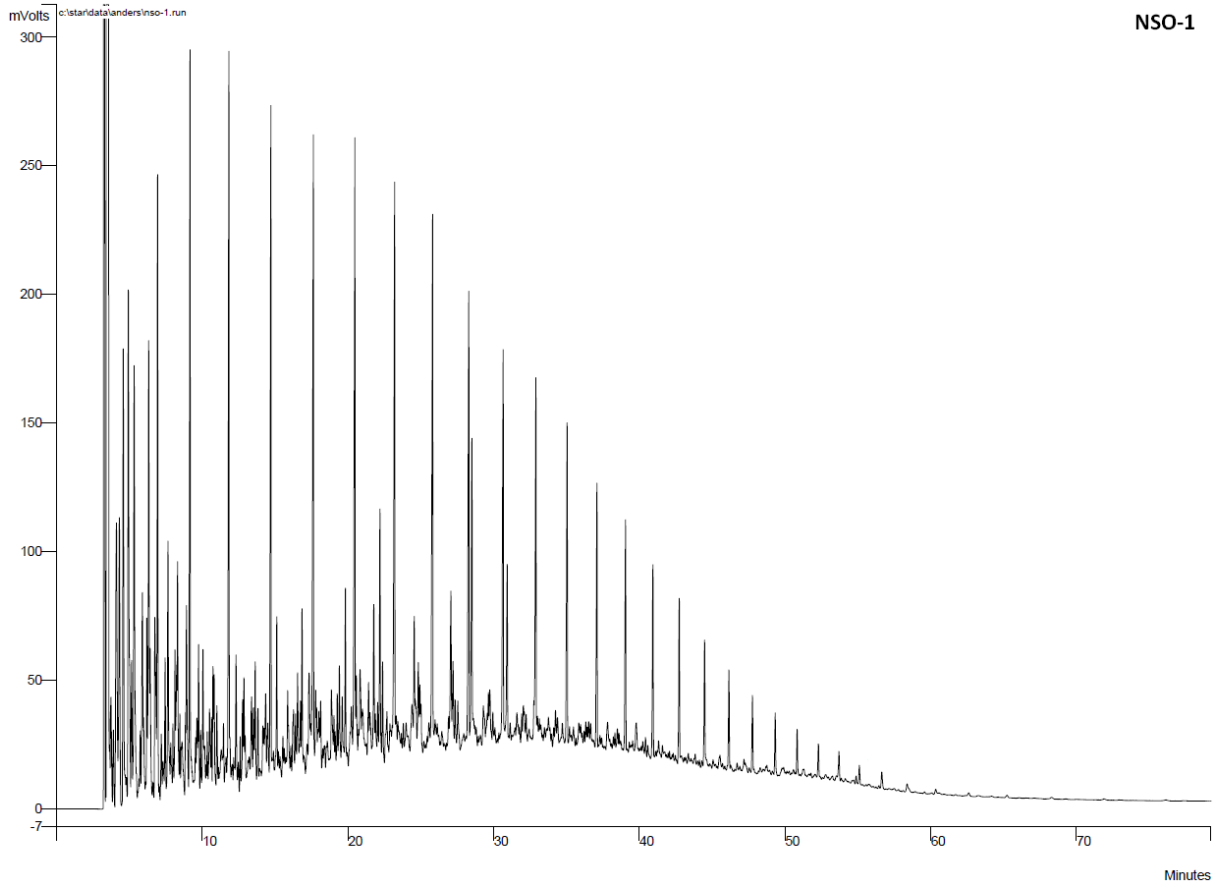
mVolts
c:\star\data\anders\nso-1.run
NSO-1
300
250
200
150
100
50
0
-7
10
20
30
40
50
60
70
Minutes

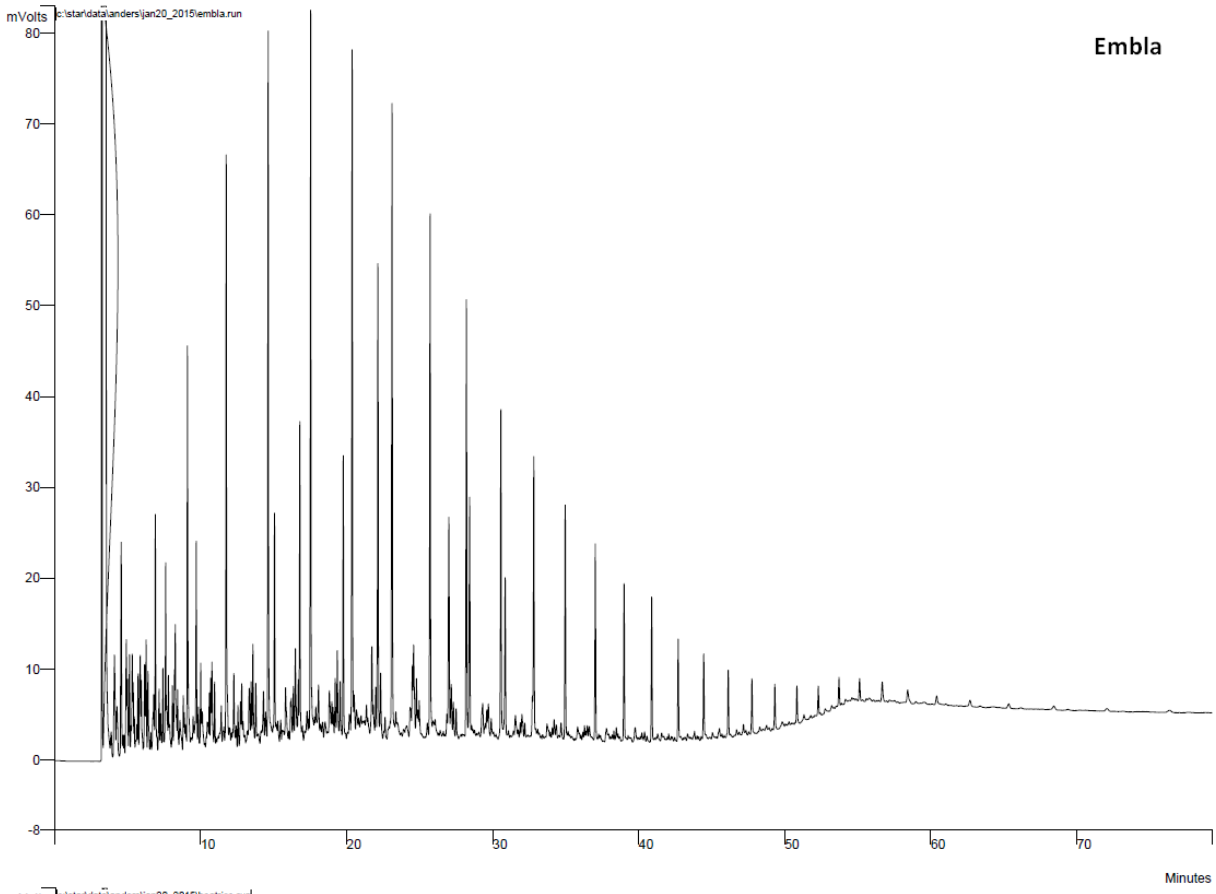
mVolts
c:\star\data\anders\jan20_2015\embla.run
Embla
80
70
60
50
40
30
20
10
0
-8
10
20
30
40
50
60
70
Minutes

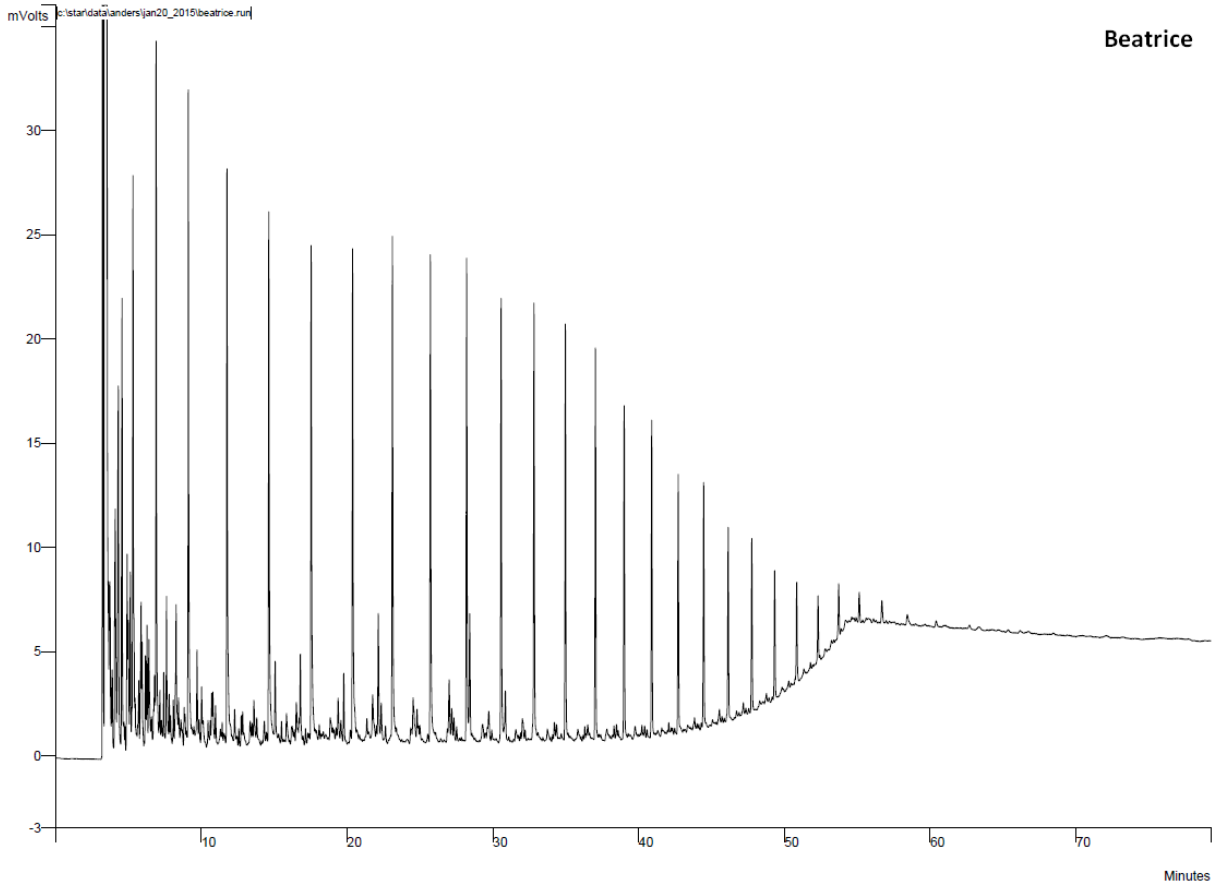
mVolts
c:\star\data\anders\jan20_2015\beatrice.run
Beatrice
30
25
20
15
10
5
0
-3
10
20
30
40
50
60
70
Minutes

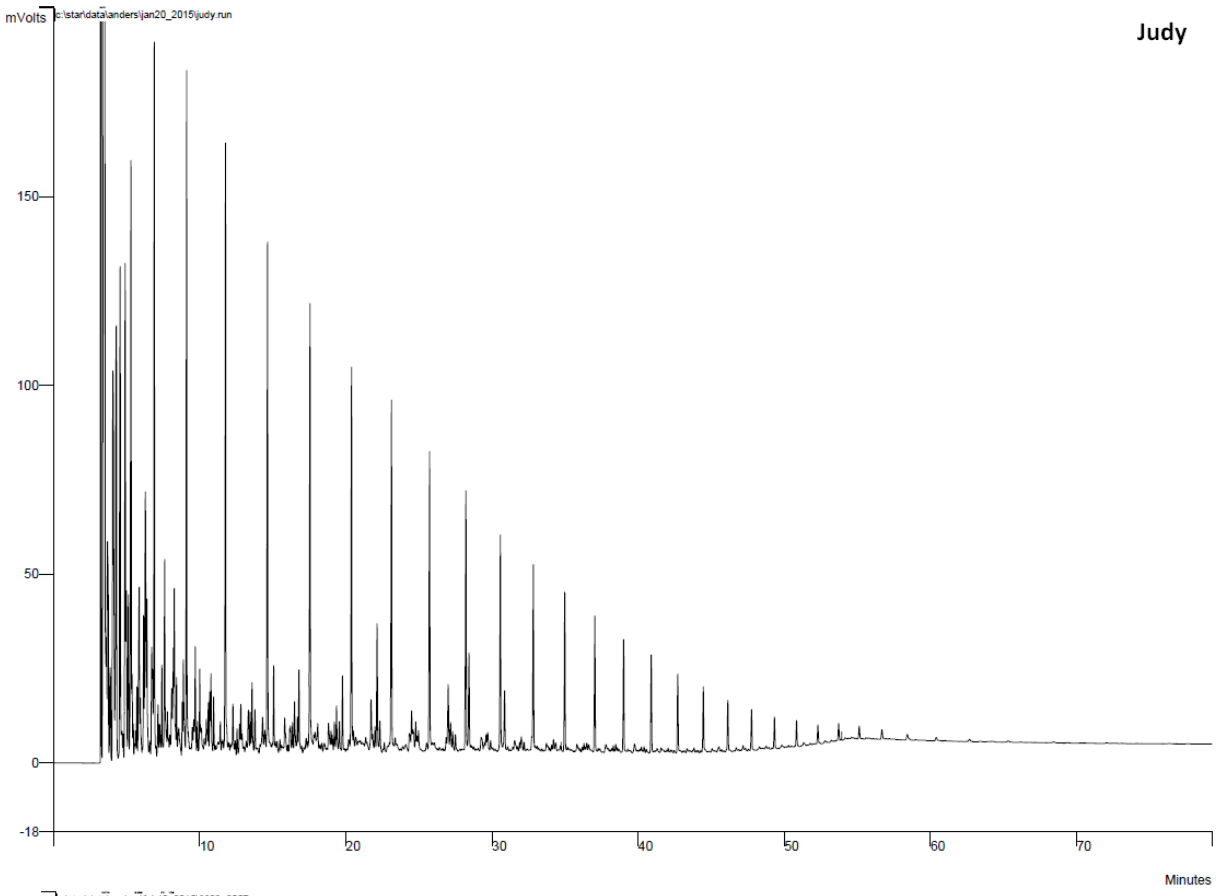
mVolts
c:\star\data\anders\jan20_2015\judy.run
Judy
150
100
50
0
-18
10
20
30
40
50
60
70
Minutes

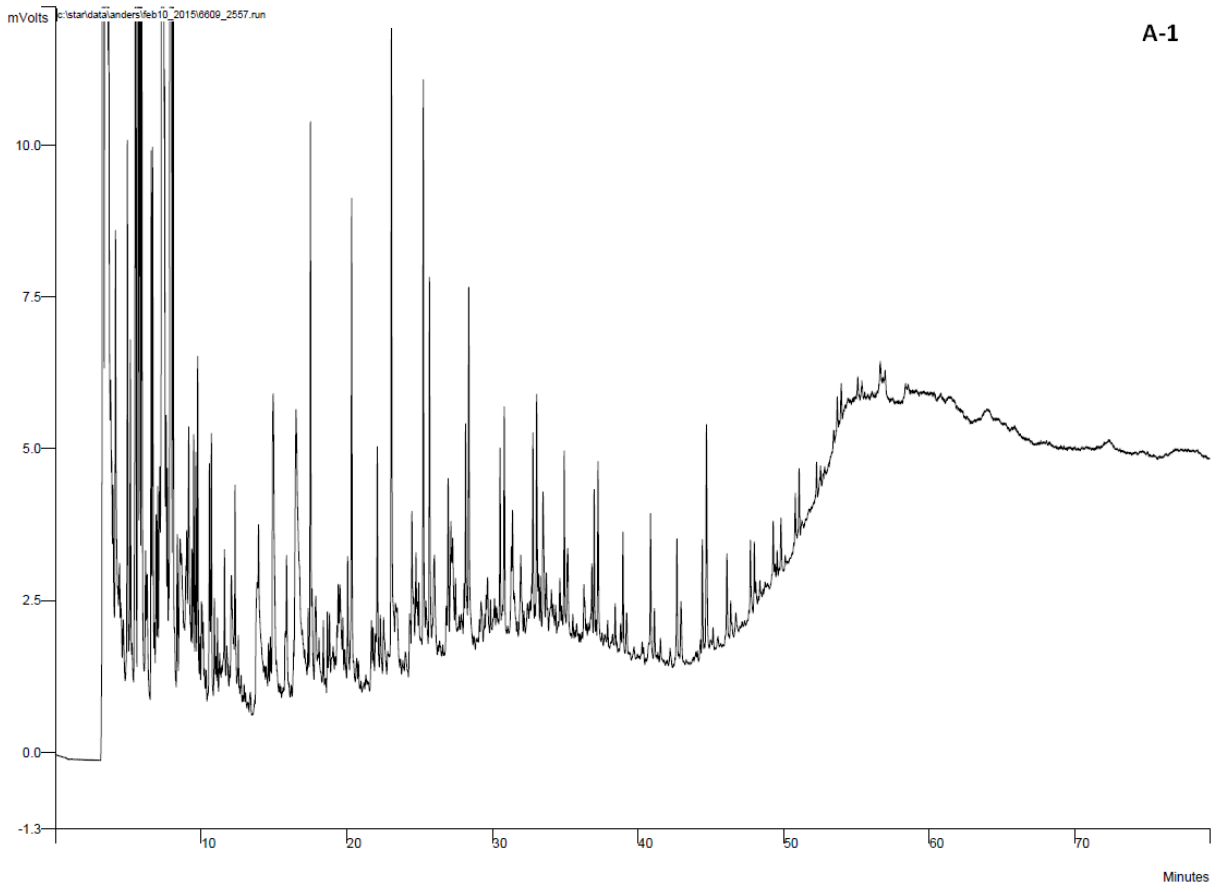
mVolts
c:\star\data\anders\feb10_2015\6609_2557.run
A-1
10.0
7.5
5.0
2.5
0.0
-1.3
10
20
30
40
50
60
70
Minutes

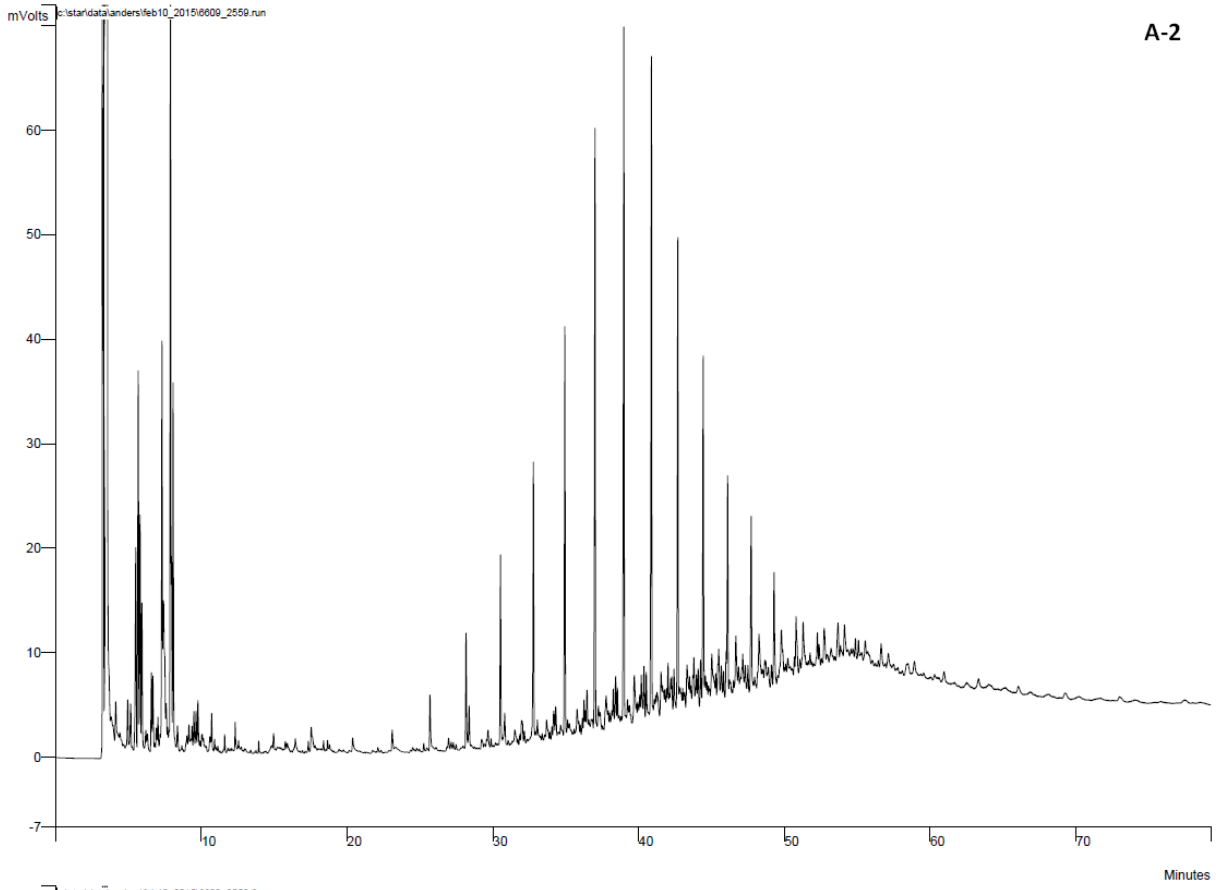
mVolts
c:\star\data\anders\feb10_2015\6609_2559.run
A-2
60
50
40
30
20
10
0
-7
10
20
30
40
50
60
70
Minutes

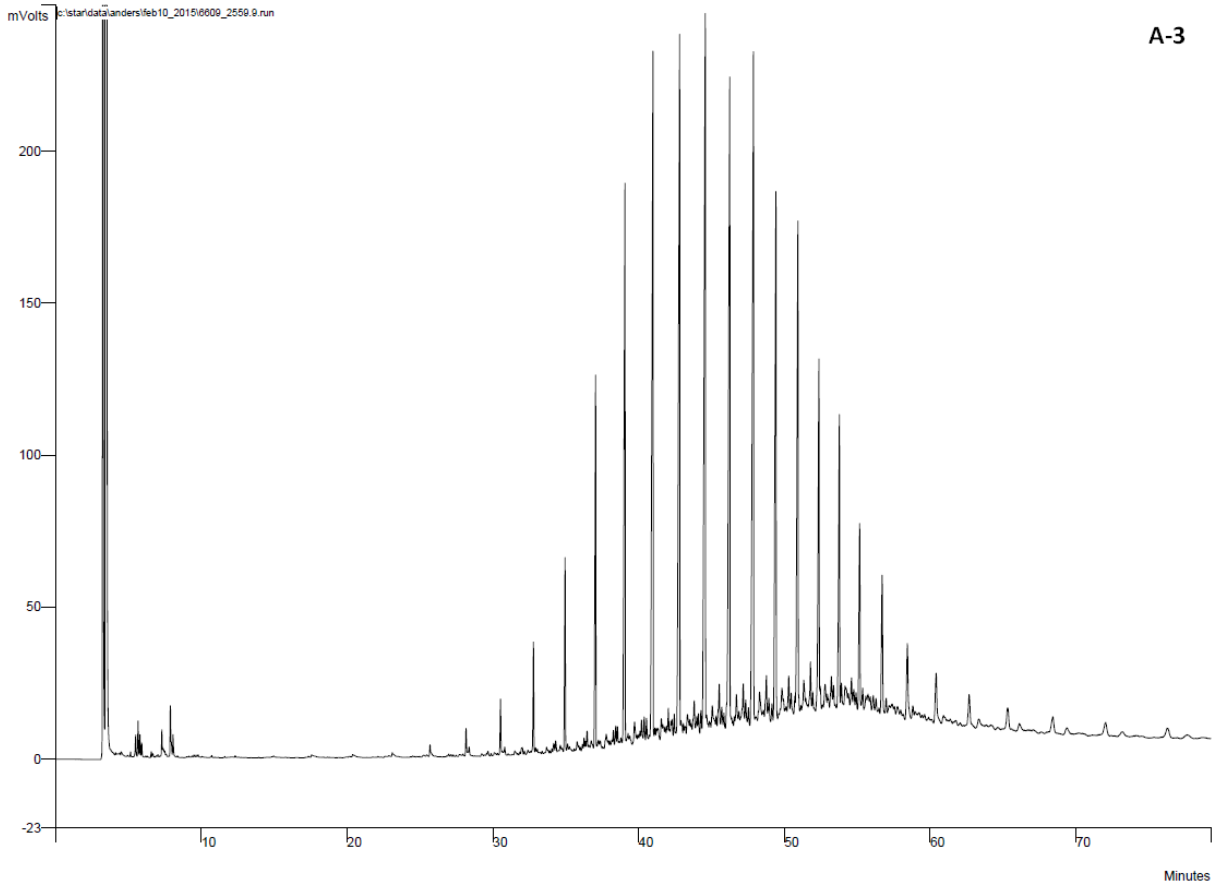
mVolts
c:\star\data\anders\feb10_2015\6609_2559.9.run
A-3
200
150
100
50
0
-23
10
20
30
40
50
60
70
Minutes

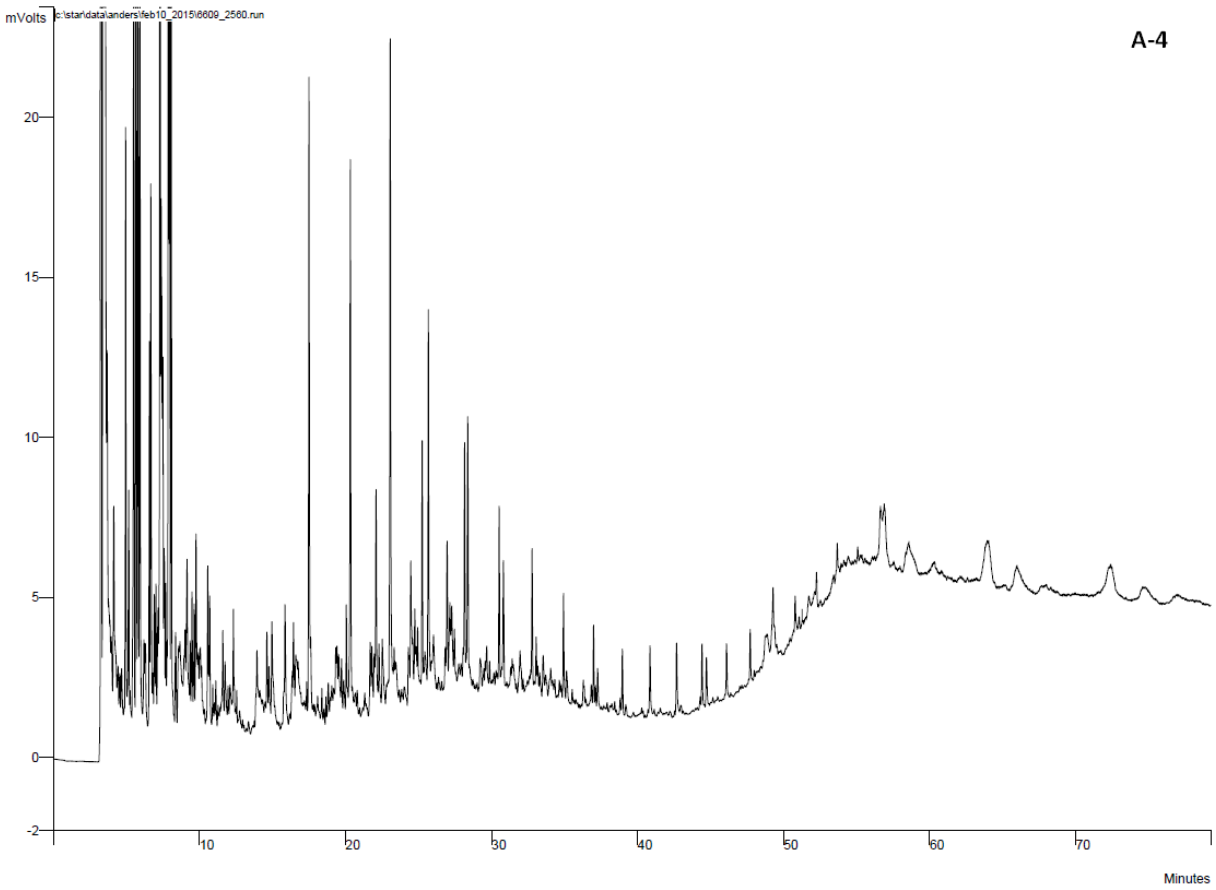
mVolts
c:\star\data\anders\feb10_2015\6609_2560.run
A-4
20
15
10
5
0
-2
10
20
30
40
50
60
70
Minutes

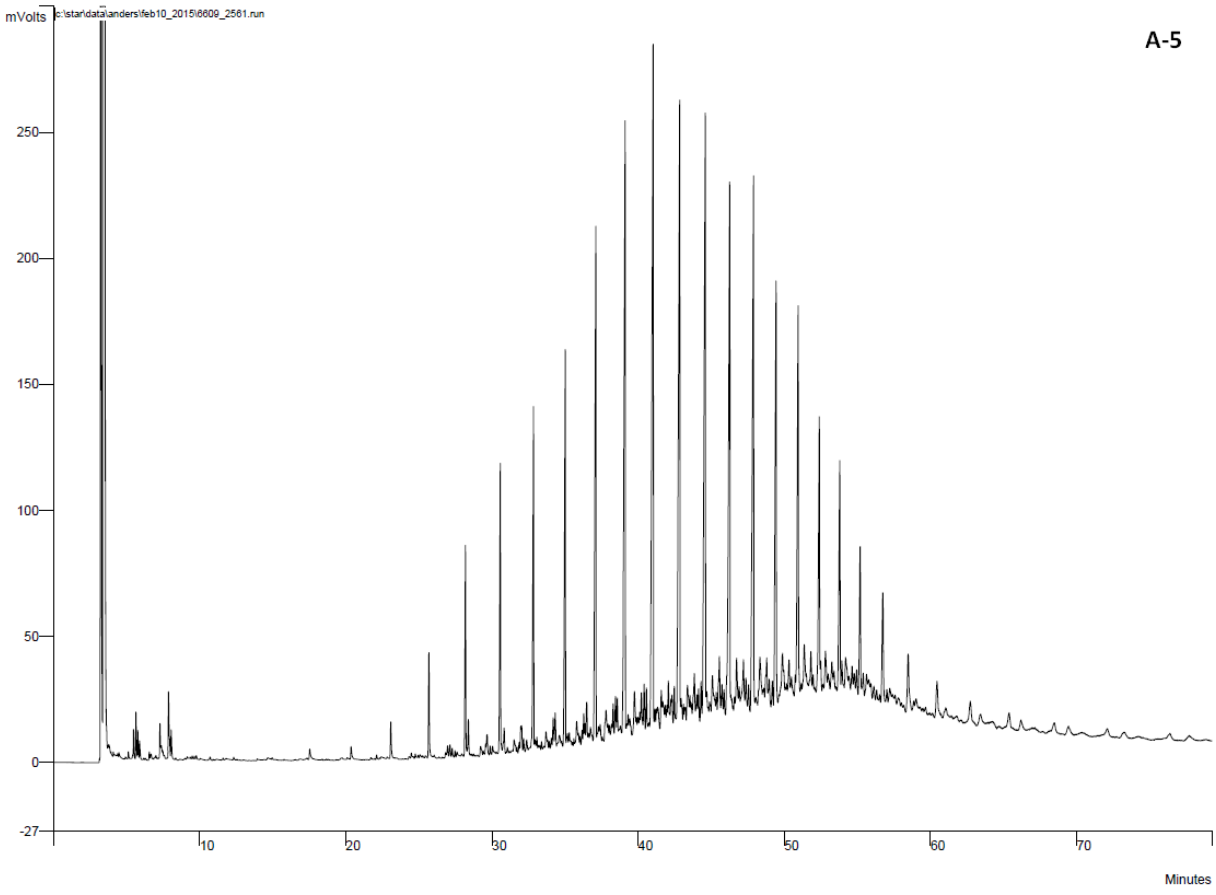
mVolts
c:\star\data\anders\feb10_2015\6609_2561.run
A-5
250
200
150
100
50
0
-27
10
20
30
40
50
60
70
Minutes

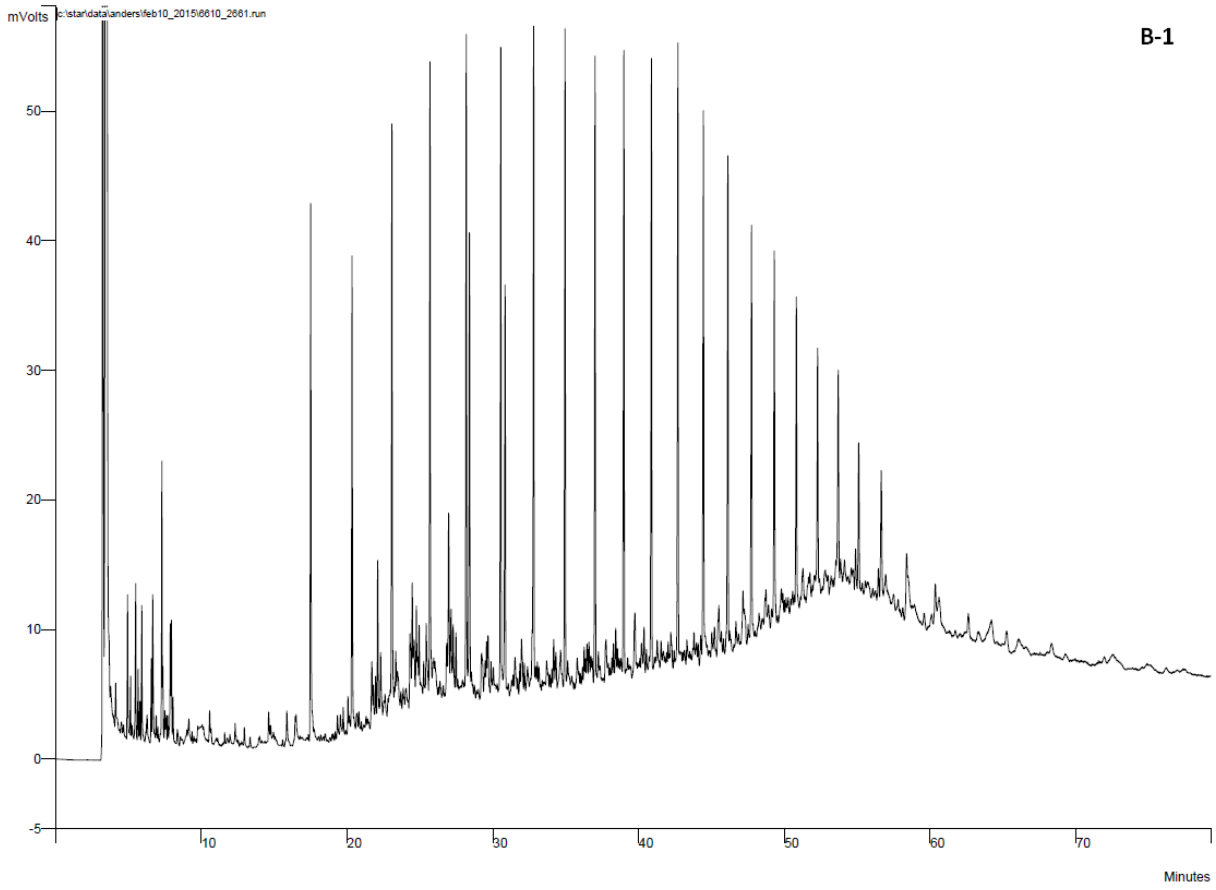
mVolts
c:\star\data\anders\feb10_2015\6610_2661.run
B-1
50
40
30
20
10
0
-5
10
20
30
40
50
60
70
Minutes

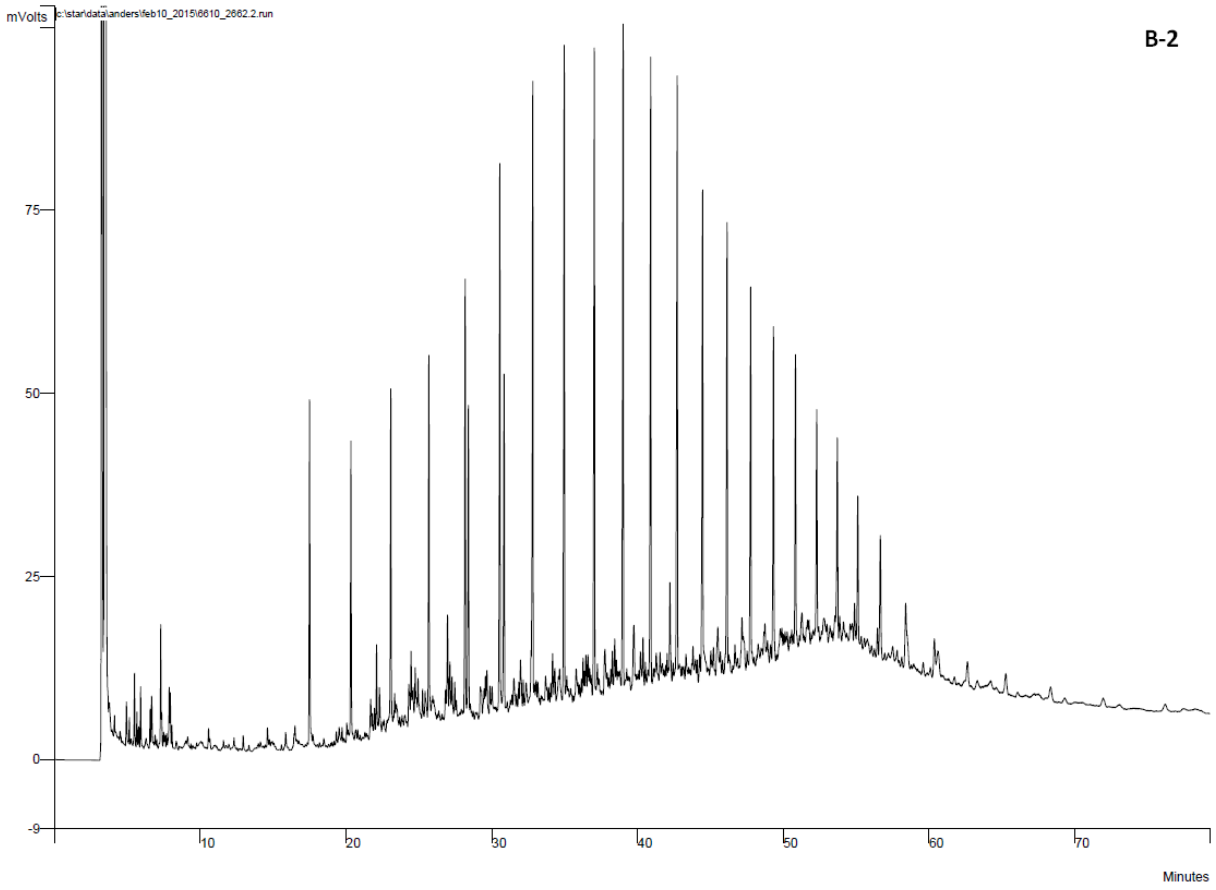
mVolts
c:\star\data\anders\feb10_2015\6610_2662.2.run
B-2
75
50
25
0
-9
10
20
30
40
50
60
70
Minutes

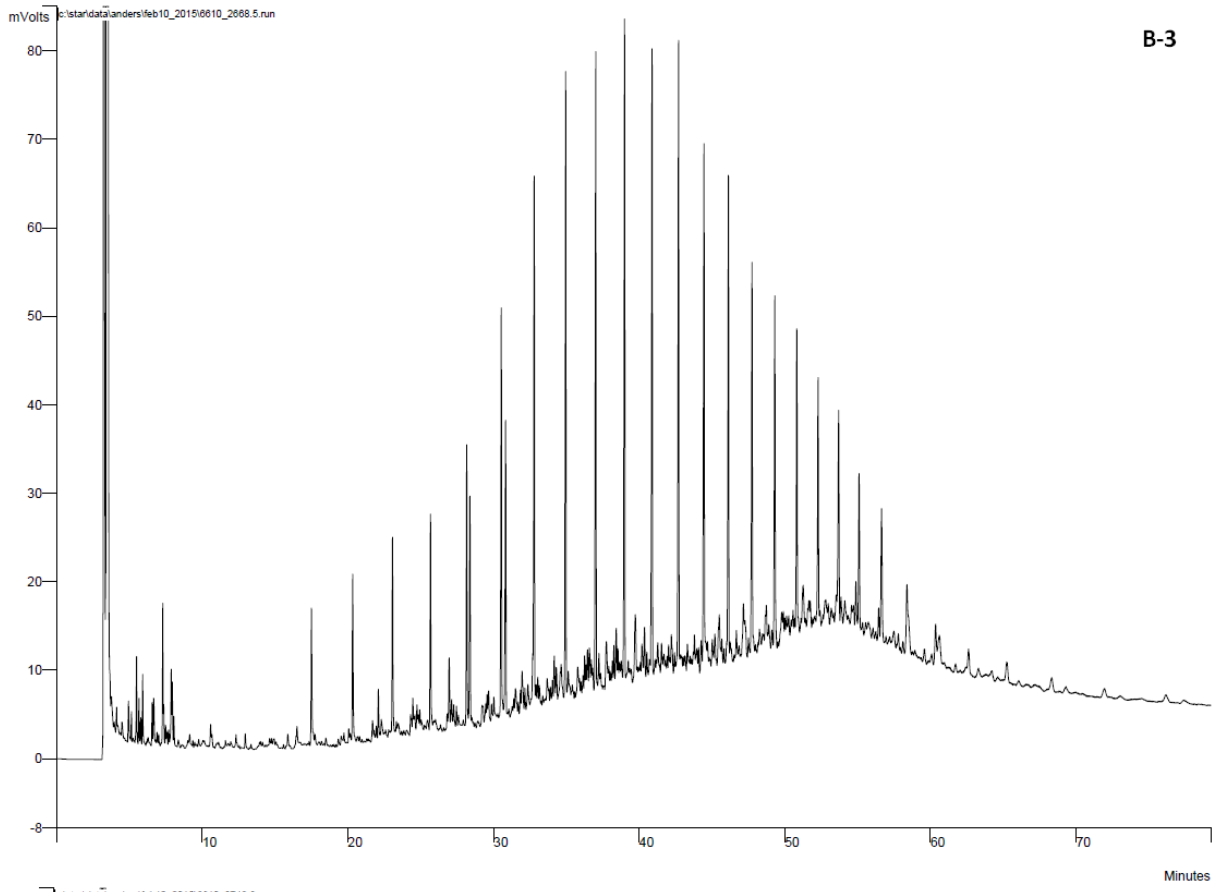
mVolts
c:\star\data\anders\feb10_2015\6610_2668.5.run
B-3
80
70
60
50
40
30
20
10
0
-8
10
20
30
40
50
60
70
Minutes

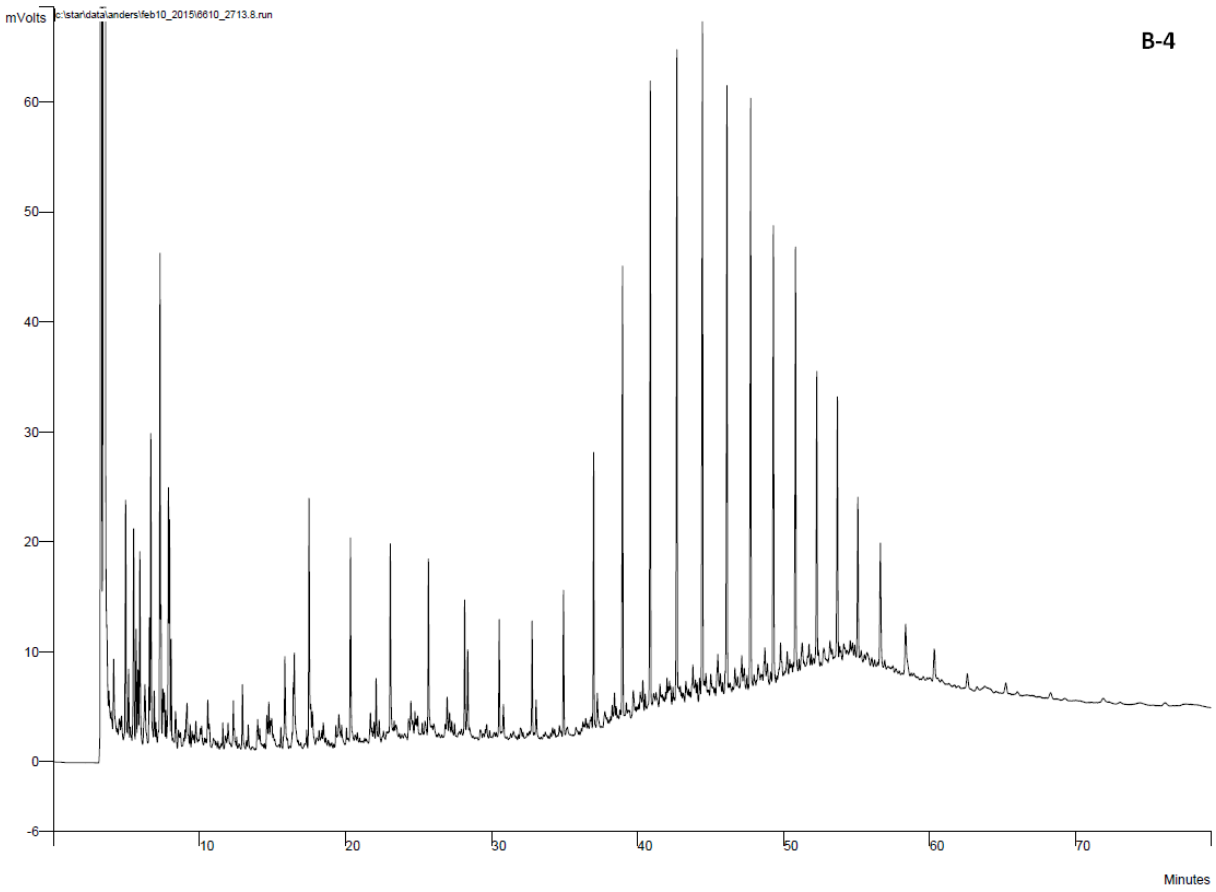
mVolts
c:\star\data\anders\feb10_2015\6610_2713.8.run
B-4
60
50
40
30
20
10
0
-6
10
20
30
40
50
60
70
Minutes

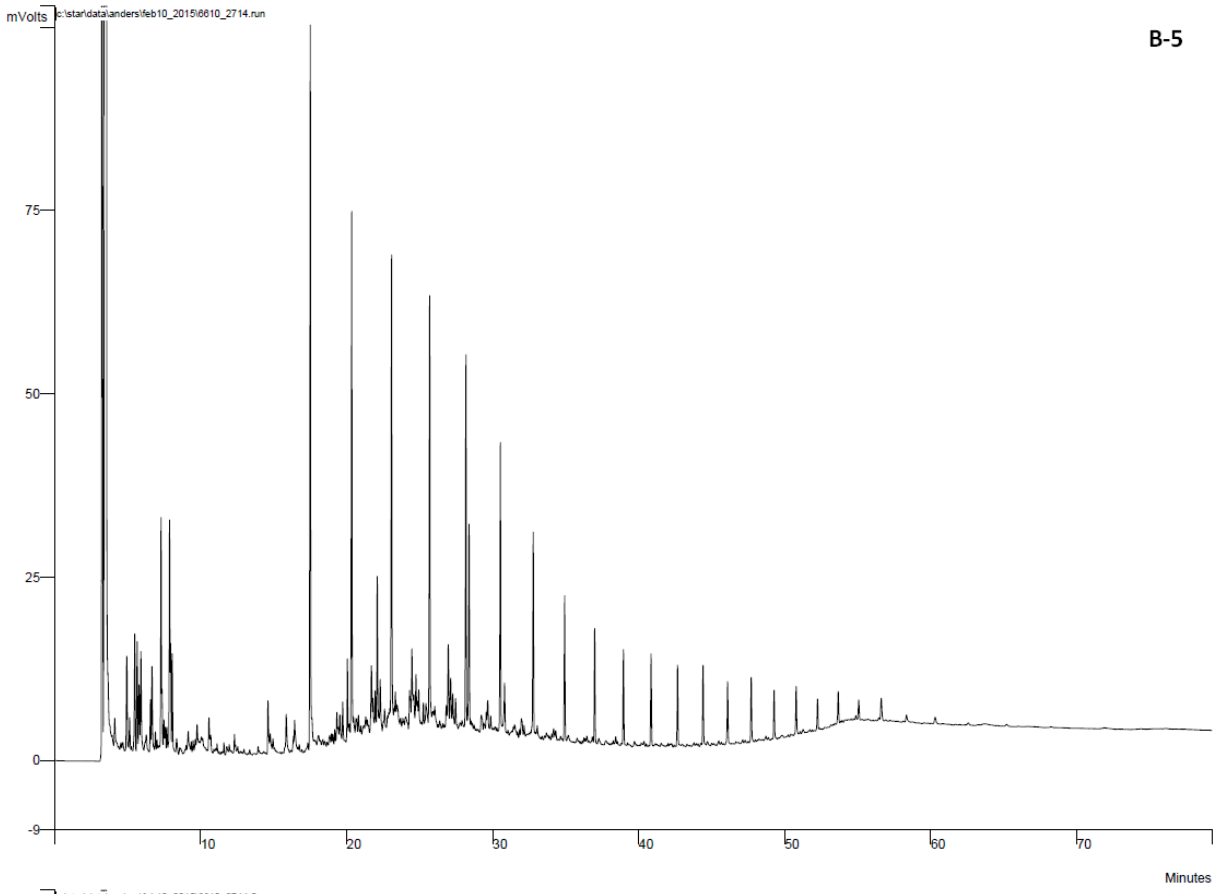
mVolts
c:\star\data\anders\feb10_2015\6610_2714.run
B-5
75
50
25
0
-9
10
20
30
40
50
60
70
Minutes

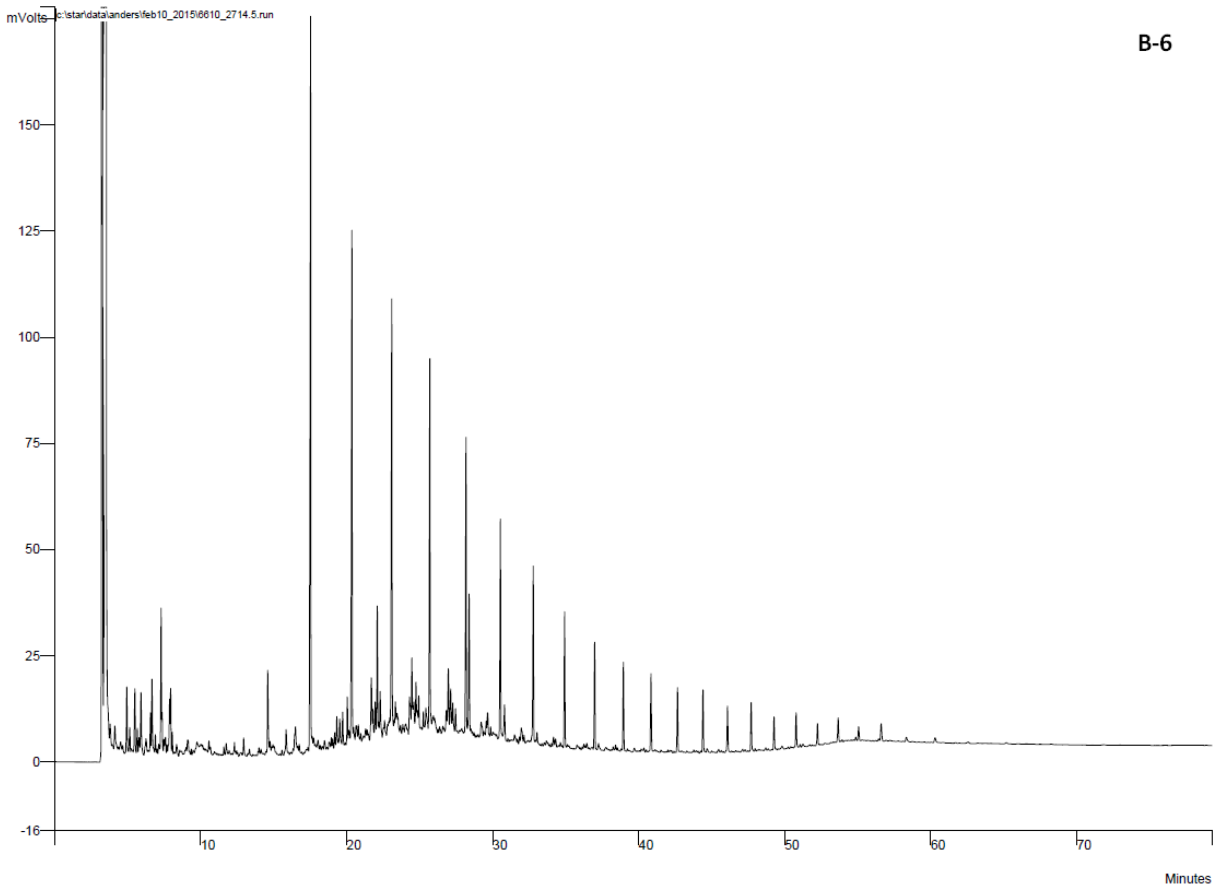
mVolts
c:\star\data\anders\feb10_2015\6610_2714.5.run
B-6
150
125
100
75
50
25
0
-16
10
20
30
40
50
60
70
Minutes

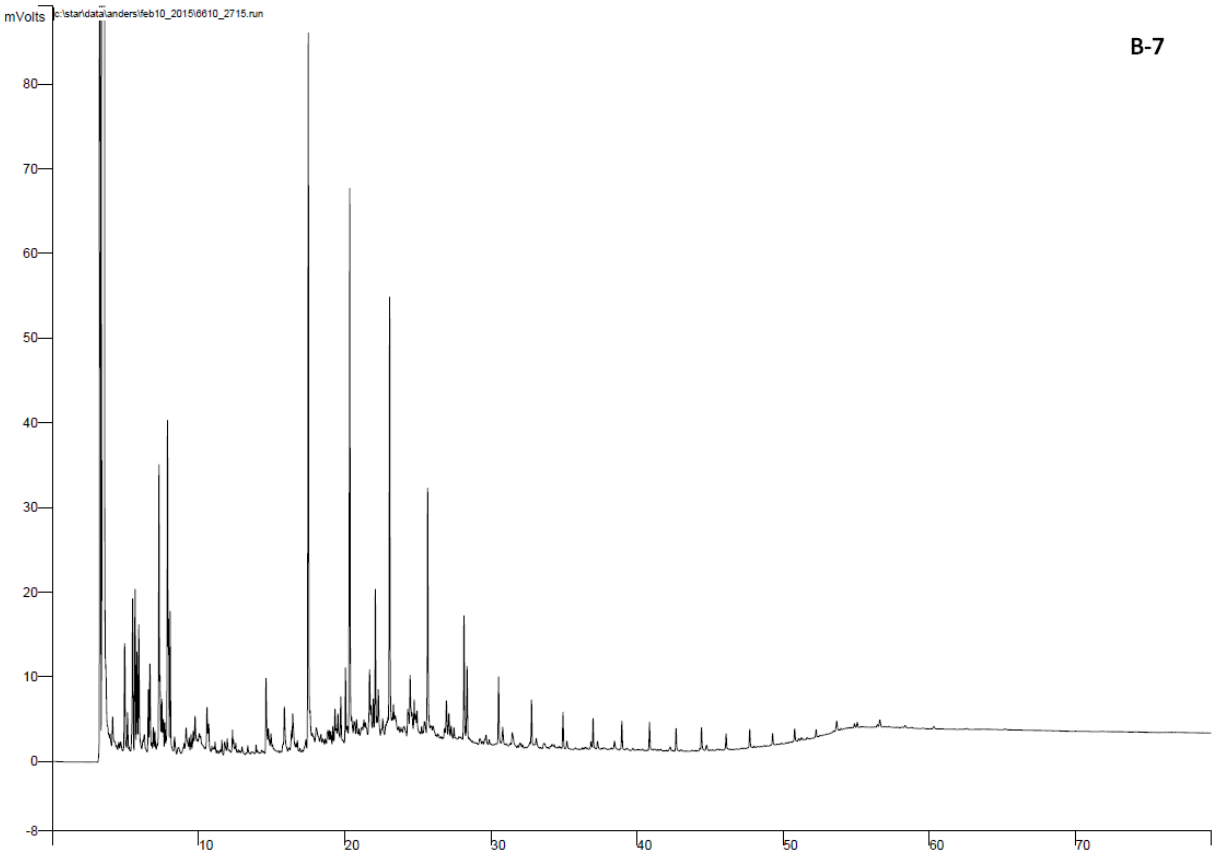
mVolts
c:\star\data\anders\feb10_2015\6610_2715.run
B-7
80
70
60
50
40
30
20
10
0
-8
10
20
30
40
50
60
70
Minutes

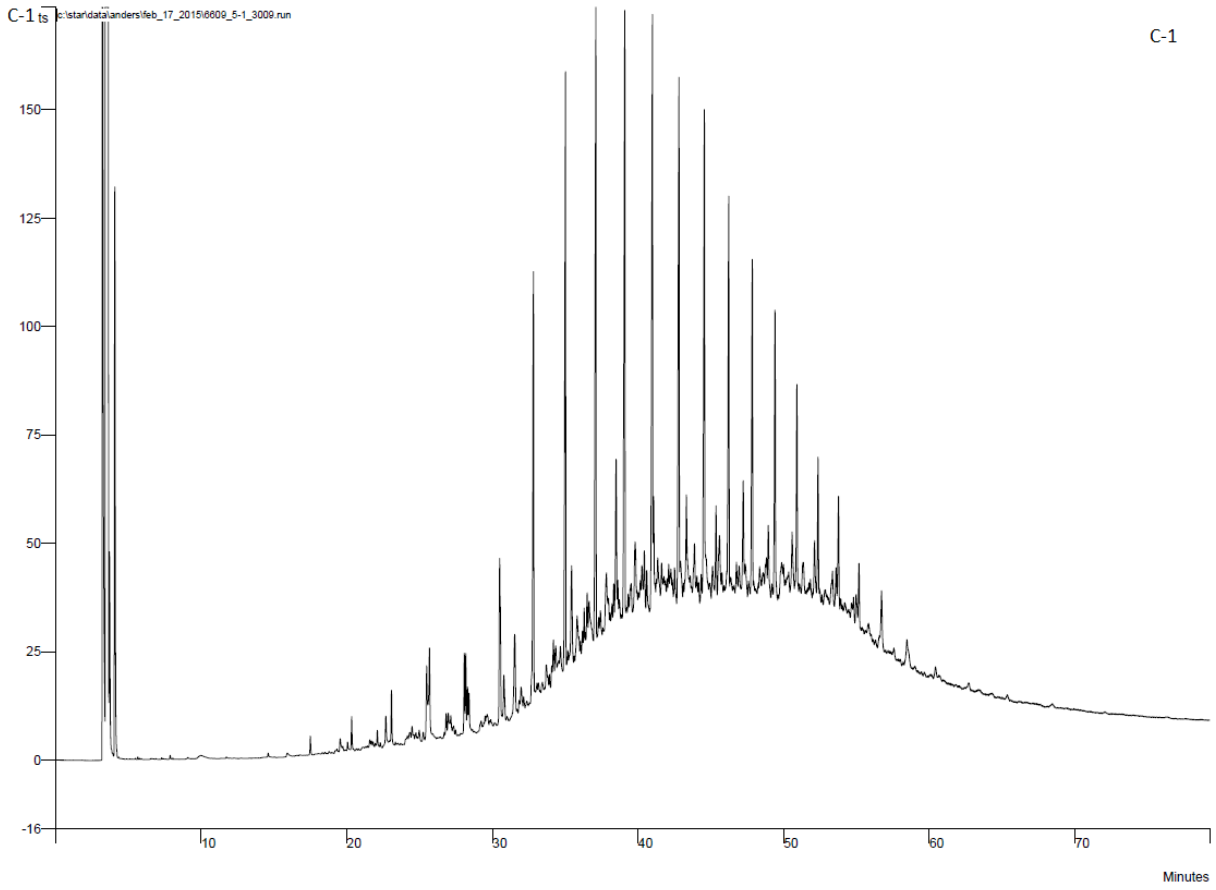
C-1 ts
c:\star\data\anders\feb_17_2015\6609_5-1_3009.run
C-1
150
125
100
75
50
25
0
-16
10
20
30
40
50
60
70
Minutes

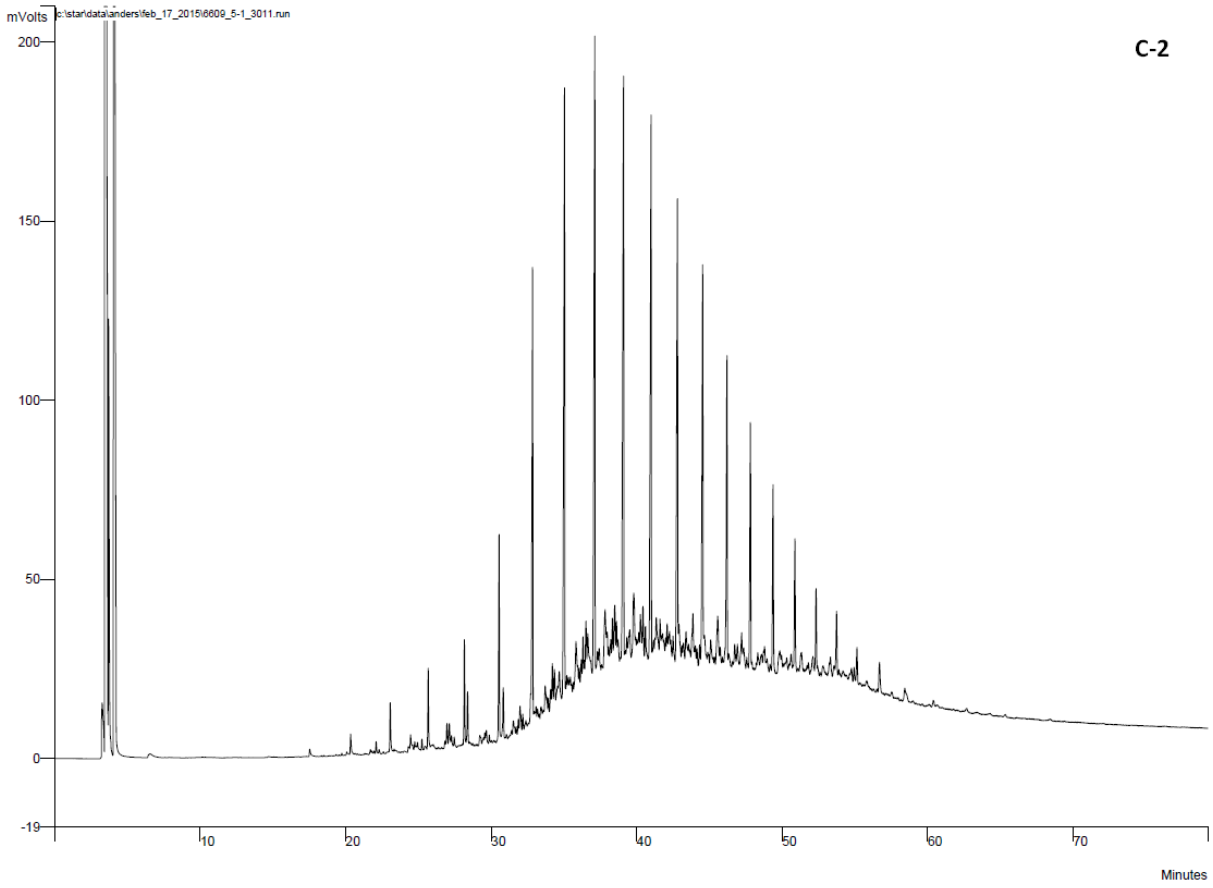
mVolts
c:\star\data\anders\feb_17_2015\6609_5-1_3011.run
C-2
200
150
100
50
0
-19
10
20
30
40
50
60
70
Minutes

Appendix B: GC-MS chromatograms

O-1

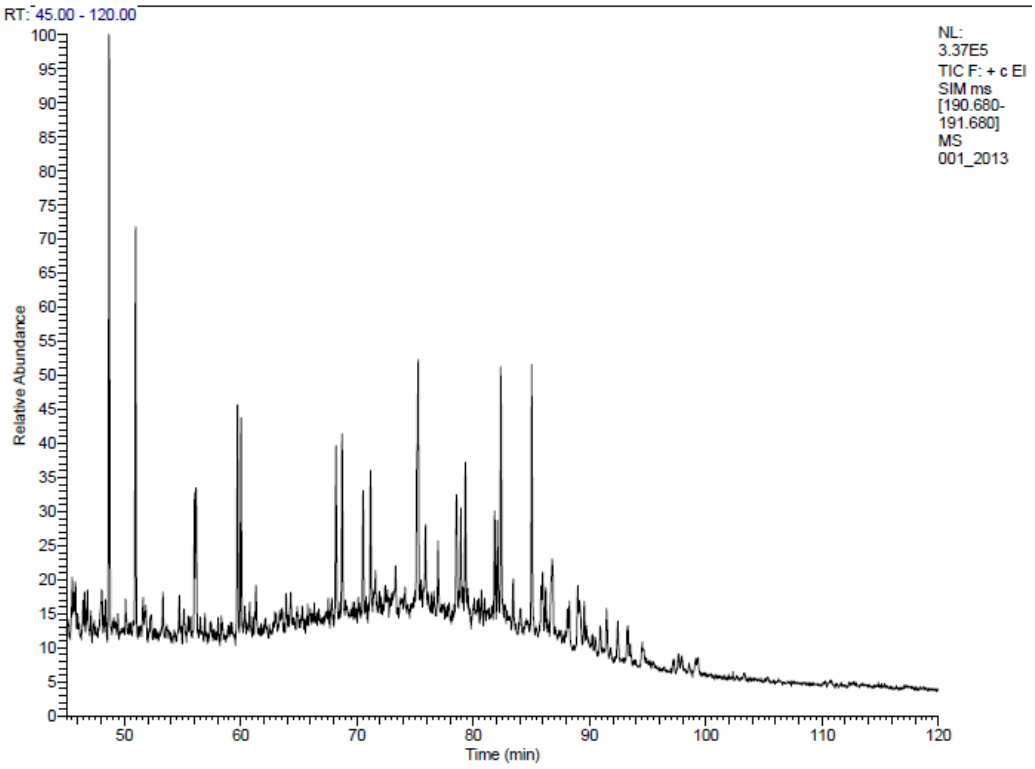

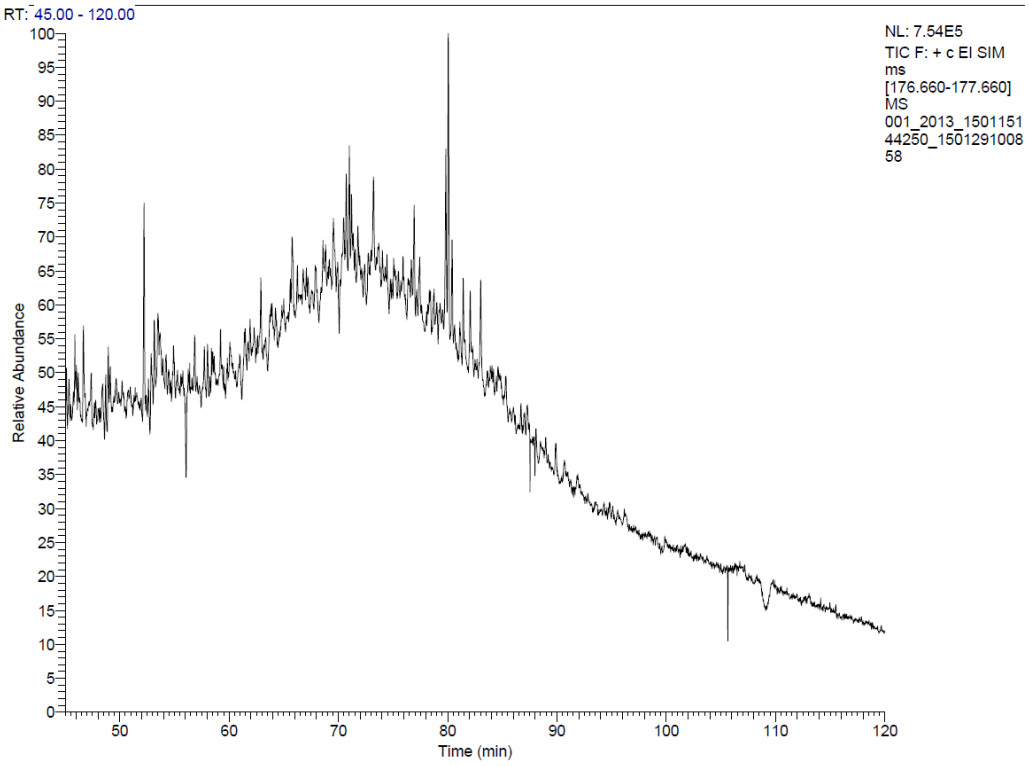

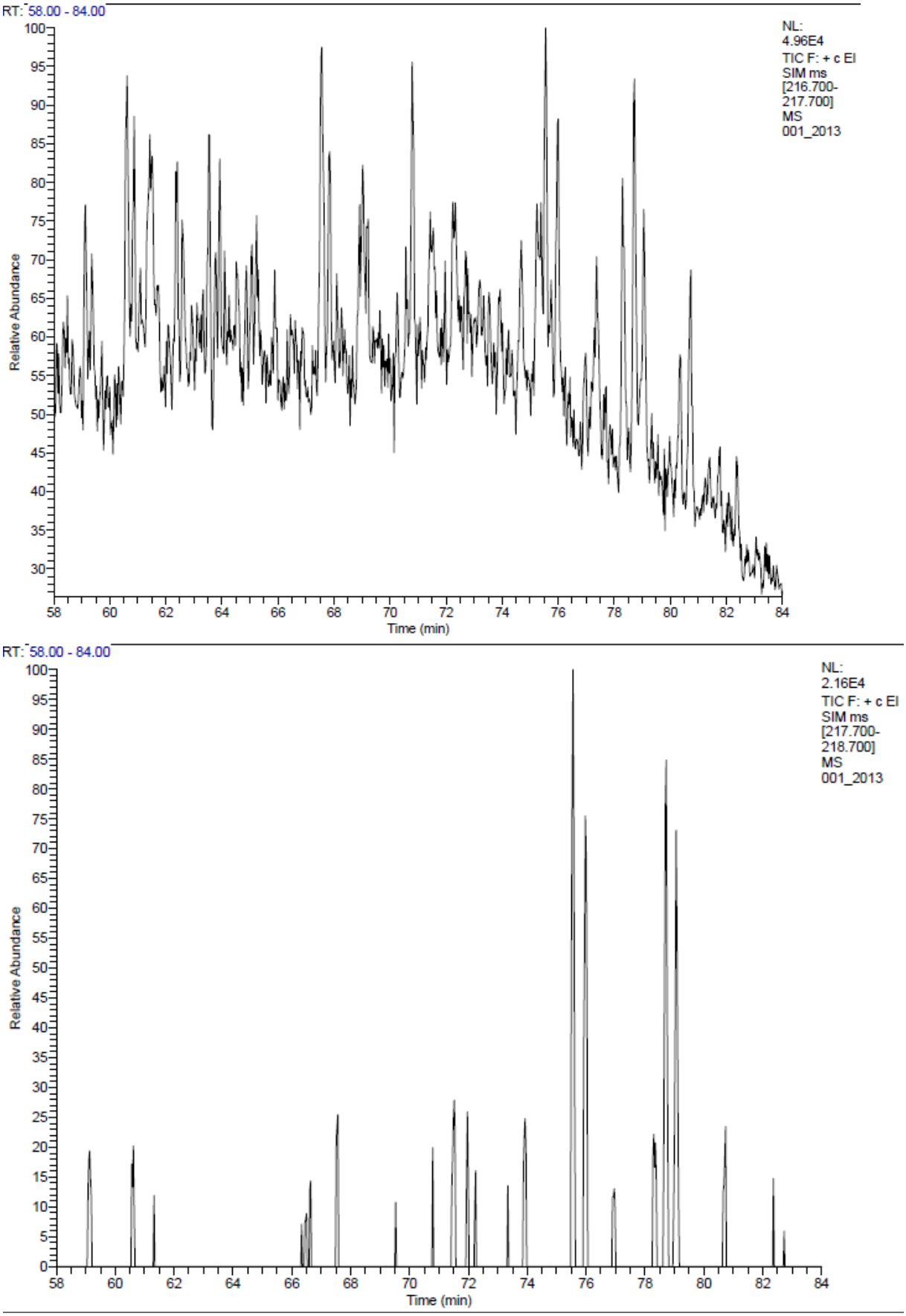
RT: 58.00 - 84.00
NL:
4.96E4
TIC F: + c EI
SIM ms
[216.700-
217.700]
MS
001_2013
Relative Abundance
Time (min)
RT: 58.00 - 84.00
NL:
2.16E4
TIC F: + c EI
SIM ms
[217.700-
218.700]
MS
001_2013
Relative Abundance
Time (min)

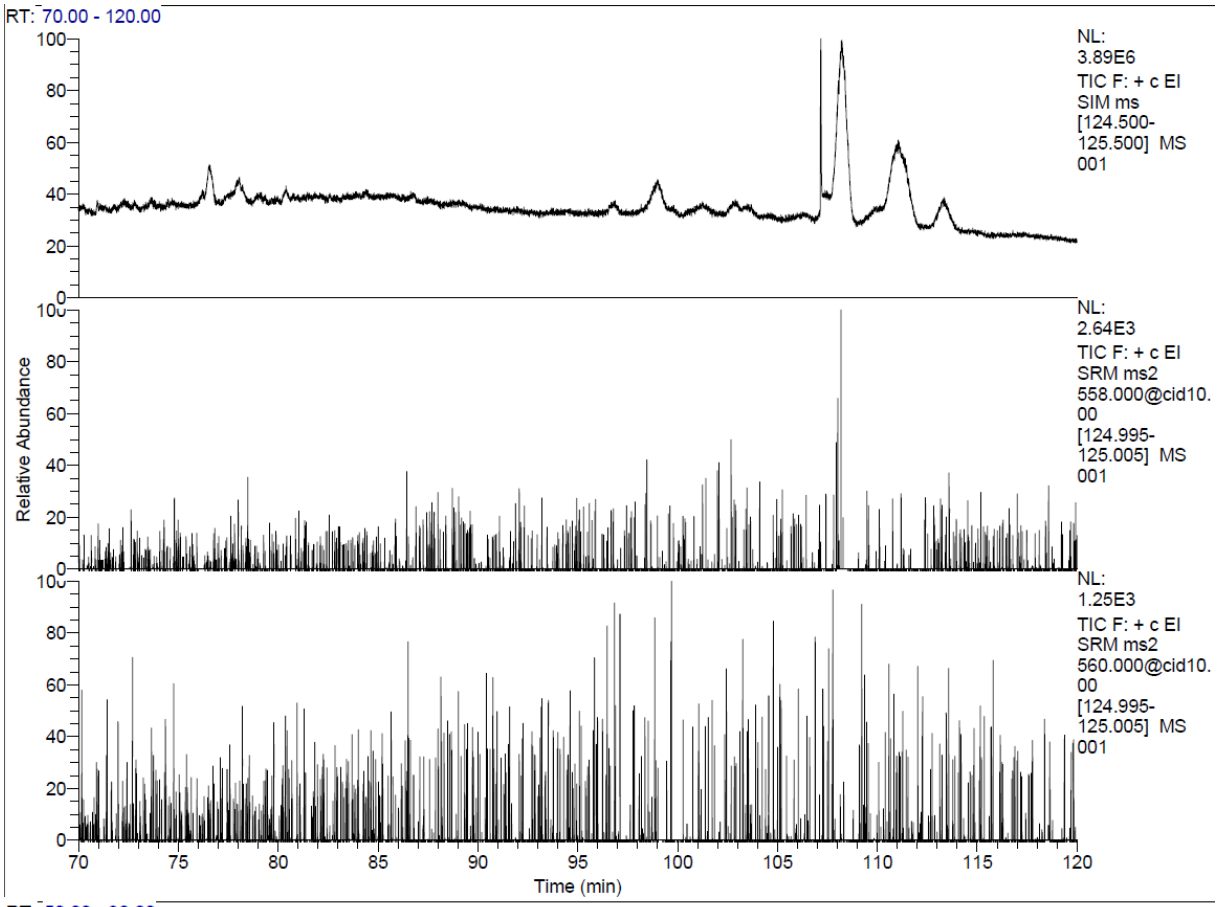
RT: 70.00 - 120.00
NL: 3.89E6 TIC F: + c EI SIM ms [124.500-125.500] MS 001
NL: 2.64E3 TIC F: + c EI SRM ms2 558.000@cid10.00 [124.995-125.005] MS 001
NL: 1.25E3 TIC F: + c EI SRM ms2 560.000@cid10.00 [124.995-125.005] MS 001
Relative Abundance
Time (min)

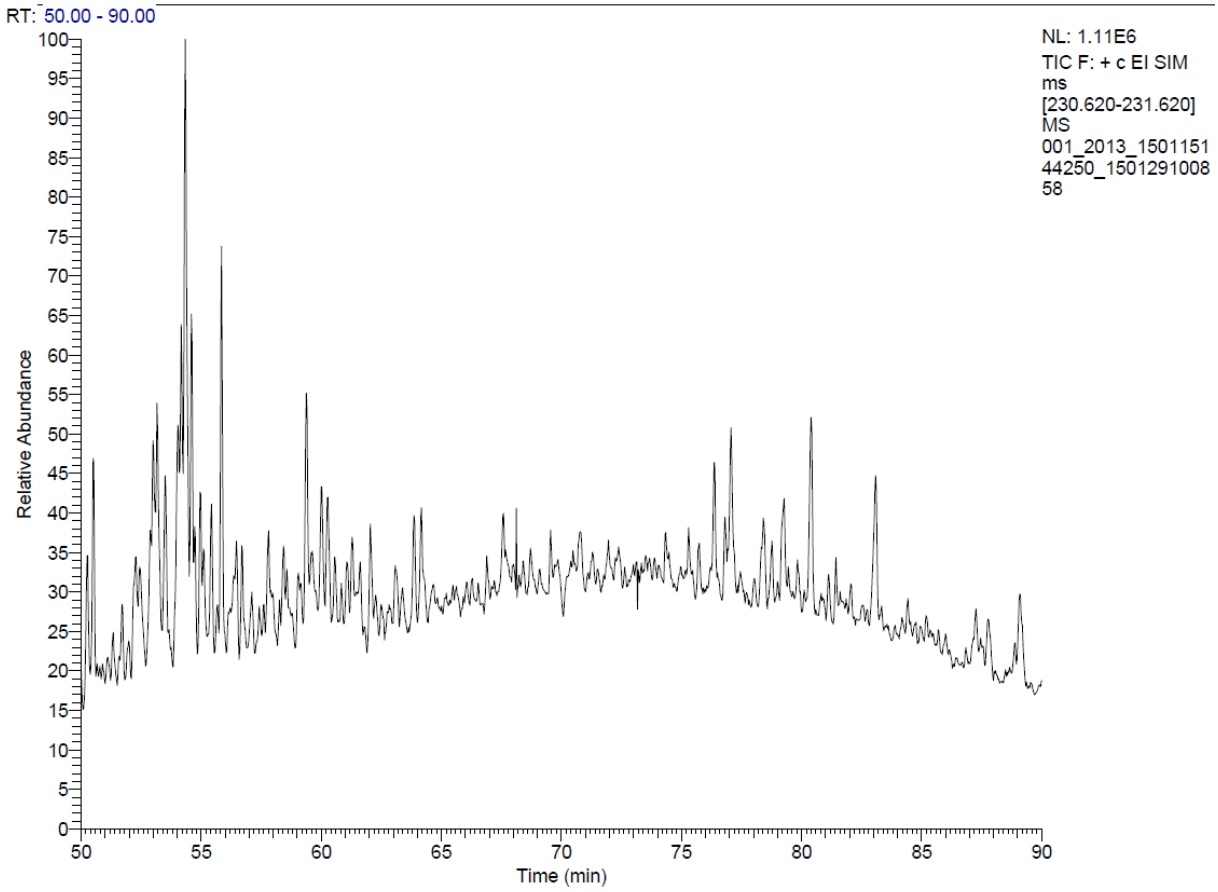
RT: 50.00 - 90.00
NL: 1.11E6 TIC F: + c EI SIM ms [230.620-231.620] MS 001_2013_150115144250_150129100858
Relative Abundance
Time (min)

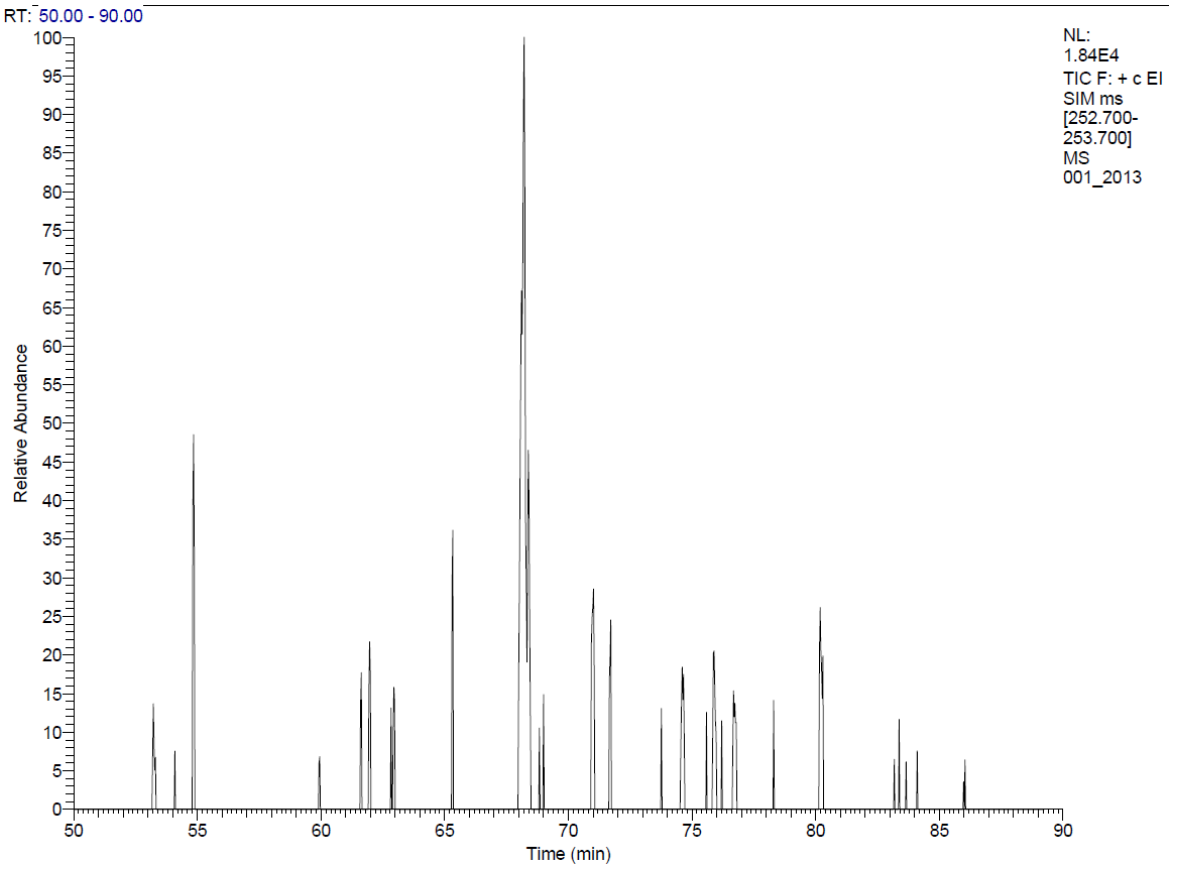
RT: 50.00 - 90.00
NL:
1.84E4
TIC F: + c EI
SIM ms
[252.700-
253.700]
MS
001_2013
Relative Abundance
Time (min)

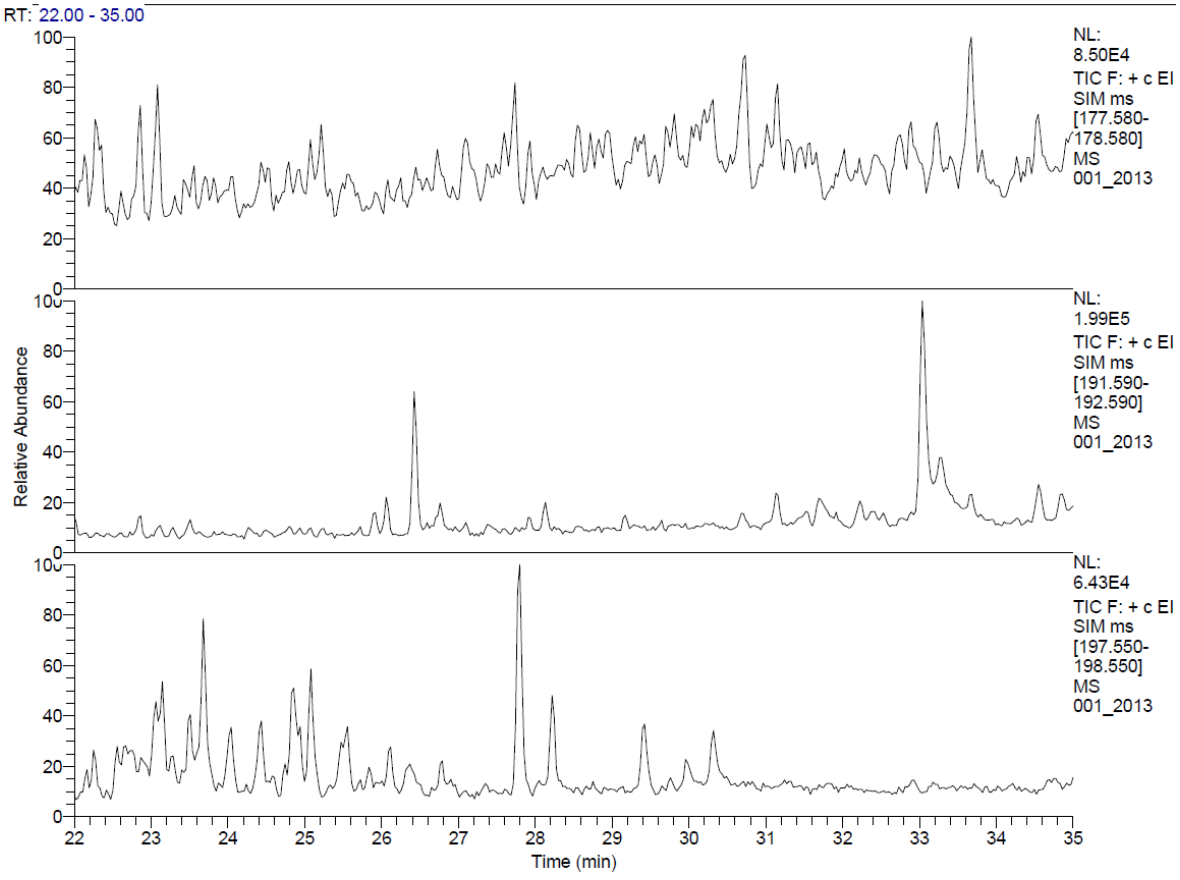
RT: 22.00 - 35.00
NL:
8.50E4
TIC F: + c EI
SIM ms
[177.580-
178.580]
MS
001_2013
NL:
1.99E5
TIC F: + c EI
SIM ms
[191.590-
192.590]
MS
001_2013
NL:
6.43E4
TIC F: + c EI
SIM ms
[197.550-
198.550]
MS
001_2013
Relative Abundance
Time (min)

O-2

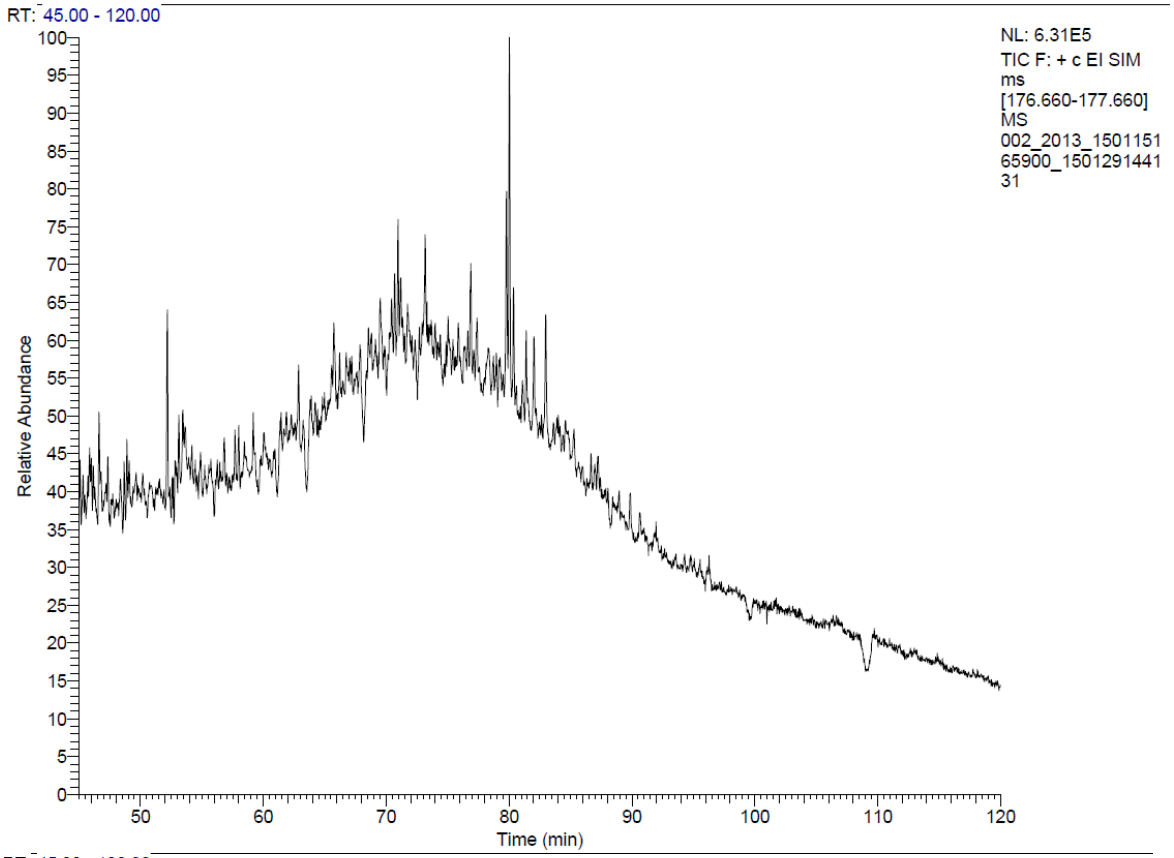
RT: 45.00 - 120.00
NL: 6.31E5
TIC F: + c EI SIM ms [176.660-177.660] MS 002_2013_150115165900_150129144131
Relative Abundance
Time (min)

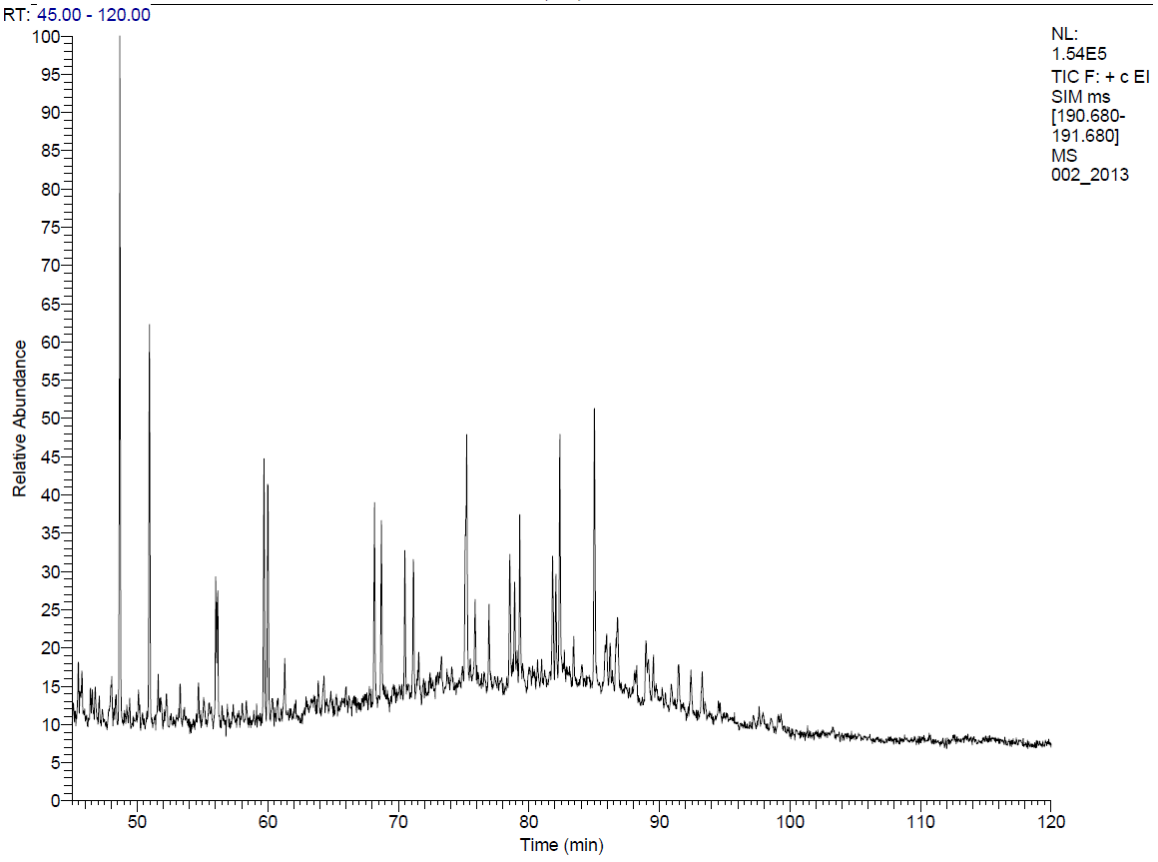
RT: 45.00 - 120.00
NL: 1.54E5
TIC F: + c EI SIM ms [190.680-191.680] MS 002_2013
Relative Abundance
Time (min)

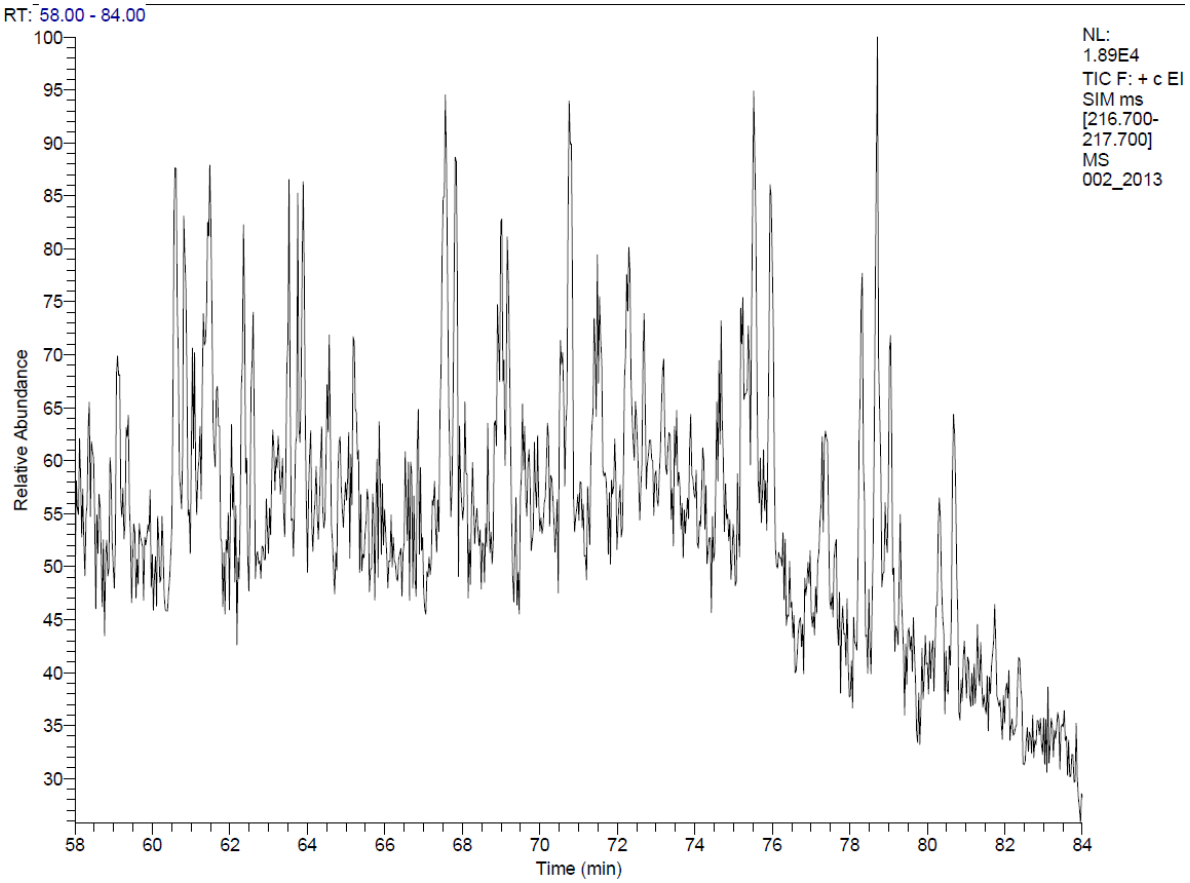
RT: 58.00 - 84.00
NL:
1.89E4
TIC F: + c EI
SIM ms
[216.700-
217.700]
MS
002_2013
Relative Abundance
Time (min)

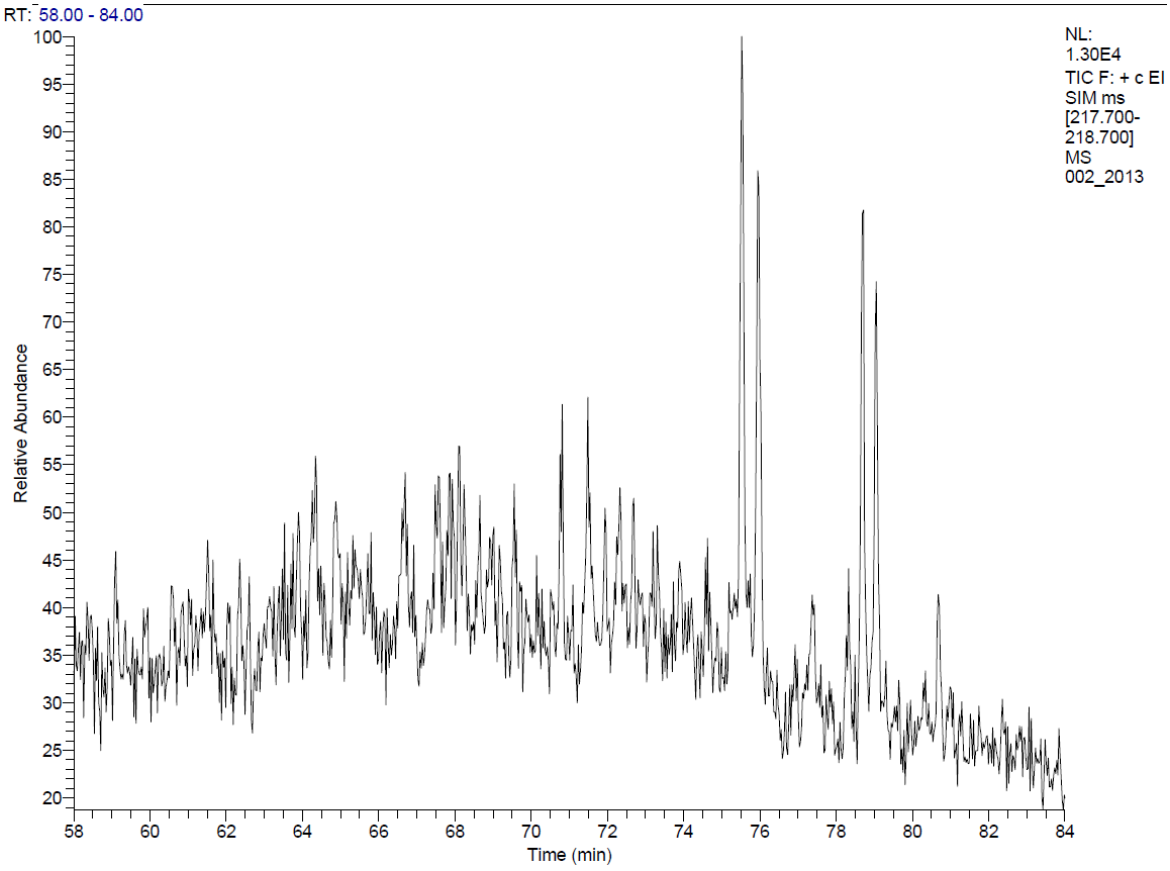
RT: 58.00 - 84.00
NL:
1.30E4
TIC F: + c EI
SIM ms
[217.700-
218.700]
MS
002_2013
Relative Abundance
Time (min)

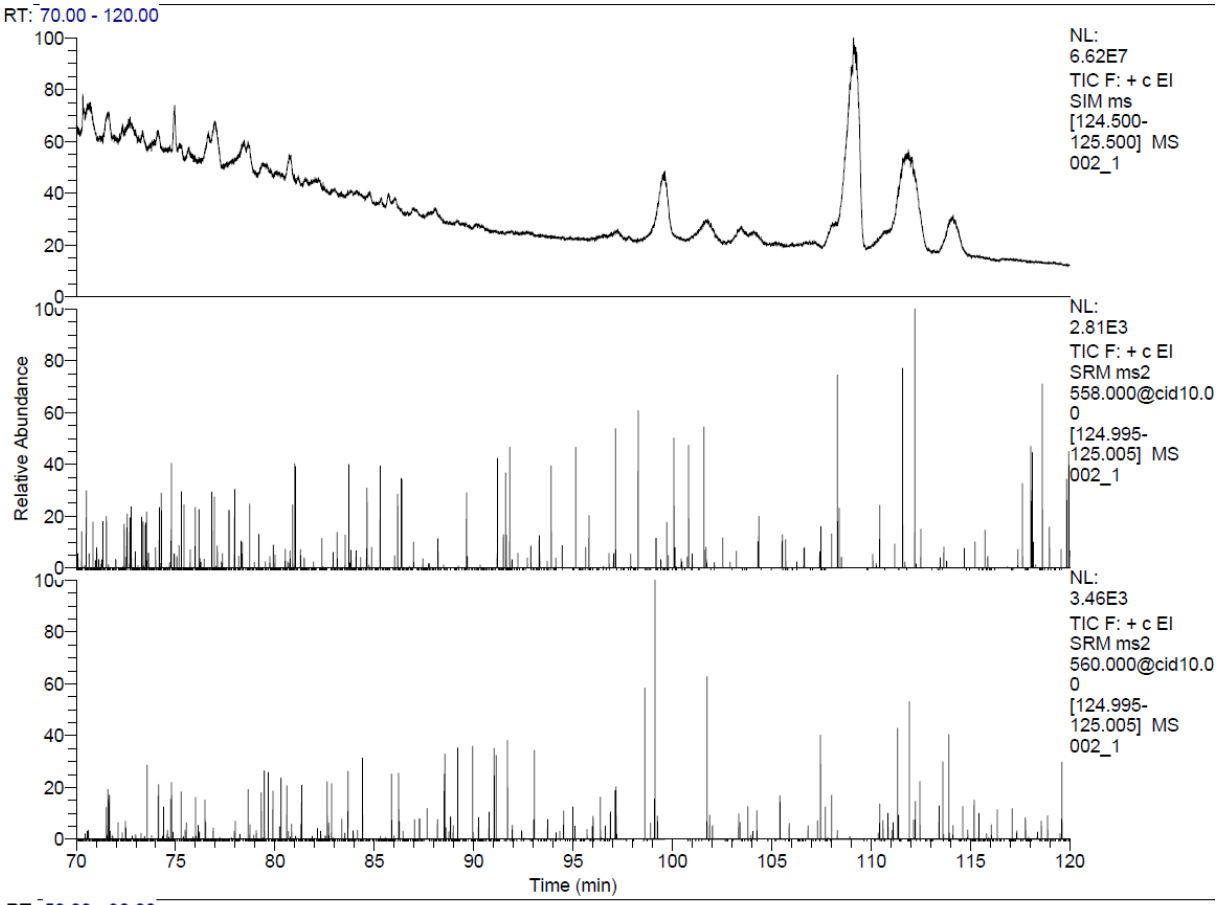
RT: 70.00 - 120.00
NL:
6.62E7
TIC F: + c EI
SIM ms
[124.500-
125.500] MS
002_1
NL:
2.81E3
TIC F: + c EI
SRM ms2
558.000@cid10.0
0
[124.995-
125.005] MS
002_1
NL:
3.46E3
TIC F: + c EI
SRM ms2
560.000@cid10.0
0
[124.995-
125.005] MS
002_1
Relative Abundance
Time (min)

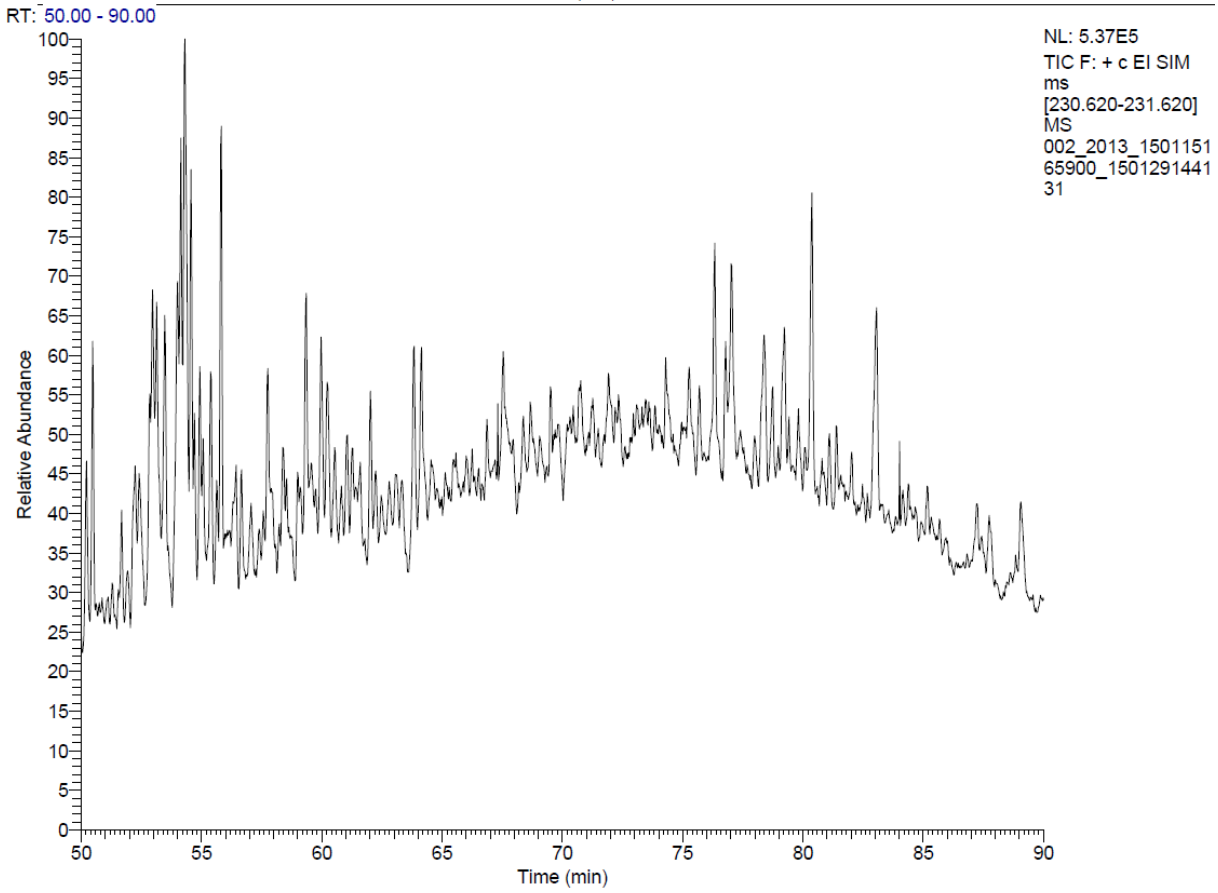
RT: 50.00 - 90.00
NL: 5.37E5
TIC F: + c EI SIM
ms
[230.620-231.620]
MS
002_2013_1501151
65900_1501291441
31
Relative Abundance
Time (min)

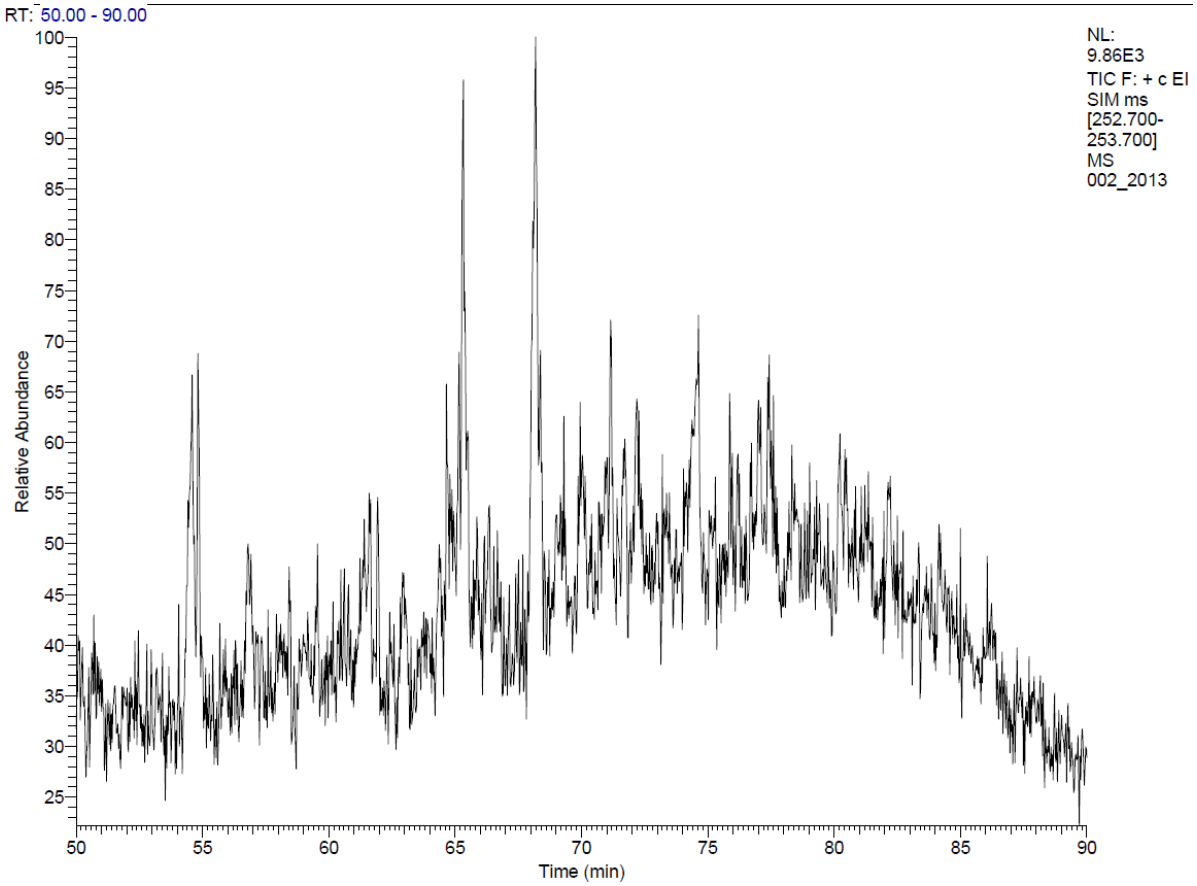
RT: 50.00 - 90.00
NL:
9.86E3
TIC F: + c EI
SIM ms
[252.700-
253.700]
MS
002_2013
Relative Abundance
Time (min)

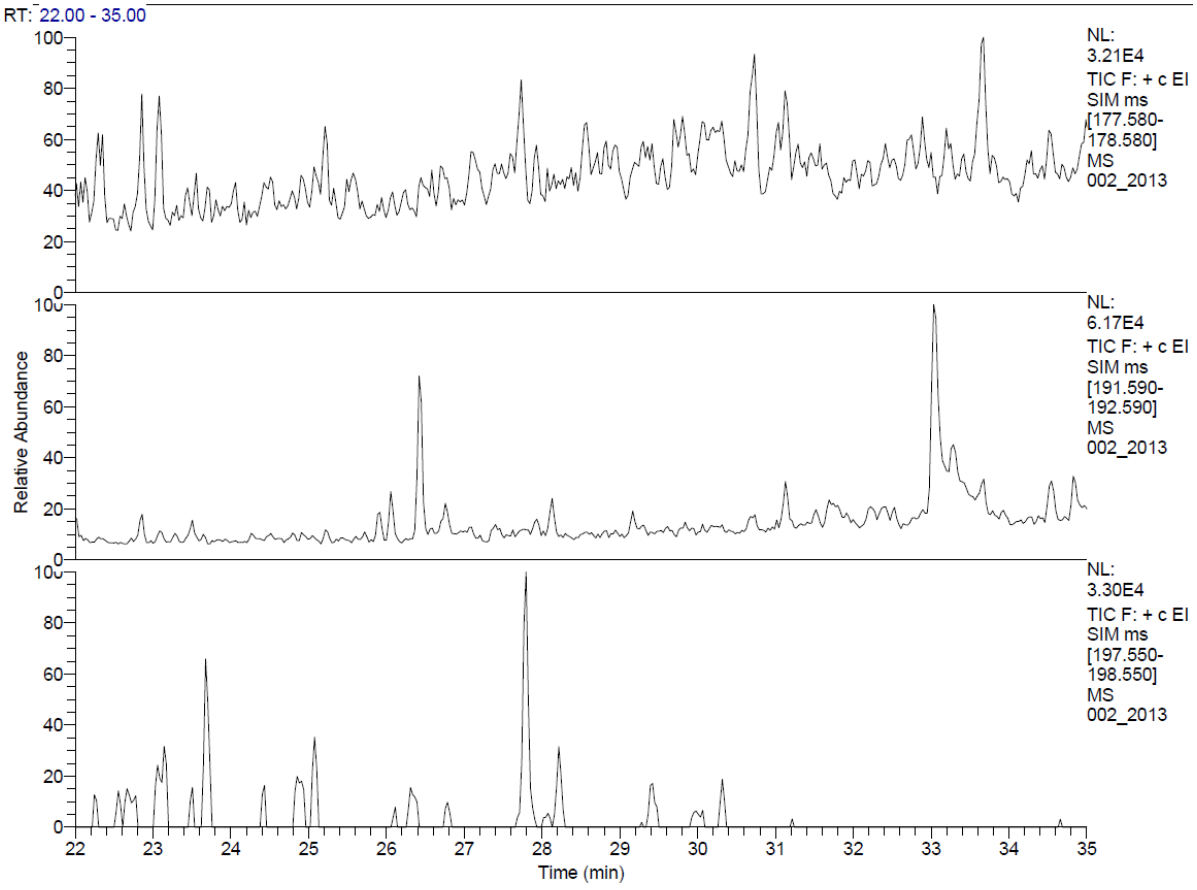
RT: 22.00 - 35.00
NL:
3.21E4
TIC F: + c EI
SIM ms
[177.580-
178.580]
MS
002_2013
NL:
6.17E4
TIC F: + c EI
SIM ms
[191.590-
192.590]
MS
002_2013
NL:
3.30E4
TIC F: + c EI
SIM ms
[197.550-
198.550]
MS
002_2013
Relative Abundance
Time (min)

O-3

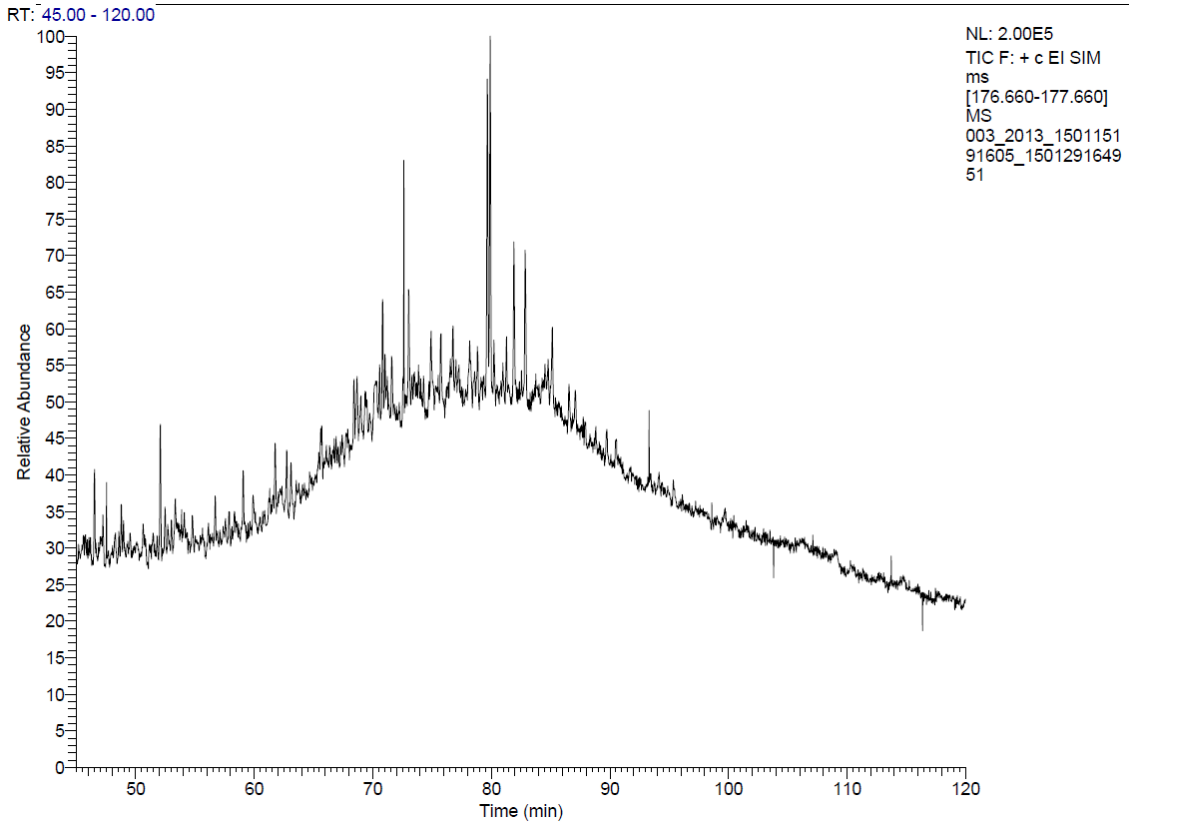
RT: 45.00 - 120.00
NL: 2.00E5
TIC F: + c EI SIM ms [176.660-177.660] MS 003_2013_150115191605_150129164951
Relative Abundance
Time (min)

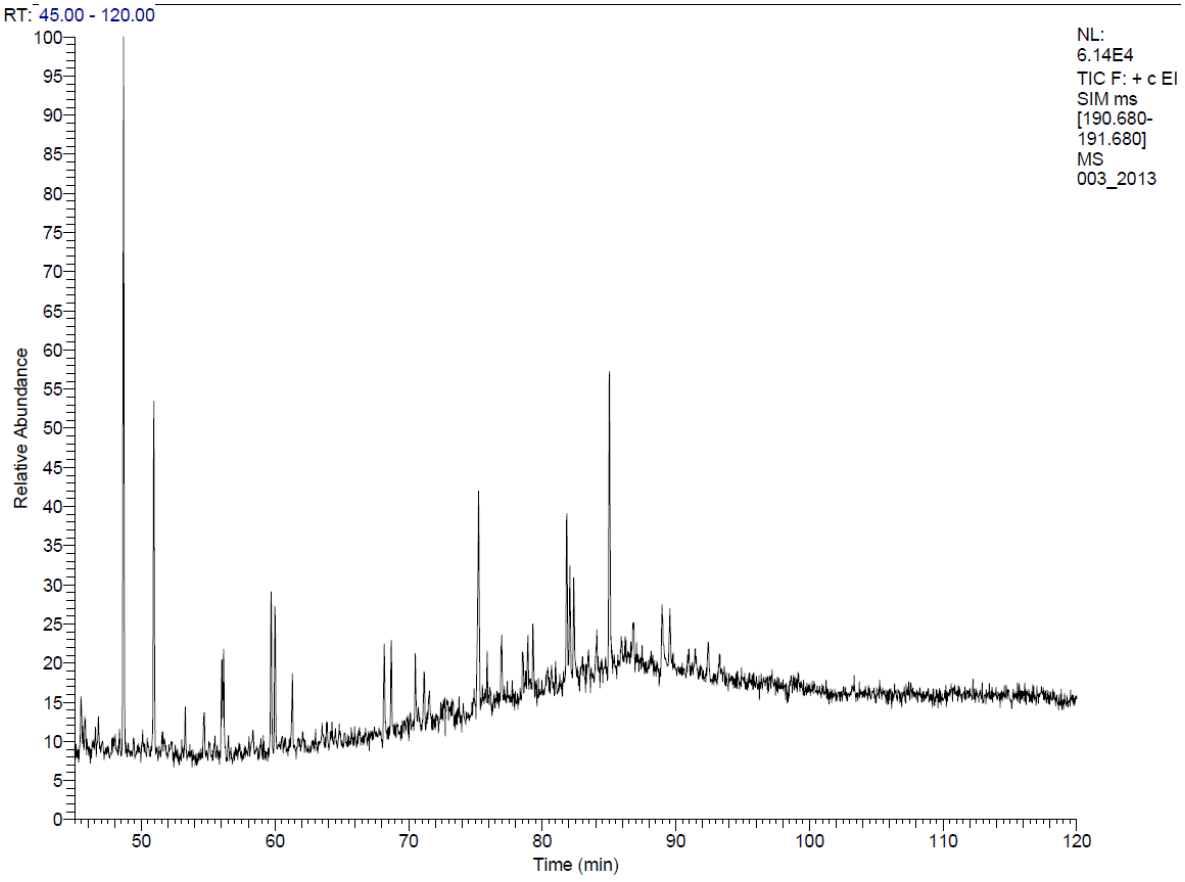
RT: 45.00 - 120.00
NL: 6.14E4
TIC F: + c EI SIM ms [190.680-191.680] MS 003_2013
Relative Abundance
Time (min)

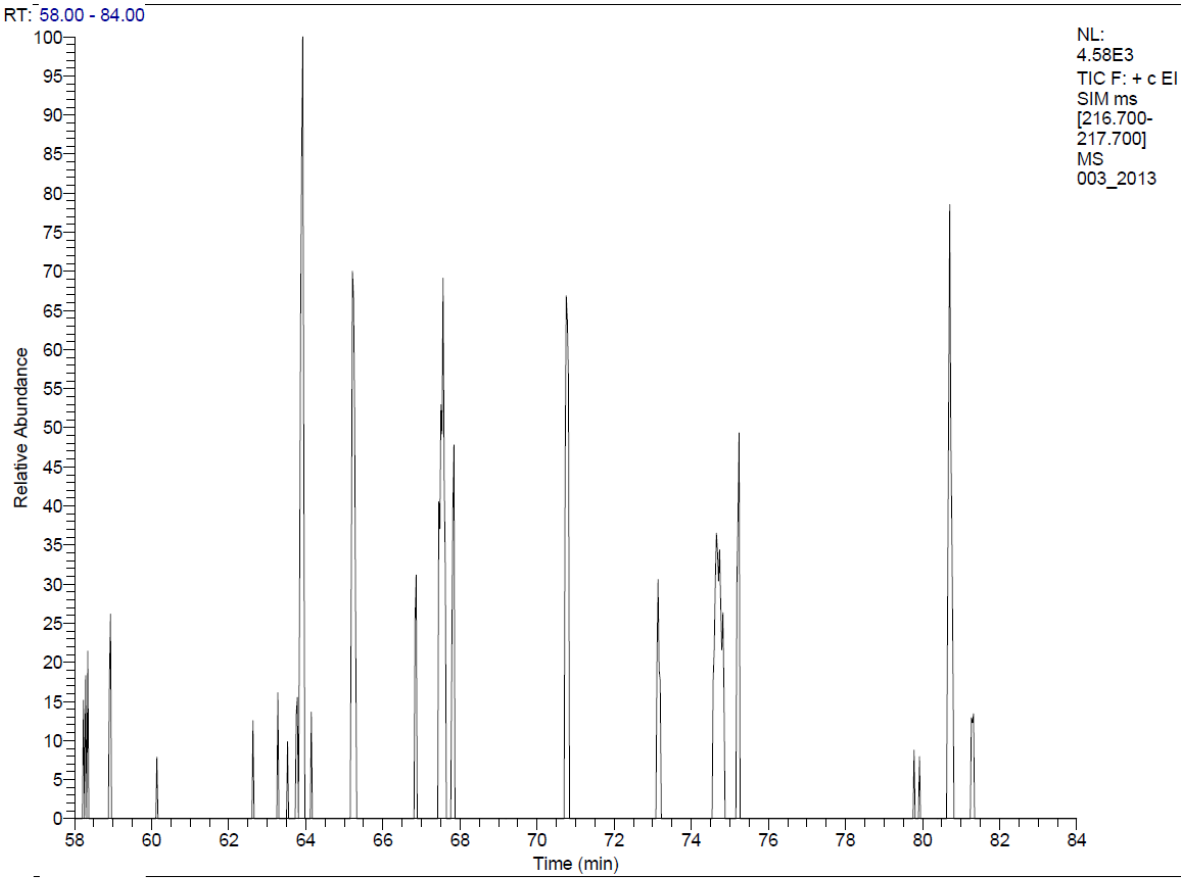
RT: 58.00 - 84.00
NL:
4.58E3
TIC F: + c EI
SIM ms
[216.700-
217.700]
MS
003_2013
Relative Abundance
Time (min)

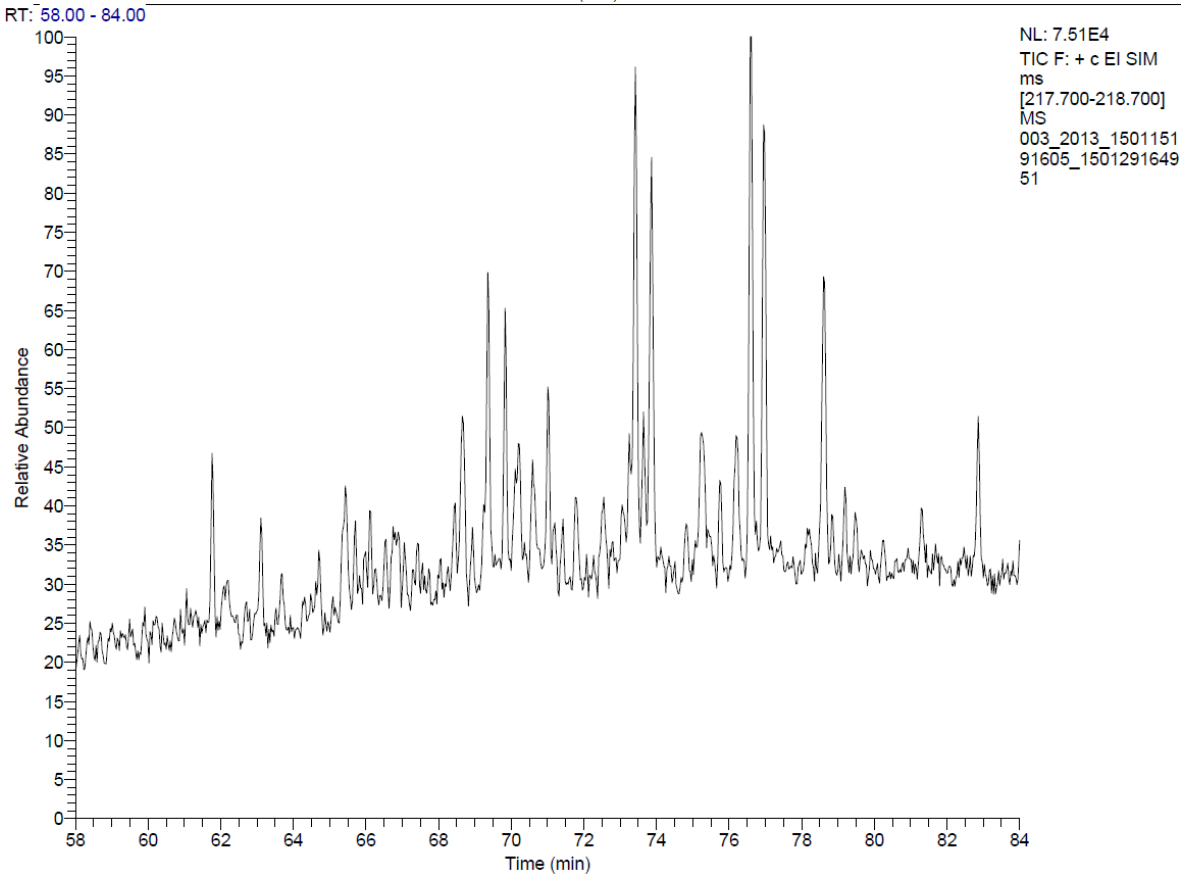
RT: 58.00 - 84.00
NL: 7.51E4
TIC F: + c EI SIM
ms
[217.700-218.700]
MS
003_2013_1501151
91605_1501291649
51
Relative Abundance
Time (min)

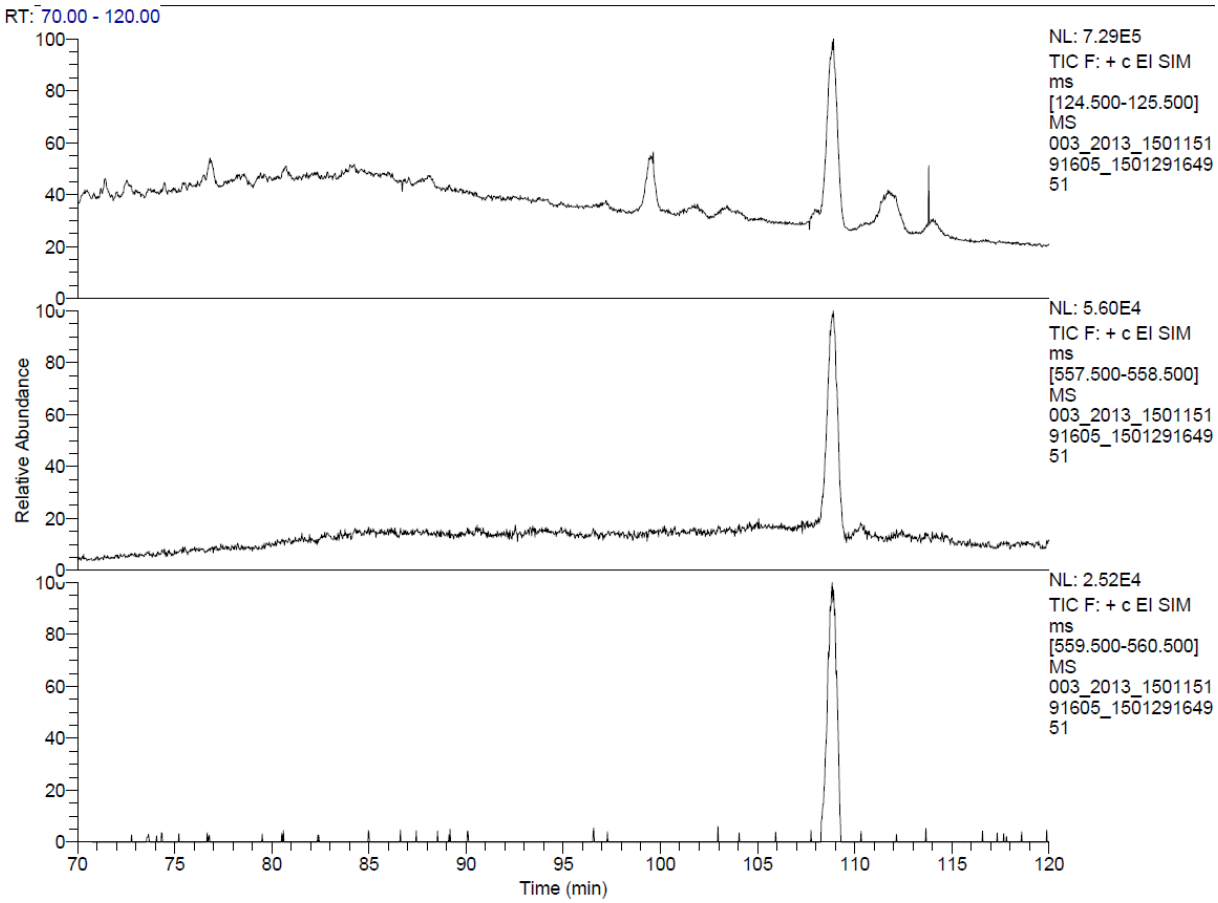
RT: 70.00 - 120.00
NL: 7.29E5
TIC F: + c EI SIM ms [124.500-125.500] MS 003_2013_150115191605_150129164951
NL: 5.60E4
TIC F: + c EI SIM ms [557.500-558.500] MS 003_2013_150115191605_150129164951
NL: 2.52E4
TIC F: + c EI SIM ms [559.500-560.500] MS 003_2013_150115191605_150129164951
Relative Abundance
Time (min)

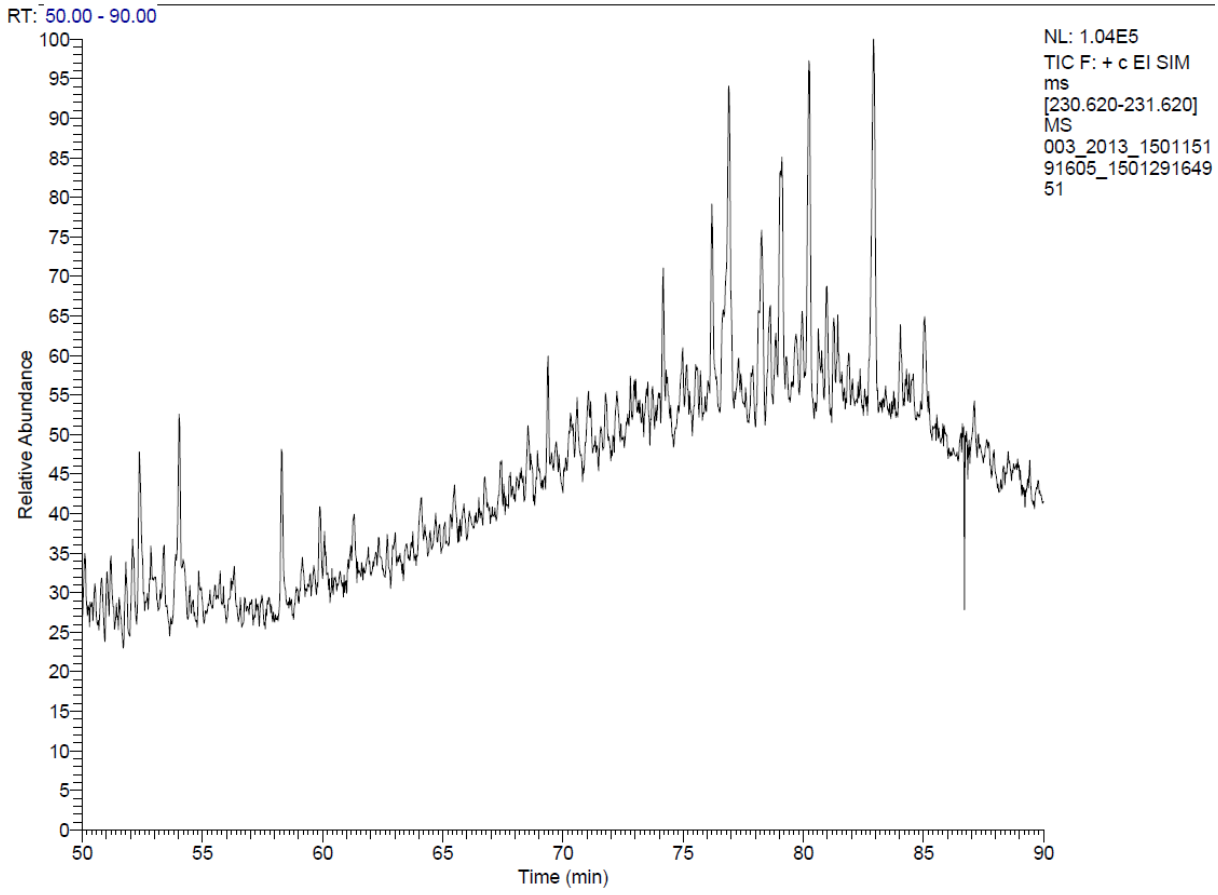
RT: 50.00 - 90.00
NL: 1.04E5
TIC F: + c EI SIM ms [230.620-231.620] MS 003_2013_150115191605_150129164951
Relative Abundance
Time (min)

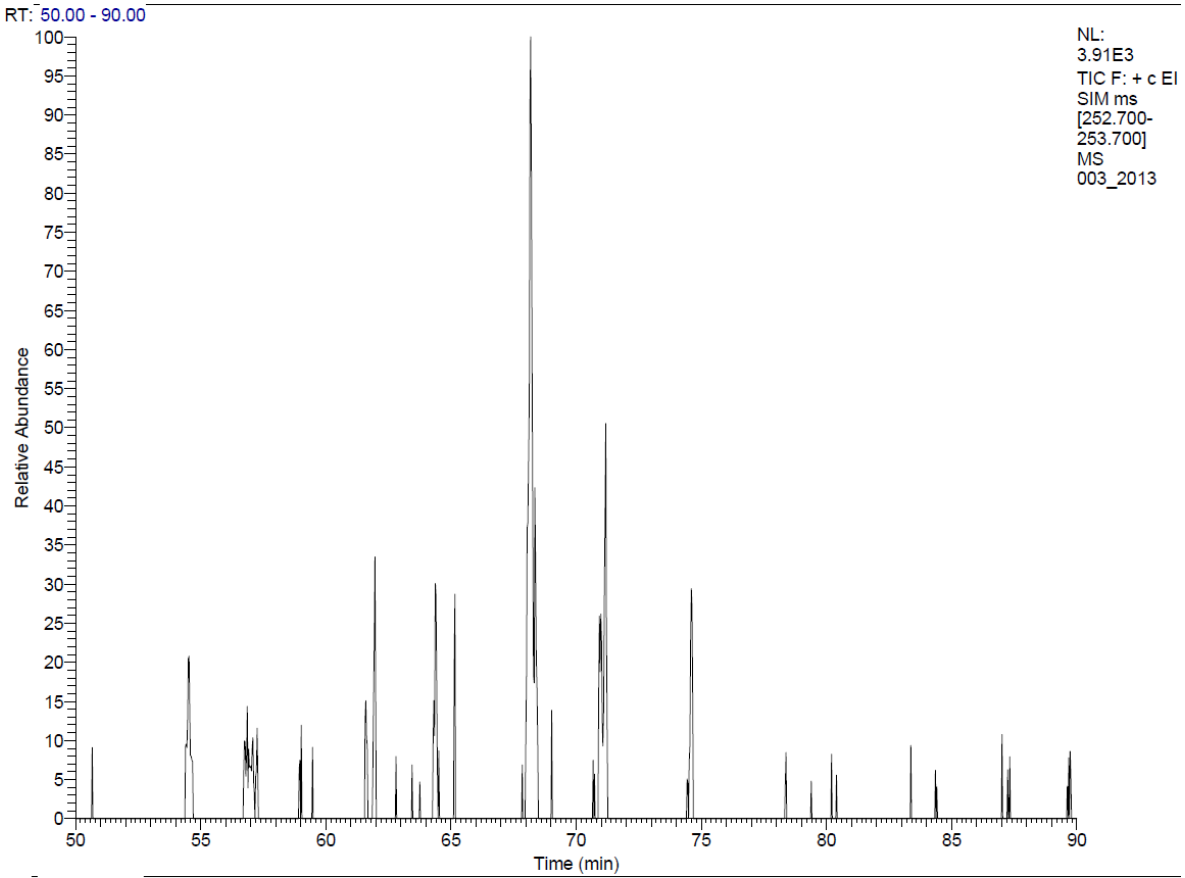
RT: 50.00 - 90.00
NL:
3.91E3
TIC F: + c EI
SIM ms
[252.700-
253.700]
MS
003_2013
Relative Abundance
Time (min)

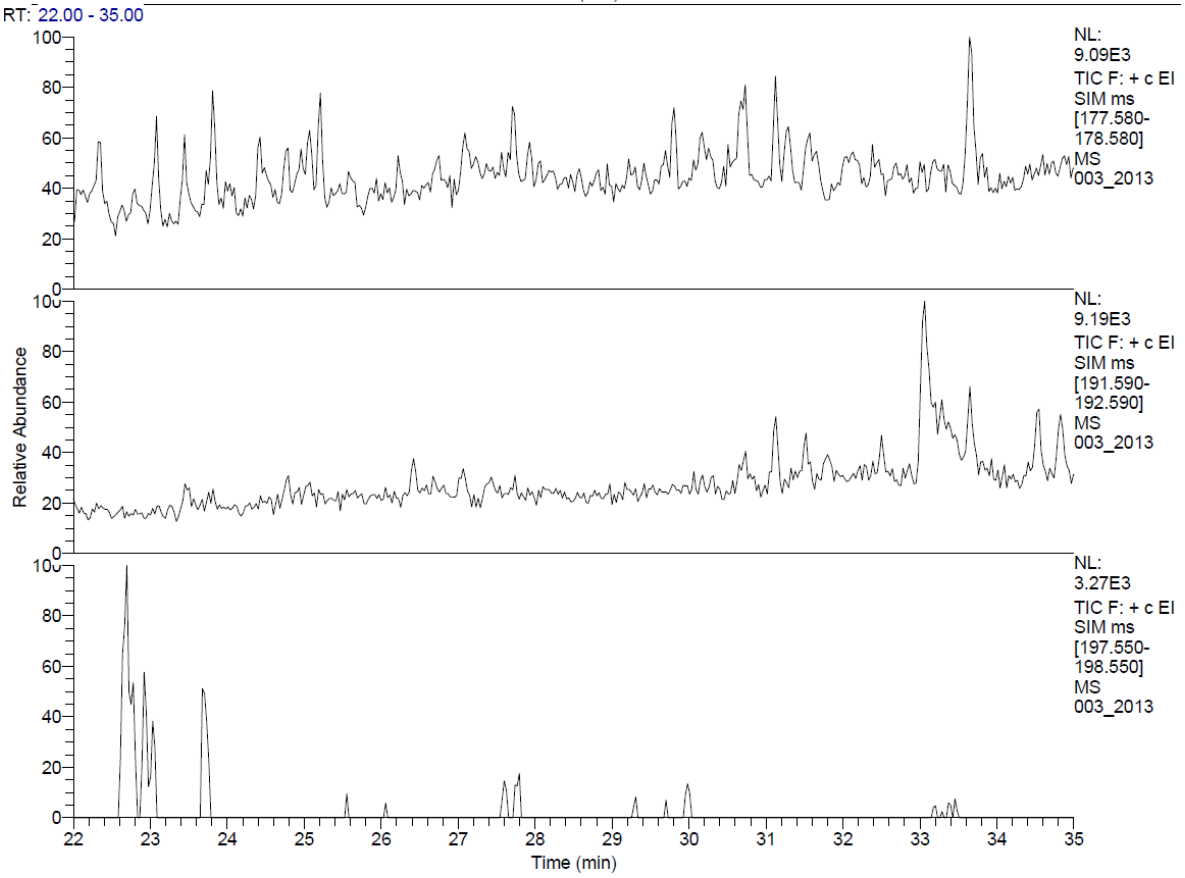
RT: 22.00 - 35.00
NL:
9.09E3
TIC F: + c EI
SIM ms
[177.580-
178.580]
MS
003_2013
NL:
9.19E3
TIC F: + c EI
SIM ms
[191.590-
192.590]
MS
003_2013
NL:
3.27E3
TIC F: + c EI
SIM ms
[197.550-
198.550]
MS
003_2013
Relative Abundance
Time (min)

O-4

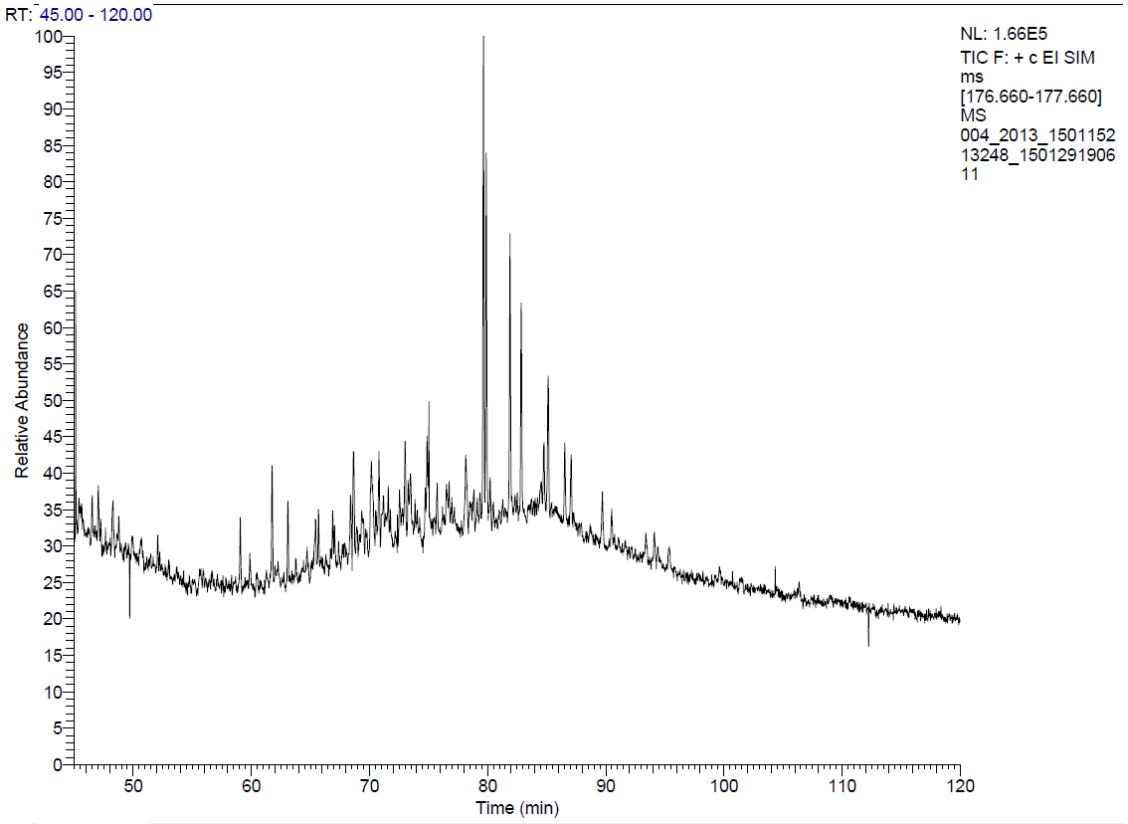
RT: 45.00 - 120.00
NL: 1.66E5
TIC F: + c EI SIM ms [176.660-177.660] MS 004_2013_150115213248_150129190611
Relative Abundance
Time (min)

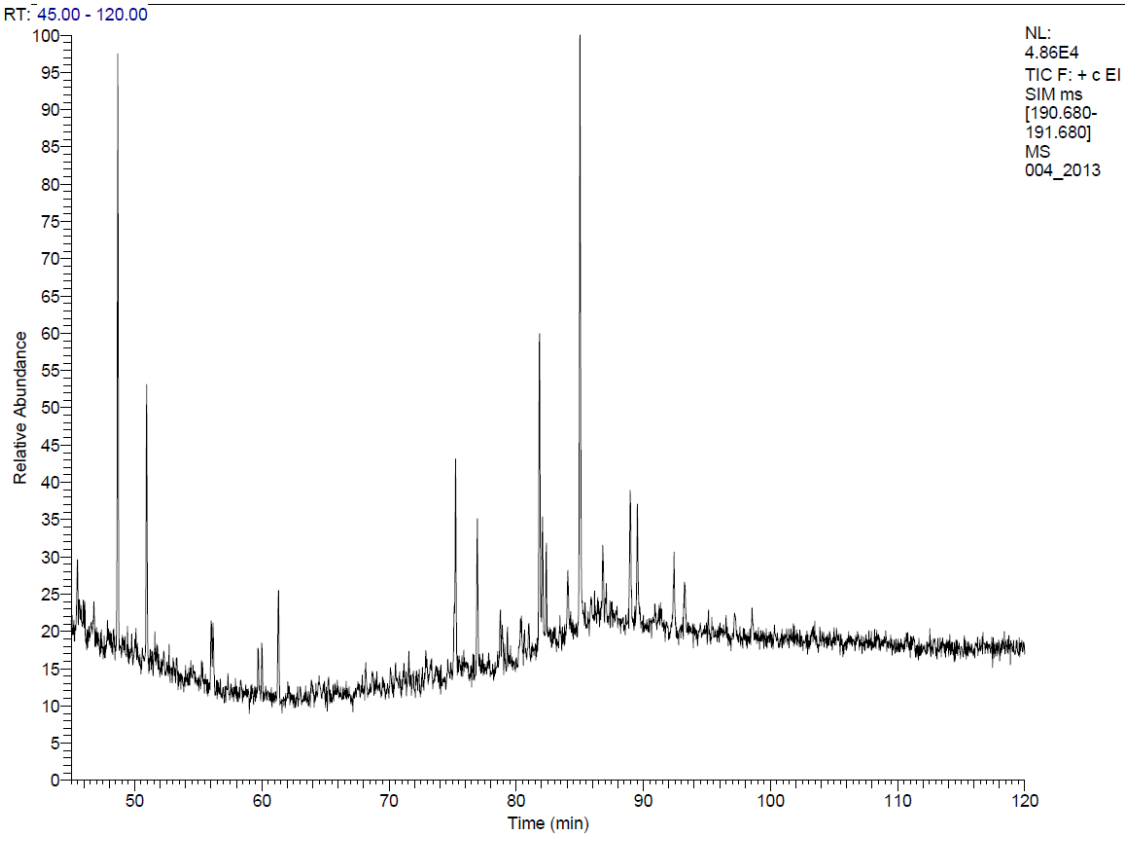
RT: 45.00 - 120.00
NL: 4.86E4
TIC F: + c EI SIM ms [190.680-191.680] MS 004_2013
Relative Abundance
Time (min)

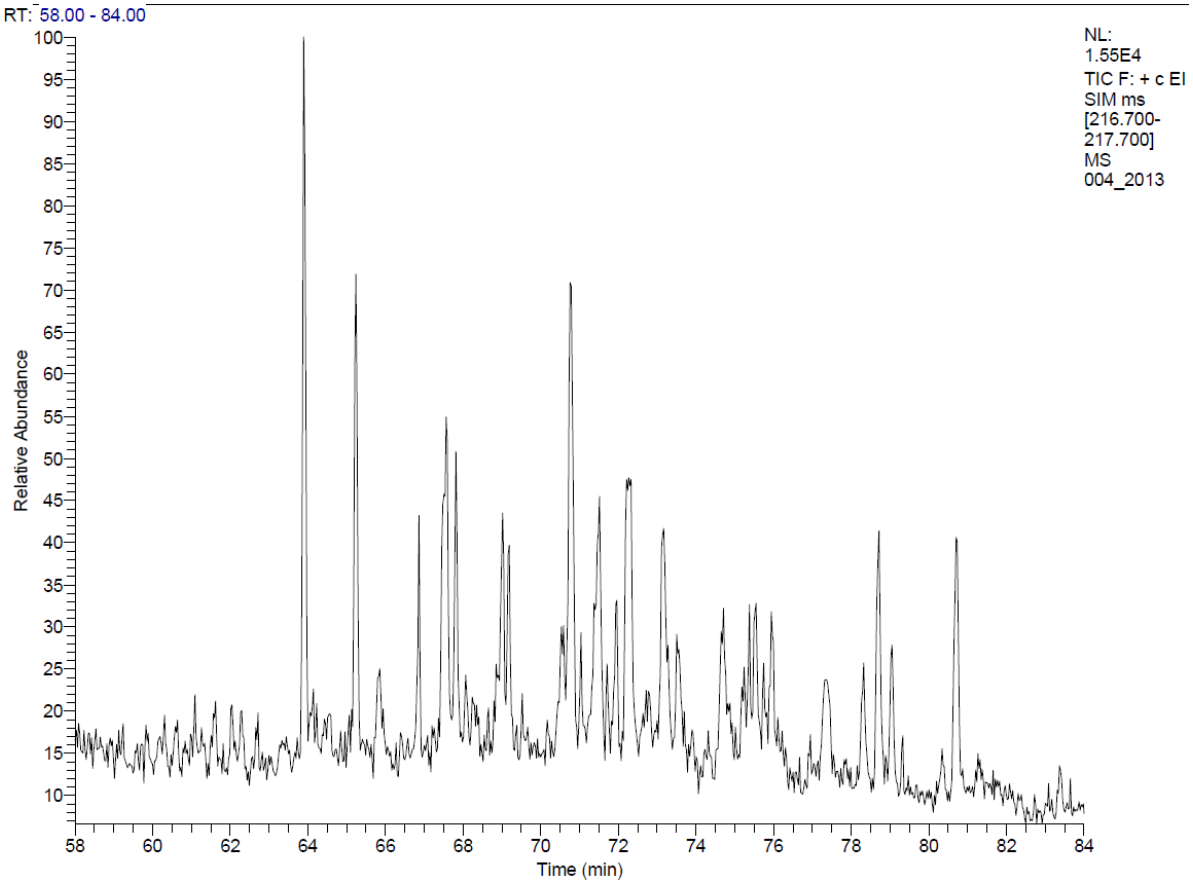
RT: 58.00 - 84.00
NL:
1.55E4
TIC F: + c EI
SIM ms
[216.700-
217.700]
MS
004_2013
Relative Abundance
Time (min)

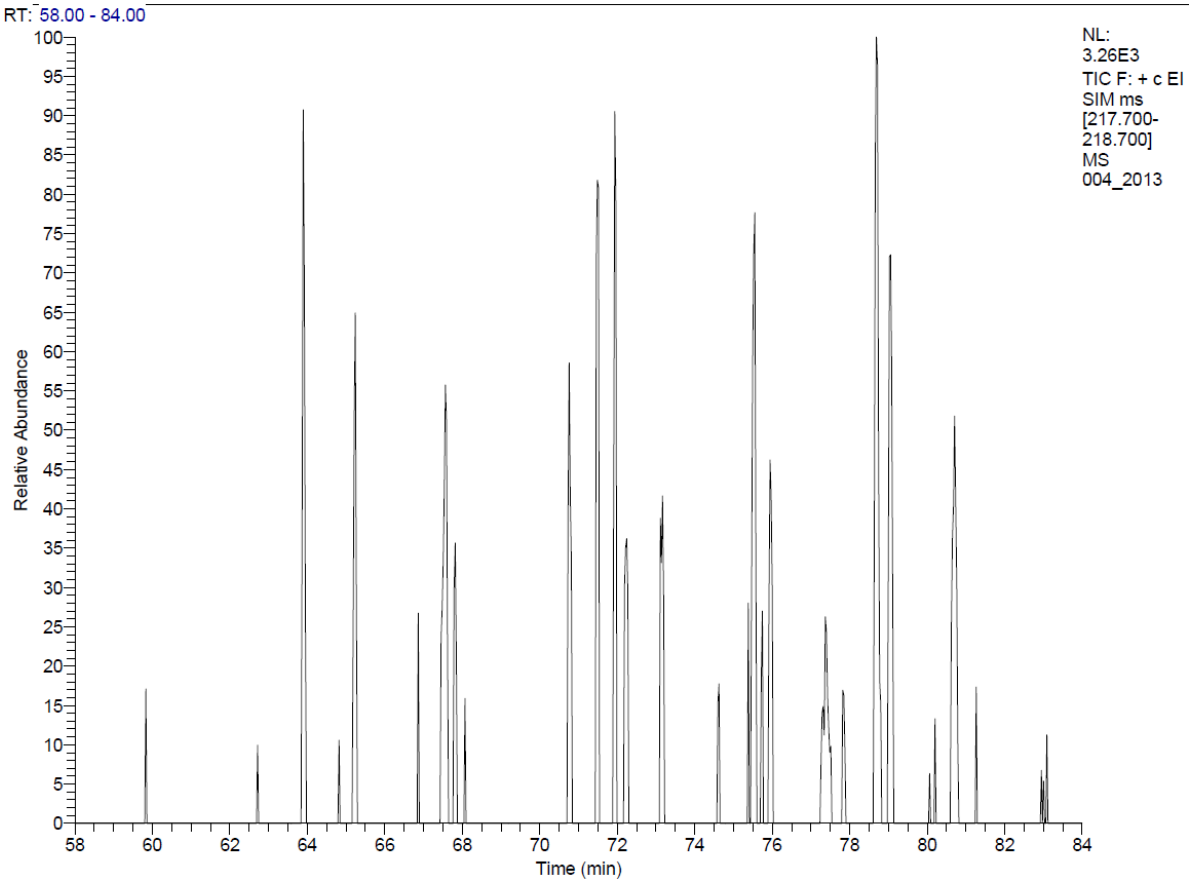
RT: 58.00 - 84.00
NL:
3.26E3
TIC F: + c EI
SIM ms
[217.700-
218.700]
MS
004_2013
Relative Abundance
Time (min)

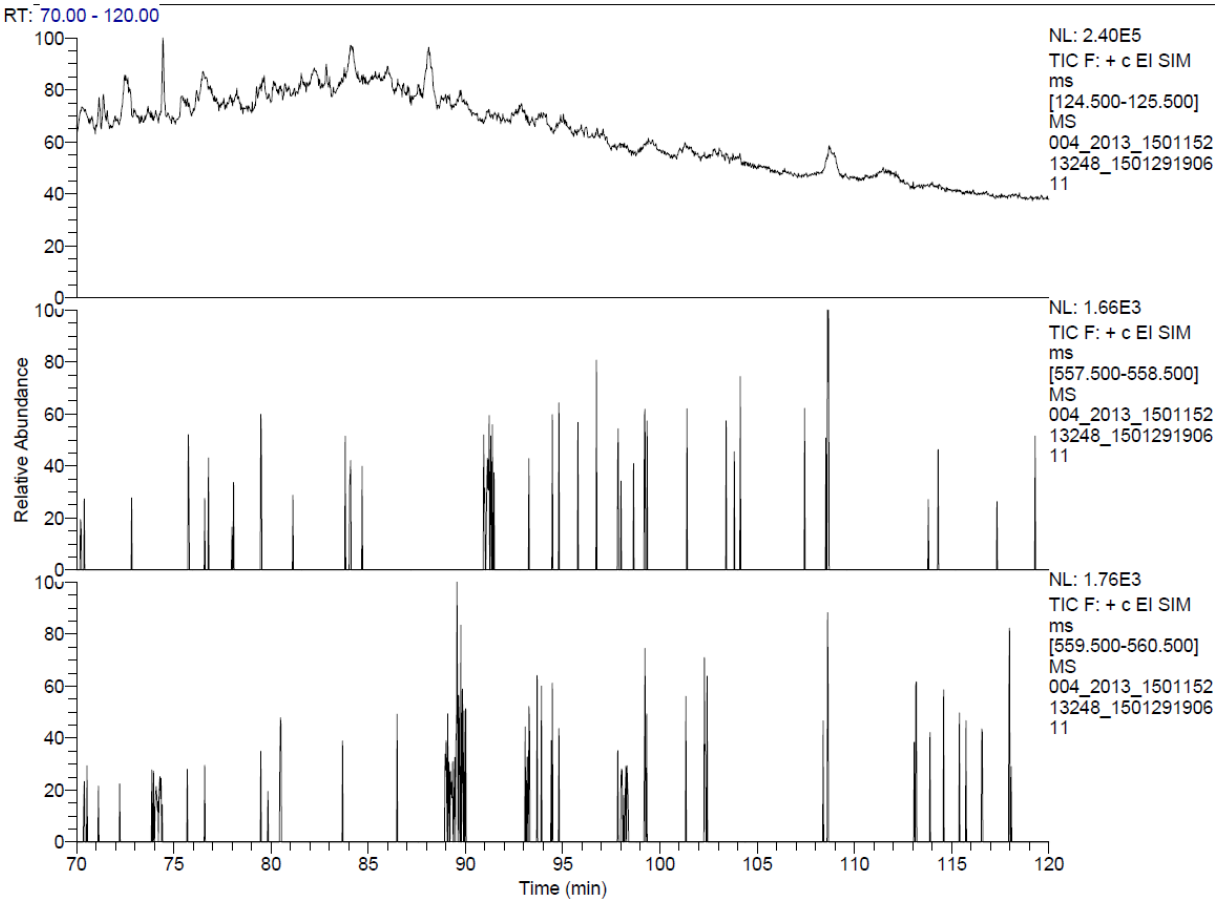
RT: 70.00 - 120.00
NL: 2.40E5
TIC F: + c EI SIM ms [124.500-125.500] MS 004_2013_150115213248_150129190611
NL: 1.66E3
TIC F: + c EI SIM ms [557.500-558.500] MS 004_2013_150115213248_150129190611
NL: 1.76E3
TIC F: + c EI SIM ms [559.500-560.500] MS 004_2013_150115213248_150129190611
Relative Abundance
Time (min)

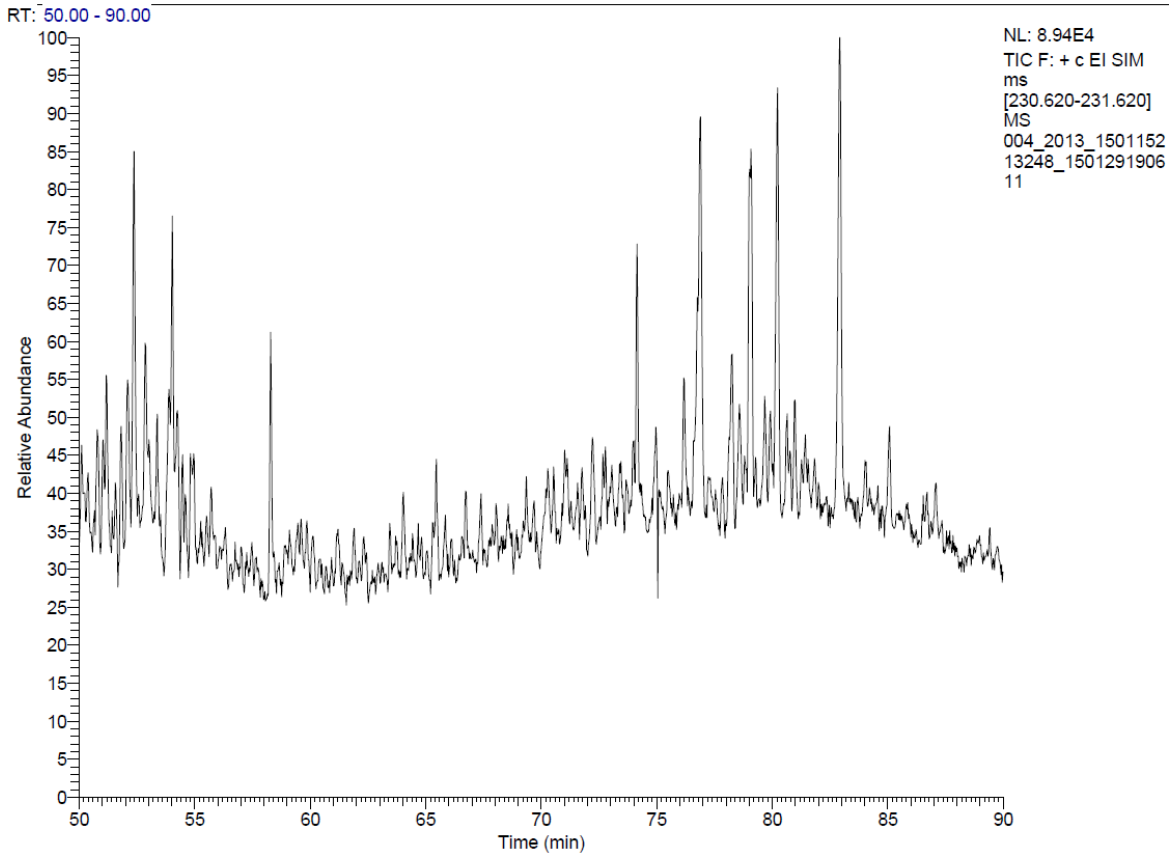
RT: 50.00 - 90.00
NL: 8.94E4
TIC F: + c EI SIM ms [230.620-231.620] MS 004_2013_150115213248_150129190611
Relative Abundance
Time (min)

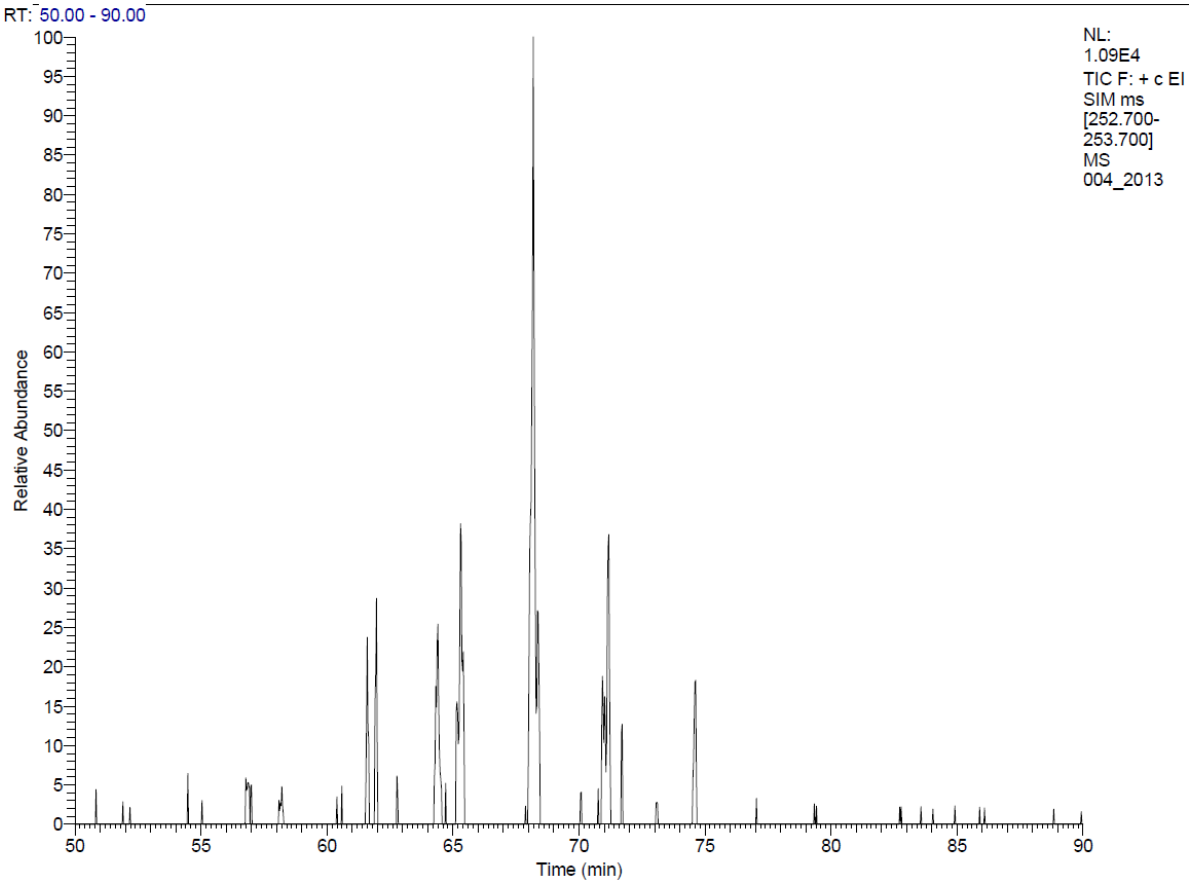
RT: 50.00 - 90.00
NL:
1.09E4
TIC F: + c EI
SIM ms
[252.700-
253.700]
MS
004_2013
Relative Abundance
Time (min)

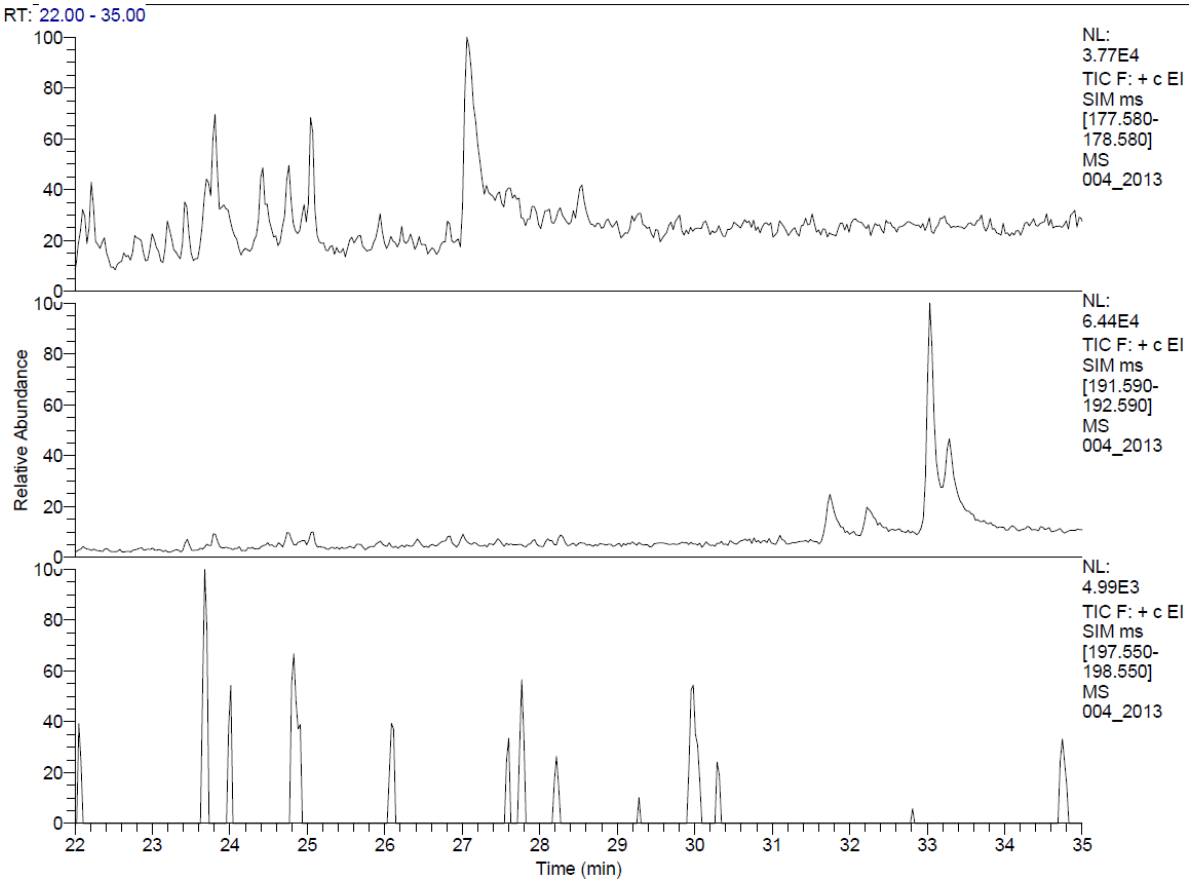
RT: 22.00 - 35.00
NL:
3.77E4
TIC F: + c EI
SIM ms
[177.580-
178.580]
MS
004_2013
NL:
6.44E4
TIC F: + c EI
SIM ms
[191.590-
192.590]
MS
004_2013
NL:
4.99E3
TIC F: + c EI
SIM ms
[197.550-
198.550]
MS
004_2013
Relative Abundance
Time (min)

O-5

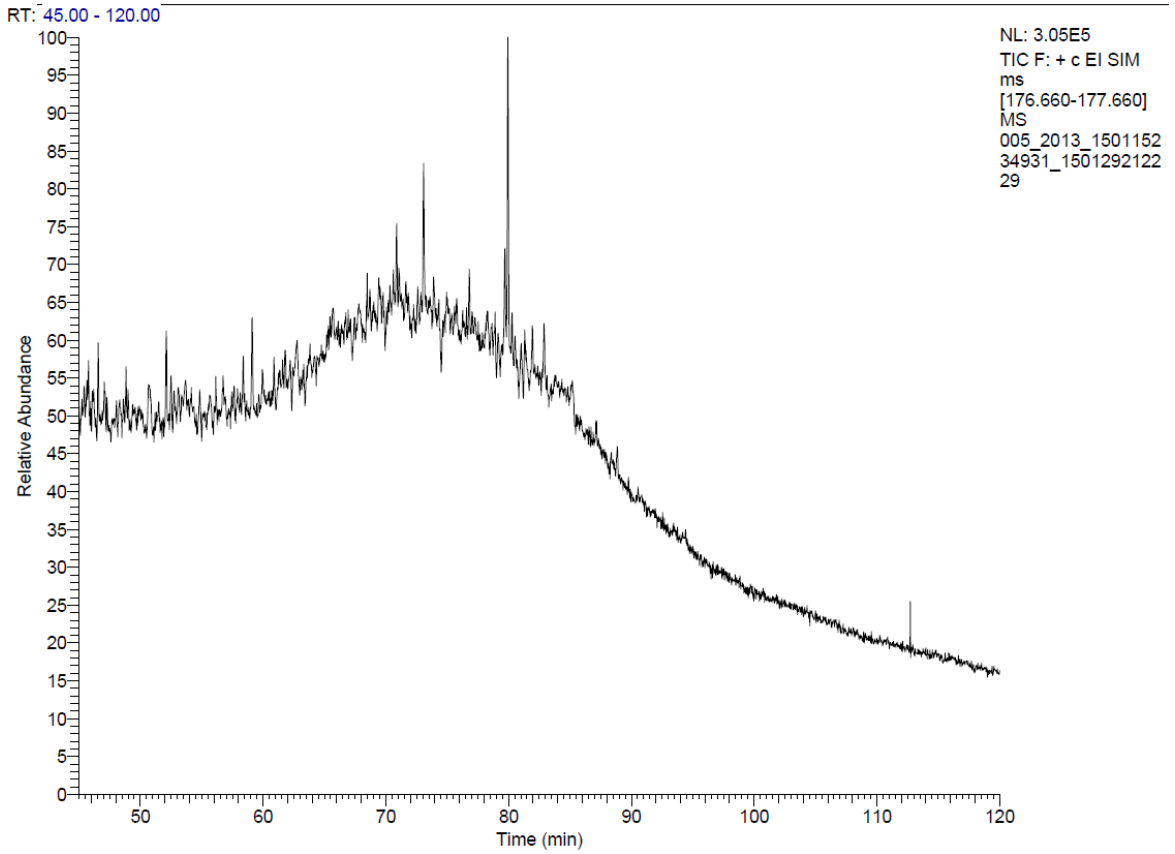
RT: 45.00 - 120.00
NL: 3.05E5
TIC F: + c EI SIM ms [176.660-177.660] MS 005_2013_150115234931_150129212229
Relative Abundance
Time (min)

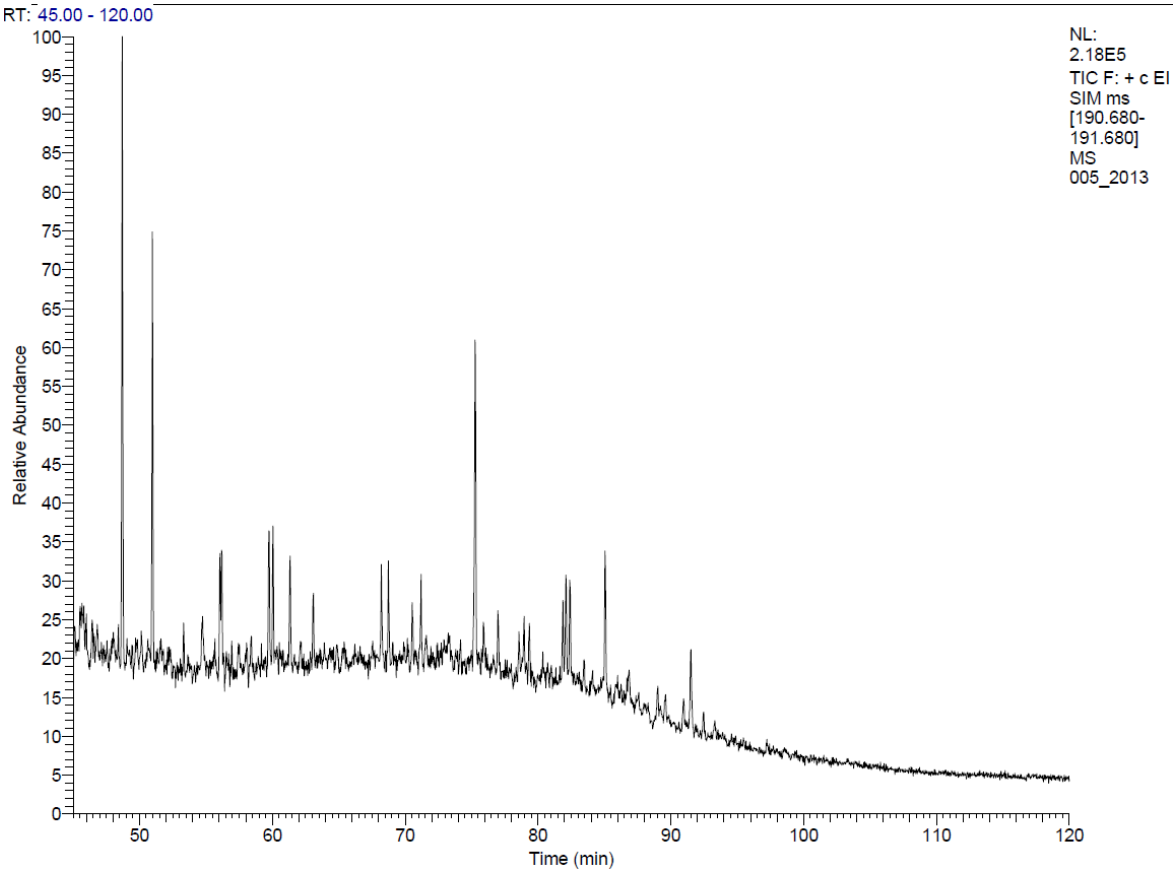
RT: 45.00 - 120.00
NL: 2.18E5
TIC F: + c EI SIM ms [190.680-191.680] MS 005_2013
Relative Abundance
Time (min)

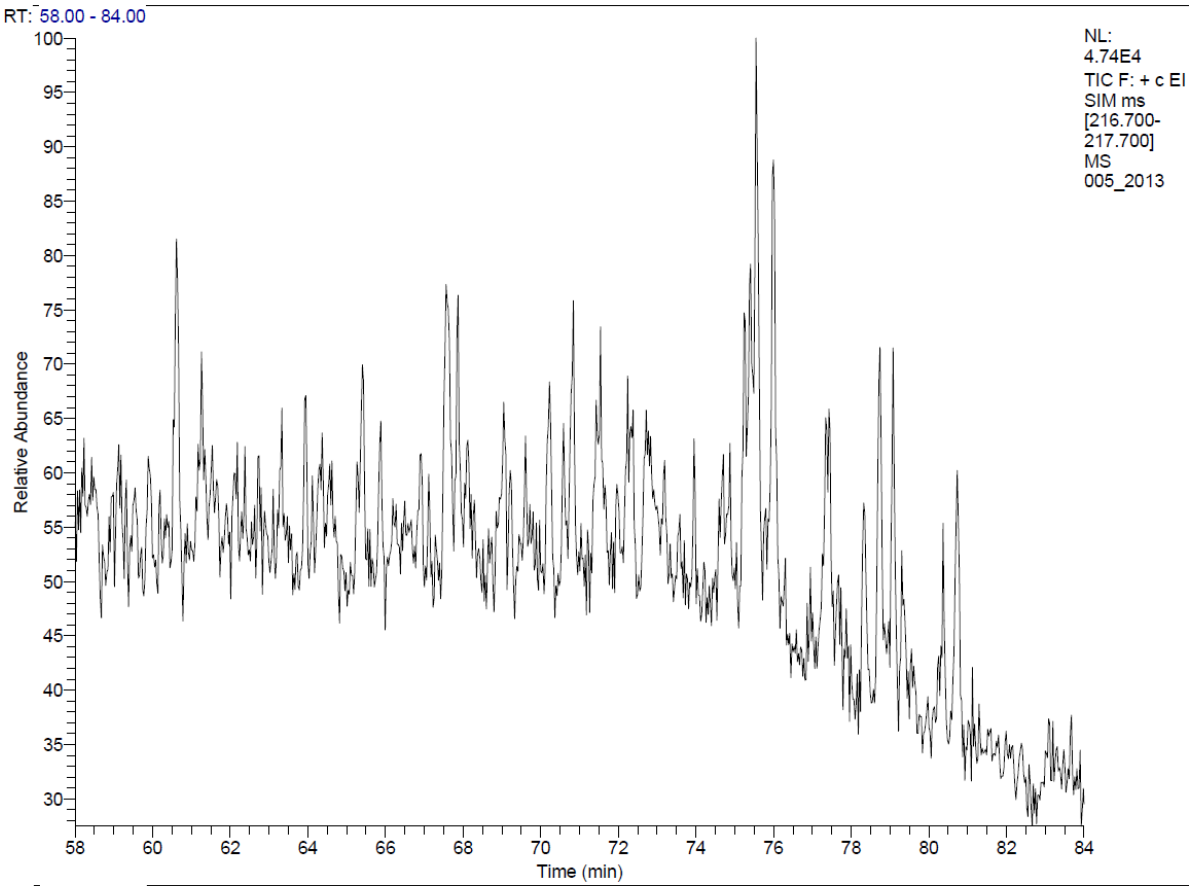
RT: 58.00 - 84.00
NL:
4.74E4
TIC F: + c EI
SIM ms
[216.700-
217.700]
MS
005_2013
Relative Abundance
Time (min)

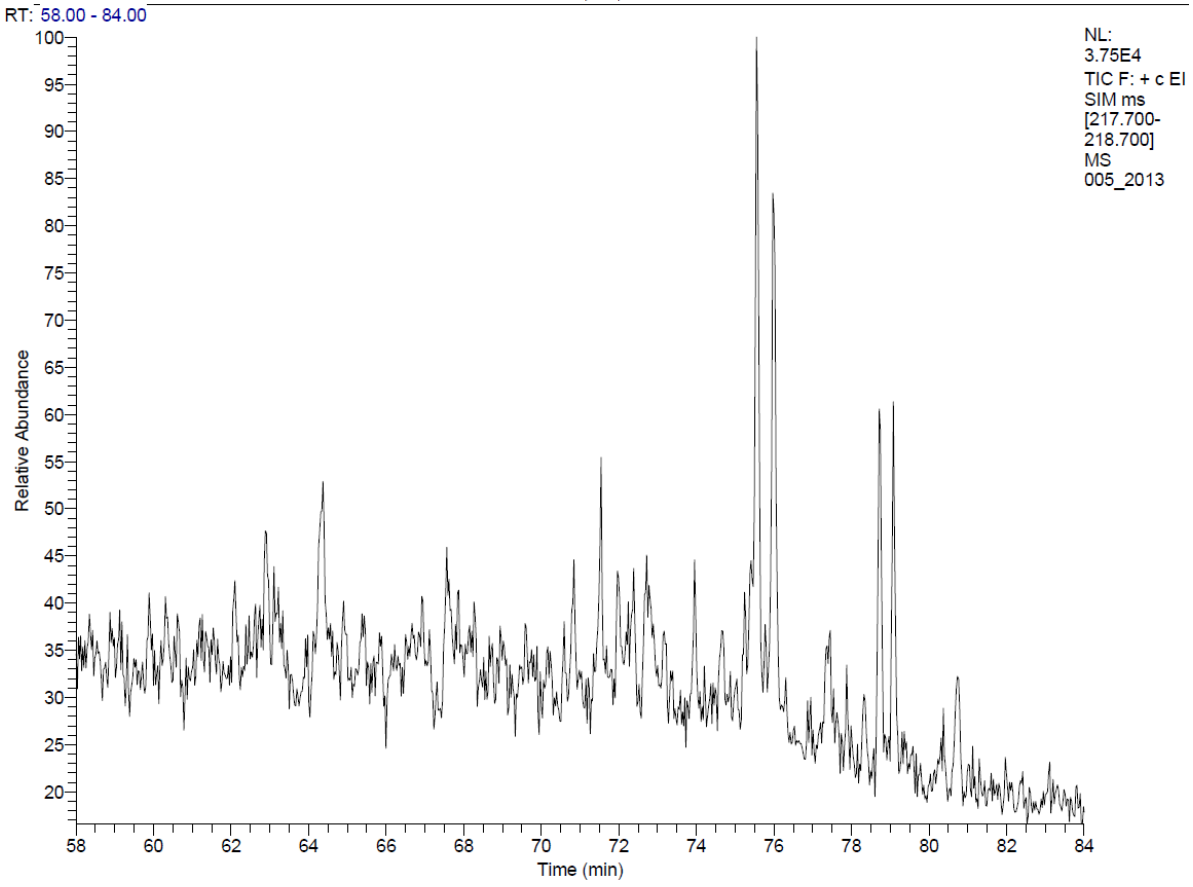
RT: 58.00 - 84.00
NL:
3.75E4
TIC F: + c EI
SIM ms
[217.700-
218.700]
MS
005_2013
Relative Abundance
Time (min)

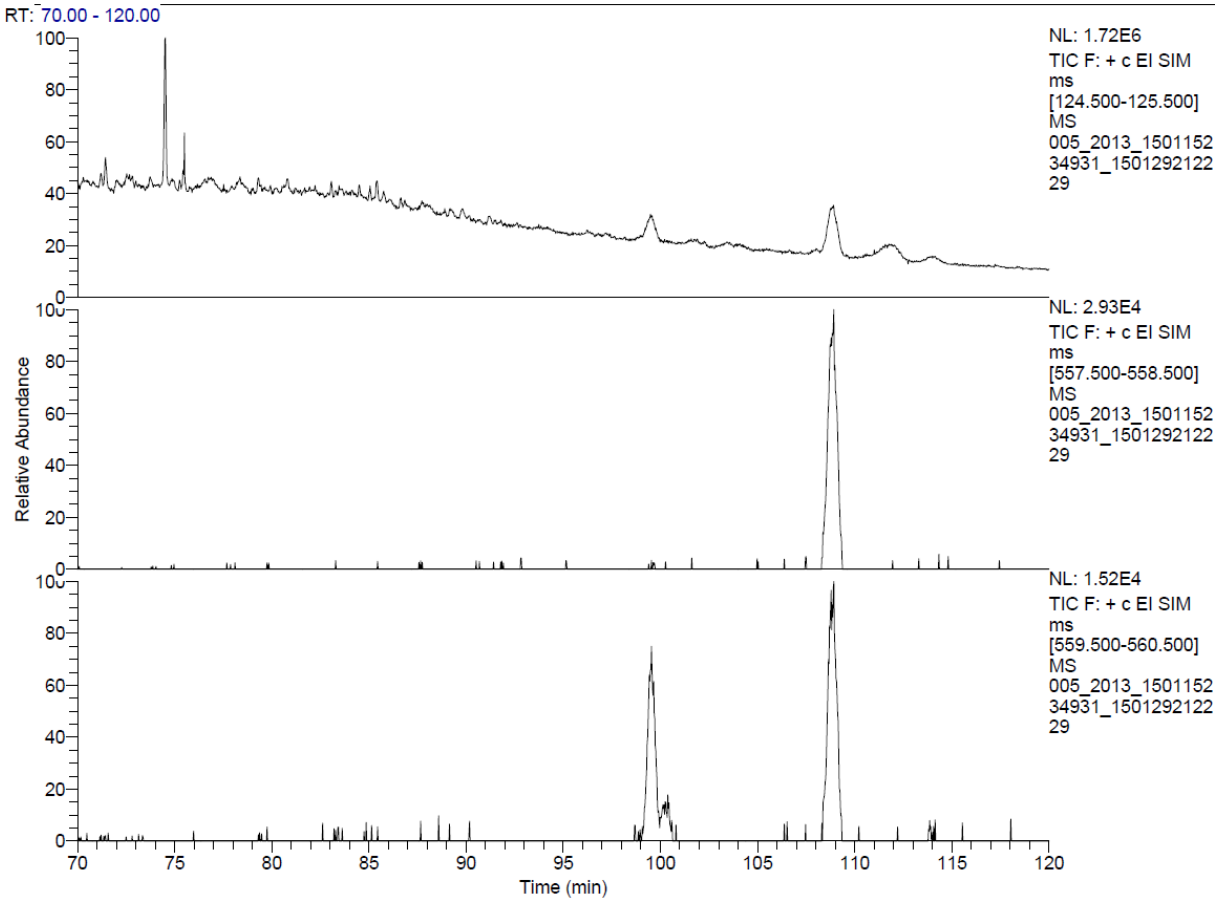
RT: 70.00 - 120.00
NL: 1.72E6
TIC F: + c EI SIM
ms
[124.500-125.500]
MS
005_2013_150115234931_150129212229
NL: 2.93E4
TIC F: + c EI SIM
ms
[557.500-558.500]
MS
005_2013_150115234931_150129212229
NL: 1.52E4
TIC F: + c EI SIM
ms
[559.500-560.500]
MS
005_2013_150115234931_150129212229
Relative Abundance
Time (min)

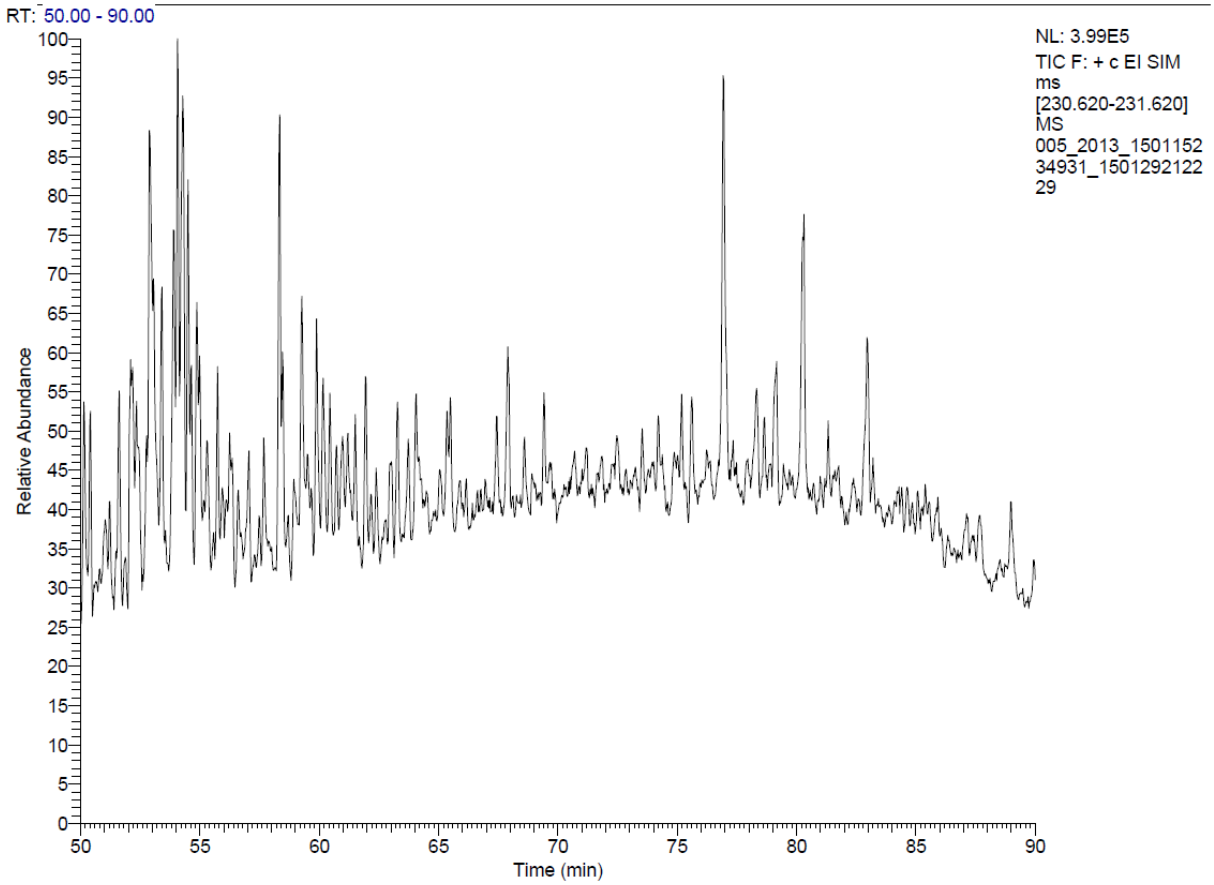
RT: 50.00 - 90.00
NL: 3.99E5
TIC F: + c EI SIM
ms
[230.620-231.620]
MS
005_2013_150115234931_150129212229
Relative Abundance
Time (min)

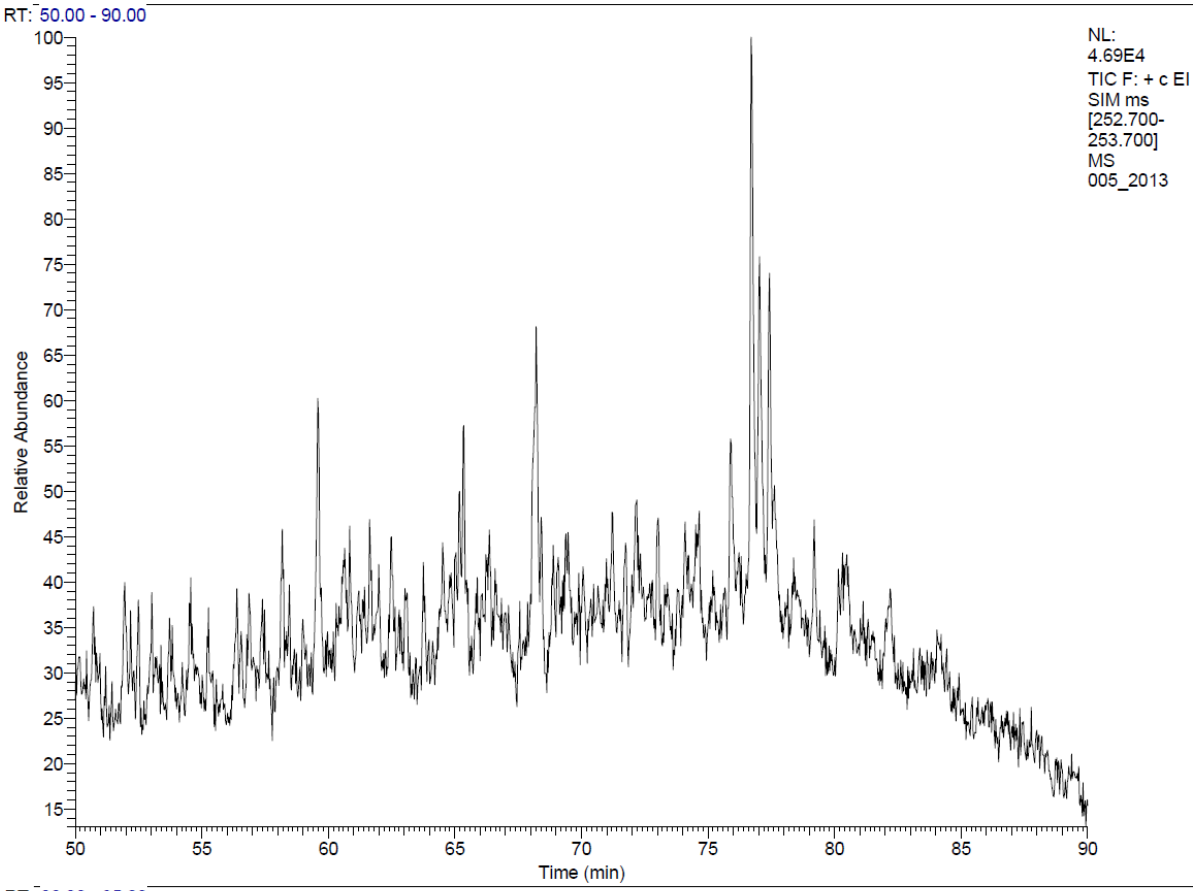
RT: 50.00 - 90.00
NL:
4.69E4
TIC F: + c EI
SIM ms
[252.700-
253.700]
MS
005_2013
Relative Abundance
Time (min)

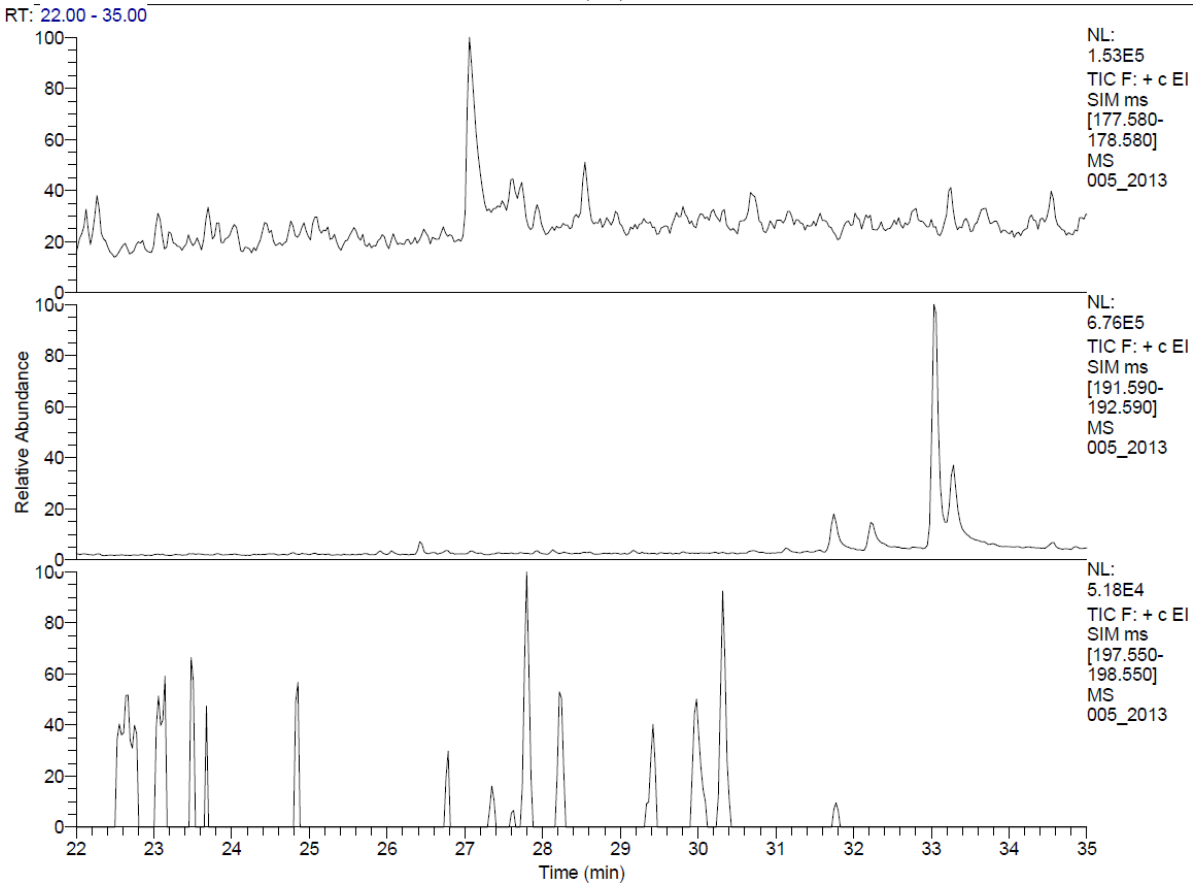
RT: 22.00 - 35.00
NL:
1.53E5
TIC F: + c EI
SIM ms
[177.580-
178.580]
MS
005_2013
NL:
6.76E5
TIC F: + c EI
SIM ms
[191.590-
192.590]
MS
005_2013
NL:
5.18E4
TIC F: + c EI
SIM ms
[197.550-
198.550]
MS
005_2013
Relative Abundance
Time (min)

O-6

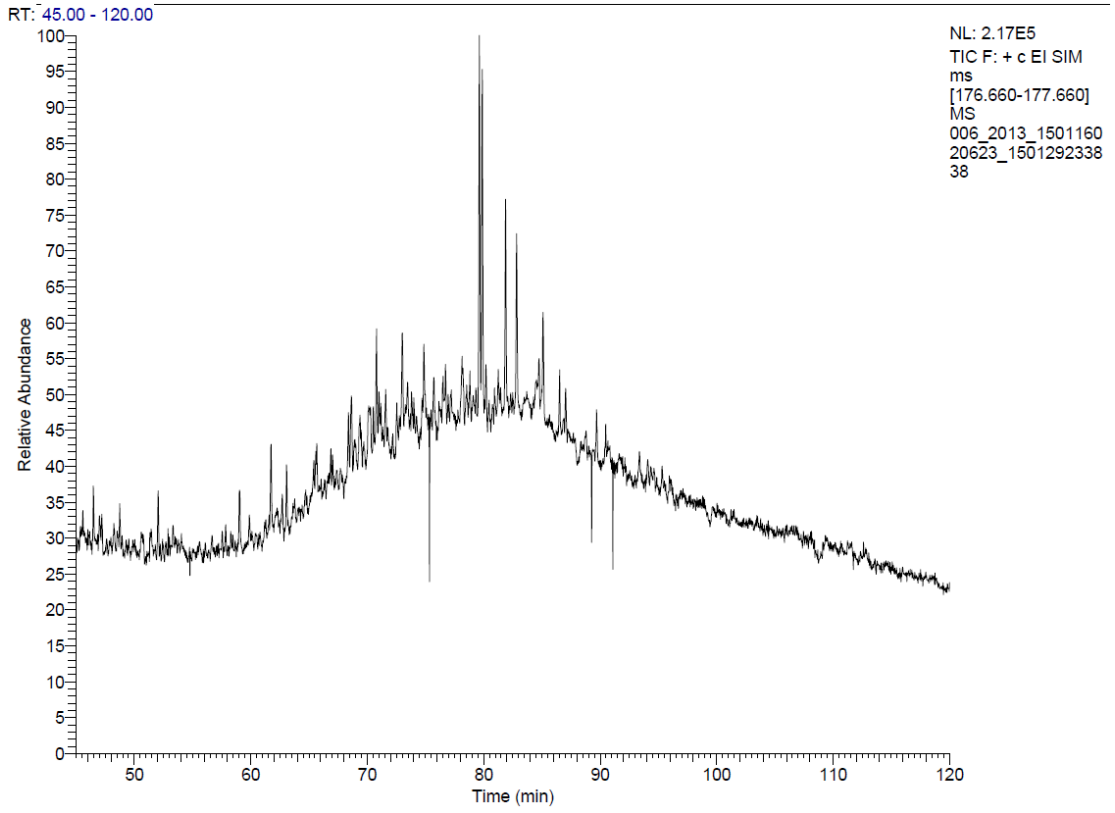
RT: 45.00 - 120.00
NL: 2.17E5
TIC F: + c EI SIM ms [176.660-177.660] MS 006_2013_150116020623_150129233838
Relative Abundance
Time (min)

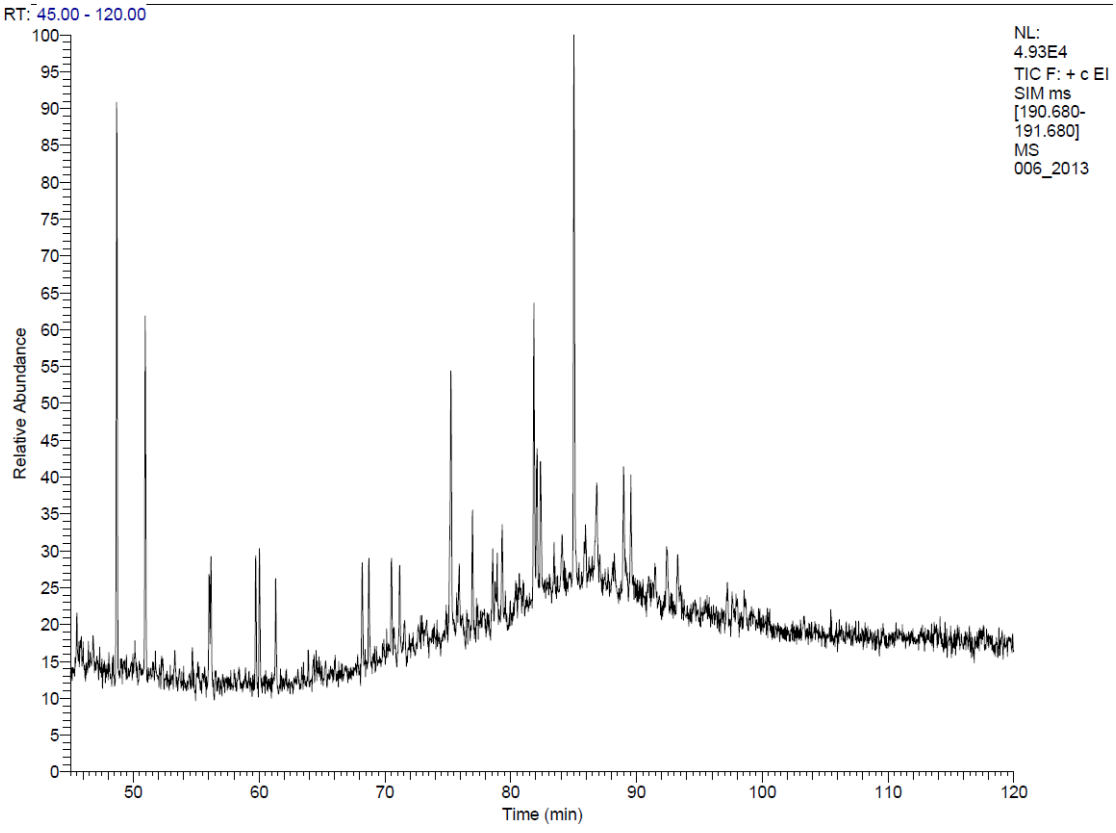
RT: 45.00 - 120.00
NL: 4.93E4
TIC F: + c EI SIM ms [190.680-191.680] MS 006_2013
Relative Abundance
Time (min)

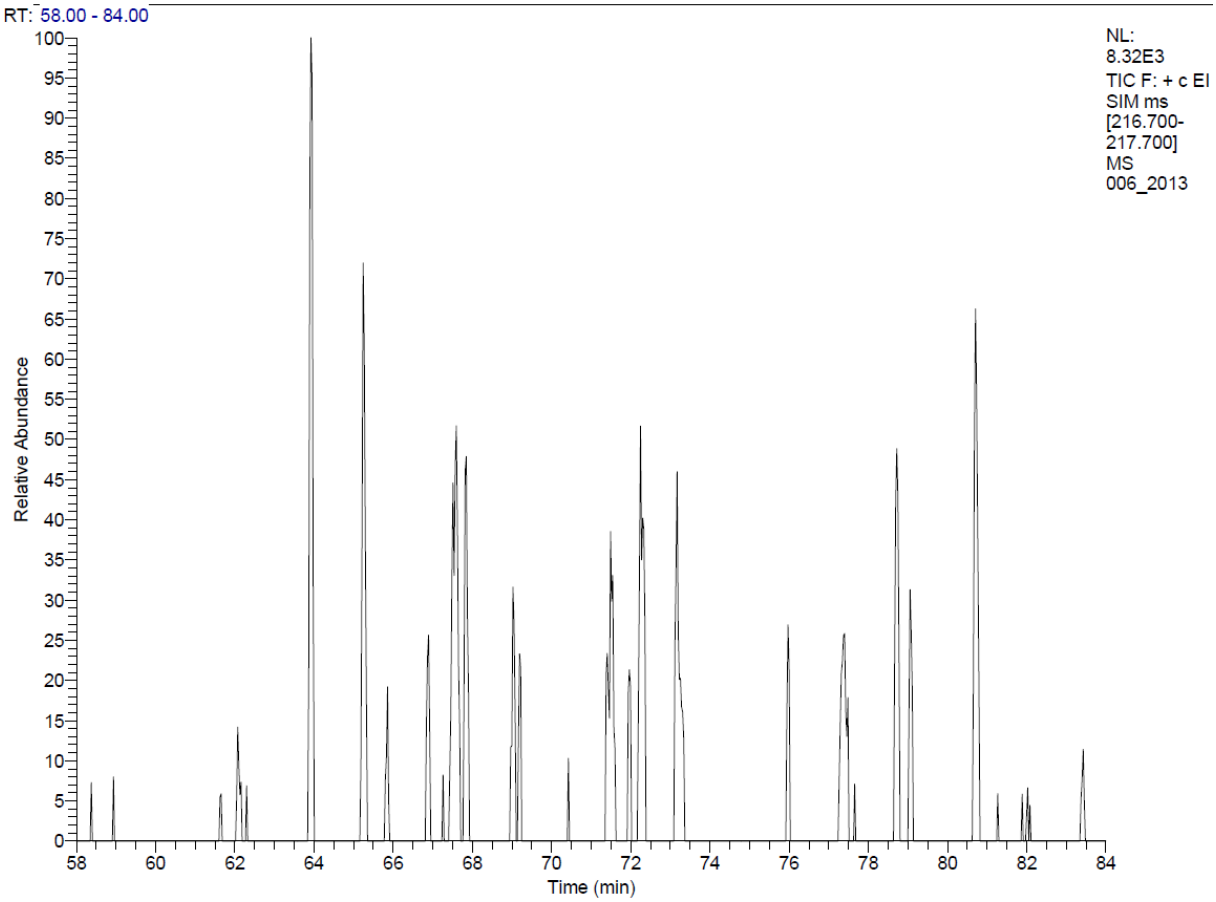
RT: 58.00 - 84.00
NL:
8.32E3
TIC F: + c EI
SIM ms
[216.700-
217.700]
MS
006_2013
Relative Abundance
Time (min)

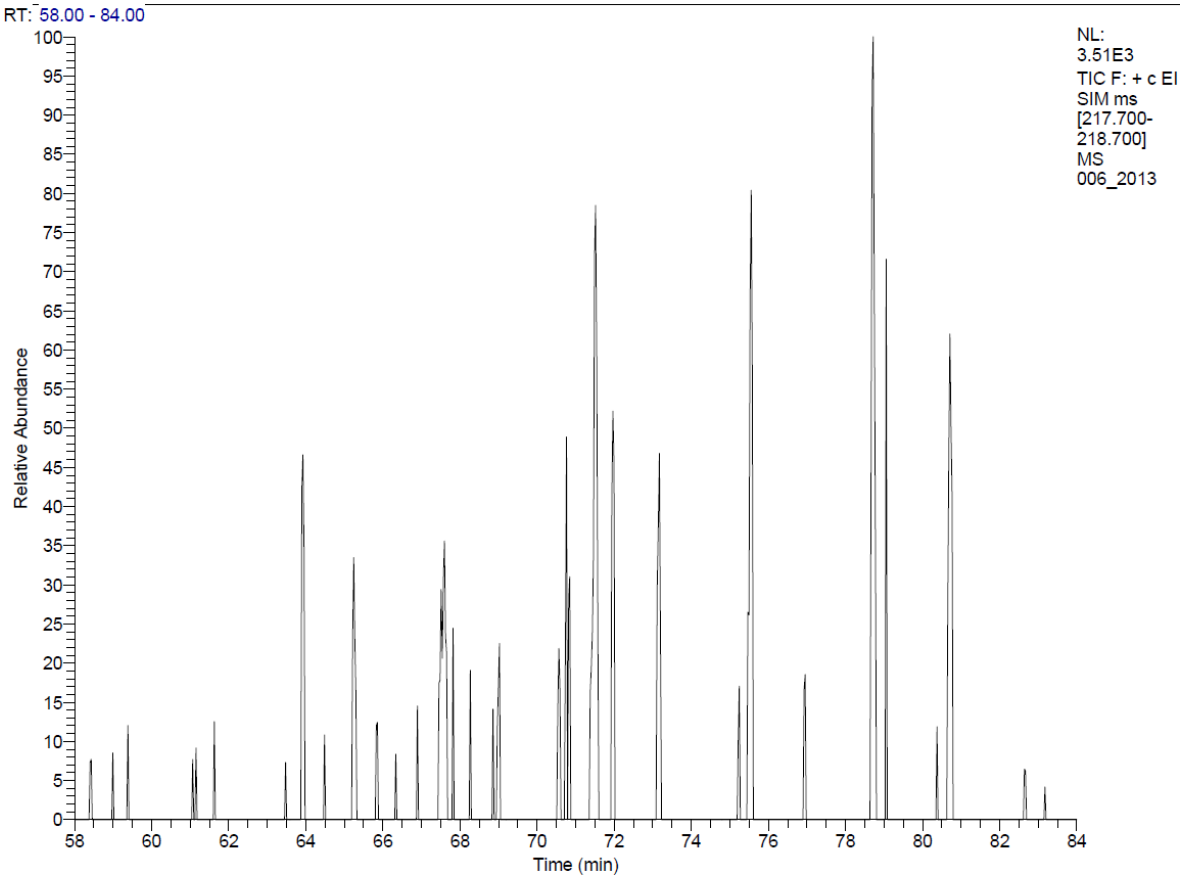
RT: 58.00 - 84.00
NL:
3.51E3
TIC F: + c EI
SIM ms
[217.700-
218.700]
MS
006_2013
Relative Abundance
Time (min)

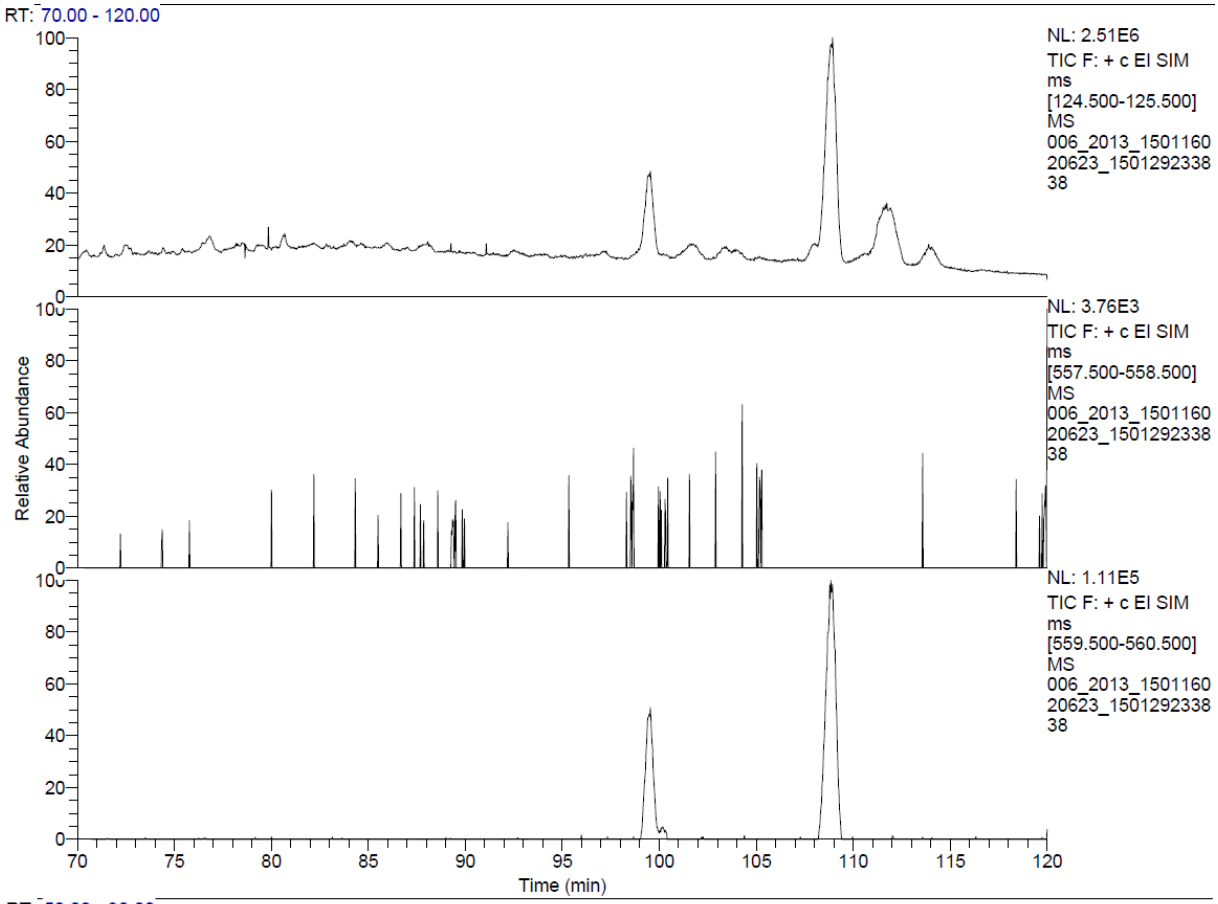
RT: 70.00 - 120.00
NL: 2.51E6
TIC F: + c EI SIM ms [124.500-125.500] MS 006_2013_150116020623_150129233838
NL: 3.76E3
TIC F: + c EI SIM ms [557.500-558.500] MS 006_2013_150116020623_150129233838
NL: 1.11E5
TIC F: + c EI SIM ms [559.500-560.500] MS 006_2013_150116020623_150129233838
Relative Abundance
Time (min)

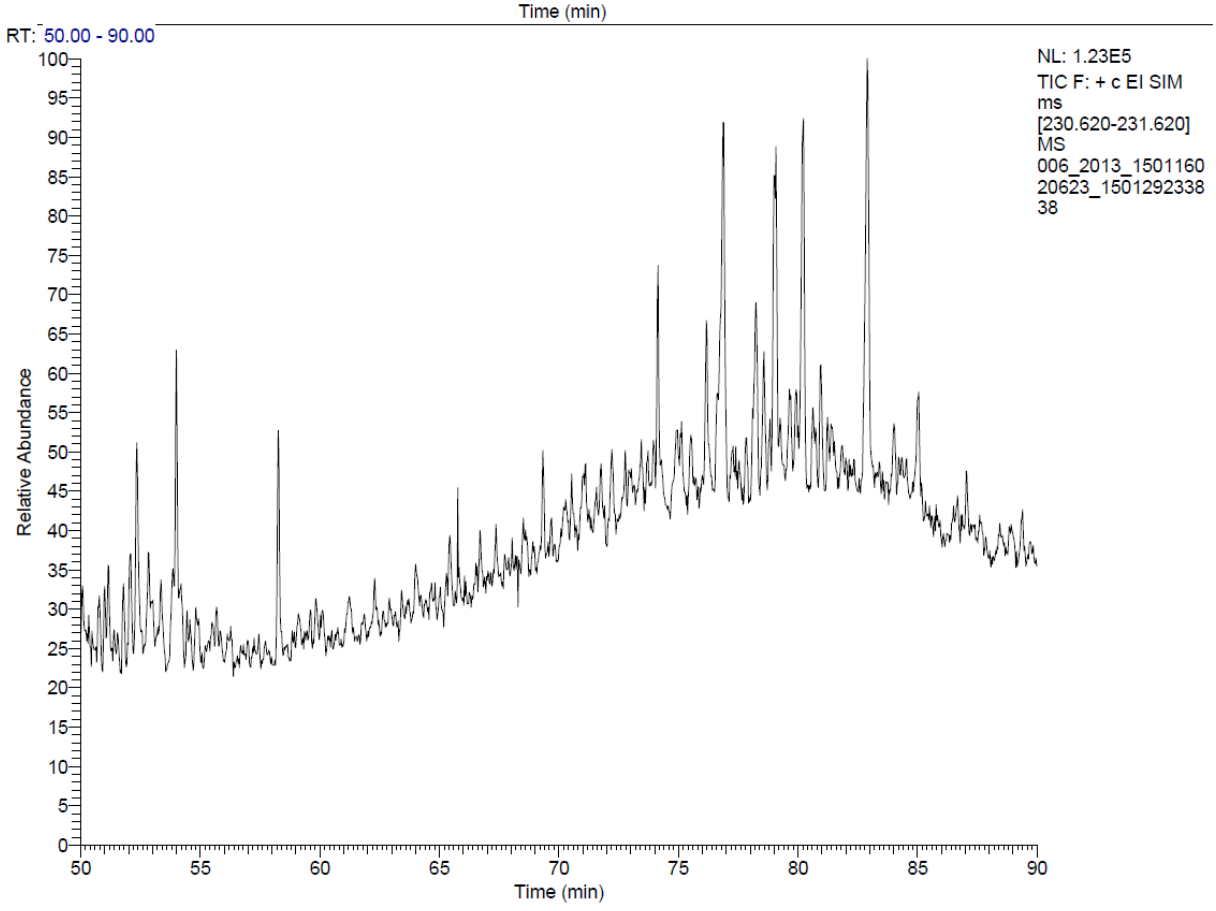
RT: 50.00 - 90.00
NL: 1.23E5
TIC F: + c EI SIM ms [230.620-231.620] MS 006_2013_150116020623_150129233838
Relative Abundance
Time (min)

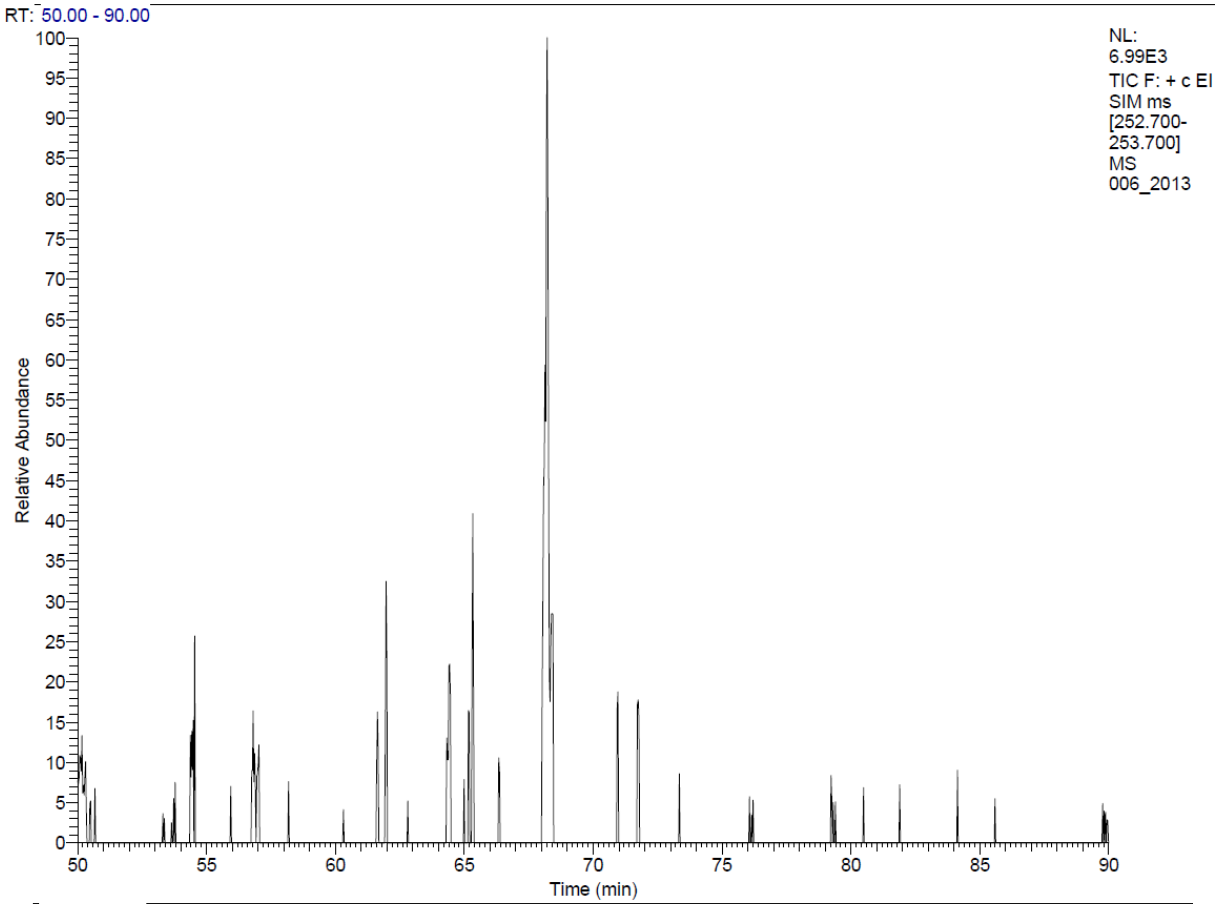
RT: 50.00 - 90.00
NL:
6.99E3
TIC F: + c EI
SIM ms
[252.700-
253.700]
MS
006_2013
Relative Abundance
Time (min)

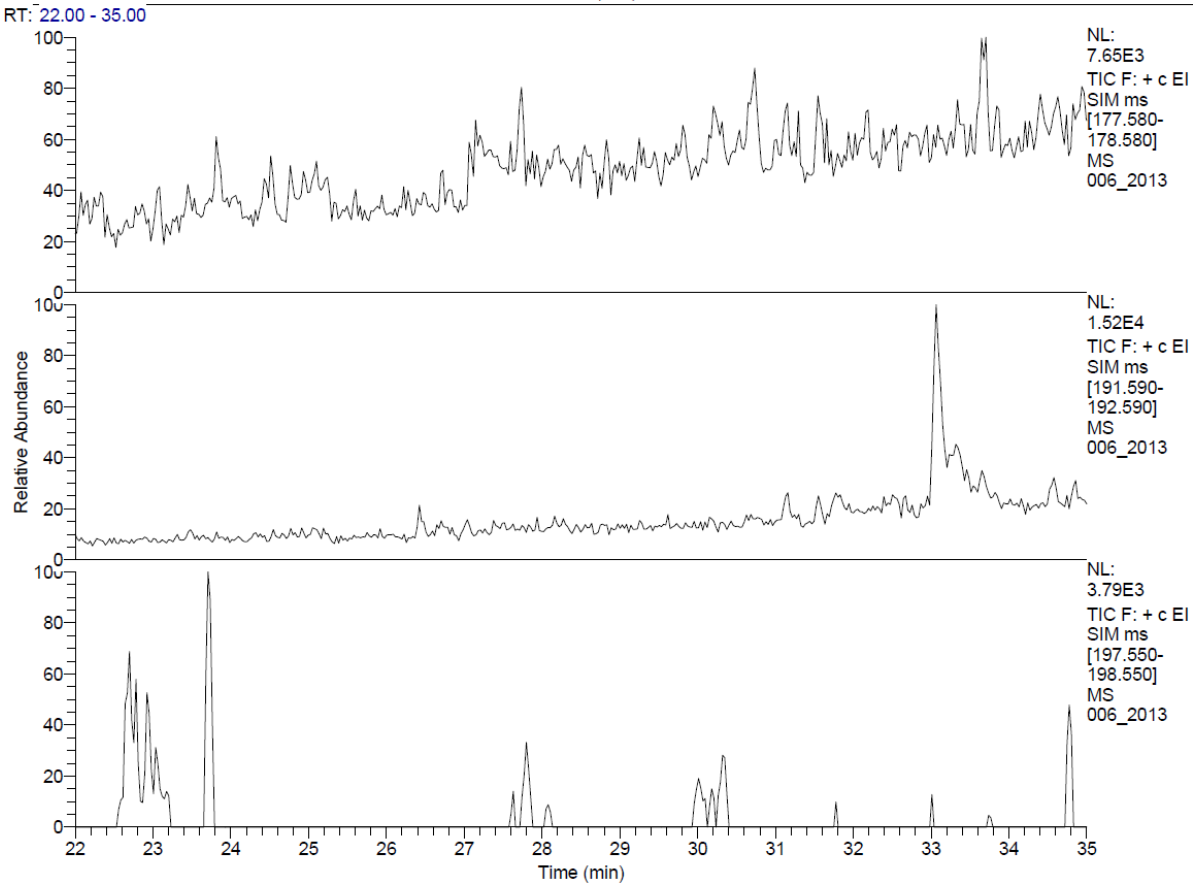
RT: 22.00 - 35.00
NL:
7.65E3
TIC F: + c EI
SIM ms
[177.580-
178.580]
MS
006_2013
NL:
1.52E4
TIC F: + c EI
SIM ms
[191.590-
192.590]
MS
006_2013
NL:
3.79E3
TIC F: + c EI
SIM ms
[197.550-
198.550]
MS
006_2013
Relative Abundance
Time (min)

O-7

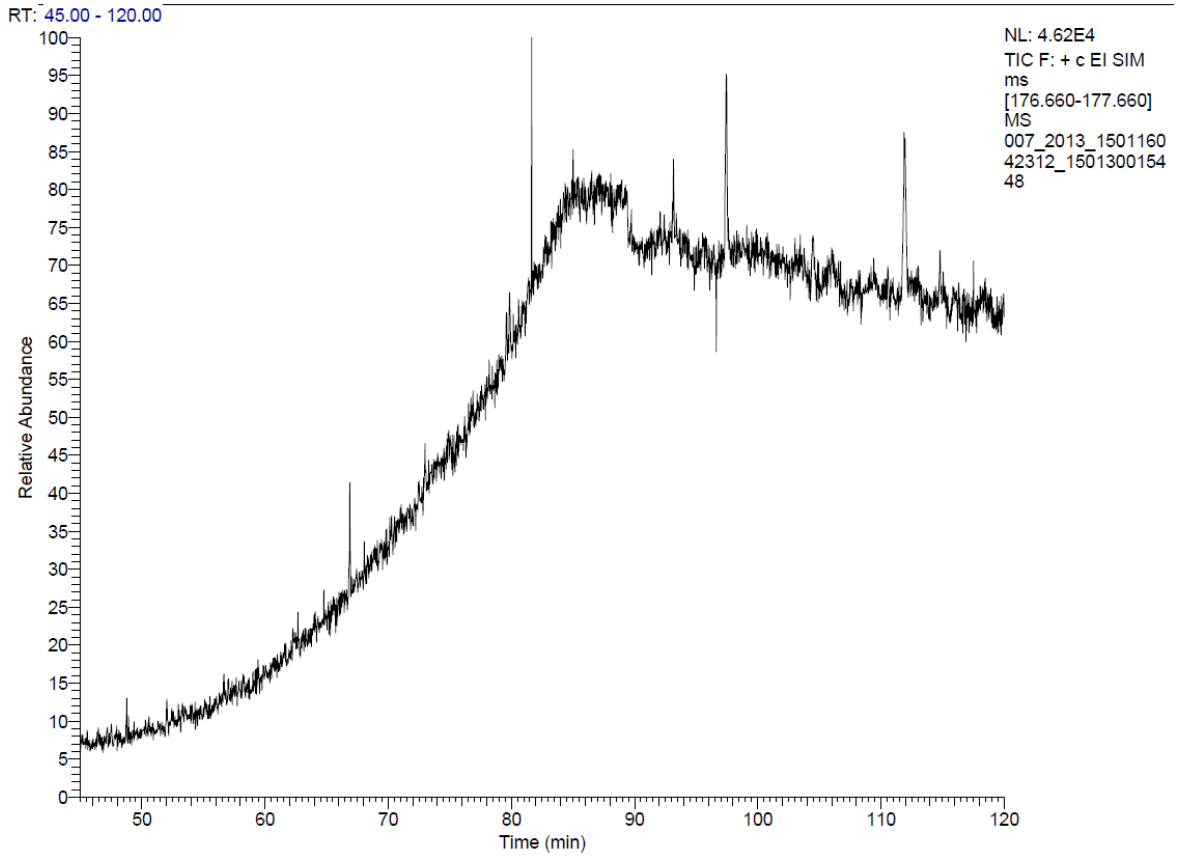
RT: 45.00 - 120.00
NL: 4.62E4
TIC F: + c EI SIM ms [176.660-177.660] MS 007_2013_150116042312_150130015448
Relative Abundance
Time (min)

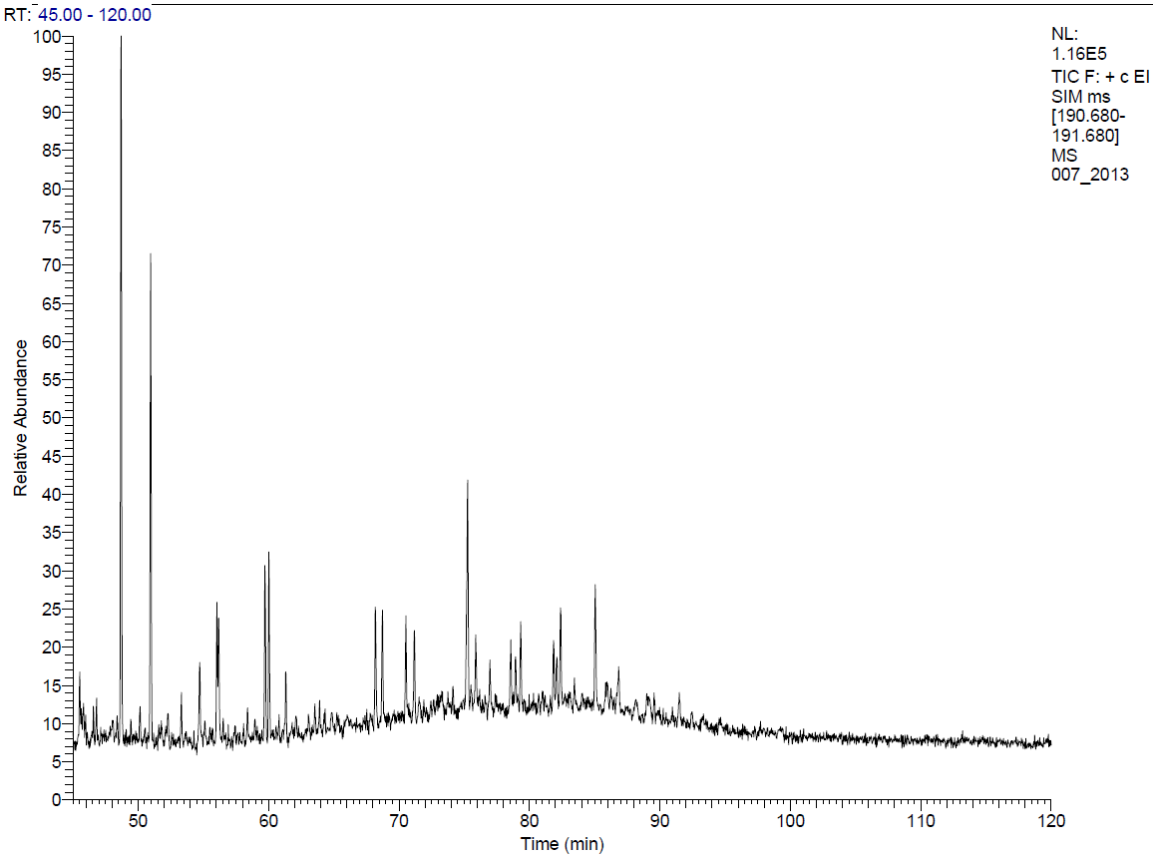
RT: 45.00 - 120.00
NL: 1.16E5
TIC F: + c EI SIM ms [190.680-191.680] MS 007_2013
Relative Abundance
Time (min)

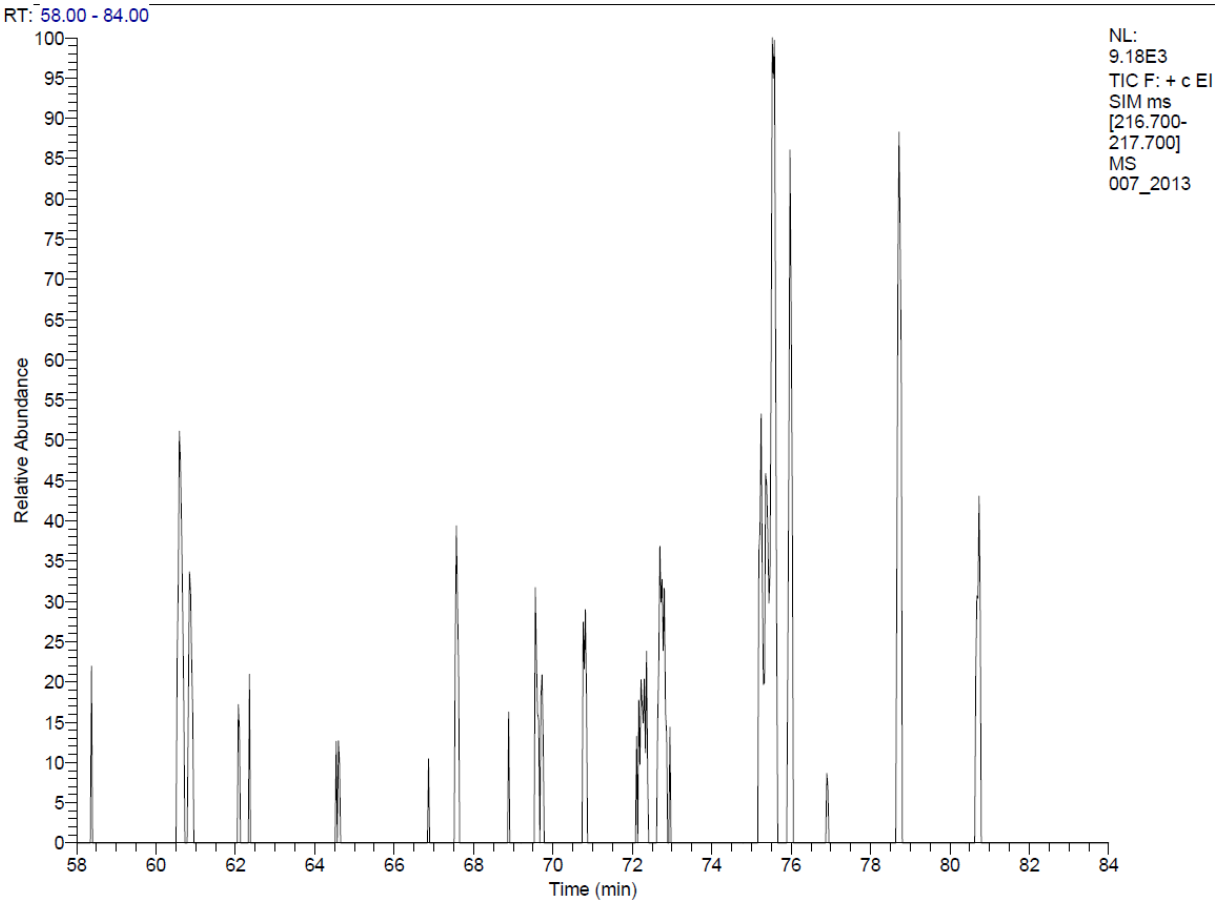
RT: 58.00 - 84.00
NL:
9.18E3
TIC F: + c EI
SIM ms
[216.700-
217.700]
MS
007_2013
Relative Abundance
Time (min)

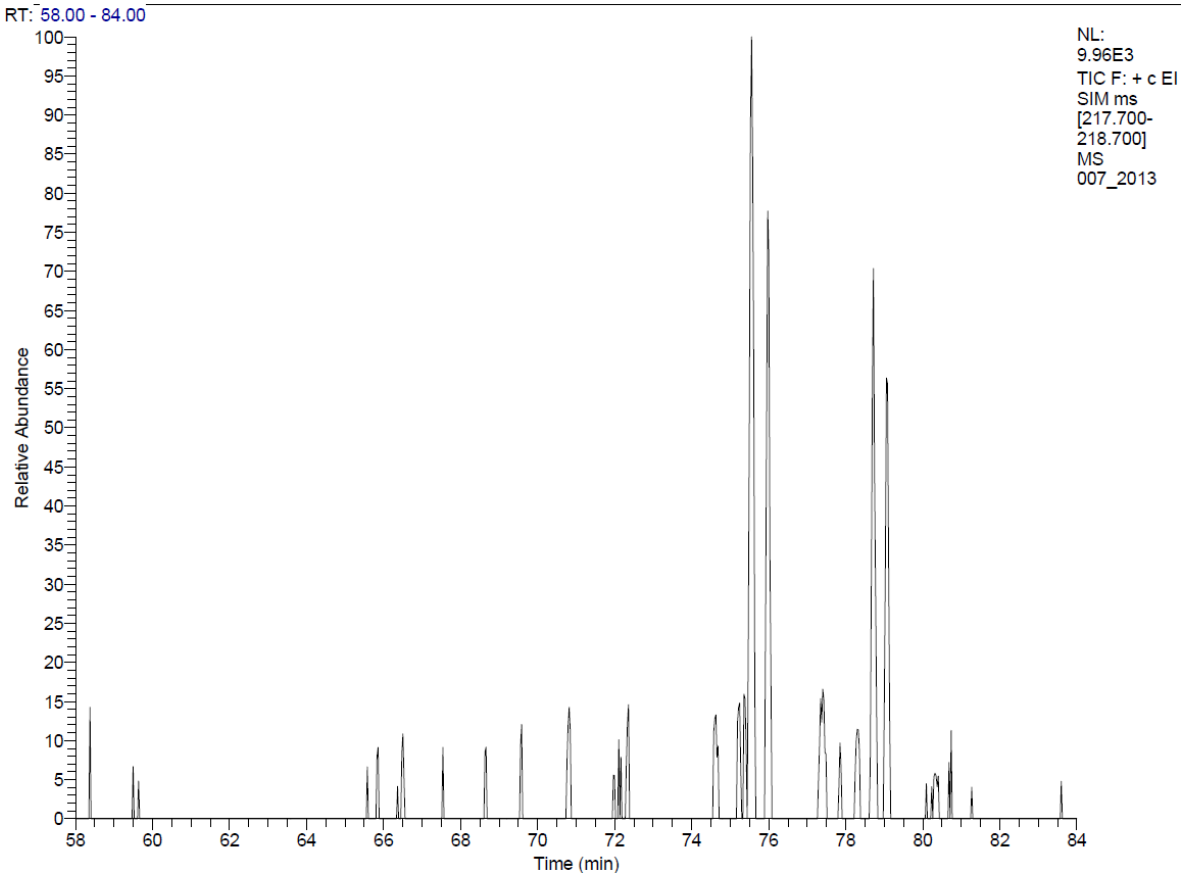
RT: 58.00 - 84.00
NL:
9.96E3
TIC F: + c EI
SIM ms
[217.700-
218.700]
MS
007_2013
Relative Abundance
Time (min)

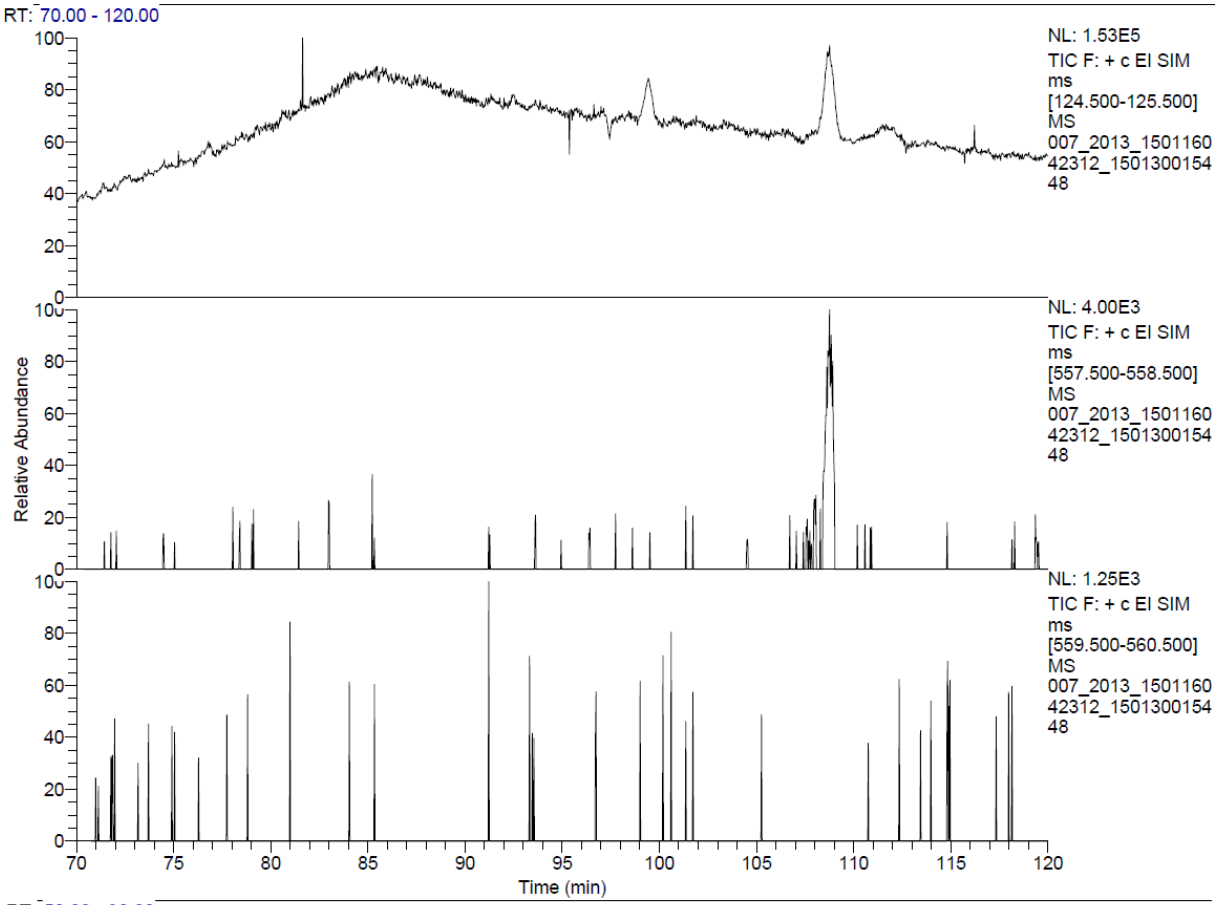
RT: 70.00 - 120.00
NL: 1.53E5
TIC F: + c EI SIM ms [124.500-125.500] MS 007_2013_150116042312_150130015448
NL: 4.00E3
TIC F: + c EI SIM ms [557.500-558.500] MS 007_2013_150116042312_150130015448
NL: 1.25E3
TIC F: + c EI SIM ms [559.500-560.500] MS 007_2013_150116042312_150130015448
Relative Abundance
Time (min)

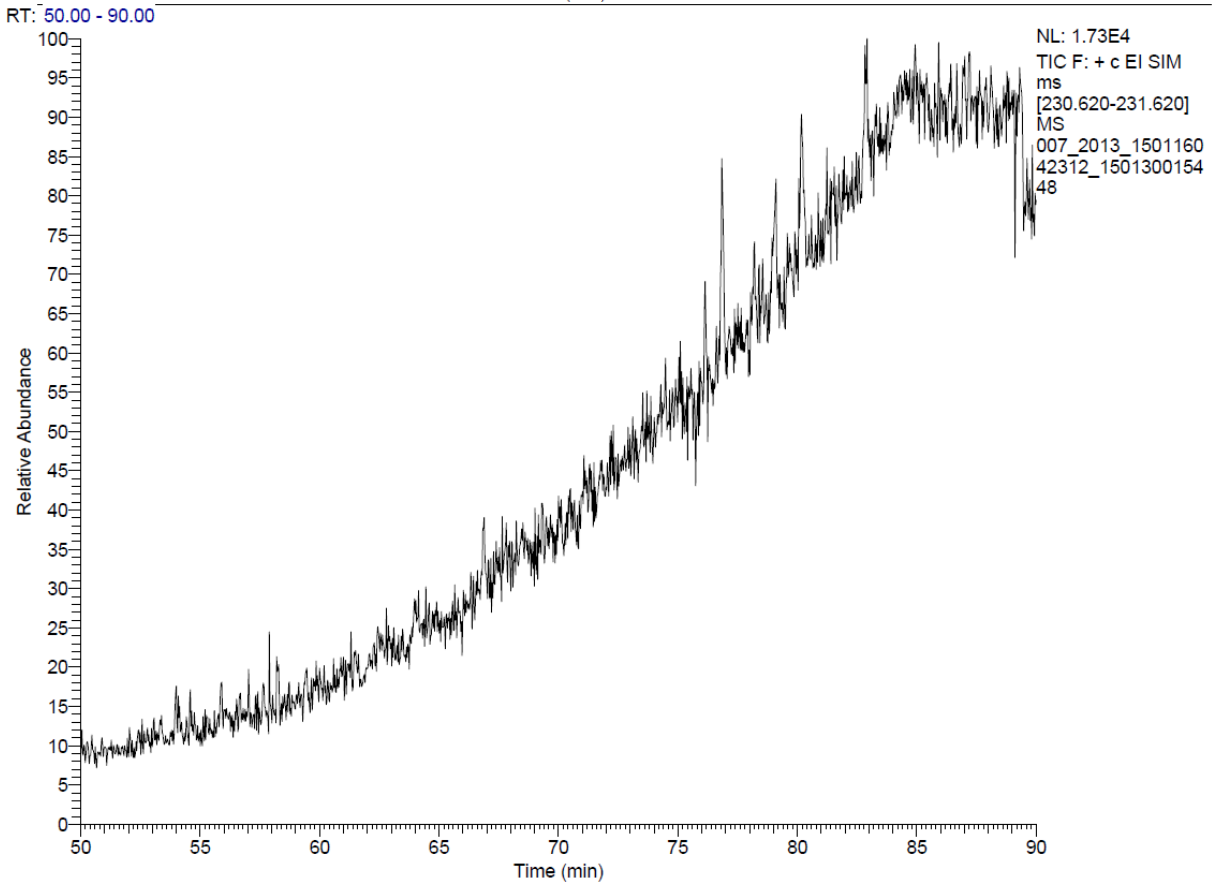
RT: 50.00 - 90.00
NL: 1.73E4
TIC F: + c EI SIM ms [230.620-231.620] MS 007_2013_150116042312_150130015448
Relative Abundance
Time (min)

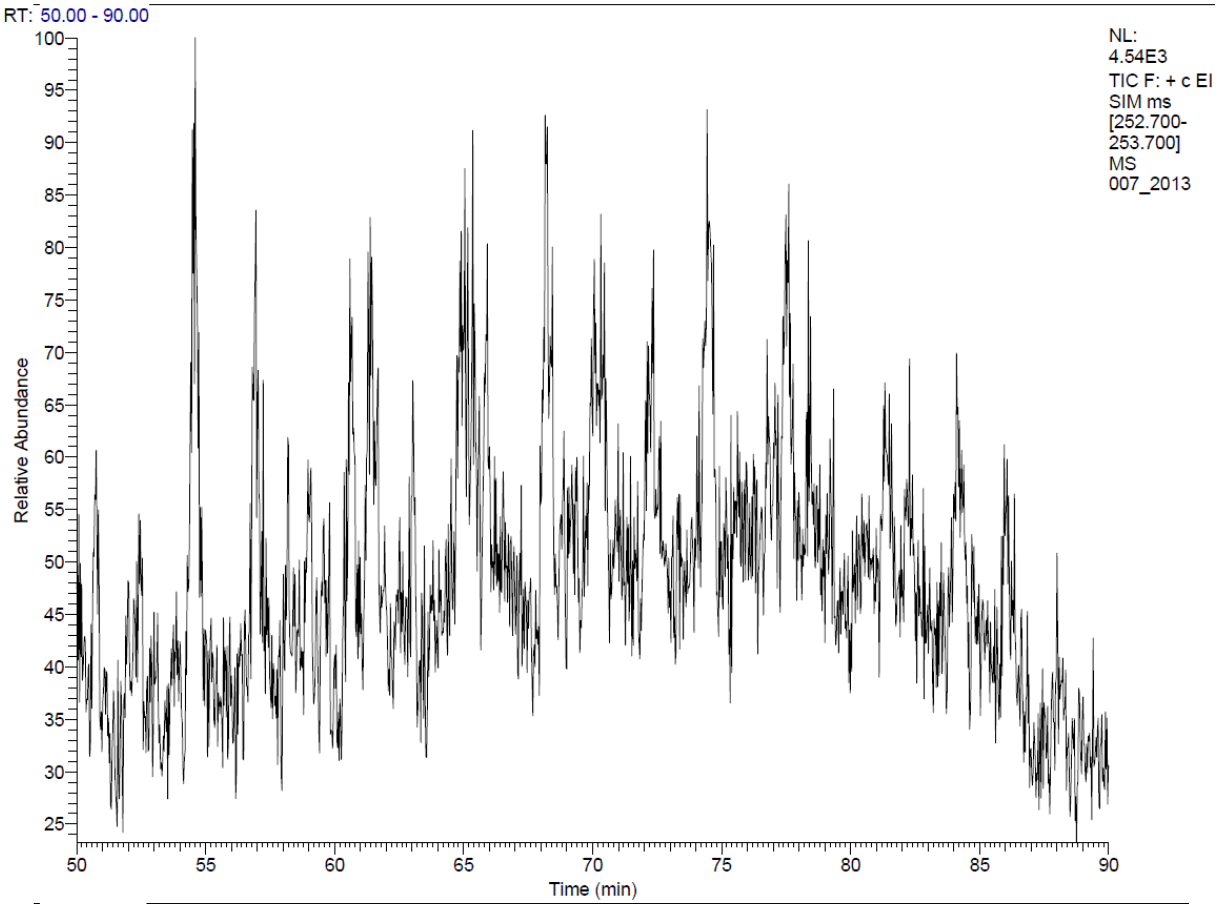
RT: 50.00 - 90.00
NL:
4.54E3
TIC F: + c EI
SIM ms
[252.700-
253.700]
MS
007_2013
Relative Abundance
Time (min)

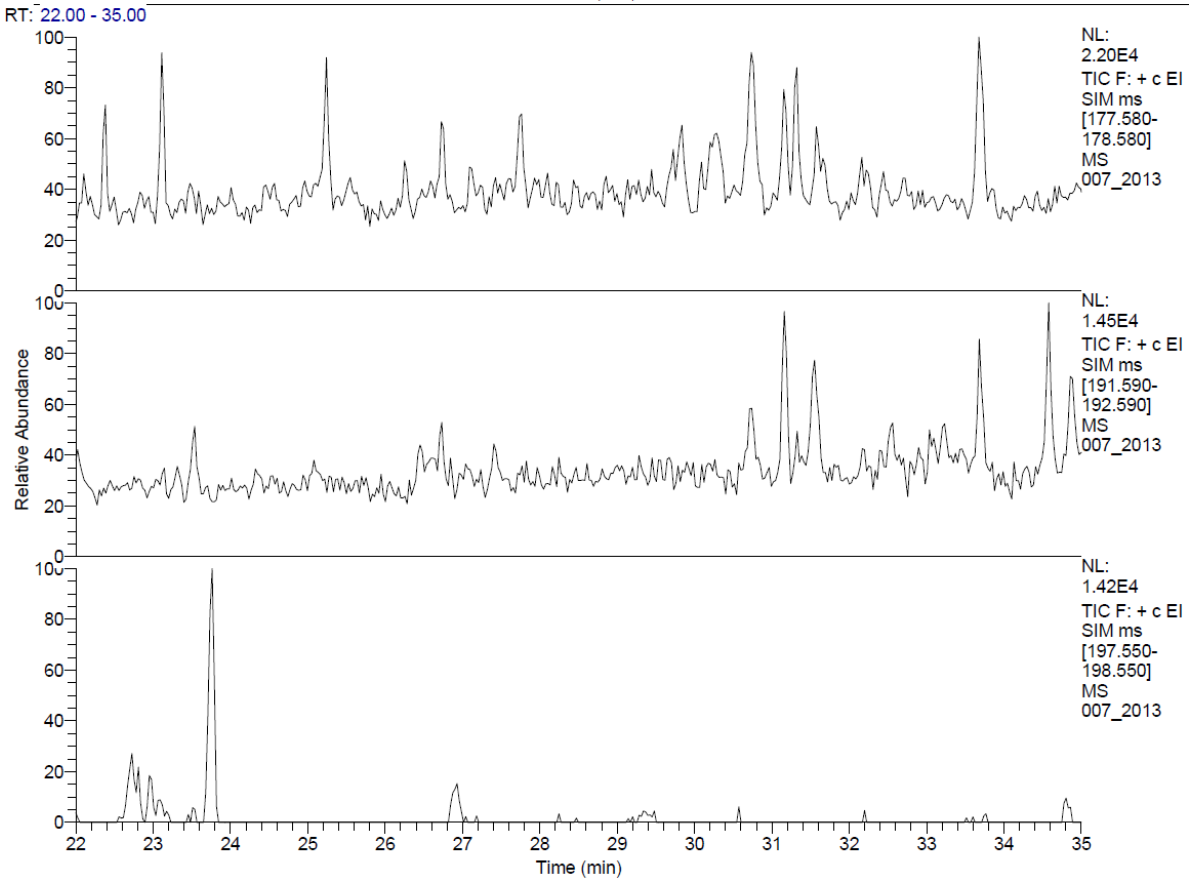
RT: 22.00 - 35.00
NL:
2.20E4
TIC F: + c EI
SIM ms
[177.580-
178.580]
MS
007_2013
NL:
1.45E4
TIC F: + c EI
SIM ms
[191.590-
192.590]
MS
007_2013
NL:
1.42E4
TIC F: + c EI
SIM ms
[197.550-
198.550]
MS
007_2013
Relative Abundance
Time (min)

O-20

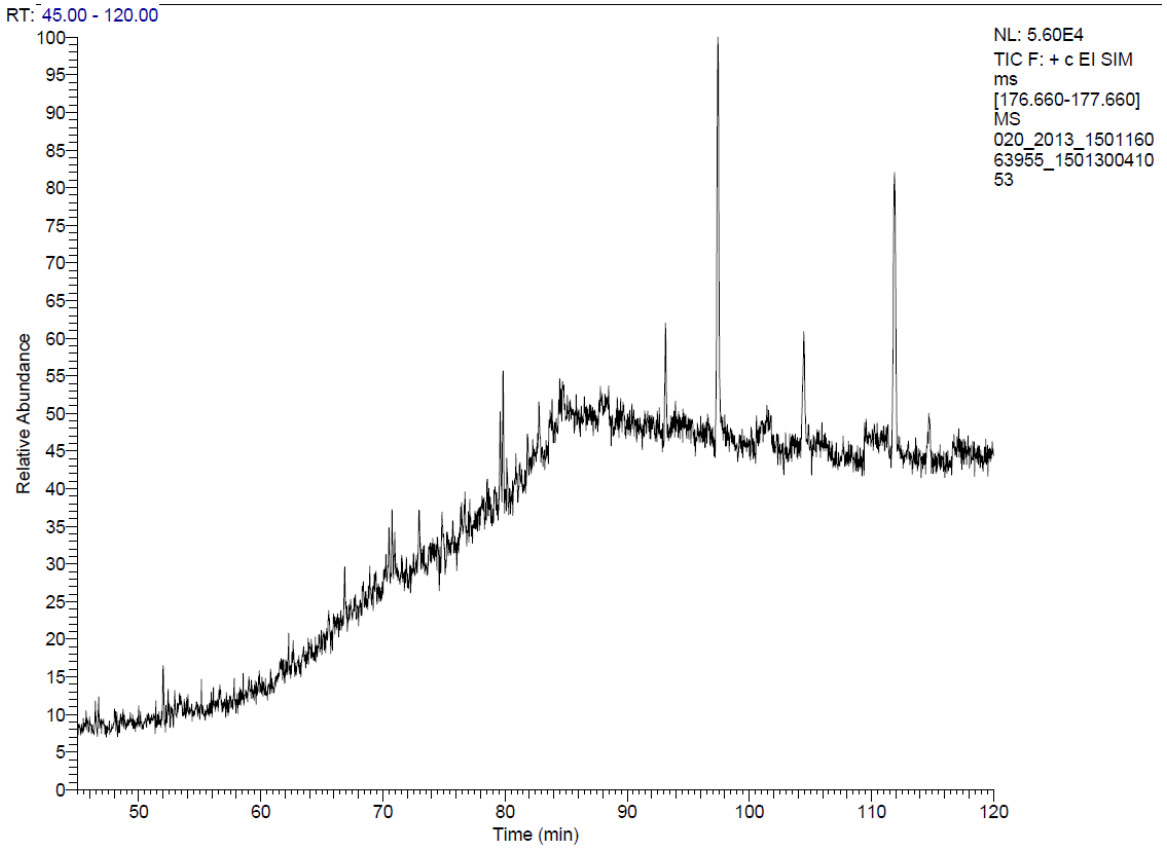
RT: 45.00 - 120.00
NL: 5.60E4
TIC F: + c EI SIM ms [176.660-177.660] MS 020_2013_150116063955_150130041053
Relative Abundance
Time (min)

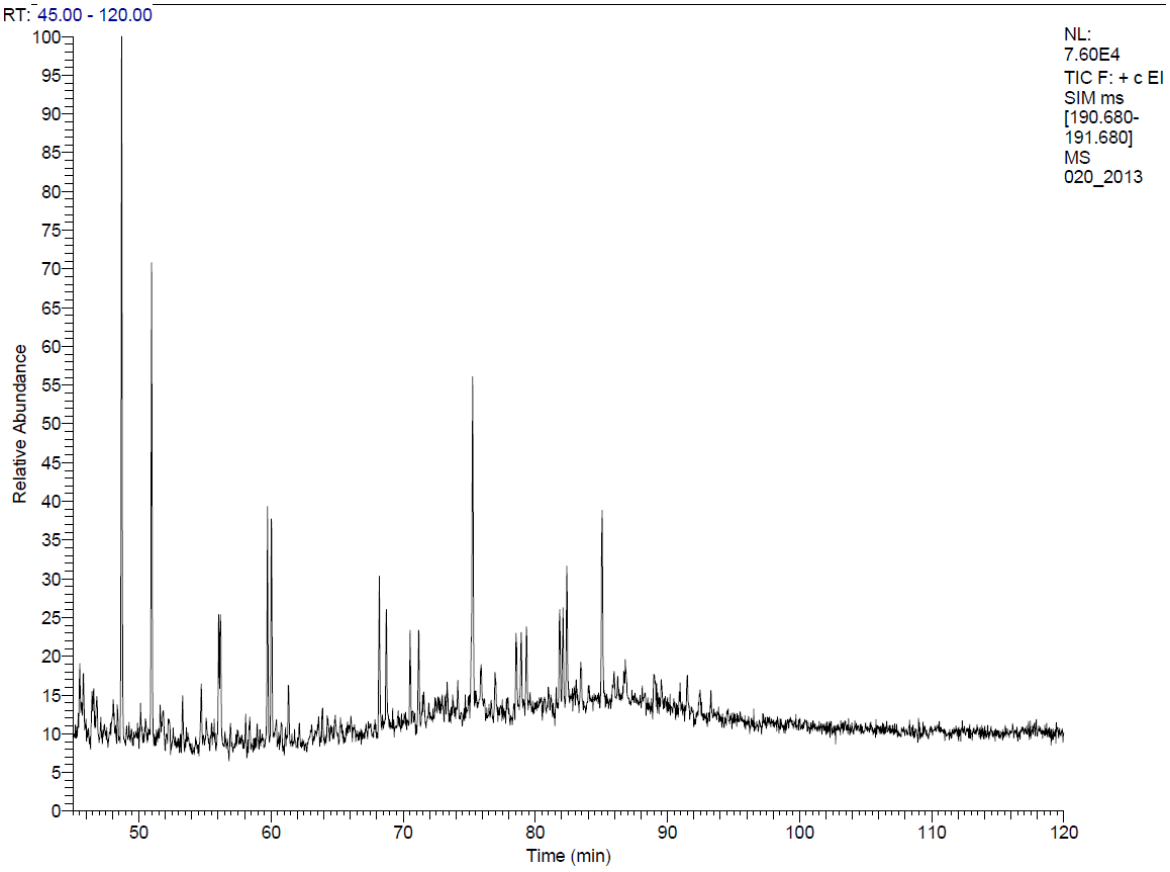
RT: 45.00 - 120.00
NL: 7.60E4
TIC F: + c EI SIM ms [190.680-191.680] MS 020_2013
Relative Abundance
Time (min)

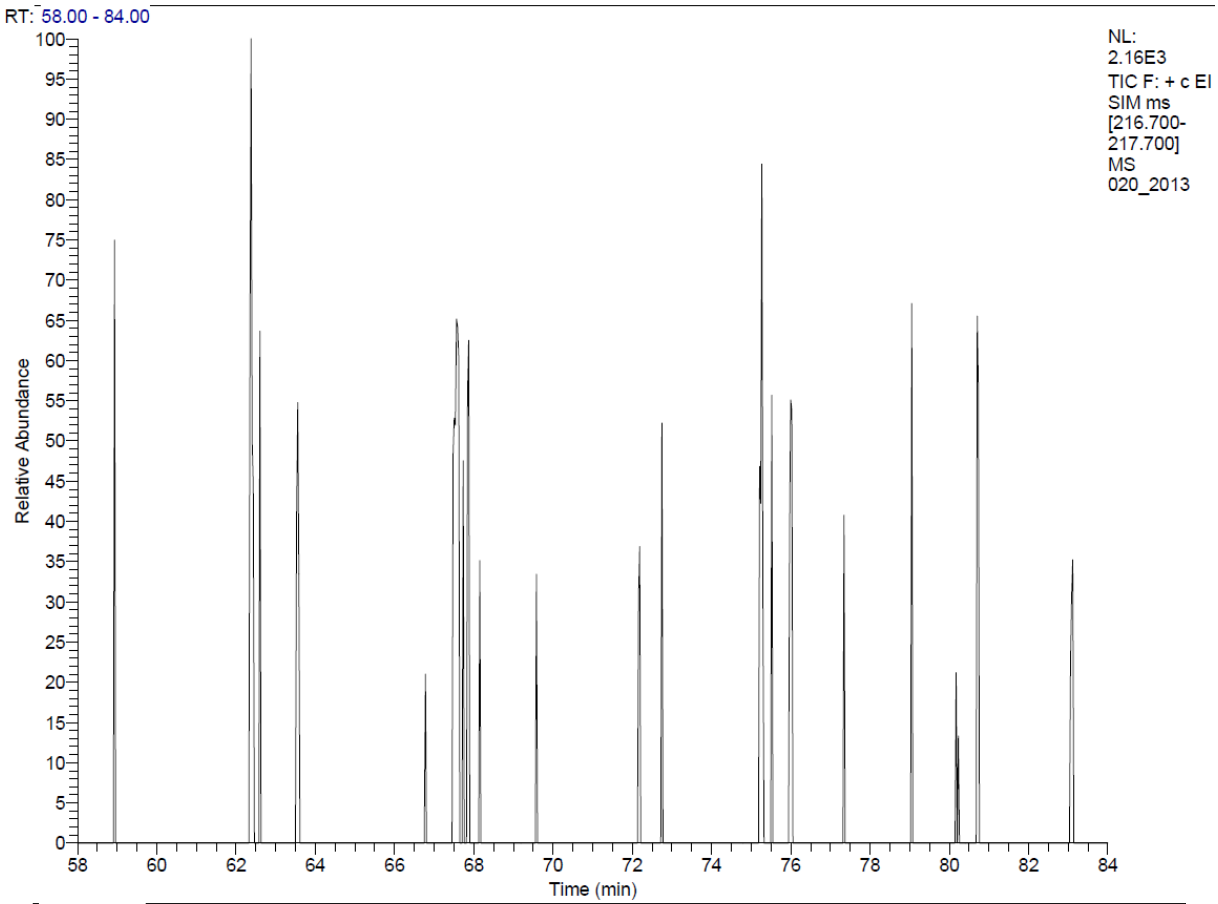
RT: 58.00 - 84.00
NL:
2.16E3
TIC F: + c EI
SIM ms
[216.700-
217.700]
MS
020_2013
Relative Abundance
Time (min)

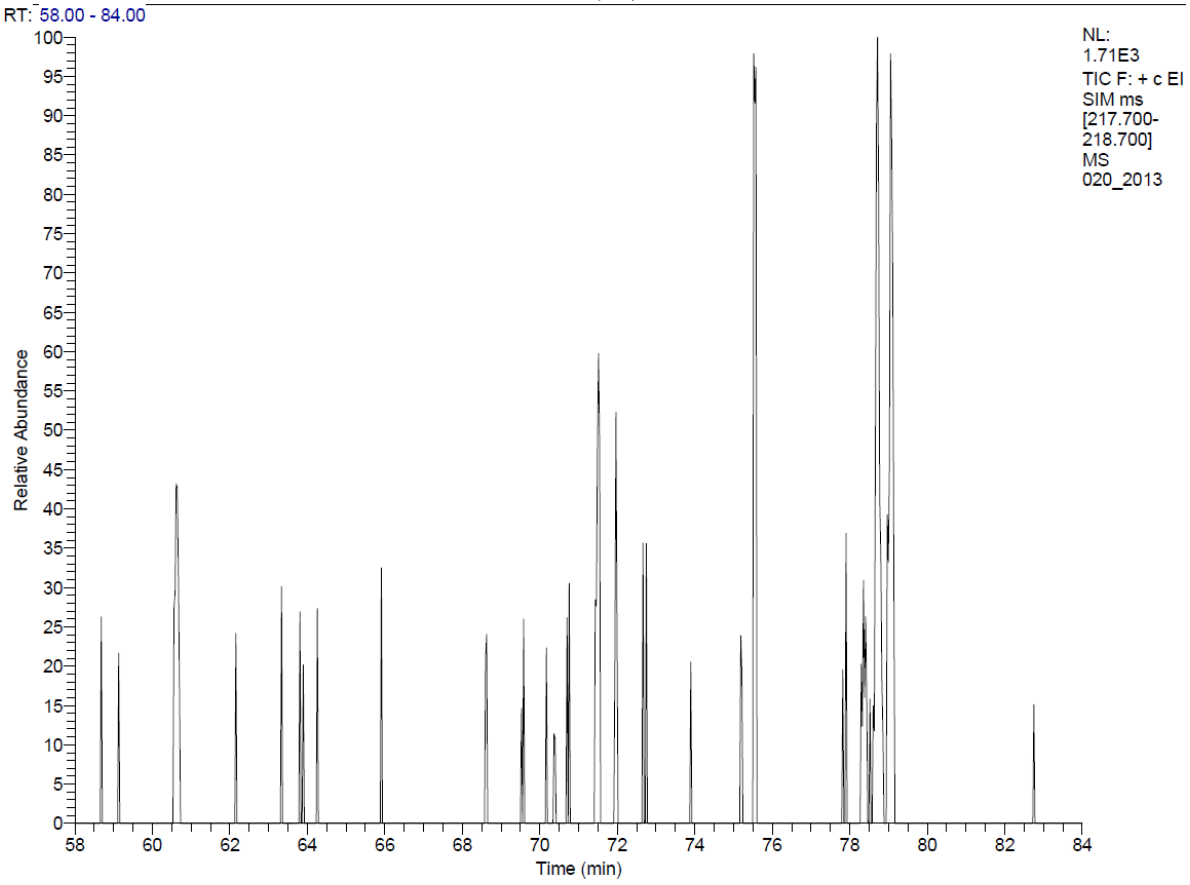
RT: 58.00 - 84.00
NL:
1.71E3
TIC F: + c EI
SIM ms
[217.700-
218.700]
MS
020_2013
Relative Abundance
Time (min)

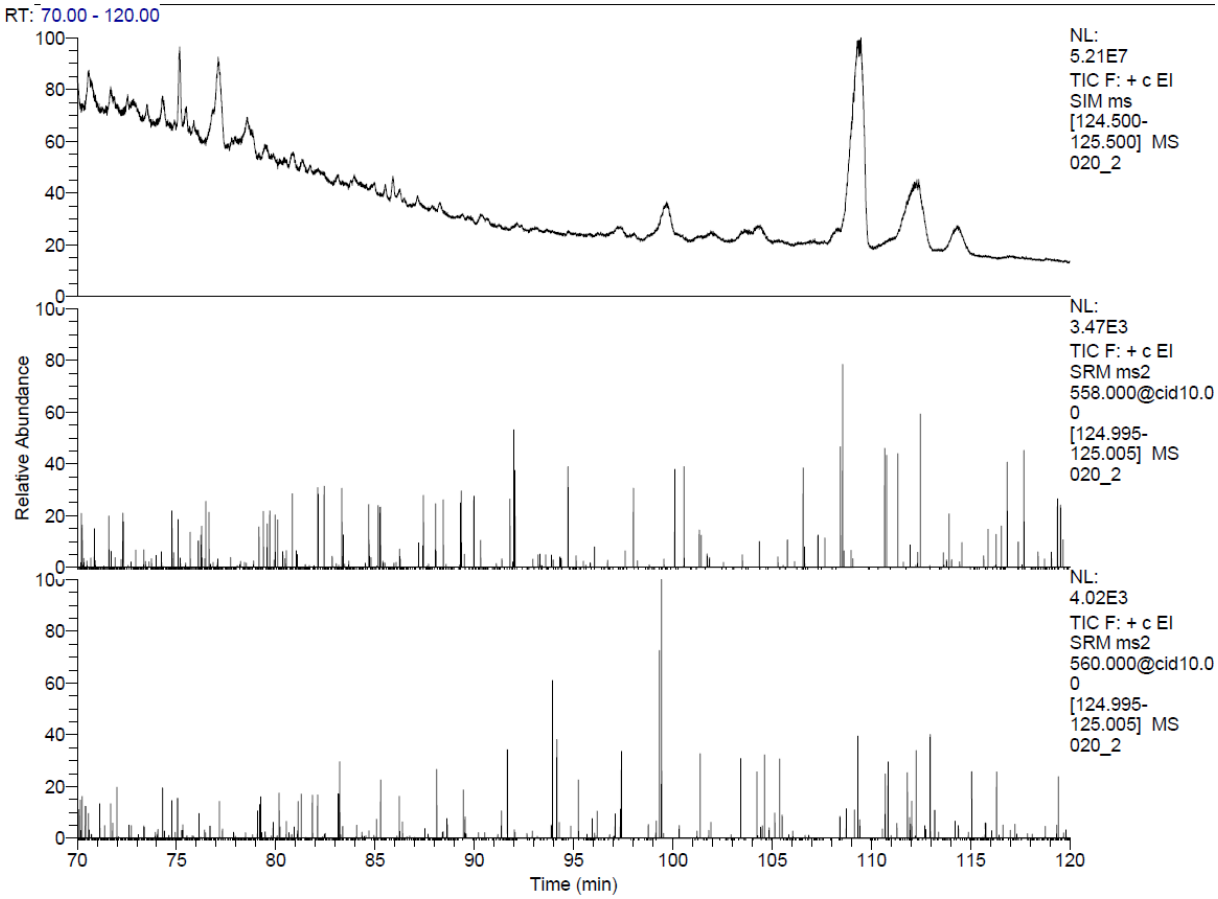
RT: 70.00 - 120.00
NL:
5.21E7
TIC F: + c EI
SIM ms
[124.500-
125.500] MS
020_2
NL:
3.47E3
TIC F: + c EI
SRM ms2
558.000@cid10.0
0
[124.995-
125.005] MS
020_2
NL:
4.02E3
TIC F: + c EI
SRM ms2
560.000@cid10.0
0
[124.995-
125.005] MS
020_2
Relative Abundance
Time (min)

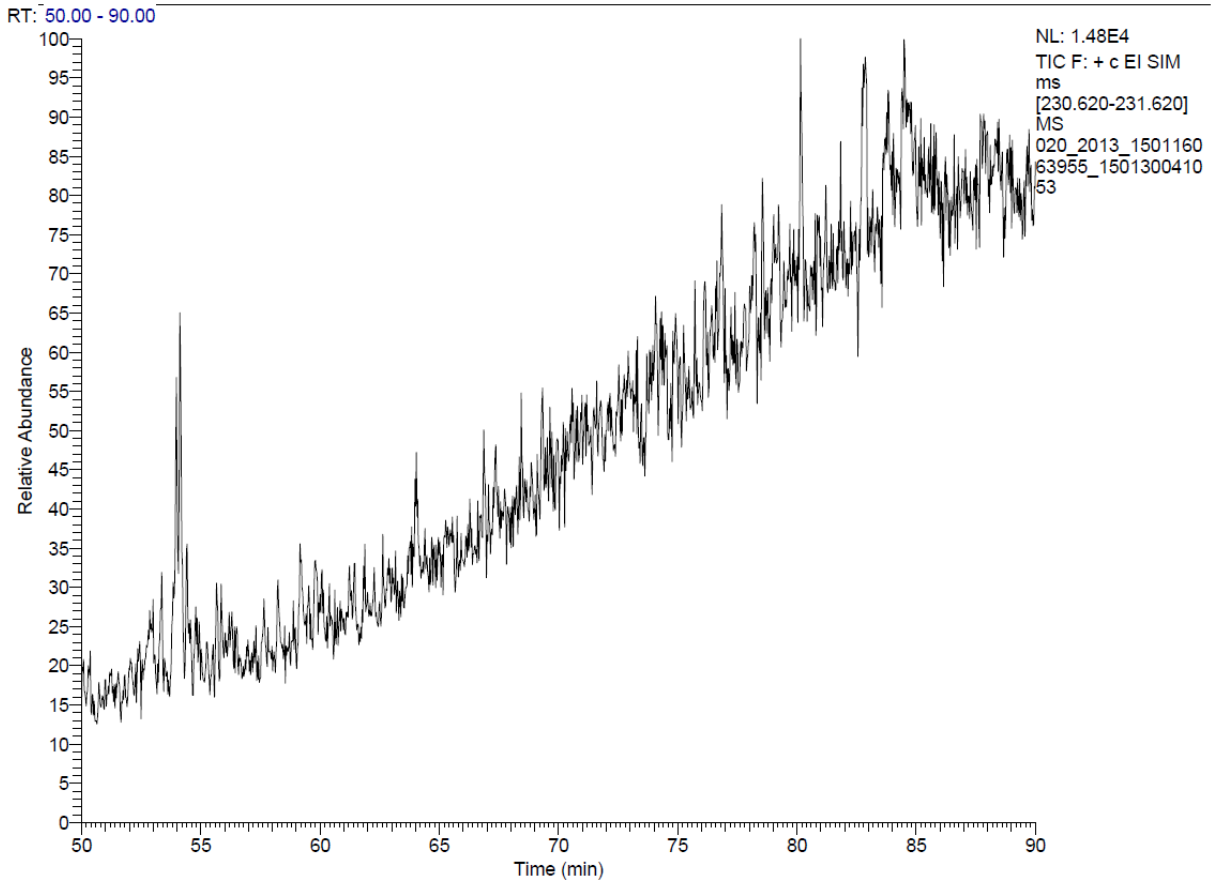
RT: 50.00 - 90.00
NL: 1.48E4
TIC F: + c EI SIM
ms
[230.620-231.620]
MS
020_2013_1501160
63955_1501300410
53
Relative Abundance
Time (min)

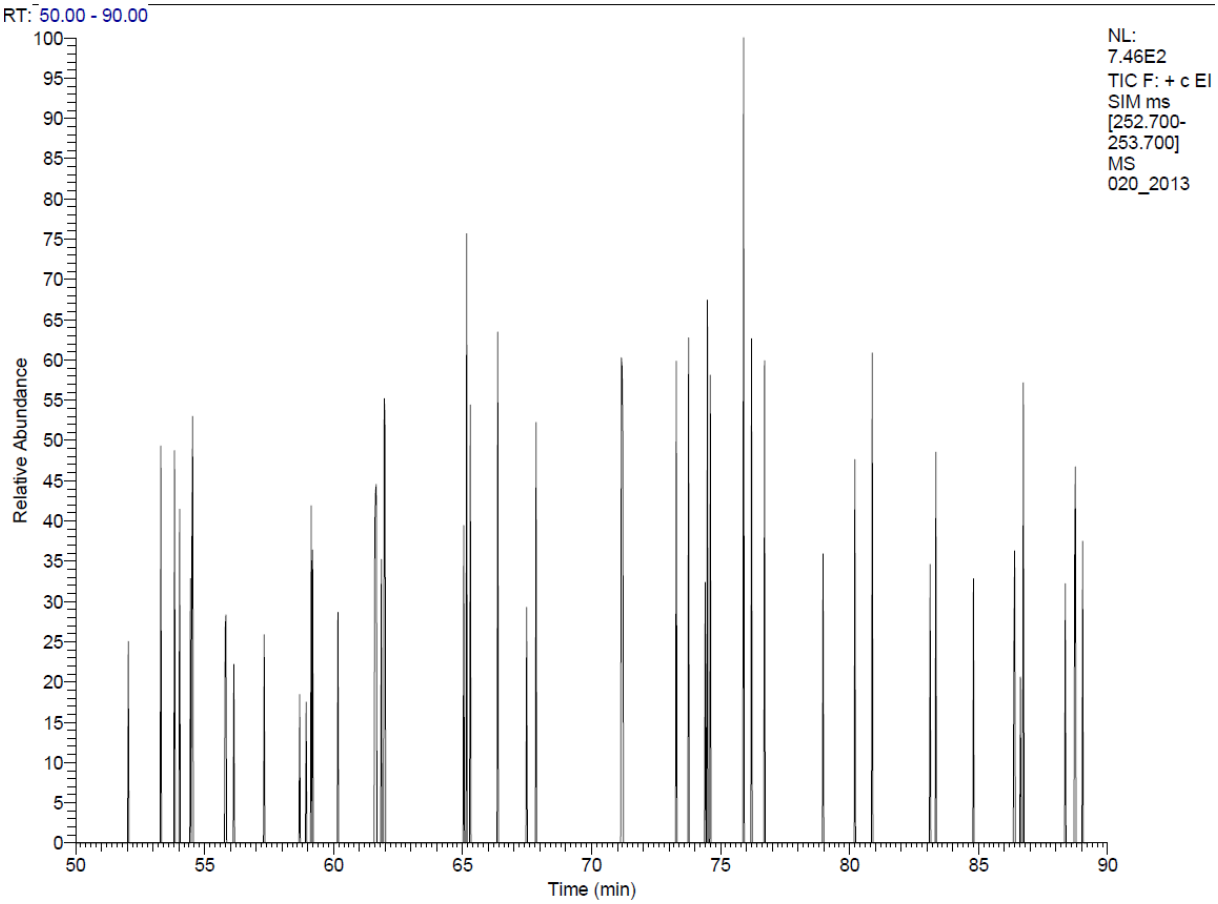
RT: 50.00 - 90.00
NL:
7.46E2
TIC F: + c EI
SIM ms
[252.700-
253.700]
MS
020_2013
Relative Abundance
Time (min)

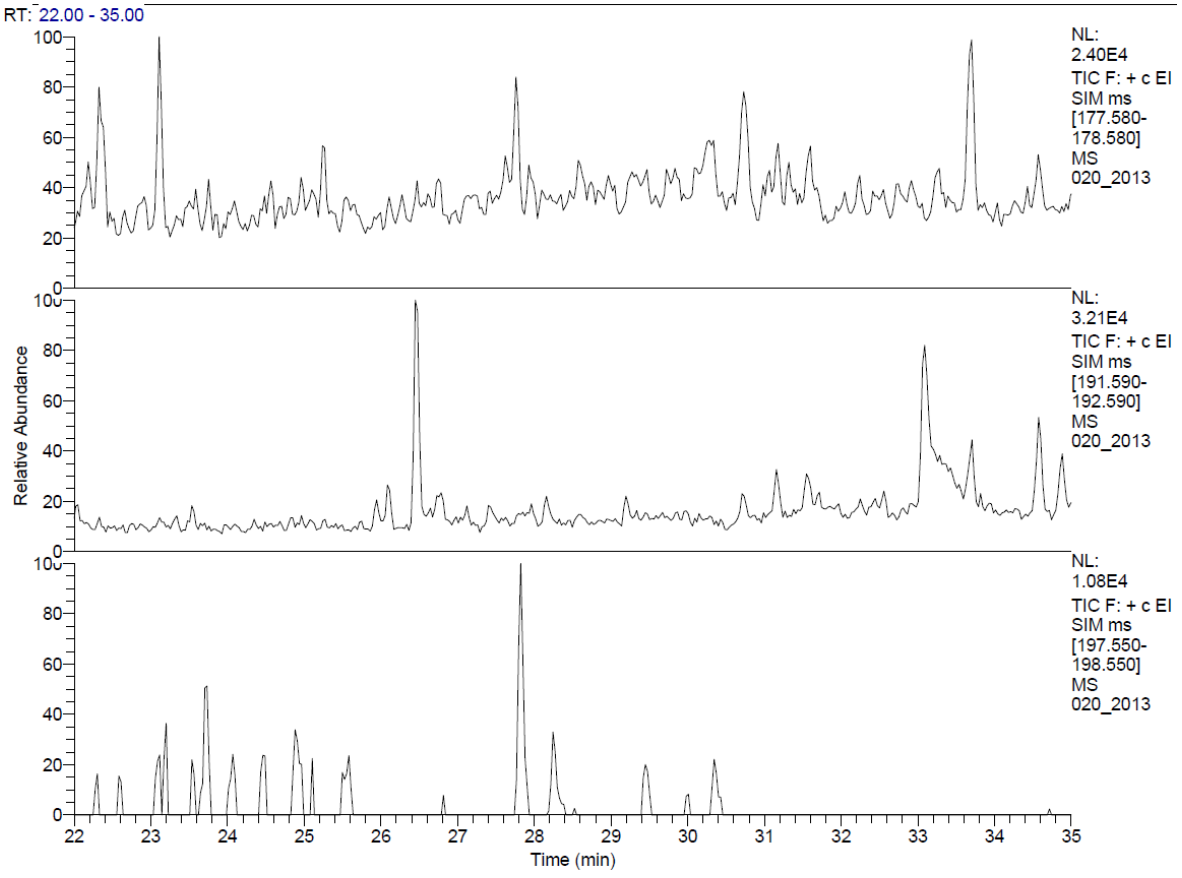
RT: 22.00 - 35.00
NL:
2.40E4
TIC F: + c EI
SIM ms
[177.580-
178.580]
MS
020_2013
NL:
3.21E4
TIC F: + c EI
SIM ms
[191.590-
192.590]
MS
020_2013
NL:
1.08E4
TIC F: + c EI
SIM ms
[197.550-
198.550]
MS
020_2013
Relative Abundance
Time (min)

O-21

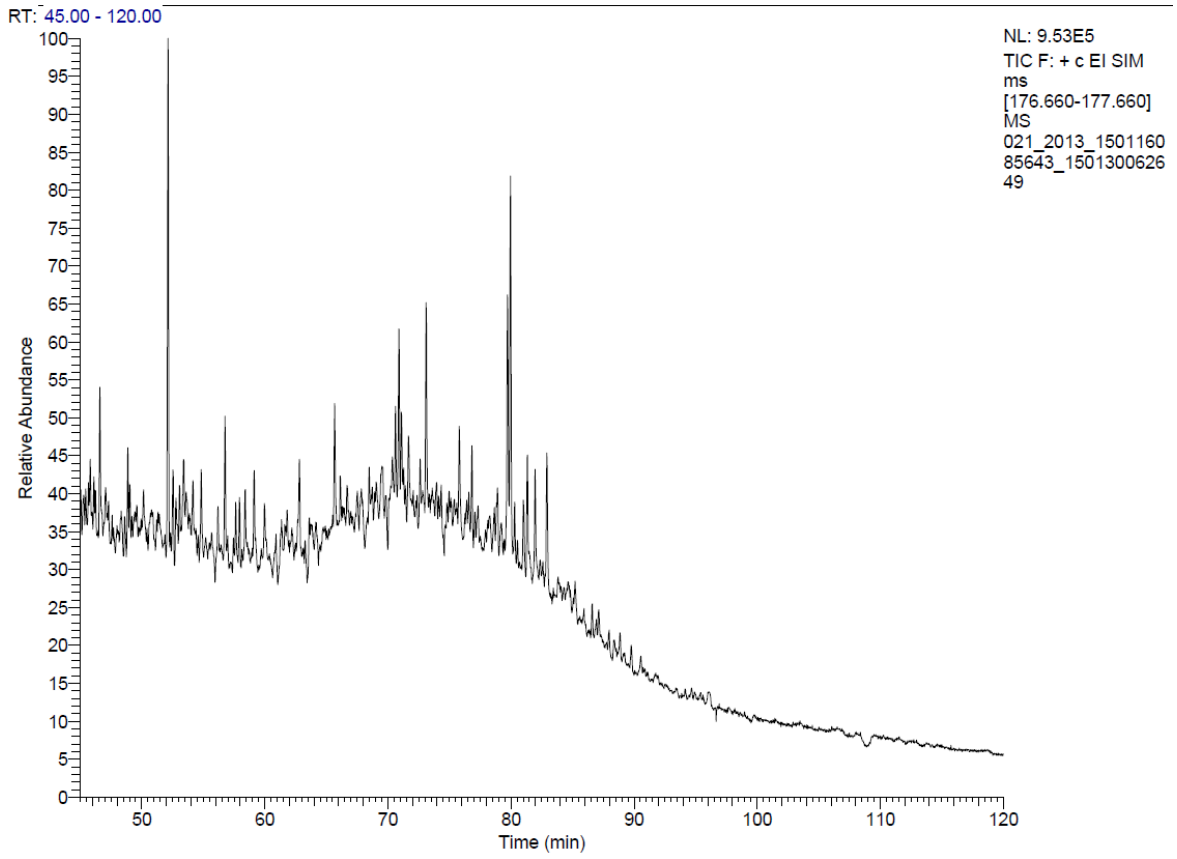
RT: 45.00 - 120.00
NL: 9.53E5
TIC F: + c EI SIM ms [176.660-177.660] MS 021_2013_150116085643_150130062649
Relative Abundance
Time (min)

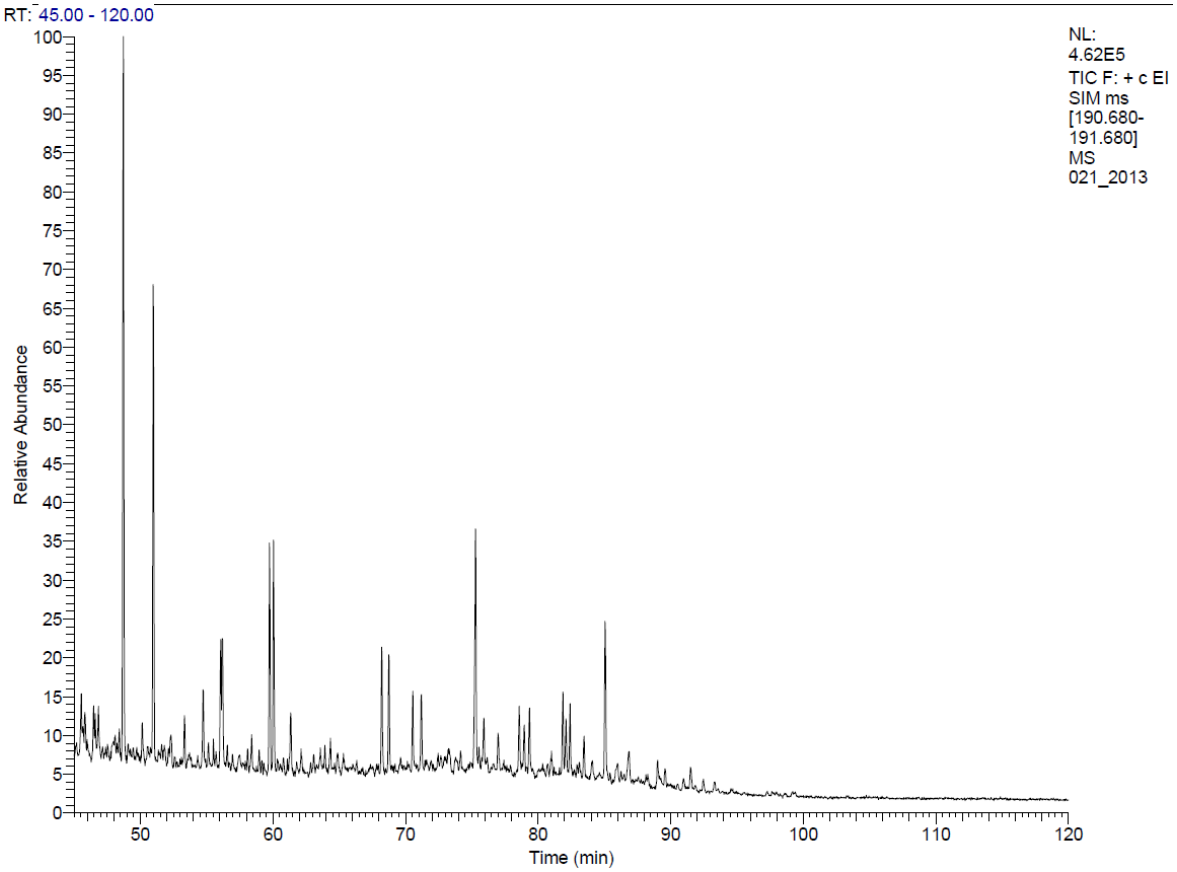
RT: 45.00 - 120.00
NL: 4.62E5
TIC F: + c EI SIM ms [190.680-191.680] MS 021_2013
Relative Abundance
Time (min)

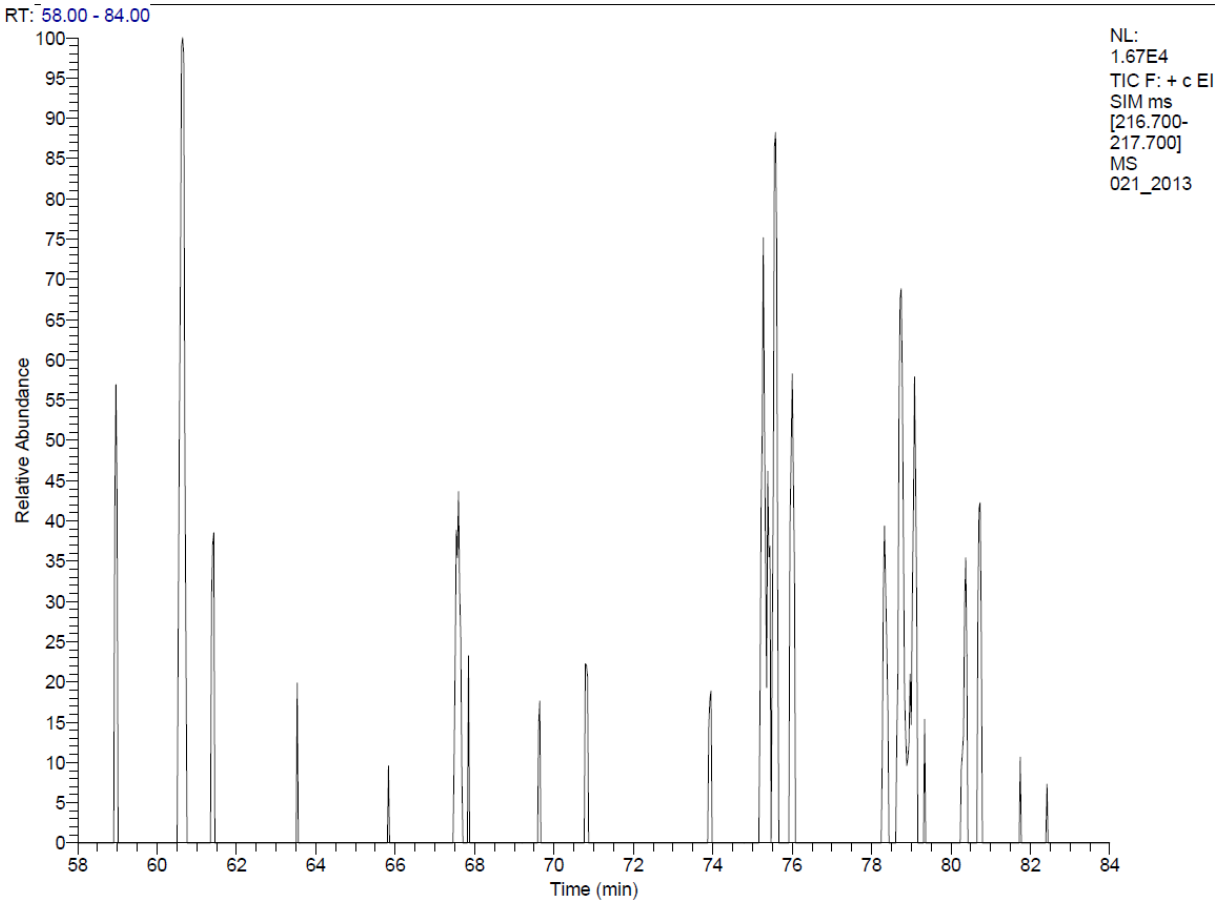
RT: 58.00 - 84.00
NL:
1.67E4
TIC F: + c EI
SIM ms
[216.700-
217.700]
MS
021_2013
Relative Abundance
Time (min)

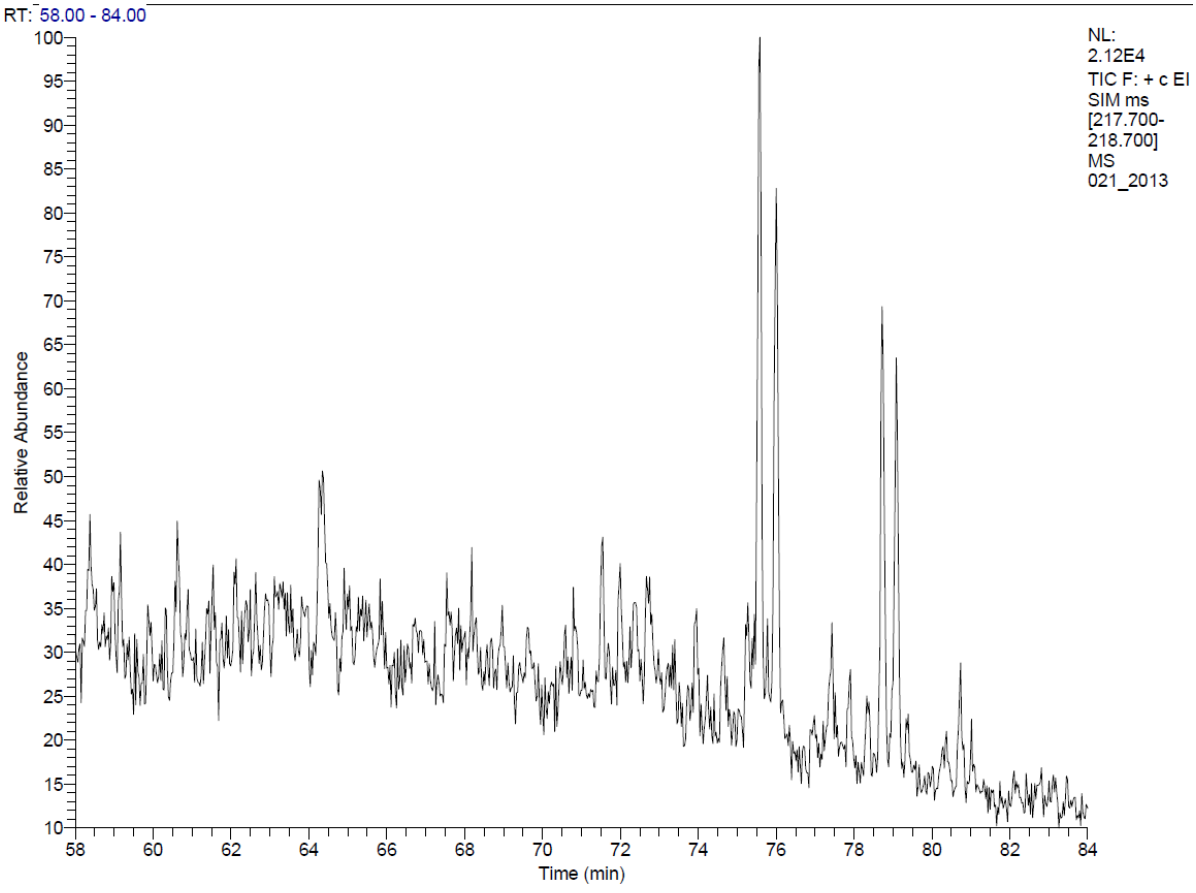
RT: 58.00 - 84.00
NL:
2.12E4
TIC F: + c EI
SIM ms
[217.700-
218.700]
MS
021_2013
Relative Abundance
Time (min)

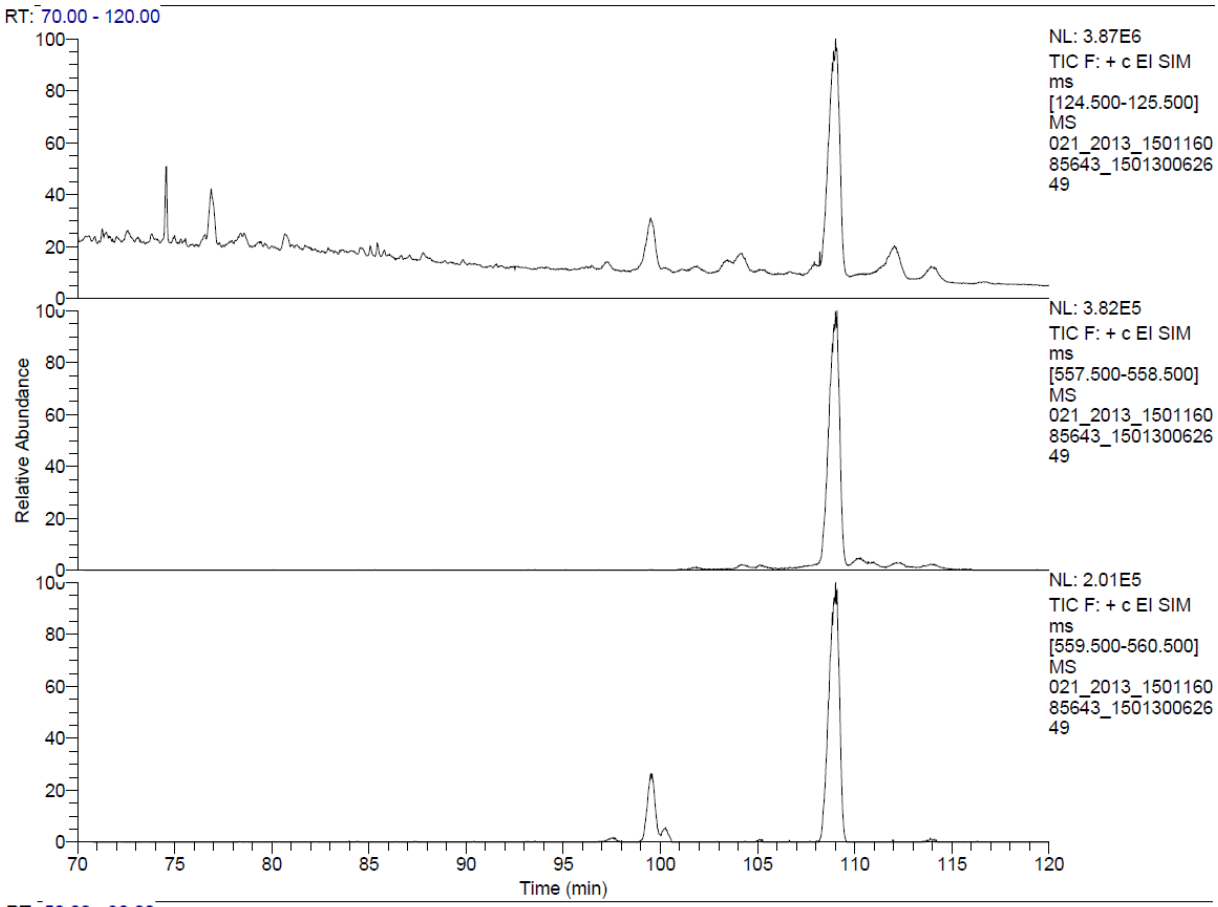
RT: 70.00 - 120.00
NL: 3.87E6
TIC F: + c EI SIM ms [124.500-125.500] MS 021_2013_150116085643_150130062649
NL: 3.82E5
TIC F: + c EI SIM ms [557.500-558.500] MS 021_2013_150116085643_150130062649
NL: 2.01E5
TIC F: + c EI SIM ms [559.500-560.500] MS 021_2013_150116085643_150130062649
Relative Abundance
Time (min)

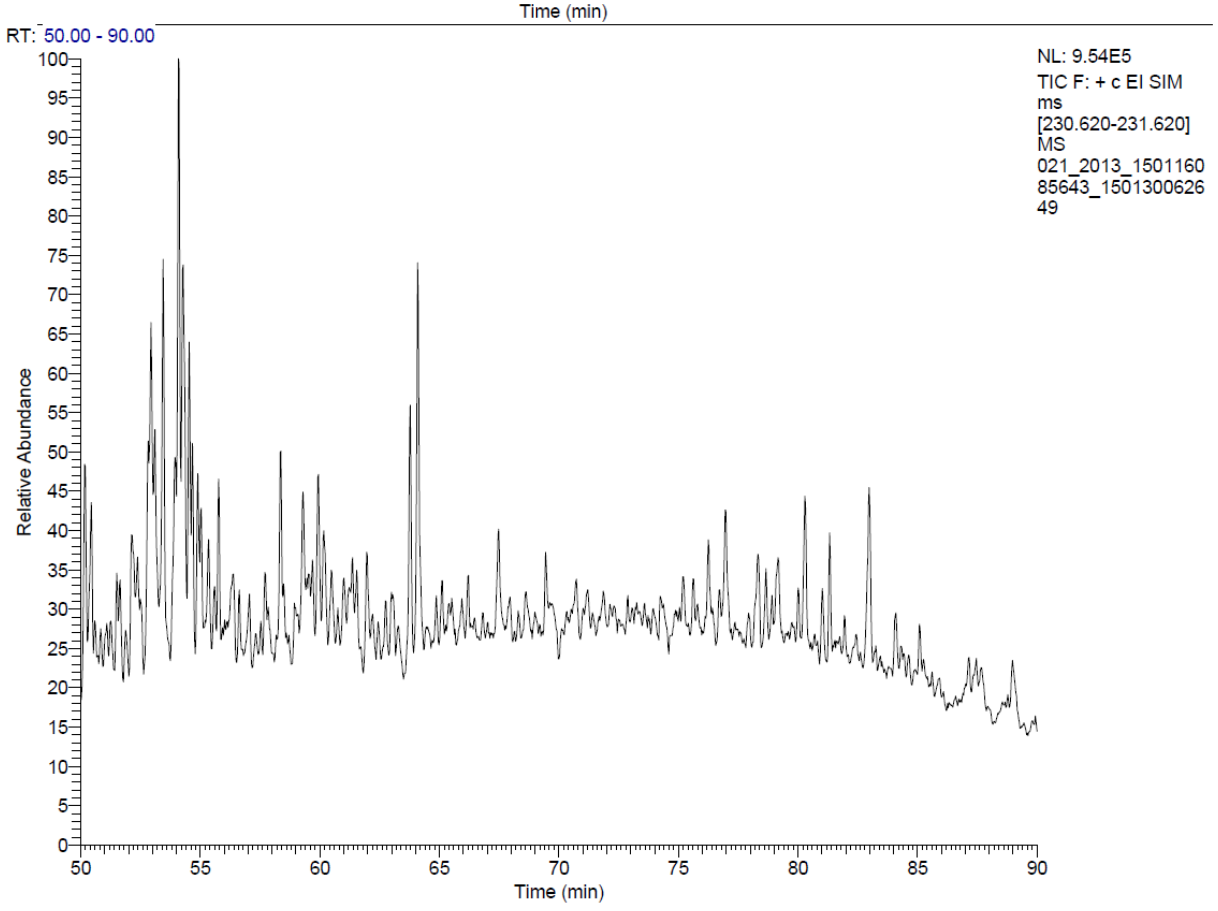
RT: 50.00 - 90.00
NL: 9.54E5
TIC F: + c EI SIM ms [230.620-231.620] MS 021_2013_150116085643_150130062649
Relative Abundance
Time (min)

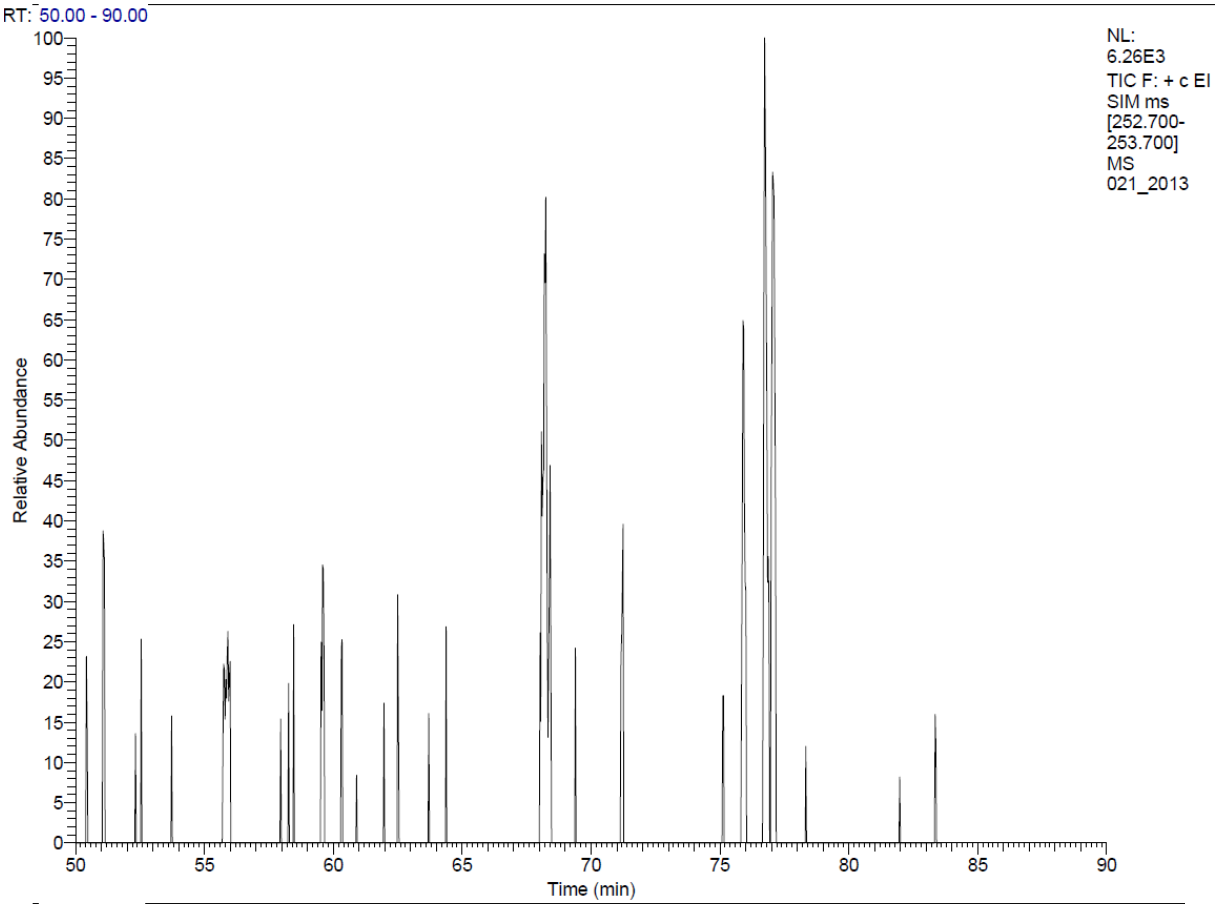
RT: 50.00 - 90.00
NL:
6.26E3
TIC F: + c EI
SIM ms
[252.700-
253.700]
MS
021_2013
Relative Abundance
Time (min)

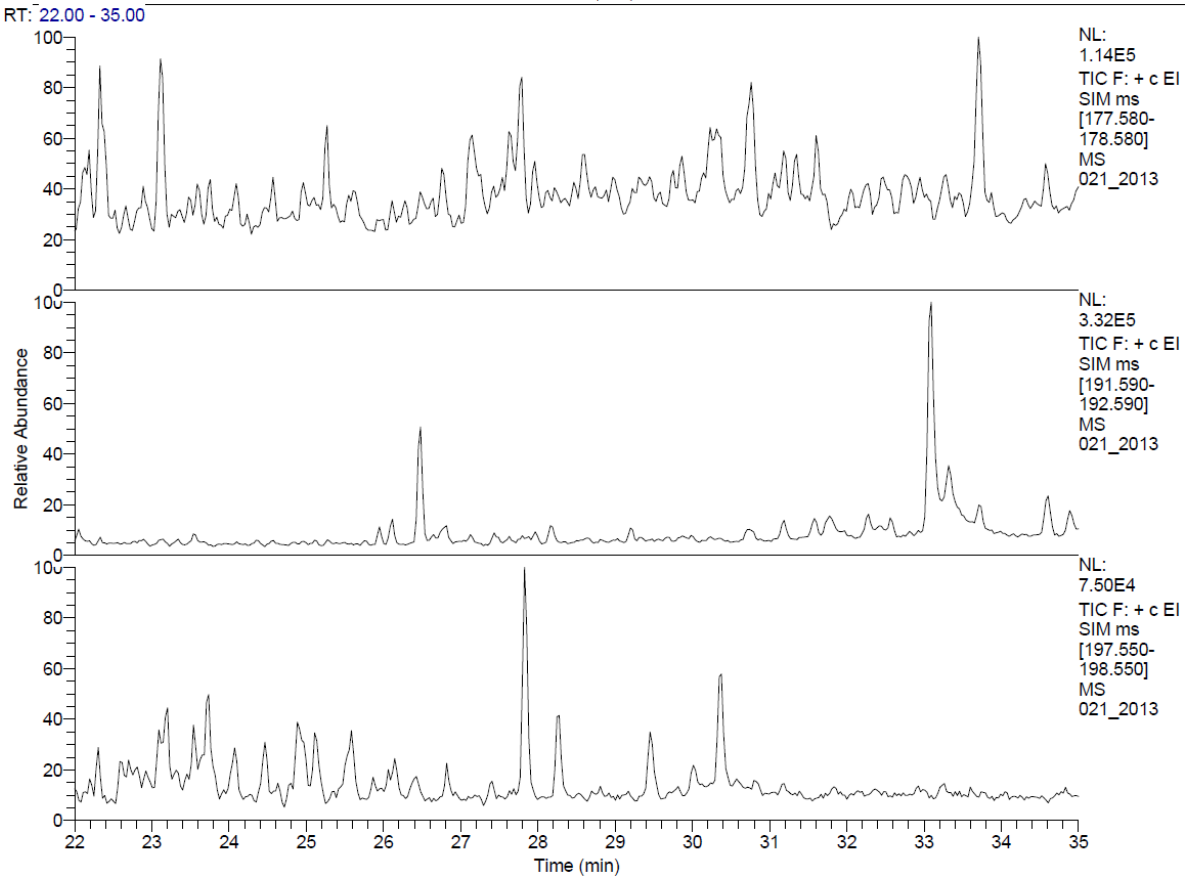
RT: 22.00 - 35.00
NL:
1.14E5
TIC F: + c EI
SIM ms
[177.580-
178.580]
MS
021_2013
NL:
3.32E5
TIC F: + c EI
SIM ms
[191.590-
192.590]
MS
021_2013
NL:
7.50E4
TIC F: + c EI
SIM ms
[197.550-
198.550]
MS
021_2013
Relative Abundance
Time (min)

NSO-1

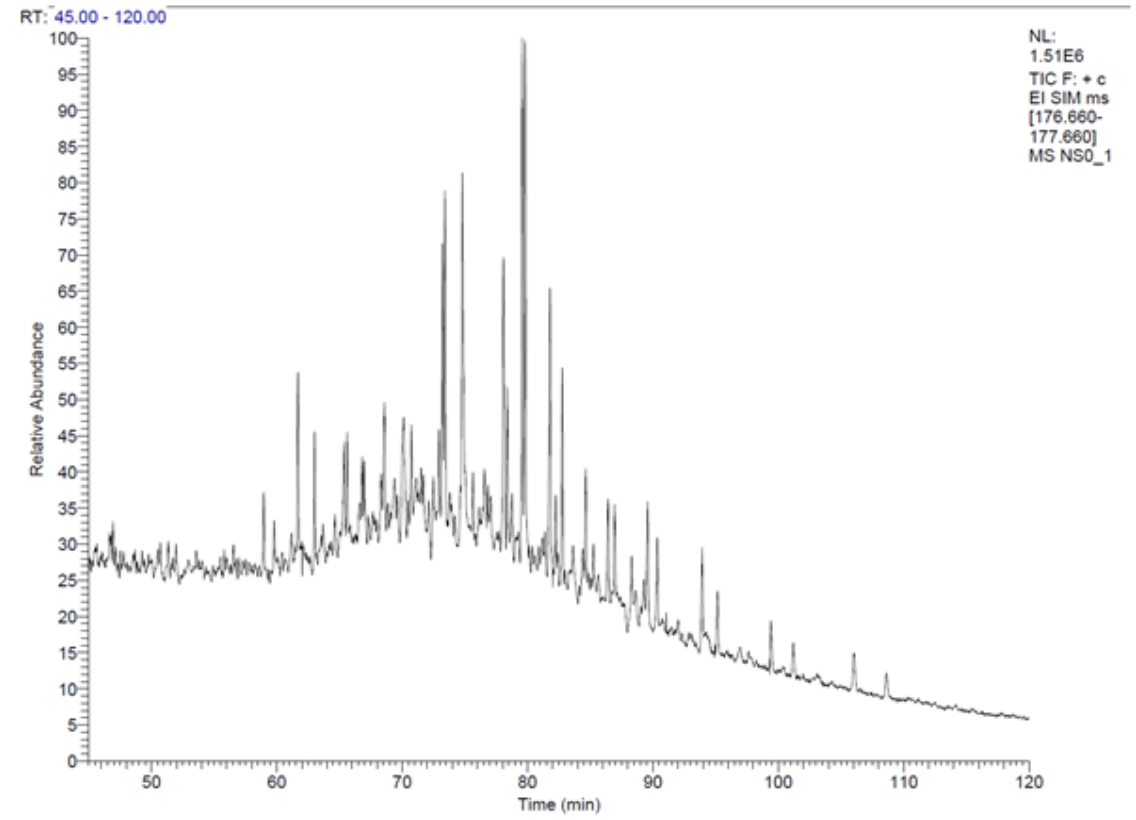
RT: 45.00 - 120.00
NL:
1.51E6
TIC F: + c
EI SIM ms
[176.660-
177.660]
MS NS0_1
Relative Abundance
Time (min)

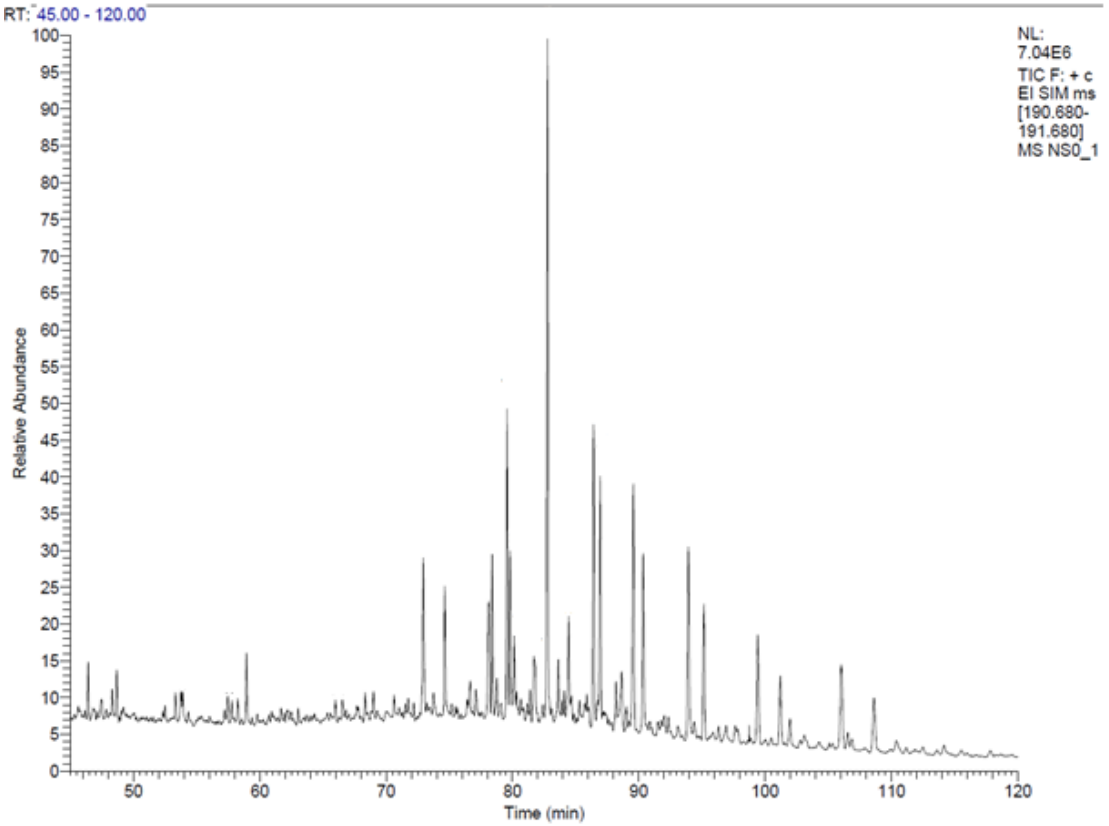
RT: 45.00 - 120.00
NL:
7.04E6
TIC F: + c
EI SIM ms
[190.680-
191.680]
MS NS0_1
Relative Abundance
Time (min)

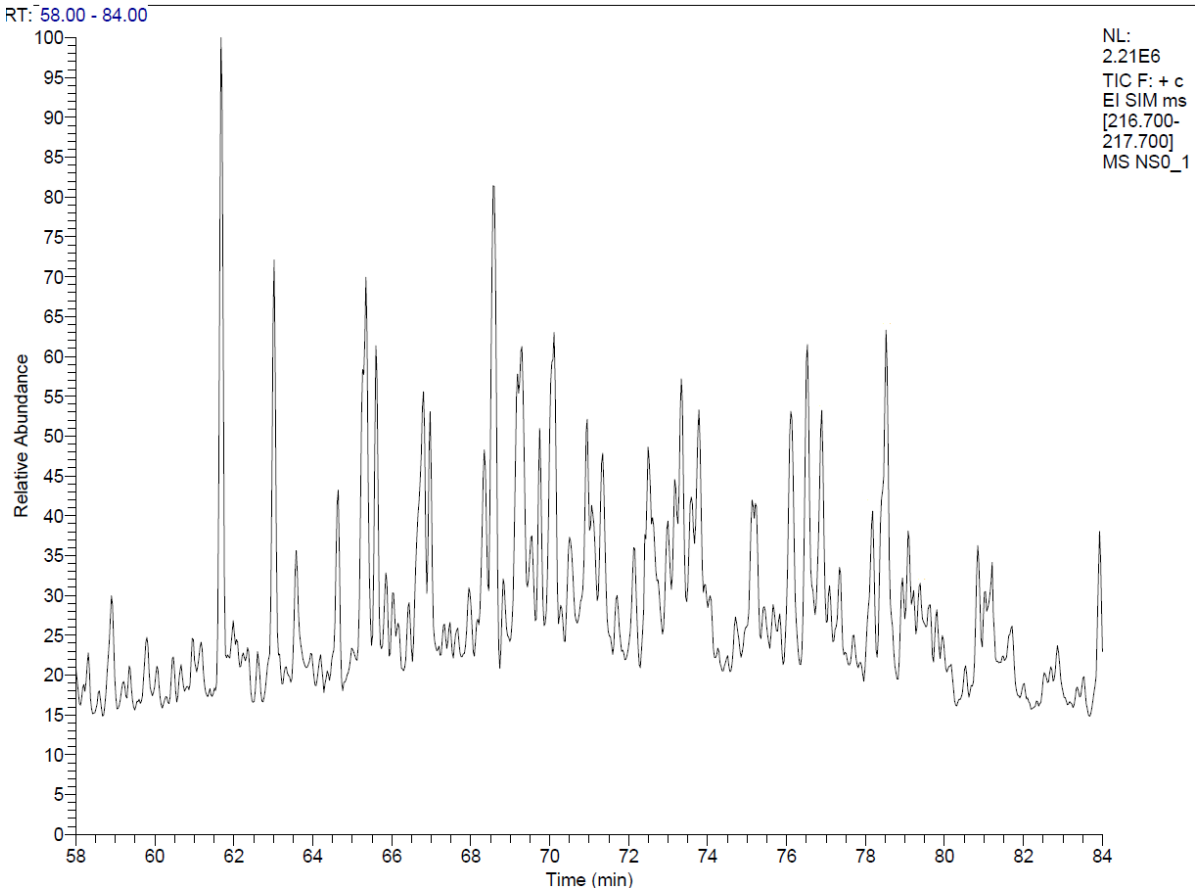
RT: 58.00 - 84.00
NL:
2.21E6
TIC F: + c
EI SIM ms
[216.700-
217.700]
MS NS0_1
Relative Abundance
Time (min)

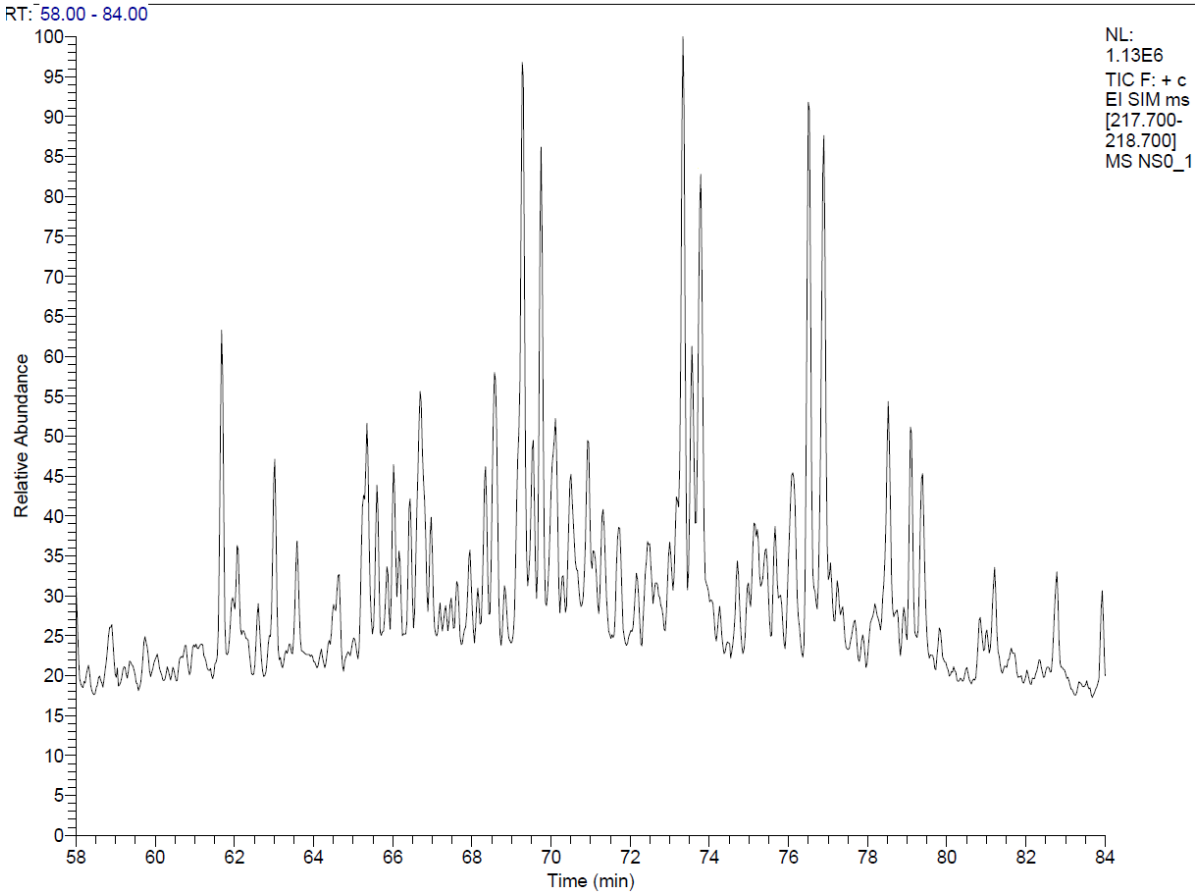
RT: 58.00 - 84.00
NL:
1.13E6
TIC F: + c
EI SIM ms
[217.700-
218.700]
MS NS0_1
Relative Abundance
Time (min)

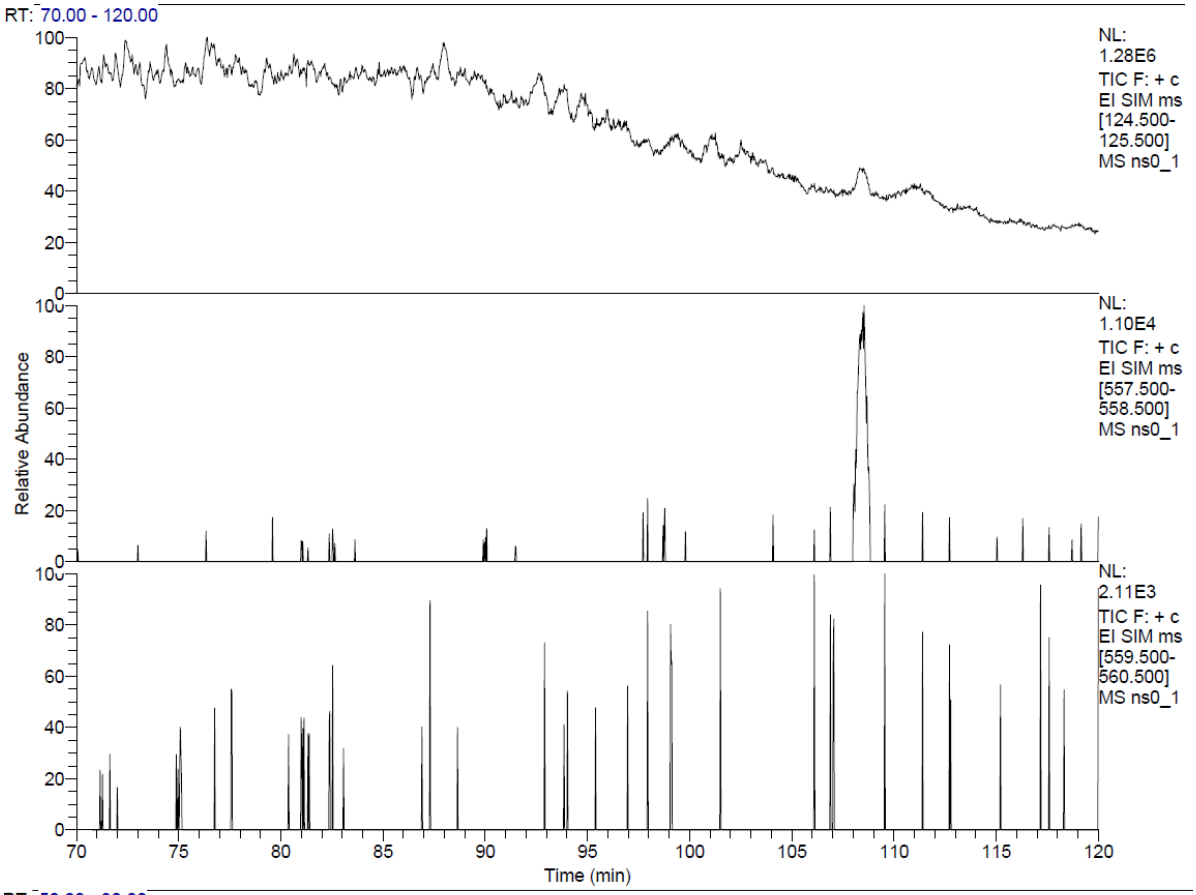
RT: 70.00 - 120.00
NL:
1.28E6
TIC F: + c
EI SIM ms
[124.500-
125.500]
MS ns0_1
NL:
1.10E4
TIC F: + c
EI SIM ms
[557.500-
558.500]
MS ns0_1
NL:
2.11E3
TIC F: + c
EI SIM ms
[559.500-
560.500]
MS ns0_1
Relative Abundance
Time (min)

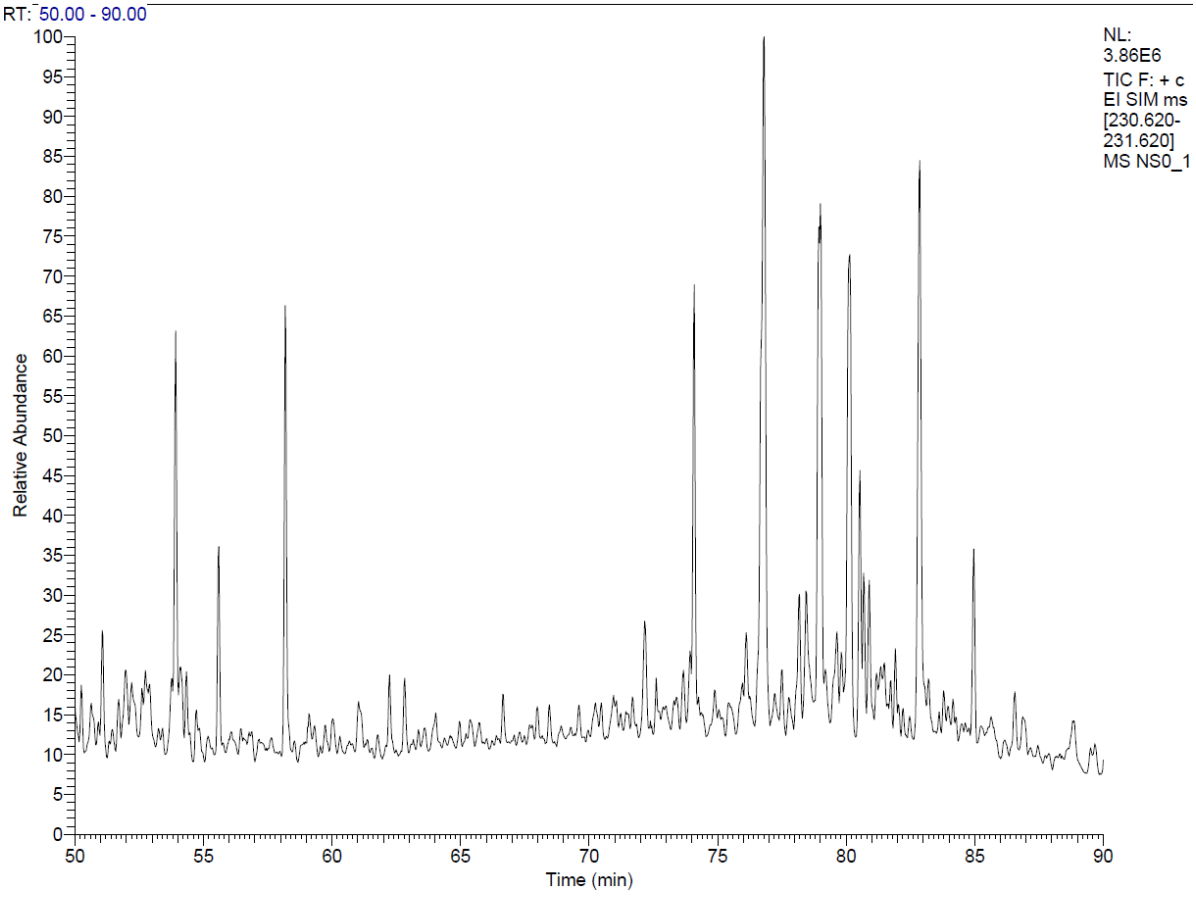
RT: 50.00 - 90.00
NL:
3.86E6
TIC F: + c
EI SIM ms
[230.620-
231.620]
MS NS0_1
Relative Abundance
Time (min)

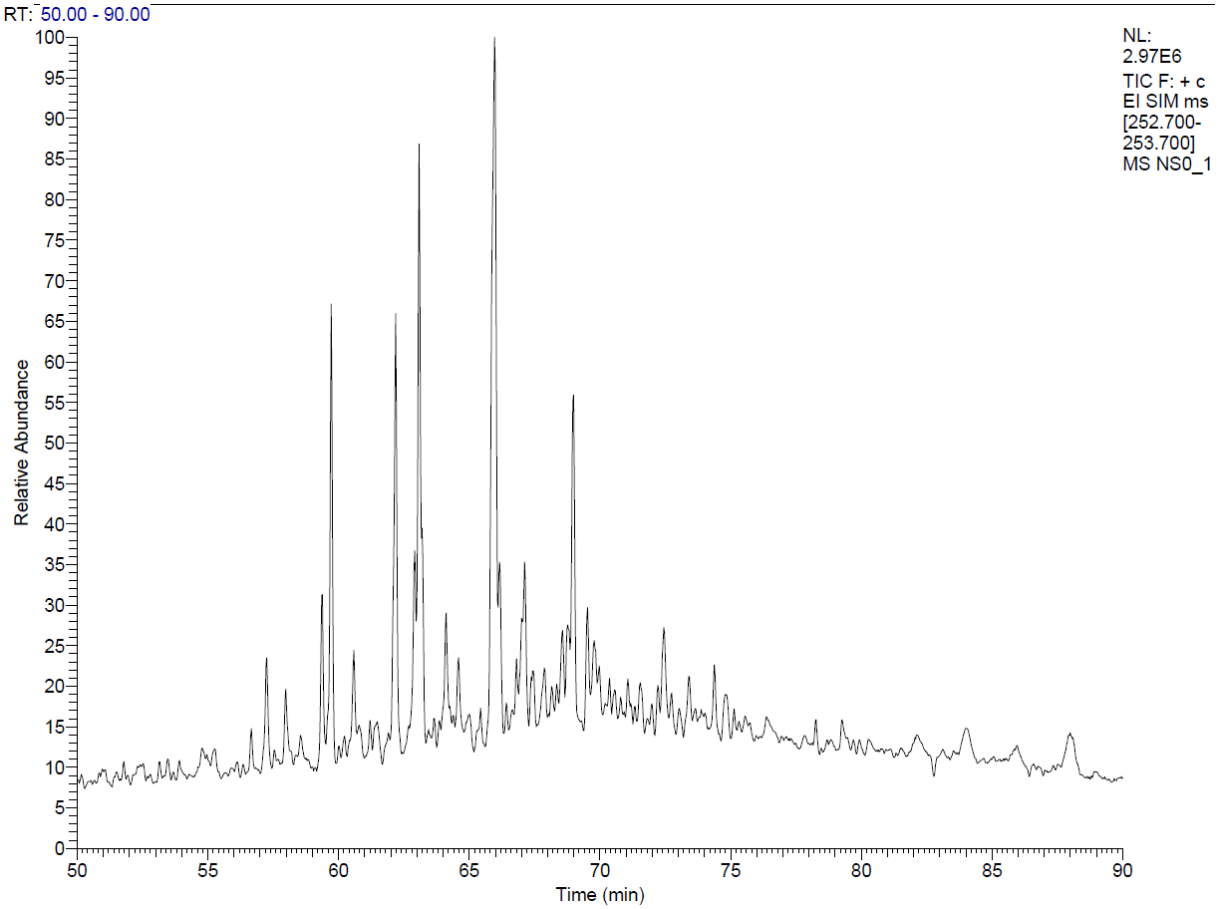
RT: 50.00 - 90.00
NL:
2.97E6
TIC F: + c
EI SIM ms
[252.700-
253.700]
MS NS0_1
Relative Abundance
Time (min)

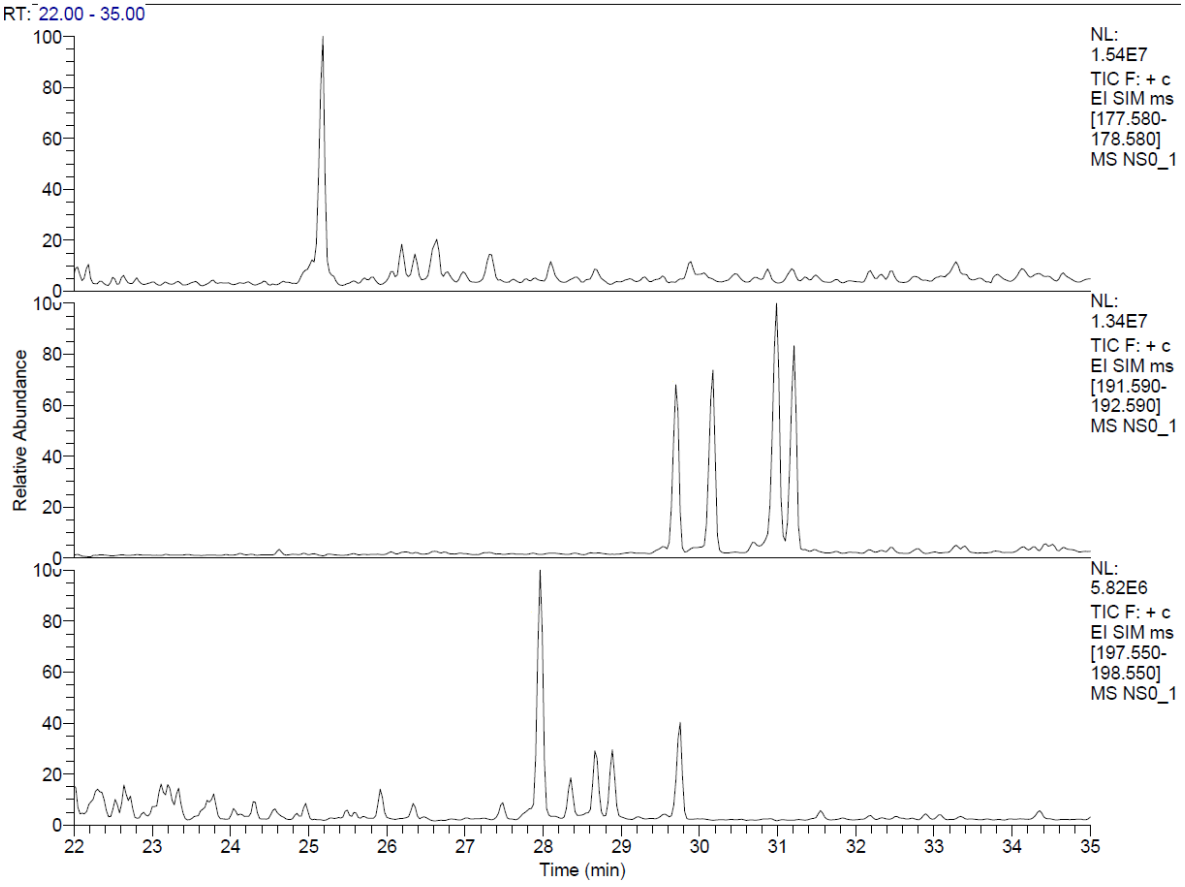
RT: 22.00 - 35.00
NL:
1.54E7
TIC F: + c
EI SIM ms
[177.580-
178.580]
MS NS0_1
NL:
1.34E7
TIC F: + c
EI SIM ms
[191.590-
192.590]
MS NS0_1
NL:
5.82E6
TIC F: + c
EI SIM ms
[197.550-
198.550]
MS NS0_1
Relative Abundance
Time (min)

Embla

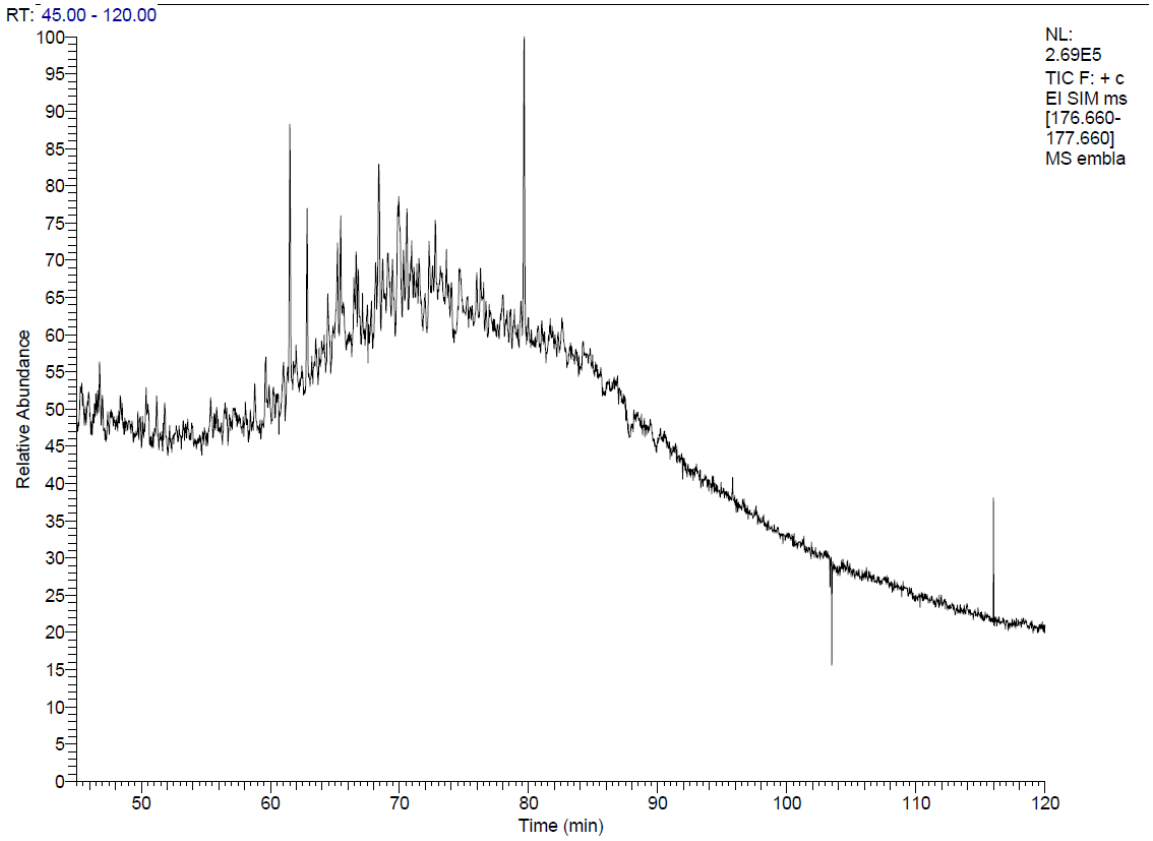
RT: 45.00 - 120.00
NL:
2.69E5
TIC F: + c
EI SIM ms
[176.660-
177.660]
MS embla
Relative Abundance
Time (min)

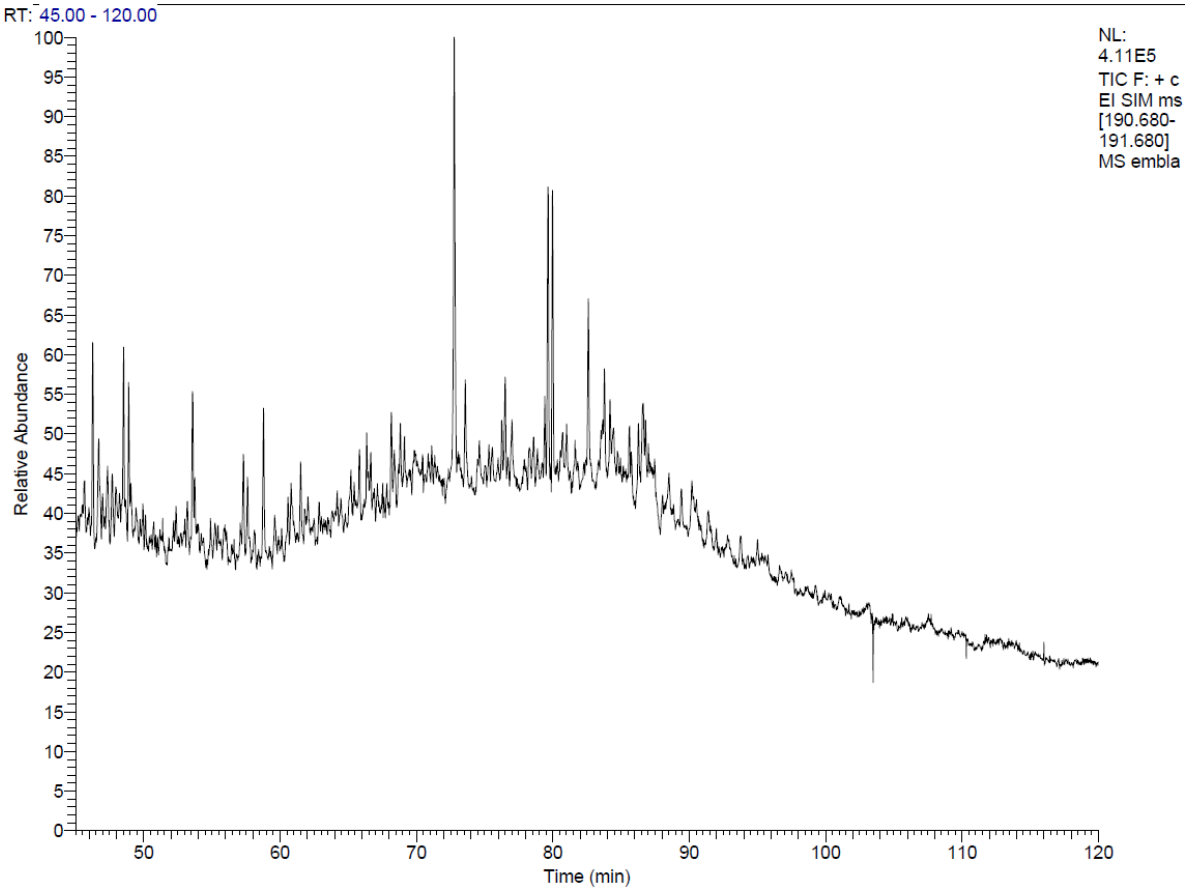
RT: 45.00 - 120.00
NL:
4.11E5
TIC F: + c
EI SIM ms
[190.680-
191.680]
MS embla
Relative Abundance
Time (min)

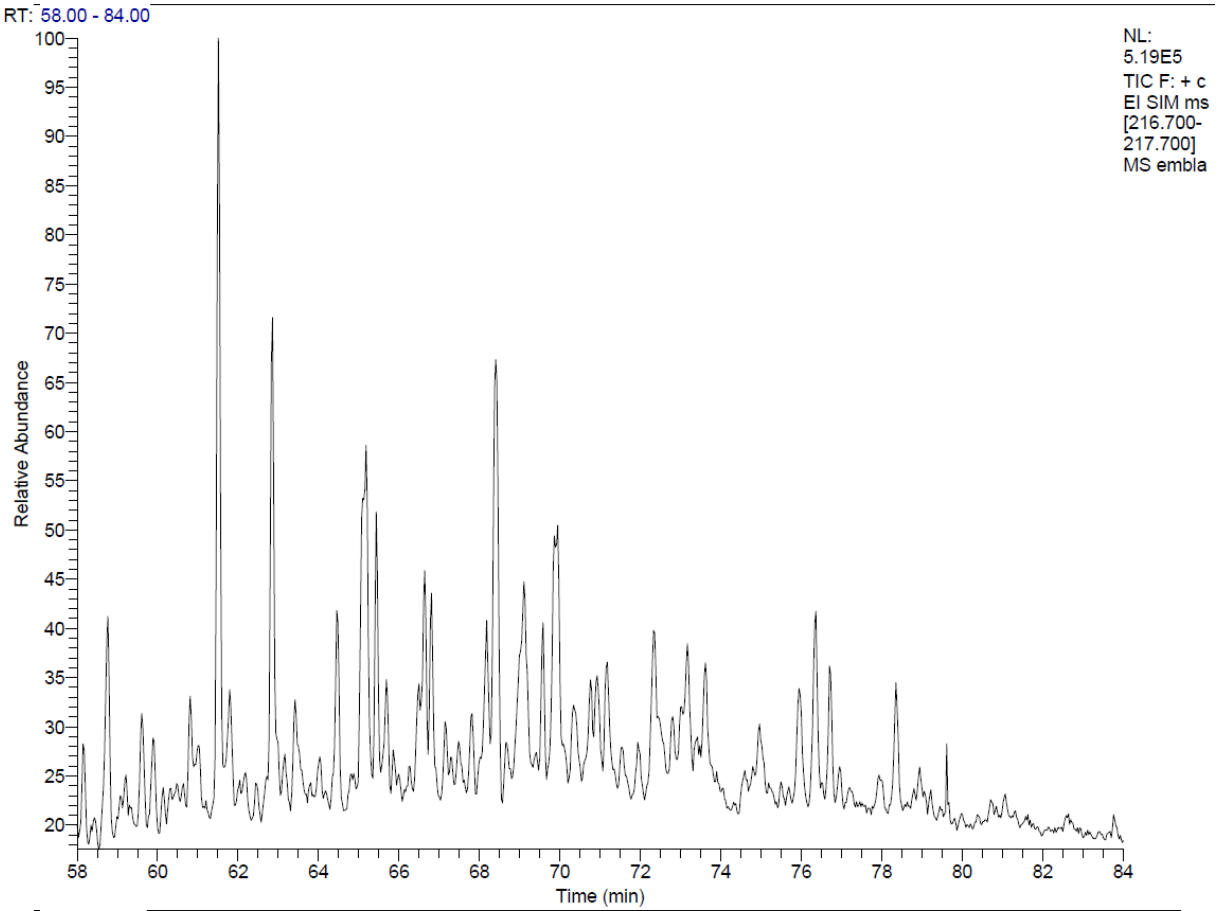
RT: 58.00 - 84.00
NL:
5.19E5
TIC F: + c
EI SIM ms
[216.700-
217.700]
MS embla
Relative Abundance
Time (min)

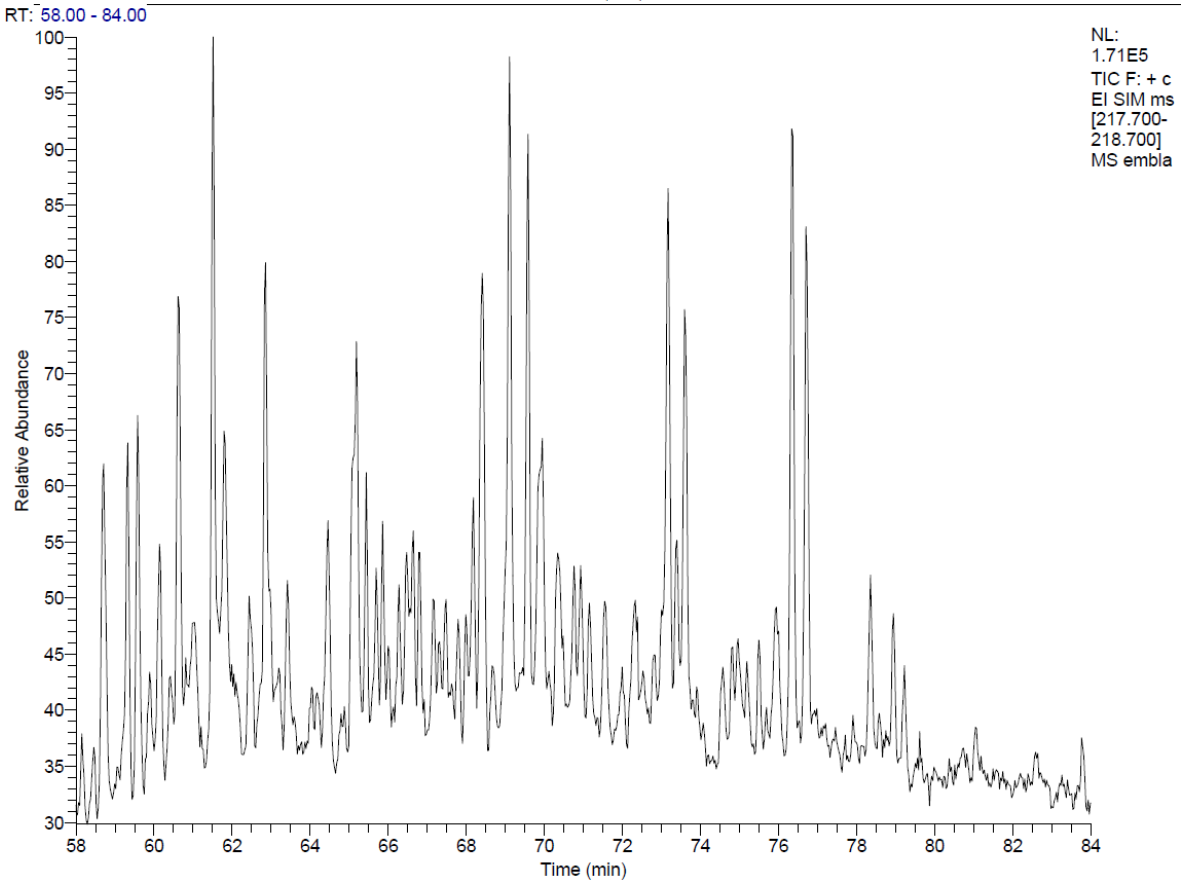
RT: 58.00 - 84.00
NL:
1.71E5
TIC F: + c
EI SIM ms
[217.700-
218.700]
MS embla
Relative Abundance
Time (min)

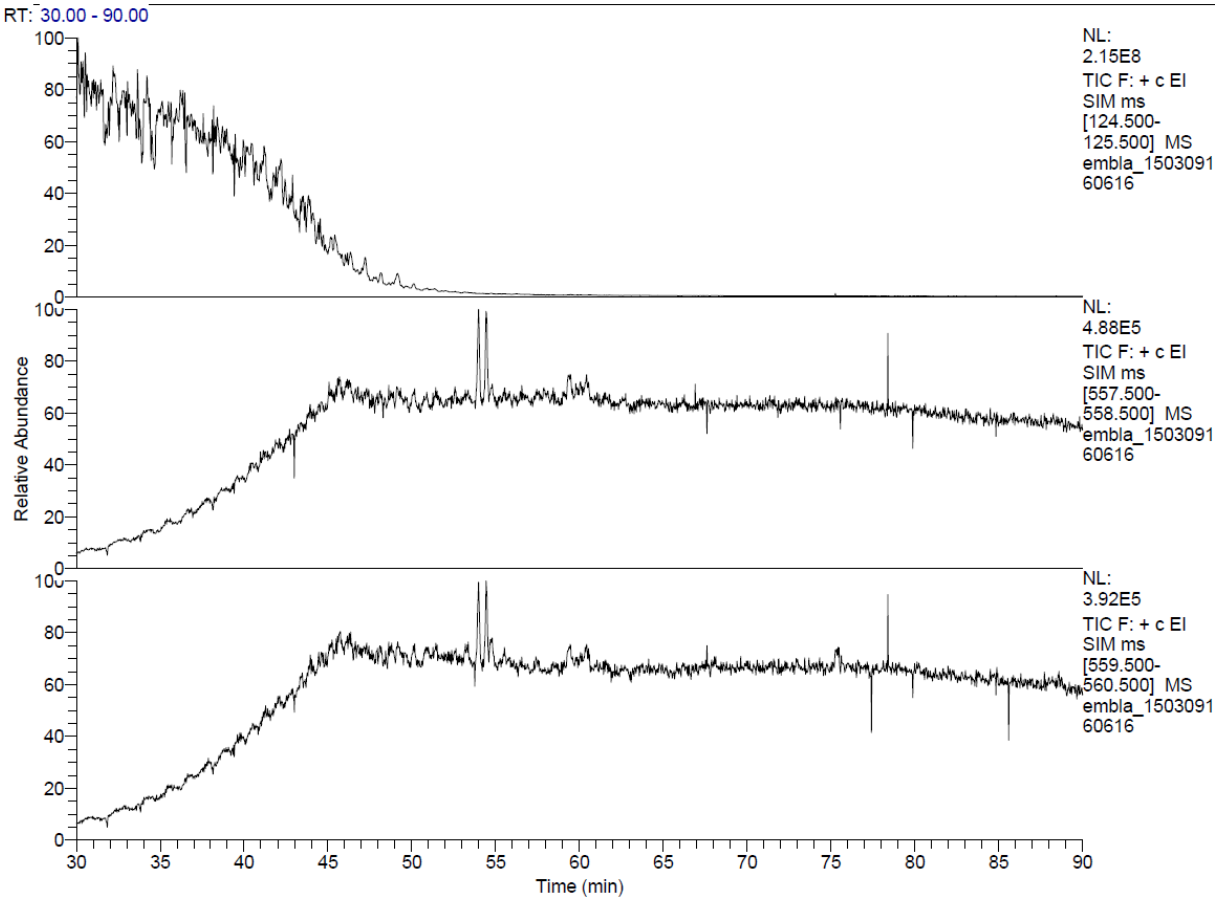
RT: 30.00 - 90.00
NL:
2.15E8
TIC F: + c EI
SIM ms
[124.500-
125.500] MS
embla_1503091
60616
NL:
4.88E5
TIC F: + c EI
SIM ms
[557.500-
558.500] MS
embla_1503091
60616
NL:
3.92E5
TIC F: + c EI
SIM ms
[559.500-
560.500] MS
embla_1503091
60616
Relative Abundance
Time (min)

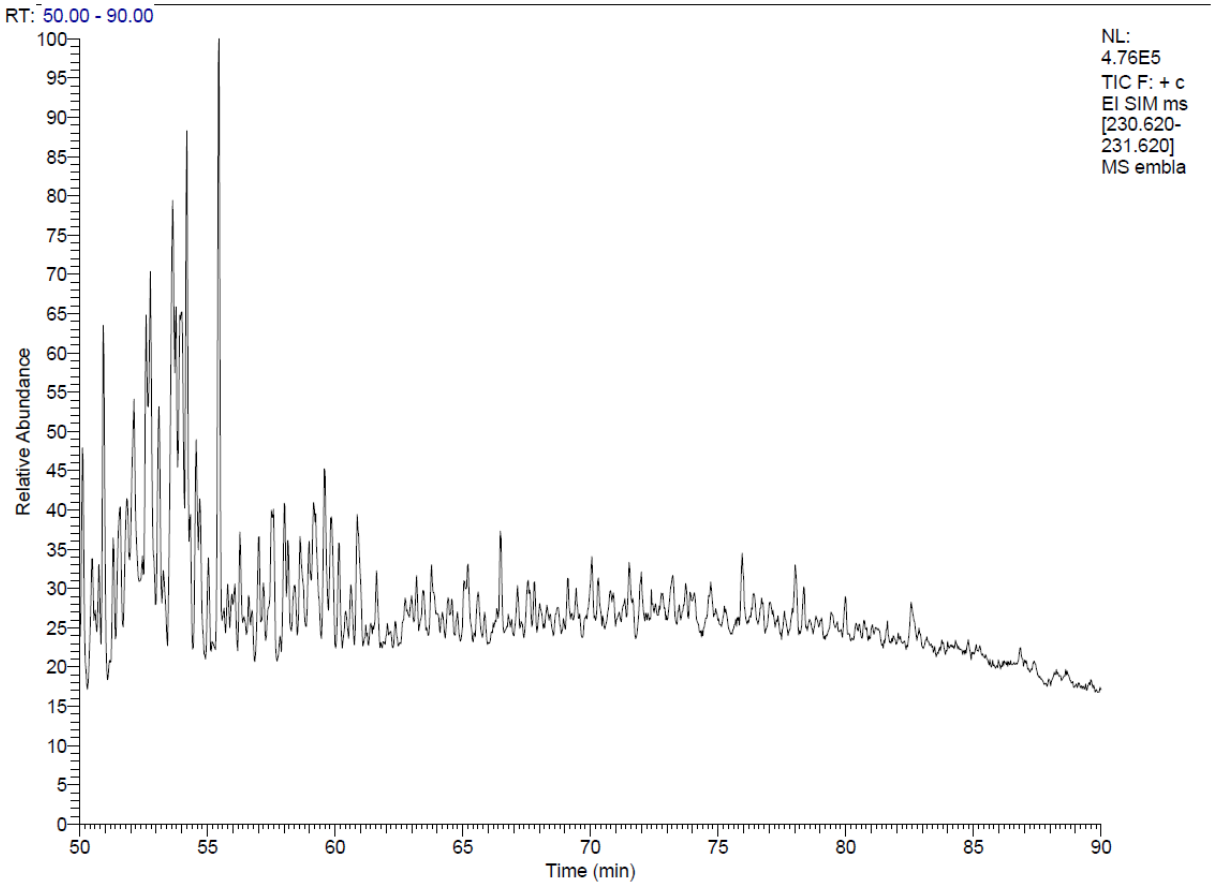
RT: 50.00 - 90.00
NL:
4.76E5
TIC F: + c
EI SIM ms
[230.620-
231.620]
MS embla
Relative Abundance
Time (min)

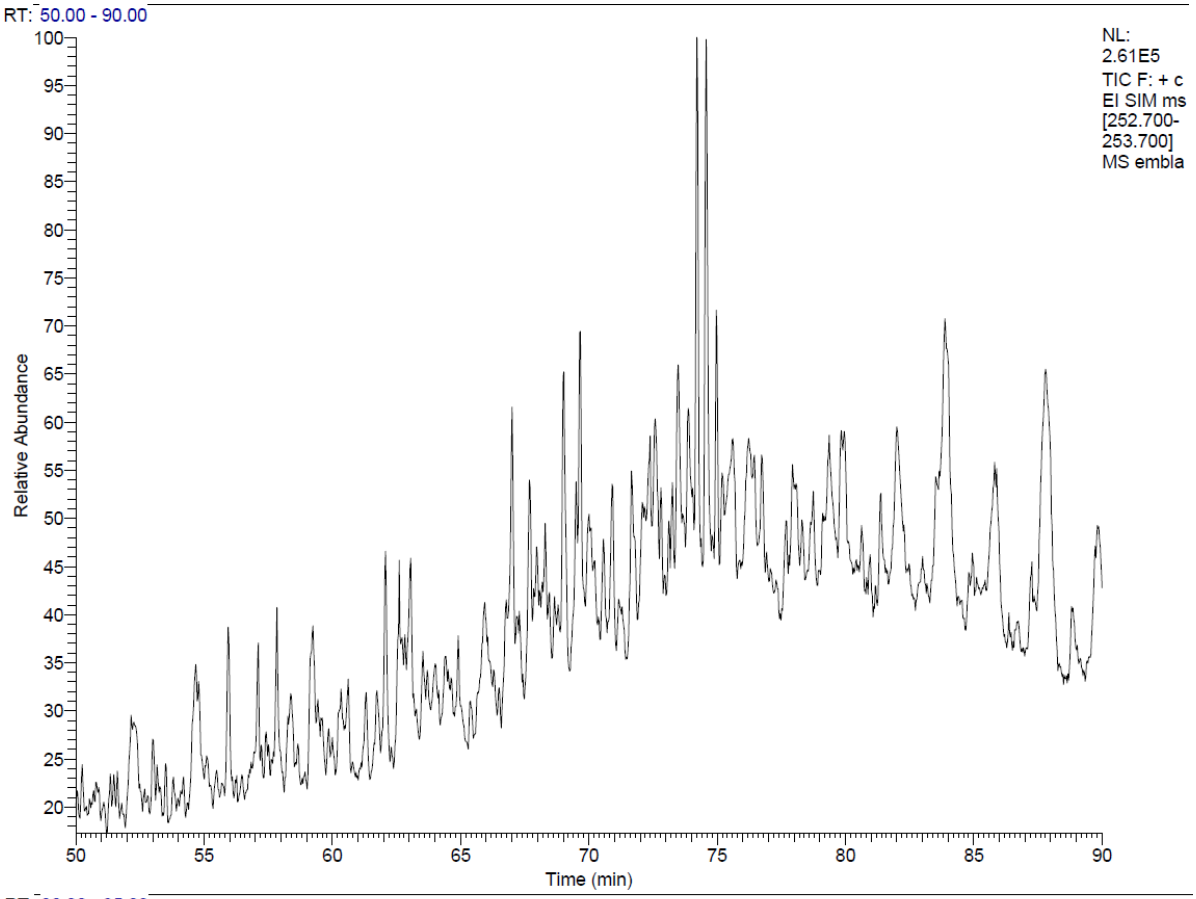
RT: 50.00 - 90.00
NL:
2.61E5
TIC F: + c
EI SIM ms
[252.700-
253.700]
MS embla
Relative Abundance
Time (min)

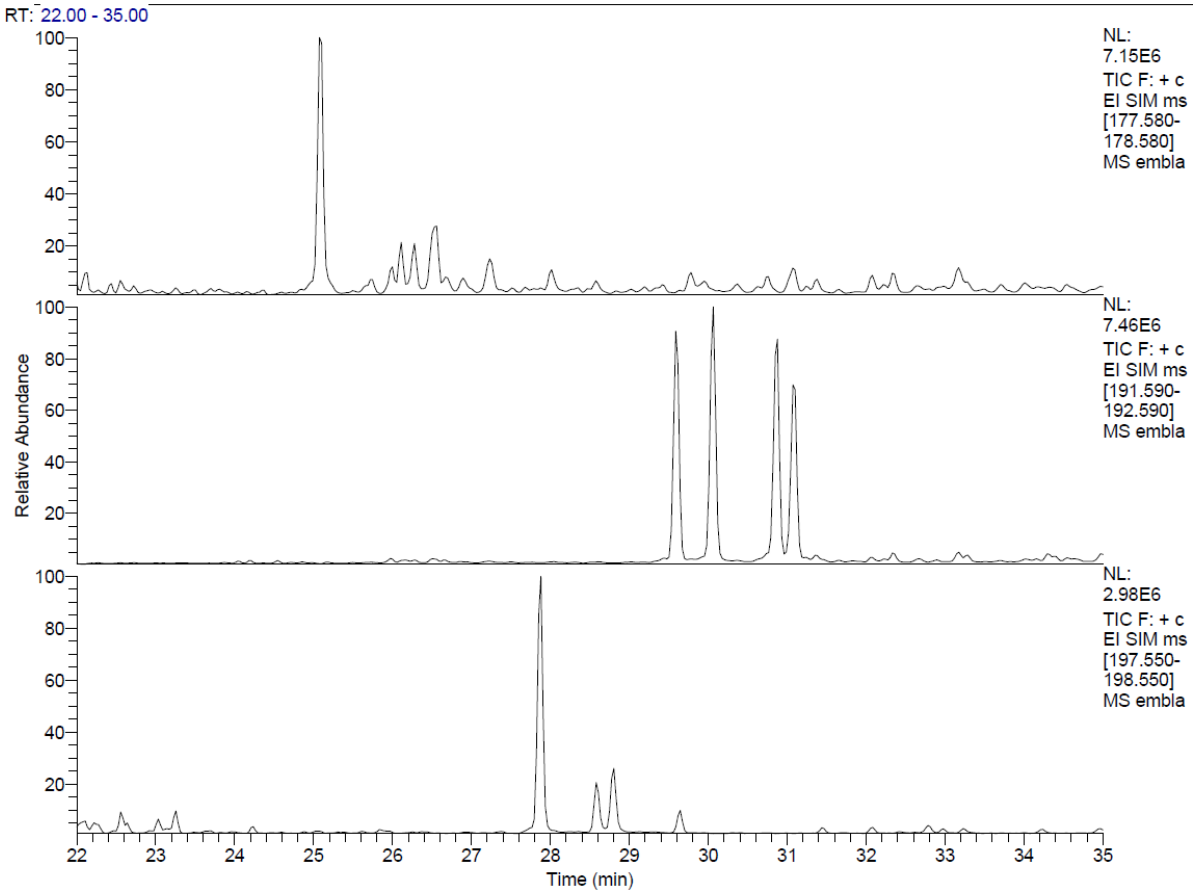
RT: 22.00 - 35.00
NL:
7.15E6
TIC F: + c
EI SIM ms
[177.580-
178.580]
MS embla
NL:
7.46E6
TIC F: + c
EI SIM ms
[191.590-
192.590]
MS embla
NL:
2.98E6
TIC F: + c
EI SIM ms
[197.550-
198.550]
MS embla
Relative Abundance
Time (min)

Beatrice

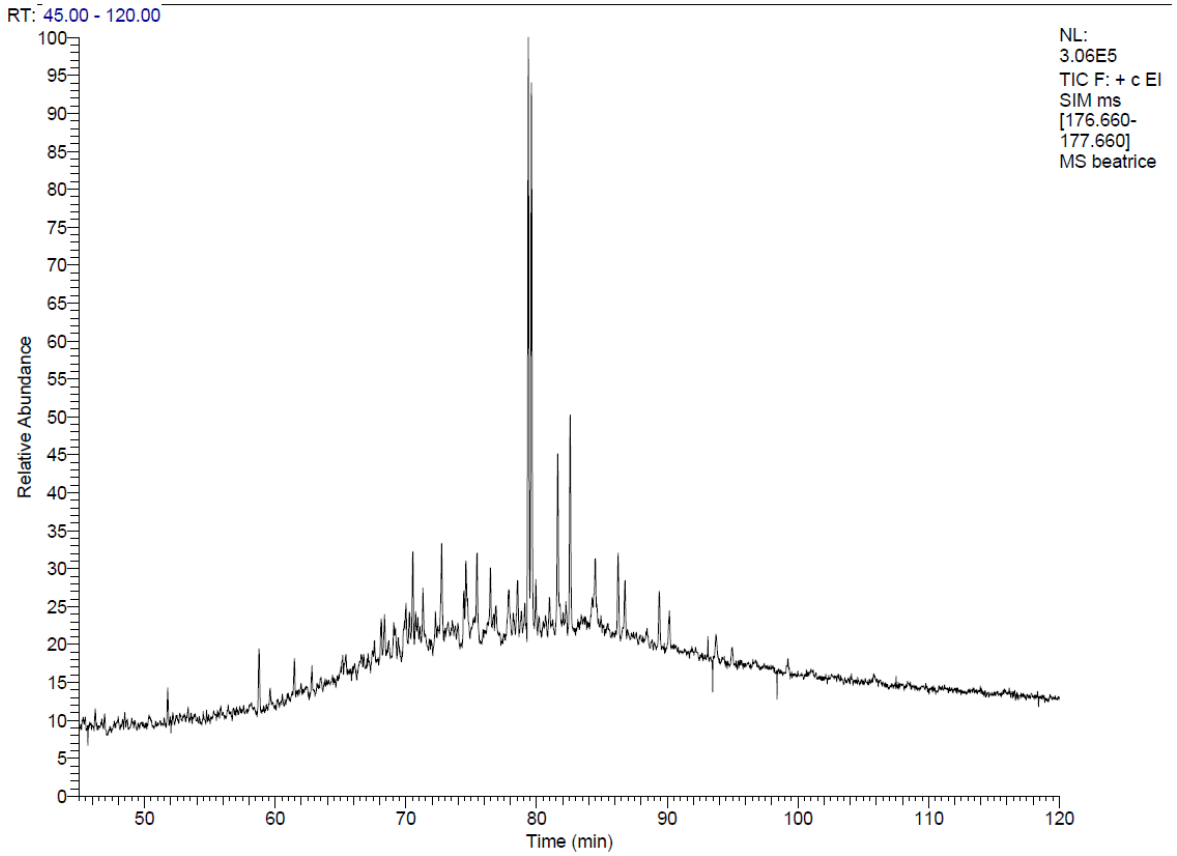
RT: 45.00 - 120.00
NL:
3.06E5
TIC F: + c EI
SIM ms
[176.660-
177.660]
MS beatrice
Relative Abundance
Time (min)

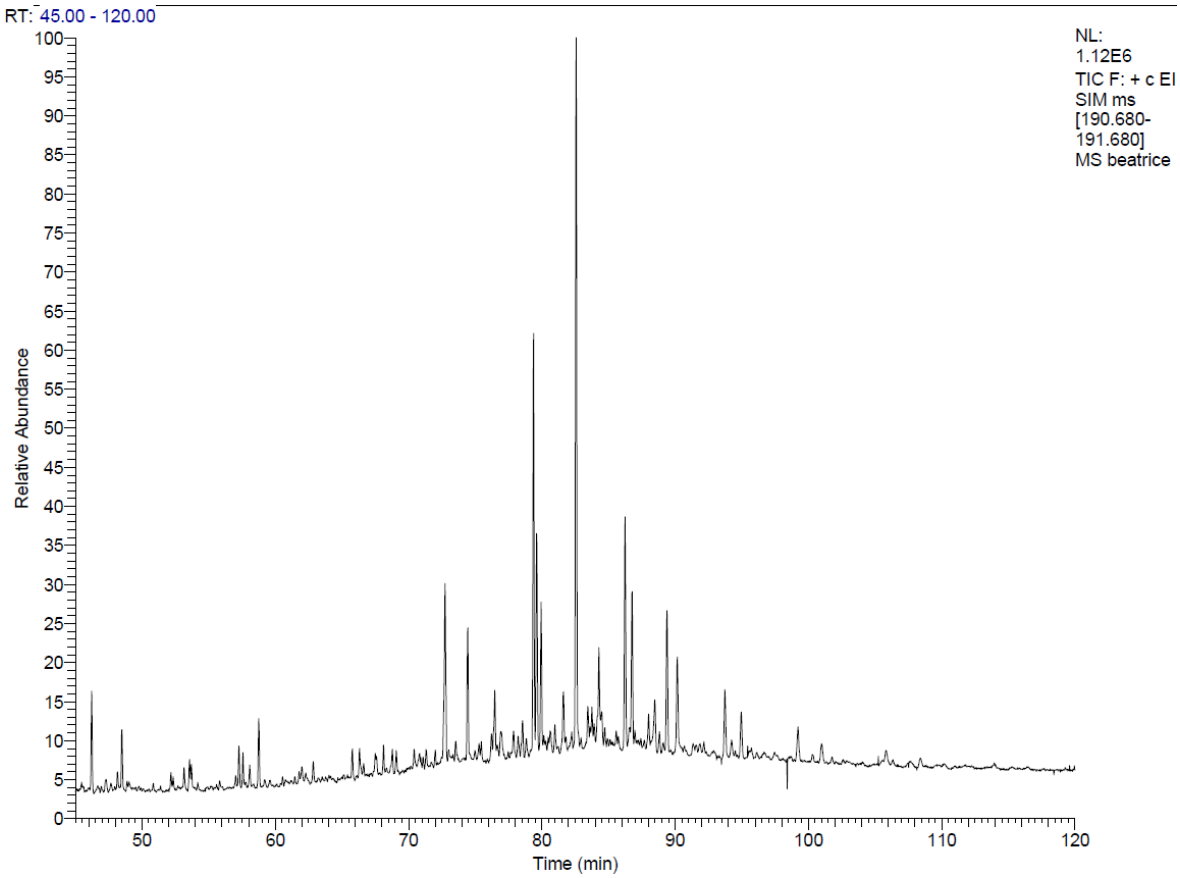
RT: 45.00 - 120.00
NL:
1.12E6
TIC F: + c EI
SIM ms
[190.680-
191.680]
MS beatrice
Relative Abundance
Time (min)

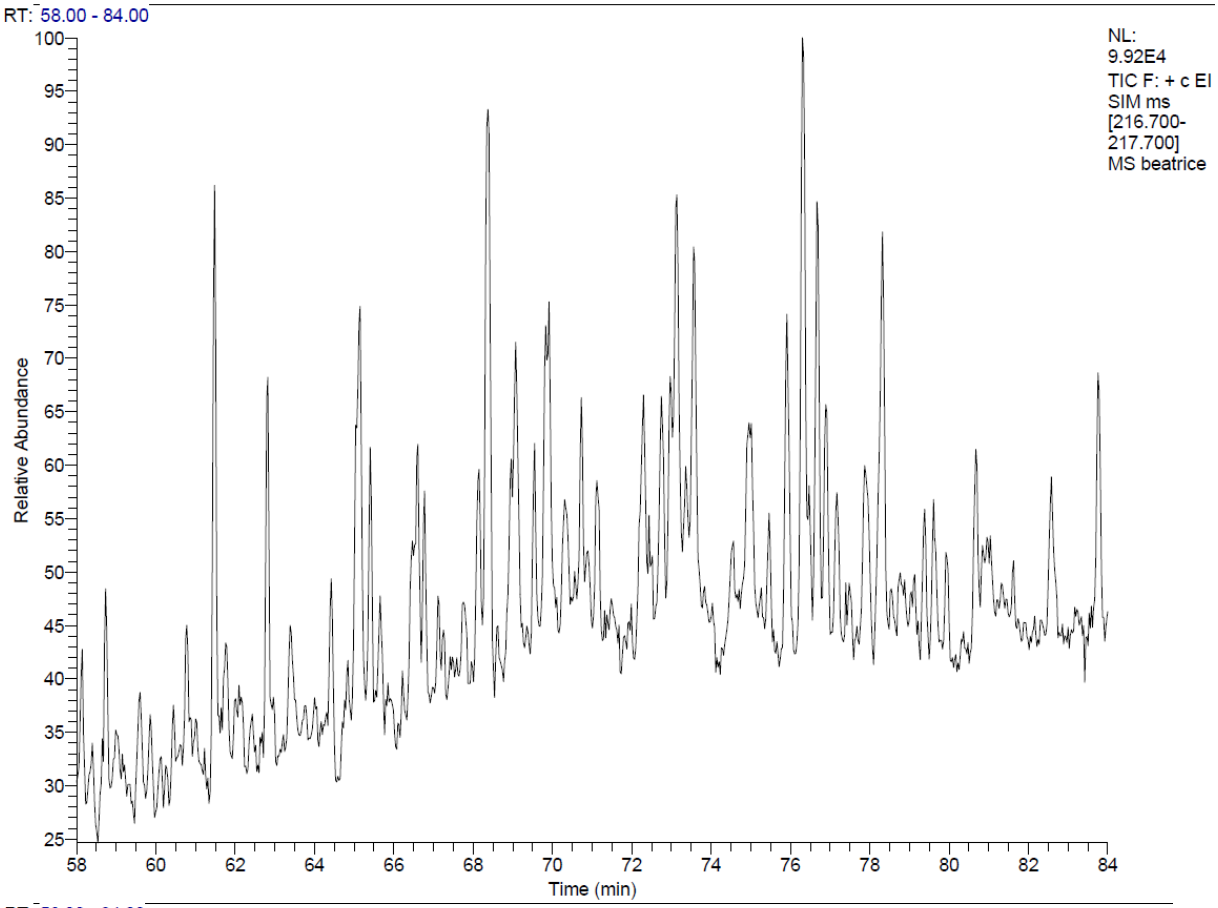
RT: 58.00 - 84.00
NL:
9.92E4
TIC F: + c EI
SIM ms
[216.700-
217.700]
MS beatrice
Relative Abundance
Time (min)

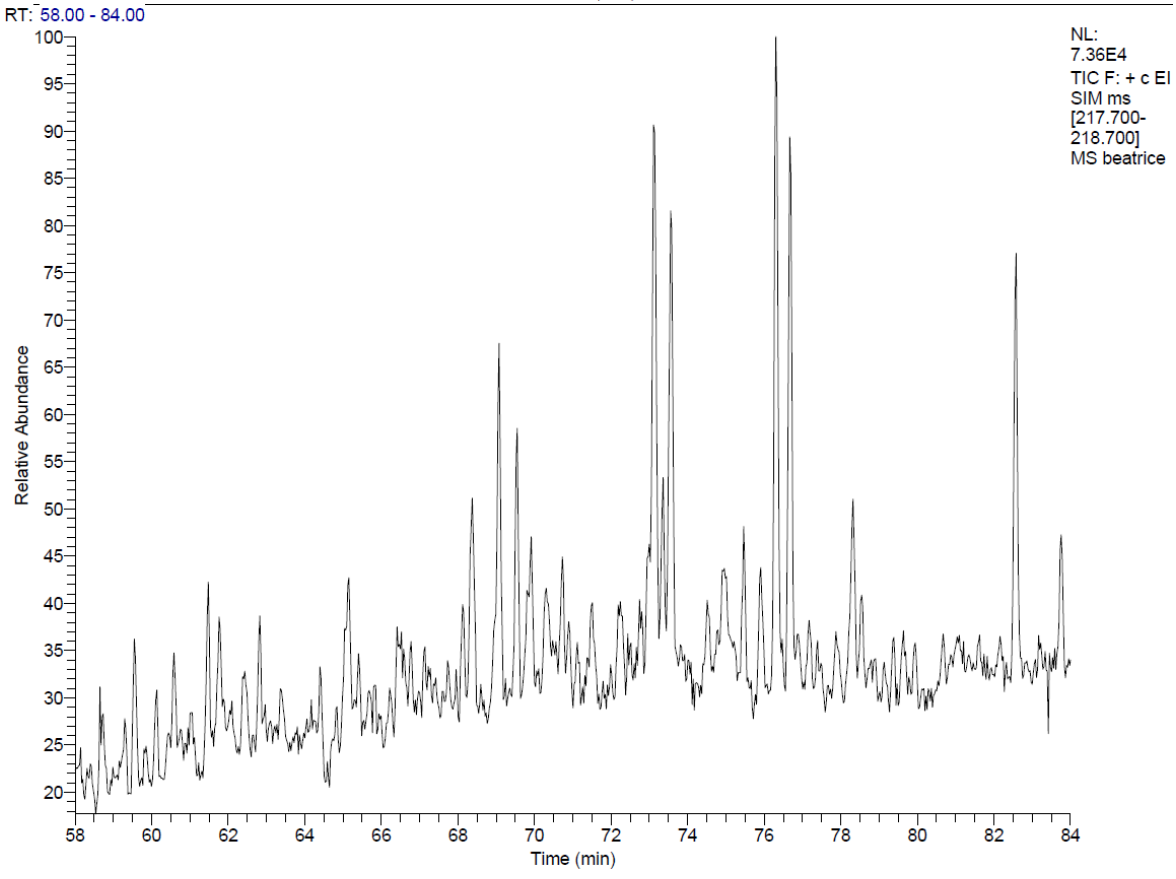
RT: 58.00 - 84.00
NL:
7.36E4
TIC F: + c EI
SIM ms
[217.700-
218.700]
MS beatrice
Relative Abundance
Time (min)

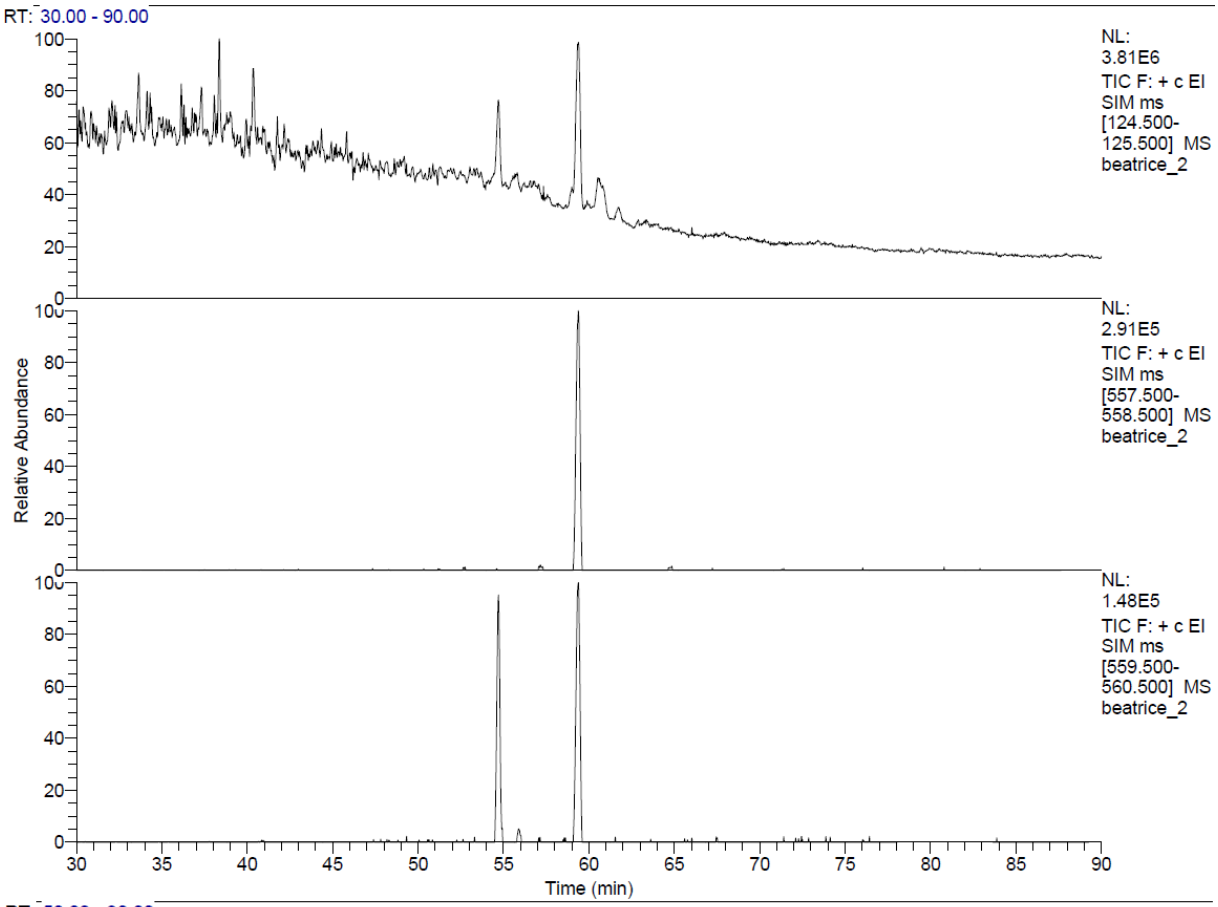
RT: 30.00 - 90.00
NL:
3.81E6
TIC F: + c EI
SIM ms
[124.500-
125.500] MS
beatrice_2
NL:
2.91E5
TIC F: + c EI
SIM ms
[557.500-
558.500] MS
beatrice_2
NL:
1.48E5
TIC F: + c EI
SIM ms
[559.500-
560.500] MS
beatrice_2
Relative Abundance
Time (min)

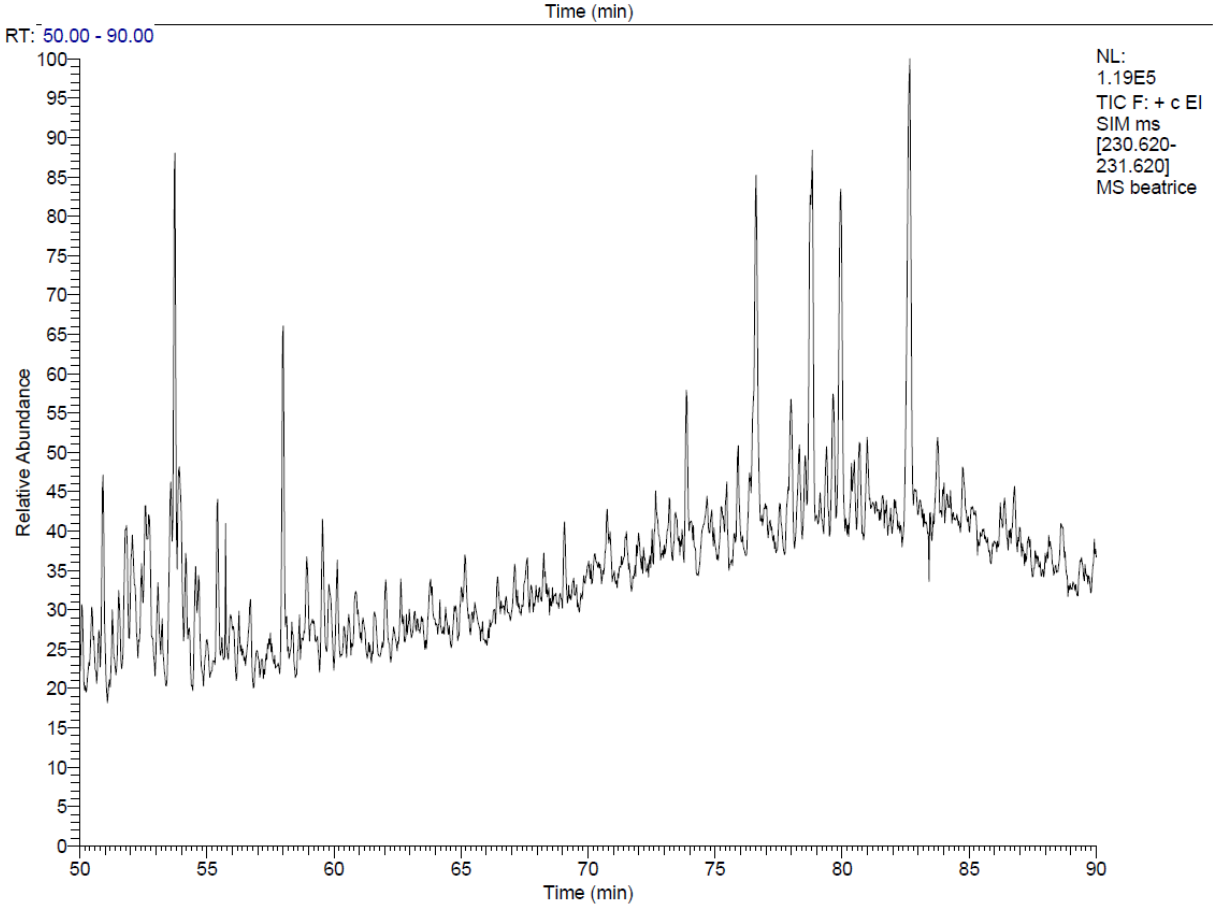
RT: 50.00 - 90.00
NL:
1.19E5
TIC F: + c EI
SIM ms
[230.620-
231.620]
MS beatrice
Relative Abundance
Time (min)

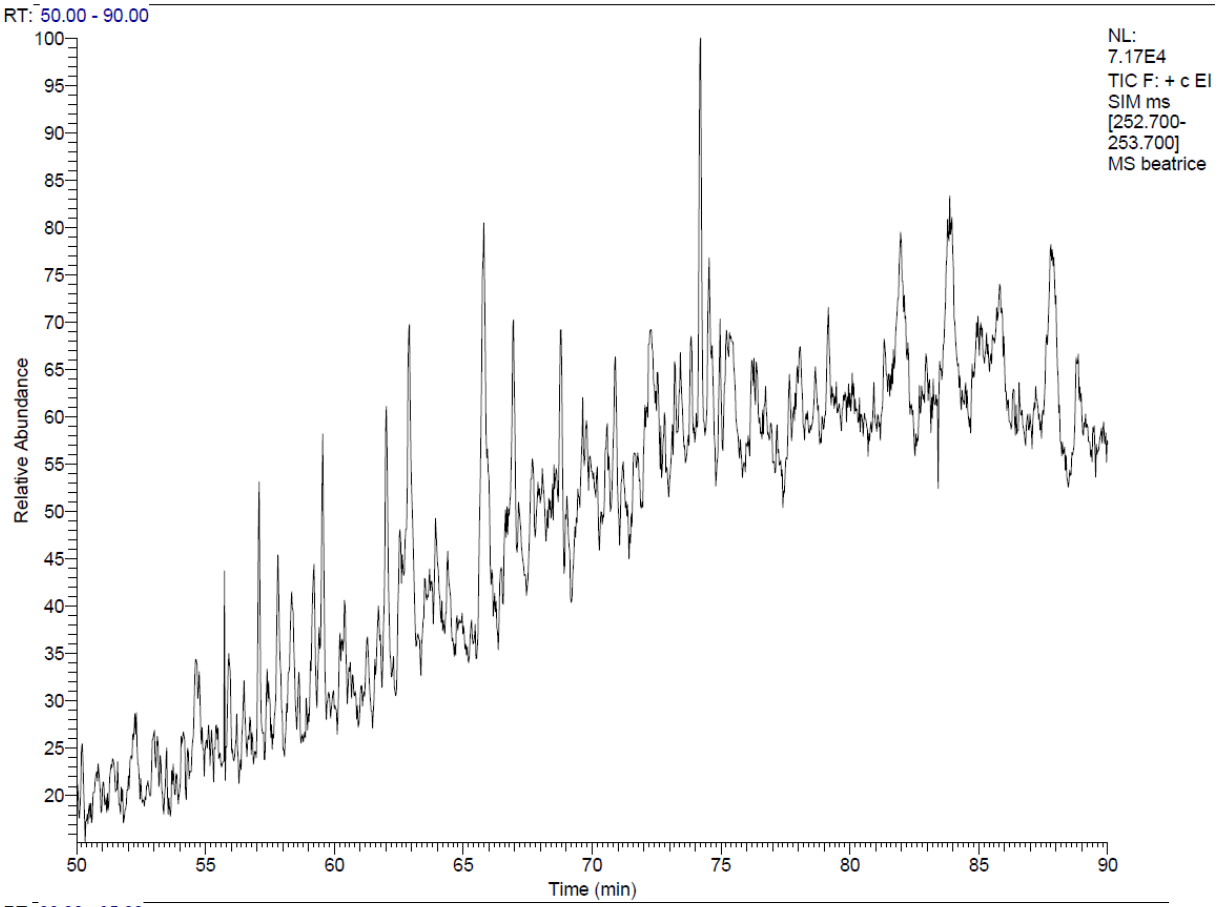
RT: 50.00 - 90.00
NL:
7.17E4
TIC F: + c EI
SIM ms
[252.700-
253.700]
MS beatrice
Relative Abundance
Time (min)

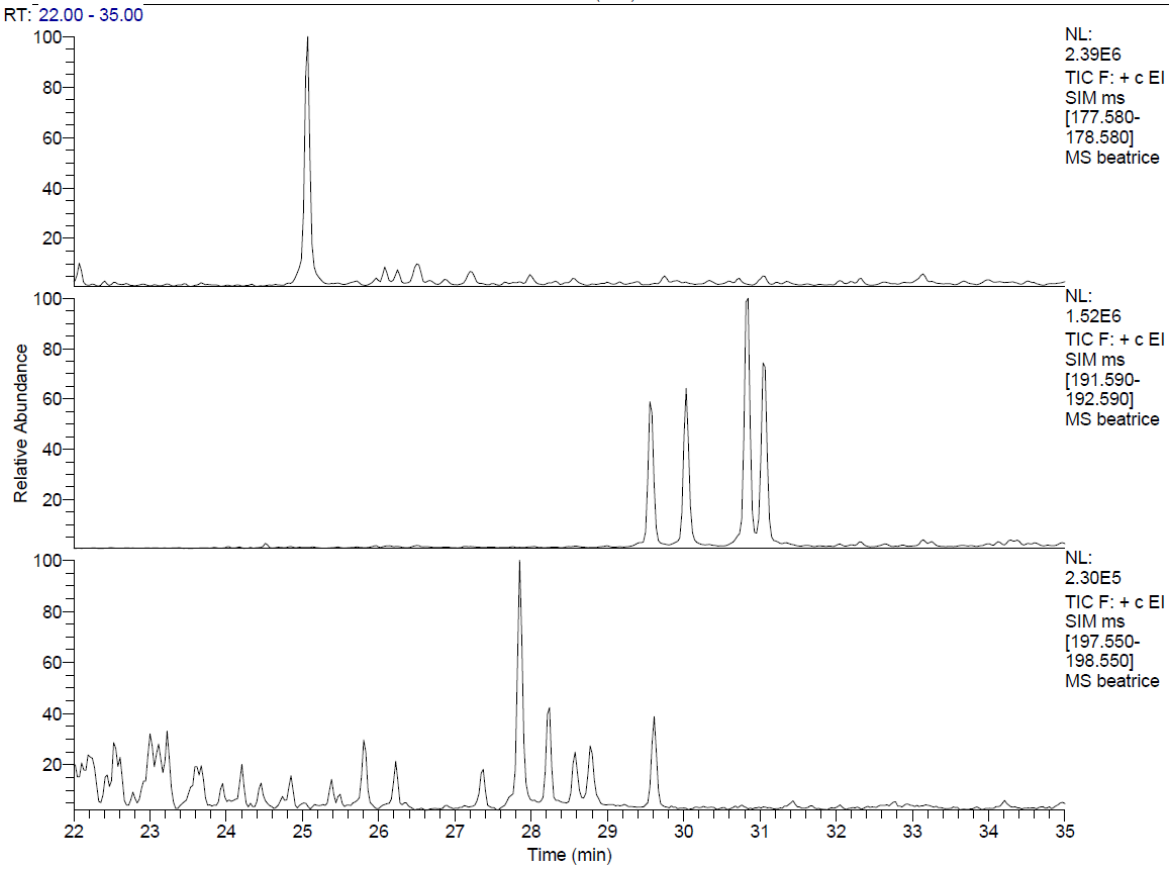
RT: 22.00 - 35.00
NL:
2.39E6
TIC F: + c EI
SIM ms
[177.580-
178.580]
MS beatrice
NL:
1.52E6
TIC F: + c EI
SIM ms
[191.590-
192.590]
MS beatrice
NL:
2.30E5
TIC F: + c EI
SIM ms
[197.550-
198.550]
MS beatrice
Relative Abundance
Time (min)

Judy

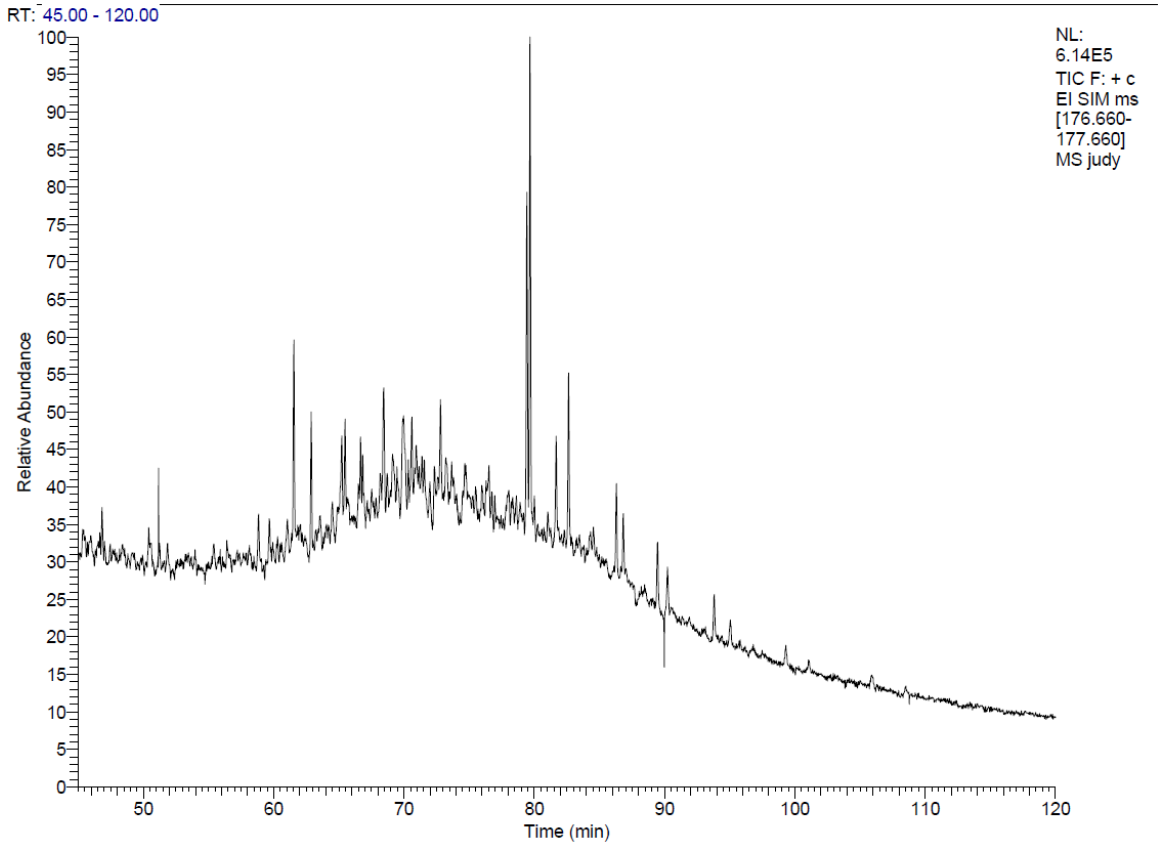
RT: 45.00 - 120.00
NL:
6.14E5
TIC F: + c
EI SIM ms
[176.660-
177.660]
MS judy
Relative Abundance
Time (min)

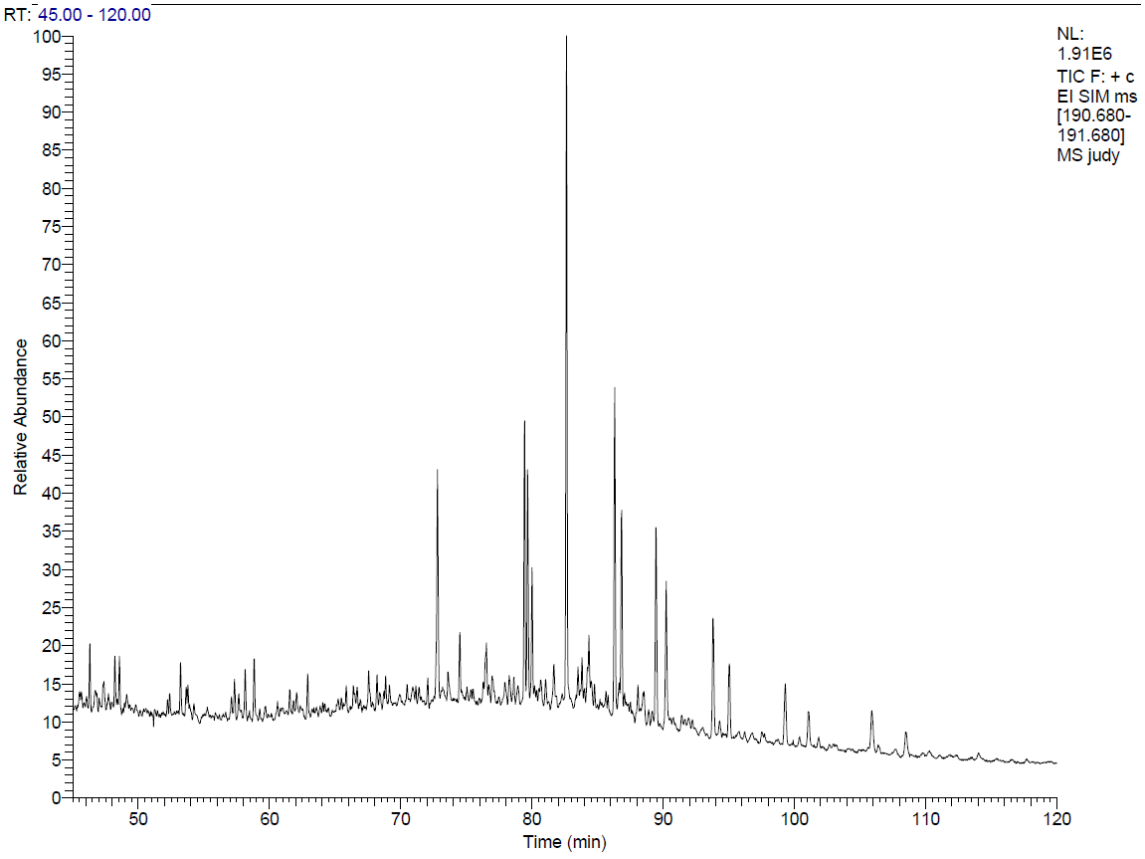
RT: 45.00 - 120.00
NL:
1.91E6
TIC F: + c
EI SIM ms
[190.680-
191.680]
MS judy
Relative Abundance
Time (min)

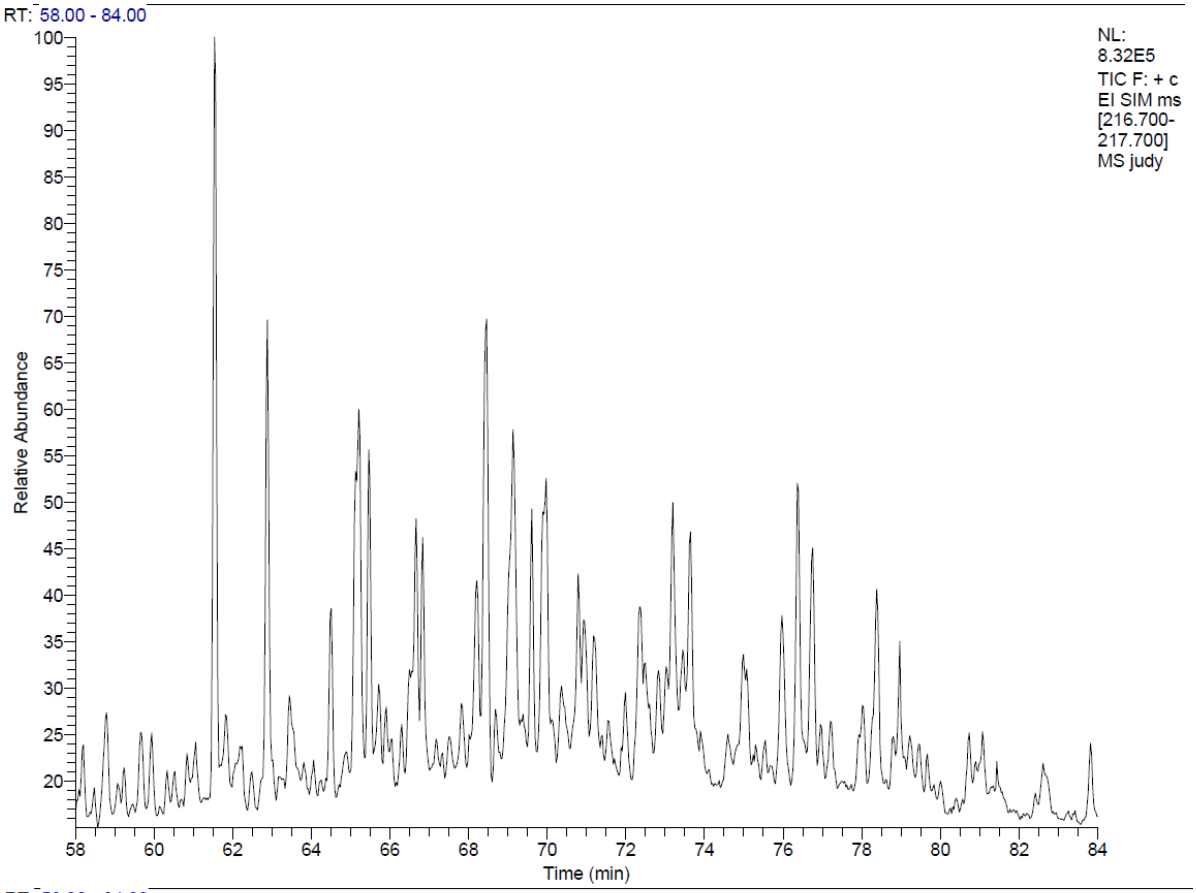
RT: 58.00 - 84.00
NL:
8.32E5
TIC F: + c
EI SIM ms
[216.700-
217.700]
MS judy
Relative Abundance
Time (min)

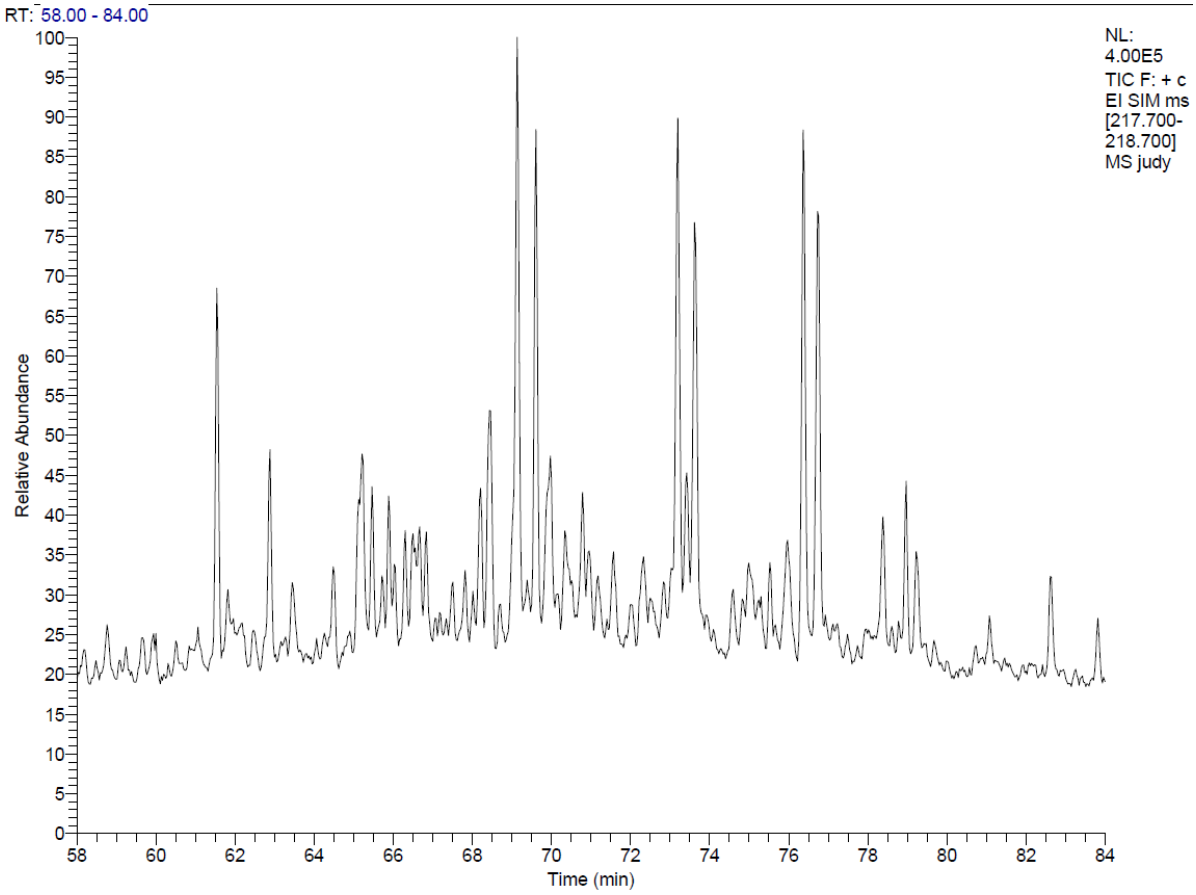
RT: 58.00 - 84.00
NL:
4.00E5
TIC F: + c
EI SIM ms
[217.700-
218.700]
MS judy
Relative Abundance
Time (min)

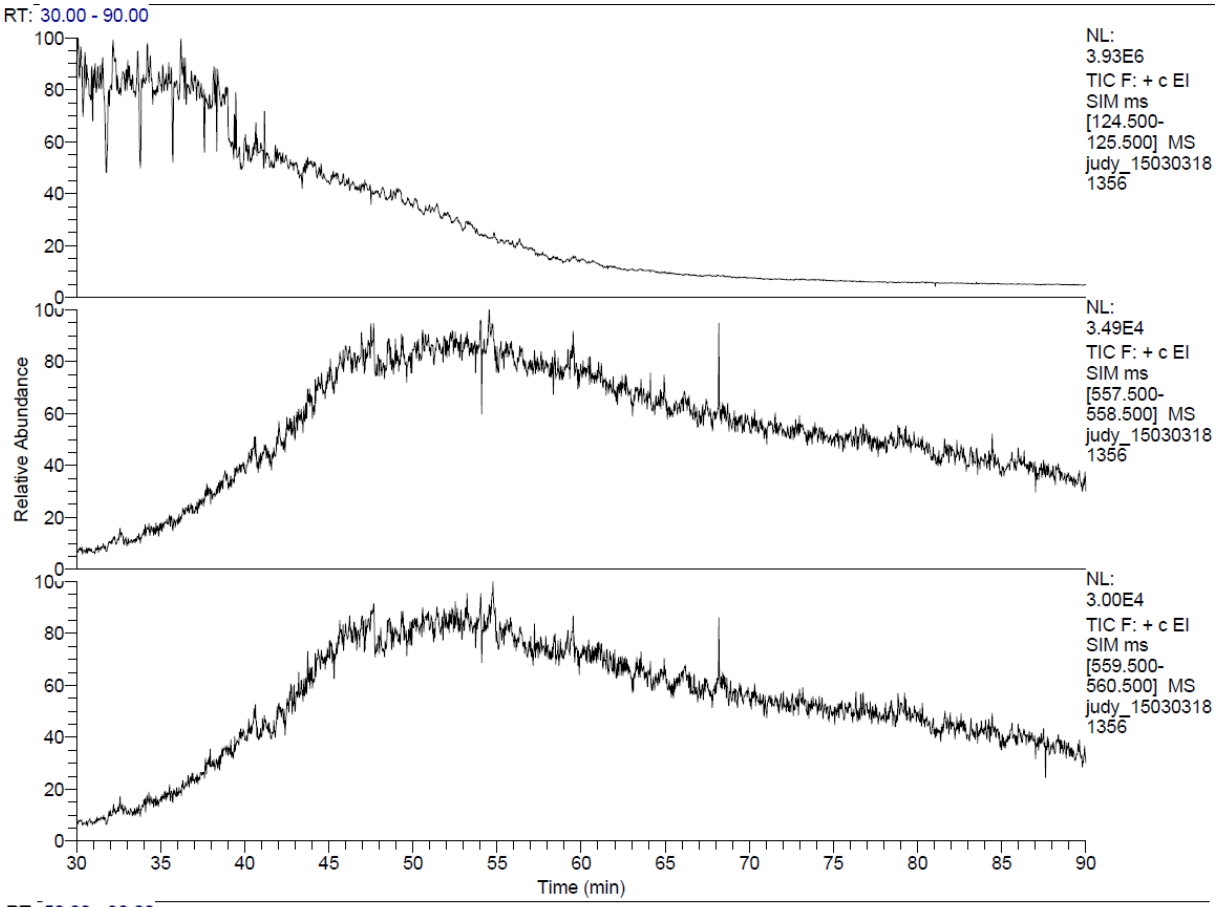
RT: 30.00 - 90.00
NL:
3.93E6
TIC F: + c EI
SIM ms
[124.500-
125.500] MS
judy_15030318
1356
NL:
3.49E4
TIC F: + c EI
SIM ms
[557.500-
558.500] MS
judy_15030318
1356
NL:
3.00E4
TIC F: + c EI
SIM ms
[559.500-
560.500] MS
judy_15030318
1356
Relative Abundance
Time (min)

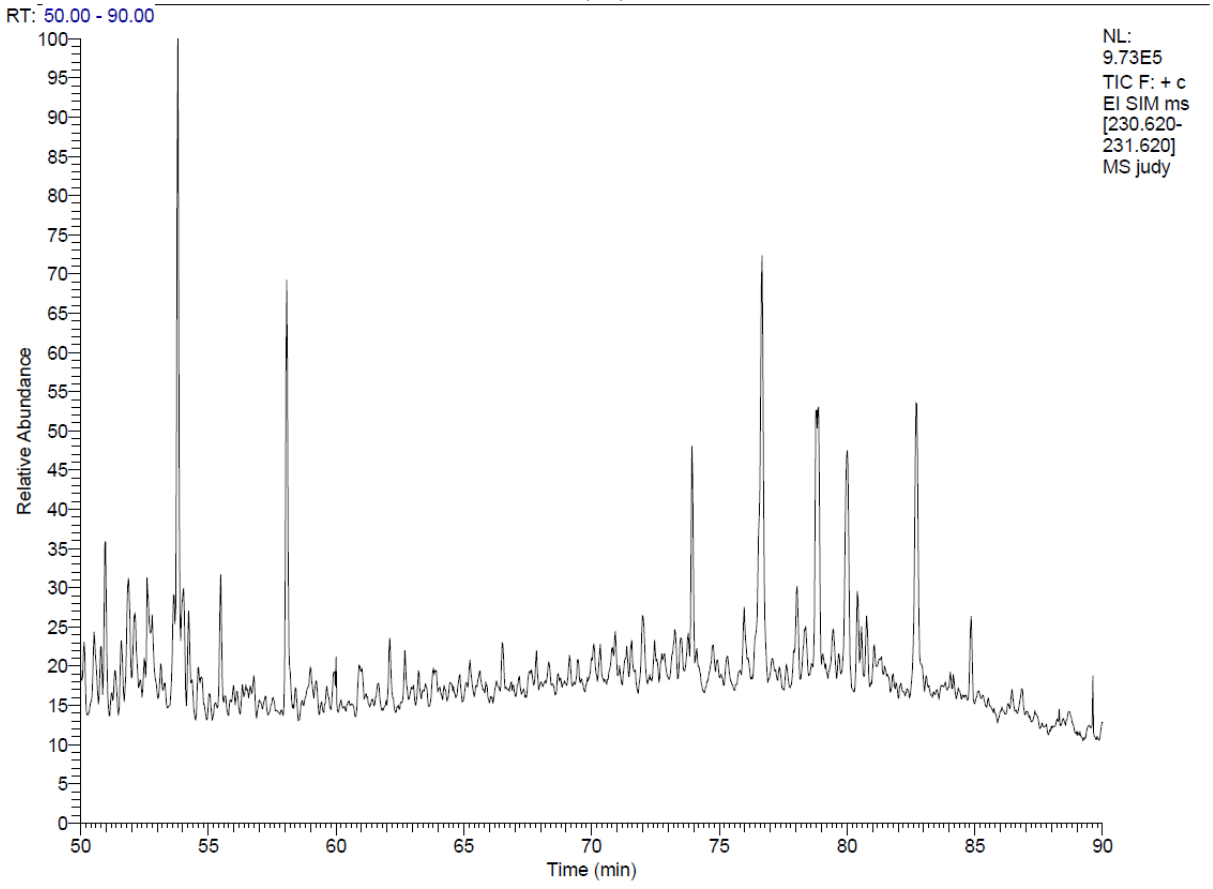
RT: 50.00 - 90.00
NL:
9.73E5
TIC F: + c
EI SIM ms
[230.620-
231.620]
MS judy
Relative Abundance
Time (min)

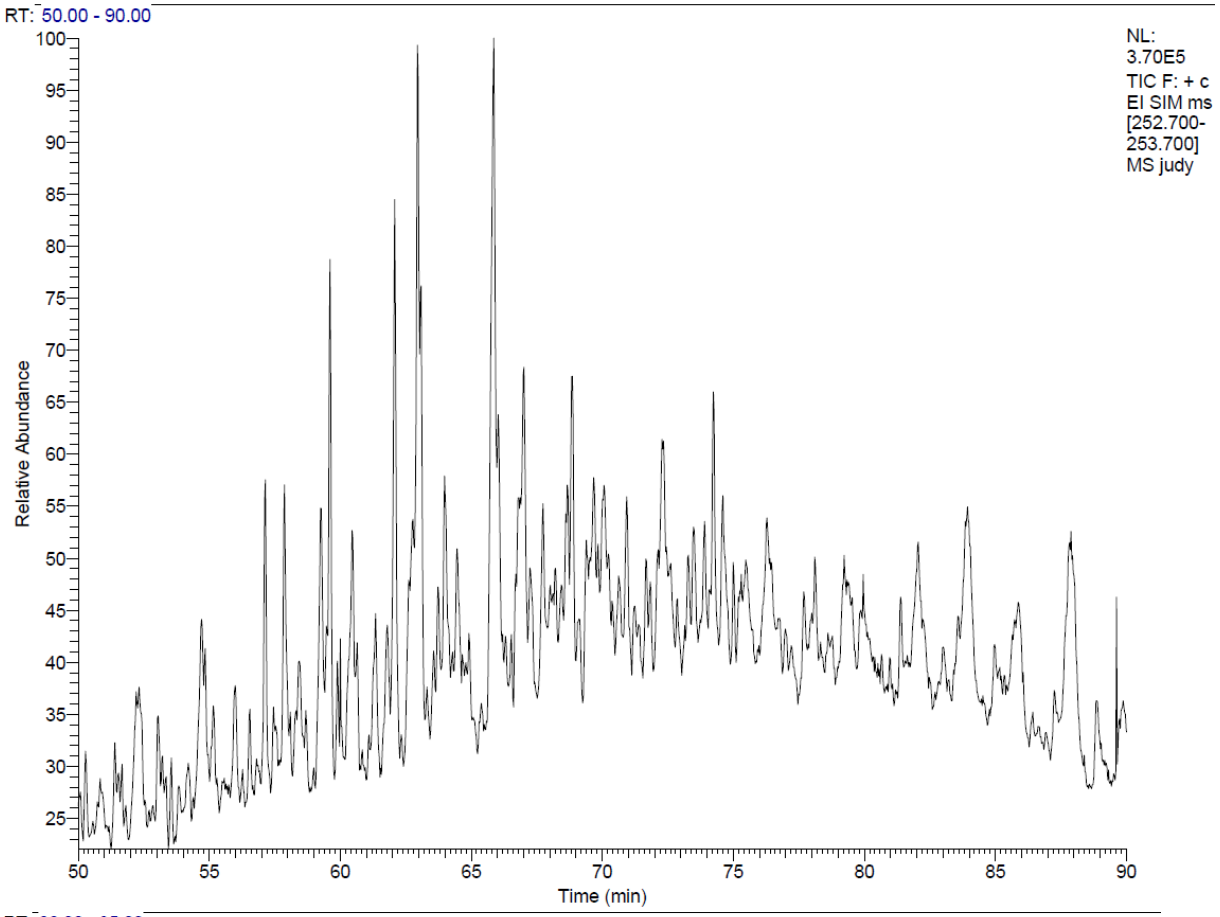
RT: 50.00 - 90.00
NL:
3.70E5
TIC F: + c
EI SIM ms
[252.700-
253.700]
MS judy
Relative Abundance
Time (min)

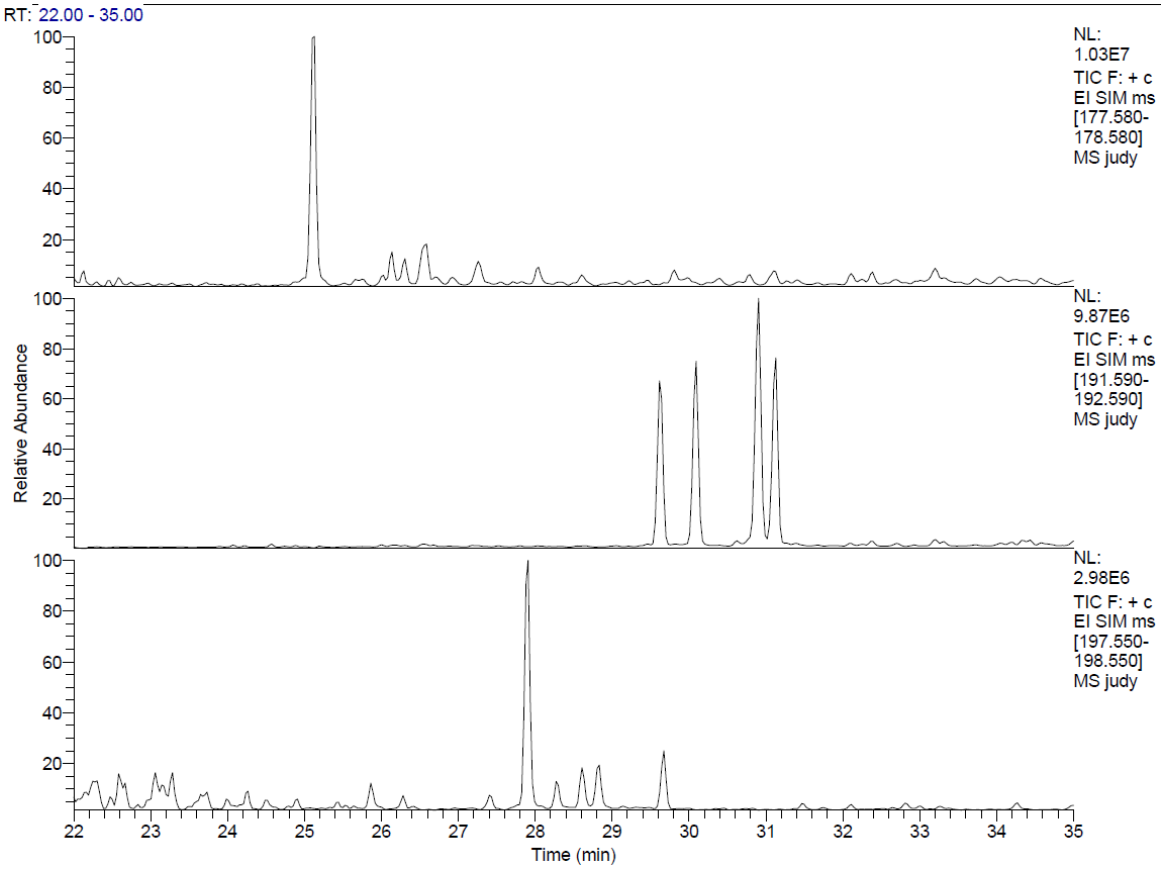
RT: 22.00 - 35.00
NL:
1.03E7
TIC F: + c
EI SIM ms
[177.580-
178.580]
MS judy
NL:
9.87E6
TIC F: + c
EI SIM ms
[191.590-
192.590]
MS judy
NL:
2.98E6
TIC F: + c
EI SIM ms
[197.550-
198.550]
MS judy
Relative Abundance
Time (min)

A-1

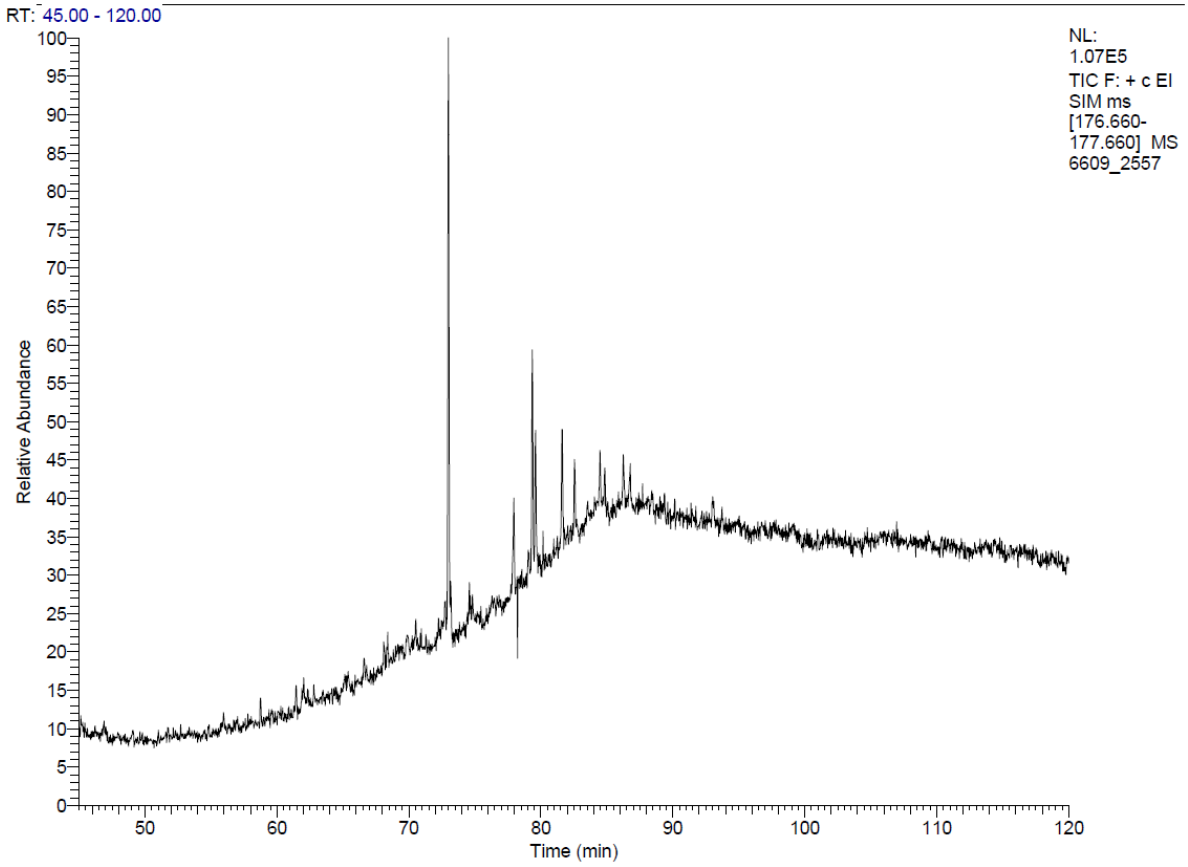
RT: 45.00 - 120.00
NL:
1.07E5
TIC F: + c EI
SIM ms
[176.660-
177.660] MS
6609_2557
Relative Abundance
Time (min)

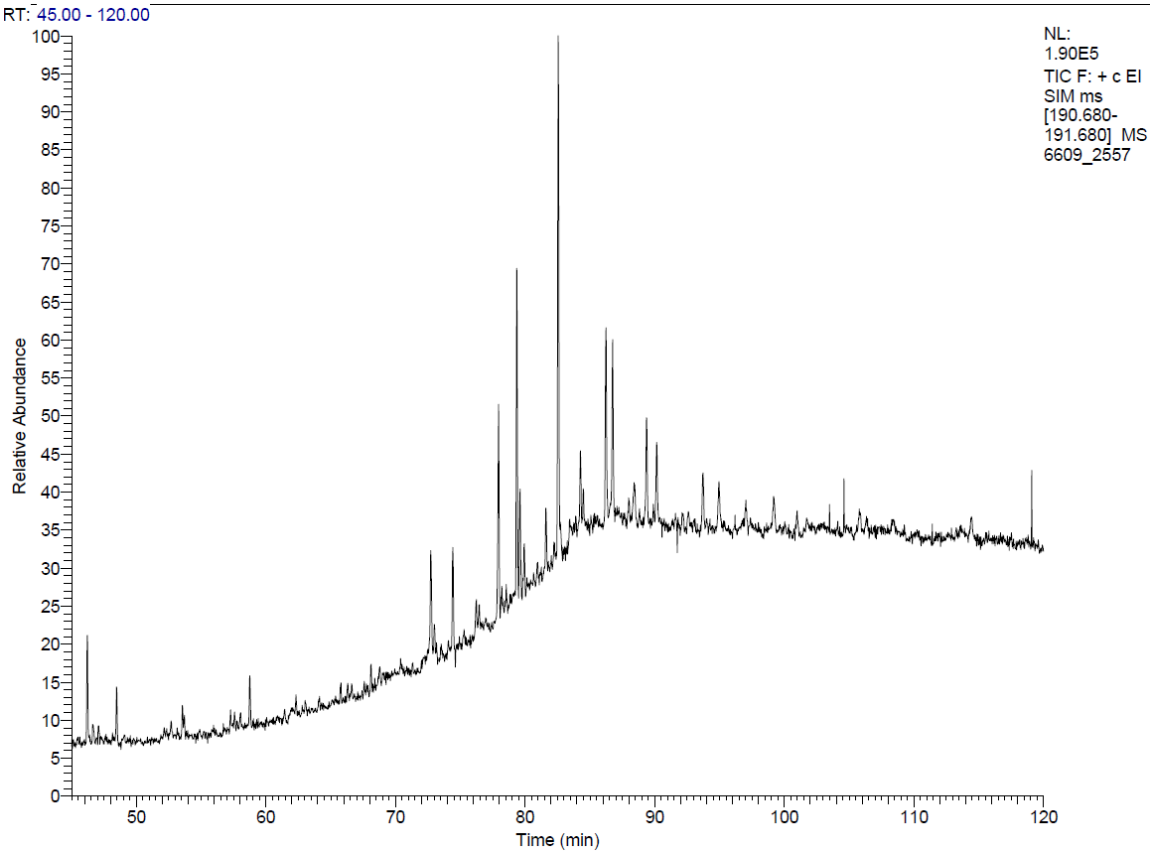
RT: 45.00 - 120.00
NL:
1.90E5
TIC F: + c EI
SIM ms
[190.680-
191.680] MS
6609_2557
Relative Abundance
Time (min)

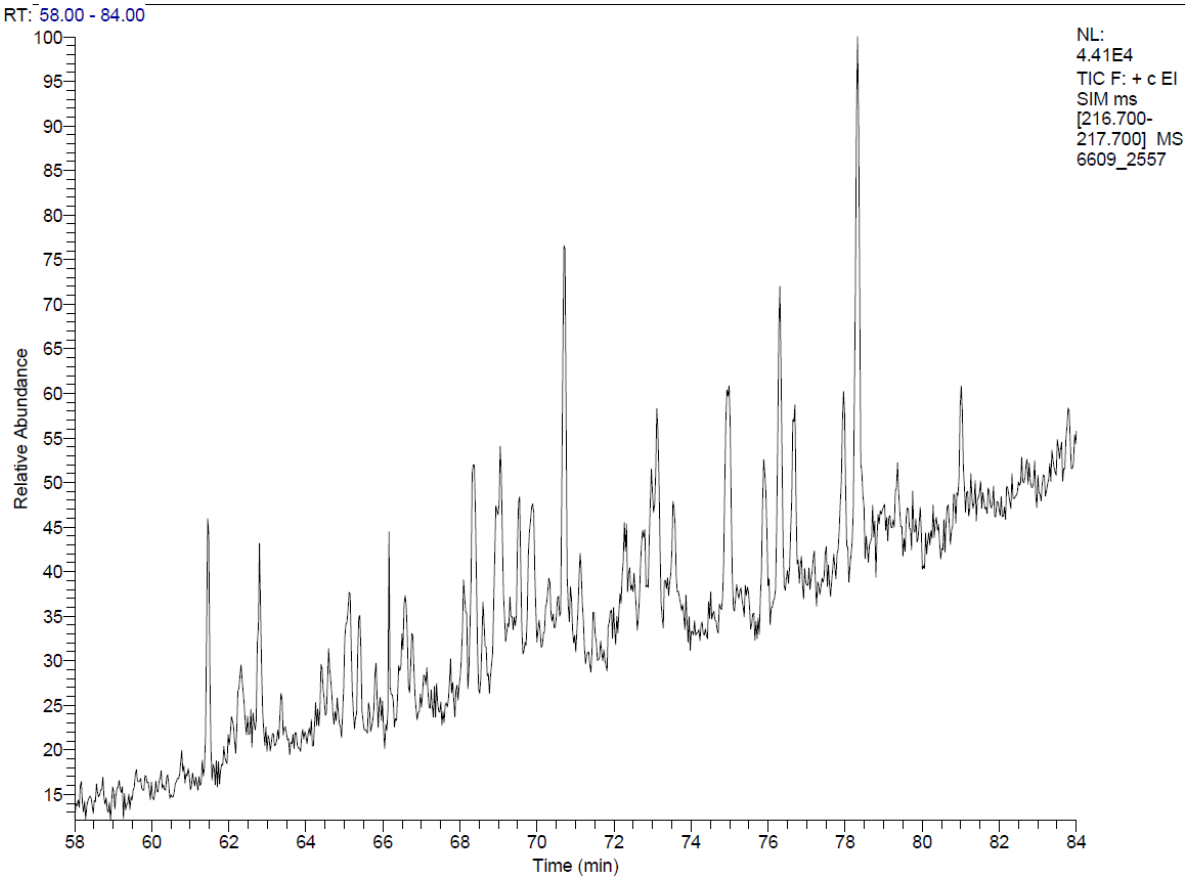
RT: 58.00 - 84.00
NL:
4.41E4
TIC F: + c EI
SIM ms
[216.700-
217.700] MS
6609_2557
Relative Abundance
Time (min)

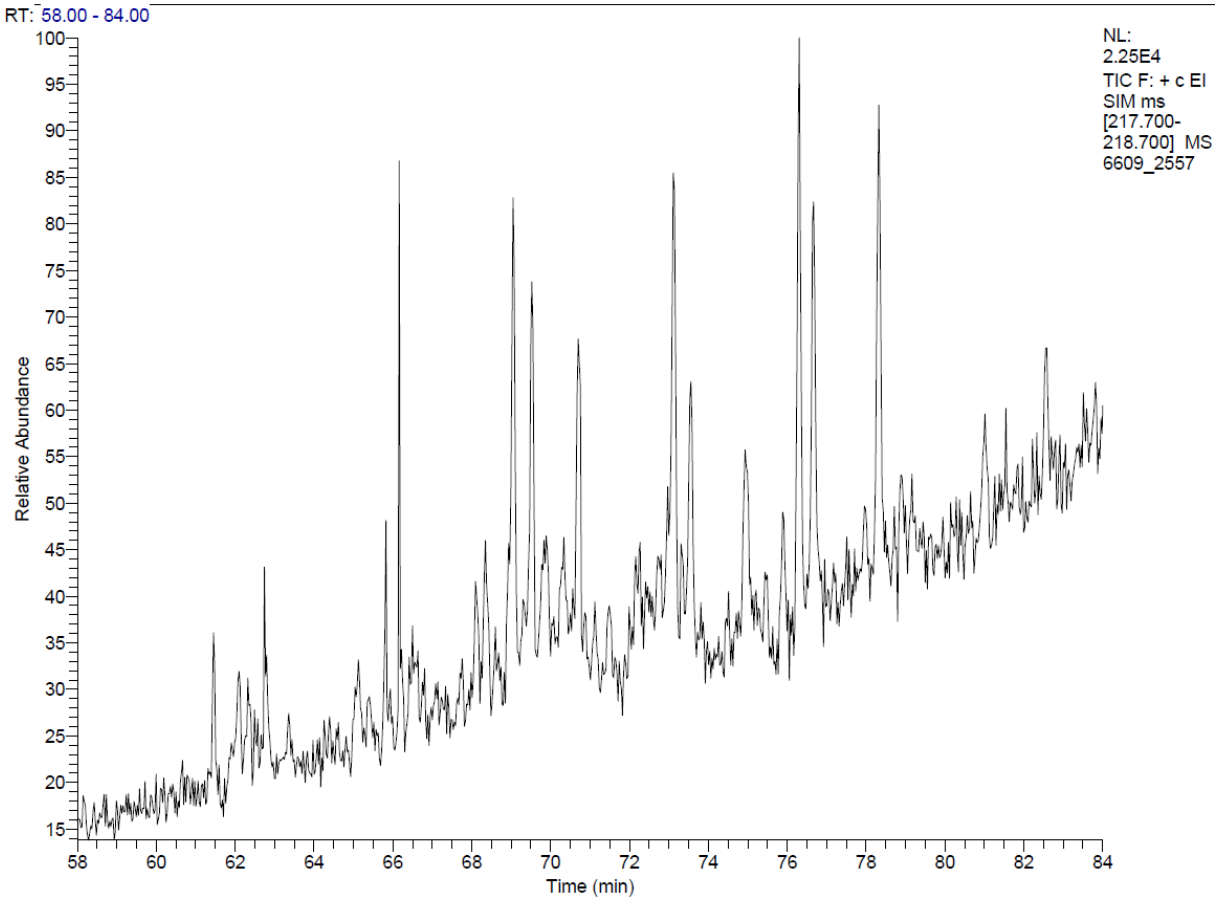
RT: 58.00 - 84.00
NL:
2.25E4
TIC F: + c EI
SIM ms
[217.700-
218.700] MS
6609_2557
Relative Abundance
Time (min)

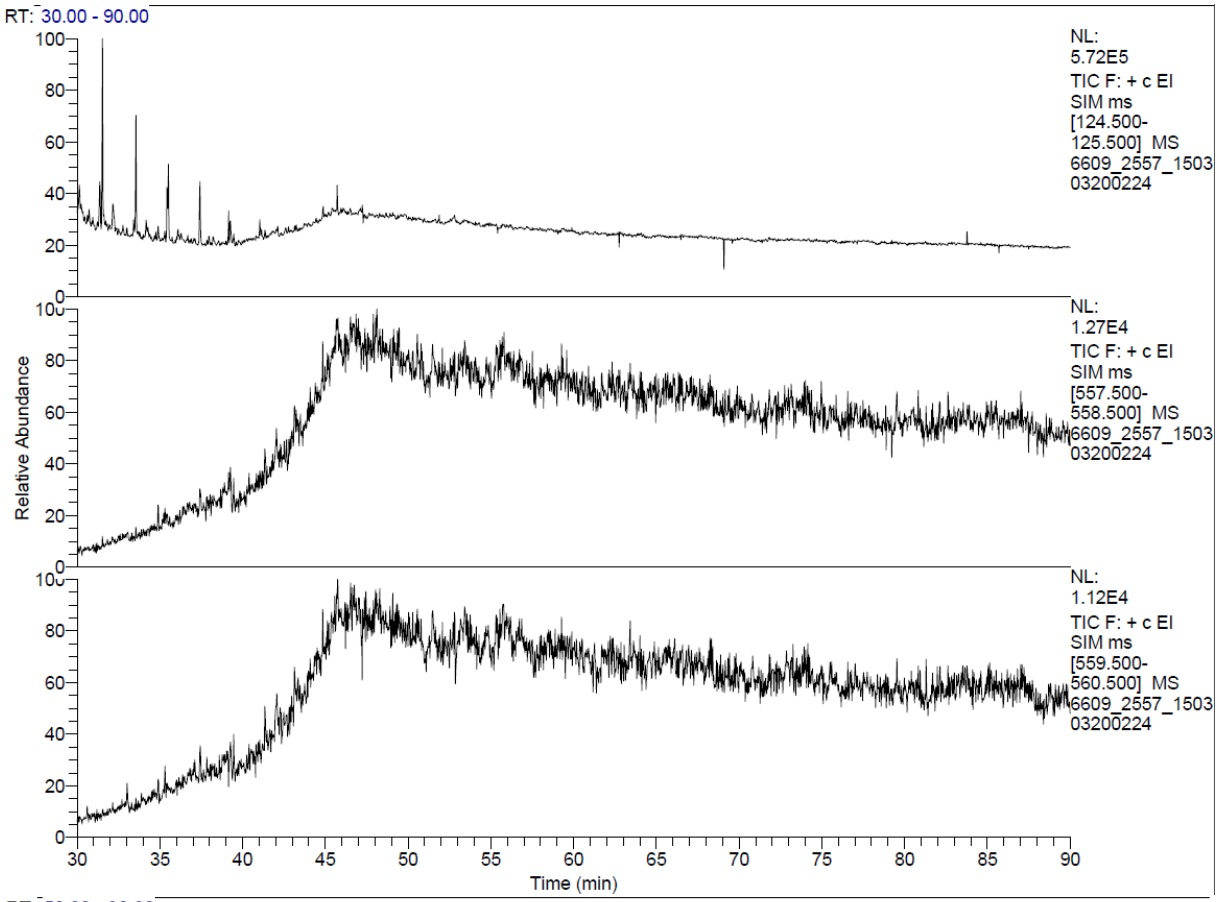
RT: 30.00 - 90.00
NL:
5.72E5
TIC F: + c EI
SIM ms
[124.500-
125.500] MS
6609_2557_1503
03200224
NL:
1.27E4
TIC F: + c EI
SIM ms
[557.500-
558.500] MS
6609_2557_1503
03200224
NL:
1.12E4
TIC F: + c EI
SIM ms
[559.500-
560.500] MS
6609_2557_1503
03200224
Relative Abundance
Time (min)

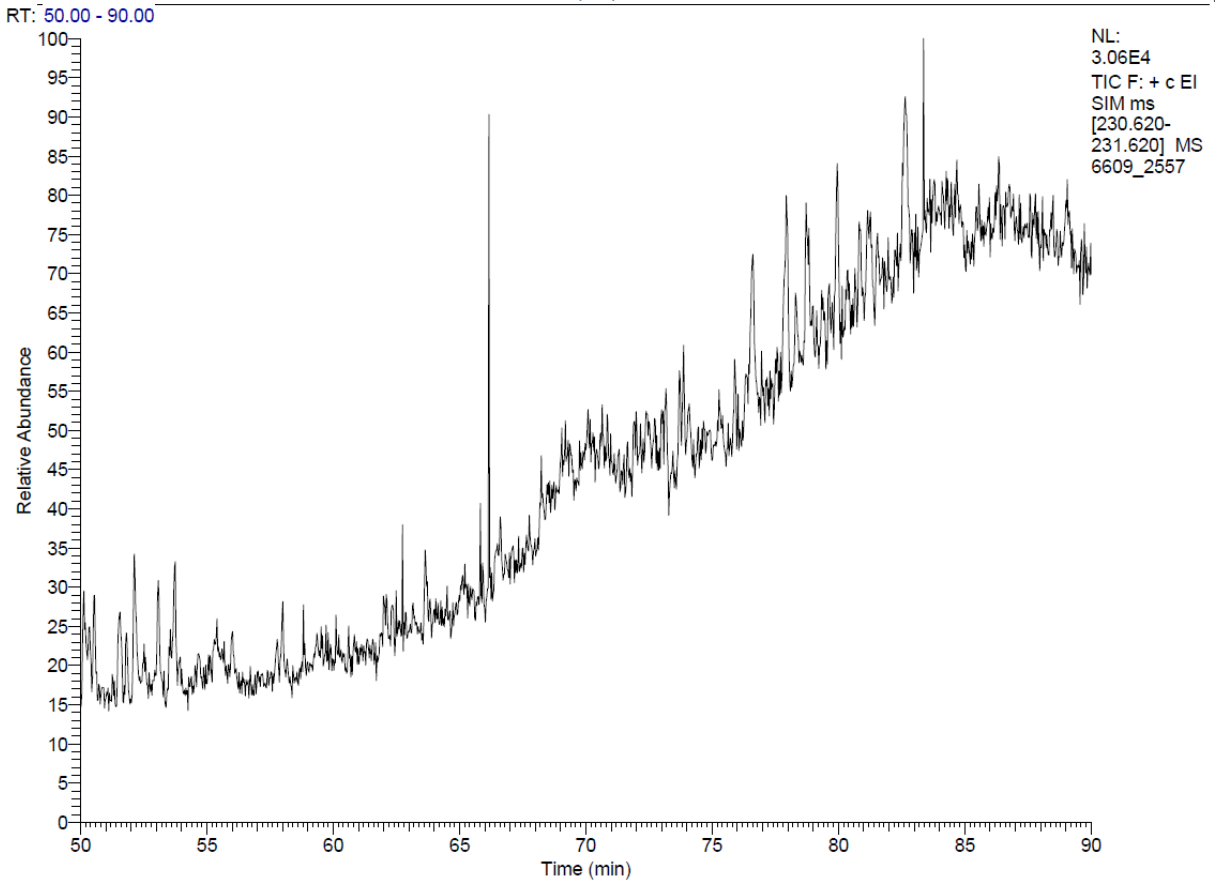
RT: 50.00 - 90.00
NL:
3.06E4
TIC F: + c EI
SIM ms
[230.620-
231.620] MS
6609_2557
Relative Abundance
Time (min)

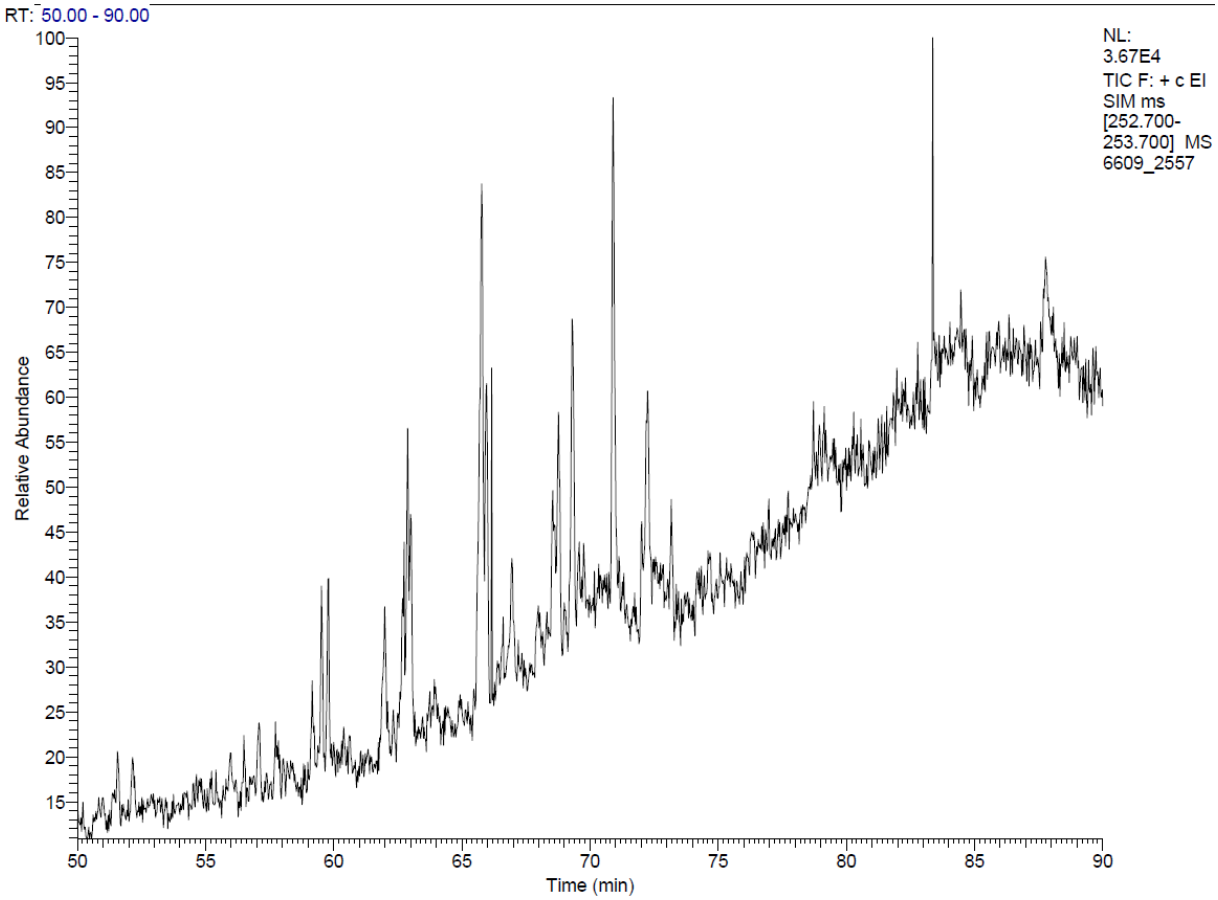
RT: 50.00 - 90.00
NL:
3.67E4
TIC F: + c EI
SIM ms
[252.700-
253.700] MS
6609_2557
Relative Abundance
Time (min)

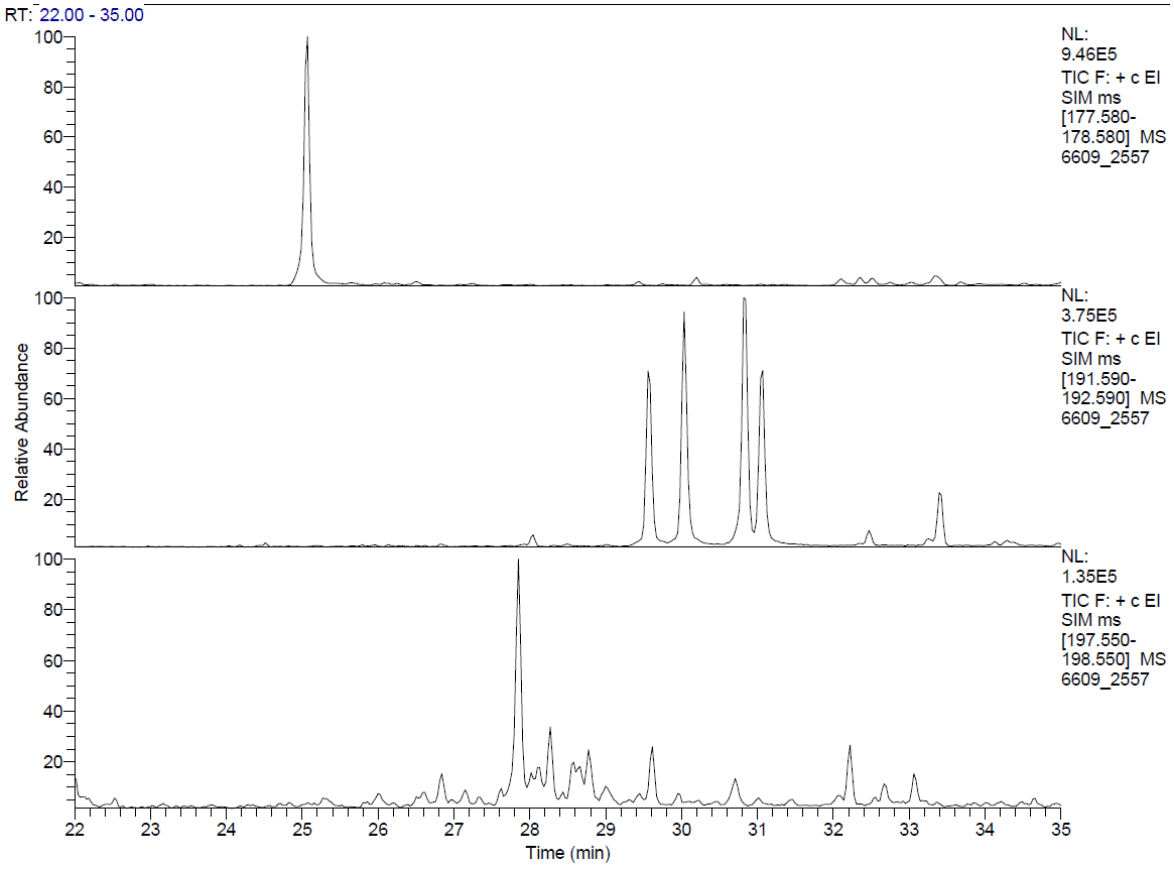
RT: 22.00 - 35.00
NL:
9.46E5
TIC F: + c EI
SIM ms
[177.580-
178.580] MS
6609_2557
NL:
3.75E5
TIC F: + c EI
SIM ms
[191.590-
192.590] MS
6609_2557
NL:
1.35E5
TIC F: + c EI
SIM ms
[197.550-
198.550] MS
6609_2557
Relative Abundance
Time (min)

A-2

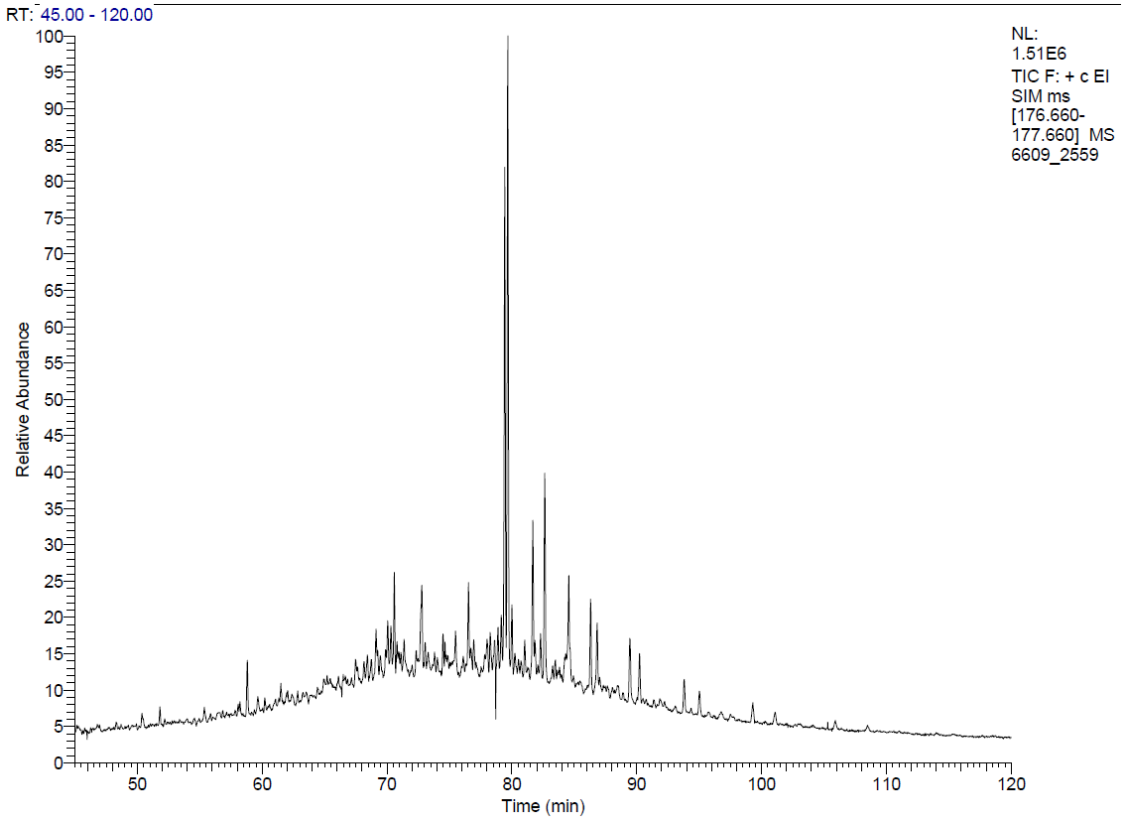
RT: 45.00 - 120.00
NL:
1.51E6
TIC F: + c EI
SIM ms
[176.660-
177.660] MS
6609_2559
Relative Abundance
Time (min)

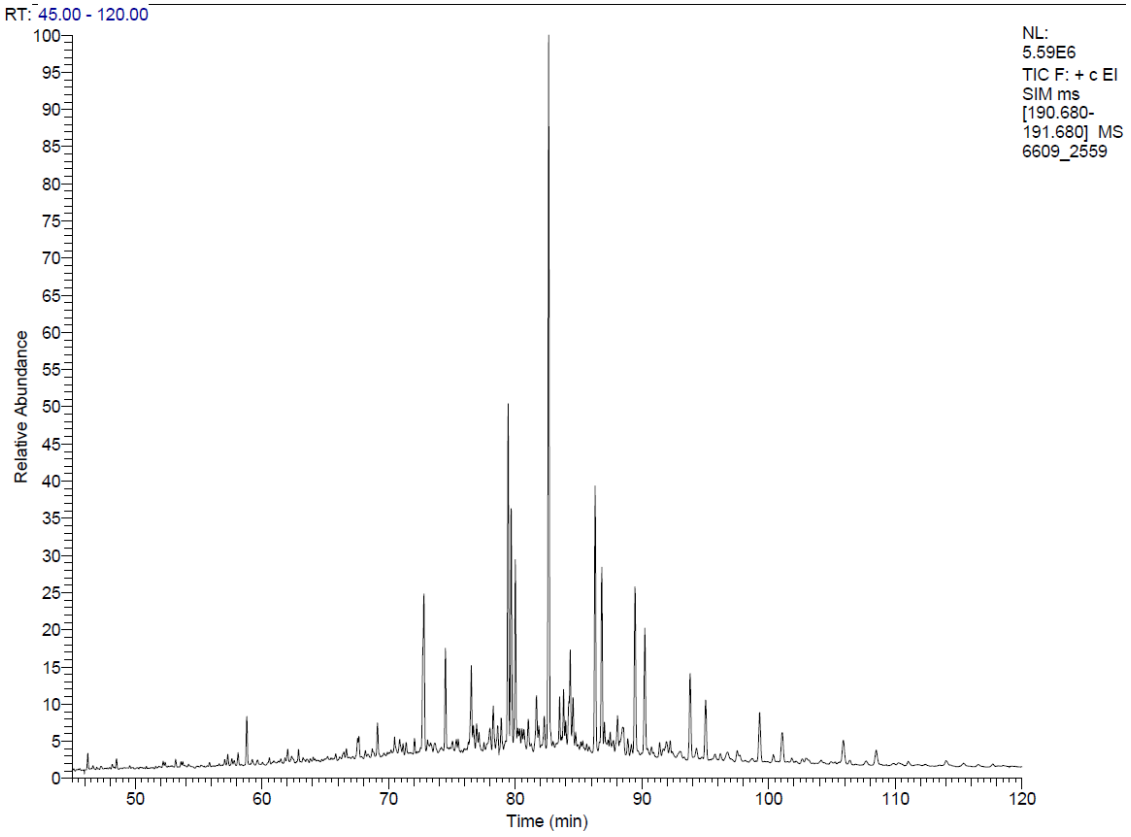
RT: 45.00 - 120.00
NL:
5.59E6
TIC F: + c EI
SIM ms
[190.680-
191.680] MS
6609_2559
Relative Abundance
Time (min)

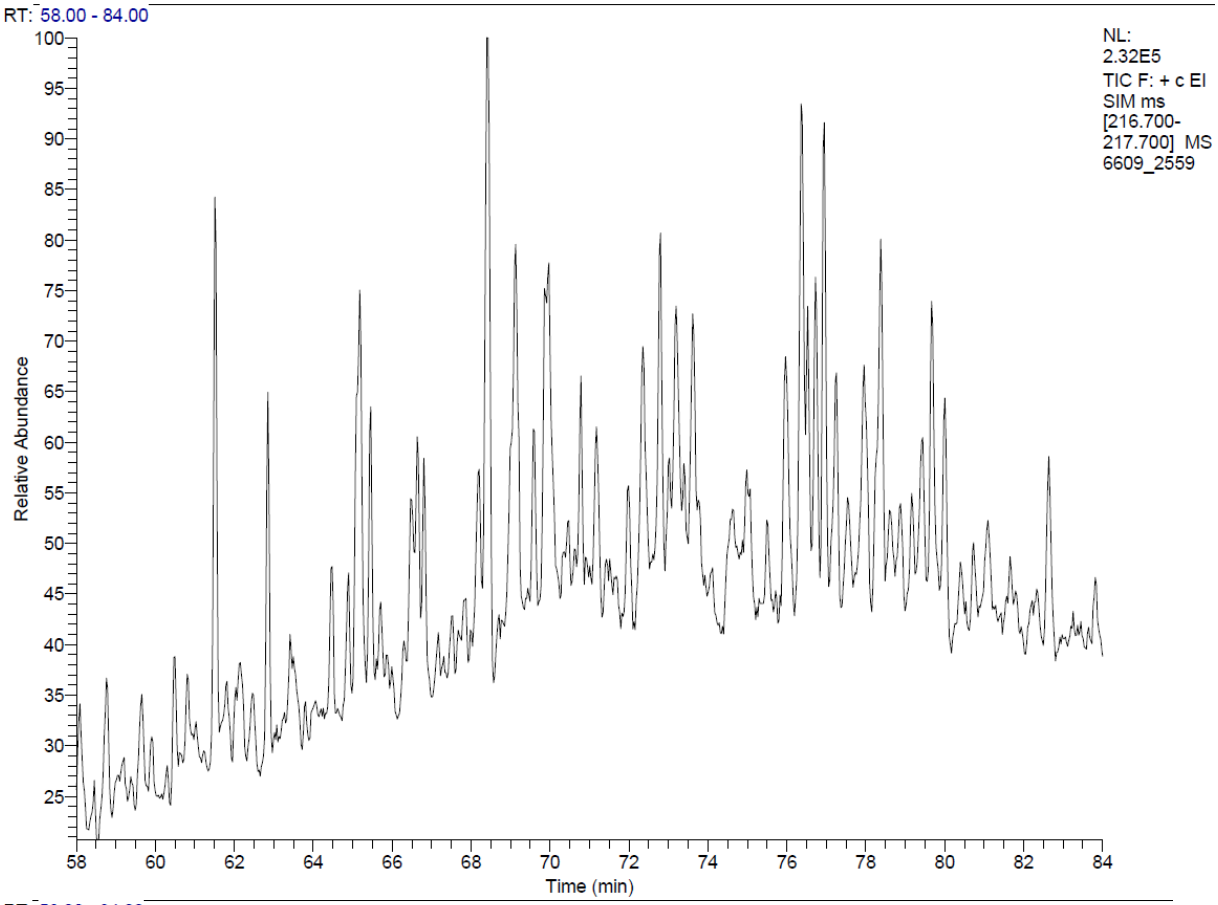
RT: 58.00 - 84.00
NL:
2.32E5
TIC F: + c EI
SIM ms
[216.700-
217.700] MS
6609_2559
Relative Abundance
Time (min)

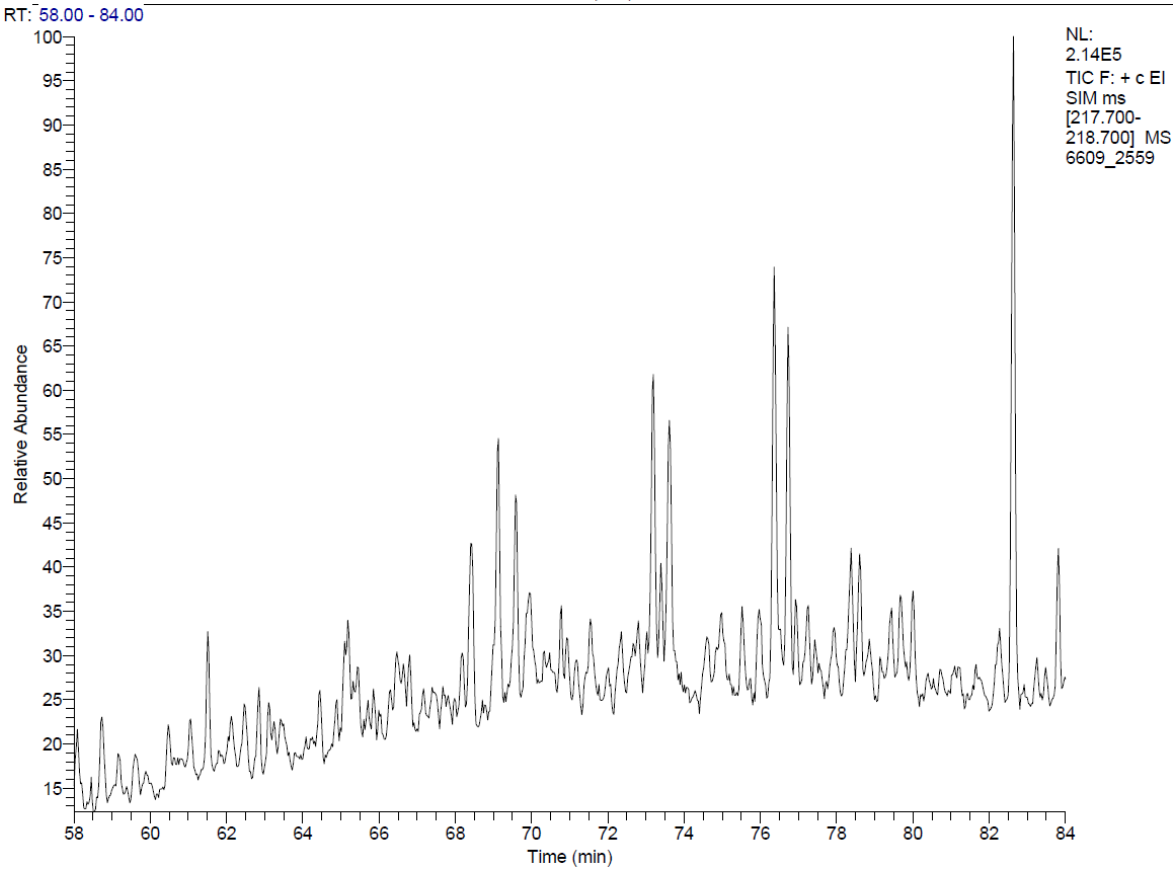
RT: 58.00 - 84.00
NL:
2.14E5
TIC F: + c EI
SIM ms
[217.700-
218.700] MS
6609_2559
Relative Abundance
Time (min)

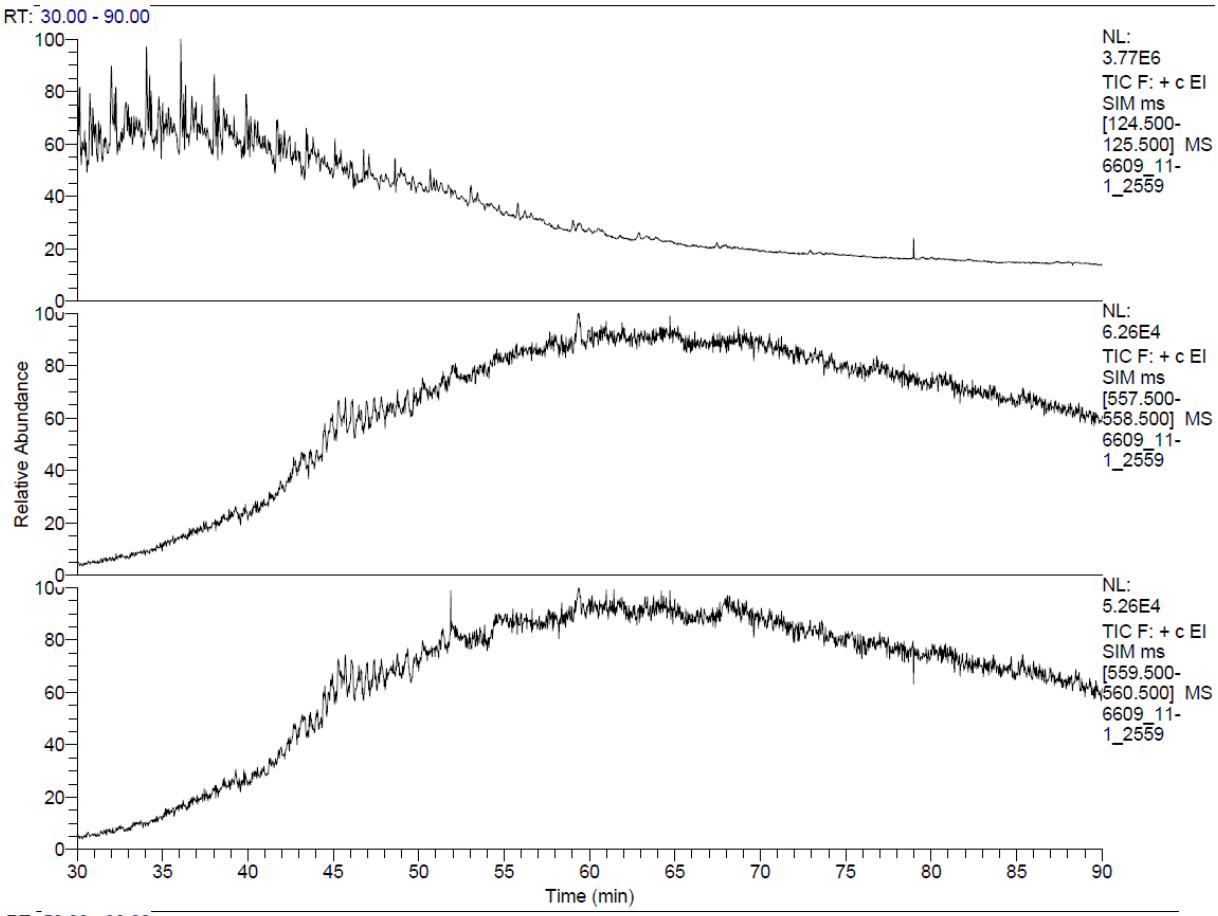
RT: 30.00 - 90.00
NL:
3.77E6
TIC F: + c EI
SIM ms
[124.500-
125.500] MS
6609_11-
1_2559
NL:
6.26E4
TIC F: + c EI
SIM ms
[557.500-
558.500] MS
6609_11-
1_2559
NL:
5.26E4
TIC F: + c EI
SIM ms
[559.500-
560.500] MS
6609_11-
1_2559
Relative Abundance
Time (min)

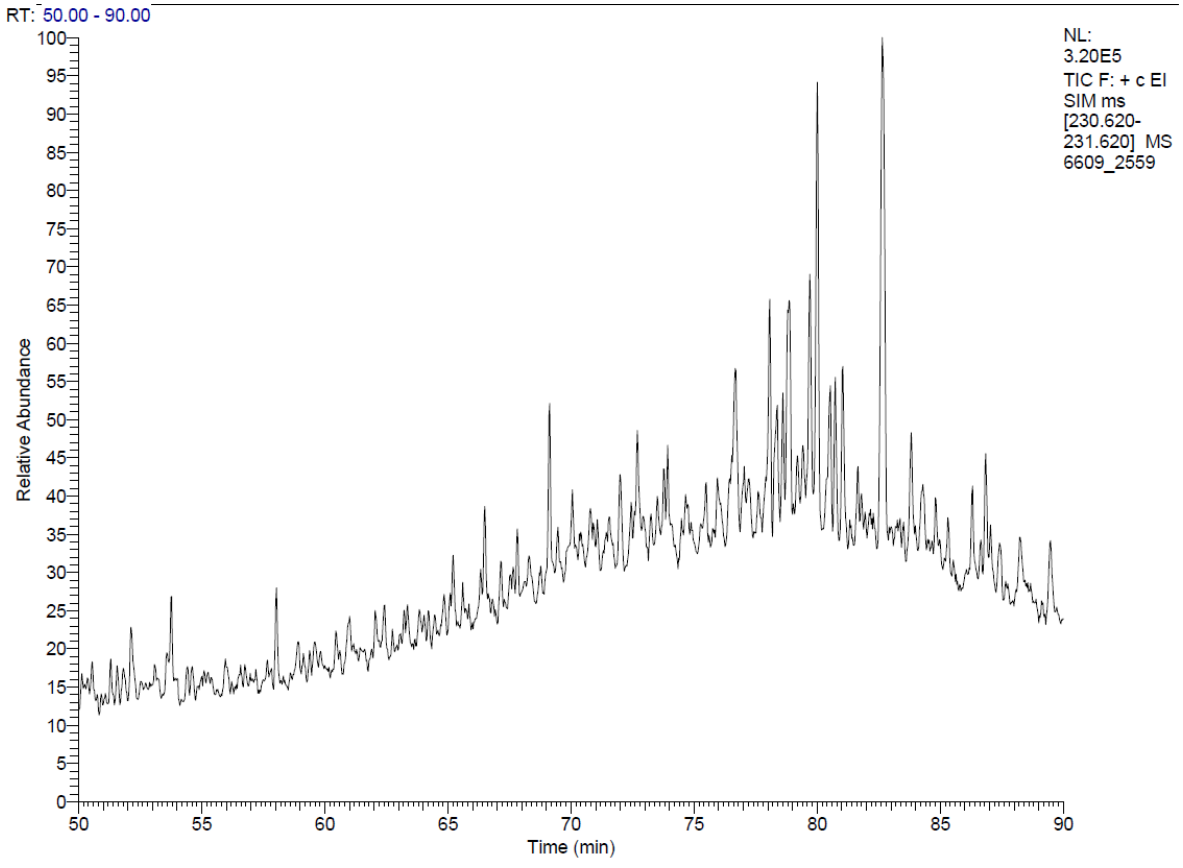
RT: 50.00 - 90.00
NL:
3.20E5
TIC F: + c EI
SIM ms
[230.620-
231.620] MS
6609_2559
Relative Abundance
Time (min)

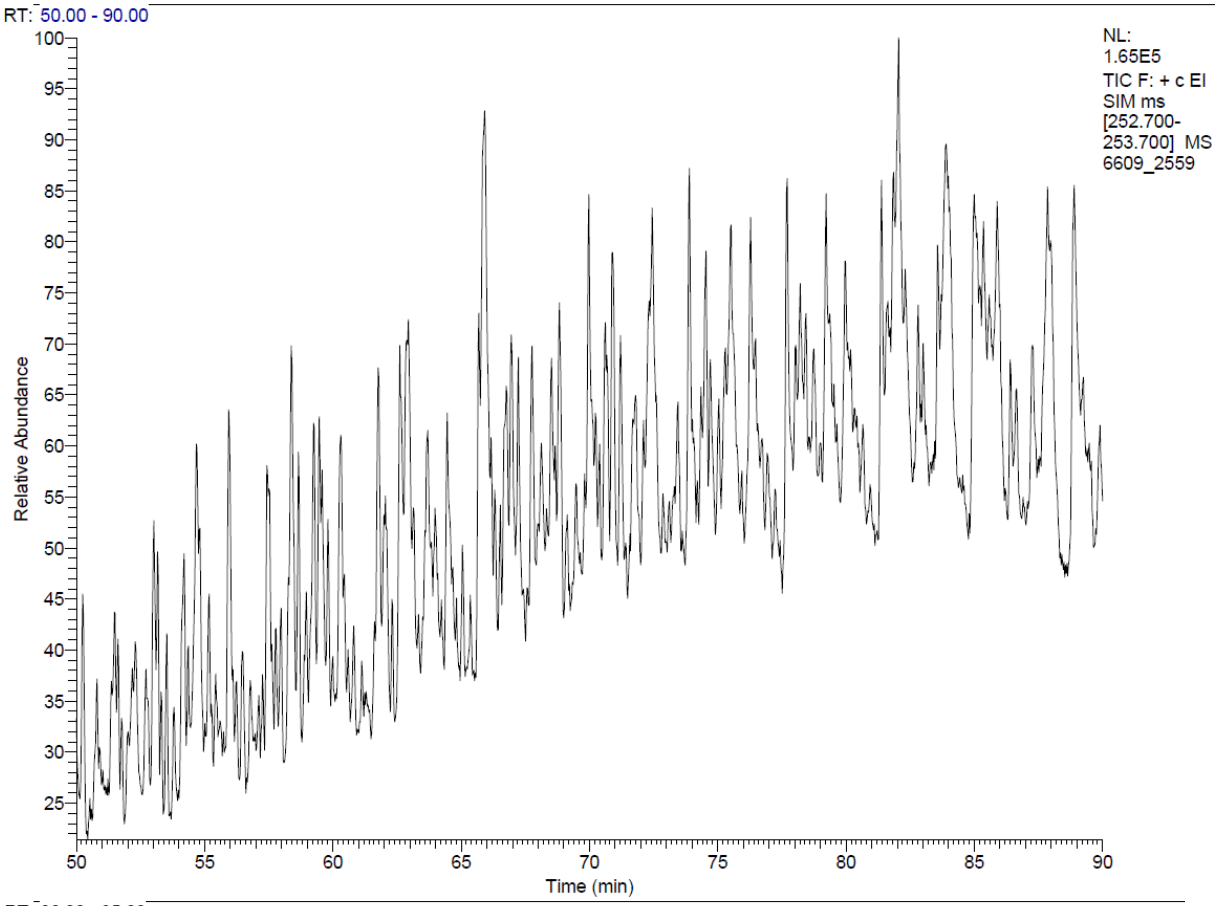
RT: 50.00 - 90.00
NL:
1.65E5
TIC F: + c EI
SIM ms
[252.700-
253.700] MS
6609_2559
Relative Abundance
Time (min)

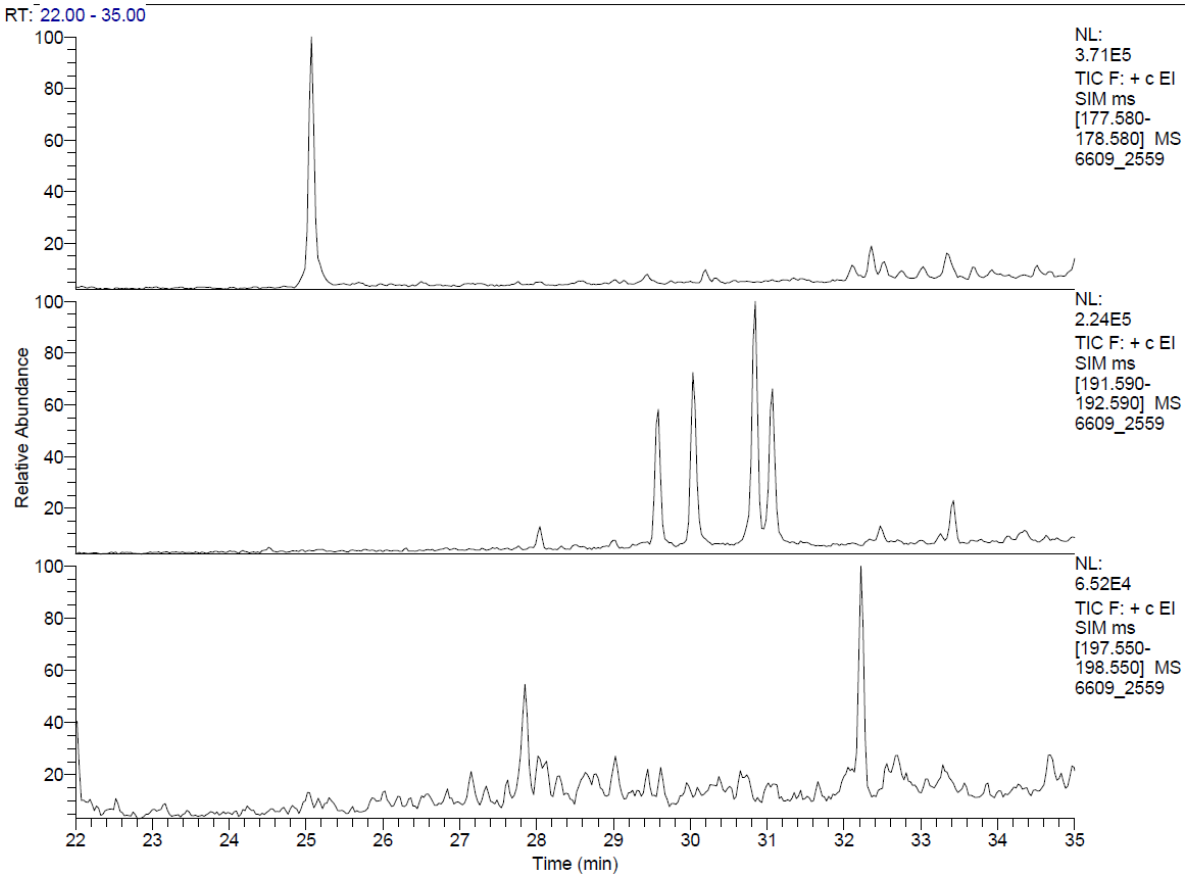
RT: 22.00 - 35.00
NL:
3.71E5
TIC F: + c EI
SIM ms
[177.580-
178.580] MS
6609_2559
NL:
2.24E5
TIC F: + c EI
SIM ms
[191.590-
192.590] MS
6609_2559
NL:
6.52E4
TIC F: + c EI
SIM ms
[197.550-
198.550] MS
6609_2559
Relative Abundance
Time (min)

A-3

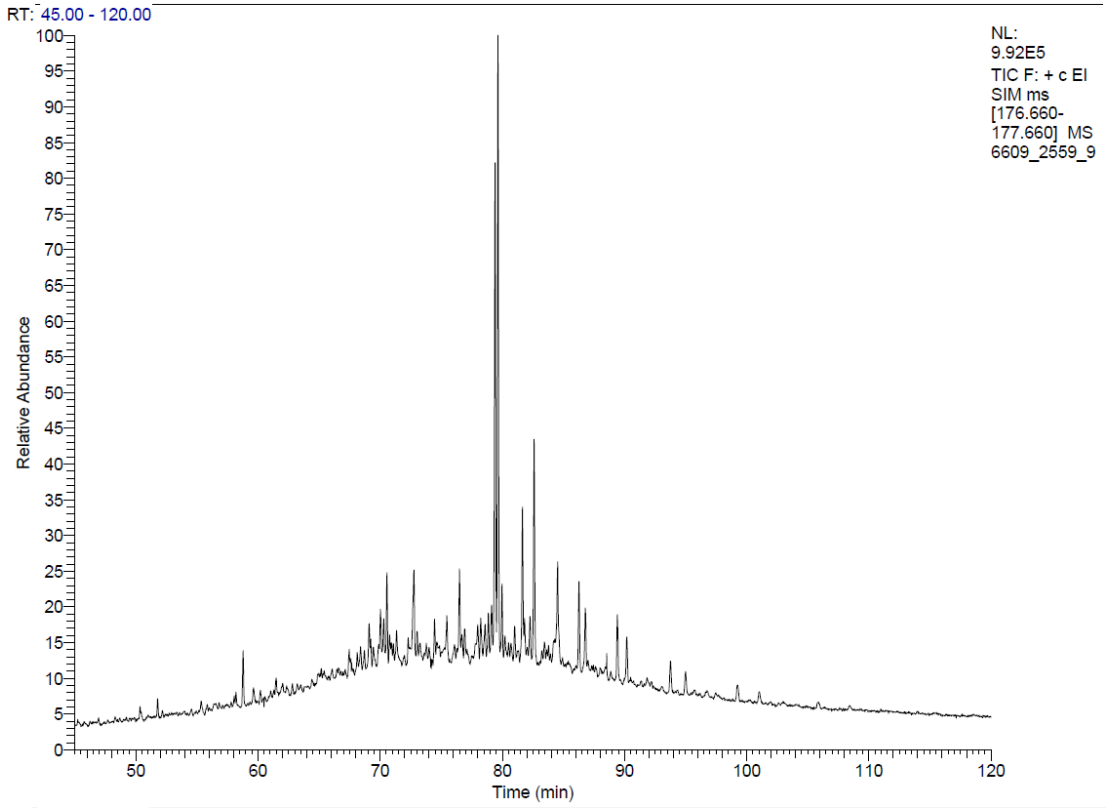
RT: 45.00 - 120.00
NL:
9.92E5
TIC F: + c EI
SIM ms
[176.660-
177.660] MS
6609_2559_9
Relative Abundance
Time (min)

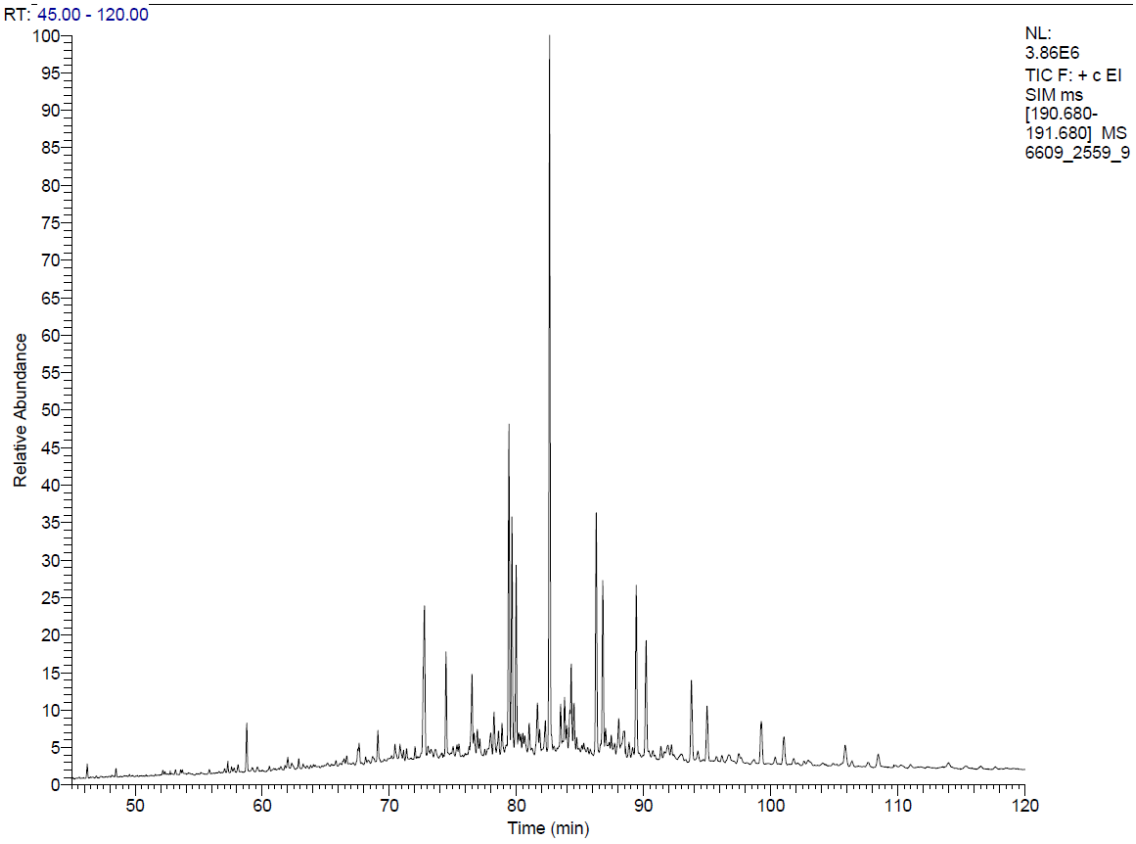
RT: 45.00 - 120.00
NL:
3.86E6
TIC F: + c EI
SIM ms
[190.680-
191.680] MS
6609_2559_9
Relative Abundance
Time (min)

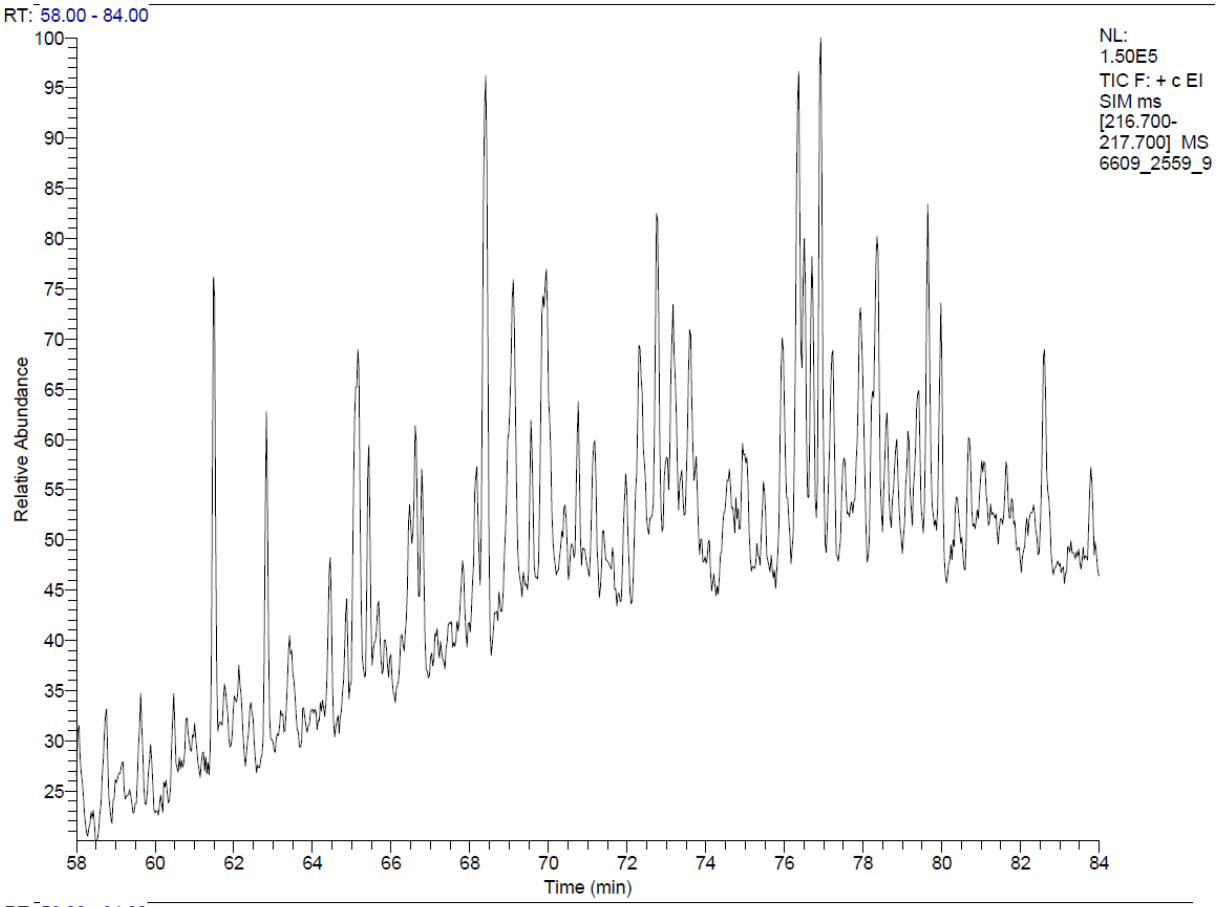
RT: 58.00 - 84.00
NL:
1.50E5
TIC F: + c EI
SIM ms
[216.700-
217.700] MS
6609_2559_9
Relative Abundance
Time (min)

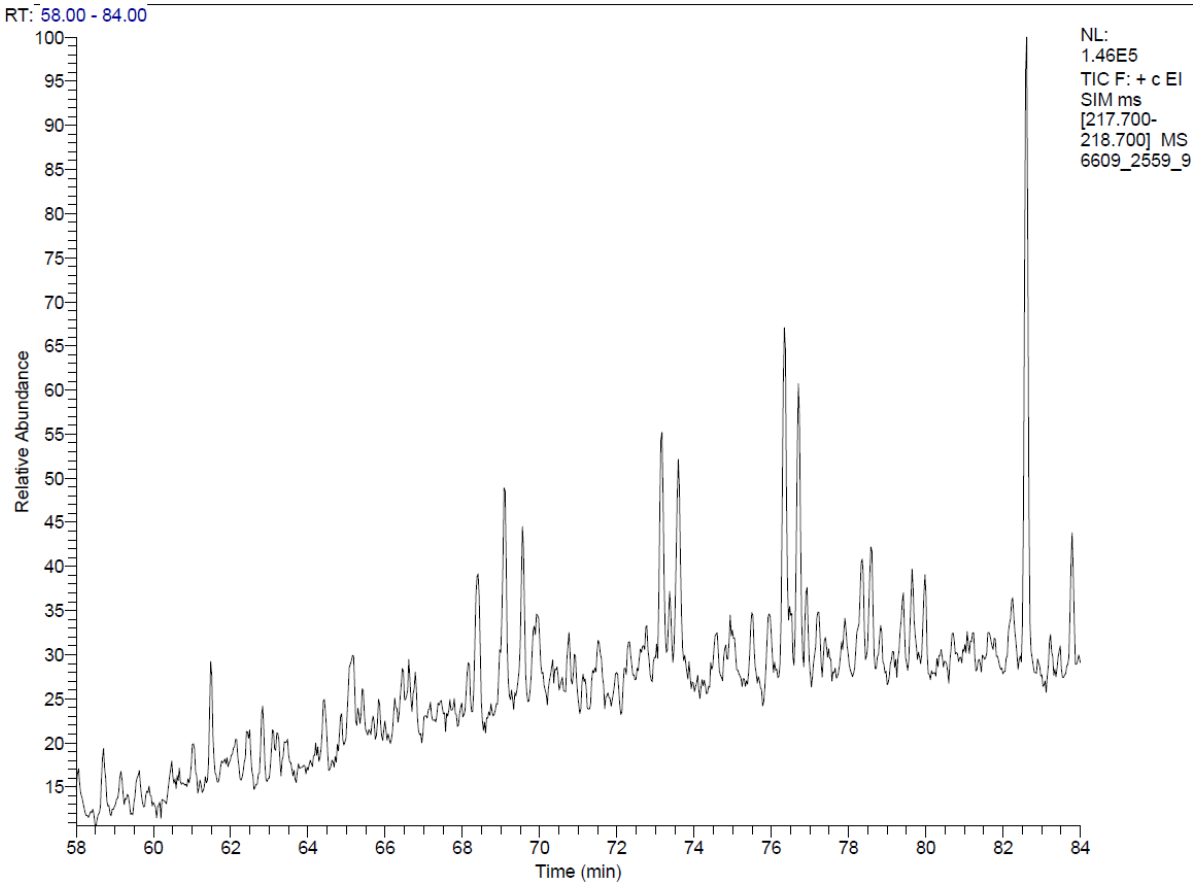
RT: 58.00 - 84.00
NL:
1.46E5
TIC F: + c EI
SIM ms
[217.700-
218.700] MS
6609_2559_9
Relative Abundance
Time (min)

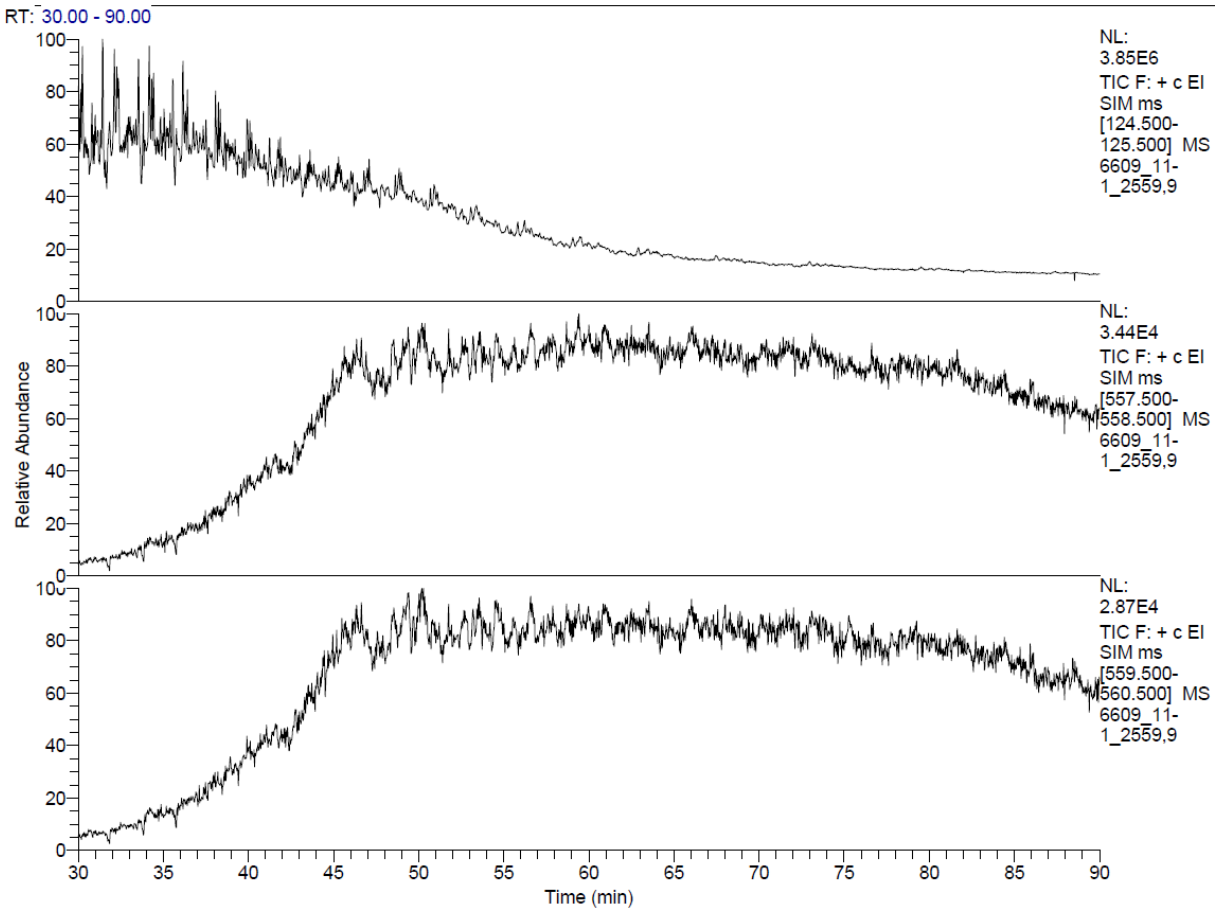
RT: 30.00 - 90.00
NL:
3.85E6
TIC F: + c EI
SIM ms
[124.500-
125.500] MS
6609_11-
1_2559,9
NL:
3.44E4
TIC F: + c EI
SIM ms
[557.500-
558.500] MS
6609_11-
1_2559,9
NL:
2.87E4
TIC F: + c EI
SIM ms
[559.500-
560.500] MS
6609_11-
1_2559,9
Relative Abundance
Time (min)

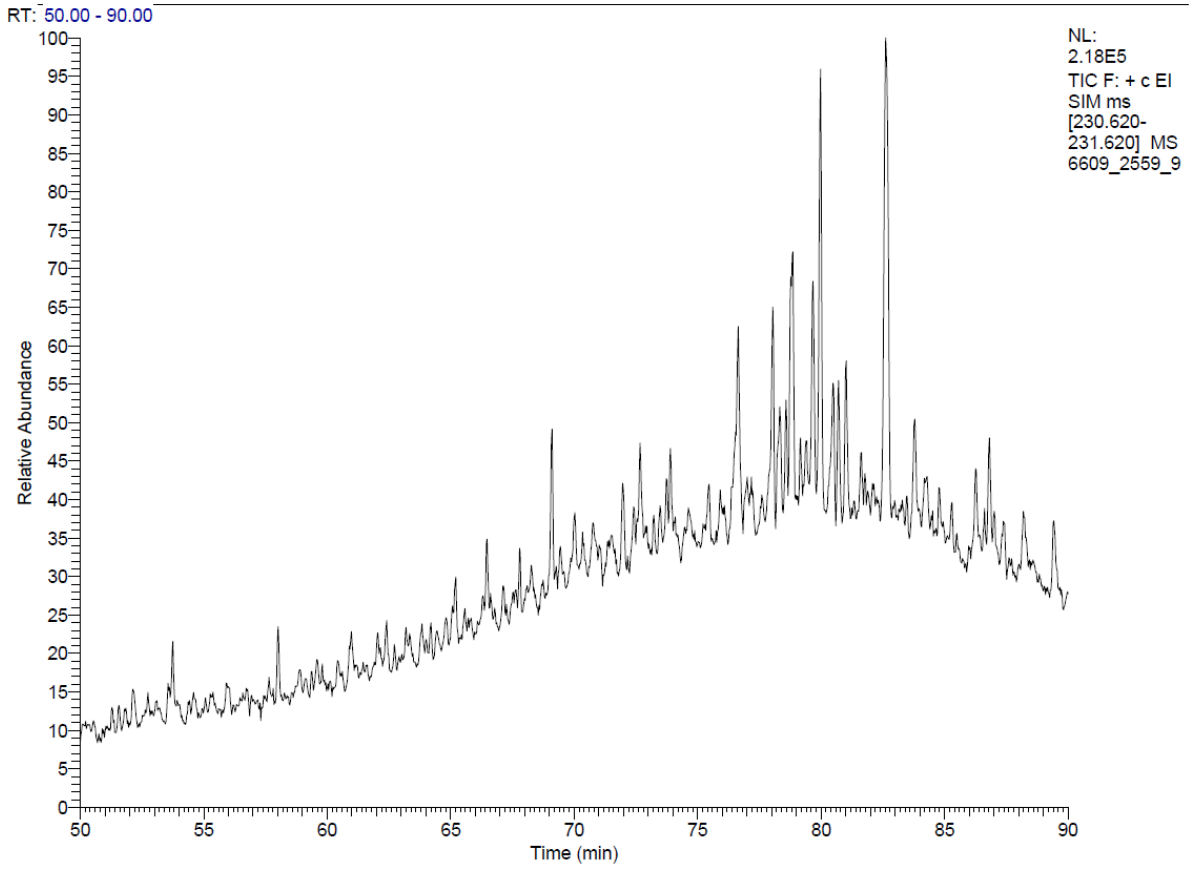
RT: 50.00 - 90.00
NL:
2.18E5
TIC F: + c EI
SIM ms
[230.620-
231.620] MS
6609_2559_9
Relative Abundance
Time (min)

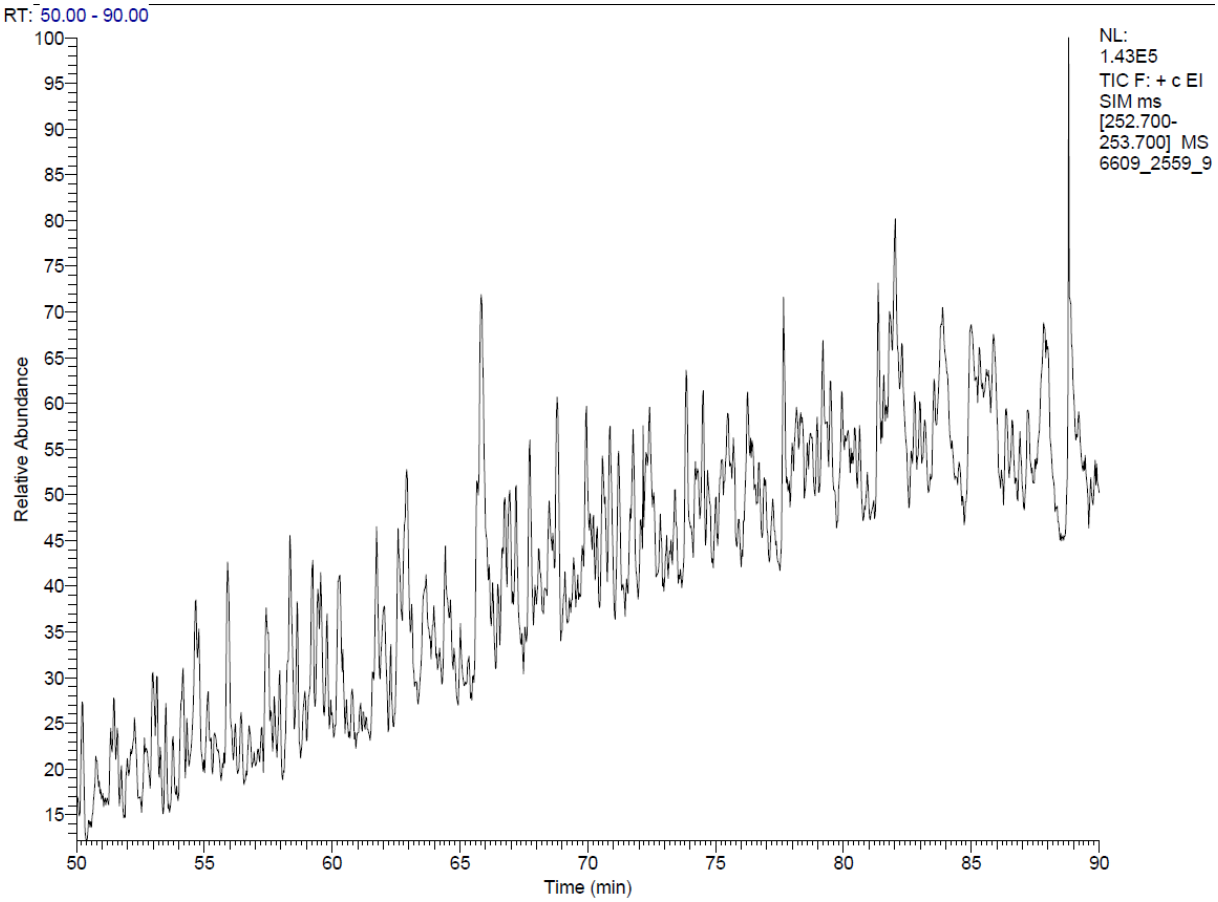
RT: 50.00 - 90.00
NL:
1.43E5
TIC F: + c EI
SIM ms
[252.700-
253.700] MS
6609_2559_9
Relative Abundance
Time (min)

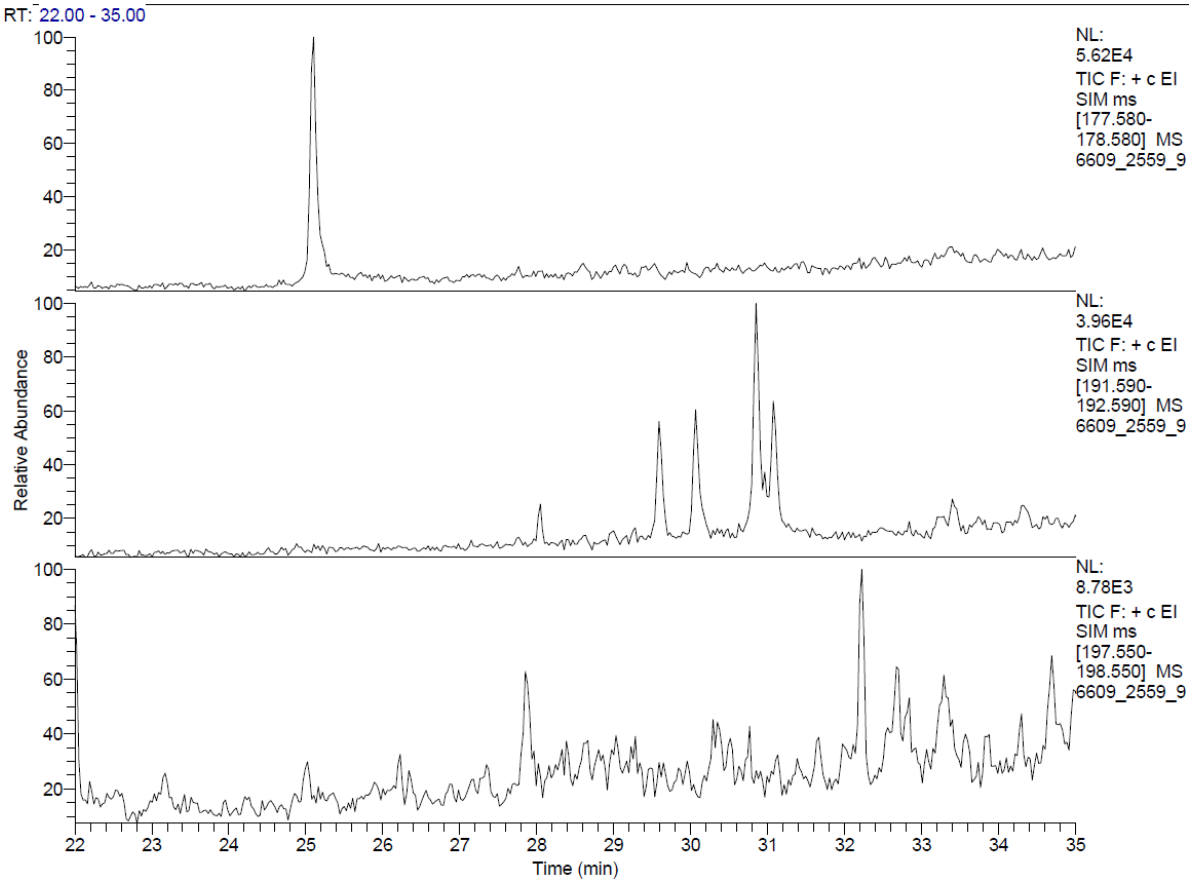
RT: 22.00 - 35.00
NL:
5.62E4
TIC F: + c EI
SIM ms
[177.580-
178.580] MS
6609_2559_9
NL:
3.96E4
TIC F: + c EI
SIM ms
[191.590-
192.590] MS
6609_2559_9
NL:
8.78E3
TIC F: + c EI
SIM ms
[197.550-
198.550] MS
6609_2559_9
Relative Abundance
Time (min)

A-4

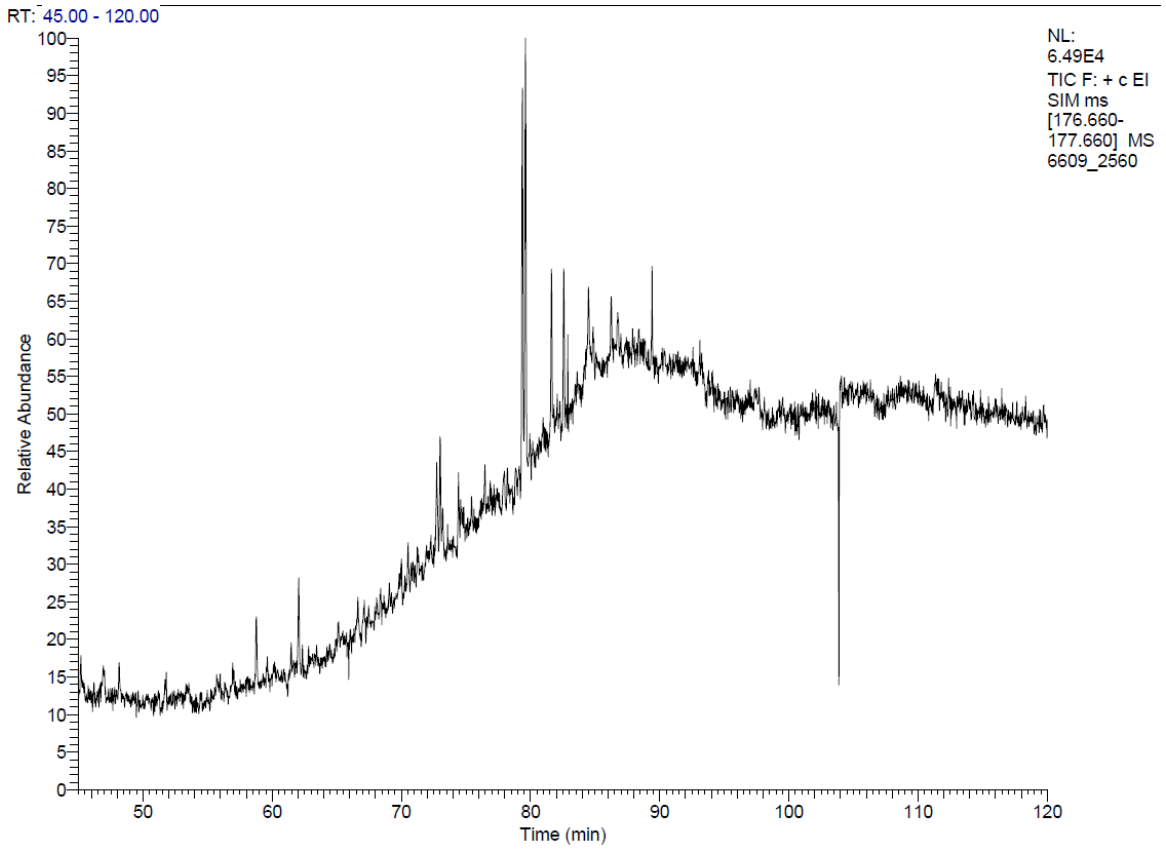
RT: 45.00 - 120.00
NL:
6.49E4
TIC F: + c EI
SIM ms
[176.660-
177.660] MS
6609_2560
Relative Abundance
Time (min)

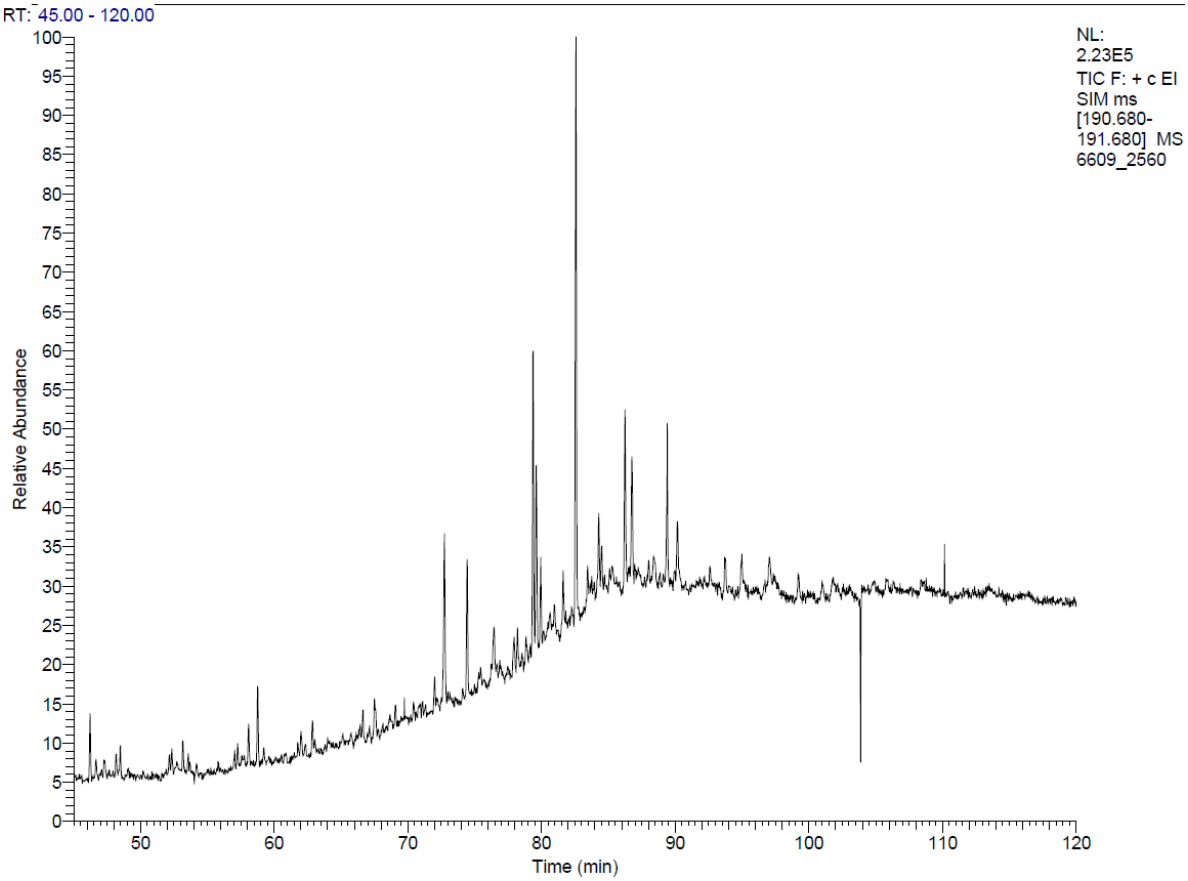
RT: 45.00 - 120.00
NL:
2.23E5
TIC F: + c EI
SIM ms
[190.680-
191.680] MS
6609_2560
Relative Abundance
Time (min)

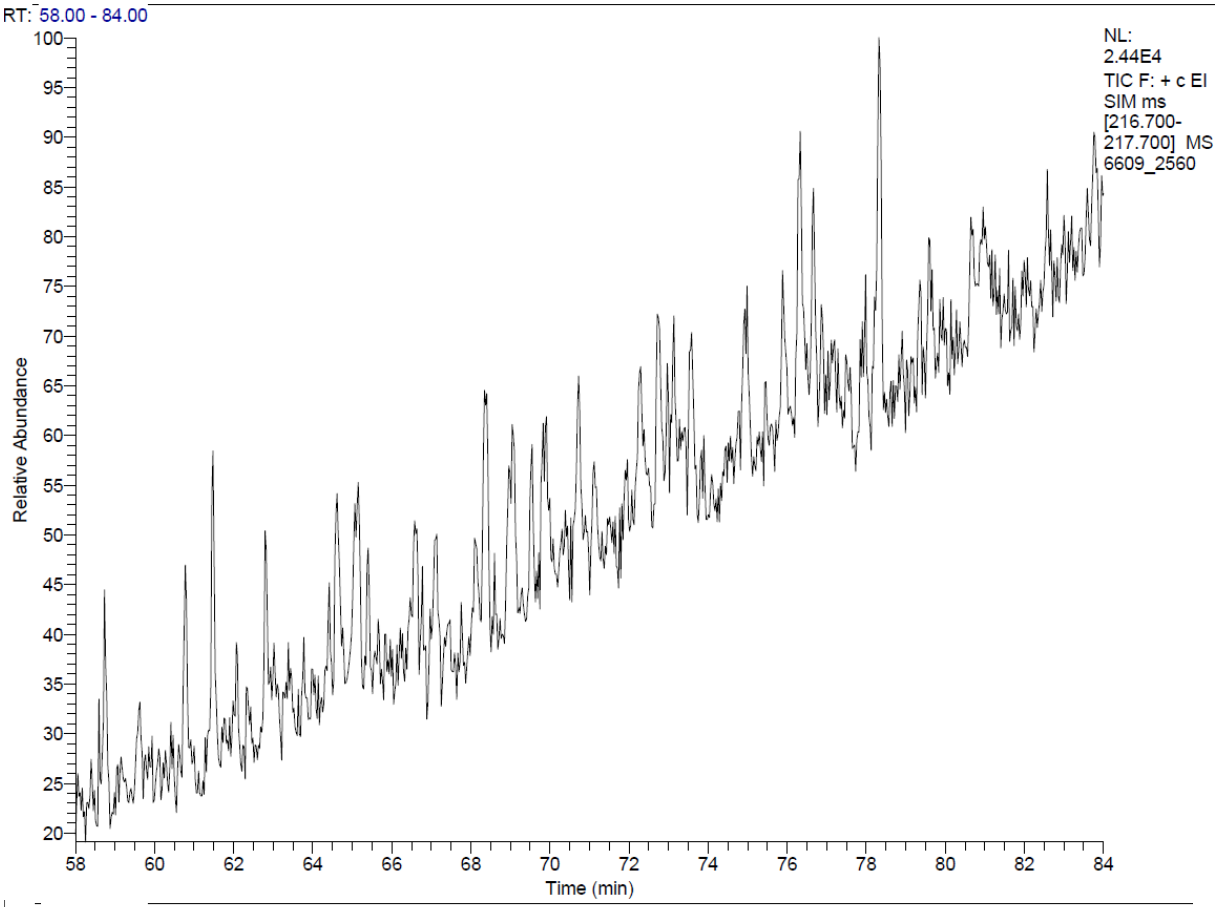
RT: 58.00 - 84.00
NL:
2.44E4
TIC F: + c EI
SIM ms
[216.700-
217.700] MS
6609_2560
Relative Abundance
Time (min)

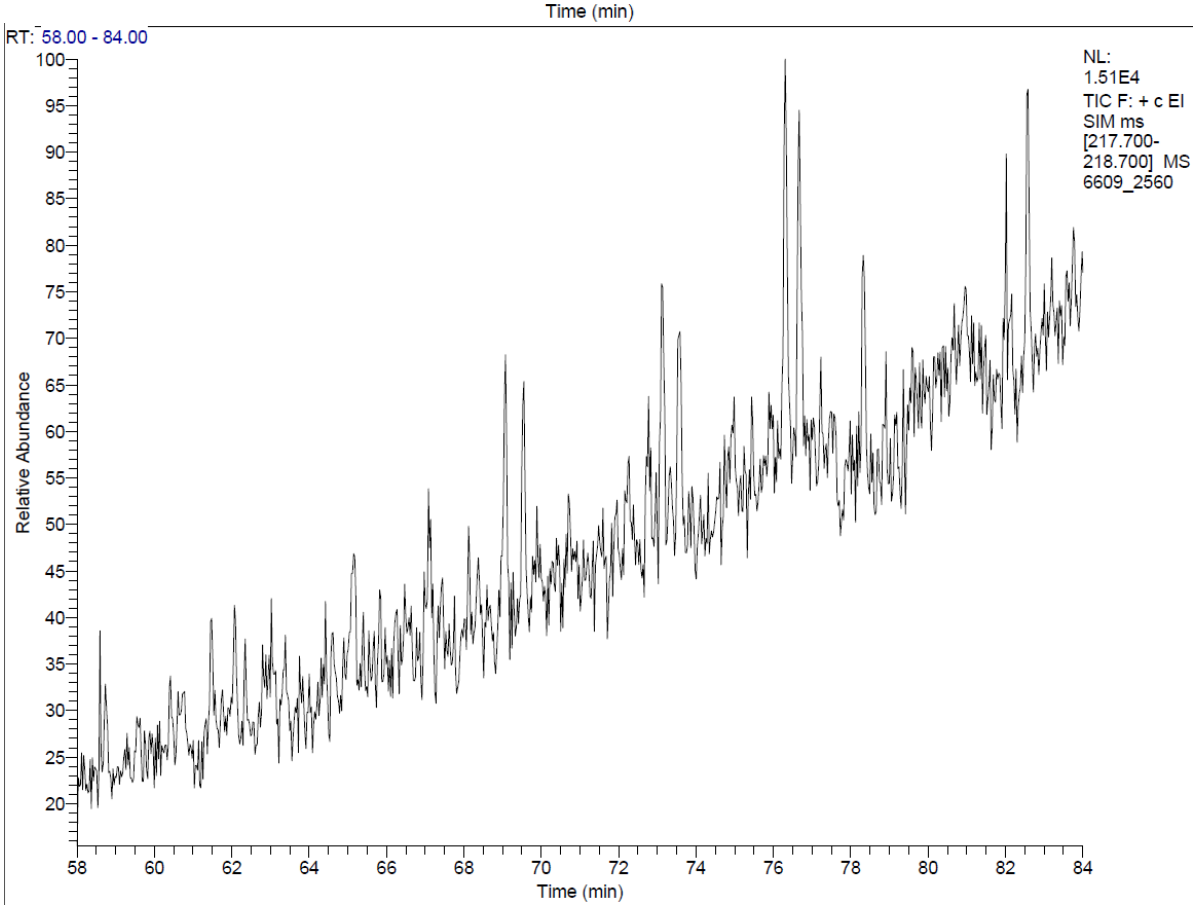
RT: 58.00 - 84.00
NL:
1.51E4
TIC F: + c EI
SIM ms
[217.700-
218.700] MS
6609_2560
Relative Abundance
Time (min)

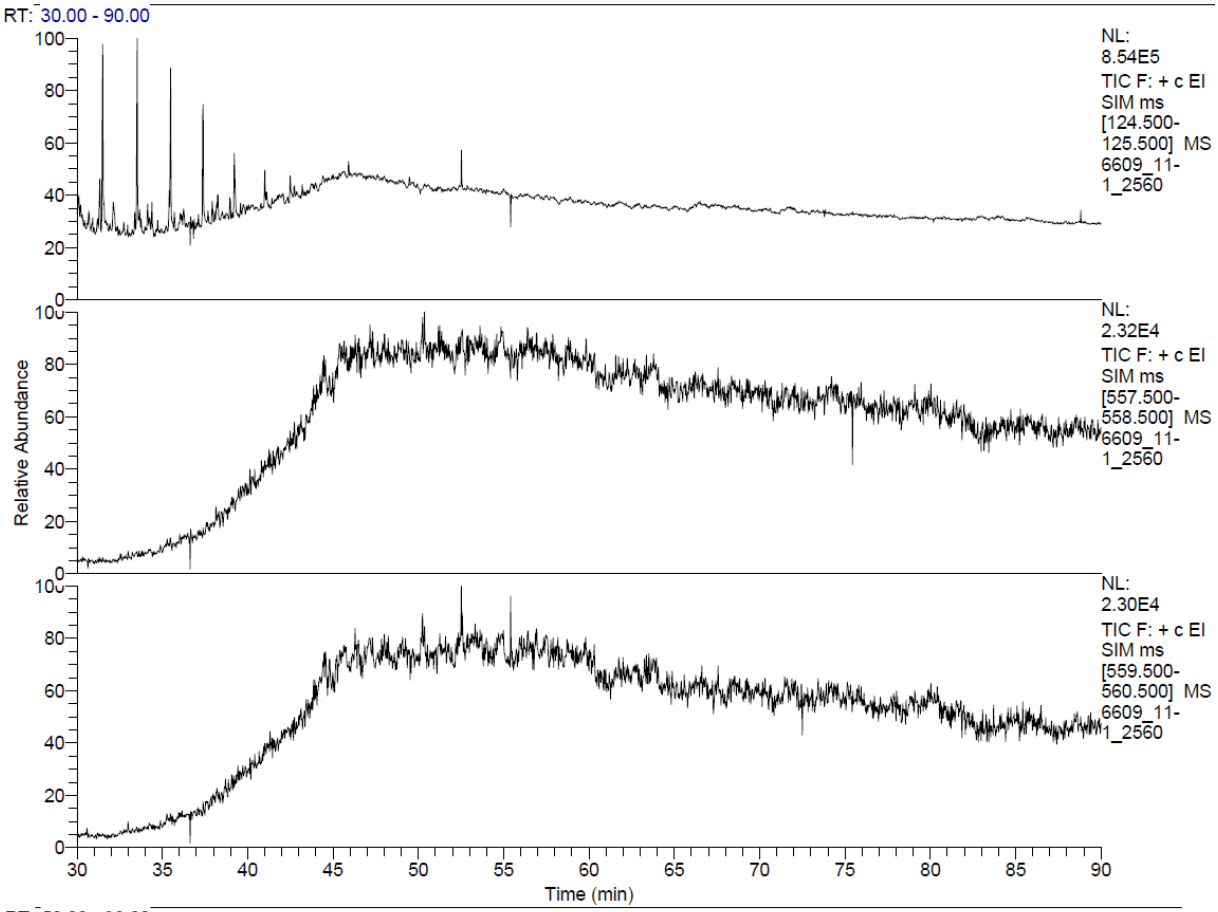
RT: 30.00 - 90.00
NL:
8.54E5
TIC F: + c EI
SIM ms
[124.500-
125.500] MS
6609_11-
1_2560
NL:
2.32E4
TIC F: + c EI
SIM ms
[557.500-
558.500] MS
6609_11-
1_2560
NL:
2.30E4
TIC F: + c EI
SIM ms
[559.500-
560.500] MS
6609_11-
1_2560
Relative Abundance
Time (min)

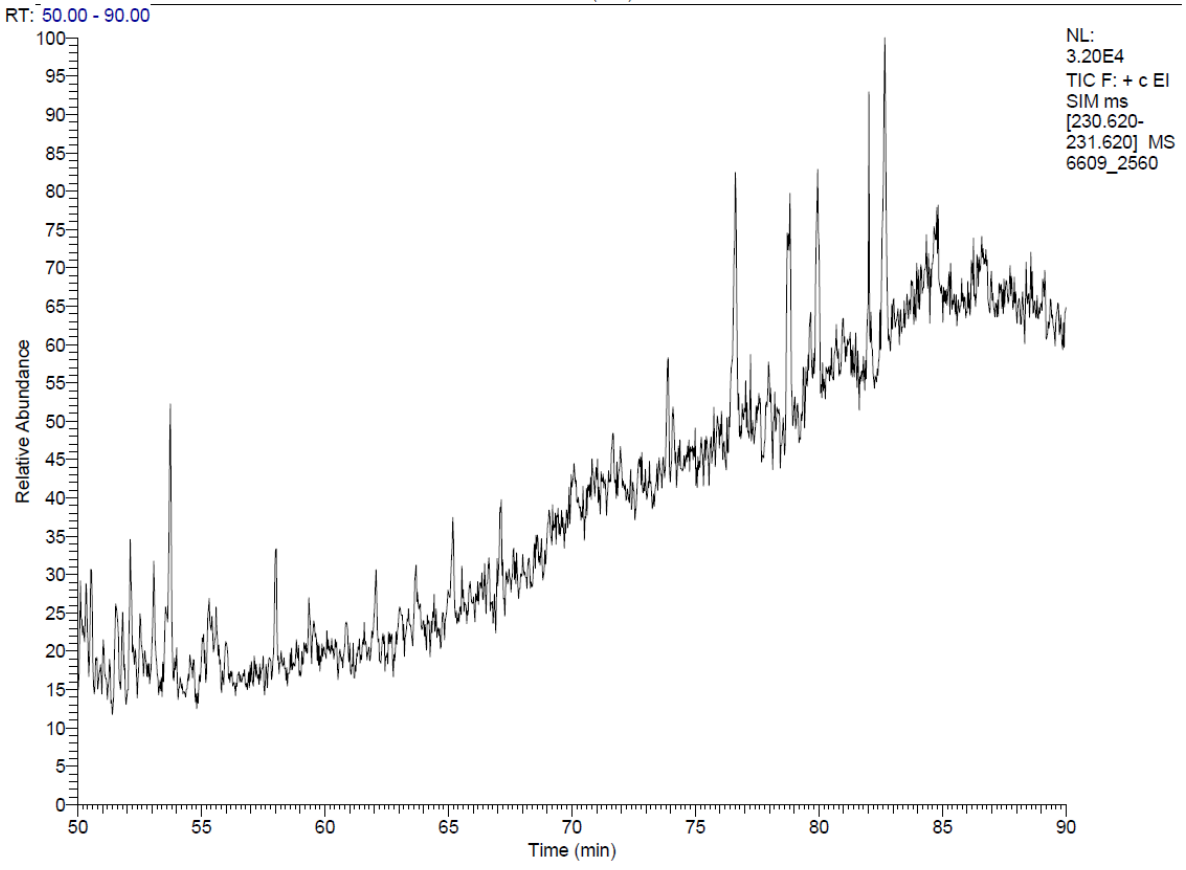
RT: 50.00 - 90.00
NL:
3.20E4
TIC F: + c EI
SIM ms
[230.620-
231.620] MS
6609_2560
Relative Abundance
Time (min)

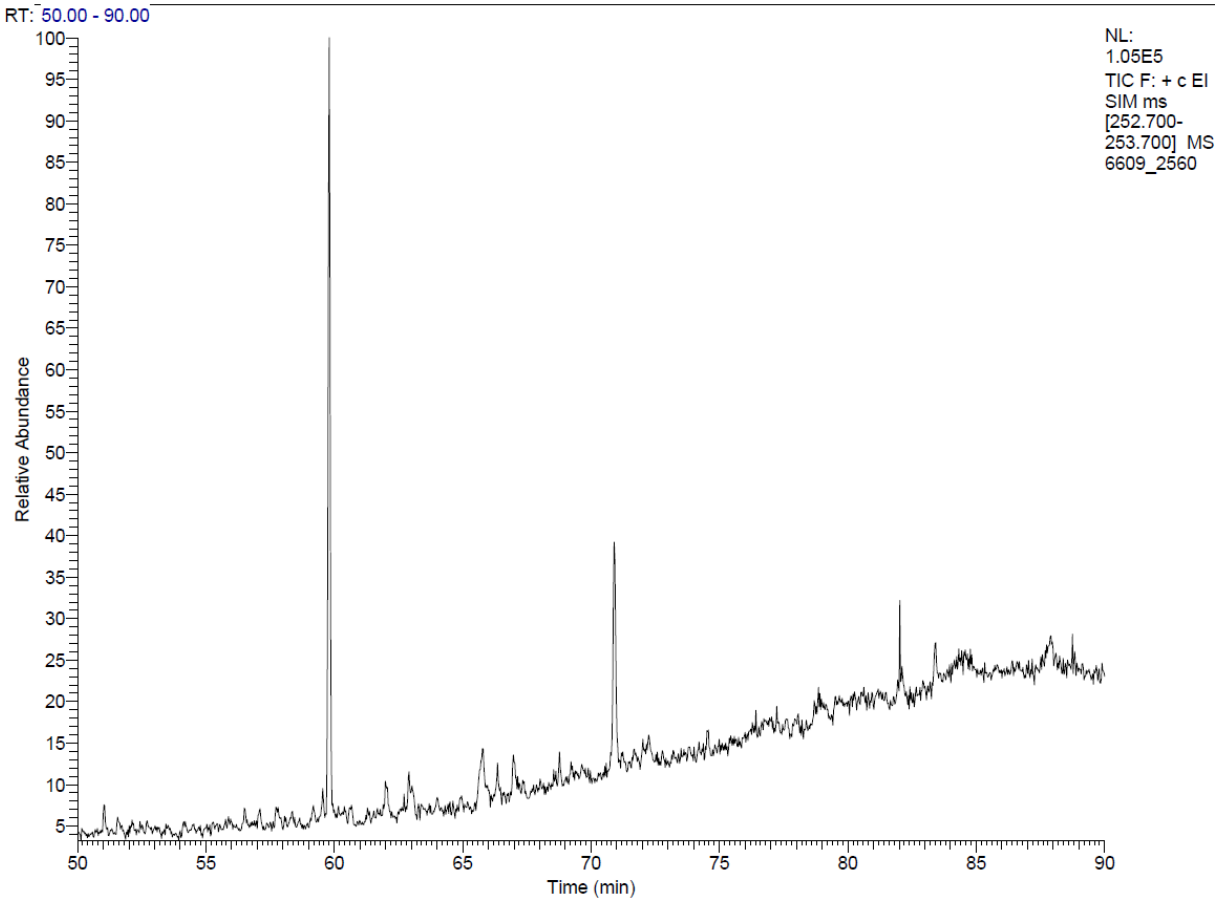
RT: 50.00 - 90.00
NL:
1.05E5
TIC F: + c EI
SIM ms
[252.700-
253.700] MS
6609_2560
Relative Abundance
Time (min)

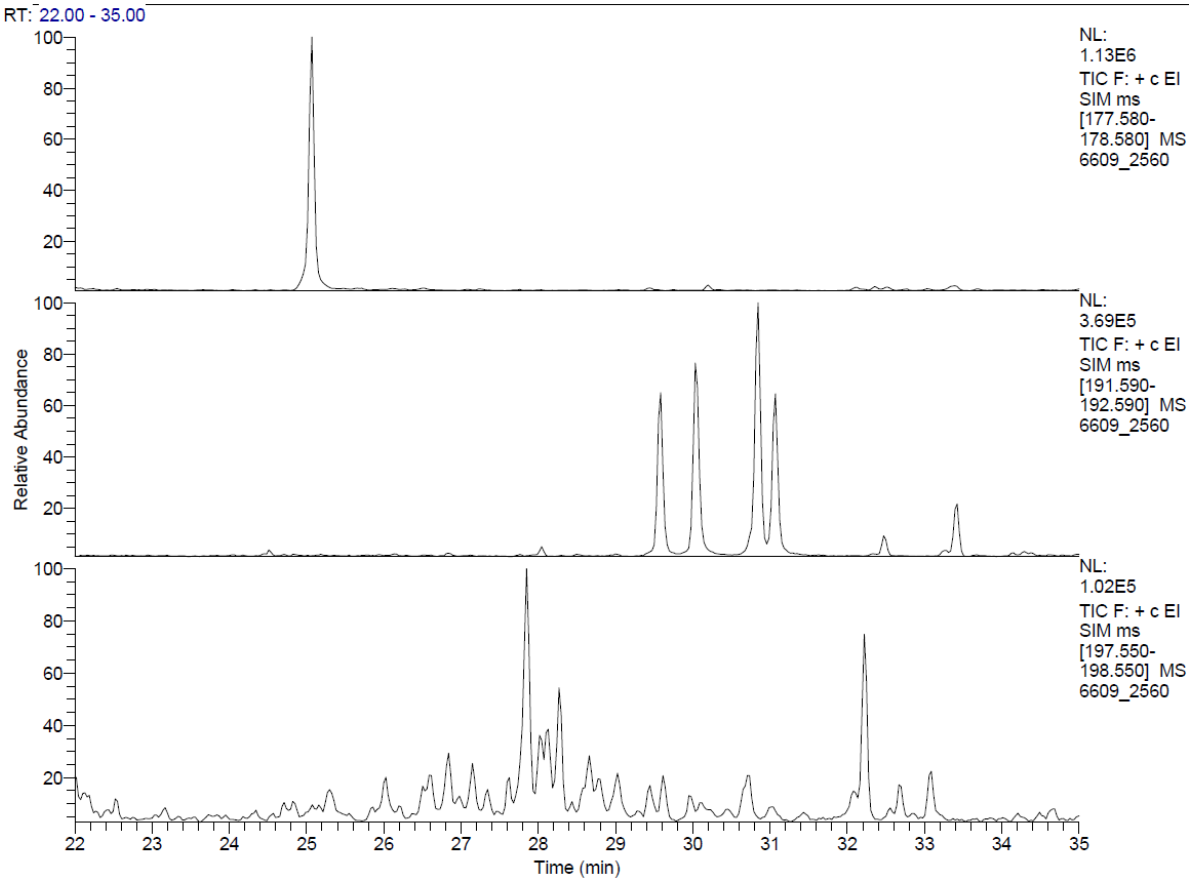
RT: 22.00 - 35.00
NL:
1.13E6
TIC F: + c EI
SIM ms
[177.580-
178.580] MS
6609_2560
NL:
3.69E5
TIC F: + c EI
SIM ms
[191.590-
192.590] MS
6609_2560
NL:
1.02E5
TIC F: + c EI
SIM ms
[197.550-
198.550] MS
6609_2560
Relative Abundance
Time (min)

A-5

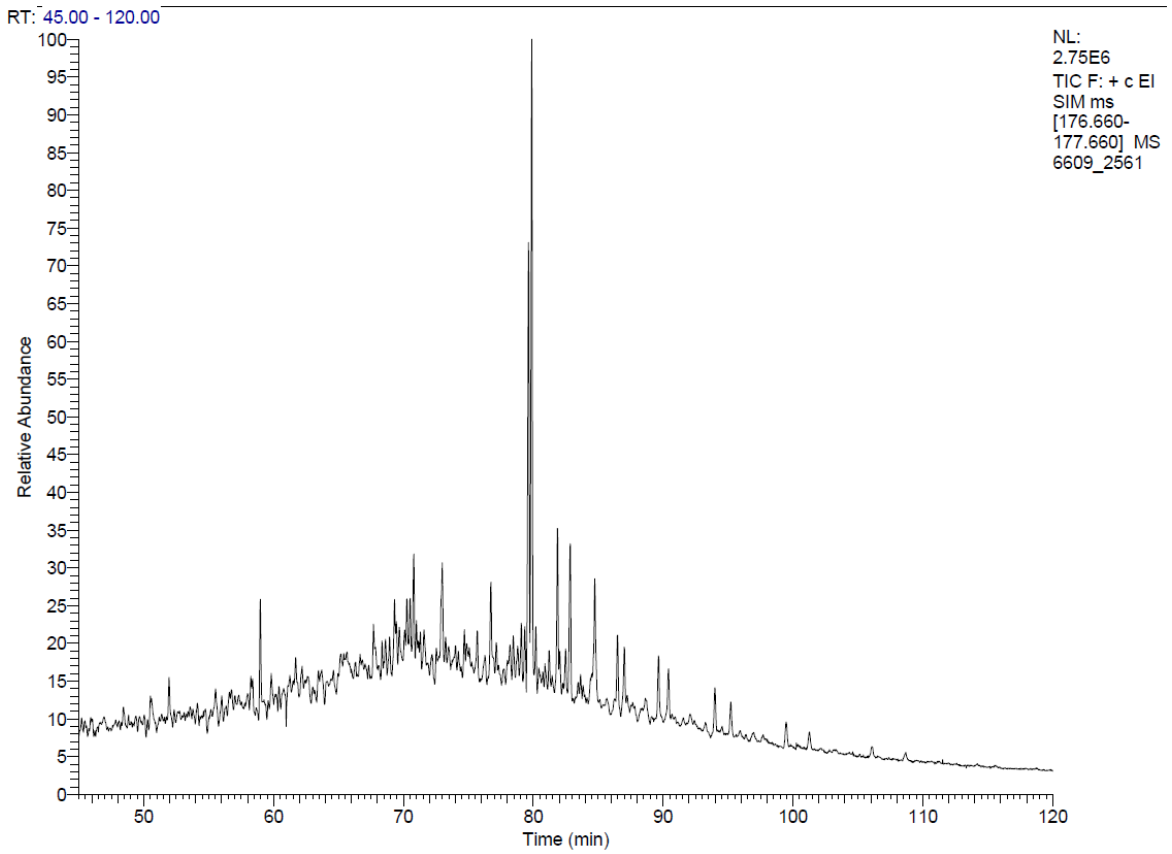
RT: 45.00 - 120.00
NL:
2.75E6
TIC F: + c EI
SIM ms
[176.660-
177.660] MS
6609_2561
Relative Abundance
Time (min)

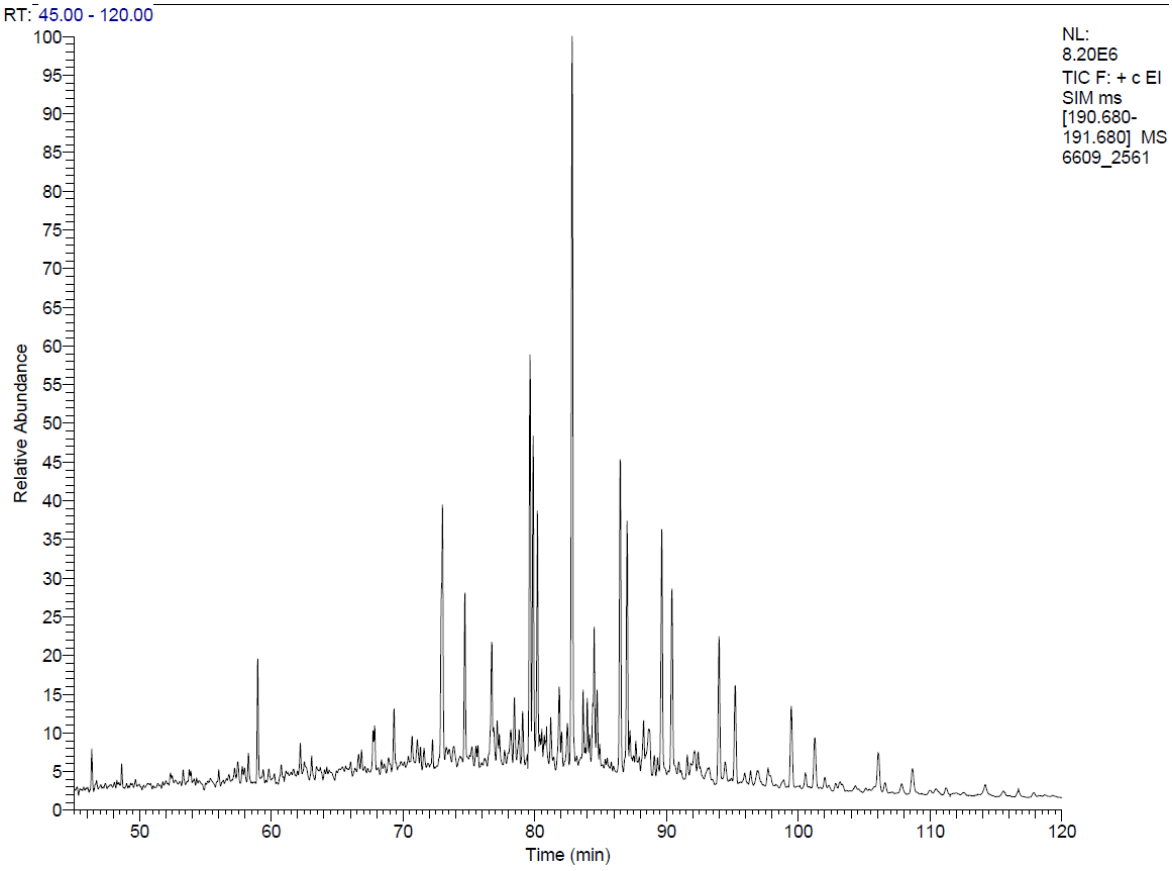
RT: 45.00 - 120.00
NL:
8.20E6
TIC F: + c EI
SIM ms
[190.680-
191.680] MS
6609_2561
Relative Abundance
Time (min)

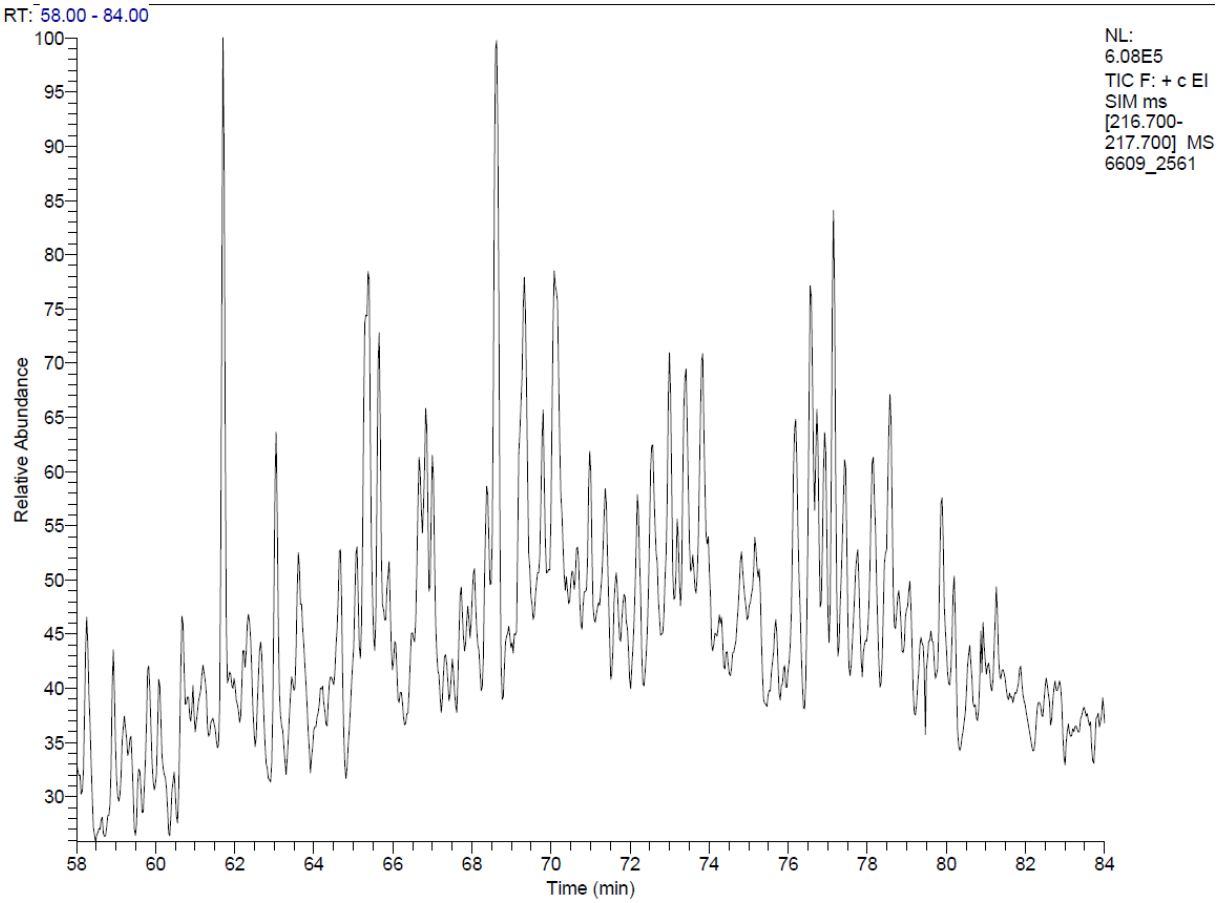
RT: 58.00 - 84.00
NL:
6.08E5
TIC F: + c EI
SIM ms
[216.700-
217.700] MS
6609_2561
Relative Abundance
Time (min)

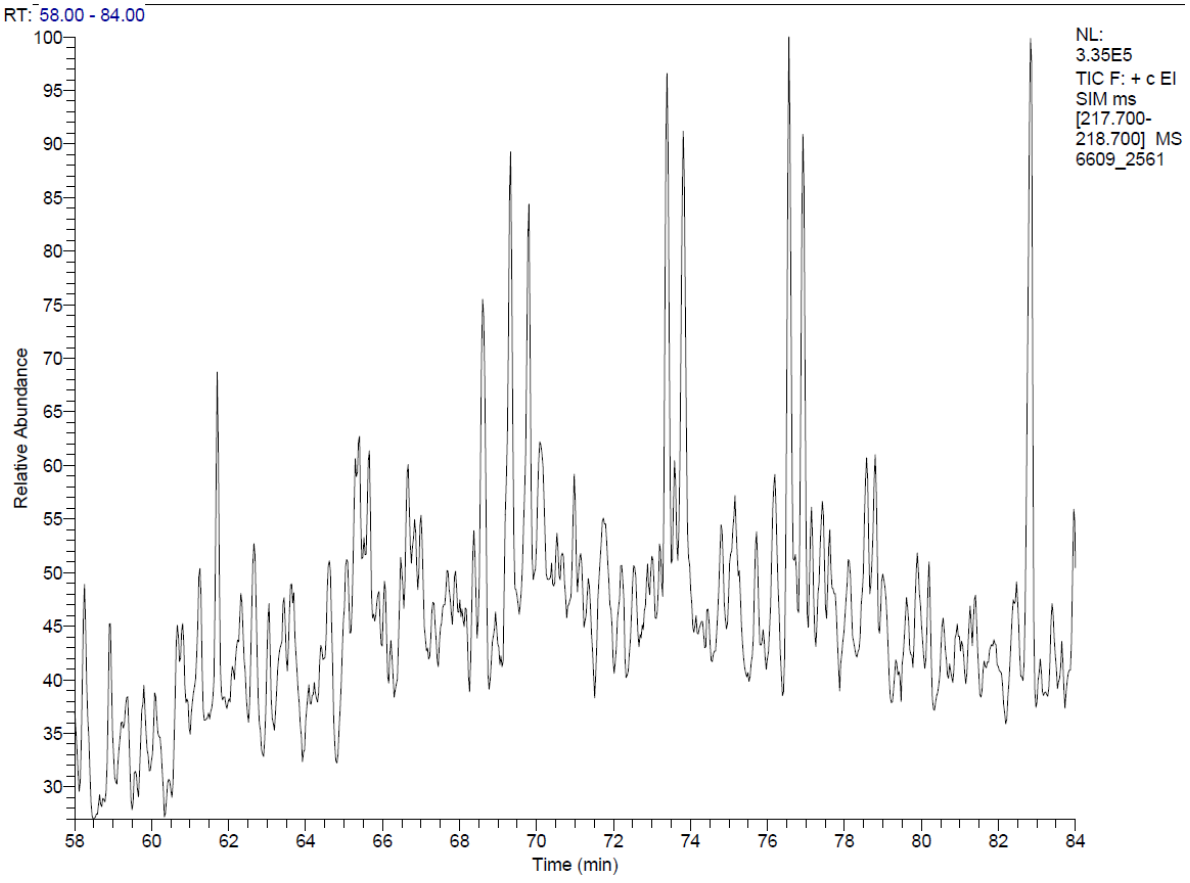
RT: 58.00 - 84.00
NL:
3.35E5
TIC F: + c EI
SIM ms
[217.700-
218.700] MS
6609_2561
Relative Abundance
Time (min)

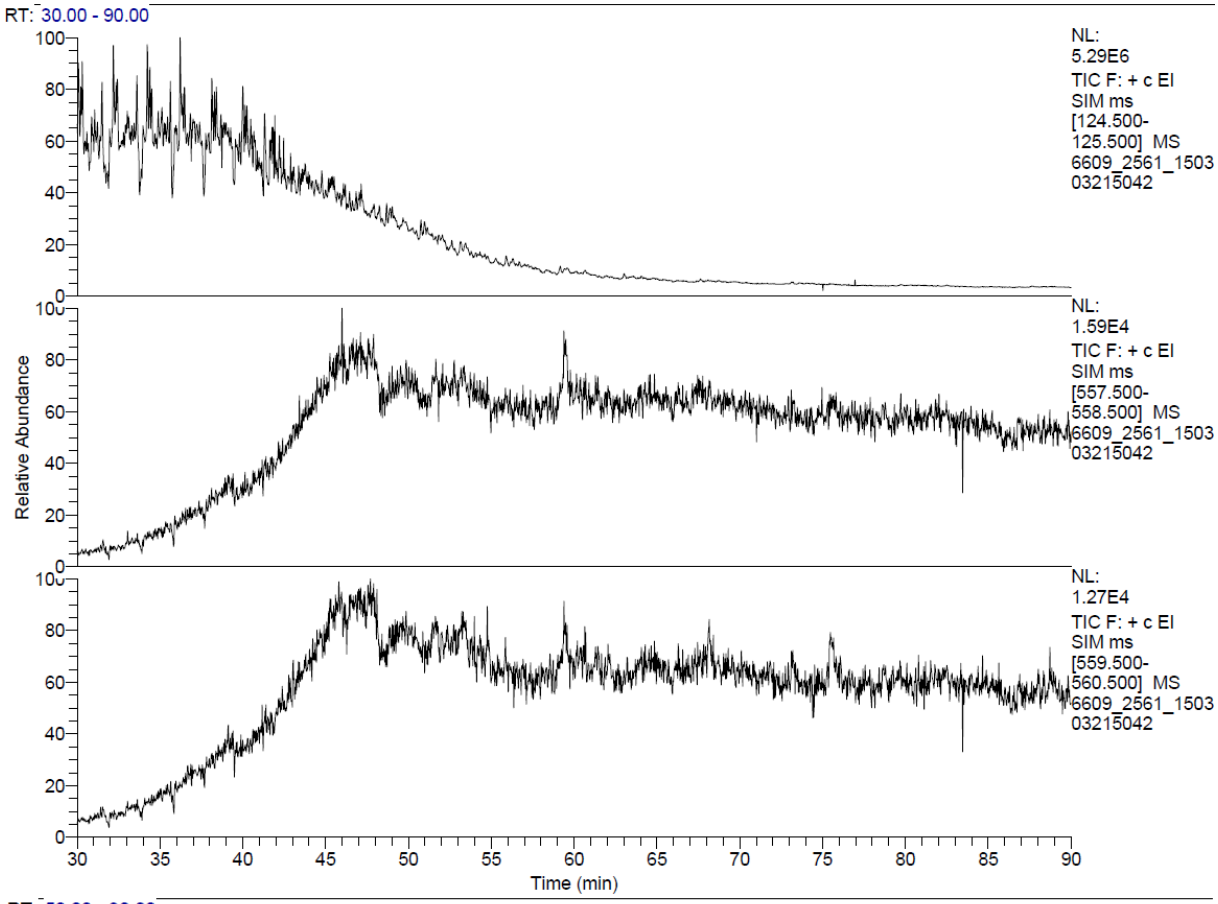
RT: 30.00 - 90.00
NL:
5.29E6
TIC F: + c EI
SIM ms
[124.500-
125.500] MS
6609_2561_1503
03215042
NL:
1.59E4
TIC F: + c EI
SIM ms
[557.500-
558.500] MS
6609_2561_1503
03215042
NL:
1.27E4
TIC F: + c EI
SIM ms
[559.500-
560.500] MS
6609_2561_1503
03215042
Relative Abundance
Time (min)

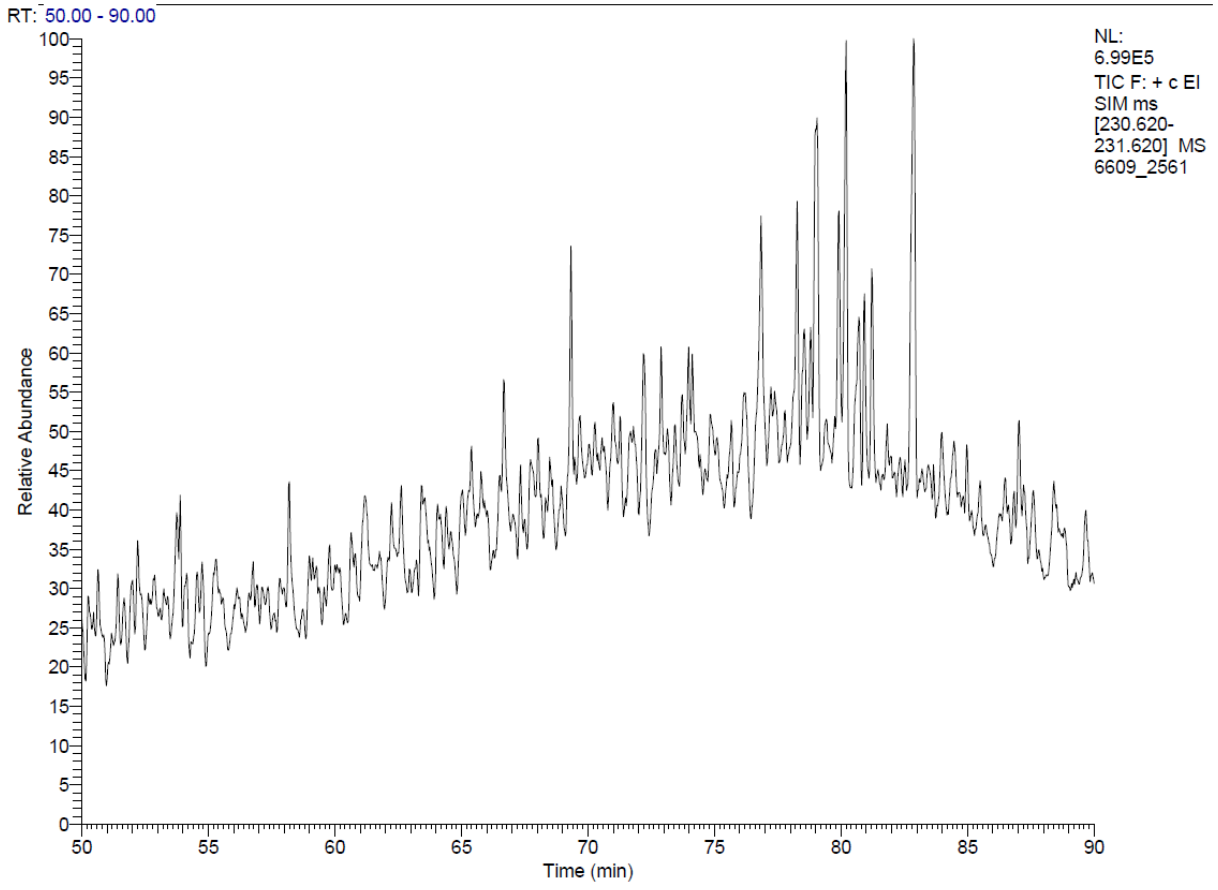
RT: 50.00 - 90.00
NL:
6.99E5
TIC F: + c EI
SIM ms
[230.620-
231.620] MS
6609_2561
Relative Abundance
Time (min)

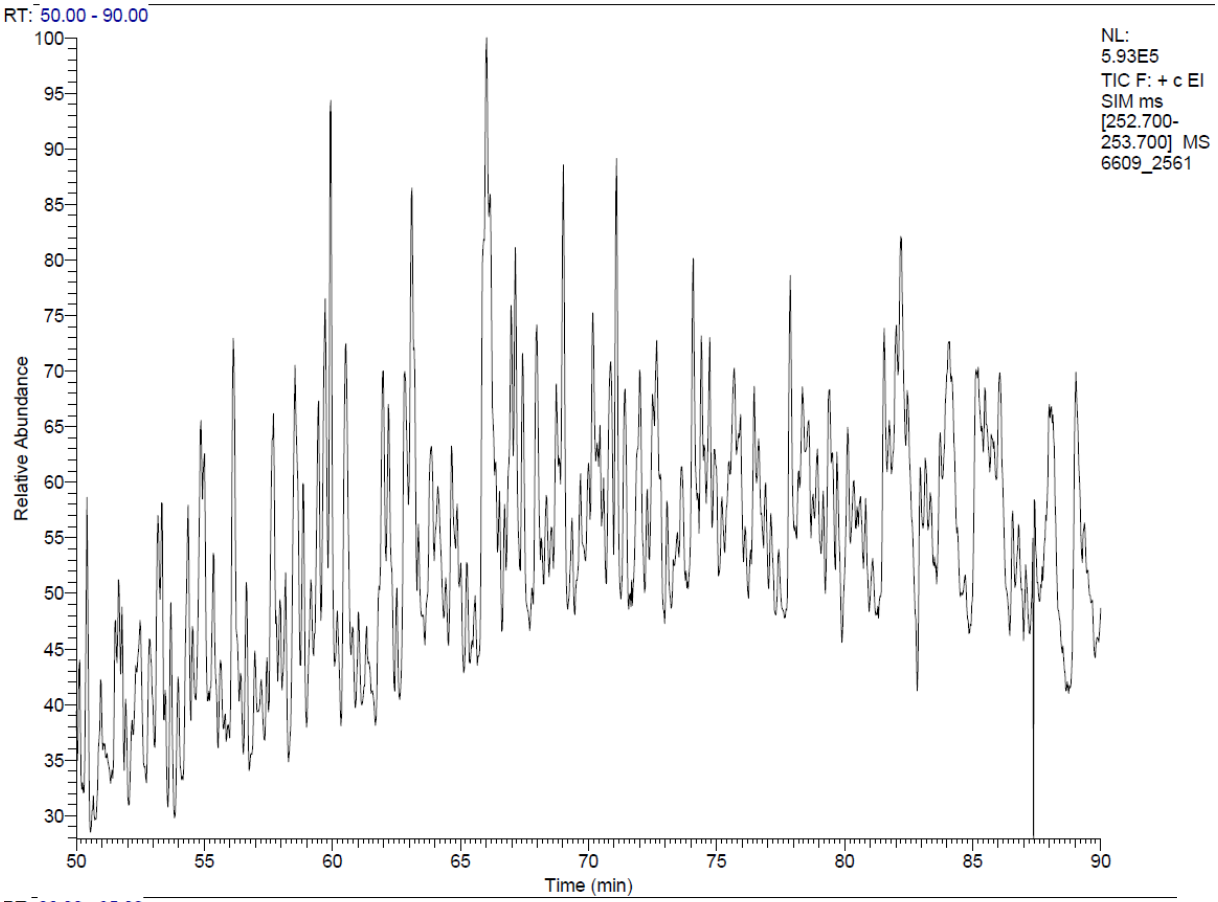
RT: 50.00 - 90.00
NL:
5.93E5
TIC F: + c EI
SIM ms
[252.700-
253.700] MS
6609_2561
Relative Abundance
Time (min)

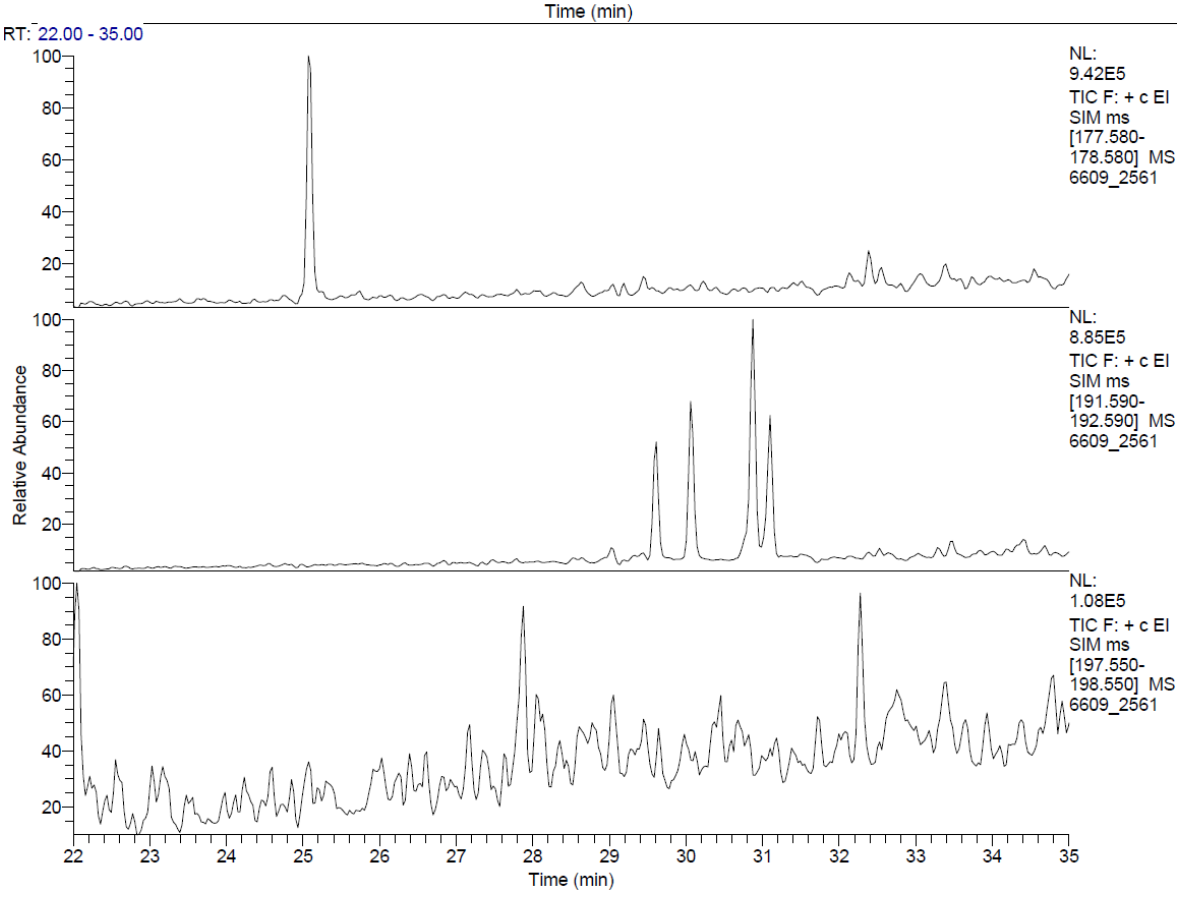
RT: 22.00 - 35.00
NL:
9.42E5
TIC F: + c EI
SIM ms
[177.580-
178.580] MS
6609_2561
NL:
8.85E5
TIC F: + c EI
SIM ms
[191.590-
192.590] MS
6609_2561
NL:
1.08E5
TIC F: + c EI
SIM ms
[197.550-
198.550] MS
6609_2561
Relative Abundance
Time (min)

B-1

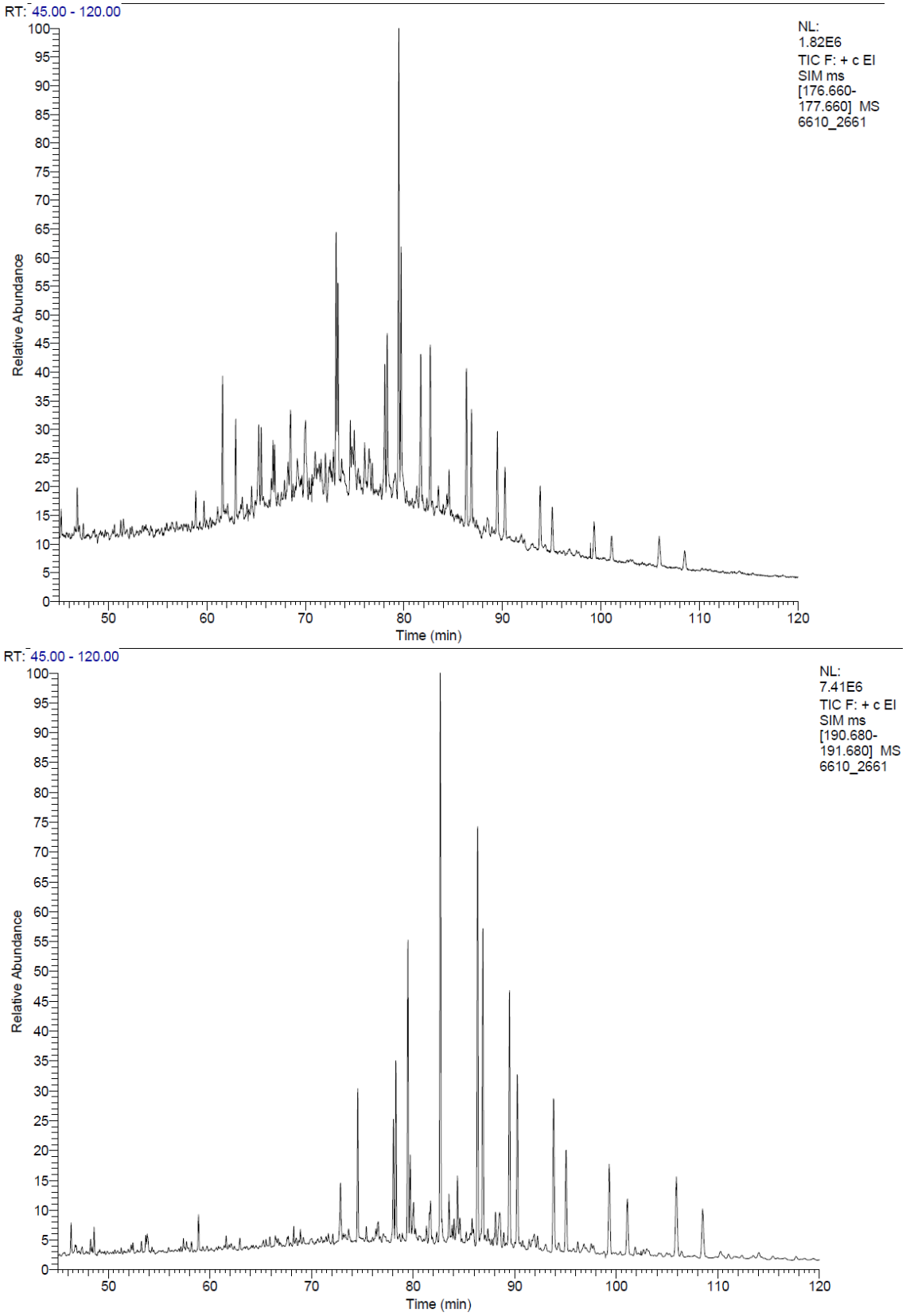
RT: 45.00 - 120.00
NL:
1.82E6
TIC F: + c EI
SIM ms
[176.660-
177.660] MS
6610_2661
Relative Abundance
Time (min)
RT: 45.00 - 120.00
NL:
7.41E6
TIC F: + c EI
SIM ms
[190.680-
191.680] MS
6610_2661
Relative Abundance
Time (min)

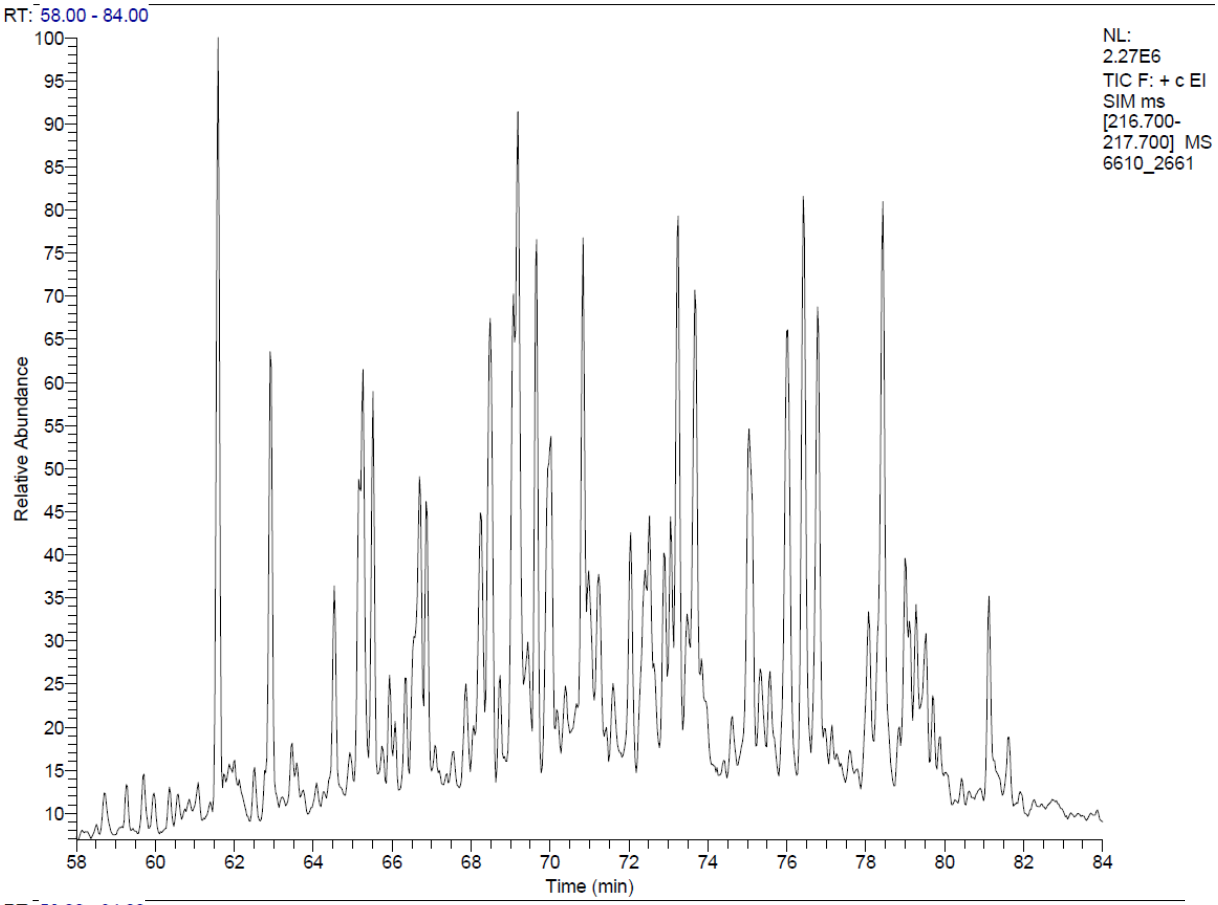
RT: 58.00 - 84.00
NL:
2.27E6
TIC F: + c EI
SIM ms
[216.700-
217.700] MS
6610_2661
Relative Abundance
Time (min)

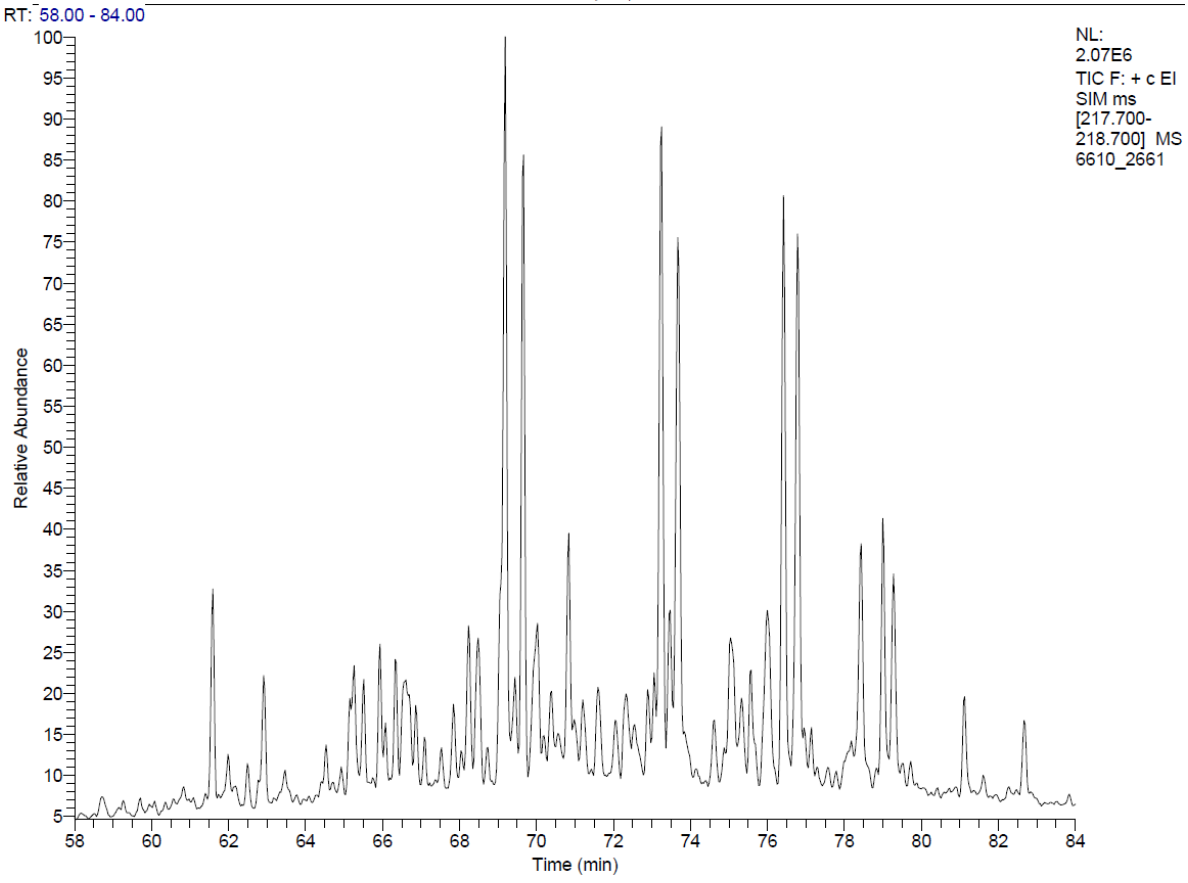
RT: 58.00 - 84.00
NL:
2.07E6
TIC F: + c EI
SIM ms
[217.700-
218.700] MS
6610_2661
Relative Abundance
Time (min)

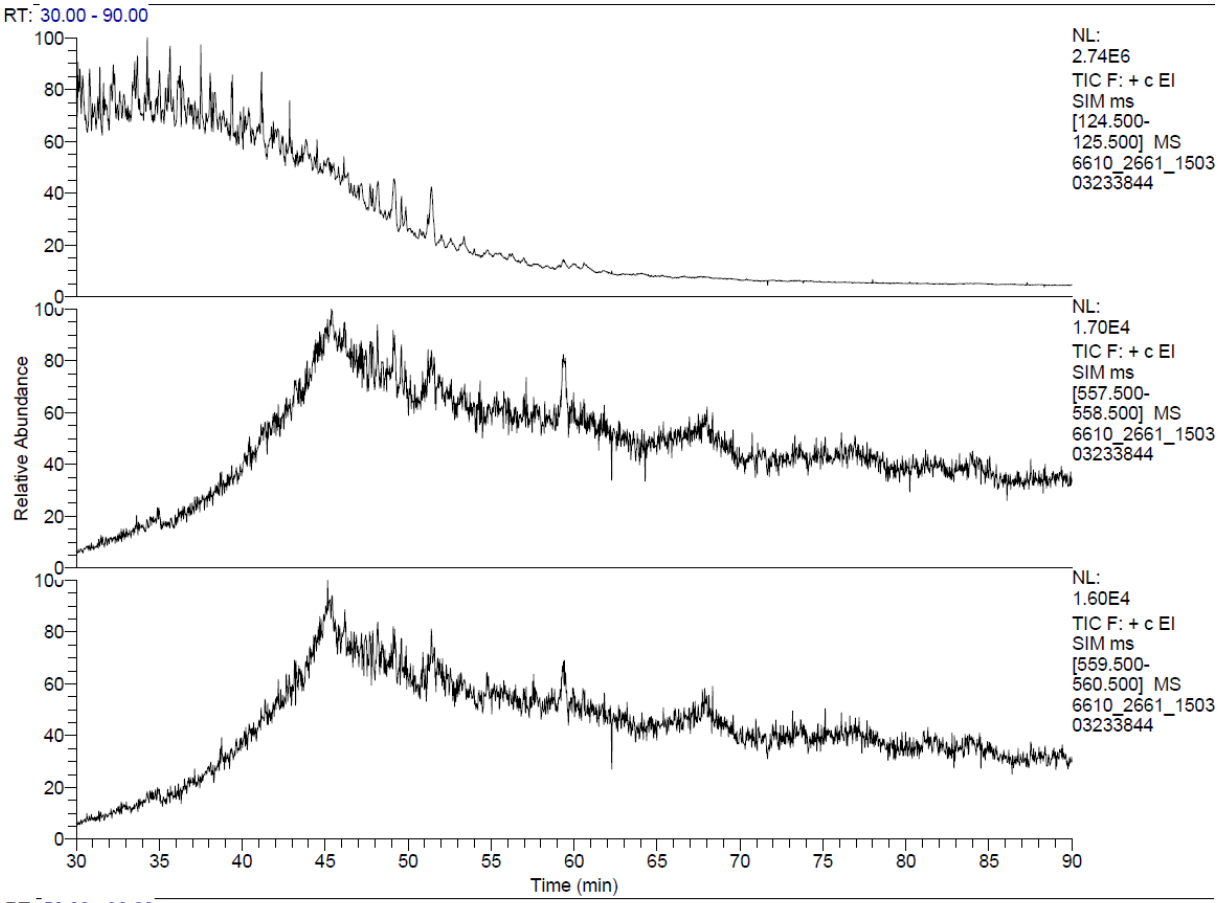
RT: 30.00 - 90.00
NL:
2.74E6
TIC F: + c EI
SIM ms
[124.500-
125.500] MS
6610_2661_1503
03233844
NL:
1.70E4
TIC F: + c EI
SIM ms
[557.500-
558.500] MS
6610_2661_1503
03233844
NL:
1.60E4
TIC F: + c EI
SIM ms
[559.500-
560.500] MS
6610_2661_1503
03233844
Relative Abundance
Time (min)

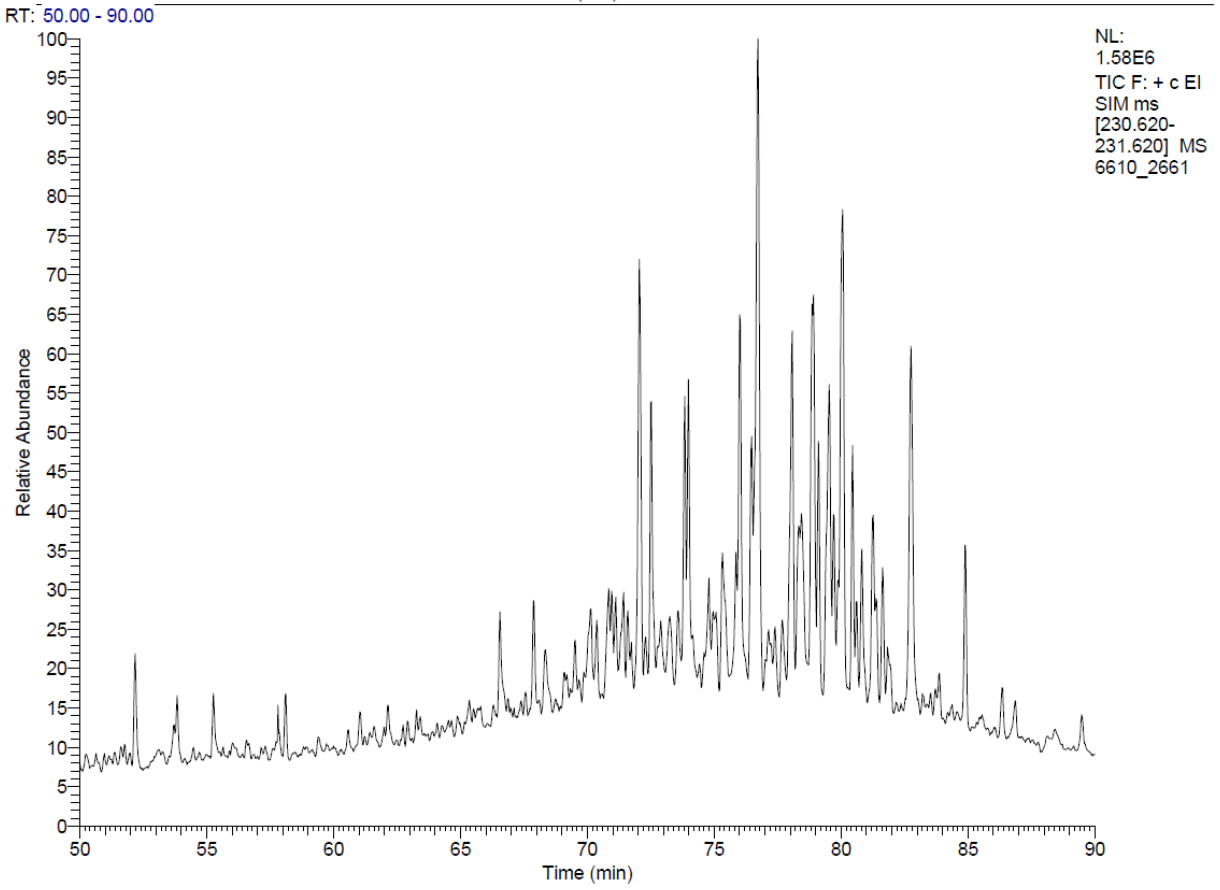
RT: 50.00 - 90.00
NL:
1.58E6
TIC F: + c EI
SIM ms
[230.620-
231.620] MS
6610_2661
Relative Abundance
Time (min)

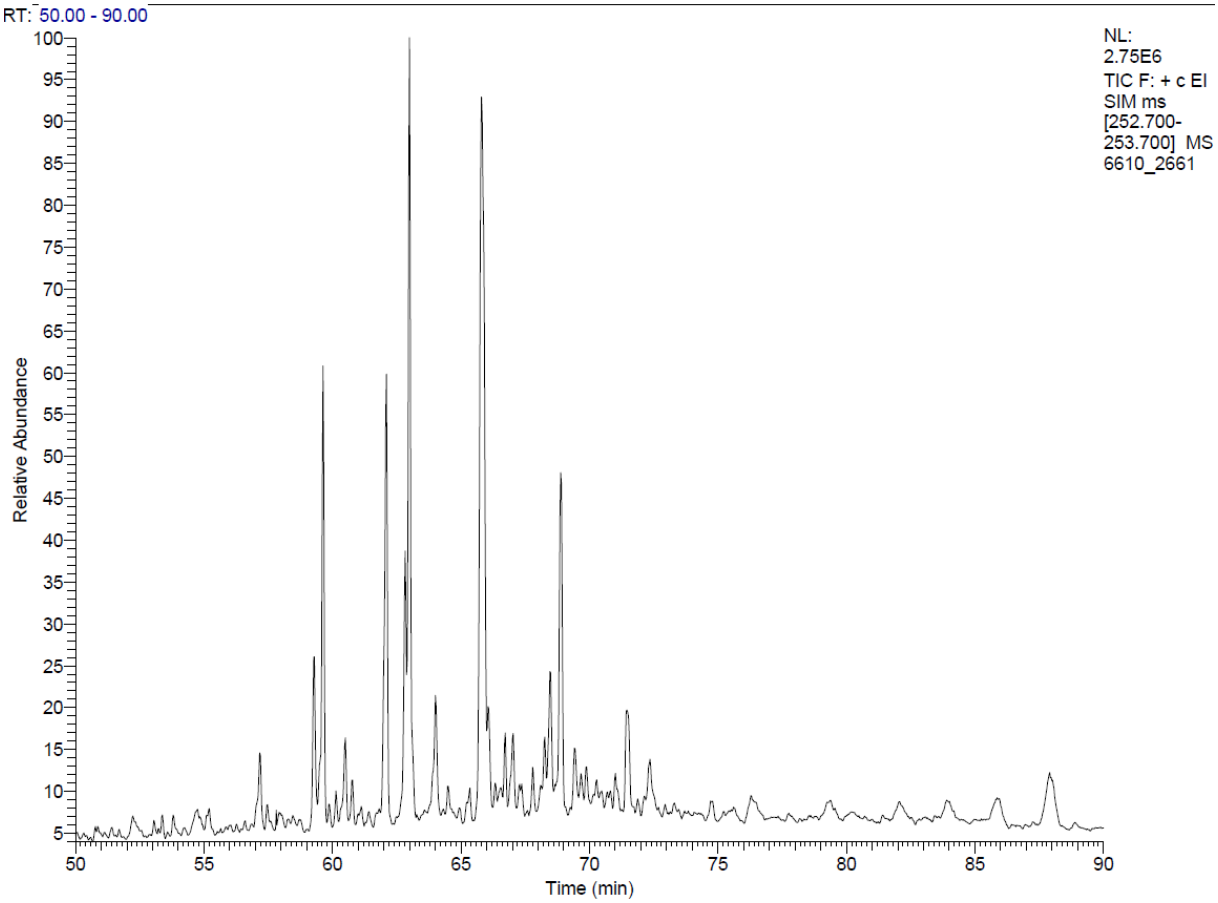
RT: 50.00 - 90.00
NL:
2.75E6
TIC F: + c EI
SIM ms
[252.700-
253.700] MS
6610_2661
Relative Abundance
Time (min)

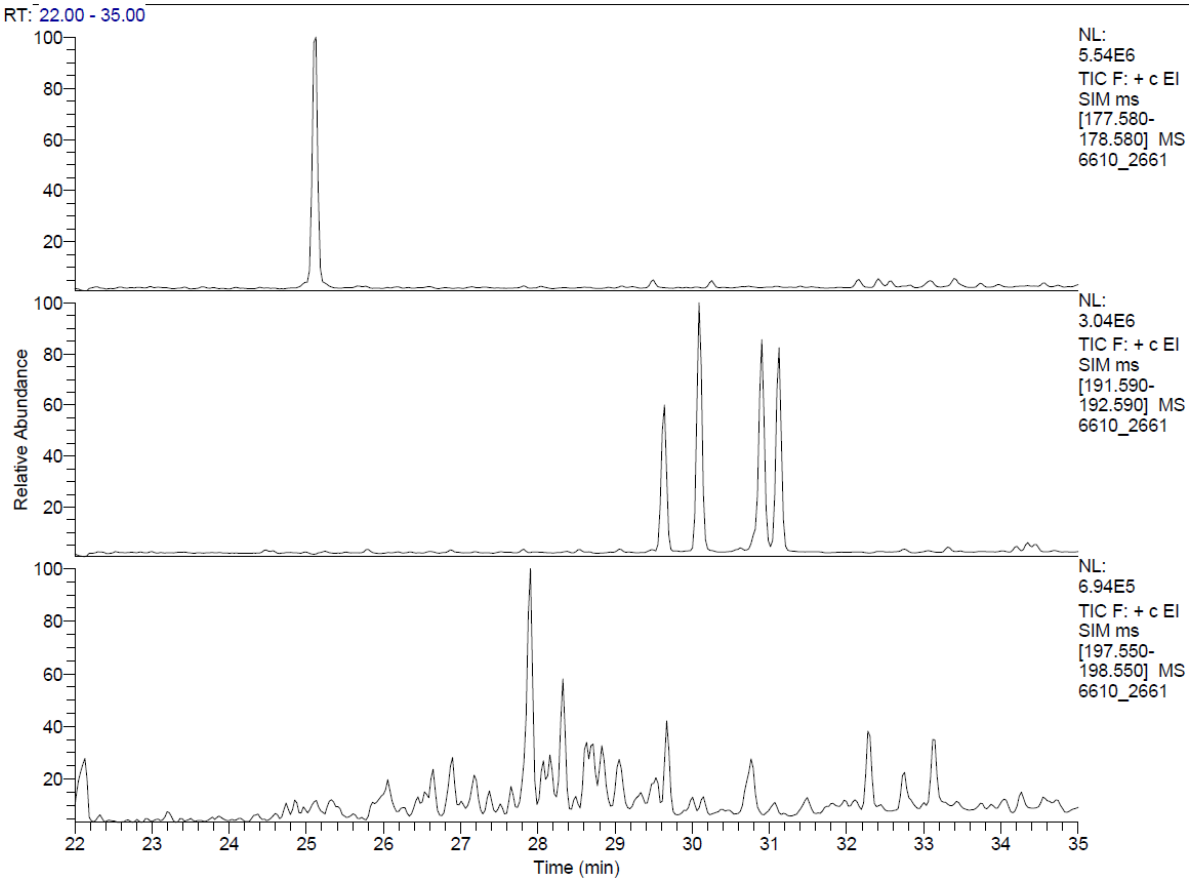
RT: 22.00 - 35.00
NL:
5.54E6
TIC F: + c EI
SIM ms
[177.580-
178.580] MS
6610_2661
NL:
3.04E6
TIC F: + c EI
SIM ms
[191.590-
192.590] MS
6610_2661
NL:
6.94E5
TIC F: + c EI
SIM ms
[197.550-
198.550] MS
6610_2661
Relative Abundance
Time (min)

B-2

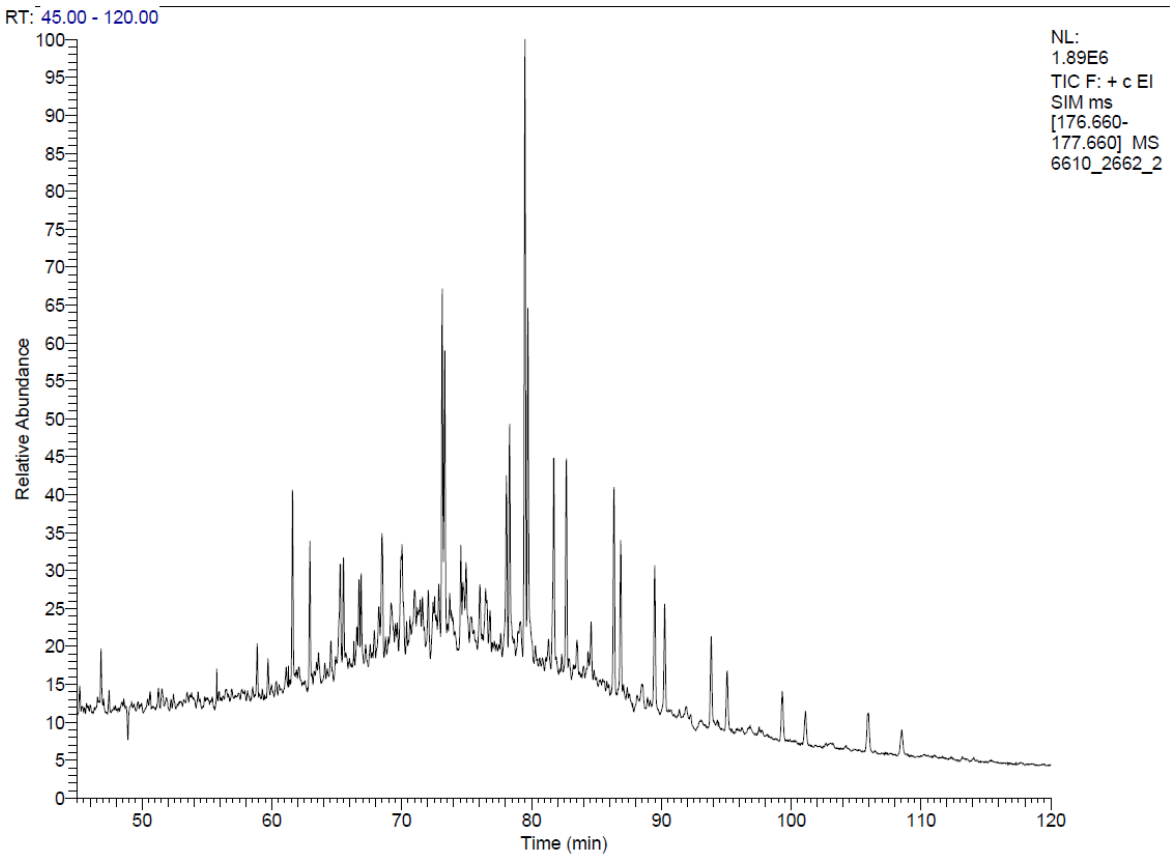
RT: 45.00 - 120.00
NL:
1.89E6
TIC F: + c EI
SIM ms
[176.660-
177.660] MS
6610_2662_2
Relative Abundance
Time (min)

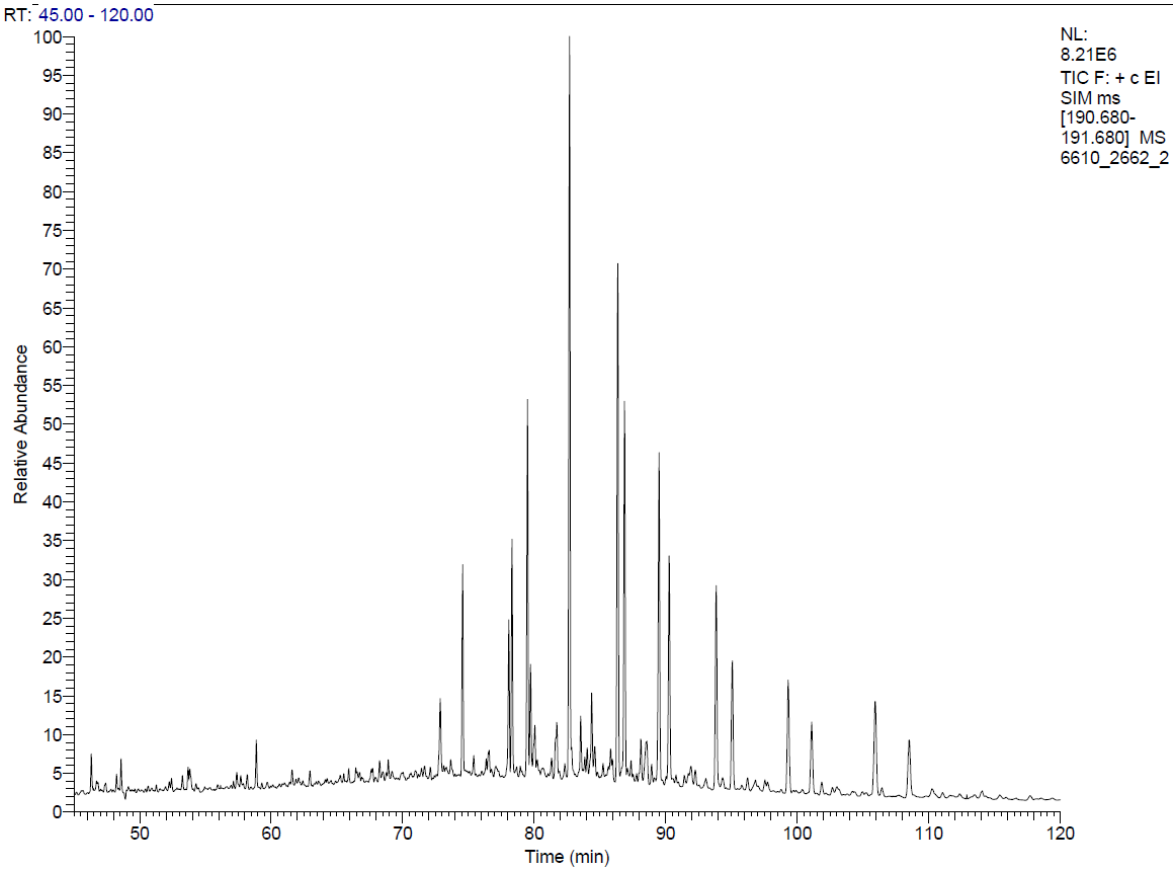
RT: 45.00 - 120.00
NL:
8.21E6
TIC F: + c EI
SIM ms
[190.680-
191.680] MS
6610_2662_2
Relative Abundance
Time (min)

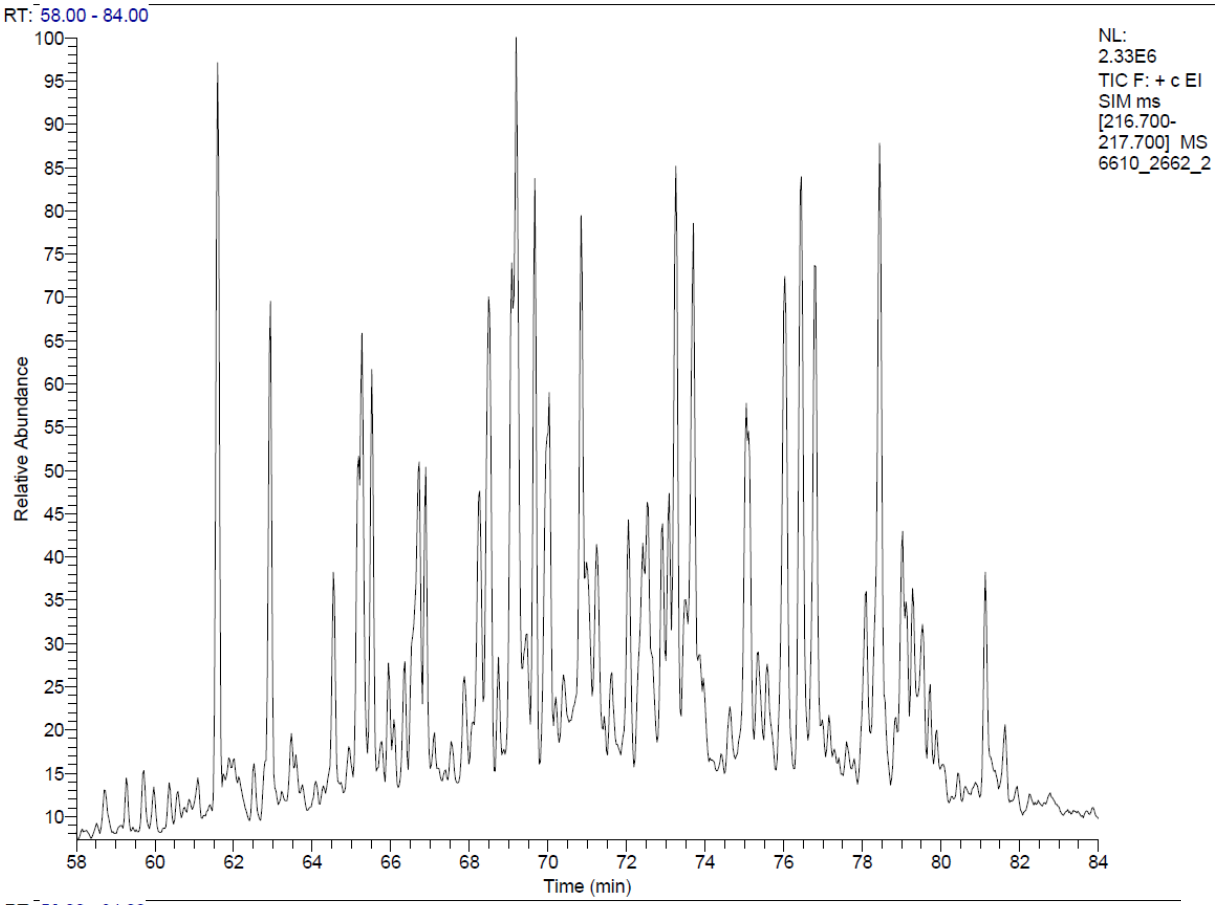
RT: 58.00 - 84.00
NL:
2.33E6
TIC F: + c EI
SIM ms
[216.700-
217.700] MS
6610_2662_2
Relative Abundance
Time (min)

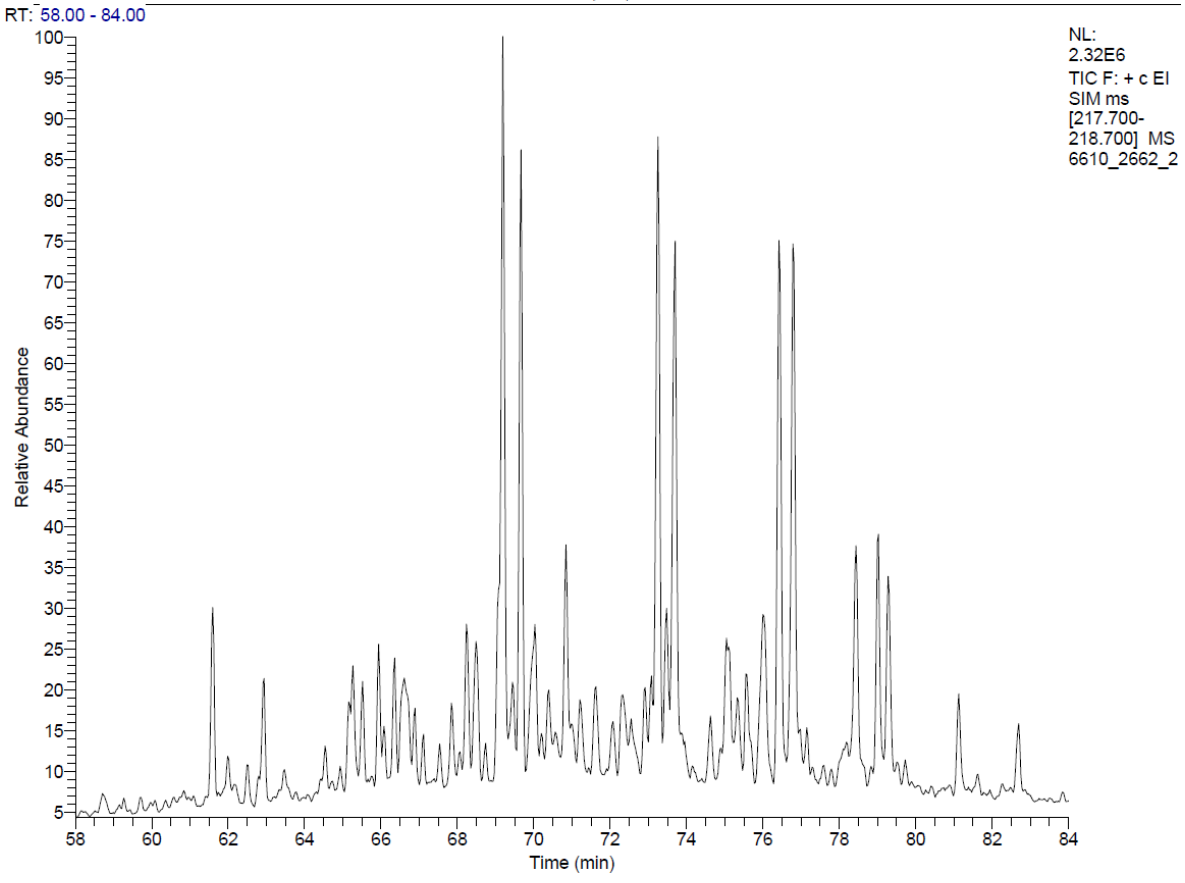
RT: 58.00 - 84.00
NL:
2.32E6
TIC F: + c EI
SIM ms
[217.700-
218.700] MS
6610_2662_2
Relative Abundance
Time (min)

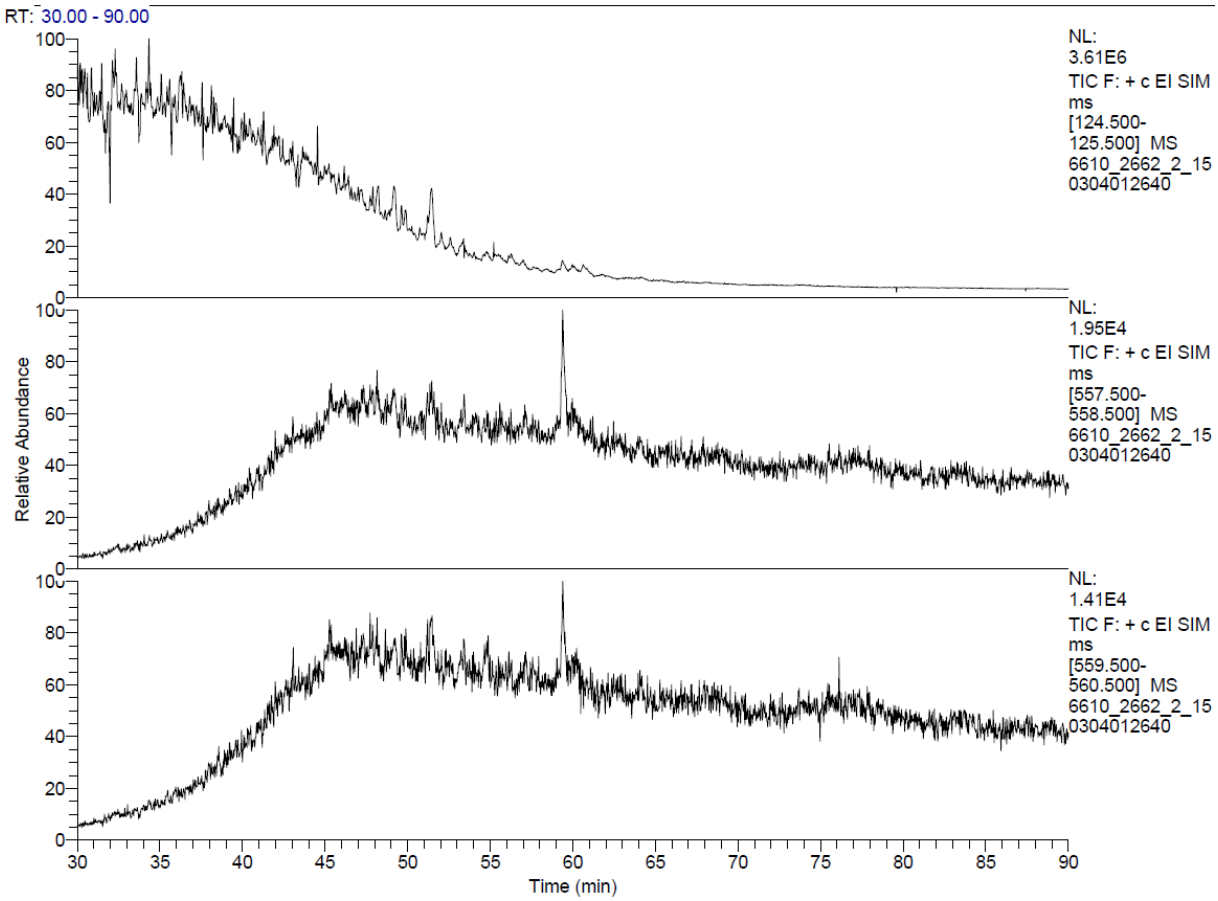
RT: 30.00 - 90.00
NL:
3.61E6
TIC F: + c EI SIM
ms
[124.500-
125.500] MS
6610_2662_2_15
0304012640
NL:
1.95E4
TIC F: + c EI SIM
ms
[557.500-
558.500] MS
6610_2662_2_15
0304012640
NL:
1.41E4
TIC F: + c EI SIM
ms
[559.500-
560.500] MS
6610_2662_2_15
0304012640
Relative Abundance
Time (min)

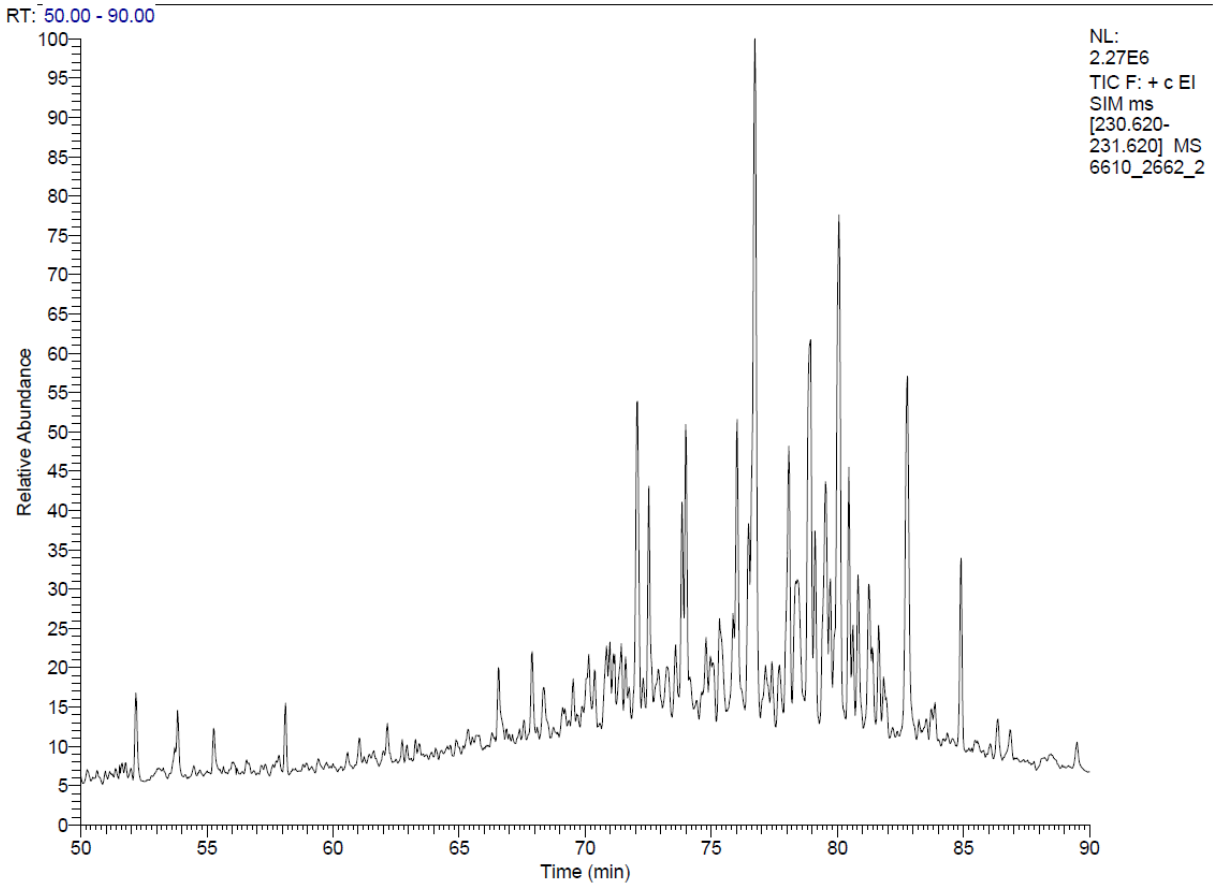
RT: 50.00 - 90.00
NL:
2.27E6
TIC F: + c EI
SIM ms
[230.620-
231.620] MS
6610_2662_2
Relative Abundance
Time (min)

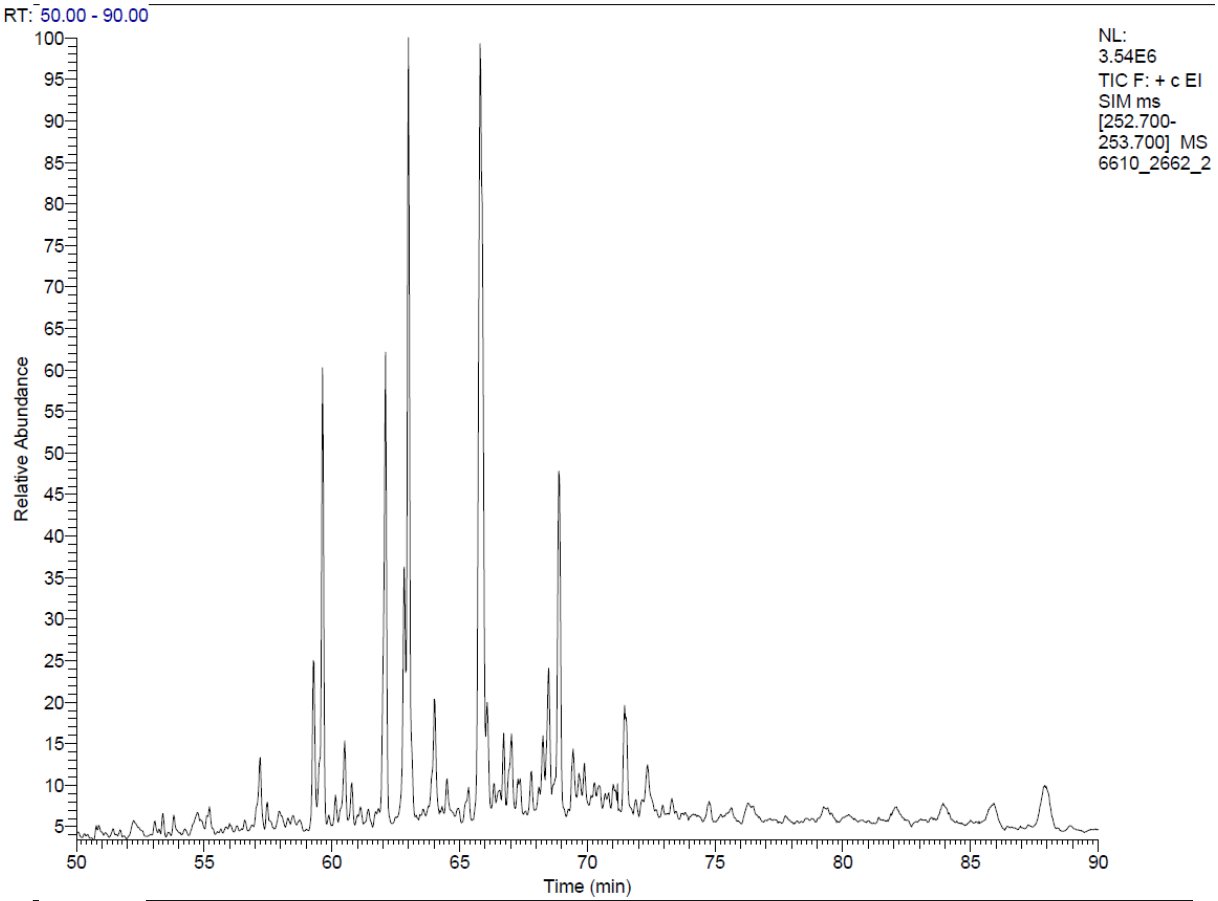
RT: 50.00 - 90.00
NL:
3.54E6
TIC F: + c EI
SIM ms
[252.700-
253.700] MS
6610_2662_2
Relative Abundance
Time (min)

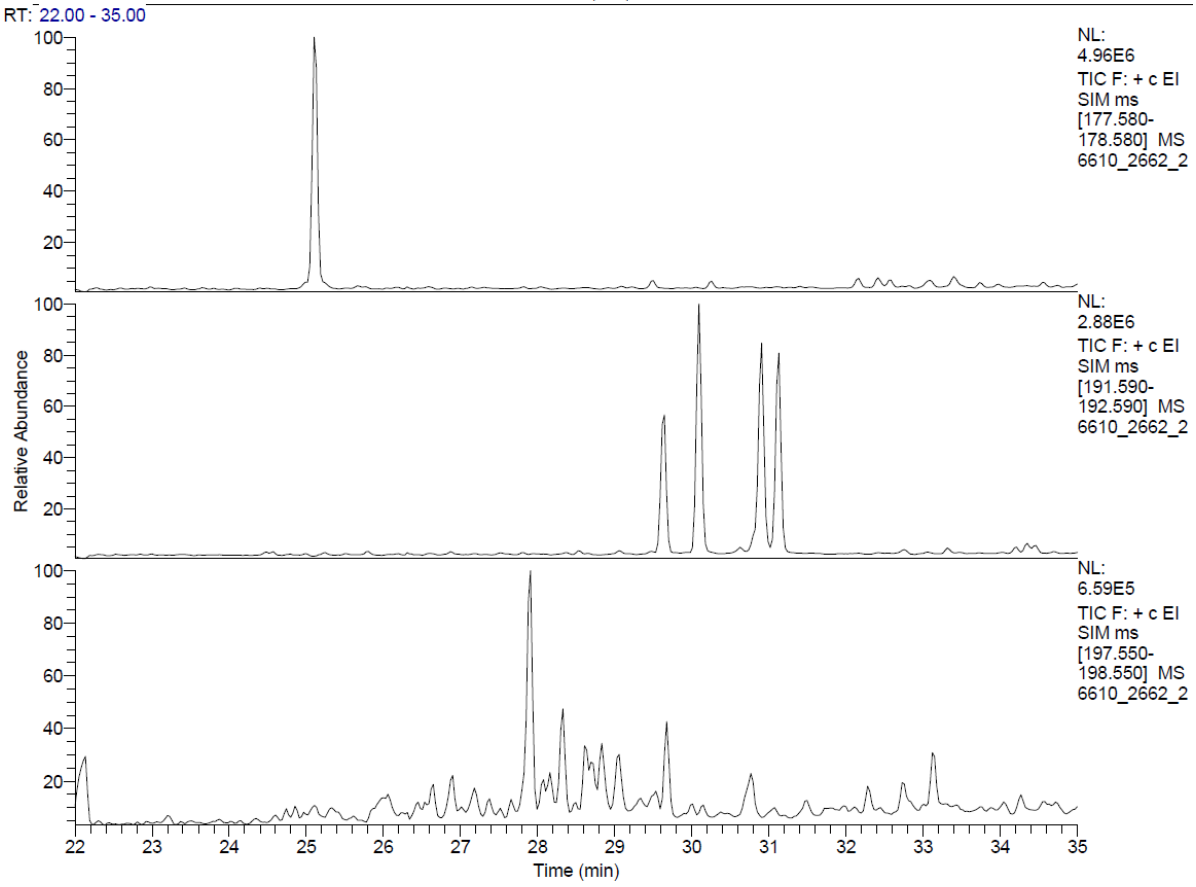
RT: 22.00 - 35.00
NL:
4.96E6
TIC F: + c EI
SIM ms
[177.580-
178.580] MS
6610_2662_2
NL:
2.88E6
TIC F: + c EI
SIM ms
[191.590-
192.590] MS
6610_2662_2
NL:
6.59E5
TIC F: + c EI
SIM ms
[197.550-
198.550] MS
6610_2662_2
Relative Abundance
Time (min)

B-3

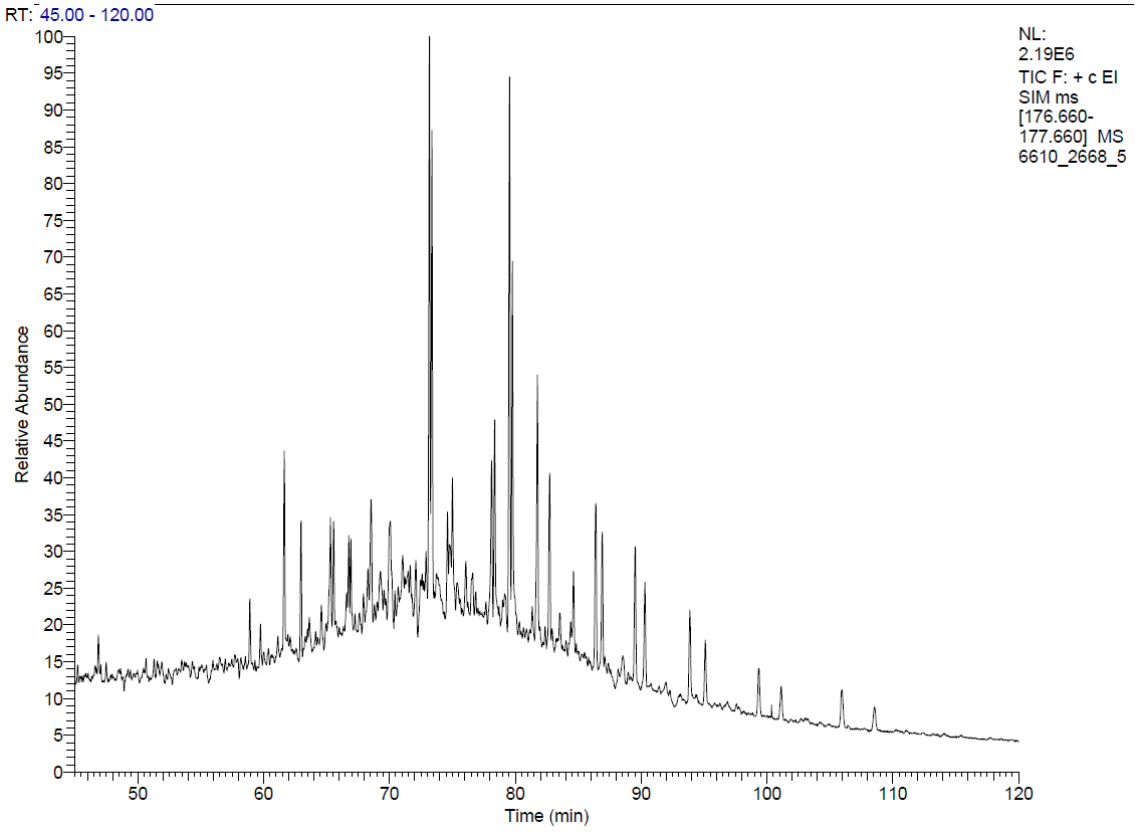
RT: 45.00 - 120.00
NL:
2.19E6
TIC F: + c EI
SIM ms
[176.660-
177.660] MS
6610_2668_5
Relative Abundance
Time (min)

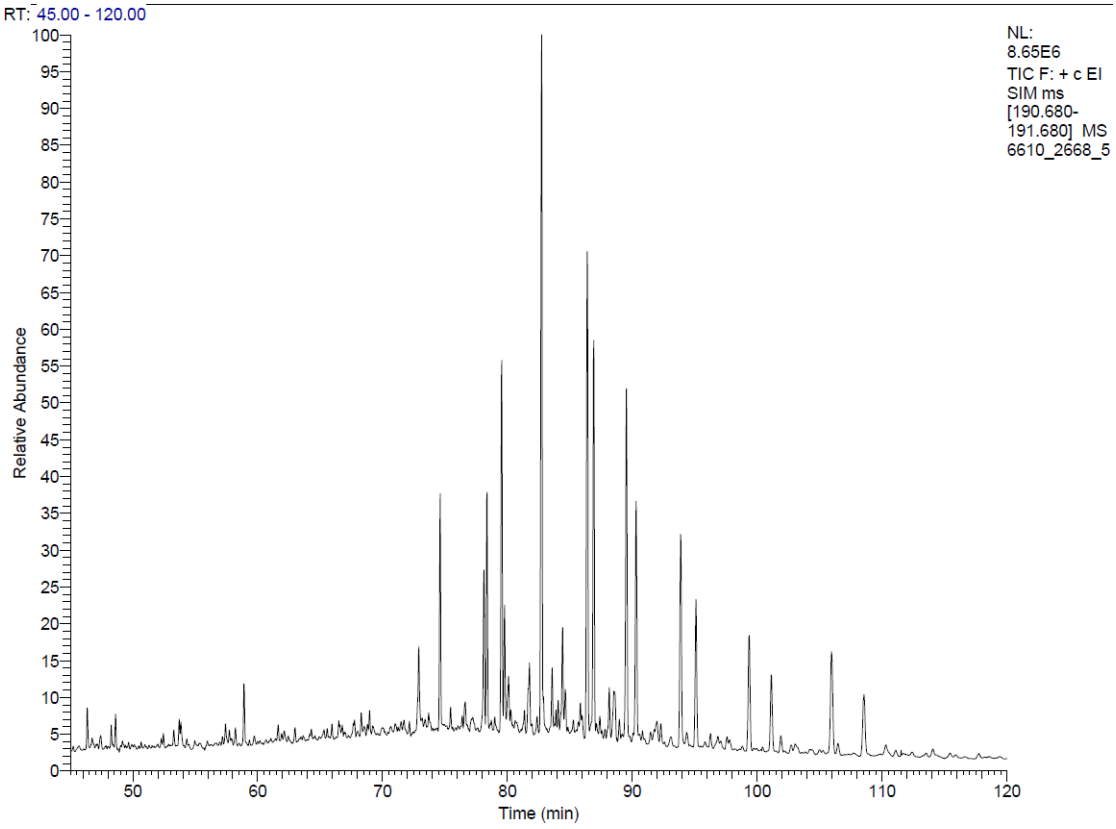
RT: 45.00 - 120.00
NL:
8.65E6
TIC F: + c EI
SIM ms
[190.680-
191.680] MS
6610_2668_5
Relative Abundance
Time (min)

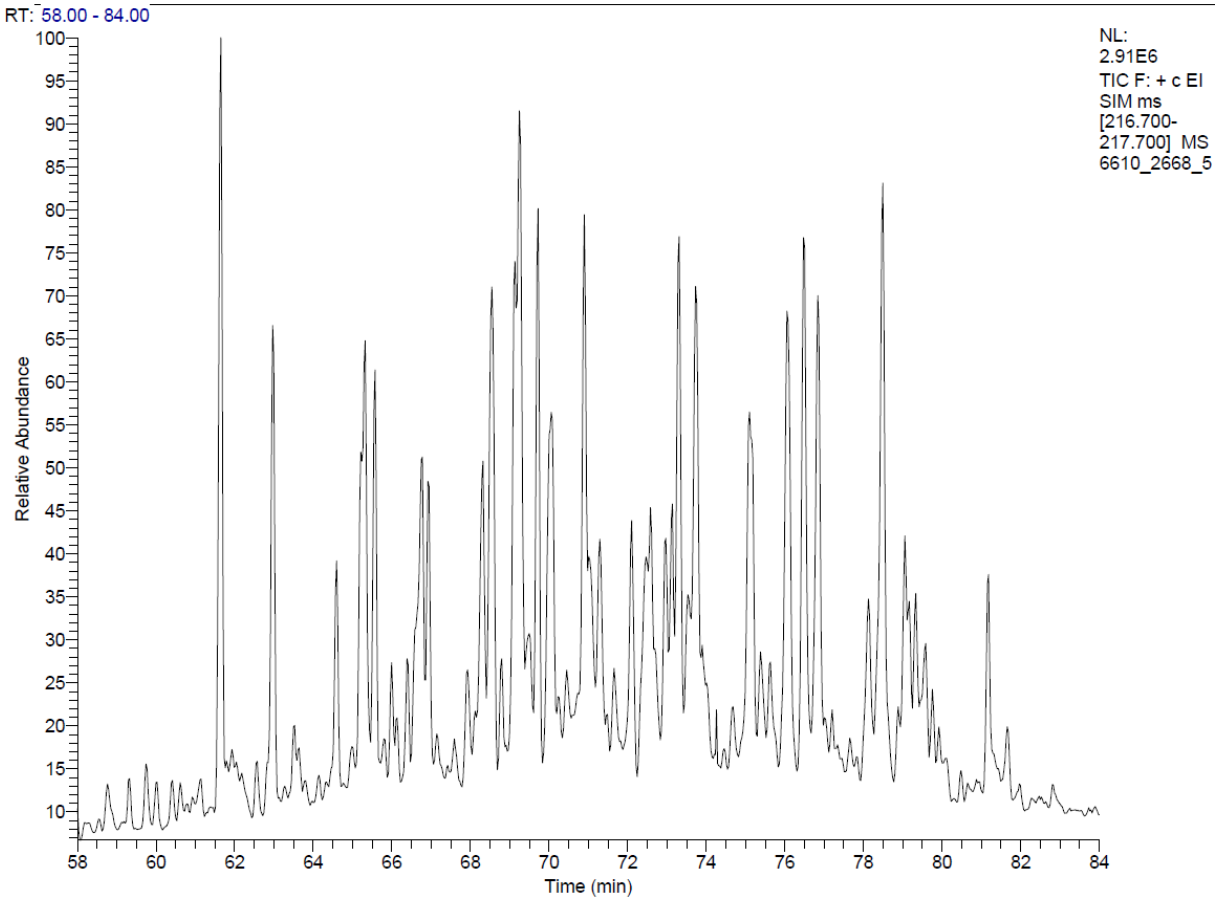
RT: 58.00 - 84.00
NL:
2.91E6
TIC F: + c EI
SIM ms
[216.700-
217.700] MS
6610_2668_5
Relative Abundance
Time (min)

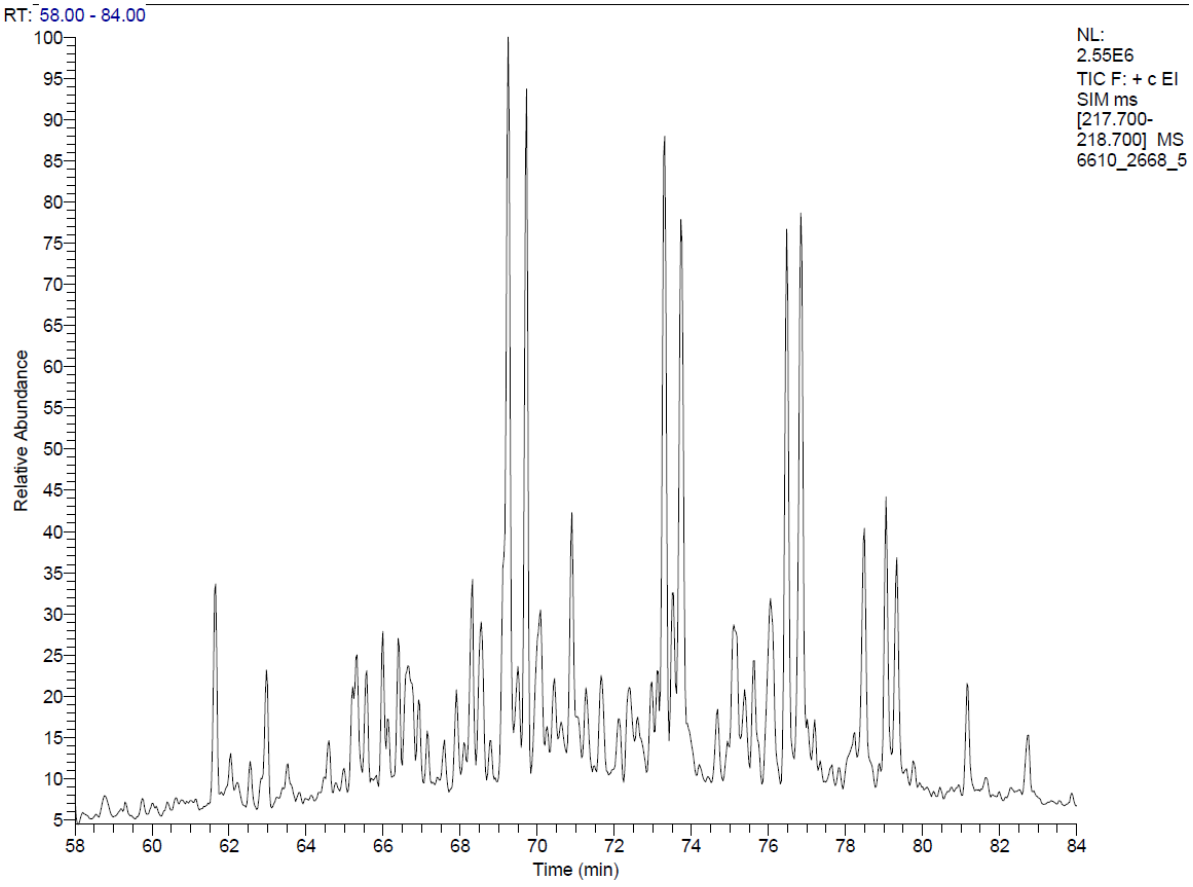
RT: 58.00 - 84.00
NL:
2.55E6
TIC F: + c EI
SIM ms
[217.700-
218.700] MS
6610_2668_5
Relative Abundance
Time (min)

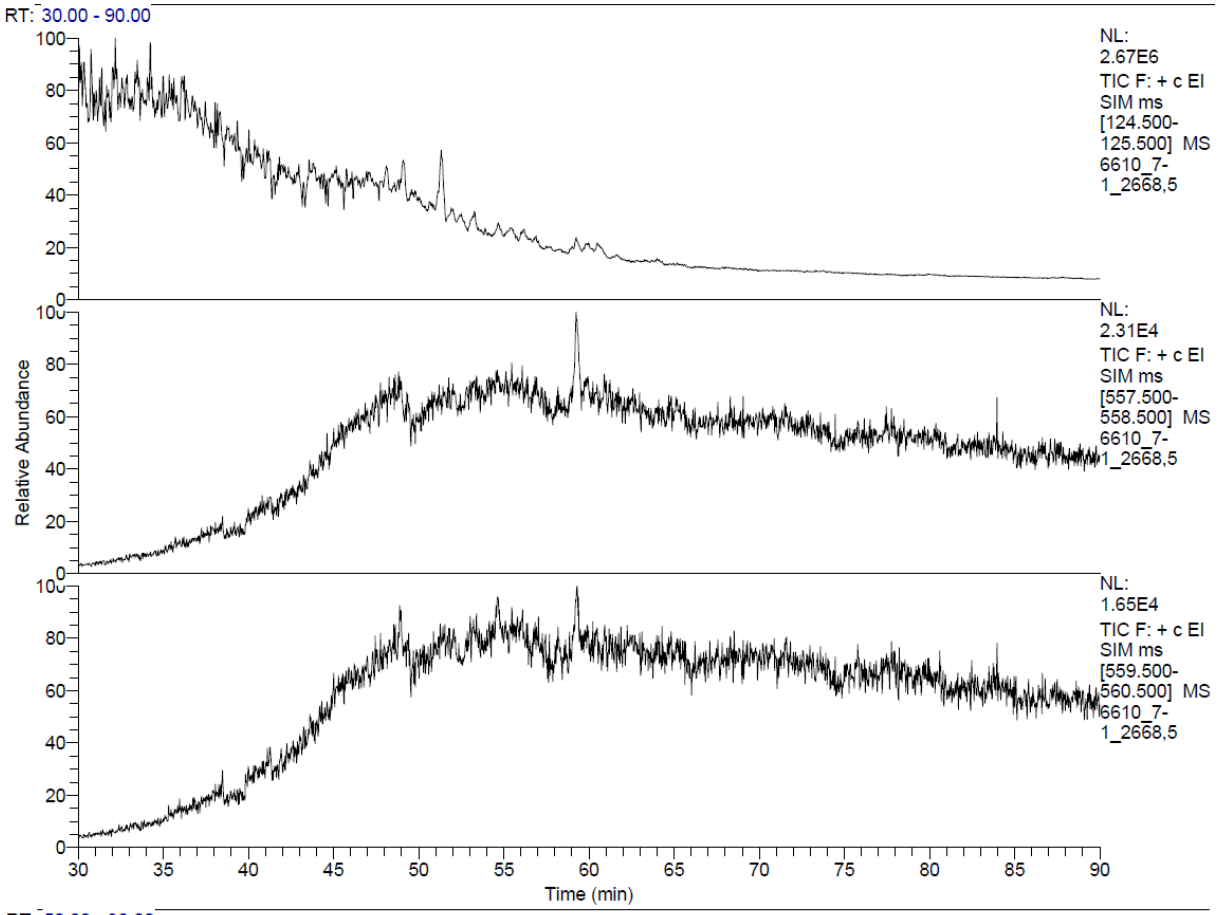
RT: 30.00 - 90.00
NL:
2.67E6
TIC F: + c EI
SIM ms
[124.500-
125.500] MS
6610_7-
1_2668,5
NL:
2.31E4
TIC F: + c EI
SIM ms
[557.500-
558.500] MS
6610_7-
1_2668,5
NL:
1.65E4
TIC F: + c EI
SIM ms
[559.500-
560.500] MS
6610_7-
1_2668,5
Relative Abundance
Time (min)

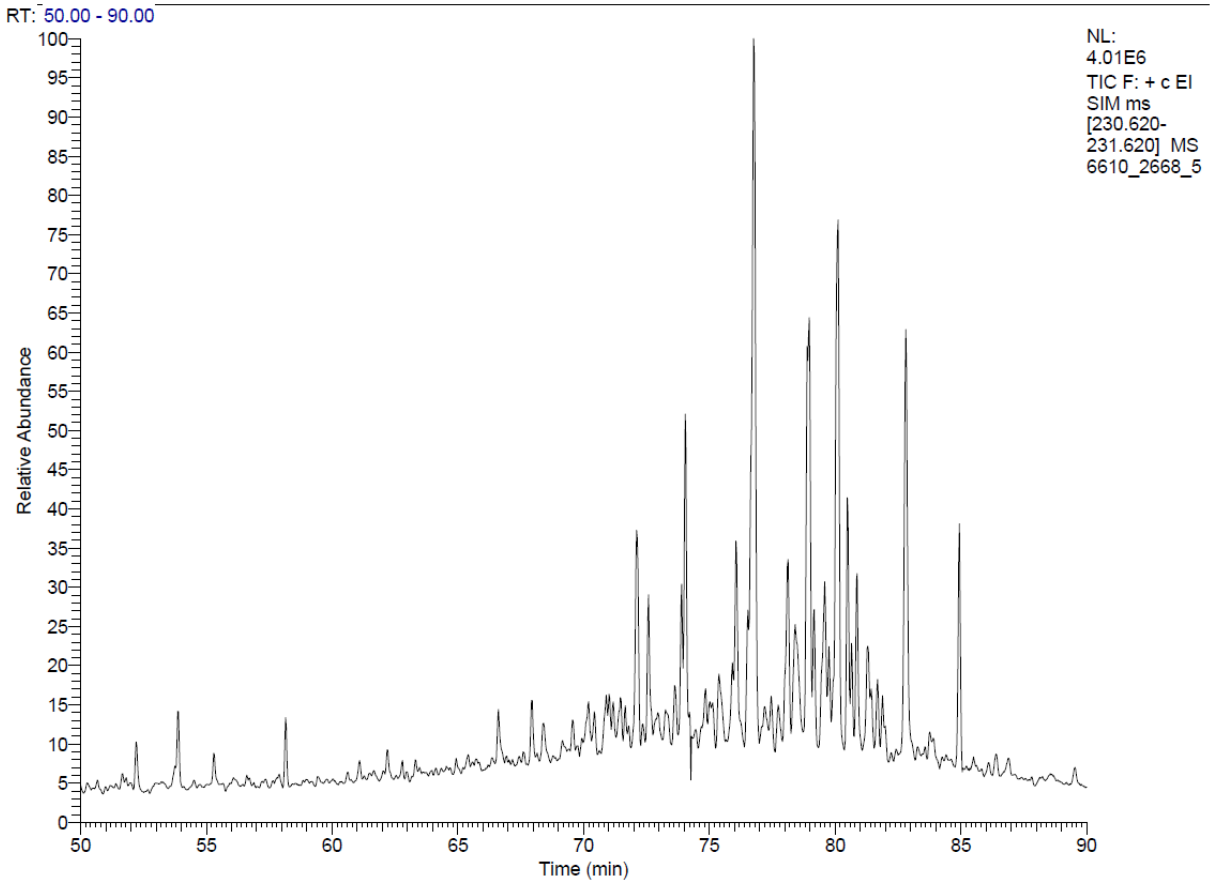
RT: 50.00 - 90.00
NL:
4.01E6
TIC F: + c EI
SIM ms
[230.620-
231.620] MS
6610_2668_5
Relative Abundance
Time (min)

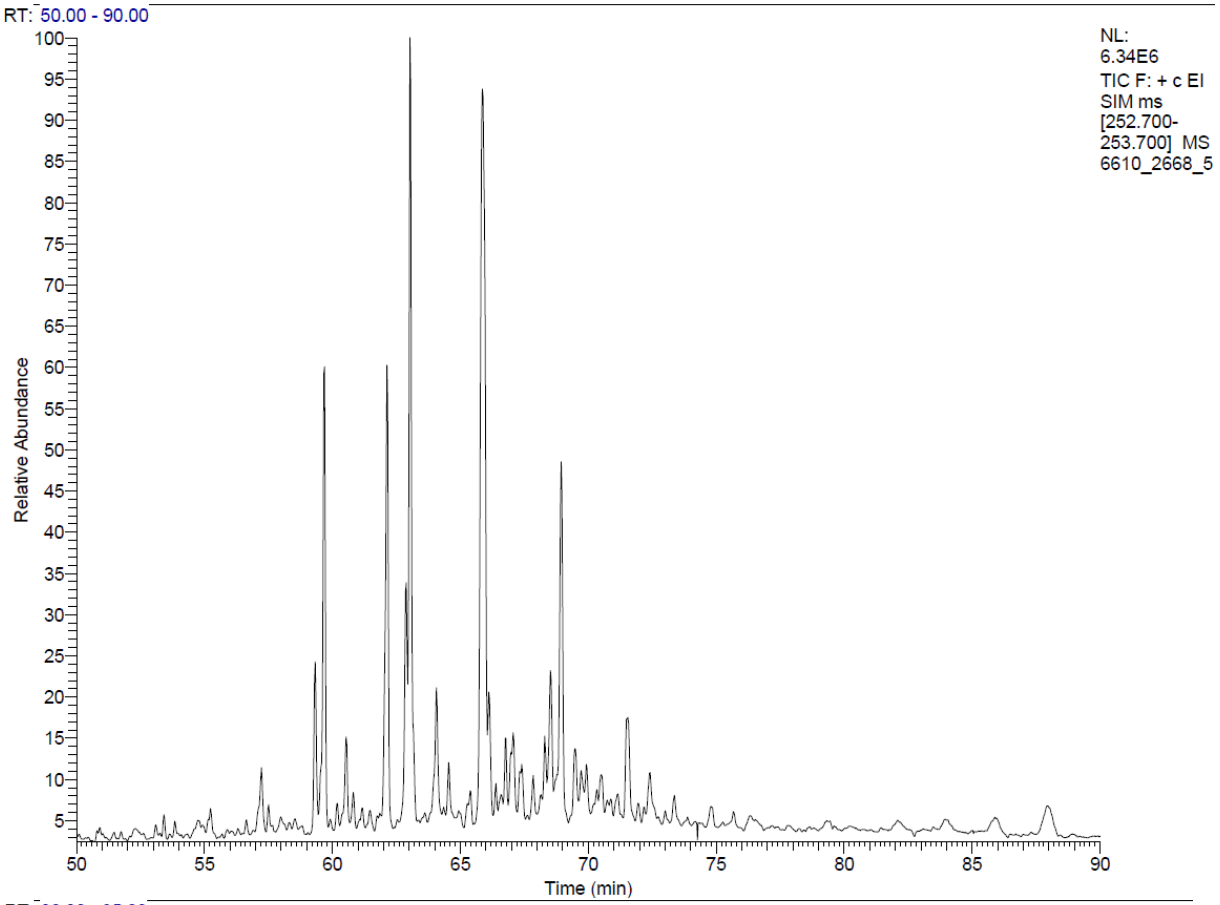
RT: 50.00 - 90.00
NL:
6.34E6
TIC F: + c EI
SIM ms
[252.700-
253.700] MS
6610_2668_5
Relative Abundance
Time (min)

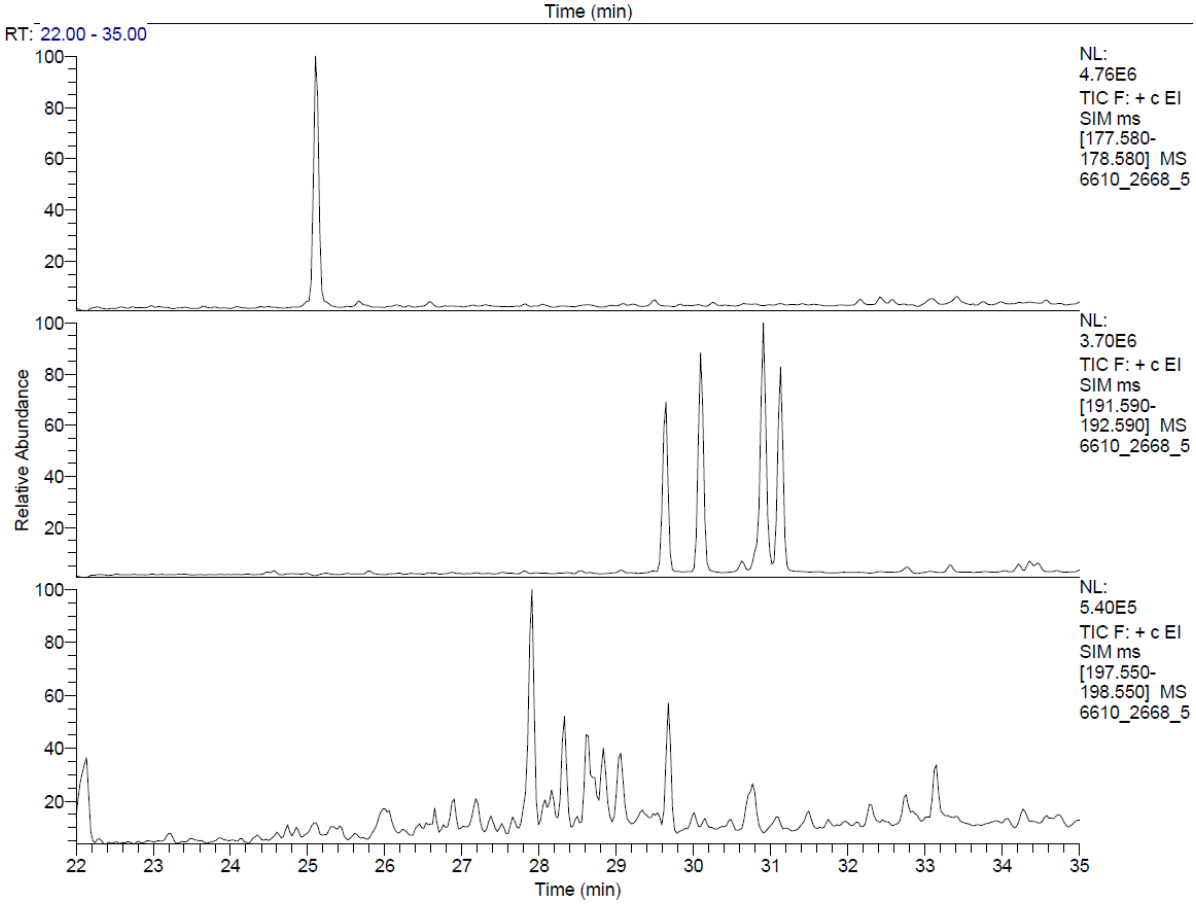
RT: 22.00 - 35.00
NL:
4.76E6
TIC F: + c EI
SIM ms
[177.580-
178.580] MS
6610_2668_5
NL:
3.70E6
TIC F: + c EI
SIM ms
[191.590-
192.590] MS
6610_2668_5
NL:
5.40E5
TIC F: + c EI
SIM ms
[197.550-
198.550] MS
6610_2668_5
Relative Abundance
Time (min)

B-4

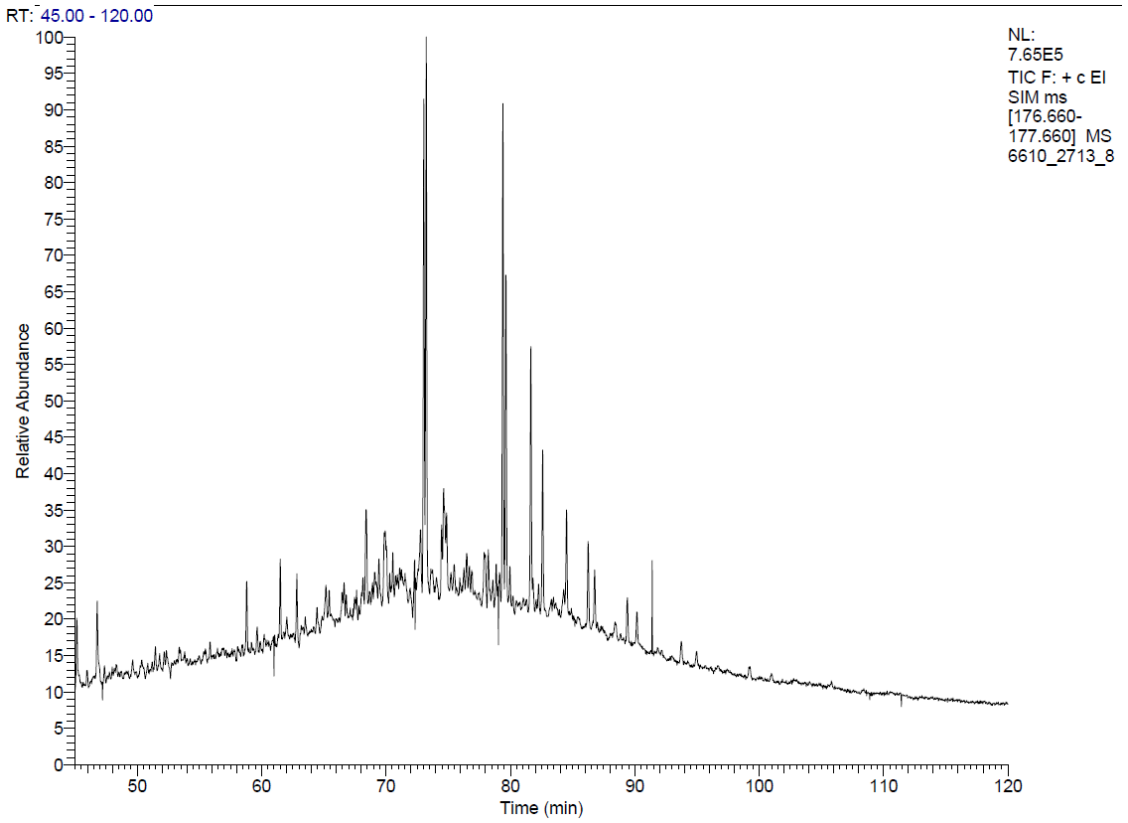
RT: 45.00 - 120.00
NL:
7.65E5
TIC F: + c EI
SIM ms
[176.660-
177.660] MS
6610_2713_8
Relative Abundance
Time (min)

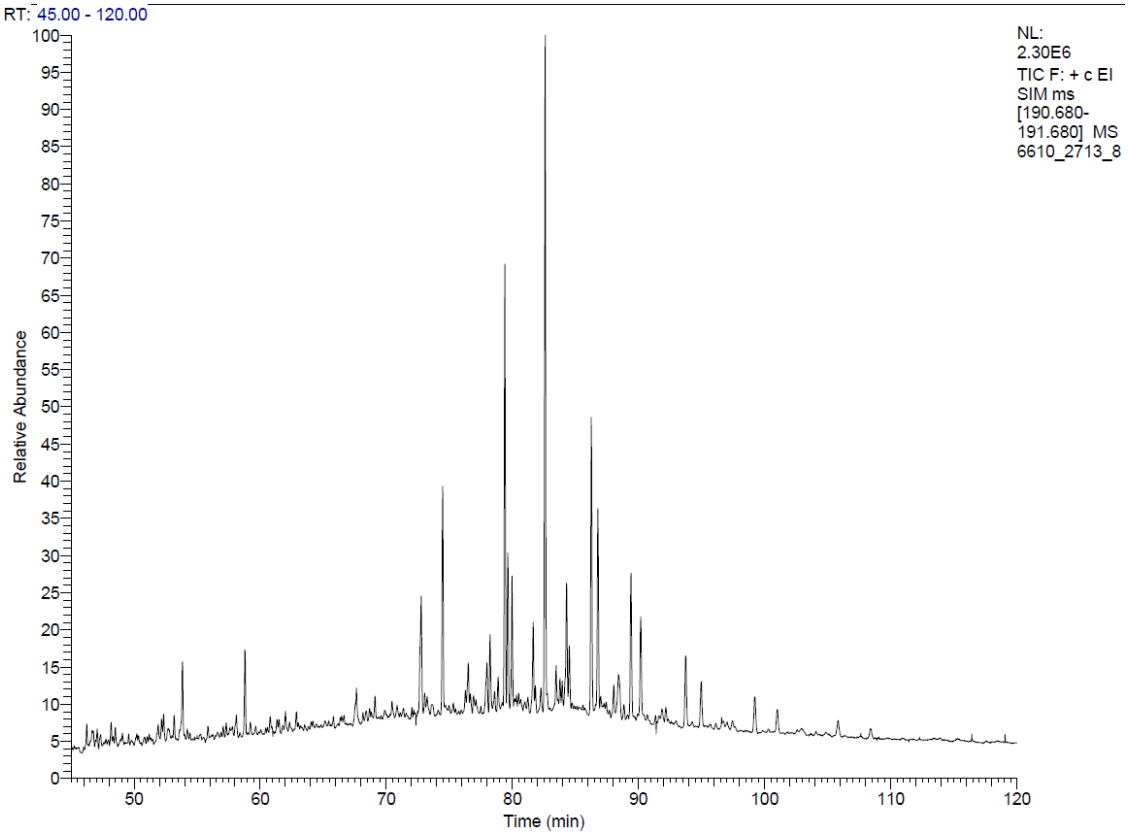
RT: 45.00 - 120.00
NL:
2.30E6
TIC F: + c EI
SIM ms
[190.680-
191.680] MS
6610_2713_8
Relative Abundance
Time (min)

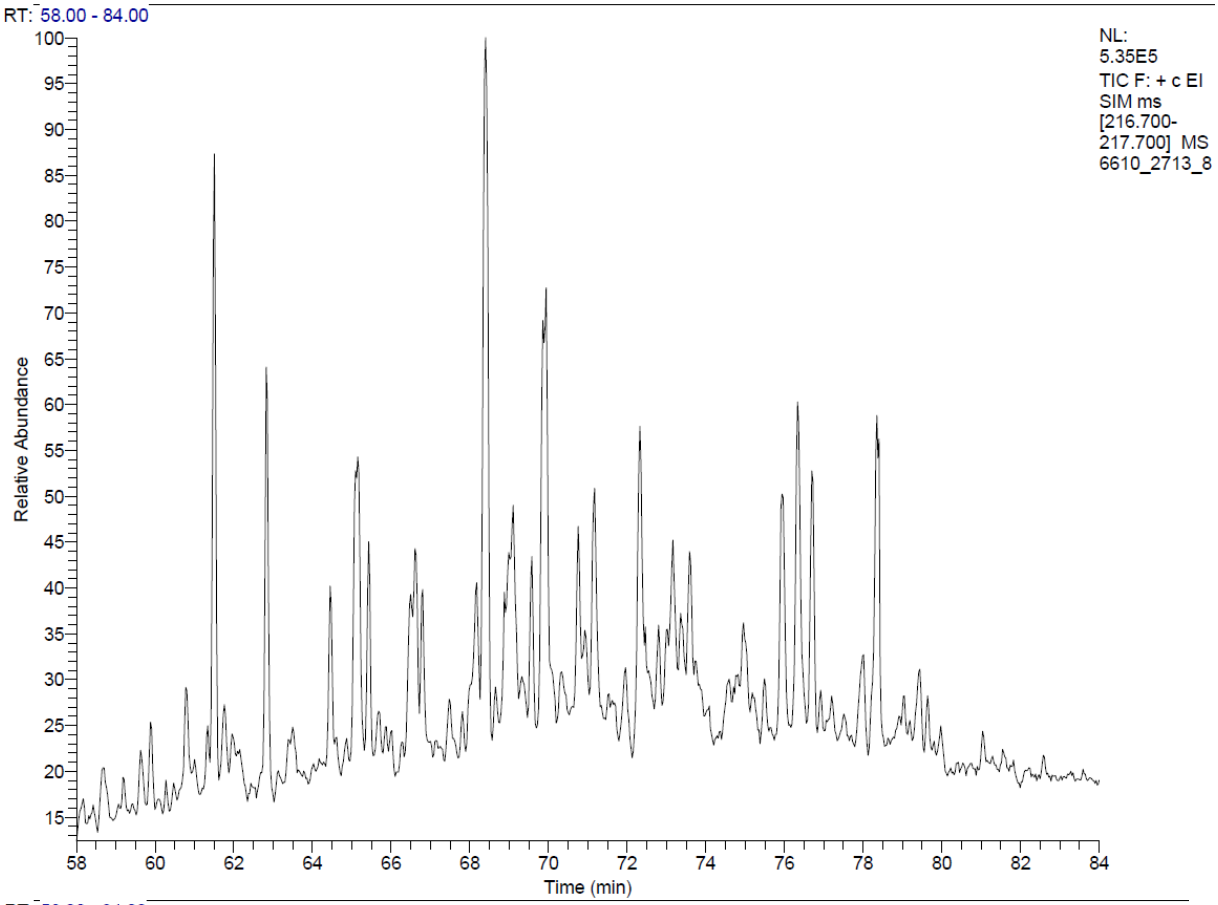
RT: 58.00 - 84.00
NL:
5.35E5
TIC F: + c EI
SIM ms
[216.700-
217.700] MS
6610_2713_8
Relative Abundance
Time (min)

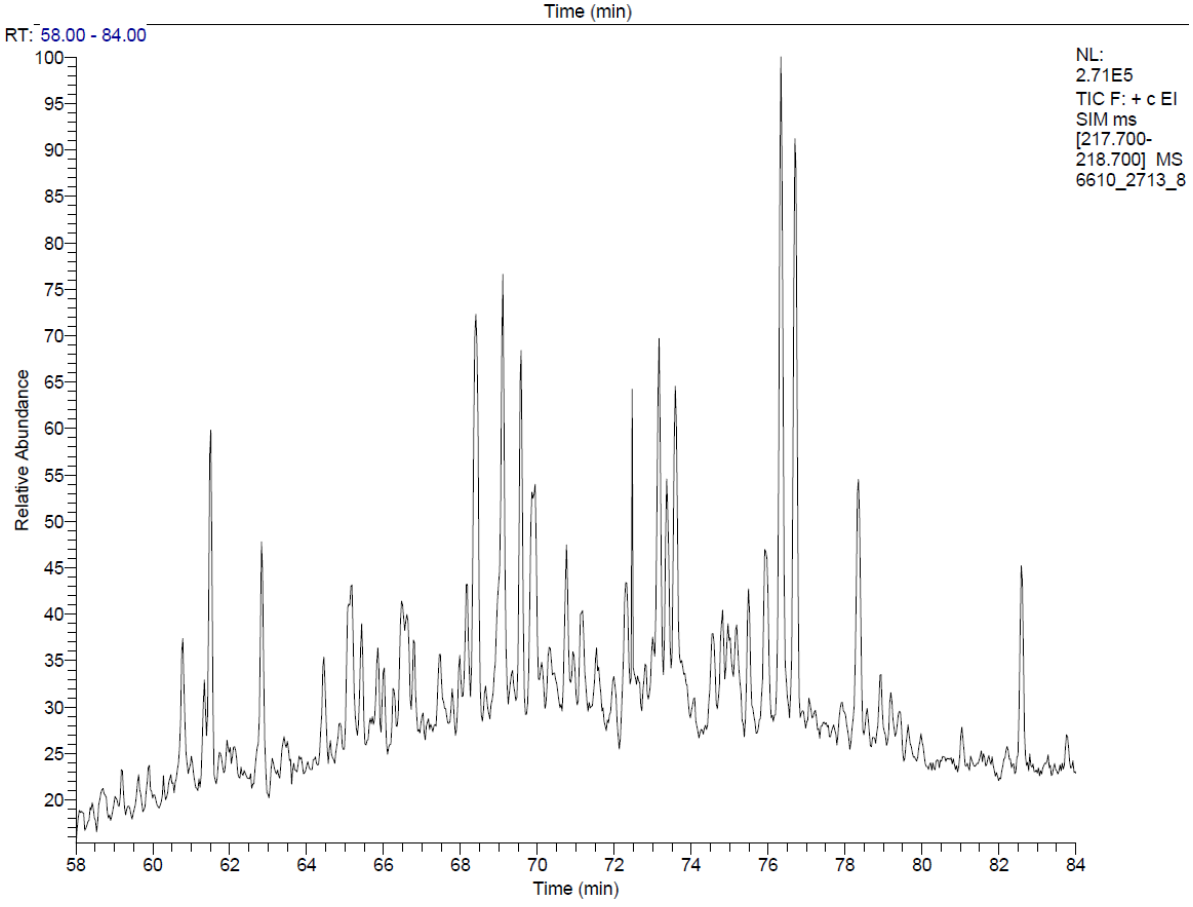
RT: 58.00 - 84.00
NL:
2.71E5
TIC F: + c EI
SIM ms
[217.700-
218.700] MS
6610_2713_8
Relative Abundance
Time (min)

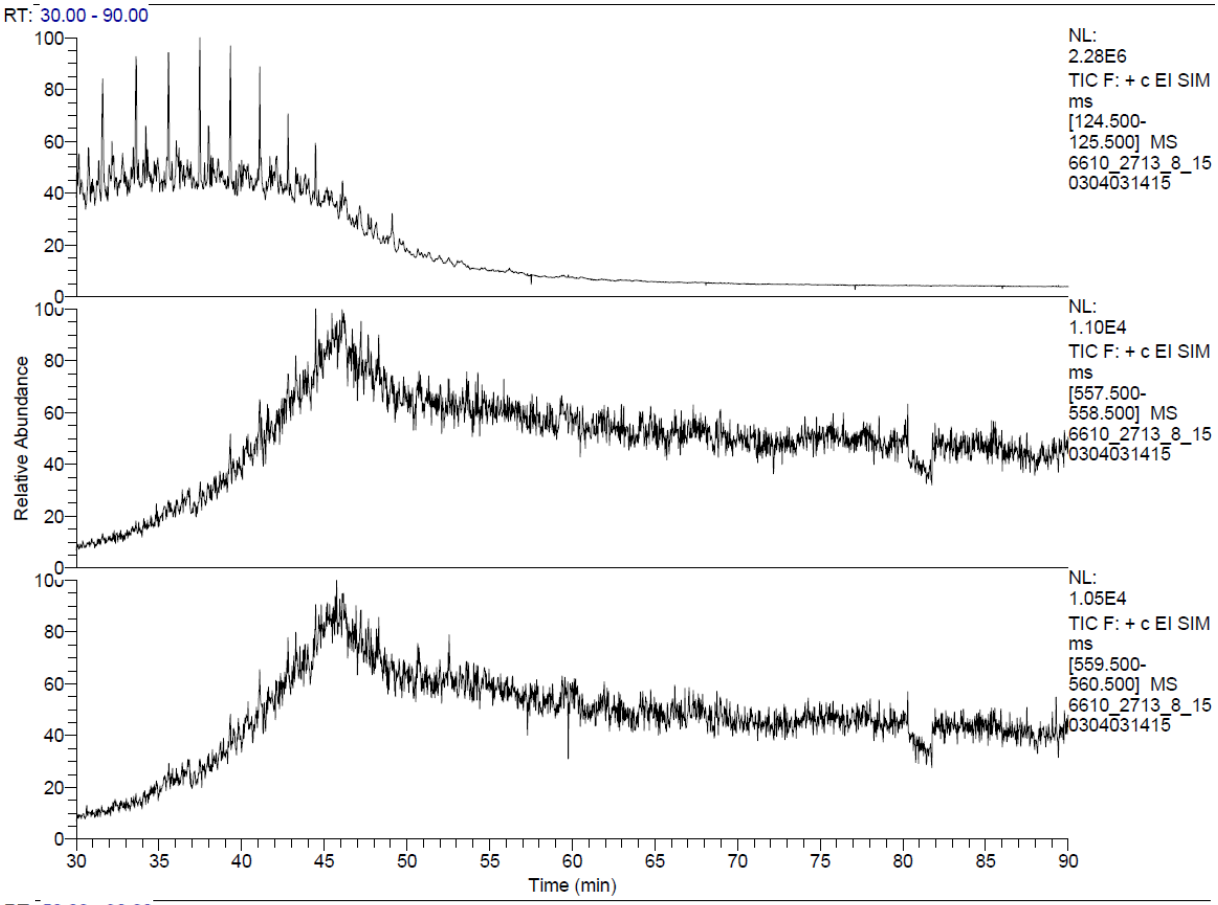
RT: 30.00 - 90.00
NL:
2.28E6
TIC F: + c EI SIM ms [124.500-125.500] MS 6610_2713_8_150304031415
NL:
1.10E4
TIC F: + c EI SIM ms [557.500-558.500] MS 6610_2713_8_150304031415
NL:
1.05E4
TIC F: + c EI SIM ms [559.500-560.500] MS 6610_2713_8_150304031415
Relative Abundance
Time (min)

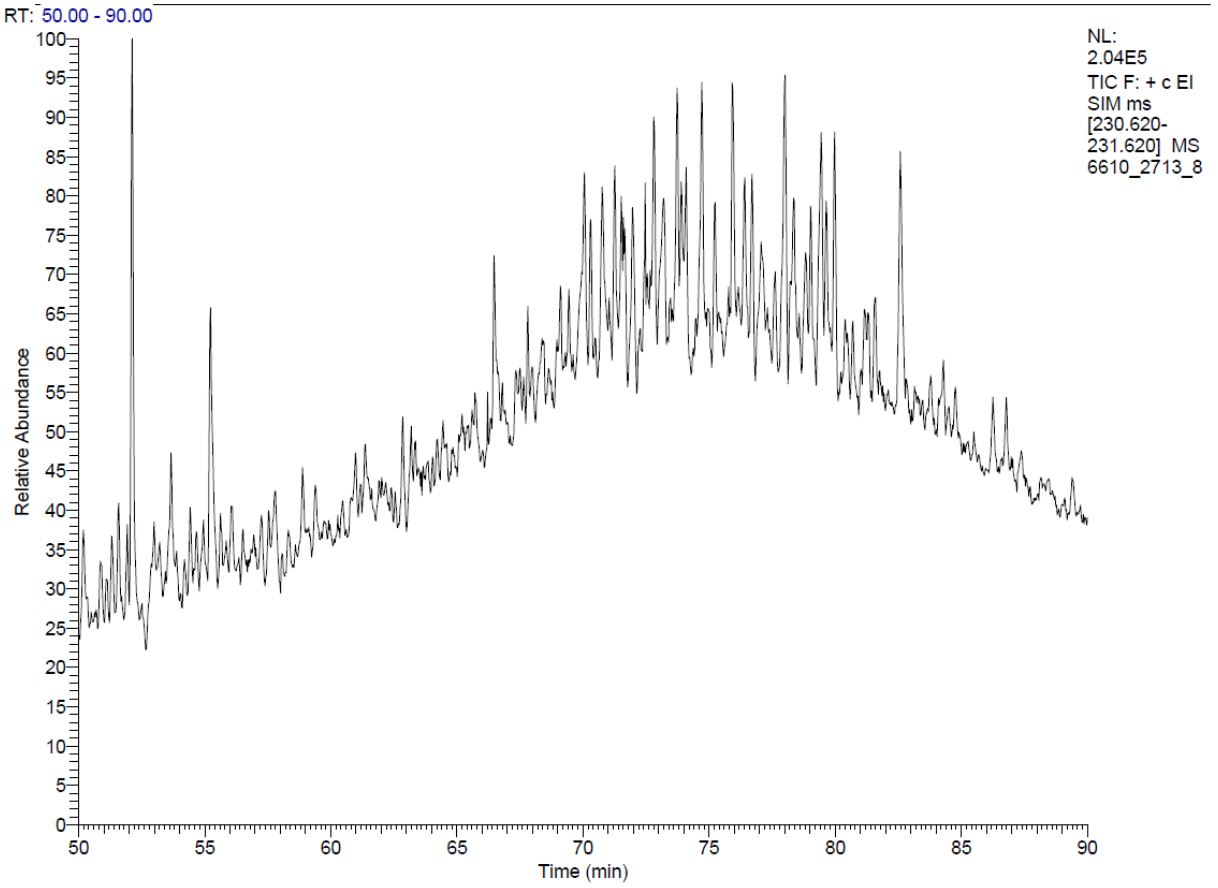
RT: 50.00 - 90.00
NL:
2.04E5
TIC F: + c EI SIM ms [230.620-231.620] MS 6610_2713_8
Relative Abundance
Time (min)

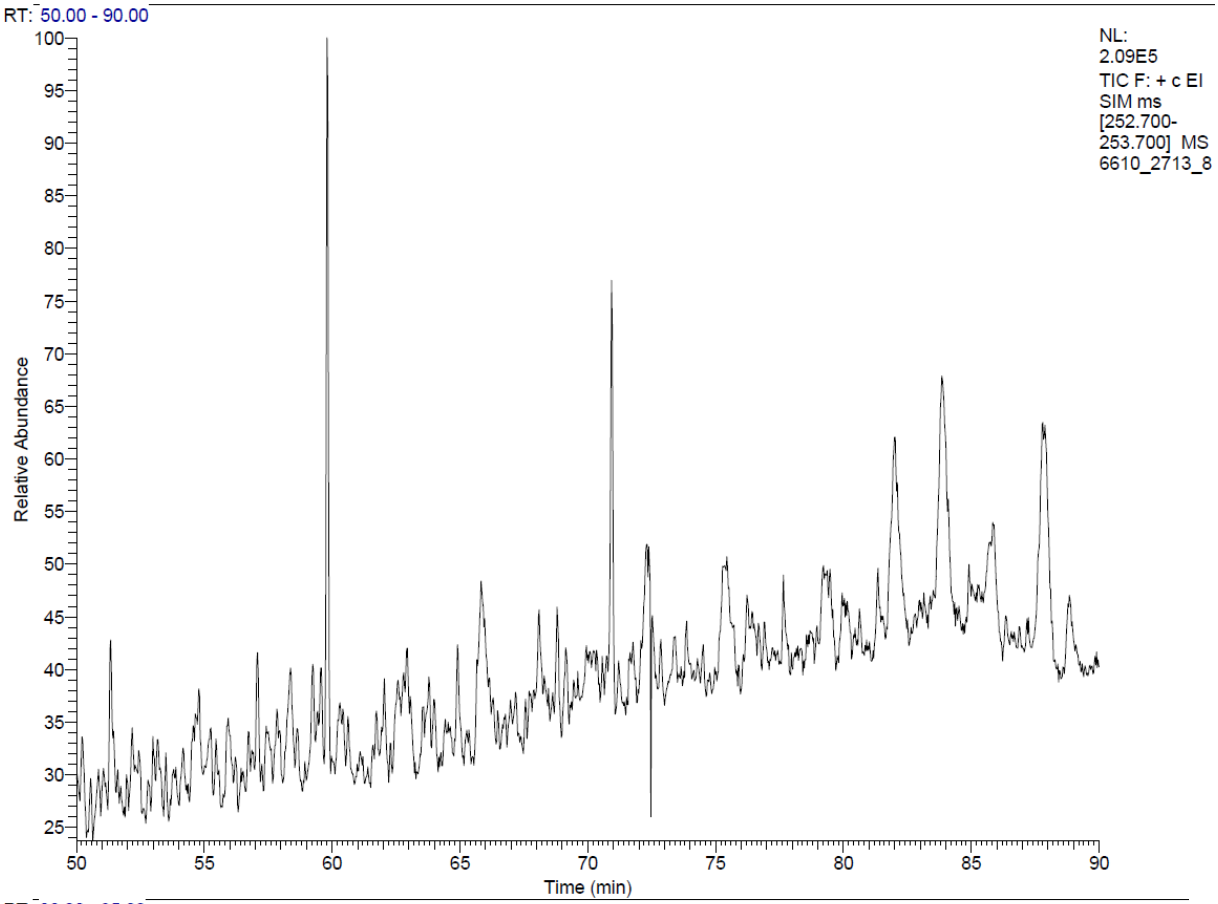
RT: 50.00 - 90.00
NL:
2.09E5
TIC F: + c EI
SIM ms
[252.700-
253.700] MS
6610_2713_8
Relative Abundance
Time (min)

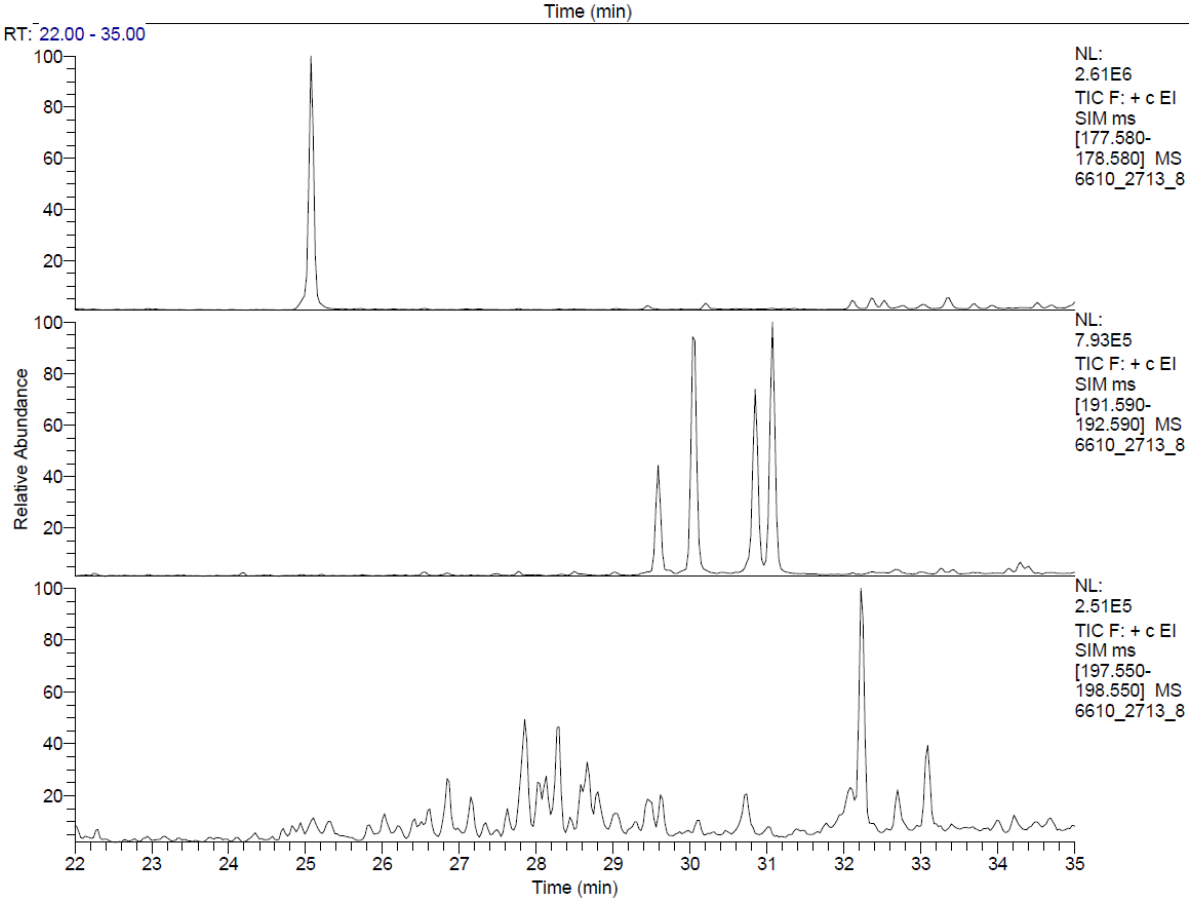
RT: 22.00 - 35.00
NL:
2.61E6
TIC F: + c EI
SIM ms
[177.580-
178.580] MS
6610_2713_8
NL:
7.93E5
TIC F: + c EI
SIM ms
[191.590-
192.590] MS
6610_2713_8
NL:
2.51E5
TIC F: + c EI
SIM ms
[197.550-
198.550] MS
6610_2713_8
Relative Abundance
Time (min)

B-5

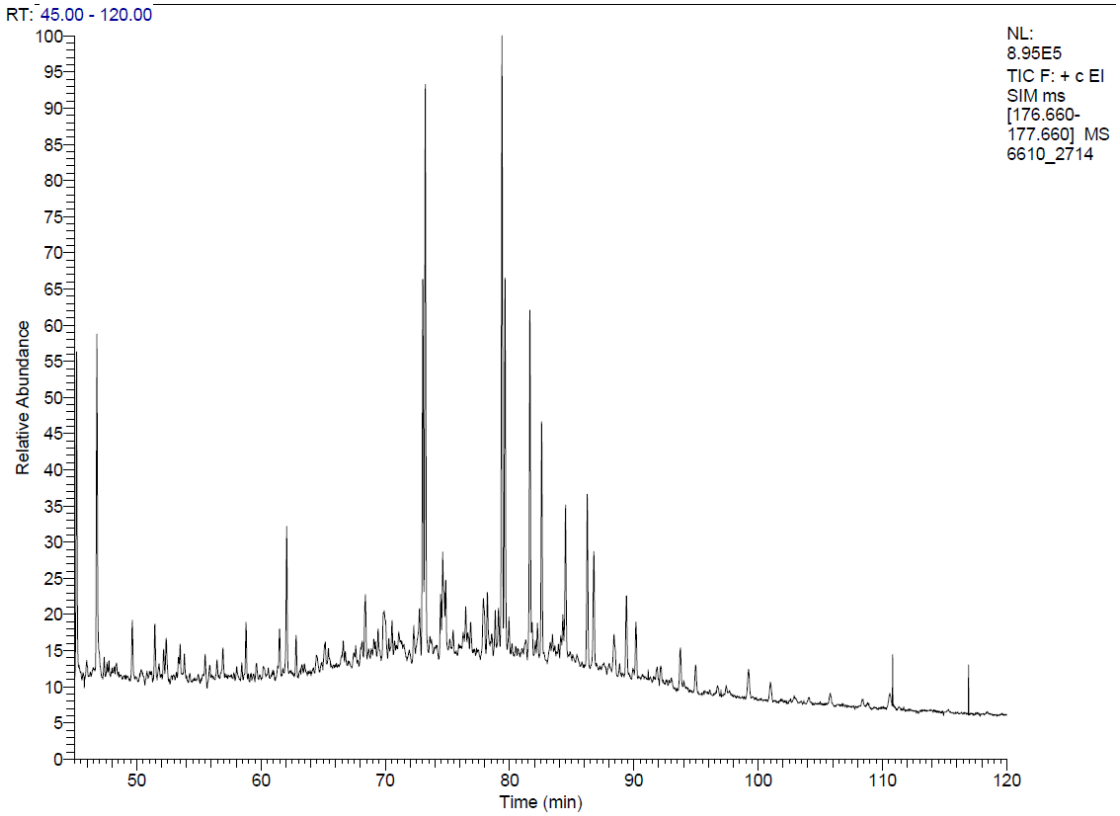
RT: 45.00 - 120.00
NL:
8.95E5
TIC F: + c EI
SIM ms
[176.660-
177.660] MS
6610_2714
Relative Abundance
Time (min)

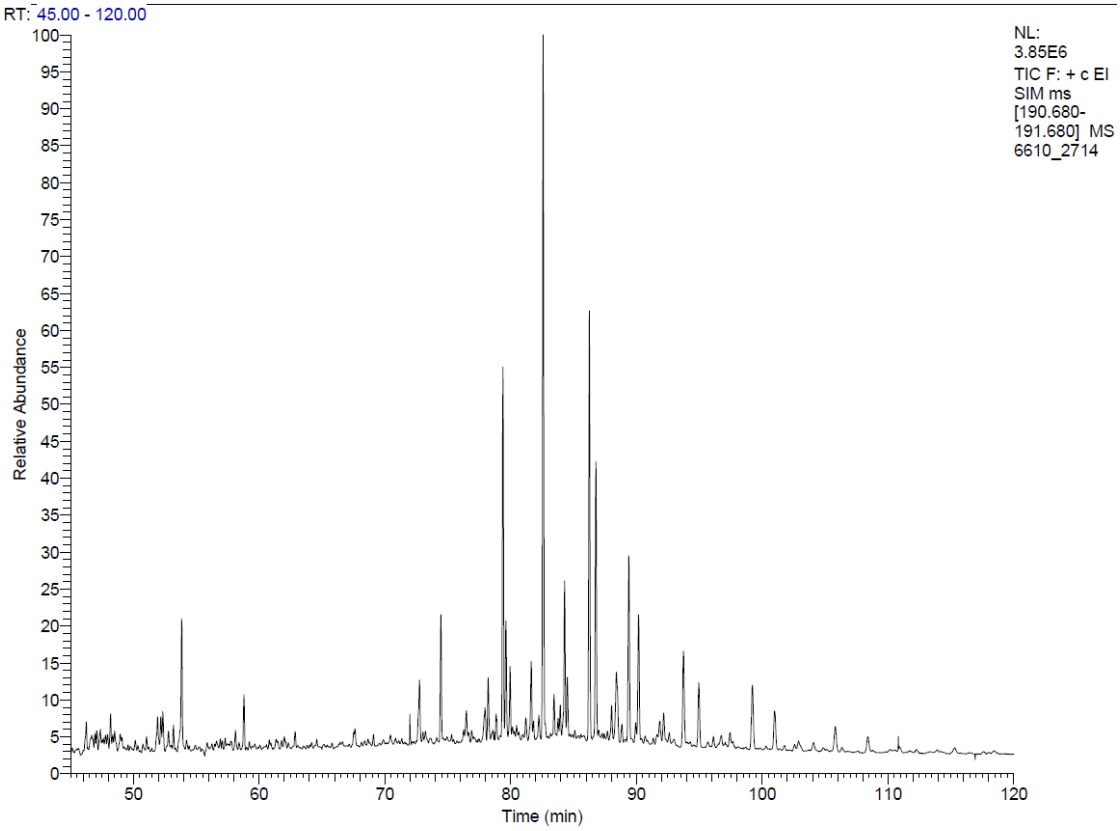
RT: 45.00 - 120.00
NL:
3.85E6
TIC F: + c EI
SIM ms
[190.680-
191.680] MS
6610_2714
Relative Abundance
Time (min)

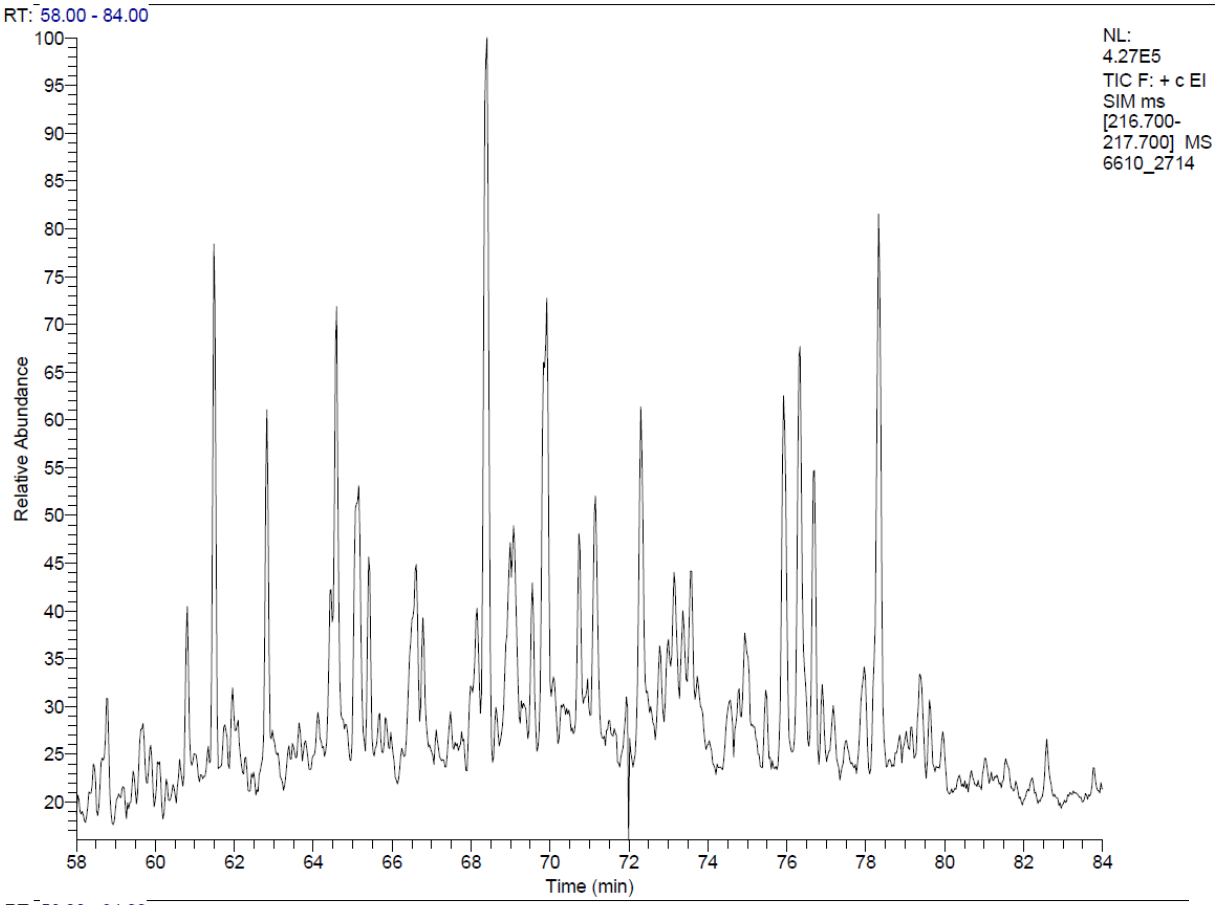
RT: 58.00 - 84.00
NL:
4.27E5
TIC F: + c EI
SIM ms
[216.700-
217.700] MS
6610_2714
Relative Abundance
Time (min)

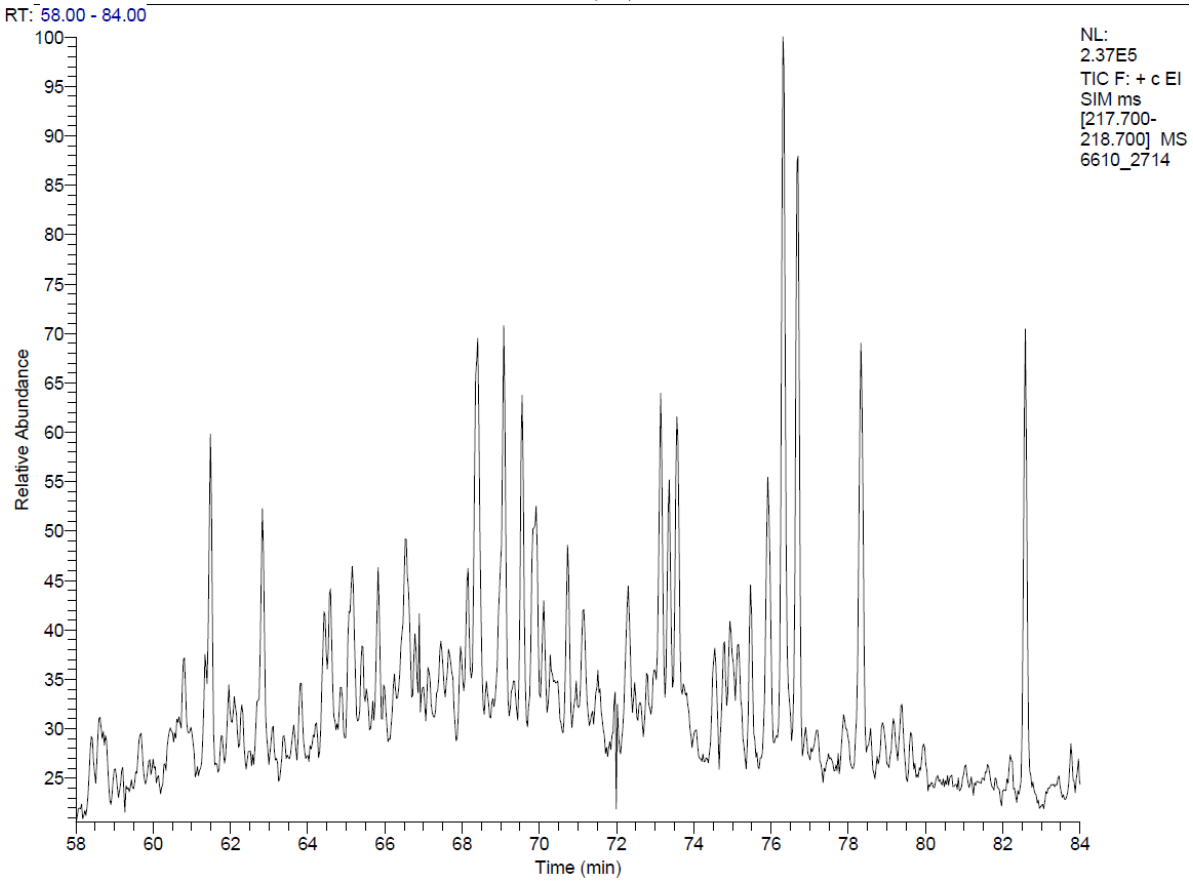
RT: 58.00 - 84.00
NL:
2.37E5
TIC F: + c EI
SIM ms
[217.700-
218.700] MS
6610_2714
Relative Abundance
Time (min)

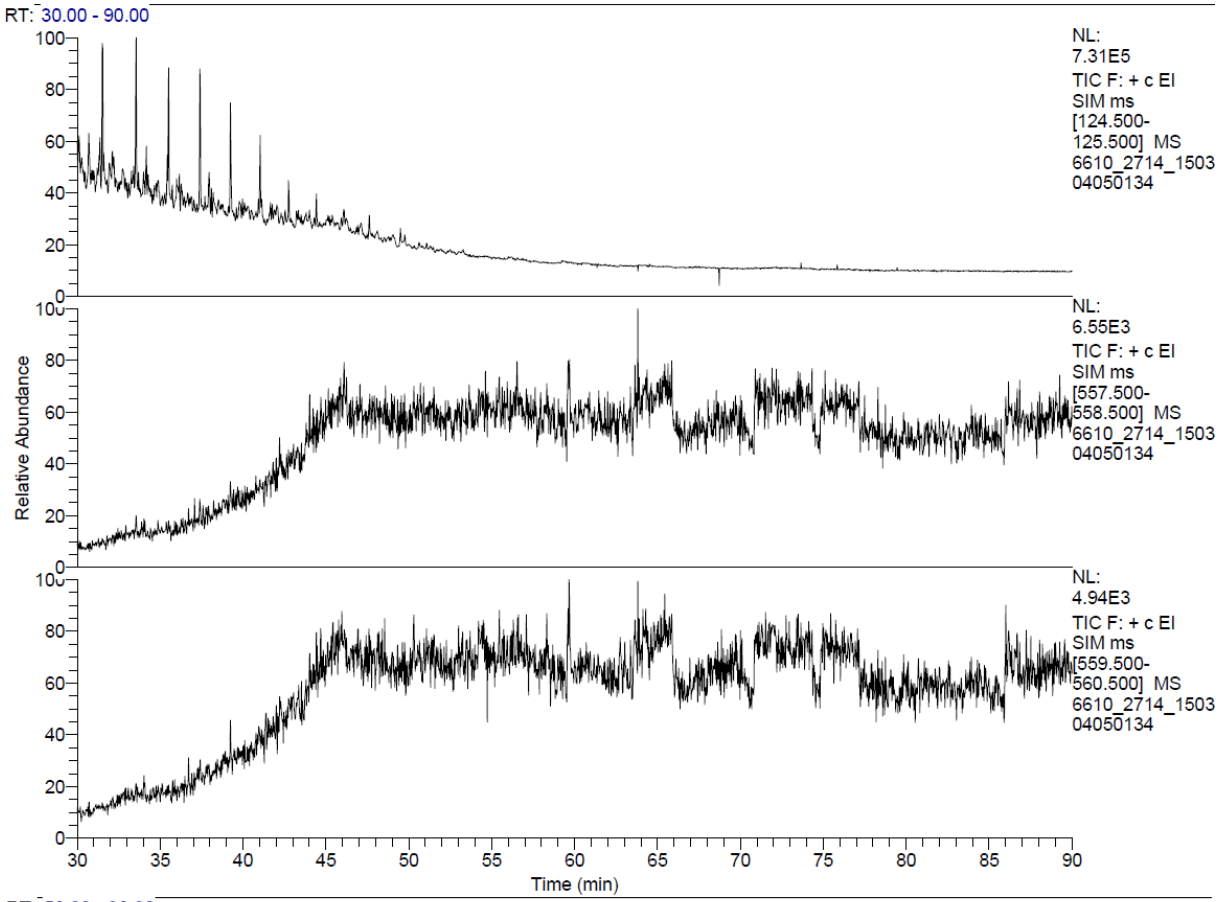
RT: 30.00 - 90.00
NL:
7.31E5
TIC F: + c EI
SIM ms
[124.500-
125.500] MS
6610_2714_1503
04050134
NL:
6.55E3
TIC F: + c EI
SIM ms
[557.500-
558.500] MS
6610_2714_1503
04050134
NL:
4.94E3
TIC F: + c EI
SIM ms
[559.500-
560.500] MS
6610_2714_1503
04050134
Relative Abundance
Time (min)

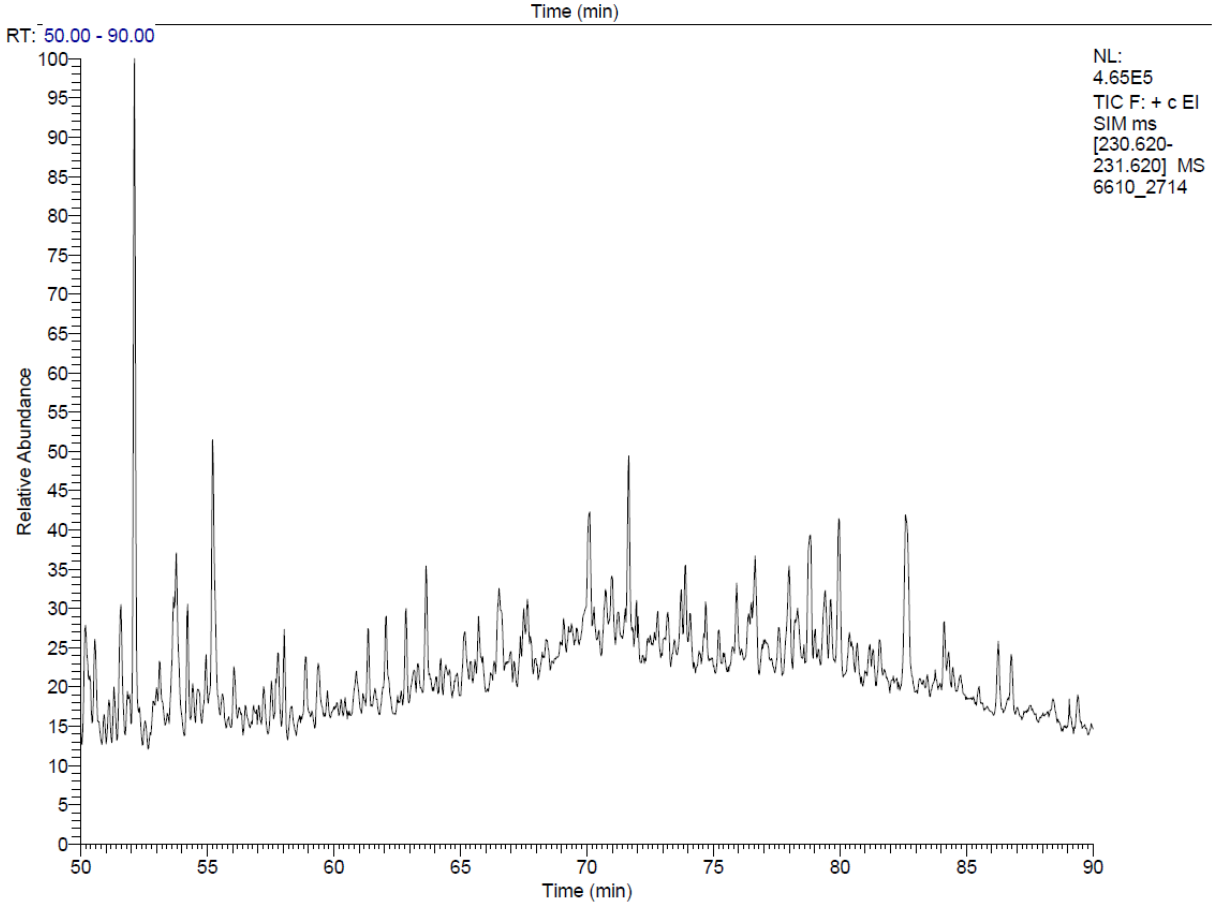
RT: 50.00 - 90.00
NL:
4.65E5
TIC F: + c EI
SIM ms
[230.620-
231.620] MS
6610_2714
Relative Abundance
Time (min)

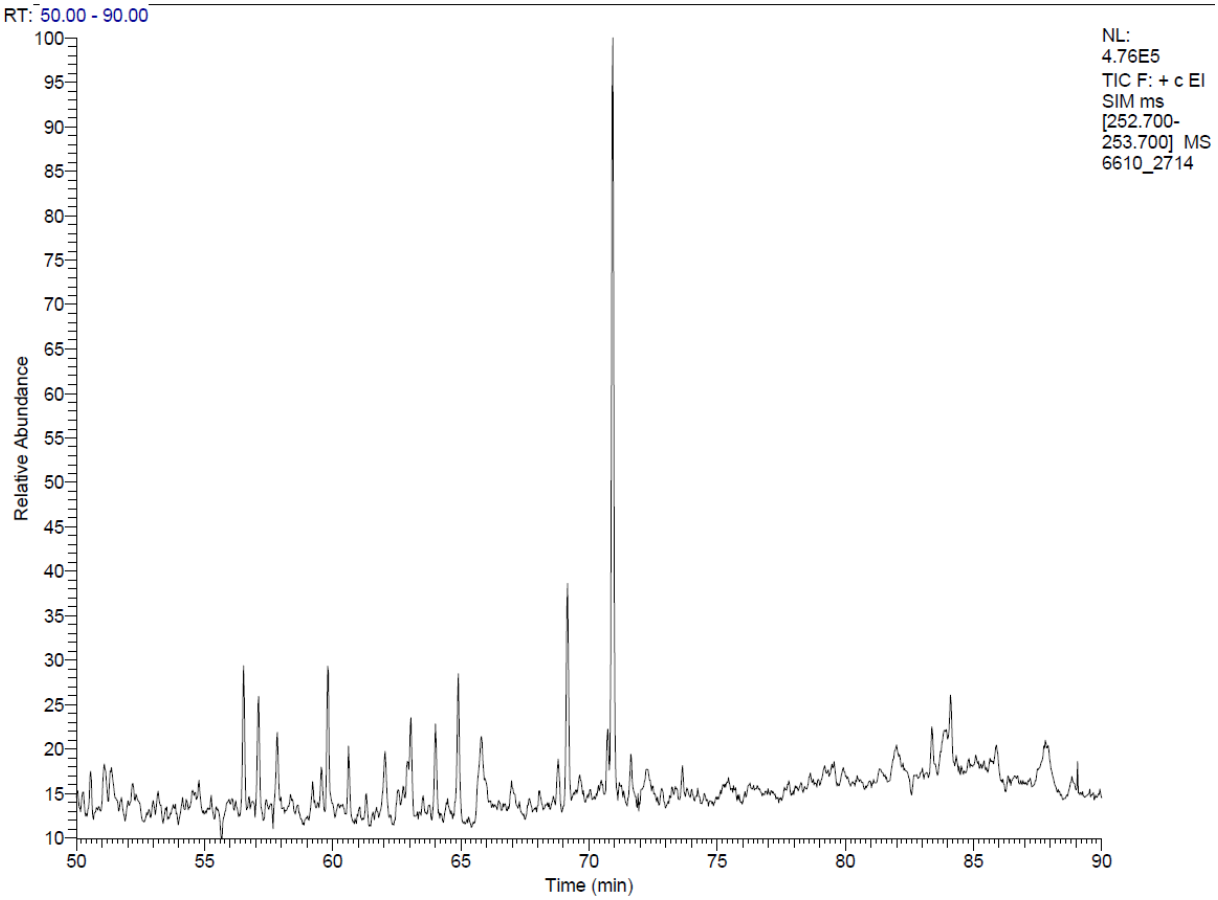
RT: 50.00 - 90.00
NL:
4.76E5
TIC F: + c EI
SIM ms
[252.700-
253.700] MS
6610_2714
Relative Abundance
Time (min)

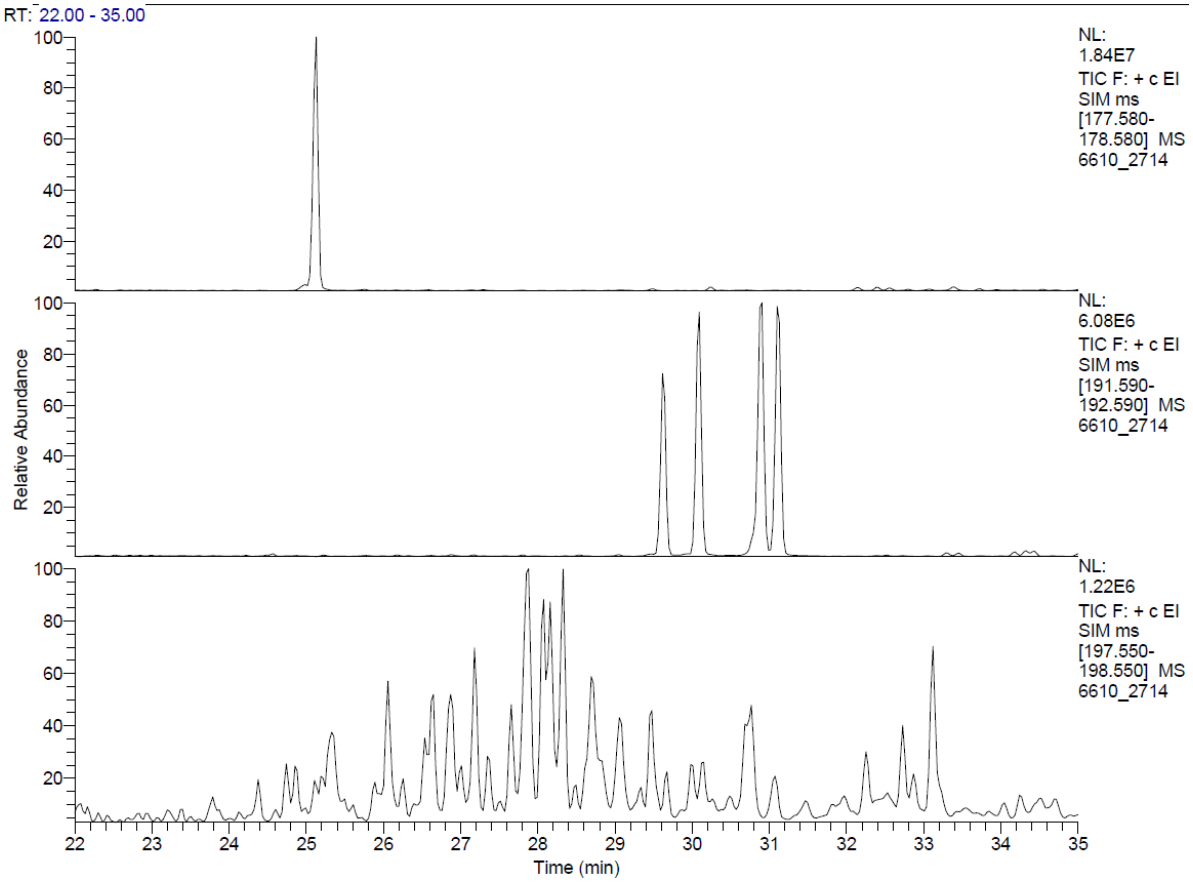
RT: 22.00 - 35.00
NL:
1.84E7
TIC F: + c EI
SIM ms
[177.580-
178.580] MS
6610_2714
NL:
6.08E6
TIC F: + c EI
SIM ms
[191.590-
192.590] MS
6610_2714
NL:
1.22E6
TIC F: + c EI
SIM ms
[197.550-
198.550] MS
6610_2714
Relative Abundance
Time (min)

B-6

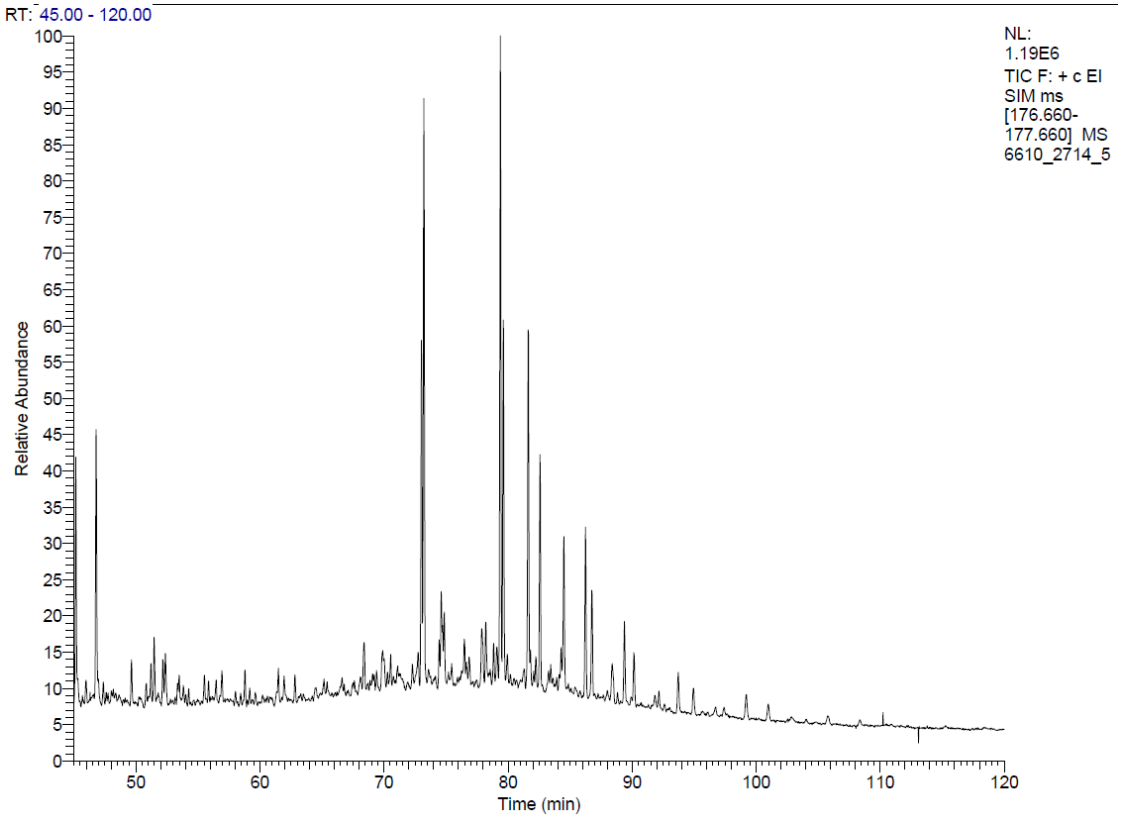
RT: 45.00 - 120.00
NL:
1.19E6
TIC F: + c EI
SIM ms
[176.660-
177.660] MS
6610_2714_5
Relative Abundance
Time (min)

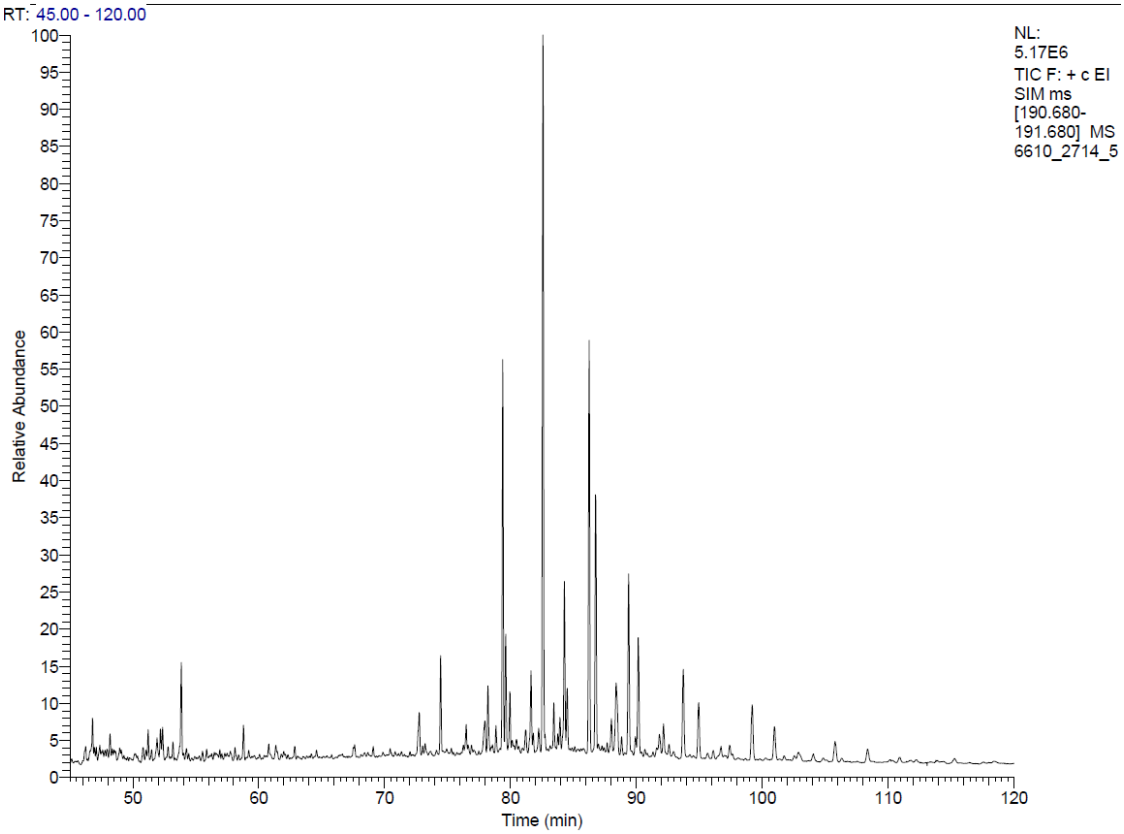
RT: 45.00 - 120.00
NL:
5.17E6
TIC F: + c EI
SIM ms
[190.680-
191.680] MS
6610_2714_5
Relative Abundance
Time (min)

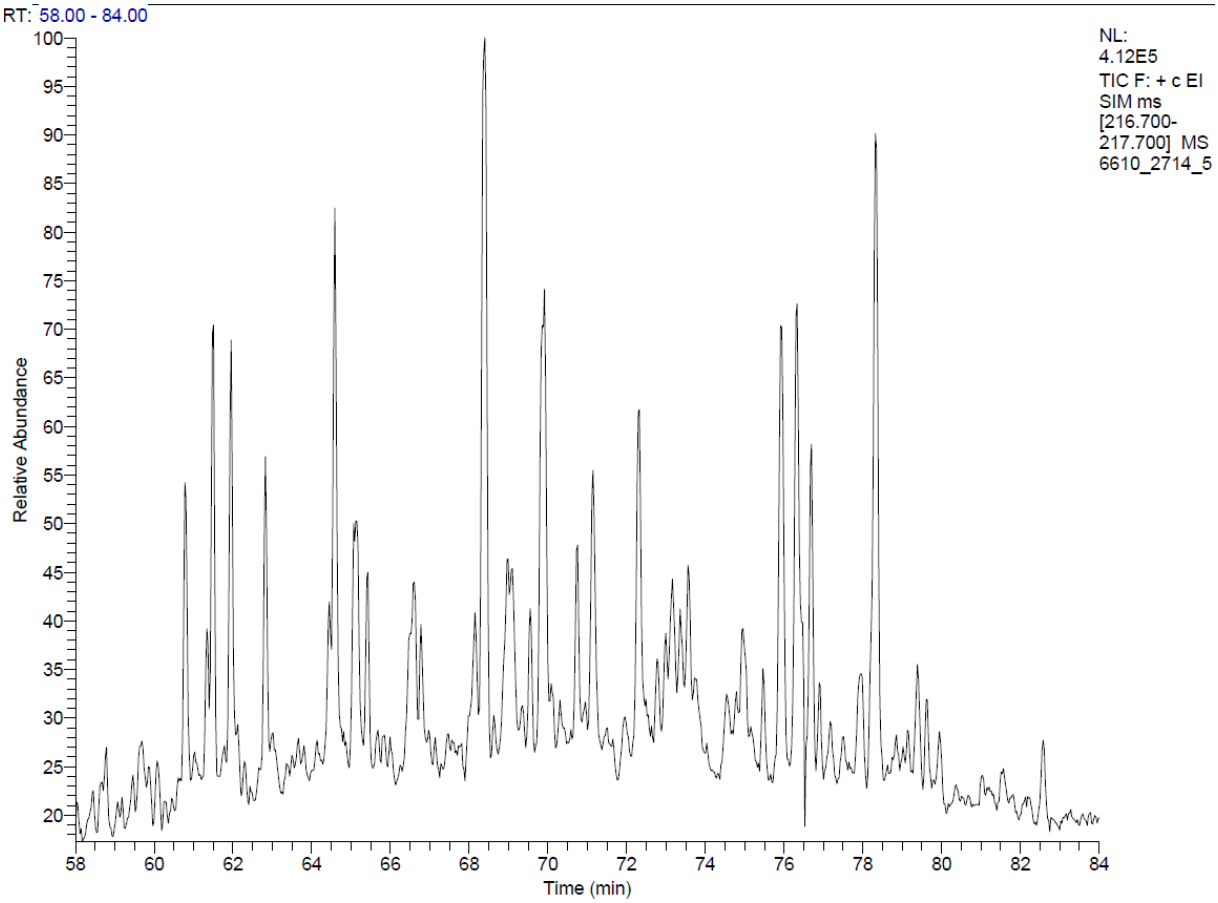
RT: 58.00 - 84.00
NL:
4.12E5
TIC F: + c EI
SIM ms
[216.700-
217.700] MS
6610_2714_5
Relative Abundance
Time (min)

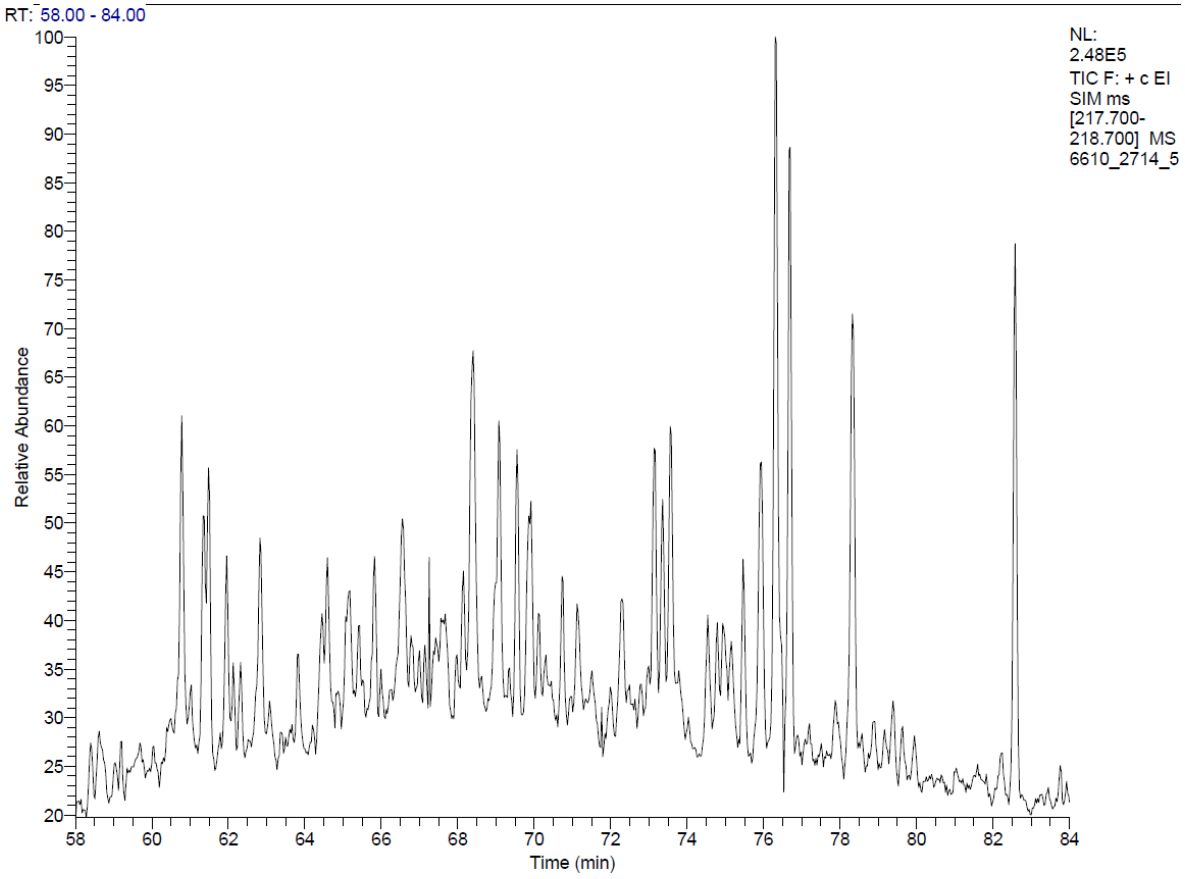
RT: 58.00 - 84.00
NL:
2.48E5
TIC F: + c EI
SIM ms
[217.700-
218.700] MS
6610_2714_5
Relative Abundance
Time (min)

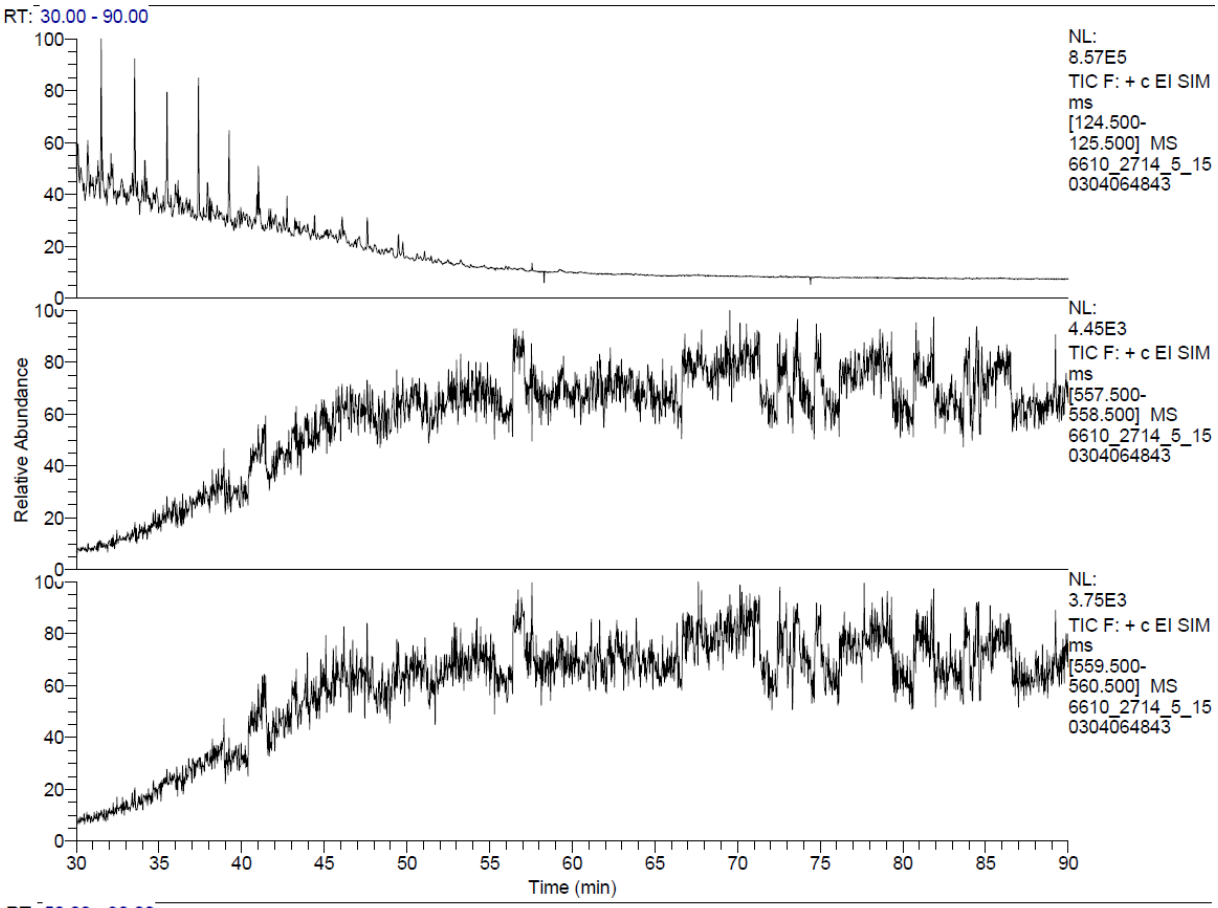
RT: 30.00 - 90.00
NL:
8.57E5
TIC F: + c EI SIM
ms
[124.500-
125.500] MS
6610_2714_5_15
0304064843
NL:
4.45E3
TIC F: + c EI SIM
ms
[557.500-
558.500] MS
6610_2714_5_15
0304064843
NL:
3.75E3
TIC F: + c EI SIM
ms
[559.500-
560.500] MS
6610_2714_5_15
0304064843
Relative Abundance
Time (min)

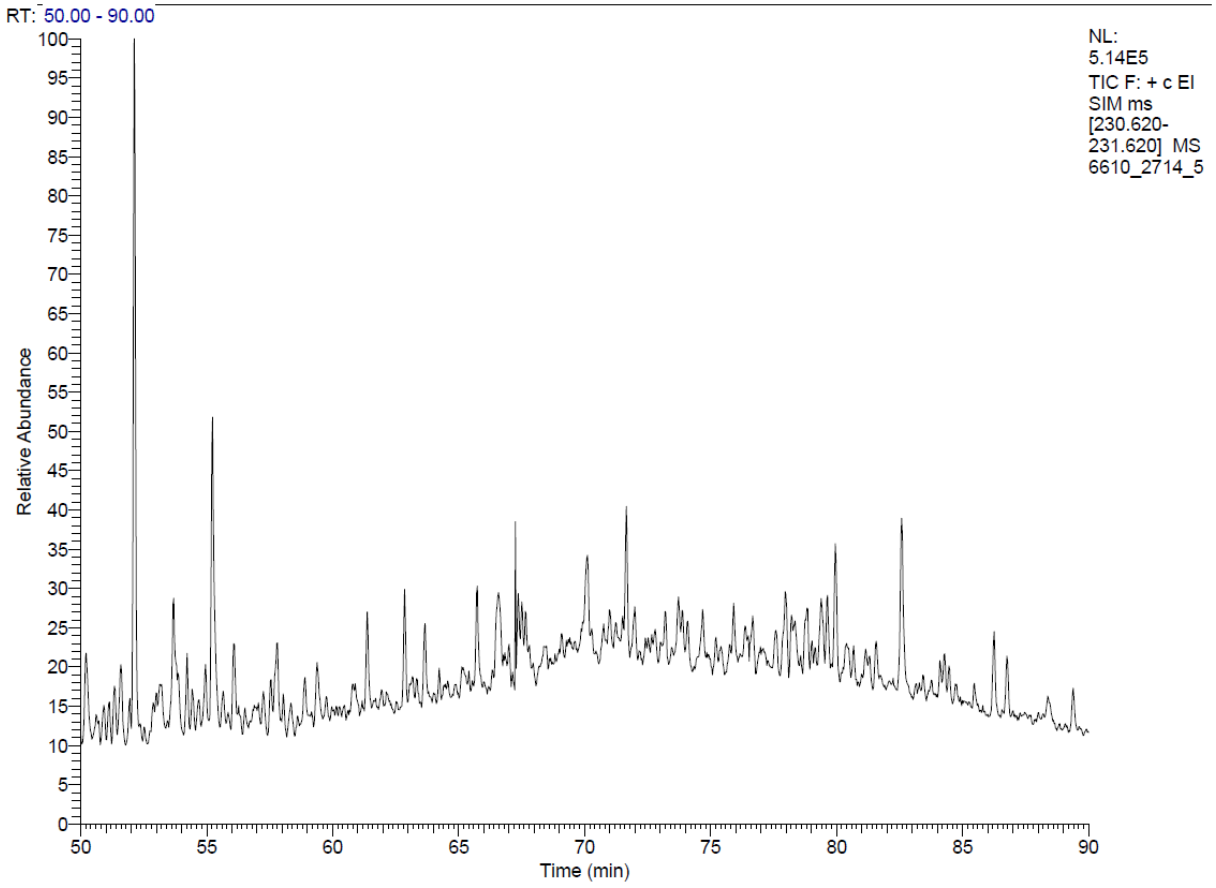
RT: 50.00 - 90.00
NL:
5.14E5
TIC F: + c EI
SIM ms
[230.620-
231.620] MS
6610_2714_5
Relative Abundance
Time (min)

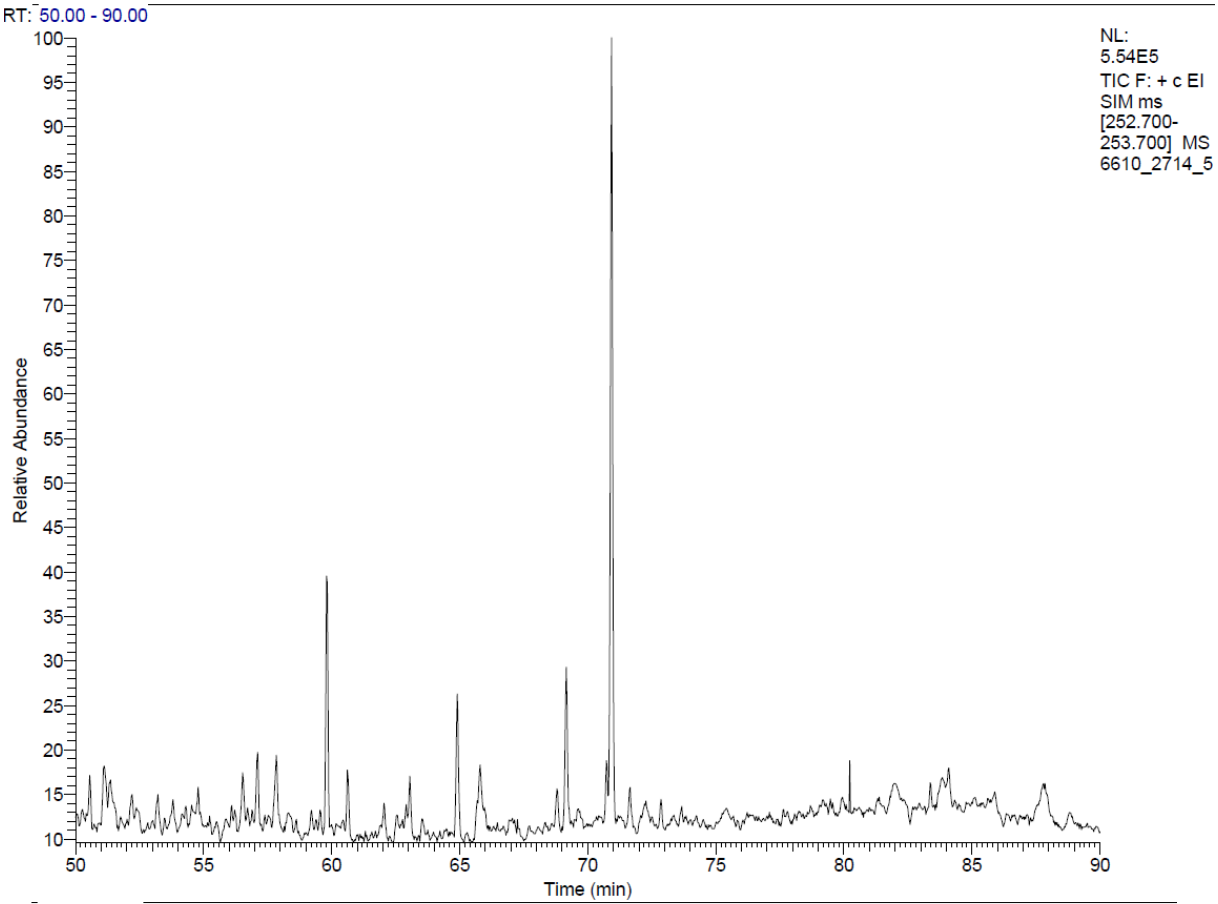
RT: 50.00 - 90.00
NL:
5.54E5
TIC F: + c EI
SIM ms
[252.700-
253.700] MS
6610_2714_5
Relative Abundance
Time (min)

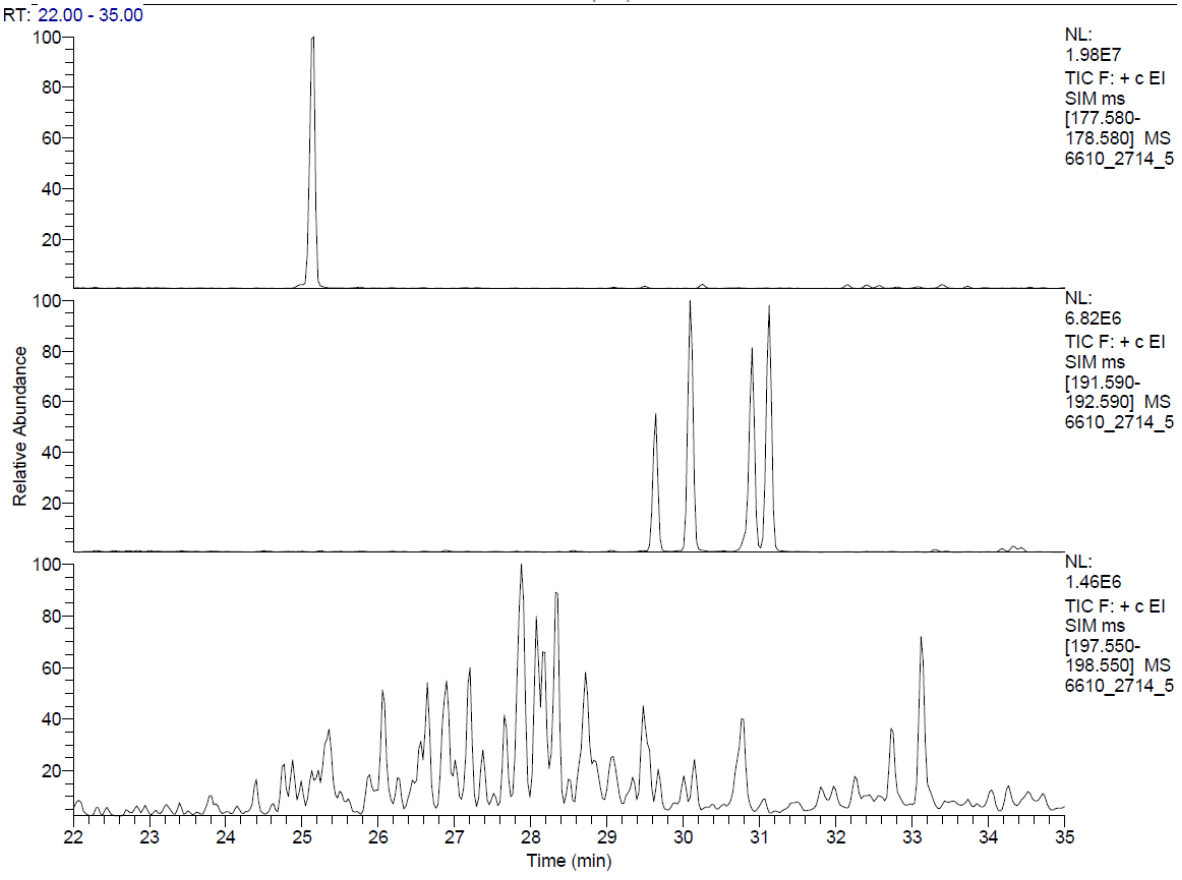
RT: 22.00 - 35.00
NL:
1.98E7
TIC F: + c EI
SIM ms
[177.580-
178.580] MS
6610_2714_5
NL:
6.82E6
TIC F: + c EI
SIM ms
[191.590-
192.590] MS
6610_2714_5
NL:
1.46E6
TIC F: + c EI
SIM ms
[197.550-
198.550] MS
6610_2714_5
Relative Abundance
Time (min)

B-7

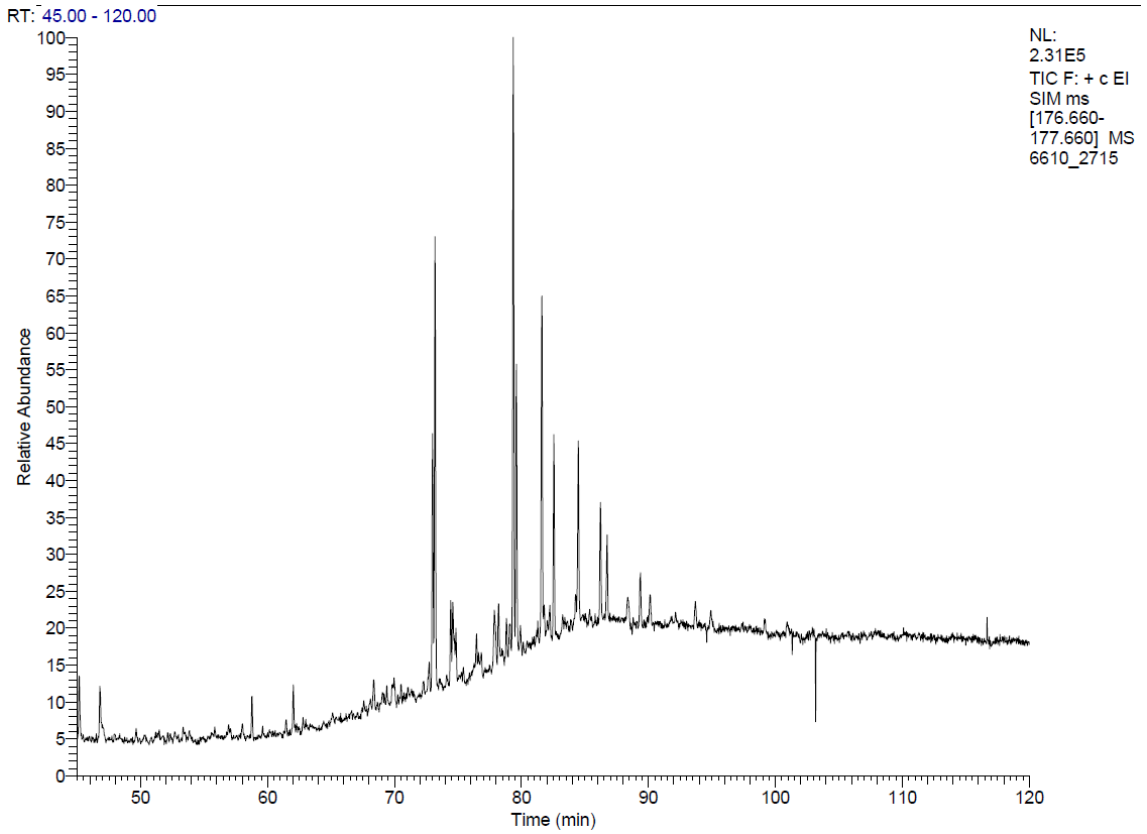
RT: 45.00 - 120.00
NL:
2.31E5
TIC F: + c EI
SIM ms
[176.660-
177.660] MS
6610_2715
Relative Abundance
Time (min)

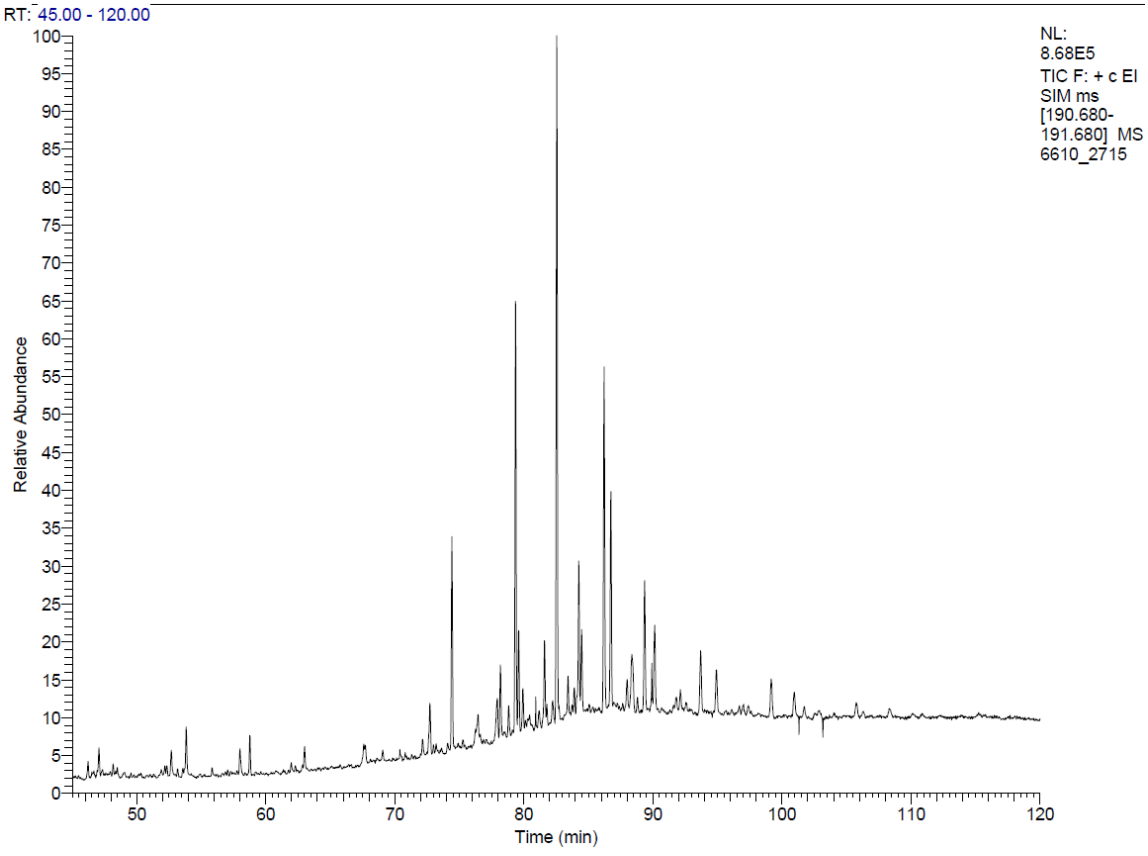
RT: 45.00 - 120.00
NL:
8.68E5
TIC F: + c EI
SIM ms
[190.680-
191.680] MS
6610_2715
Relative Abundance
Time (min)

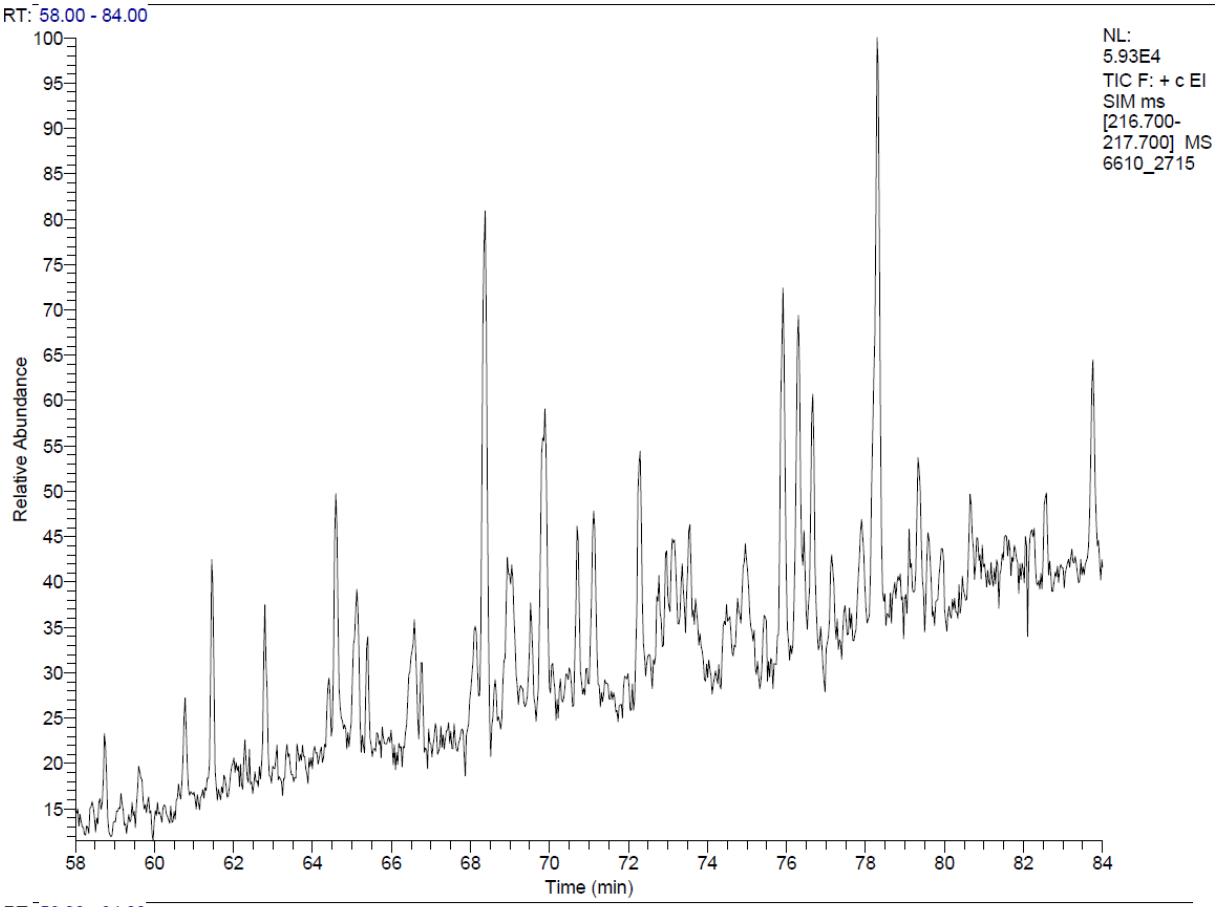
RT: 58.00 - 84.00
NL:
5.93E4
TIC F: + c EI
SIM ms
[216.700-
217.700] MS
6610_2715
Relative Abundance
Time (min)

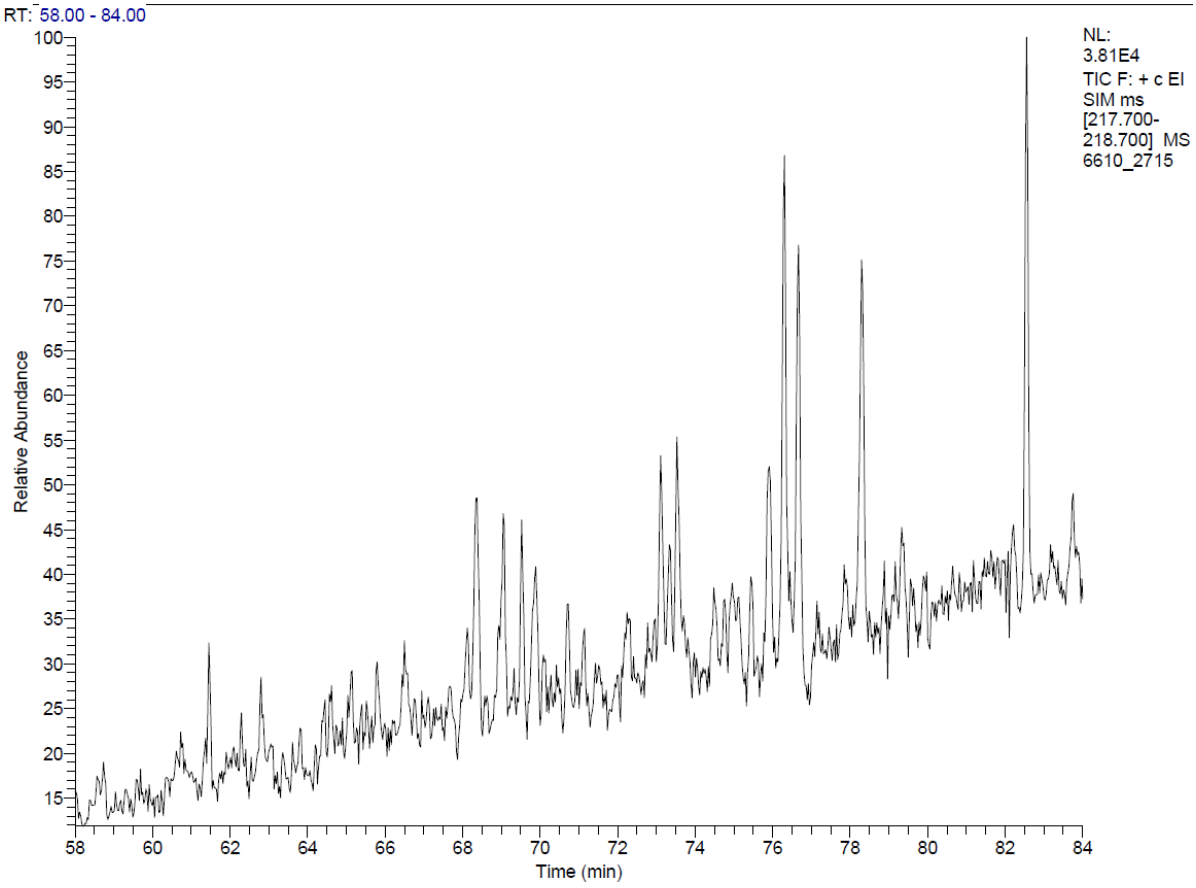
RT: 58.00 - 84.00
NL:
3.81E4
TIC F: + c EI
SIM ms
[217.700-
218.700] MS
6610_2715
Relative Abundance
Time (min)

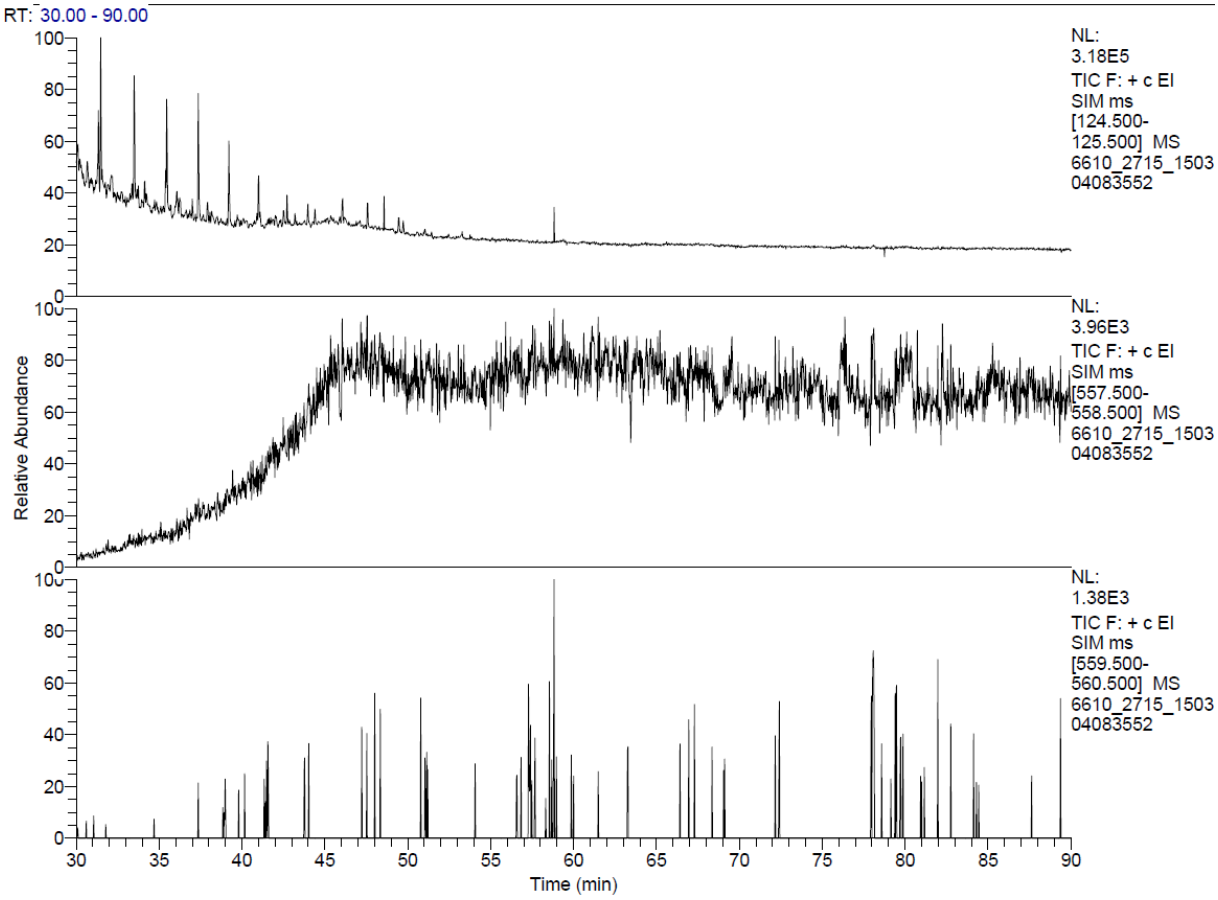
RT: 30.00 - 90.00
NL:
3.18E5
TIC F: + c EI
SIM ms
[124.500-
125.500] MS
6610_2715_1503
04083552
NL:
3.96E3
TIC F: + c EI
SIM ms
[557.500-
558.500] MS
6610_2715_1503
04083552
NL:
1.38E3
TIC F: + c EI
SIM ms
[559.500-
560.500] MS
6610_2715_1503
04083552
Relative Abundance
Time (min)

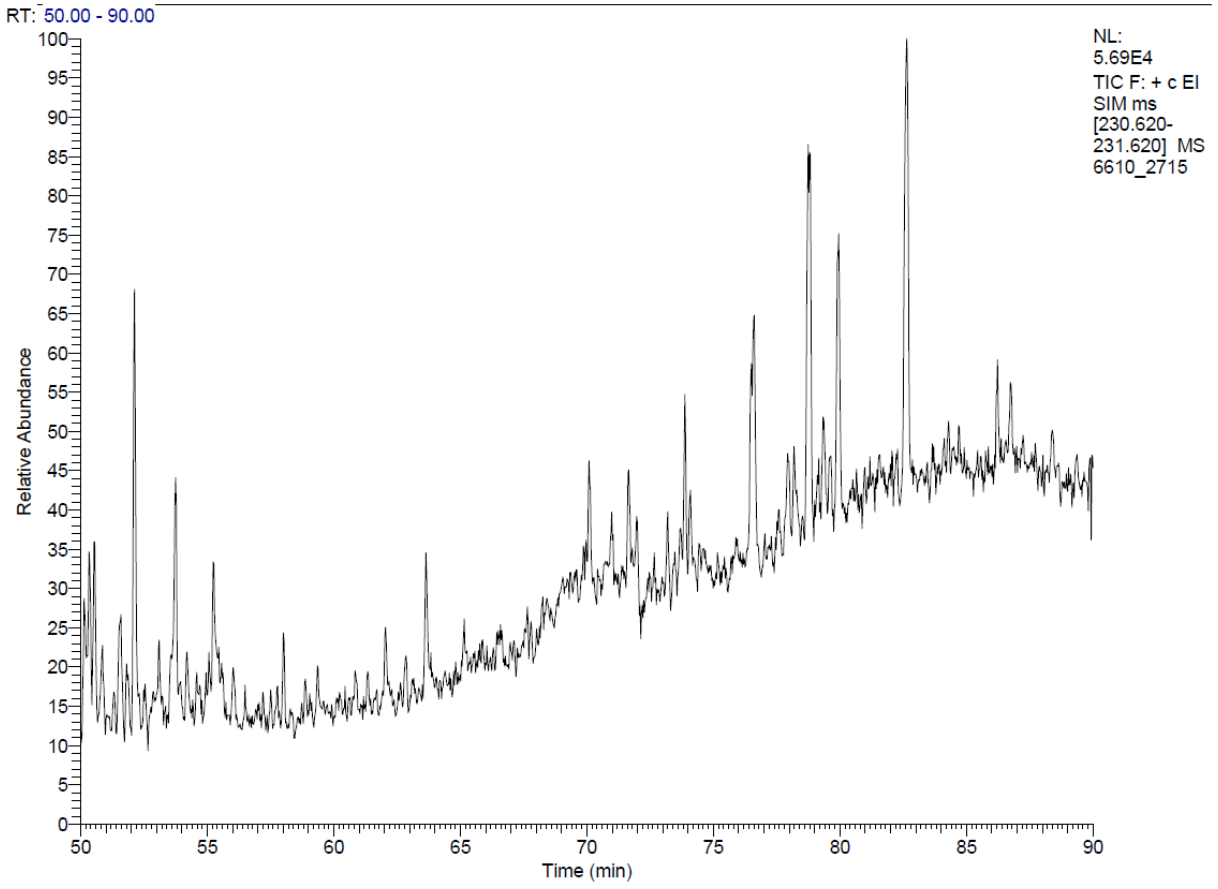
RT: 50.00 - 90.00
NL:
5.69E4
TIC F: + c EI
SIM ms
[230.620-
231.620] MS
6610_2715
Relative Abundance
Time (min)

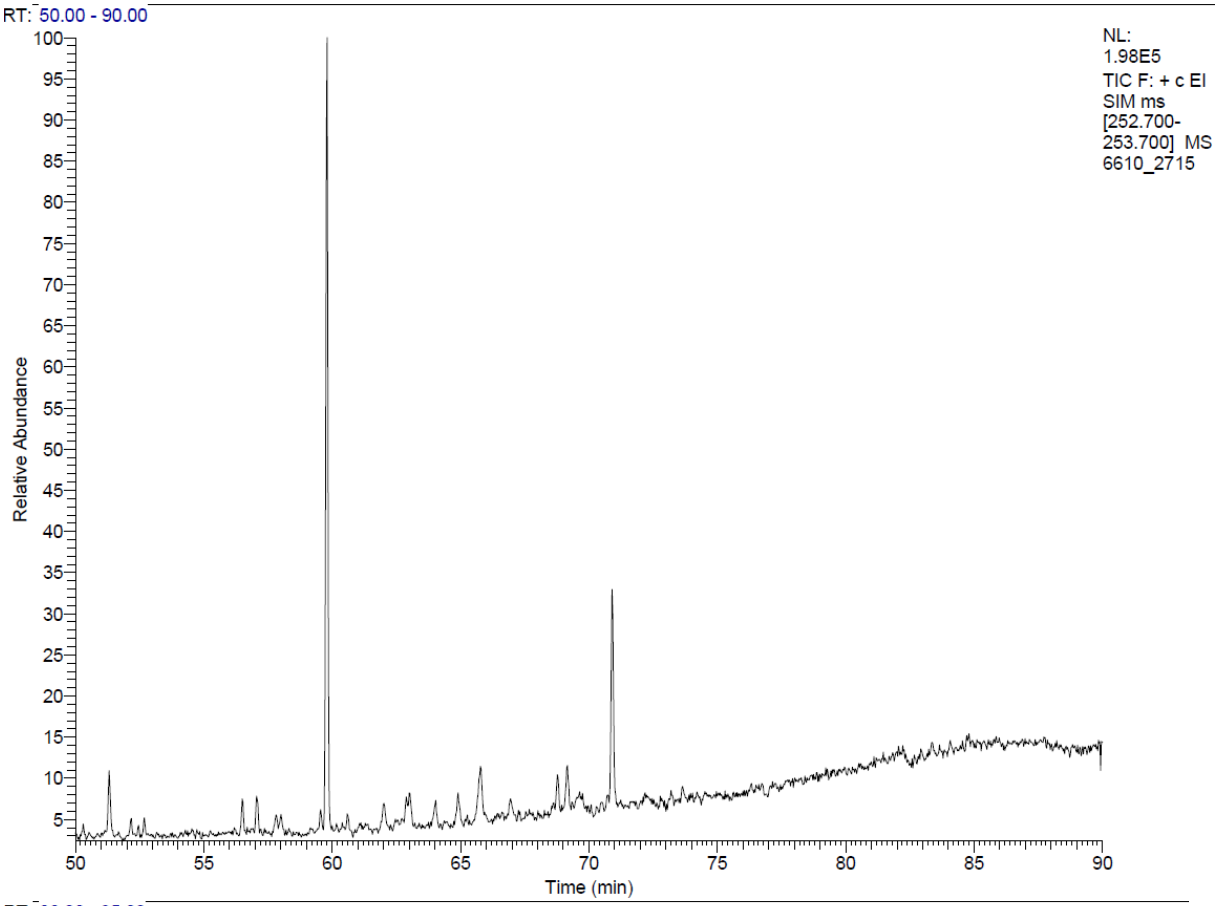
RT: 50.00 - 90.00
NL:
1.98E5
TIC F: + c EI
SIM ms
[252.700-
253.700] MS
6610_2715
Relative Abundance
Time (min)

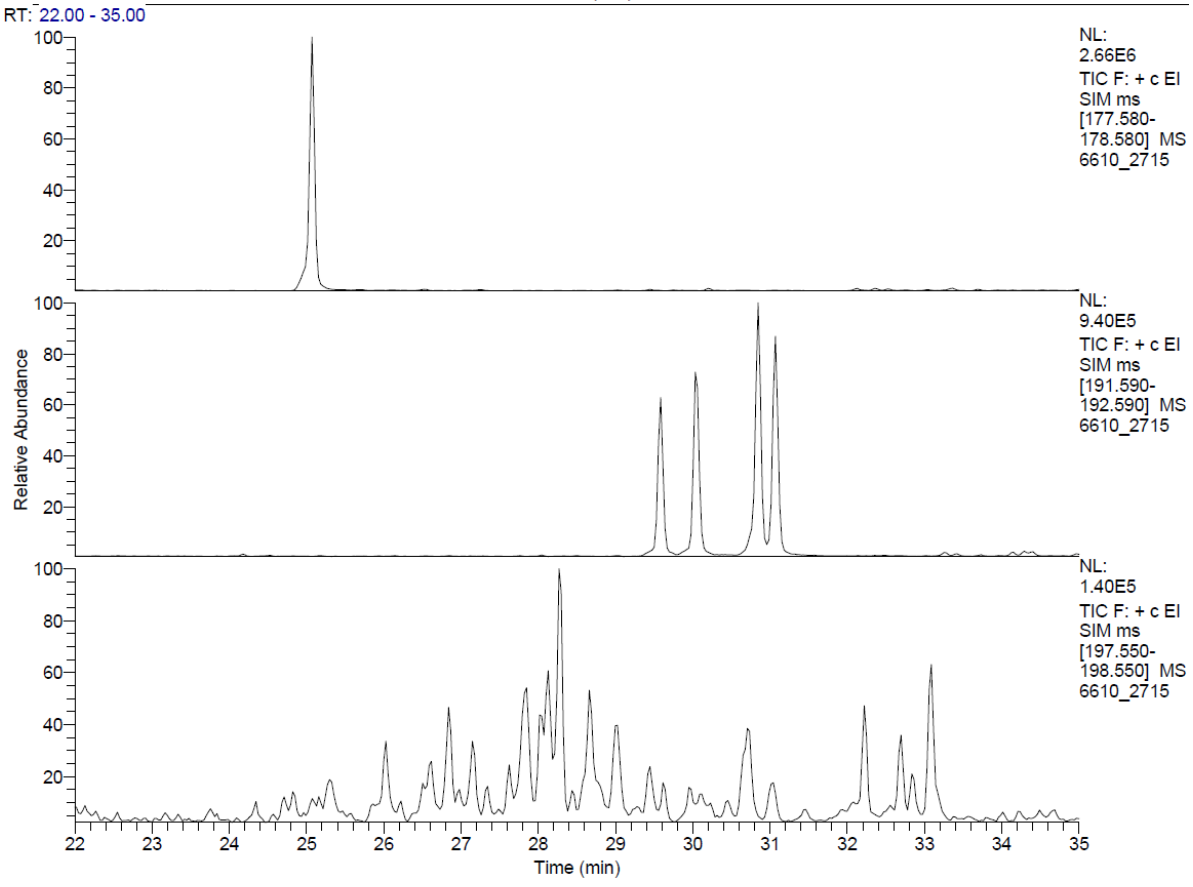
RT: 22.00 - 35.00
NL:
2.66E6
TIC F: + c EI
SIM ms
[177.580-
178.580] MS
6610_2715
NL:
9.40E5
TIC F: + c EI
SIM ms
[191.590-
192.590] MS
6610_2715
NL:
1.40E5
TIC F: + c EI
SIM ms
[197.550-
198.550] MS
6610_2715
Relative Abundance
Time (min)

C-1

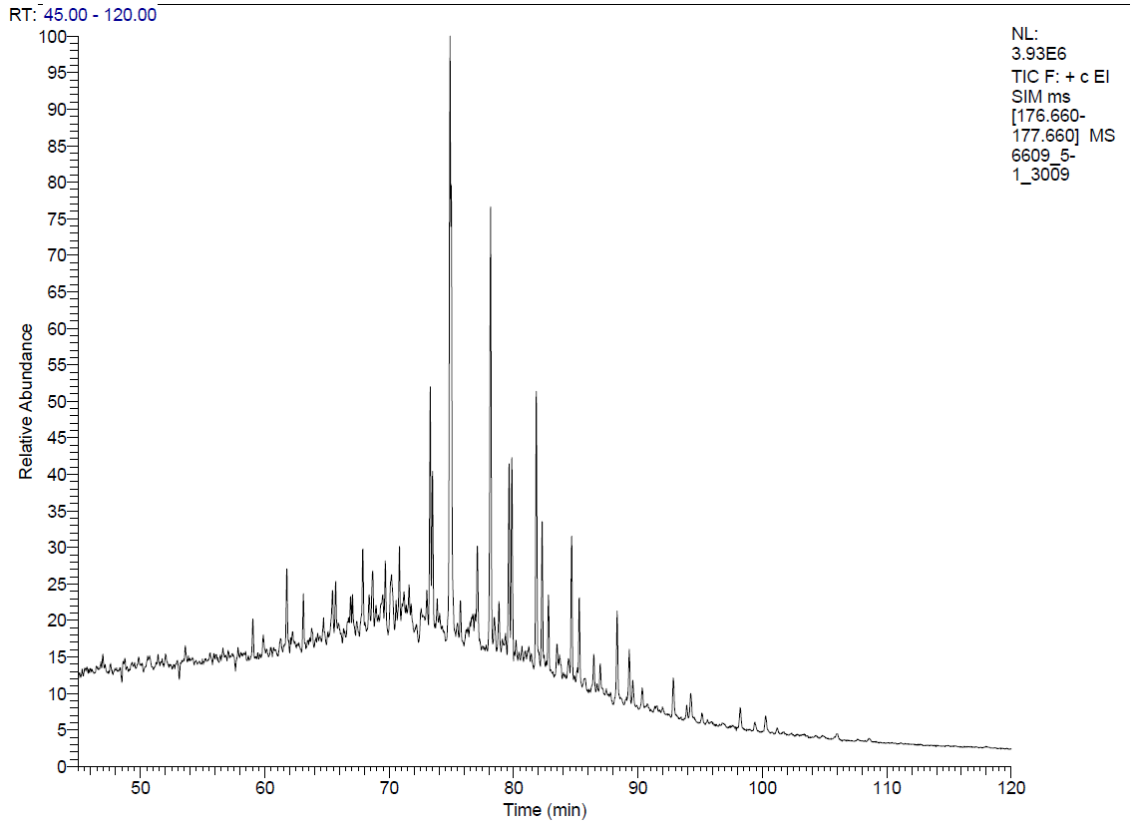
RT: 45.00 - 120.00
NL:
3.93E6
TIC F: + c EI
SIM ms
[176.660-
177.660] MS
6609_5-
1_3009
Relative Abundance
Time (min)

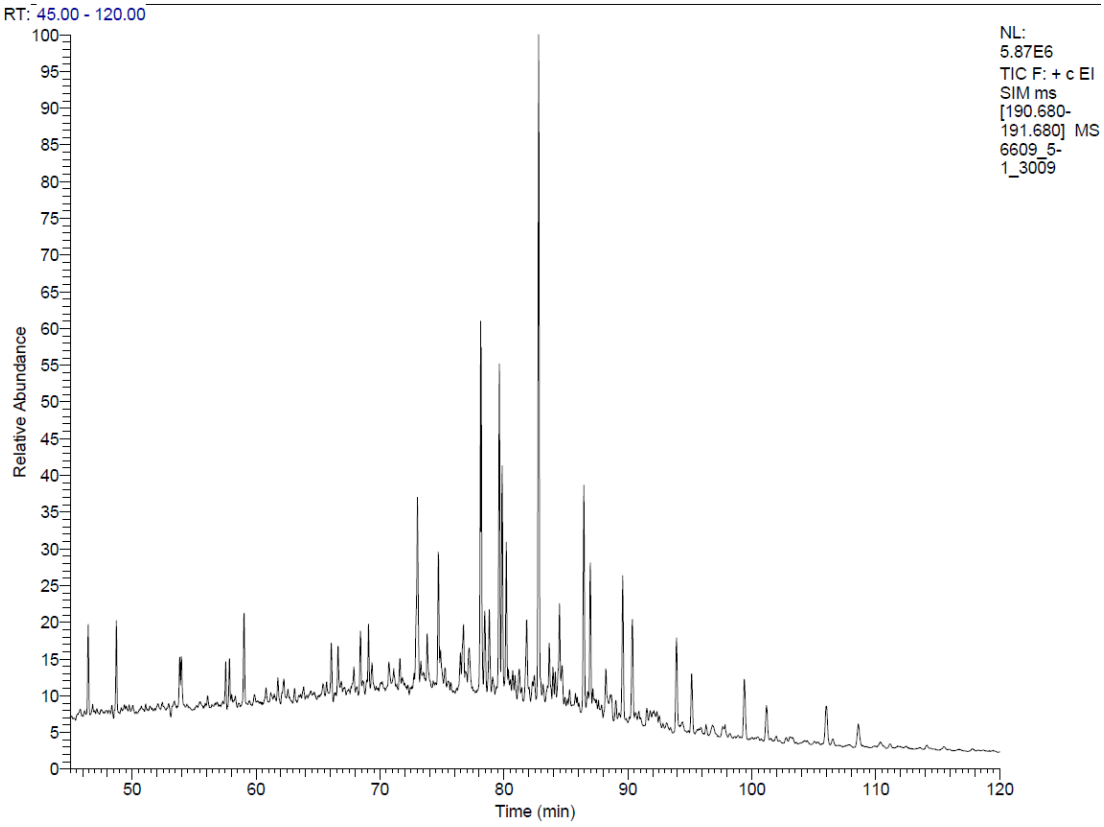
RT: 45.00 - 120.00
NL:
5.87E6
TIC F: + c EI
SIM ms
[190.680-
191.680] MS
6609_5-
1_3009
Relative Abundance
Time (min)

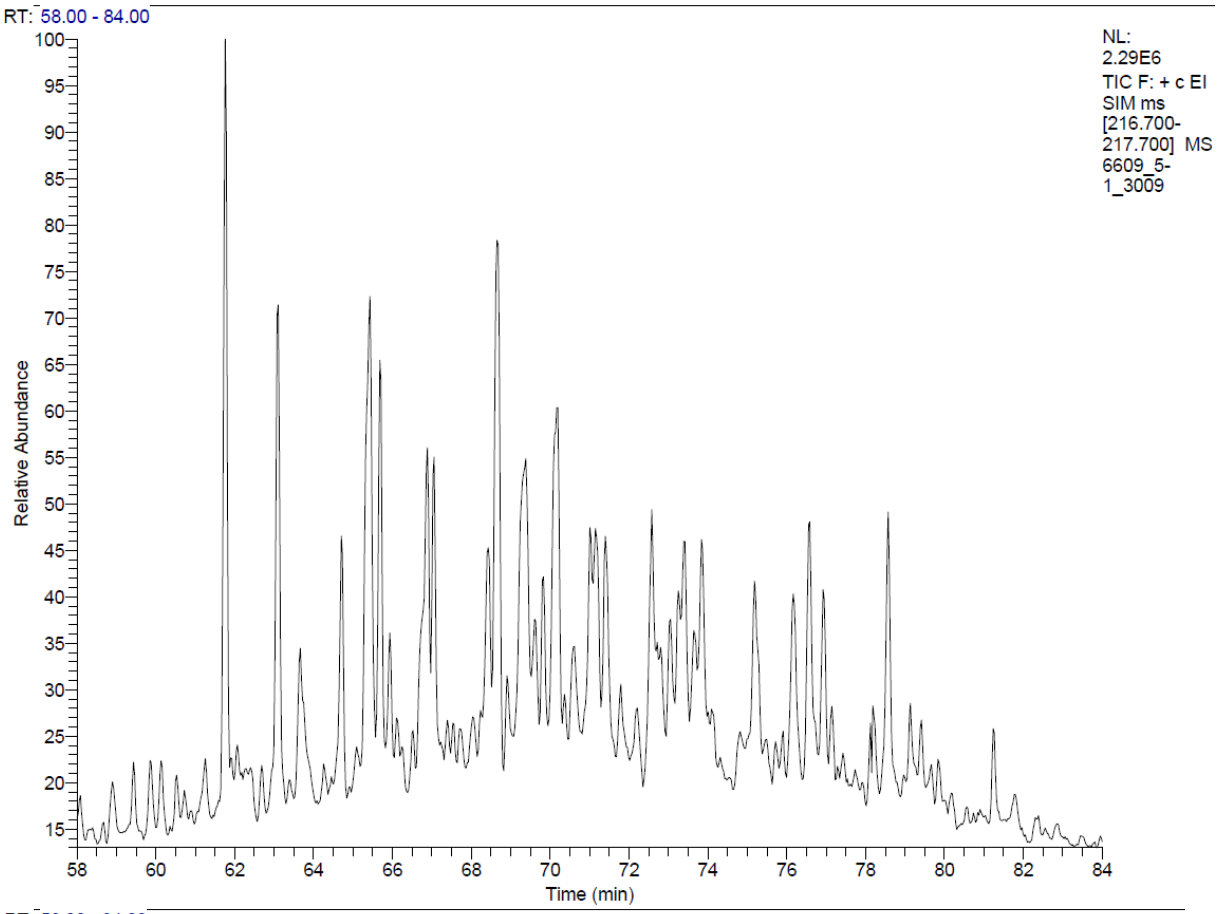
RT: 58.00 - 84.00
NL:
2.29E6
TIC F: + c EI
SIM ms
[216.700-
217.700] MS
6609_5-
1_3009
Relative Abundance
Time (min)

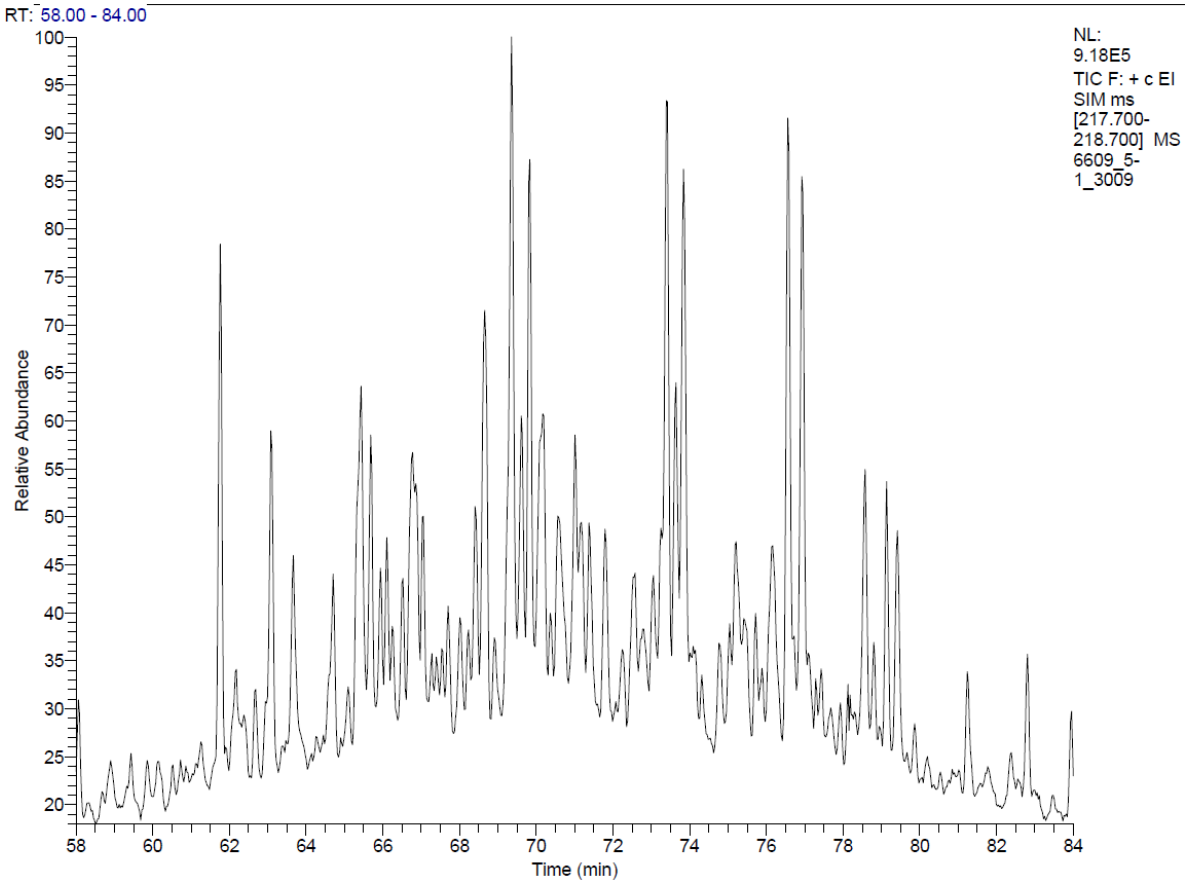
RT: 58.00 - 84.00
NL:
9.18E5
TIC F: + c EI
SIM ms
[217.700-
218.700] MS
6609_5-
1_3009
Relative Abundance
Time (min)

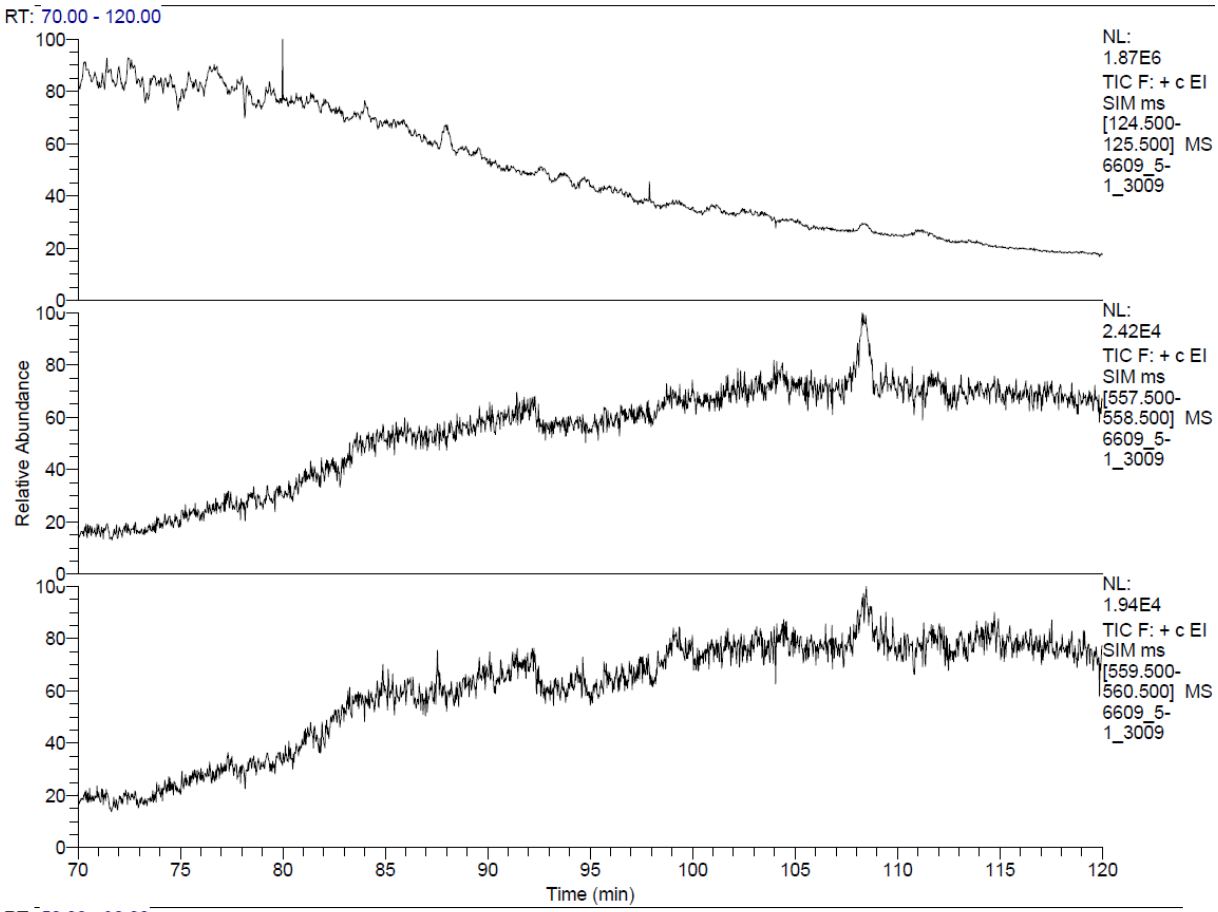
RT: 70.00 - 120.00
NL:
1.87E6
TIC F: + c EI
SIM ms
[124.500-
125.500] MS
6609_5-
1_3009
NL:
2.42E4
TIC F: + c EI
SIM ms
[557.500-
558.500] MS
6609_5-
1_3009
NL:
1.94E4
TIC F: + c EI
SIM ms
[559.500-
560.500] MS
6609_5-
1_3009
Relative Abundance
Time (min)

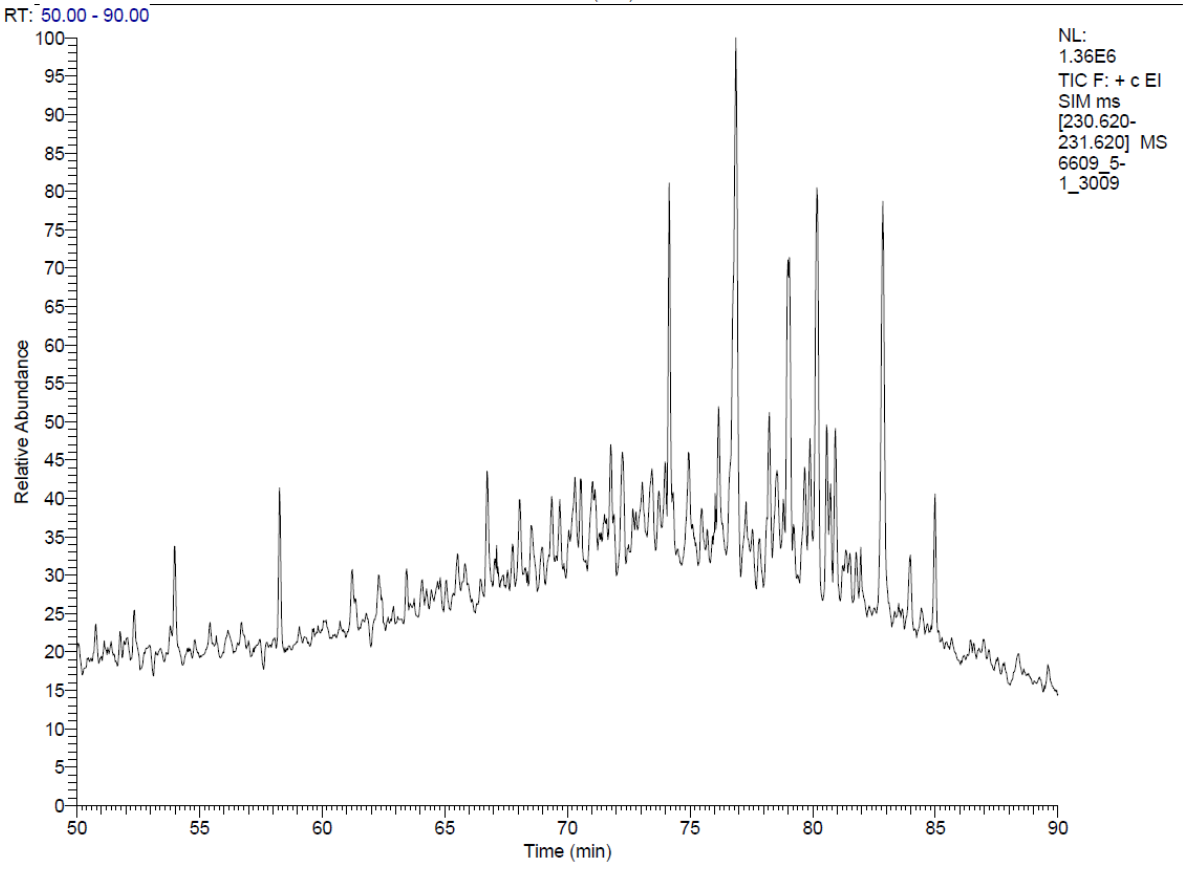
RT: 50.00 - 90.00
NL:
1.36E6
TIC F: + c EI
SIM ms
[230.620-
231.620] MS
6609_5-
1_3009
Relative Abundance
Time (min)

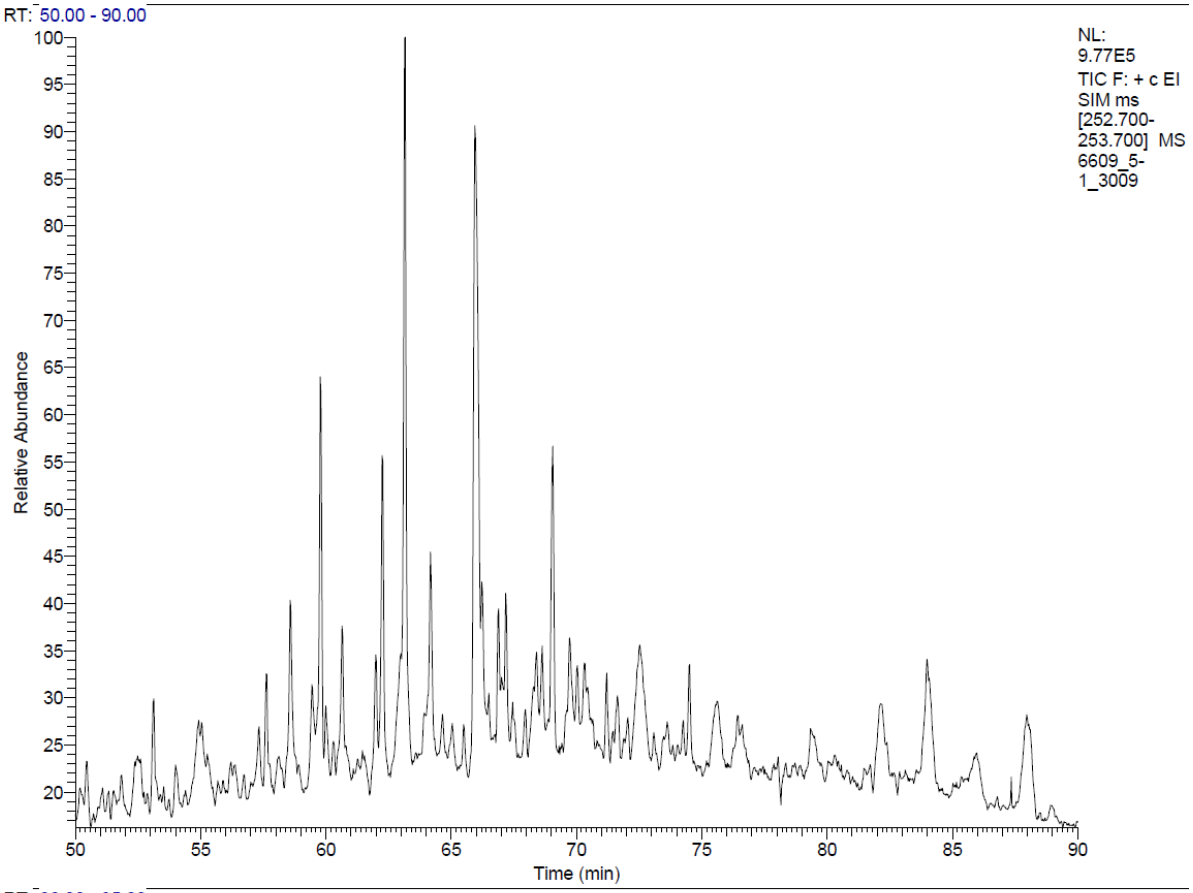
RT: 50.00 - 90.00
NL:
9.77E5
TIC F: + c EI
SIM ms
[252.700-
253.700] MS
6609_5-
1_3009
Relative Abundance
Time (min)

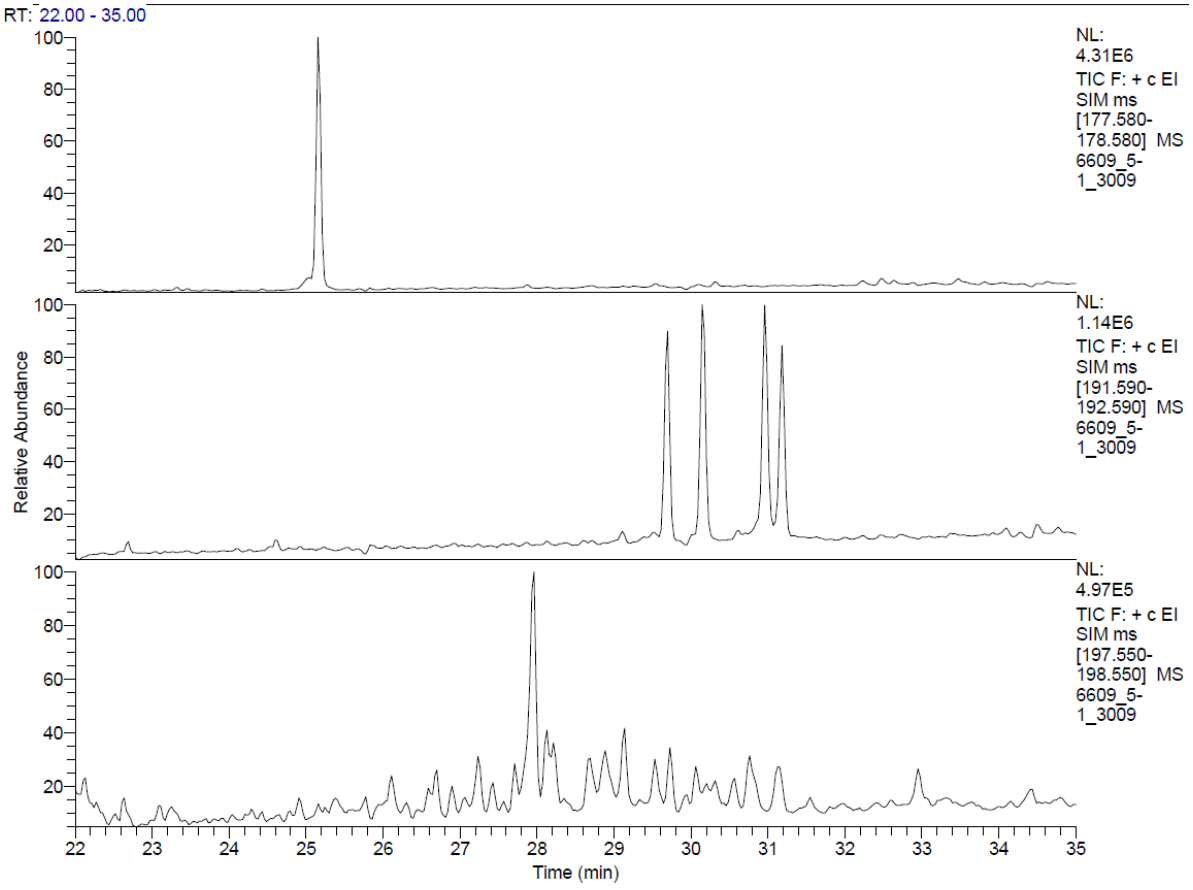
RT: 22.00 - 35.00
NL:
4.31E6
TIC F: + c EI
SIM ms
[177.580-
178.580] MS
6609_5-
1_3009
NL:
1.14E6
TIC F: + c EI
SIM ms
[191.590-
192.590] MS
6609_5-
1_3009
NL:
4.97E5
TIC F: + c EI
SIM ms
[197.550-
198.550] MS
6609_5-
1_3009
Relative Abundance
Time (min)

C-2

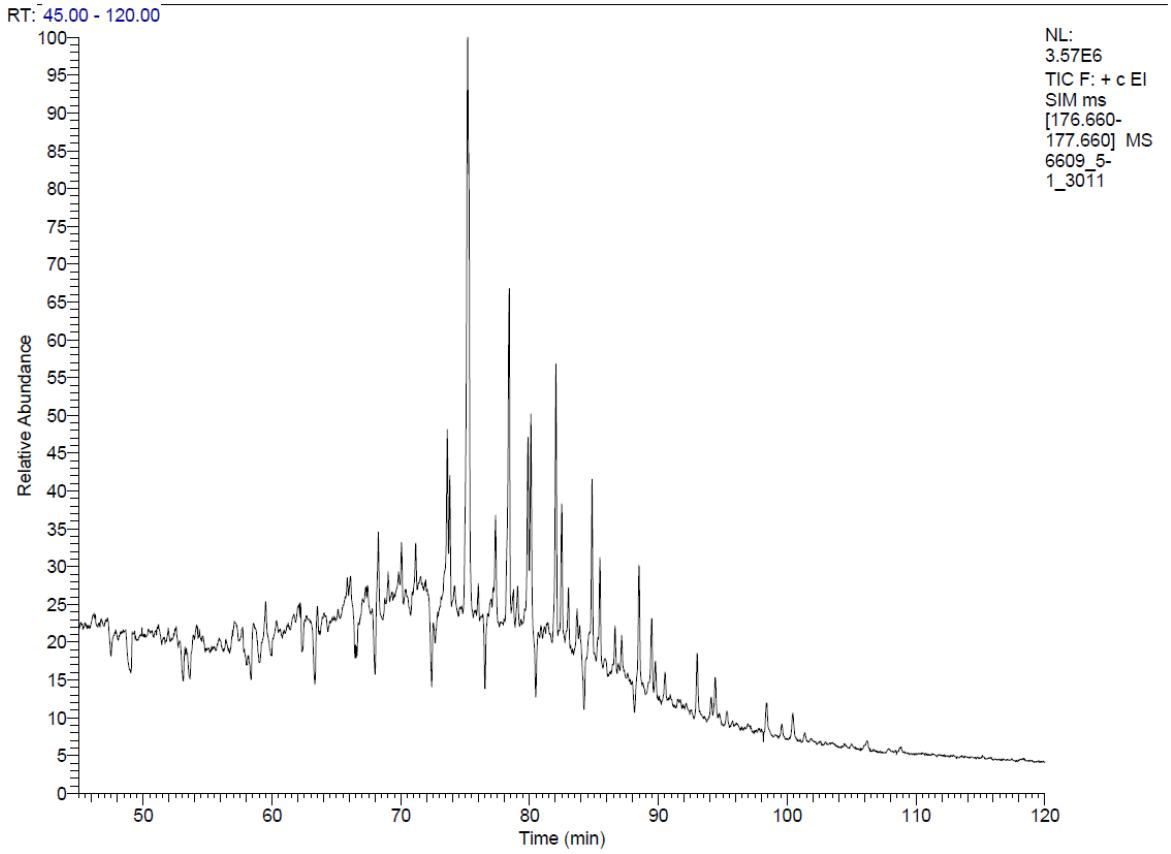
RT: 45.00 - 120.00
NL:
3.57E6
TIC F: + c EI
SIM ms
[176.660-
177.660] MS
6609_5-
1_3011
Relative Abundance
Time (min)

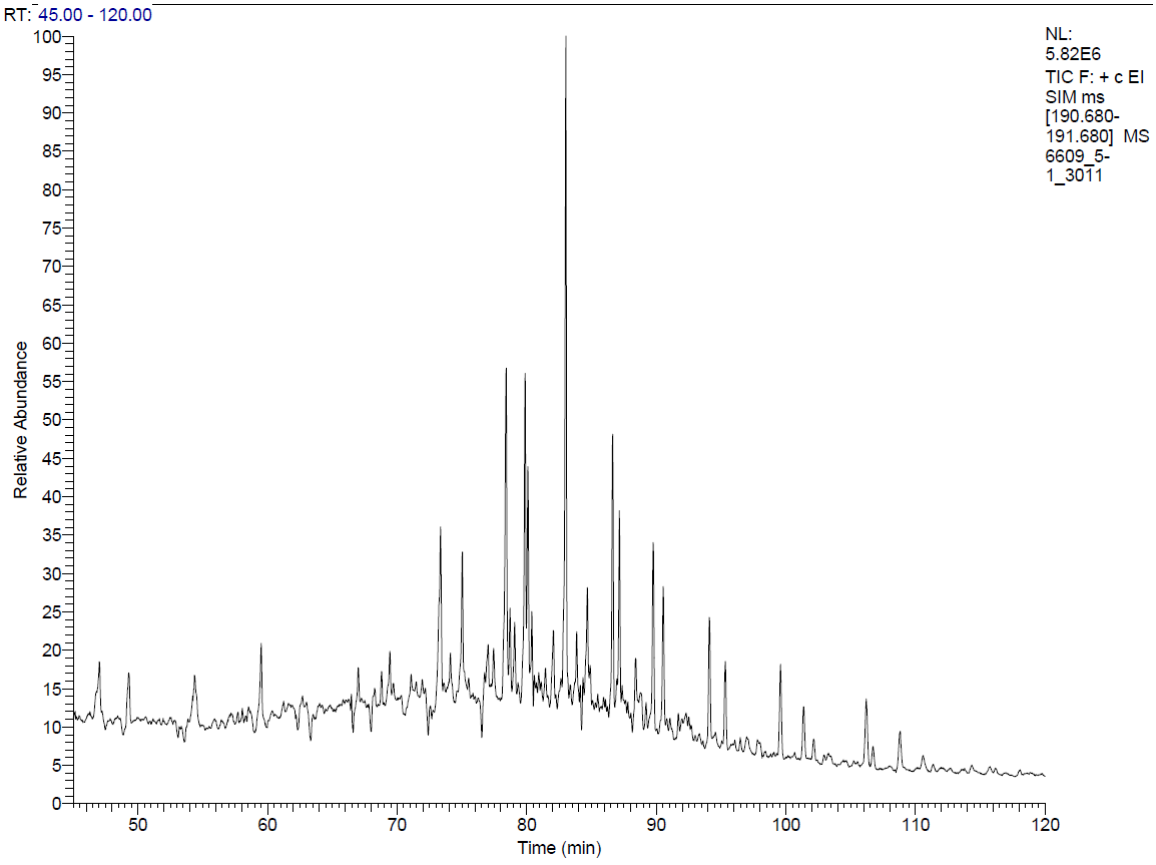
RT: 45.00 - 120.00
NL:
5.82E6
TIC F: + c EI
SIM ms
[190.680-
191.680] MS
6609_5-
1_3011
Relative Abundance
Time (min)

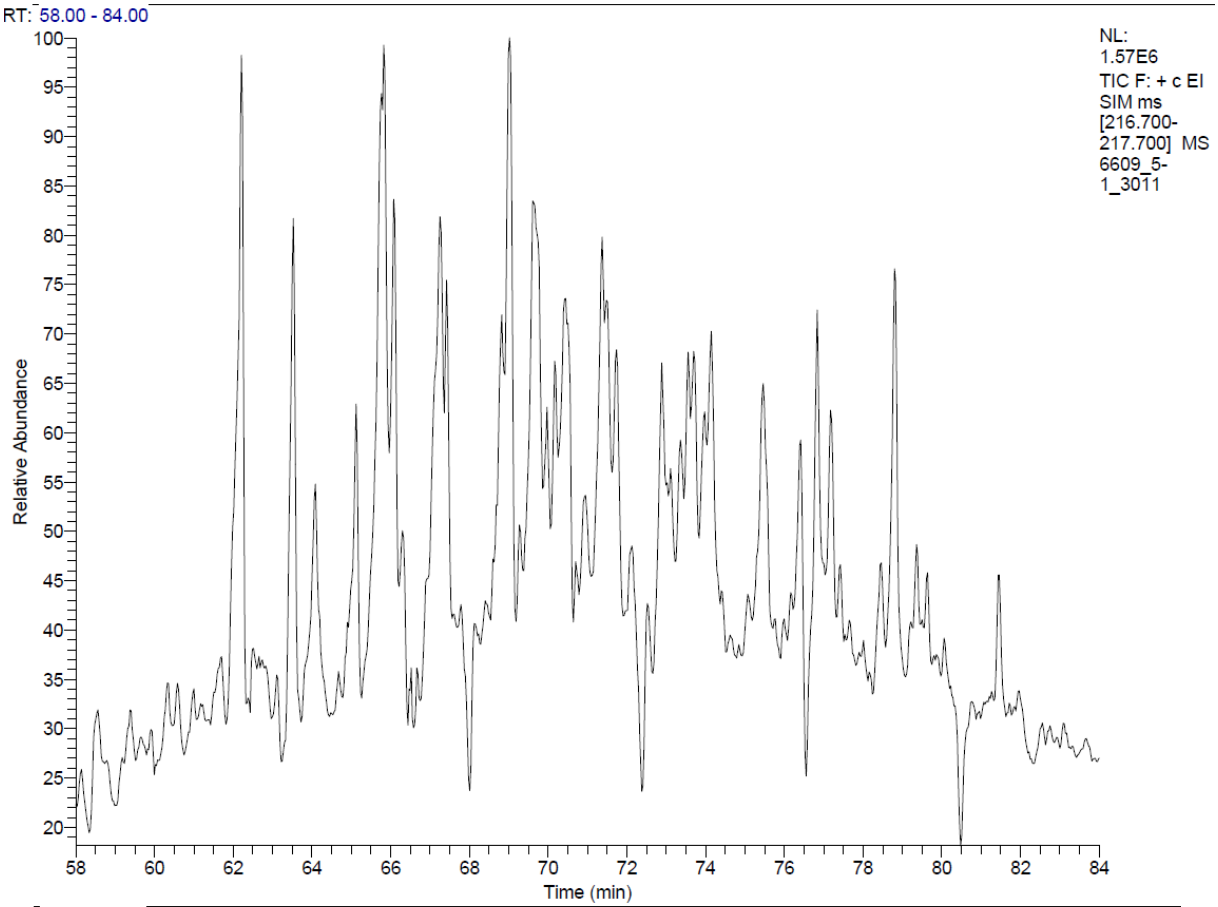
RT: 58.00 - 84.00
NL:
1.57E6
TIC F: + c EI
SIM ms
[216.700-
217.700] MS
6609_5-
1_3011
Relative Abundance
Time (min)

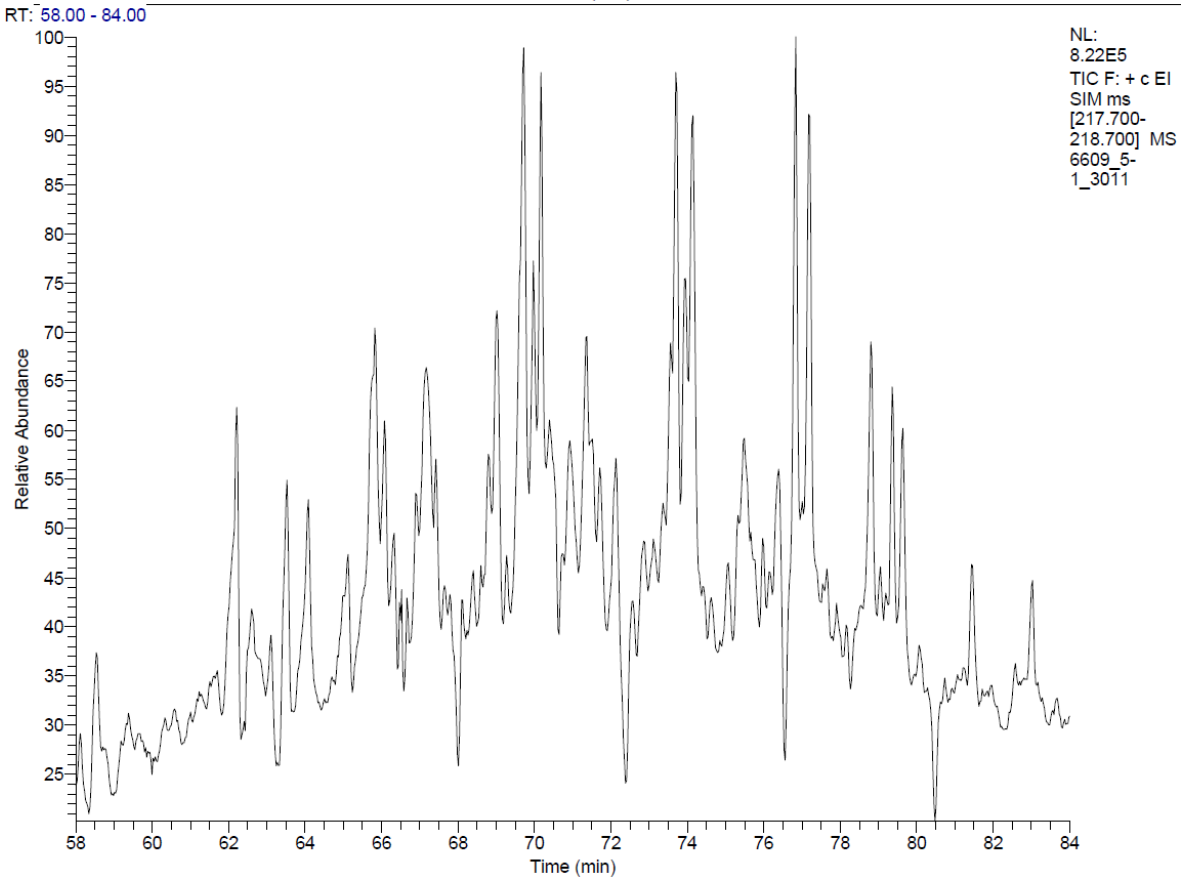
RT: 58.00 - 84.00
NL:
8.22E5
TIC F: + c EI
SIM ms
[217.700-
218.700] MS
6609_5-
1_3011
Relative Abundance
Time (min)

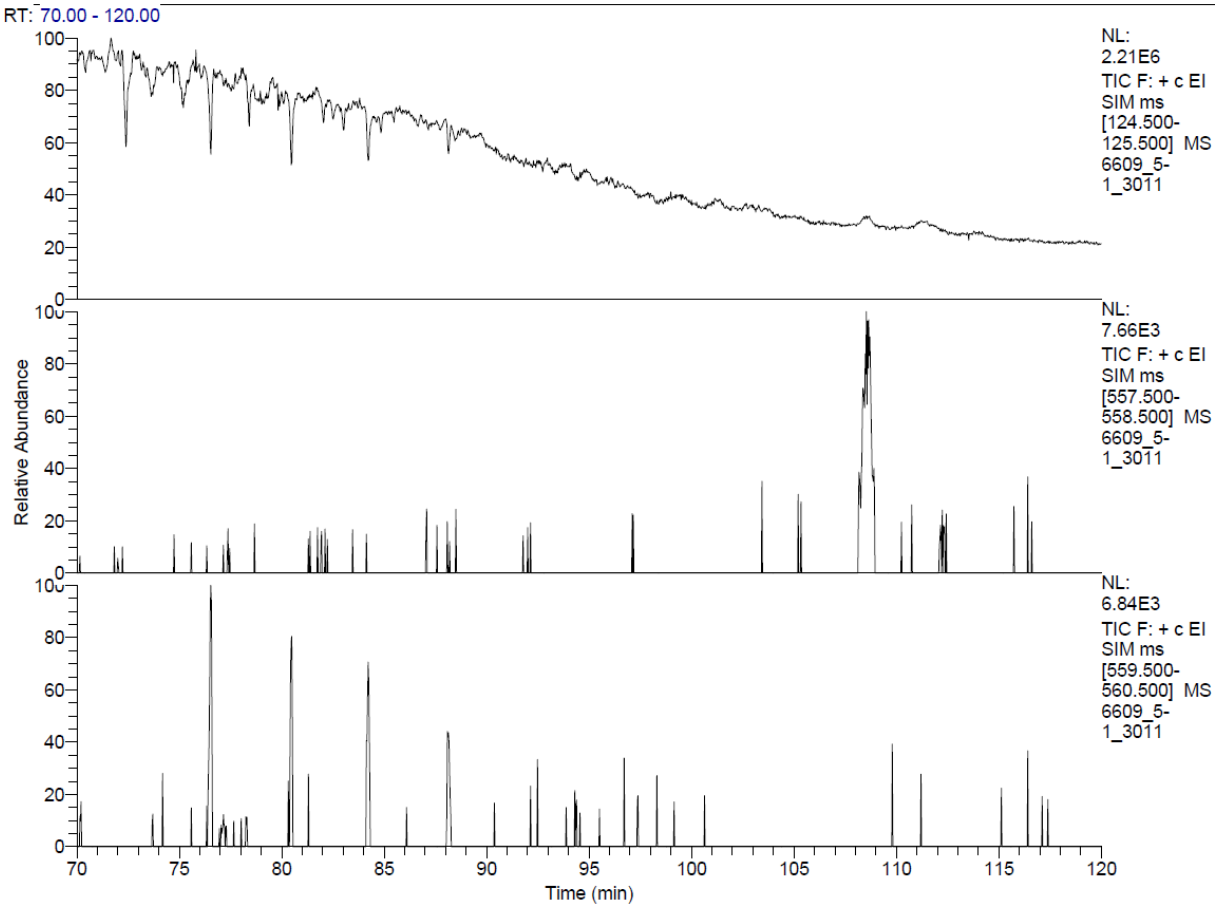
RT: 70.00 - 120.00
NL:
2.21E6
TIC F: + c EI
SIM ms
[124.500-
125.500] MS
6609_5-
1_3011
NL:
7.66E3
TIC F: + c EI
SIM ms
[557.500-
558.500] MS
6609_5-
1_3011
NL:
6.84E3
TIC F: + c EI
SIM ms
[559.500-
560.500] MS
6609_5-
1_3011
Relative Abundance
Time (min)

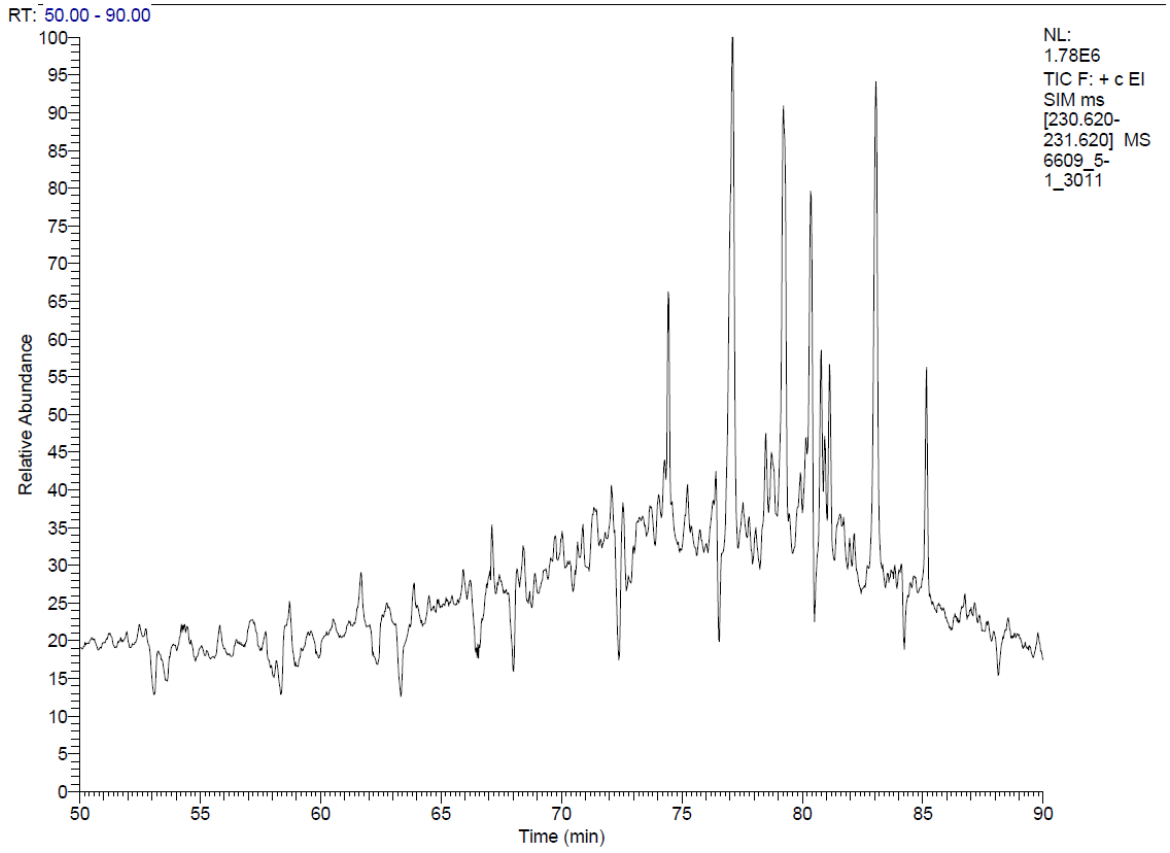
RT: 50.00 - 90.00
NL:
1.78E6
TIC F: + c EI
SIM ms
[230.620-
231.620] MS
6609_5-
1_3011
Relative Abundance
Time (min)

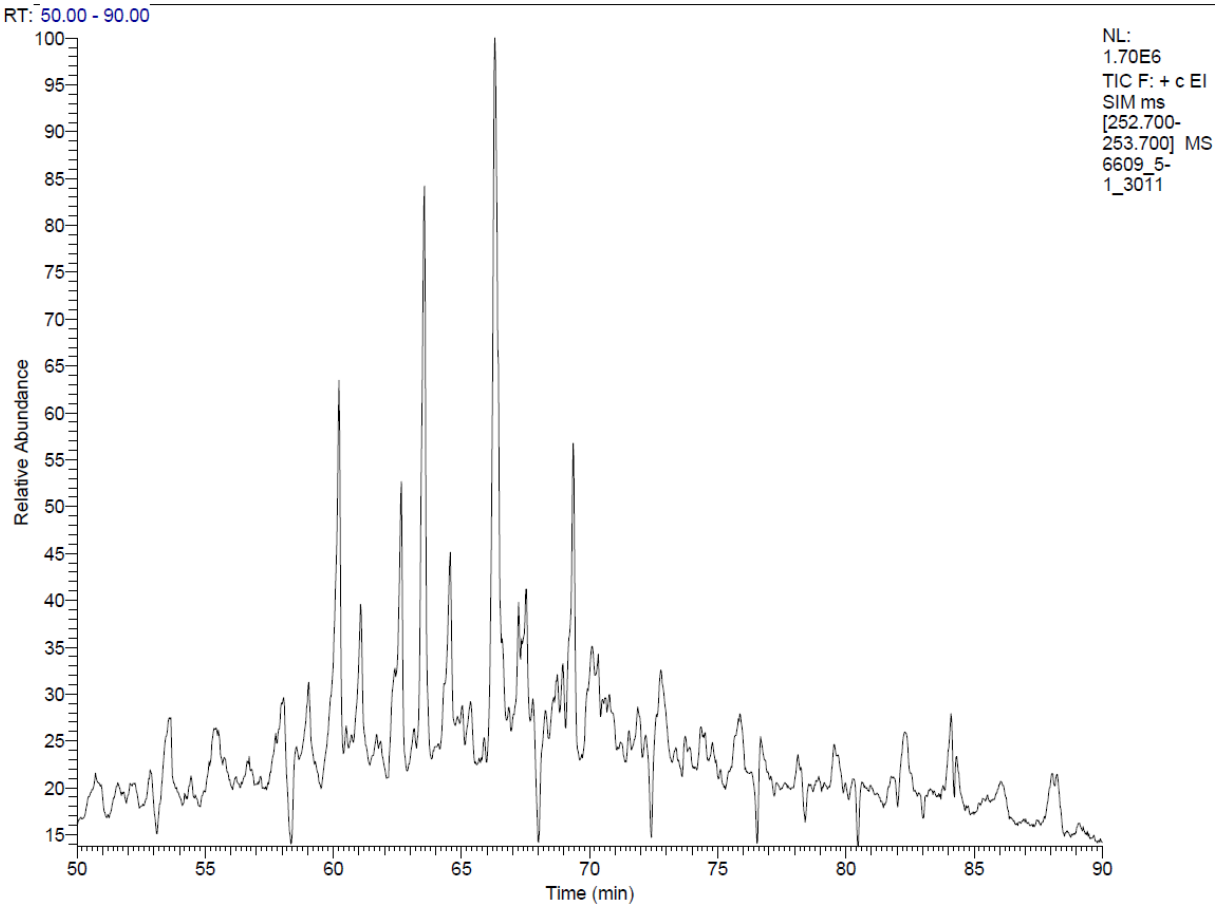
RT: 50.00 - 90.00
NL:
1.70E6
TIC F: + c EI
SIM ms
[252.700-
253.700] MS
6609_5-
1_3011
Relative Abundance
Time (min)

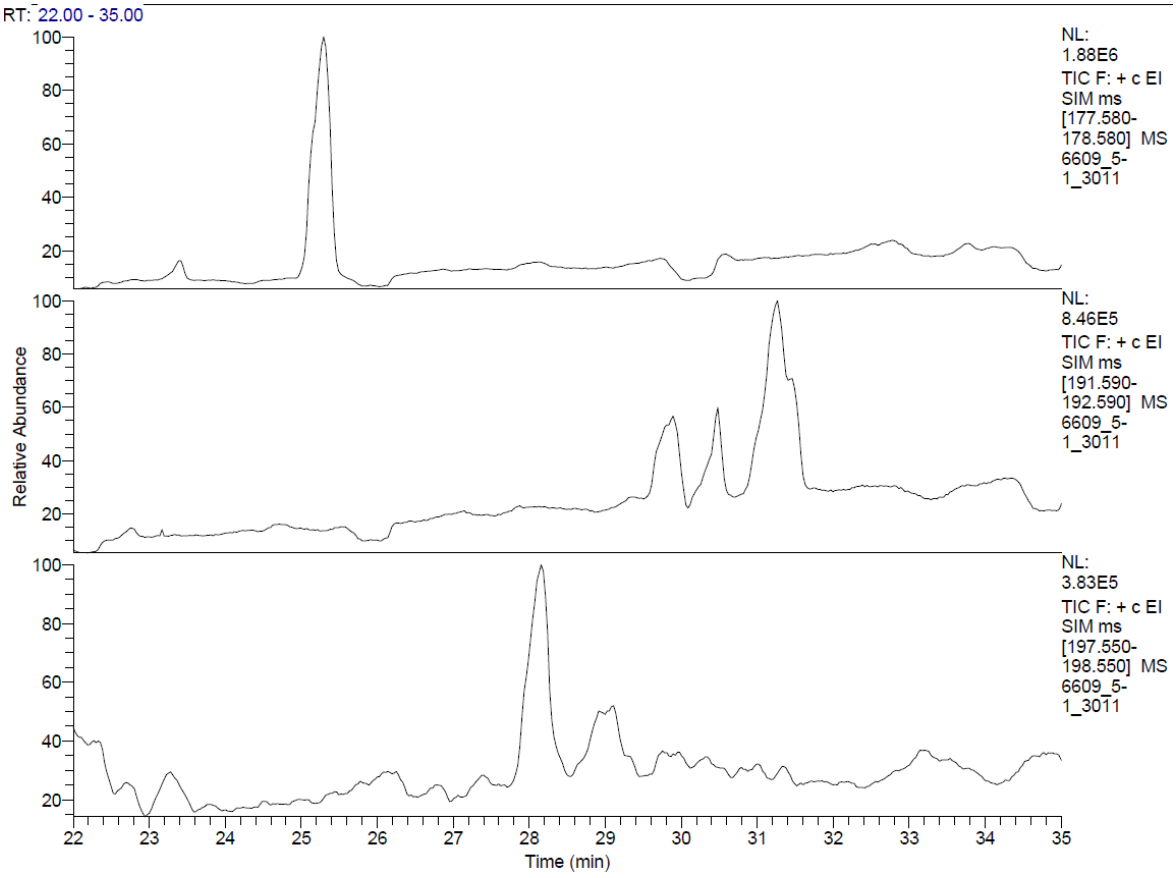
RT: 22.00 - 35.00
NL:
1.88E6
TIC F: + c EI
SIM ms
[177.580-
178.580] MS
6609_5-
1_3011
NL:
8.46E5
TIC F: + c EI
SIM ms
[191.590-
192.590] MS
6609_5-
1_3011
NL:
3.83E5
TIC F: + c EI
SIM ms
[197.550-
198.550] MS
6609_5-
1_3011
Relative Abundance
Time (min)